LIQUID BIOPSY: A TOOL FOR BETTER UNDERSTANDING OF THE METASTATIC PROCESS ECOSYSTEM

EDITED BY: Elisabetta Rossi, Matteo Bocci, Francesco Fabbri and Rui P. L. Neves

PUBLISHED IN: Frontiers in Oncology

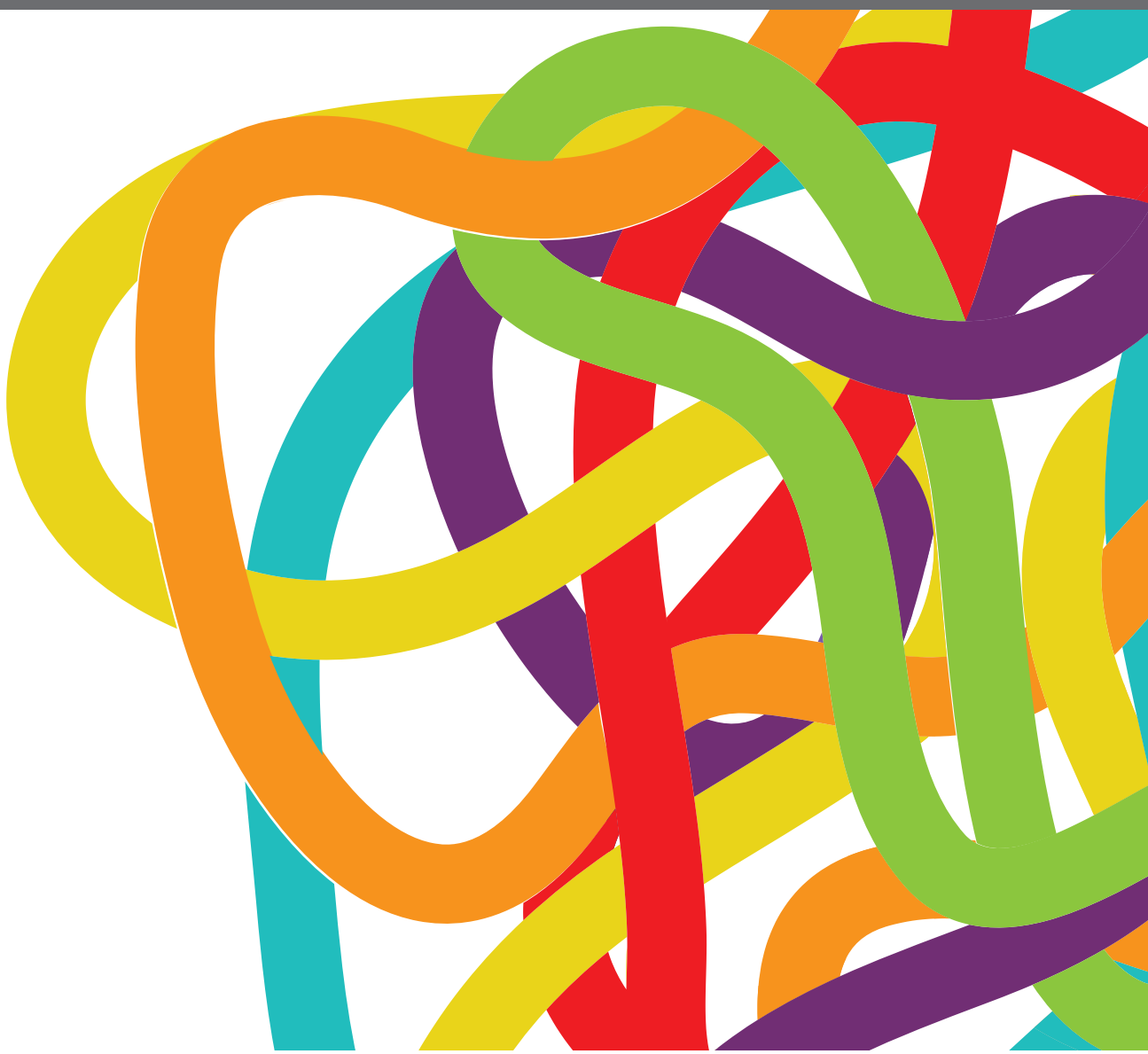

frontiers Research Topics

ISSN 1664-8714
ISBN 978-2-83250-019-4
DOI 10.3389/978-2-83250-019-4

About Frontiers

Frontiers is more than just an open-access publisher of scholarly articles: it is a pioneering approach to the world of academia, radically improving the way scholarly research is managed. The grand vision of Frontiers is a world where all people have an equal opportunity to seek, share and generate knowledge. Frontiers provides immediate and permanent online open access to all its publications, but this alone is not enough to realize our grand goals.

Frontiers Journal Series

The Frontiers Journal Series is a multi-tier and interdisciplinary set of open-access, online journals, promising a paradigm shift from the current review, selection and dissemination processes in academic publishing. All Frontiers journals are driven by researchers for researchers; therefore, they constitute a service to the scholarly community. At the same time, the Frontiers Journal Series operates on a revolutionary invention, the tiered publishing system, initially addressing specific communities of scholars, and gradually climbing up to broader public understanding, thus serving the interests of the lay society, too.

Dedication to Quality

Each Frontiers article is a landmark of the highest quality, thanks to genuinely collaborative interactions between authors and review editors, who include some of the world's best academicians. Research must be certified by peers before entering a stream of knowledge that may eventually reach the public - and shape society; therefore, Frontiers only applies the most rigorous and unbiased reviews.
Frontiers revolutionizes research publishing by freely delivering the most outstanding research, evaluated with no bias from both the academic and social point of view. By applying the most advanced information technologies, Frontiers is catapulting scholarly publishing into a new generation.

What are Frontiers Research Topics?

Frontiers Research Topics are very popular trademarks of the Frontiers Journals Series: they are collections of at least ten articles, all centered on a particular subject. With their unique mix of varied contributions from Original Research to Review Articles, Frontiers Research Topics unify the most influential researchers, the latest key findings and historical advances in a hot research area! Find out more on how to host your own Frontiers Research Topic or contribute to one as an author by contacting the Frontiers Editorial Office: frontiersin.org/about/contact

LIQUID BIOPSY: A TOOL FOR BETTER UNDERSTANDING OF THE METASTATIC PROCESS ECOSYSTEM

Topic Editors:
Elisabetta Rossi, University of Padua, Italy
Matteo Bocci, Lund University, Sweden
Francesco Fabbri, Scientific Institute of Romagna for the Study and Treatment of Tumors (IRCCS), Italy
Rui P. L. Neves, University Hospital Düsseldorf, Germany

Citation: Rossi, E., Bocci, M., Fabbri, F., Neves, R. P. L., eds. (2022). Liquid Biopsy: a Tool for Better Understanding of the Metastatic Process Ecosystem. Lausanne: Frontiers Media SA. doi: 10.3389/978-2-83250-019-4

Table of Contents

frontiers | Frontiers in Oncology

TYPE Editorial
PUBLISHED 10 August 2022
DOI 10.3389/fonc.2022.951158

OPEN ACCESS

EDITED AND REVIEWED BY
Massimo Fantini,
Precision Biologics, Inc., United States

*CORRESPONDENCE
Matteo Bocci
matteo.bocci@med.lu.se

†These authors have contributed equally to this work

SPECIALTY SECTION
This article was submitted to Cancer Molecular Targets and Therapeutics, a section of the journal Frontiers in Oncology

RECEIVED 23 May 2022
ACCEPTED 26 July 2022
PUBLISHED 10 August 2022

CITATION
Bocci M, Fabbri F, Neves RPL and Rossi E (2022) Editorial: Liquid biopsy: A tool for better understanding of the metastatic process ecosystem. *Front. Oncol.* 12:951158. doi: 10.3389/fonc.2022.951158

Editorial: Liquid biopsy: A tool for better understanding of the metastatic process ecosystem

Matteo Bocci[1*†], Francesco Fabbri[2†], Rui P.L. Neves[3†] and Elisabetta Rossi[4,5†]

[1]Department of Laboratory Medicine, Division of Translational Cancer Research, Lund University Cancer Centre, Medicon Village, Lund University, Lund, Sweden, [2]Biosciences Laboratory, IRCCS Istituto Romagnolo per lo Studio dei Tumori (IRST) "Dino Amadori", Meldola, Italy, [3]Department of General, Visceral and Pediatric Surgery, University Hospital and Medical Faculty of the Heinrich-Heine University Düsseldorf, Düsseldorf, Germany, [4]Department of Surgery, Oncology and Gastroenterology, Oncology Section, University of Padua, Padua, Italy, [5]Veneto Institute of Oncology IOV-IRCCS, Padua, Italy

KEYWORDS

liquid biopsy, metastatic cancer, cancer, tumor ecosystem, circulating tumor

Editorial on the Research Topic
Liquid biopsy: A tool for better understanding of the metastatic process ecosystem

Liquid biopsy is a non- or minimally-invasive procedure that allows retrieving analytes of different nature and different origins from body fluids including blood, urine, and cerebrospinal fluid (CSF). In the field of oncology, this sampling strategy has gained considerable attention and a growing number of technologies have been developed to inspect —in a fairly quick and economical way— circulating tumor cells (CTCs), extracellular vesicles (EVs), circulating-free tumor (ct) DNA, RNA, and a variety of non-coding RNAs from blood. Initially, these biomarkers have been gauged for their value as clinical indicators for diagnosis, prognosis as well as biomarkers for response to therapeutic regimens (1, 2). However, CTCs, ct nucleic acids, and EVs also play an active role in the metastatic process (3, 4), suggesting that liquid biopsy might also provide new opportunities to explore the biological and molecular mechanisms of tumor dissemination. On the one hand, CTCs have proven metastasis-initiating properties, indicating that these cells have the potential to inform on the molecular features necessary to reach and colonize distant organs. On the other hand, the ability of primary tumors to successfully spread to distant organs is dependent on interactions with microenvironments in distinct niches, and both CTCs (either alone, in clusters or aggregated with platelets/lymphocytes) and tumor-derived genetic material have been previously established as pivotal players in shaping such communication cues (5–8). Thus, the opportunity to detect blood-borne analytes should have a profound impact on our understanding of the systemic disease, and consequently on the management and monitoring of human malignancies.

This Research Topic comprises a series of 16 independent contributions addressing the potential utility of liquid biopsy as a complementary means to tackle specific, sorely needed, and unresolved clinical issues.

One such example comes from the inherent difficulty of detecting the presence of specific tumor types (9), which are often only diagnosed when they have already systemically spread in the organism. Xu et al. developed a prediction tool based on a regression model that integrates data from sequencing and epigenetic analysis of urine samples, and further identified the methylation status of the *ONECUT2* gene as a prospective biomarker for the detection of upper tract urinary carcinomas. With a similar goal in mind, Rikkert et al. reported on the efforts of a Dutch consortium to assess the available technologies for the recognition, classification, characterization and enumeration of the different types of tumor-derived (td)EVs in blood samples when using prostate cancer cell lines as a reference.

The availability of approved companion diagnostic tools is a reality for some tumor types with specific mutational patterns. Indeed, already in 2013, the Food and Drug Administration (FDA) agency approved the use of CellSearch for the detection of CTCs in metastatic breast, colorectal and prostate cancer (10). More recently, the same federal bureau cleared Foundation Medicine's FoundationOne®Liquid CDx platform to monitor the response to standard of care by evaluating the rearrangements, mutations, single nucleotide variants (SNVs), and *Indels* in ctDNA in breast, prostate, ovarian and non-small cell lung cancer (NSCLC). In this special issue, two papers focus on EGFR mutations specifically in NSCLC: Nardo et al. performed a retrospective droplet qPCR analysis on co-existing *KRAS* alterations in EGFR-mutated NSCLC patients post-first-line tyrosine kinase inhibitor (TKI) treatment. Despite the low number of samples that will require further validation, low-frequency co-mutations seemed to reduce the efficacy of targeted EGFR therapy. In addition to such events, uncovering secondary mutations that might emerge *de novo* or through the selection of pre-existing clones is a fundamental aspect to offer patients the best available therapeutic option. In the context of this framework, Liu et al. presented the results of a pipeline which had a twofold purpose: first, to compare EGFR mutations in primary tissue and circulation (in ctDNA and CTCs); second, to develop a multimodal analysis of secondary mutational events from a single blood sample, to spare additional invasive sampling in patients.

However, the actual role of liquid biopsy-based protocols for early detection of lung cancer seems more nebulous: as highlighted in the review article by Freitas et al., sensitivity and specificity of current technologies are still the limiting factors for the ambitioned transition from research environments to clinical routines. These aspects become even more challenging for tumor types with scarce evidence-based literature: a case in point is the underlooked role of tdEVs in the biology of gynecological malignancies, which is the ground zero for the perspective paper by Herrero et al. In a similar fashion, taking advantage of the tumor-specific circulome is not up to par in clear cell renal cell carcinoma (ccRCC), with Lakshminarayanan et al. detailing how the current strategies have fallen short of the promised revolution.

Together with driver genetic mutations, additional factors contribute to the broad spectrum of progression and response to treatment. From a clinical standpoint, these biological components represent —if validated— attractive biomarkers with diagnostic, predictive or prognostic value. One interesting approach is described by Gu et al., as a specific tRNA-derived fragment seemed to bear diagnostic and post-operative capabilities in gastric cancer. Notably, this marker correlated with disease progression and showed a gradient expression allowing to distinguish healthy donors from patients affected by different pathologies of the stomach, including inflammation-driven gastritis and cancer. Furthermore, molecular profiling can aid the traditional histopathological classification of tumors. For example, breast cancer taxonomy is clinically very well defined, with a series of markers that guide treatment decisions, and are indicative of clinical performance, outcome, and risk of metastatic disease. As the name suggests, triple-negative breast cancer (TNBC) lacks the expression of three major drivers of the proliferation of the malignant compartment, namely hormone receptors (Estrogen and Progesterone) as well as the Human Epidermal growth factor receptor (HER)2. Therefore, these tumors are currently not eligible for targeted drugs, with chemo- and radiation therapy still representing the mainstay offer. Nonetheless, through gene expression profiling, a subset of the TNBC tumors is further characterized by an enrichment for an androgen receptor (AR) signature, suggesting a functional signalling that might be exploited for therapeutic gain. The study led by Kasimir-Bauer et al. determined that in primary non-metastatic TNBC, AR-related genes can be found in CTCs that are effectively wiped out by chemotherapy. However, these markers seemed to confer an intrinsic higher risk of early relapse as well as an association with reduced overall survival. Additionally, the authors noted that the CTCs also harbored a specific AR splice variant, which is known to be associated with therapeutic resistance.

In parallel, the above-mentioned obstacles curb the use of liquid biopsy for the early detection of metastatic disease. It is indeed conceivable that tumor-derived circulating components could be found at any given time throughout tumorigenesis, including metastatic disease. At the same time, it is important to stress that a curative intent is much more likely to succeed before systemic spread occurs (11). Eslami-S et al. authored a comprehensive review of the contribution of liquid biopsy analytes in every step of the metastatic cascade, thereby serving as a backbone for many of the original articles collected in this special issue. For instance, Gurioli et al. followed castration-resistant prostate cancer patients exposed to standard of care to assess the impact of copy number status

for AR on clinical outcomes. Jiang et al. compared a panel of somatic mutations that affect pancreatic adenocarcinoma development and progression in primary tumors and plasma-borne ctDNA, and their results were further correlated to clinical parameters like tumor size, disease-free survival, and vascular invasion to predict recurrence.

Alongside these more established biomarkers, another set of papers proposes a broader range of prognostic markers based on circulating catabolites, micro (mi)RNAs as well as other hallmarks of cancer. In the context of metastatic prostate cancer, Sharova et al. aimed to identify blood-borne cell-free miRNAs that could predict the response to two different AR-targeting agents that are currently available for patients, while Crotti et al. employed mass spectrometry to determine the significance of tryptophan catabolism as a prognostic factor in locally advanced rectal cancer prior to preoperative chemotherapy. Interestingly, the authors found that tryptophan levels were differentially regulated in responsive *vs.* non-responsive patients. By expanding the analysis to the enzymes that are involved in the catabolism of this amino acid, discordant results were obtained between plasma and primary tissue, thus warranting further investigations. Finally, two studies shed light on capturing genetic events such as allelic imbalance and genomic instability. The former, led by Boldrin et al. used a panel of microsatellite and single nucleotide polymorphisms (SNPs) in blood as a readout for tumor burden during treatment in a cohort of patients diagnosed with locally advanced esophageal cancer. In agreement with the intended chief use of liquid-based screening, a longitudinal follow-up in a few selected patients further revealed that tumor-specific alterations could be detected in the circulation before symptomatic or overt clinical signs of relapse. In the latter, Wu et al. compared ctDNA in matched plasma and CSF from NSCLC patients with leptomeningeal metastases (LM). This work highlights the gain on sensitivity for mutation detection obtained by analysis of CSF and, intriguingly, this analysis revealed the enrichment of a specific mutation linked to acquired resistance to TKO inhibitors exclusively in the CSF, suggesting different mechanisms of cancer evolution between LM and extracranial lesions.

Even though the body of work presented in this collection focuses on pivotal aspects of liquid biopsy with a clear clinical application, outstanding questions remain unanswered. Among these is the overall issue of validation, as preliminary analyses are often performed in cohorts that are not sufficiently large to make solid and substantial claims from a statistical perspective. This goes hand in hand with the aforementioned specificity and sensitivity barrier of certain approaches. Nonetheless, it is also fundamental to acknowledge how dynamic the field of liquid biopsy has been, which is well reflected by the exponentially growing number of publications, particularly in the last decade. Importantly, the knowledge produced so far has resulted in great technological advances that are already reducing the gap between the bench and the bed, as highlighted before. Two of the key strengths of liquid biopsy are its power to inform about tumor features even when conventional tissue biopsy is not possible, and to shed light about residual disease long before overt clinical symptomatology. Indeed, this feature could be exploited in large-scale prevention screenings, *e.g.* together with mammographic examination for breast cancer or the fecal immunochemical test for colon cancer. Additionally, we believe that monitoring tumor *via* liquid biopsy will be an indispensable companion tool during treatment to offer more dynamic and proactive personalized regimens. Conceivably, this approach could minimize the risk of therapeutic resistance that afflicts many patients as the tumor progresses in an active state of selective pressure. An additional element central to the implementation of liquid biopsy is the notable increase in the quality and depth of sampling as the technology progresses, allowing for the selection of mutations with clear clinical relevance. This might overcome certain limitations peculiar to the early disease, a stage characterized by a limited concentration of blood-borne tumor-derived material. In this scenario, assays could be developed to identify and distinguish selective mutations rather than indiscriminately fishing out analytes without a clear clinical annotation that shed from primary tumors. Further promising assays are currently under development or awaiting clinical approval, including *e.g.* the "one tube fits all" CancerSEEK for multi-analytes for pan-cancer discovery (12), the SAGA Diagnostics' SAGAsafe for the longitudinal monitoring of EGFRT790M mutations in lung cancer (13), or the Illumina's TruSight Oncology 500 portfolio (14). These developments are good indicatives and we are positive about a gradually stronger impact of liquid biopsy in the clinics. In connection with the real implementation of liquid biopsy in the clinical setting, this procedure offers an unprecedented opportunity to sample the systemic disease and address questions related to the biology of cancer. One subject of paramount interest is whether this approach could help discriminate which organs are affected by metastatic colonization, as already suggested for EVs (15), thereby implying a differential composition of tumor-derived particles and catabolites dispersed in circulation.

Author contributions

All authors listed have made a substantial, direct, and intellectual contribution to the work and approved it for publication.

Conflict of interest

The authors declare that the research was conducted in the absence of any commercial or financial relationships that could be construed as a potential conflict of interest.

Publisher's note

References

1. Murtaza M, Dawson SJ, Tsui DW, Gale D, Forshew T, Piskorz AM, et al. Non-invasive analysis of acquired resistance to cancer therapy by sequencing of plasma DNA. *Nature* (2013) 497(7447):108–12.

2. Olsson E, Winter C, George A, Chen Y, Howlin J, Tang MH, et al. Serial monitoring of circulating tumor DNA in patients with primary breast cancer for detection of occult metastatic disease. *EMBO Mol Med* (2015) 7(8):1034–47.

3. Dawson SJ, Tsui DW, Murtaza M, Biggs H, Rueda OM, Chin SF, et al. Analysis of circulating tumor DNA to monitor metastatic breast cancer. *N Engl J Med* (2013) 368(13):1199–209.

4. Magbanua MJM, Savenkov O, Asmus EJ, Ballman KV, Scott JH, Park JW, et al. Clinical significance of circulating tumor cells in hormone receptor-positive metastatic breast cancer patients who received letrozole with or without bevacizumab. *Clin Cancer Res* (2020) 26(18):4911–20.

5. Heidrich I, Ackar L, Mossahebi Mohammadi P, Pantel K. Liquid biopsies: Potential and challenges. *Int J Cancer* (2021) 148(3):528–45.

6. Alix-Panabieres C, Pantel K. Liquid biopsy: From discovery to clinical application. *Cancer Discovery* (2021) 11(4):858–73.

7. Wortzel I, Dror S, Kenific CM, Lyden D. Exosome-mediated metastasis: Communication from a distance. *Dev Cell* (2019) 49(3):347–60. doi: 10.1016/j.devcel.2019.04.011

8. Jerabkova-Roda K, Dupas A, Osmani N, Hyenne V, Goetz JG. Circulating extracellular vesicles and tumor cells: sticky partners in metastasis. *Trends Cancer* (2022) S2405-8033(22):00113–3. doi: 10.1016/j.trecan.2022.05.002

9. Siravegna G, Marsoni S, Siena S, Bardelli A. Integrating liquid biopsies into the management of cancer. *Nat Rev Clin Oncol* (2017) 14(9):531–48. doi: 10.1038/nrclinonc.2017.14

10. Available at: https://www.cellsearchctc.com.

11. Crosby D. Delivering on the promise of early detection with liquid biopsies. *Br J Cancer* (2022) 126(3):313–5. doi: 10.1038/s41416-021-01646-w

12. Cohen JD, Li L, Wang Y, Thoburn C, Afsari B, Danilova L, et al. Detection and localization of surgically resectable cancers with a multi-analyte blood test. *Science* (2018) 359(6378):926–30.

13. Available at: https://sagadiagnostics.com/t790m/.

14. Available at: https://emea.illumina.com/products/by-type/clinical-research-products/trusight-oncology-500-ctdna.htmlhttps://emea.illumina.com/products/by-type/clinical-research-products/trusight-oncology-500-ctdna.html.

15. Rezaie J, Ahmadi M, Ravanbakhsh R, Mojarad B, Mahbubfam S, Shaban SA, et al. Tumor-derived extracellular vesicles: The metastatic organotropism drivers. *Life Sci* (2022) 289:120216. doi: 10.1016/j.lfs.2021.120216

frontiers in Oncology

METHODS
published: 04 June 2020
doi: 10.3389/fonc.2020.00608

Cancer-ID: Toward Identification of Cancer by Tumor-Derived Extracellular Vesicles in Blood

*L. G. Rikkert[1,2,3], P. Beekman[1,4,5], J. Caro[6], F. A. W. Coumans[2,3], A. Enciso-Martinez[1], G. Jenster[7], S. Le Gac[5], W. Lee[8], T. G. van Leeuwen[3,9], G. B. Loozen[6], A. Nanou[1], R. Nieuwland[2,3], H. L. Offerhaus[8], C. Otto[1], D. M. Pegtel[10], M. C. Piontek[11], E. van der Pol[2,3,9], L. de Rond[2,3,9], W. H. Roos[11], R. B. M. Schasfoort[1], M. H. M. Wauben[12], H. Zuilhof[4,13] and L. W. M. M. Terstappen[1]**

[1] Department of Medical Cell Biophysics, University of Twente, Enschede, Netherlands, [2] Laboratory of Experimental Clinical Chemistry, Amsterdam UMC, University of Amsterdam, Amsterdam, Netherlands, [3] Vesicle Observation Center, Amsterdam UMC, University of Amsterdam, Amsterdam, Netherlands, [4] Laboratory of Organic Chemistry, Wageningen University, Wageningen, Netherlands, [5] Applied Microfluidics for Bioengineering Research, University of Twente, Enschede, Netherlands, [6] Department of Imaging Physics, Delft University of Technology, Delft, Netherlands, [7] Department of Urology, Erasmus University Medical Center, Rotterdam, Netherlands, [8] Optical Sciences Group, Department of Science and Technology, University of Twente, Enschede, Netherlands, [9] Biomedical Engineering and Physics, Amsterdam UMC, University of Amsterdam, Amsterdam, Netherlands, [10] Department of Pathology, Amsterdam UMC, VU University Amsterdam, Amsterdam, Netherlands, [11] Molecular Biophysics, Zernike Institute, University of Groningen, Groningen, Netherlands, [12] Department of Biochemistry and Cell Biology, Faculty of Veterinary Medicine, Utrecht University, Utrecht, Netherlands, [13] School of Pharmaceutical Sciences and Technology, Tianjin University, Tianjin, China

OPEN ACCESS

Edited by:
Elisabetta Rossi, University of Padova, Italy

Reviewed by:
Masaki Terabe, National Cancer Institute, National Institutes of Health (NIH), United States
Victor C. Kok, Asia University, Taiwan

***Correspondence:**
L. W. M. M. Terstappen
l.w.m.m.terstappen@utwente.nl

Specialty section:
This article was submitted to Cancer Molecular Targets and Therapeutics, a section of the journal Frontiers in Oncology

Received: *21 January 2020*
Accepted: *02 April 2020*
Published: *04 June 2020*

Citation:
Rikkert LG, Beekman P, Caro J, Coumans FAW, Enciso-Martinez A, Jenster G, Le Gac S, Lee W, van Leeuwen TG, Loozen GB, Nanou A, Nieuwland R, Offerhaus HL, Otto C, Pegtel DM, Piontek MC, van der Pol E, de Rond L, Roos WH, Schasfoort RBM, Wauben MHM, Zuilhof H and Terstappen LWMM (2020) Cancer-ID: Toward Identification of Cancer by Tumor-Derived Extracellular Vesicles in Blood. Front. Oncol. 10:608. doi: 10.3389/fonc.2020.00608

Extracellular vesicles (EVs) have great potential as biomarkers since their composition and concentration in biofluids are disease state dependent and their cargo can contain disease-related information. Large tumor-derived EVs (tdEVs, $>1\,\mu m$) in blood from cancer patients are associated with poor outcome, and changes in their number can be used to monitor therapy effectiveness. Whereas, small tumor-derived EVs ($<1\,\mu m$) are likely to outnumber their larger counterparts, thereby offering better statistical significance, identification and quantification of small tdEVs are more challenging. In the blood of cancer patients, a subpopulation of EVs originate from tumor cells, but these EVs are outnumbered by non-EV particles and EVs from other origin. In the Dutch NWO Perspectief Cancer-ID program, we developed and evaluated detection and characterization techniques to distinguish EVs from non-EV particles and other EVs. Despite low signal amplitudes, we identified characteristics of these small tdEVs that may enable the enumeration of small tdEVs and extract relevant information. The insights obtained from Cancer-ID can help to explore the full potential of tdEVs in the clinic.

Keywords: atomic force microscopy, electrochemistry, electron microscopy, extracellular vesicles, flow cytometry, fluorescence microscopy, Raman spectrum analysis, surface plasmon resonance imaging

INTRODUCTION

Extracellular vesicles (EVs) are cell-derived particles with a phospholipid membrane. Because the membrane composition and content of EVs reflect the origin and state of the parental cells, EVs have become promising disease biomarkers (1–4). Participants from eight universities and 21 companies, who collaborate in the Dutch NWO Perspectief program Cancer-ID,

aim to develop and evaluate technology to detect tumor-derived EVs (tdEVs) in blood as biomarker for cancer.

Throughout the project, two main challenges involved in the detection of EVs in blood became apparent. First, EV detection is hampered because EVs are outnumbered by the presence of non-EV particles in blood, like soluble proteins and lipoprotein particles at the low end of the EV size and density range, and platelets at the high end of the EV size and density range (5–7). Moreover, the concentration of larger lipoproteins, such as chylomicrons, depends on food intake, thereby emphasizing the need to discriminate EVs from other such particles. To illustrate this challenge, we determined that 1 ml of human blood of metastatic castration-resistant prostate cancer patients contains about 10 large (>1 μm) tdEVs (8, 9), and we extrapolated this to encompass the small tdEVs to arrive at an estimated 10^4 tdEVs per 1 ml. Furthermore, the blood contains up to 10^{16} lipoproteins, up to 10^9 platelets, and up to 10^{11} other EVs (5, 7, 10–12), see **Figure 1**. The second challenge is the heterogeneity of EVs in many aspects, including morphology (13), size (13, 14), membrane composition (8, 15–19), and refractive index (20, 21), which complicates EV isolation, detection, and enumeration.

In sum, utilization of tdEVs as cancer biomarker requires (i) the discrimination of EVs from non-EV particles, (ii) identification of their cellular origin, and/or (iii) analysis of the EV molecular content. The insight that an EV-based cancer biomarker requires the ability to detect, identify, and enumerate tdEVs among other particles' plasma is an essential Cancer-ID outcome because it defines the state-of-the-art. Therefore, we will use this definition to evaluate the 10 techniques that were developed or improved throughout the project. The project includes techniques that (i) detect single particles attached to a surface, such as atomic force microscopy (AFM), electrochemical (EC) detection, scanning electron microscopy (SEM), and transmission electron microscopy (TEM); (ii) detect an ensemble of EVs attached to a surface, such as surface plasmon resonance imaging (SPRi); (iii) detect single EVs in suspension, such as flow cytometry (FCM); or (iv) can measure either single or multiple EVs attached to a substrate or in a suspension, such as Raman microspectroscopy. The other evaluated technologies are integrated photonics lab-on-chip devices for Raman spectroscopy, hybrid AFM–SEM–Raman, and immunomagnetic epithelial cell adhesion molecule (EpCAM) enrichment followed by fluorescence microscopic (FM) detection. The evaluated techniques including key characteristics are listed in **Table 1**. This table also gives an estimate of tdEV throughput from each technique applied in a clinical setting, taking into consideration the vast majority of non-tdEV particles in plasma that may or may not contribute to the signal.

To compare all techniques, EVs derived from prostate cancer cell lines and EVs derived from platelet and red blood cell concentrates were distributed among the participants and measured. Based on the aforementioned requirements, we aimed to qualify the ability of a technique to (i) detect or image EVs, (ii) identify tdEVs, which involves differentiation of tdEVs from EVs and non-EV particles, and (iii) relate the measured signal or count to the concentration of tdEVs in plasma.

PREPARATION OF EV SAMPLES

Two prostate cancer cell lines (PC3 and LNCaP) purchased from the American Type Culture Collection (ATCC, Manassas, VA) were used to obtain prostate-cancer-derived EVs. The cell lines were cultured at 37°C and 5% CO_2 in Roswell Park Memorial Institute (RPMI)-1640 with L-glutamine (Lonza, Basel, Switzerland) supplemented with 10% *v*/*v* fetal bovine serum (FBS) and 1% *v*/*v* penicillin and streptomycin (Lonza). Medium was refreshed every second day. The initial cell density was 10,000 cells/cm^2 as recommended by the ATCC. The cells were washed three times with phosphate-buffered saline (PBS; Sigma, Saint Louis, MO) when they reached 80–90% confluence. Next, FBS-free RPMI medium supplemented with 0.1% *v*/*v* penicillin and streptomycin was added to the cells. After 48 h of cell culture, the cell supernatant was collected and centrifuged for 30 min at 1,000 *g*. The supernatant was collected, and aliquots were snap frozen in liquid nitrogen and stored at −80°C.

Red blood cell concentrate (150 ml) obtained from Sanquin (Amsterdam, Netherlands) was diluted in a 1:1 ratio with filtered PBS [154 mM NaCl, 1.24 mM $Na_2HPO_4{\cdot}2H_2O$, 0.2 mM $NaH_2PO_4{\cdot}2H_2O$, pH 7.4; 0.22 μm filter (Merck Chemicals BV, Darmstadt, Germany)] and centrifuged three times for 20 min at 1,560 *g*. Platelet concentrate (100 ml) obtained from Sanquin was diluted in a 1:1 ratio with filtered PBS. Next, 40 ml acid of citrate dextrose (ACD; 0.85 M trisodiumcitrate, 0.11 M D-glucose, and 0.071 M citric acid) was added, and the suspension was centrifuged for 20 min at 800 *g*. Thereafter, the supernatant was centrifuged three times (20 min at 1,560 *g*) to ensure removal of platelets. The supernatant was collected, and aliquots of 50 μl were snap frozen in liquid nitrogen and stored at −80°C.

The particle size distributions of the EV samples were obtained using nanoparticle tracking analysis (NTA NS500; Nanosight, Amesbury, UK), equipped with an electron multiplying charge-coupled device (EMCCD) camera and a 405-nm diode laser (**Figure 2A**). Silica beads (105 nm; Microspheres–Nanospheres, Cold Spring, NY) were used to focus the microscope objective. Samples were diluted 10–2,000 times in filtered PBS to ensure that the number of particles in the field of view was below 200 per image. Of each sample, 10 videos of 30 s were captured with the camera shutter set at 33.31 ms and the camera gain set at 400. All samples were analyzed with the instrument software (NTA 2.3.0.15) using a threshold of 10, which was based on the exponential decay constant of the summed intensity histogram of all frames in each movie (MATLAB, v.7.9.0.529; Mathworks, Natick, MA).

Figure 2B shows the measured particle size distributions of the EV samples. We estimate the smallest detectable EV for NTA to be 70–90 nm (24).

TRANSMISSION ELECTRON MICROSCOPY

Cancer-ID Specific Method and Operating Principle

TEM has become the standard technique to confirm the presence of EVs in samples (27). TEM transmits electrons through

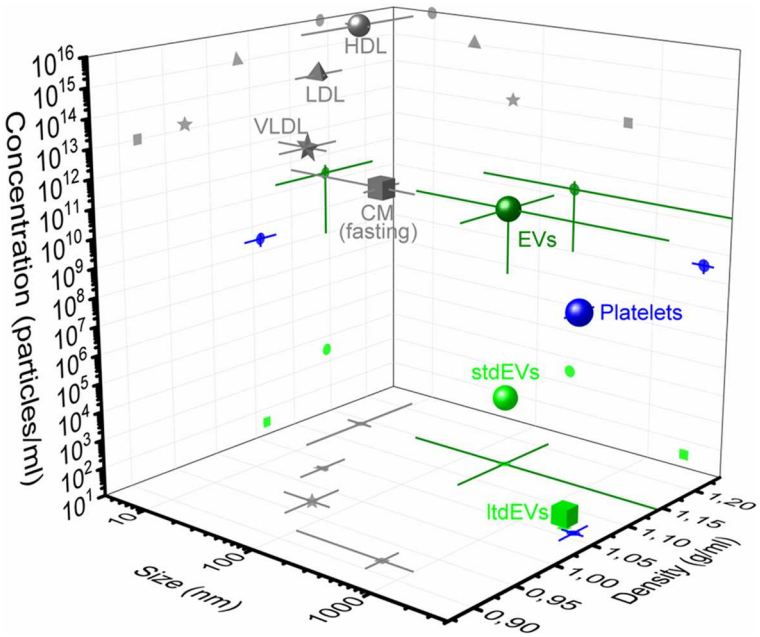

FIGURE 1 | Concentration, size, and density of plasma particles. 3D representation of concentration, size, and density of extracellular vesicles (dark green circle), platelets (blue), and the high-density lipoproteins (HDLs, gray circle), low-density lipoproteins (LDL, gray triangle), very low-density lipoproteins (VLDLs, gray star), and chylomicrons (CM, gray square) during fasting in blood. The average and standard deviation (lines) of the three parameters are indicated in the figure. Values are derived from the literature (5, 7, 11). The frequency of the large tumor-derived extracellular vesicles (ltdEVs, light green circle) determined in the Cancer-ID program and the small tdEVs (stdEVs, light green square) estimated using the frequency of ltdEVs (8–10).

sufficiently thin (<100–200 nm for biological materials) samples to make images with possibly subnanometer resolution (28). Particles from the sample are adhered to a carbon-coated formvar grid. Because EVs compete with other negatively charged particles for space on the grid, removal of soluble proteins and/or salts, for example by size exclusion chromatography (SEC) (29) and/or concentration, is required prior to incubation with EV samples. In addition, because TEM is performed in vacuum, EV samples are fixed with paraformaldehyde. After fixation and adhesion, the grid is placed on a droplet of contrast agent (uranyl acetate). A filter paper is used to remove the excess of contrast agent, and the grid is dried at room temperature (30).

Next, the grid is placed in the vacuum chamber of a FEI Tecnai 12 transmission electron microscope (FEI, Eindhoven, Netherlands). The sample is exposed to an electron beam, and images are constructed based on the detected transmitted electrons (**Figure 3A**). The contrast agent scatters electrons efficiently and stains the background more efficiently than the EVs. Consequently, EVs appear as bright particles on top of a dark background.

EV Definition

Water, the main cargo of an EV, is evaporated upon TEM resulting in a deformation of EVs, which often appear as "cup-shaped" (31–34) or "saucer/doughnut-shaped" particles (35–37) (**Figures 3C–F**). Particles, not having water as their major component, maintain their original structure during TEM. For example, lipoproteins appear spherical, and protein aggregates have an irregular shape. Therefore, we define EVs as cup-shaped particles larger than 30 nm (13).

Value Added by Cancer-ID

We show that TEM images taken by operator selection, the current standard within the EV field, can be used to demonstrate the presence of EVs in a sample. However, the examination of the morphology of EVs by TEM shows an operator bias in their identification (13), which may lead to "cherry picking" and emphasizes the importance of an automated and objective assessment of EV identification. Two important steps to improve the comparability and reproducibility of TEM for monitoring the quality of EV samples are (1) to take images at predefined locations and (2) provision of both close-up and wide-field images, as adopted by MISEV2018 (38).

Relevance for Cancer Diagnostics

Although with appropriate sample preparation, TEM can image EVs down to 30 nm, the contrast of TEM images is often insufficient to distinguish EVs from similar sized non-EV particles (**Figure 3B**). Moreover, to identify detection markers on tdEVs, immuno-gold labeling (34) is necessary. However, the main limitation of TEM for tdEV detection is the low throughput because of the scarcity of tdEVs among other abundant particles in plasma (see **Table 1**). Therefore, TEM can be used to evaluate the quality and presence of EVs but is not a relevant technique for identification of tdEVs in plasma samples.

TABLE 1 | Overview of the techniques used in Cancer-ID.

	Method	References	§	Information obtained	DL* (nm)	Thr* (prt/h)	T* (h)[a]
SURFACE							
Single	TEM	(13)	Transmission Electron Microscopy	Morphology, size	30	9×10^3	2×10^7
	SEM	(15)	Scanning Electron Microscopy	Topography, size	50	50	4×10^2
	AFM	(15)	Atomic Force Microscopy	Morphology, bending modulus	30	3×10^3	50
	Raman	(15)	Integrated Photonics Lab-on-Chip Devices for Raman Spectroscopy	Chemical composition	80	100	2×10^3
	Electrochemistry	(19)	AFM-SEM-Raman	Concentration, antigen expression	–	2×10^7	0.5
Bulk	SPRi	(22)	Electrochemistry	Antigen expression	–	30×10^7	3×10^{-2},b
SUSPENSION							
Single	NTA	(23)	Preparation of EV Samples	Particle size distribution	30	400	9×10^8
	Raman	(18)	Raman Microspectroscopy in Suspension	Chemical composition	80	9×10^4	6×10^7
	FCM	(21)	Surface Plasmon Resonance Imaging	Antigen expression, refractive index	200	6×10^6	4×10^6
	FM	(8)	Flow Cytometry	Antigen expression	1,000	4×10^6	2×10^{11}

*DL, detection limit; Thr, throughput in total number of (generic) particles per hour; T, expected time needed to find 1 tdEV (specifically) in a typical plasma sample.
[a]This column clarifies the need for in situ enrichment and sensitive detection for diagnostic applications. Nonenriched techniques are expected to process a third of all particles in 1 μl individually or spread out over a flat surface before encountering 1 tdEV. Considering that the total area of all particles (lipoproteins and EVs, see ***Figure 1***) distributed over a densely packed monolayer is ∼36 cm^2, the following assumptions were made:.
TEM: 2.2 × 2.2 μm^2 imaging area, imaged in 1 min, with a capturing efficiency of 21%. SEM: 25 μl sample, 50 μm × 7 mm capturing area, 10% capturing efficiency, 10% detected fraction (due to sensitivity limitations), 5 min per 10 × 10 μm^2 image. AFM: 25 μl sample, 50 μm × 7 mm capturing area, 10% capturing efficiency, 45 min per 25 × 25 μm^2 image. Raman on surface: 25 μl sample, 50 μm × 7 mm capturing area, 10% capturing efficiency, 1% detected fraction (due to sensitivity limitations), 17 min per 30 × 30 μm^2 image. Electrochemistry: Processing any sample takes ∼30 min regardless of the number of tdEVs. [b]SPRi: Processing time is 2 min. NTA: This technique can process 100 particles in 15 min, i.e., 10^{10} measurements have to be performed to find all tdEVs in 1 μl of plasma. Raman in suspension: ∼ 10^{12} measurements of 38 ms; 50% of particles fall below the detection limit. Flow cytometry: The sample must be diluted 10^9 times to ensure that one detection event corresponds to one particle; 3 μl can be processed in 1 min; 50% of particles fall below the detection limit. Fluorescence microscopy: An area of 100 × 100 μm^2 can be imaged in 0.2 s with an automated stage; 99% of particles fall below the detection limit.
Please note that 200 μl of sample is needed before the 10^4 EVs/μl limit of detection is reached.

SCANNING ELECTRON MICROSCOPY

Cancer-ID Specific Method and Operating Principle

EV samples are fixed in paraformaldehyde, followed by gradual dehydration from 70 to 100% ethanol in water with a 10% concentration increment step every 5–10 min. Subsequently, chemical drying of the sample can be achieved using 1:1 hexamethyldisilazane (HMDS) in ethanol for 3–5 min, followed by 100% HMDS for 3–5 min more. EVs are dehydrated and dried to maintain their morphological and surface features with minimal deformation in the vacuum chamber of the SEM (39, 40). EV samples are coated with gold to increase the image contrast and avoid surface charging. Furthermore, the sample must be placed on a conductive substrate during imaging. The entire procedure is conducted at room temperature.

In SEM imaging, a focused beam of electrons scans the surface of a sample interacting with all atoms in the sample (**Figures 4A, B**). Detection of the secondary electrons, originating from the outer layers of the sample, enables to visualize the topography of a sample. The amount of backscattered electrons, originating from the deeper layers of the sample, is associated with the atomic number of the atoms in the sample.

EV Definition

Since the LNCaP EV sample is derived from cell culture, we do not expect particles like lipoproteins to be present in this sample. **Figure 4B** shows round particles (white arrows) in lower and higher magnification, which we define as EVs.

Value Added by Cancer-ID

We show that cells and EVs captured on functionalized substrates and in solution can be imaged by SEM.

Relevance for Cancer Diagnostics

SEM can be used to visualize the topography of tdEVs, as small as 50 nm, but is unable to discriminate EVs from non-EV particles with a similar morphology. In order to confirm the nature of the particles, immunogold labeling or correlative techniques are required such as AFM, Raman, or fluorescence imaging. Cryo-TEM and cryo-SEM have been suggested superior techniques in retaining the EV morphology when compared to TEM and SEM because of the effect of fixation and air dehydration in the vacuum chamber (34); however, our results (**Figure 4**) support that gradual dehydration of EV samples in ethanol series prior to SEM imaging allows the maintenance of EV morphology. The main limitation of SEM similarly to TEM is the low throughput, as a large area needs to be processed before tdEVs are encountered

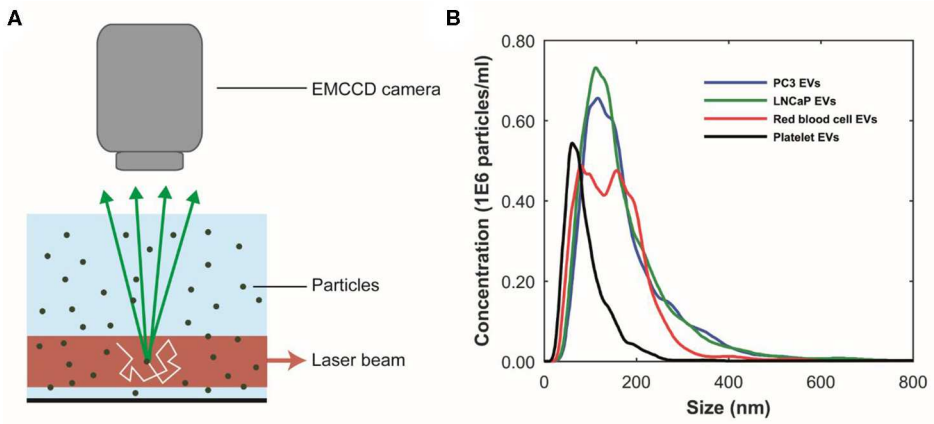

FIGURE 2 | Particle size distributions of extracellular vesicle (EV) samples measured using nanoparticle tracking analysis (NTA). **(A)** Schematic representation of the NTA setup. A laser beam illuminates the particles in suspension. The light scattered by particles undergoing random motion (white arrow) is collected by a microscope objective and detected by an multiplying charge-coupled device (EMCCD) camera. The random motion of the particles under Brownian motion can be related to their size. **(B)** NTA analysis results of the PC3 EV (blue), LNCaP EV (green), red blood cell EV (red), and the platelet (black) EV samples, respectively. The bin width is 10 nm. The mean particle size and concentration in the PC3 EV sample are 172 ± 4 nm and 1E8 particles/ml, respectively. The mean particle size and concentration in the LnCaP EV sample are 167 ± 4 nm and 1E8 particles/ml, respectively. The mean particle size and concentration in the red blood cell EV sample are 148 ± 4 nm and 1E8 particles/ml, respectively. The mean particle size and concentration in the platelet EV sample are 89 ± 5 nm and 4E7 particles/ml, respectively. Because the uncertainty in the determined concentration with NTA is unknown, the determined concentration should be interpreted as an order of magnitude estimate (24). Images adapted from Lee et al. (25) and van der Pol et al. (26).

(see **Table 1**). Therefore, SEM is not a relevant technique for the detection of tdEVs in plasma samples.

ATOMIC FORCE MICROSCOPY

Cancer-ID Specific Method and Operating Principle

EVs are added onto a poly-L-lysine-coated coverslip (41–44). Next, the sample chamber is filled with filtered PBS (0.2 μm filter; VWR International, Radnor, PA) and placed on the AFM. During AFM imaging, a cantilever with a nanometer-sized tip probes the sample surface (**Figure 5A**) (45). Deflection of the cantilever is measured with a laser and photodiode. AFM images are acquired in PeakForce Tapping mode on a Bruker Bioscope catalyst setup using minimal imaging force providing information about the topography of the samples surface. Mechanical properties can be obtained by applying a defined force perpendicular to the surface (indentation), providing force–indentation curves, as presented in **Figure 5B**.

EV Definition

With AFM, we characterize an EV as a particle of at least 25 nm in height with a spherical shape. Aggregates typically have a nonspherical shape and therefore can be excluded. The nanoindentation response is used to identify single EVs (42, 44). A typical indentation curve is characterized by a (close-to) linear initial increase in force followed by a softening and finally bilayer pinching close to the substrate (**Figure 5B**, red curve).

Value Added by Cancer-ID

Unique characteristics, like deformability, of tdEVs compared to EVs of other origin still need to be explored. Examples of AFM measurements of LNCaP EVs and platelet EVs are shown in **Figures 5C,D**. Importantly, it should be noted that AFM imaging *per se* is not distinguishing between EVs and lipoproteins. Therefore, a good purification protocol is necessary (combining gradient- and size-based isolation methods) in order to assure only EVs are present.

Relevance for Cancer Diagnostics

Because of the nanometer position sensitivity and subpiconewton force sensitivity, AFM can be used to determine the topography, morphology, and mechanical characteristics of single EVs, and differences between EVs of different origins can be investigated (42, 44). AFM is a low-throughput technique since only several particles can be observed at a time. For the moment AFM has not been shown to be a suitable technique for tdEV identification and enumeration in plasma samples (see **Table 1**).

RAMAN MICROSPECTROSCOPY IN SUSPENSION

Cancer-ID Specific Method and Operating Principle

EV samples are diluted in PBS to a concentration of $\sim 10^9$ particles/ml (as measured by NTA) and placed on a well glass slide, covered with a glass cover slip, and sealed with glue. Next, the glass slide is placed under the microscope objective (**Figure 6A**). A Raman optical tweezers [home-built system as described in Enciso-Martinez et al. (18)] is used to (i) trap single particles diffusing near the high intensity

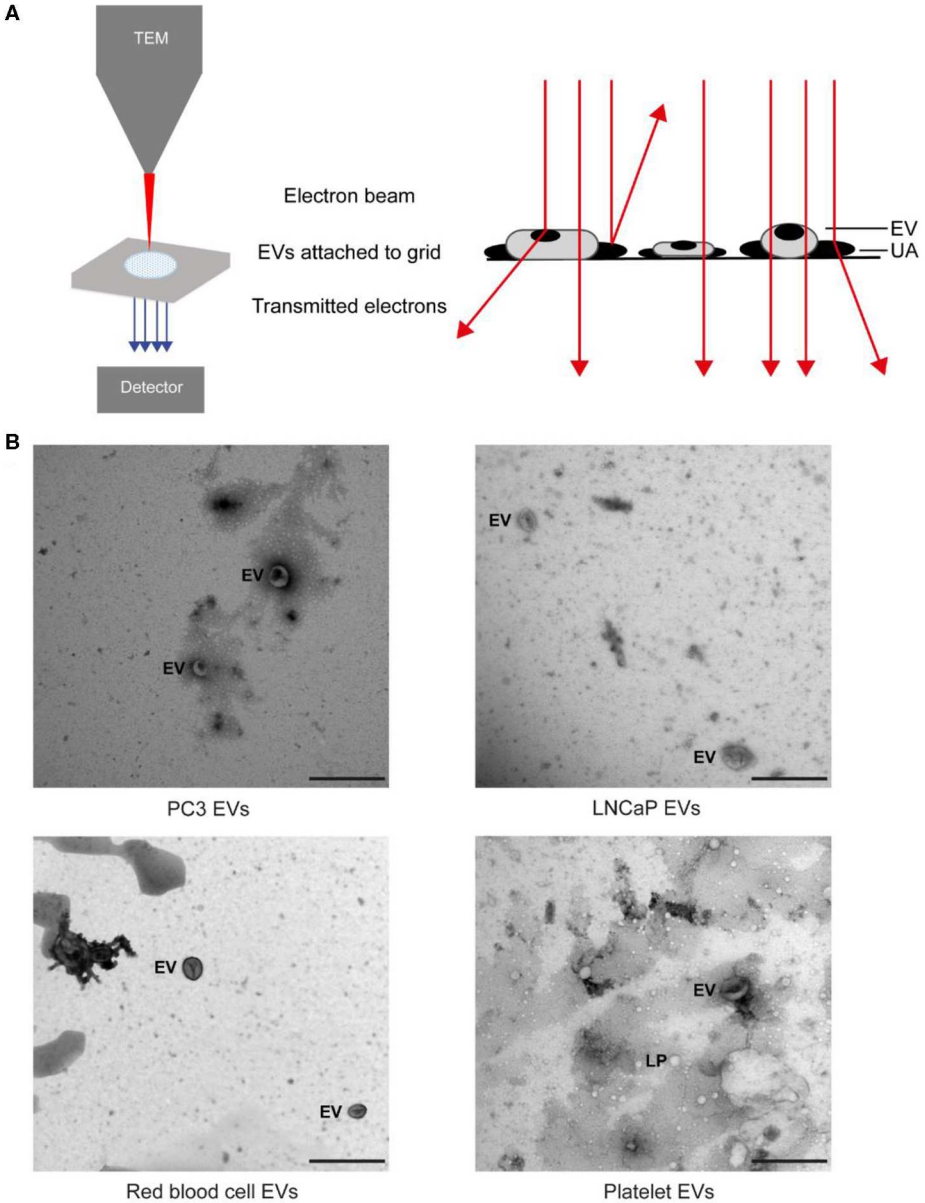

FIGURE 3 | Transmission electron microscopy (TEM) of extracellular vesicle (EV) samples. **(A)** Schematic representation of TEM imaging for EV samples. The sample on a grid is exposed to an electron beam, and images are constructed based on the detected transmitted electrons. The uranyl acetate (UA) scatters electrons efficiently, which results in negative contrast. EVs and lipoproteins (LPs) have a low electron density and are seen as bright particles in a dark background (13). **(B)** TEM images of the EV samples from PC3 and LNCaP and of red blood cells and platelets after size exclusion chromatography. The scale bar corresponds to 500 nm (25).

part of the focus (**Figure 6A**) and (ii) detect both Rayleigh and Raman scattered photons synchronously. The trapping of a single particle is detected by Rayleigh scattering, and the corresponding Raman spectrum discloses the chemical composition (18, 46).

EV Definition

The Raman spectra of submicrometer particles in biofluids have distinct spectral features depending on the nature of the particle or the source of EVs.

Value Added by Cancer-ID

The procedure to trap, release, and acquire sequentially the spectrum of single EVs in the focal volume is automated (18). Furthermore, EVs can be distinguished from lipoproteins and EVs from different sources, like PC3 EVs, LNCaP EVs, and red blood cell EVs. EVs show distinctive peaks at 1,004 and 1,607 cm^{-1} (phenylalanine) and a larger protein contribution at 2,811–3,023 cm^{-1} than lipoproteins (**Figures 6B**,**C**) (25, 46). The Raman spectrum of red blood cell EVs is different from PC3 EVs and LNCaP EVs around 1,200–1,385 cm^{-1} and

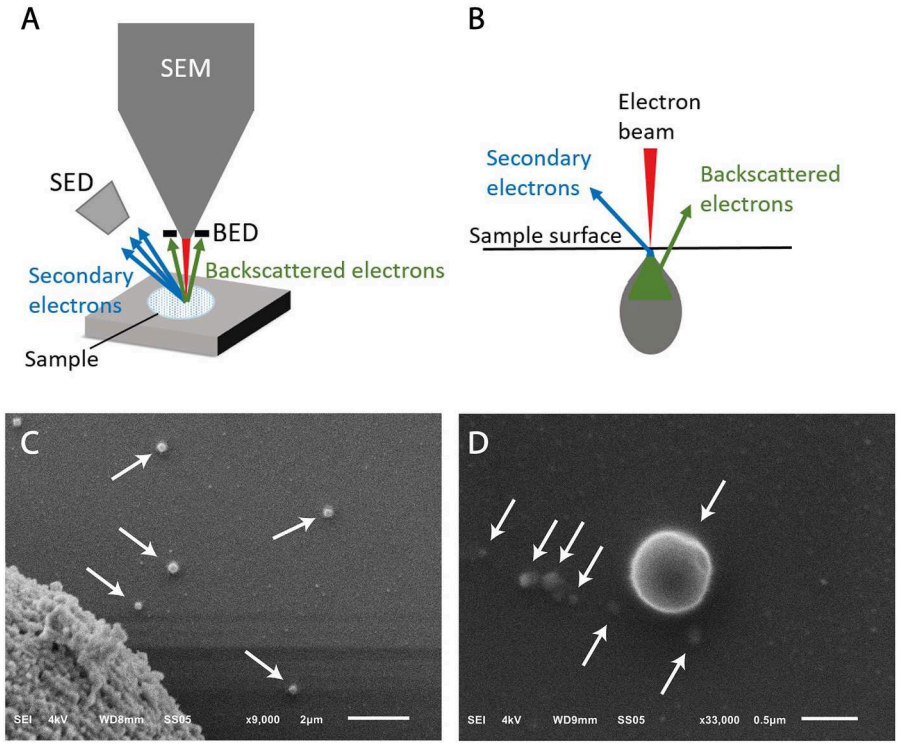

FIGURE 4 | Scanning electron microscopy (SEM) of extracellular vesicle (EV) samples. **(A)** Schematic representation of a SEM setup. SED, secondary electron detector; BED, backscatter electron detector. **(B)** The sample is illuminated by the electron beam. Electrons interact with the sample at different depths, resulting in emitted electrons from the surface (secondary electrons) and from deeper layers (backscattered electrons). **(C)** SEM image of LNCaP EVs indicated by arrows. The large object in the left lower corner is part of a LNCaP cell floating in the cell supernatant and was imaged to show that the contrast of EVs is similar to cells. The scale bar represents 2 μm. **(D)** Higher magnification allows imaging of smaller particles, possibly EVs, with lower contrast. The scale bar represents 500 nm.

1,510–1,631 cm^{-1} (46). Further classification of EVs and lipoproteins was achieved by multivariate analysis and convolutional neural networks analysis (25, 47).

Relevance for Cancer Diagnostics

Differences in chemical composition are shown between EVs and lipoproteins, and tdEVs compared to red blood cell EVs. However, a limitation of Raman is the throughput. As an example, a typical acquisition time per EV is 1 s (18). Hence, it has become clear that enrichment of tdEVs is needed prior to Raman analysis. Nevertheless, spontaneous Raman spectroscopy provides information on the chemical composition of single or multiple EVs in solution or on a surface in a noninvasive and label-free manner (18, 25, 46, 48–52).

INTEGRATED PHOTONICS LAB-ON-CHIP DEVICES FOR RAMAN SPECTROSCOPY

Cancer-ID Specific Method and Operating Principle

Two types of lab-on-chip devices were developed by Cancer-ID and fabricated in the cleanroom of the MESA+ Institute of Technology. From a technological perspective, Cancer-ID exploits the possibility of lab-on-a-chip devices to localize light in ways that are impossible with traditional optics. For example, compared to optical trapping using a microscope objective (*Raman Microspectroscopy in Suspension*), we expect that combining multiple beams will result in higher field gradients and therefore trapping of smaller single EVs. To proof the principle, device type 1 contains multiple waveguides, each of which emits a narrow beam of light towards the center of a fluidic microbath, as shown in **Figure 7A**. The resulting multiple beams combine coherently to form an interference pattern with multiple spots of high light intensity, each serving as an optical trap sufficiently strong to trap single submicrometer particles near the microbath center. The same concentrated light induces a Raman spectrum from the trapped particle for label-free identification. To increase the throughput, the well may be replaced by a flow cell in future versions.

To increase throughput compared to optical trapping using a microscope objective (section *Raman Microspectroscopy in Suspension*), device type 2 combines an enrichment step with the simultaneous detection of Rayleigh and Raman scattered light from multiple EVs. EVs in suspension bind to antibodies at the surface of a spiral waveguide, which is placed at the bottom of a microfluidic channel as shown in **Figure 7B** (54). A laser field propagates inside the waveguide and produces an evanescent field that probes the attached EVs simultaneously. The EVs will scatter some of this light with characteristic Raman shifts. A

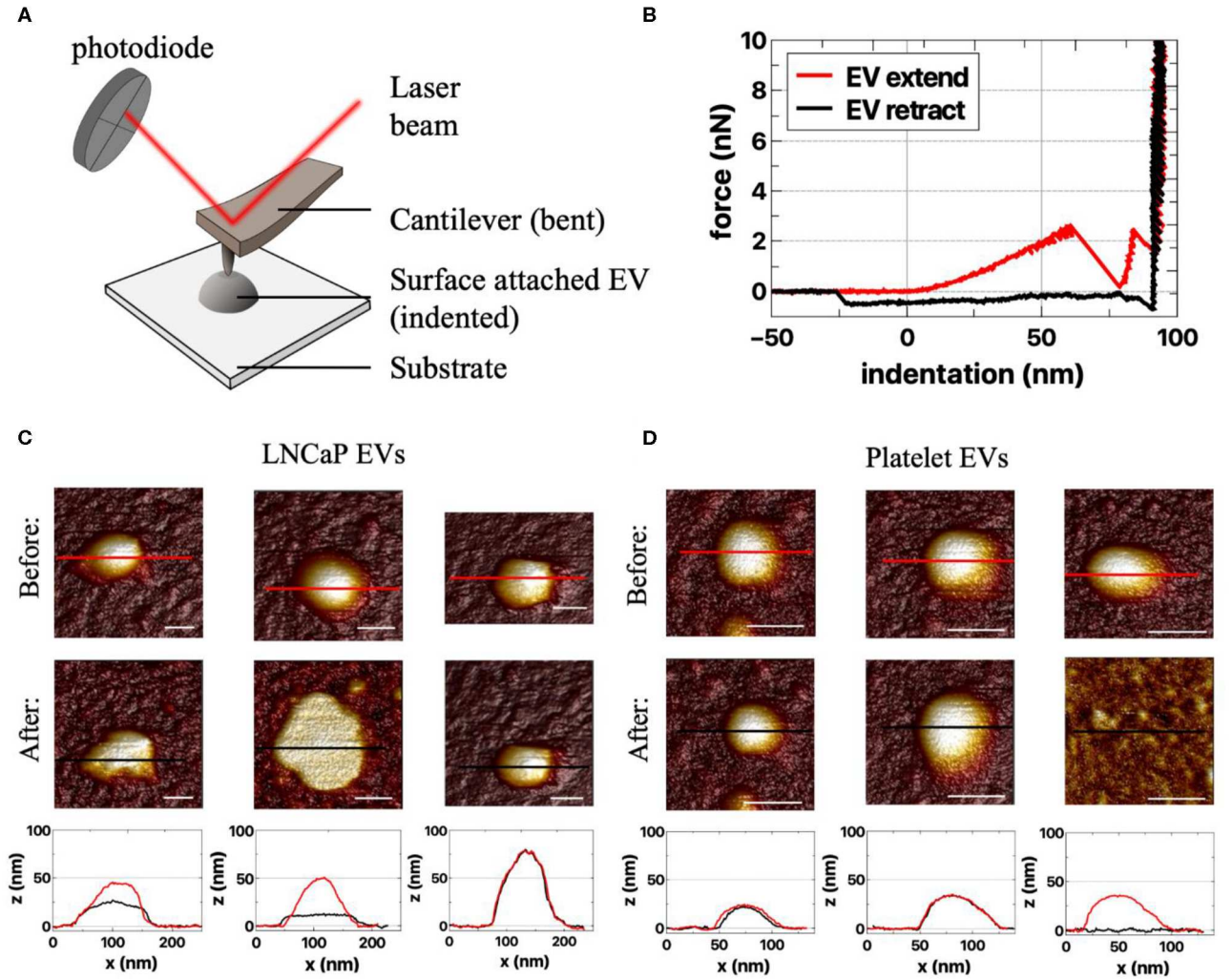

FIGURE 5 | Atomic force microscopy (AFM) of extracellular vesicle (EV) samples. **(A)** Schematic representation of the AFM setup. In AFM, a cantilever interacts with the sample, and the reflected laser beam is detected by a photodiode (45). The experiments are performed in liquid (not depicted). **(B)** Example of force–indentation curves (distance *z*) of the extend and retract response on an EV (45). AFM images of responses of **(C)** LNCaP EVs and **(D)** platelet EVs to an applied force before (first row) and after indentation (second row). Both the LNCaP and the platelet EVs can change shape upon indentation. The different responses are illustrated by the cross-sections (bottom row), taken at the indicated spots in the corresponding AFM images above (red, before indentation; black, after indentation). Scale bars represent 50 nm.

significant portion of this light re-enters the waveguide and can be collected from the entrance through the same objective that launched the excitation light.

EV Definition

An EV is identified based on the acquired Raman spectrum of the trapped particle. The obtained spectra may be cross-referenced with EV spectra already acquired with standard spontaneous Raman tweezers (*Raman Microspectroscopy in Suspension*). Furthermore, using device type 2, EVs are bound to the surface of a spiral waveguide by a specific antibody.

Value Added by Cancer-ID

Both device types are still under development. So the throughput and detection limit remain to be determined. In device type 1, integration of the multiple beam trap with a microfluidic channel opens new possibilities of controlled particle delivery to the trap and particle sorting with pressure-driven flow, which may allow the detection of smaller EVs. In device type 2, specific capture of tdEVs from the plasma is possible by the use of antibodies coated on the surface of a spiral waveguide using the chemistry used in *AFM-SEM-Raman* and *Electrochemistry*.

Relevance for Cancer Diagnostics

Based on the differences in chemical composition, tdEVs can be distinguished from non-EV particles like lipoproteins and EVs from other origin. Furthermore, enrichment can be achieved by the use of antibodies bound to the surface of a waveguide. Raman spectroscopy of EVs provides

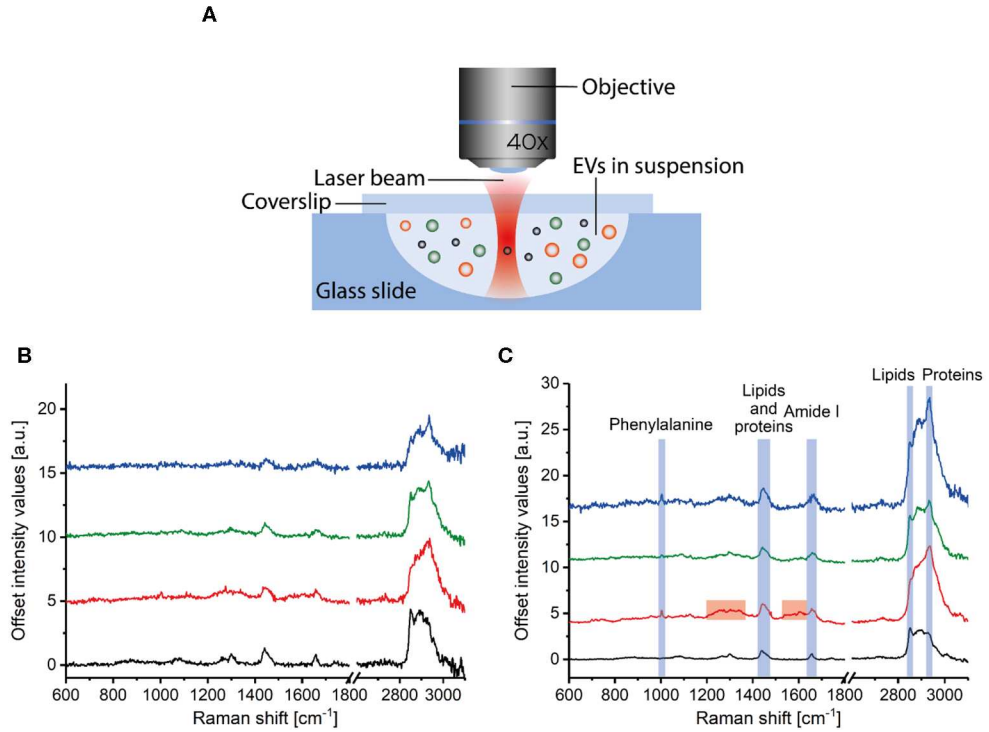

FIGURE 6 | Raman spectroscopy of extracellular vesicle (EV) samples. **(A)** Particles in suspension are loaded in a well glass slide that is mounted under a microscope objective. Incident light illuminates the sample, and both Raman and Rayleigh light are backscattered, collected by the lens, and detected by a spectrograph. Raman spectra corresponding to **(B)** single and **(C)** multiple PC3 EVs (blue), LNCaP EVs (green), red blood cell EVs (red), and lipoproteins in plasma (black). **(A)** is adapted from Enciso-Martinez et al. (18).

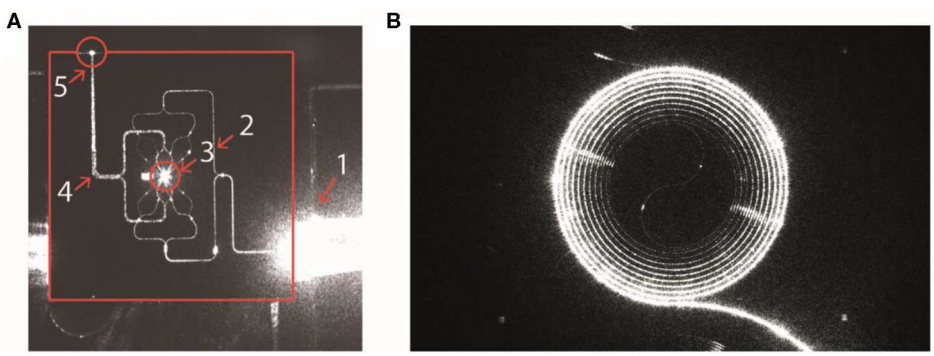

FIGURE 7 | Integrated photonics based lab-on-a-chip Raman spectroscopy. **(A)** Device type 1: Camera image of a device with 16 waveguides for trapping and four waveguides for detection. The device is actuated with light from an input fiber that is embedded in a fiber array unit (FAU) at the lower right-hand side. The various structures light up as a result of light scattering, causing some saturation of the camera. The solid red lines indicate the chip edges. 1, FAU; 2, excitation-waveguide circuitry; 3, microfluidic bath with the central trapping region; 4, detection-waveguide circuitry; 5, light from the trap that is coupled out by the detection waveguides. Here, the detection waveguides collect light as a result of direct illumination and scattering (from Loozen et al. (53)). **(B)** Device type 2: Spiral waveguide with the Raman pump light traveling inside the waveguide. The Raman signal is (partially) scattered back into the waveguide and collected at the front entrance. Reproduced with permission from Lee (54).

information on the chemical composition of single or multiple EVs in a noninvasive and label-free manner and may be simplified using integrated photonics lab-on-a-chip devices. The analysis time per particle remains to be measured before estimating the tdEV throughput and potential of the specific technique.

AFM–SEM–RAMAN

Cancer-ID Specific Method and Operating Principle

The surface of stainless-steel substrates is modified with a carboxydecyl phosphonic acid monolayer to covalently link

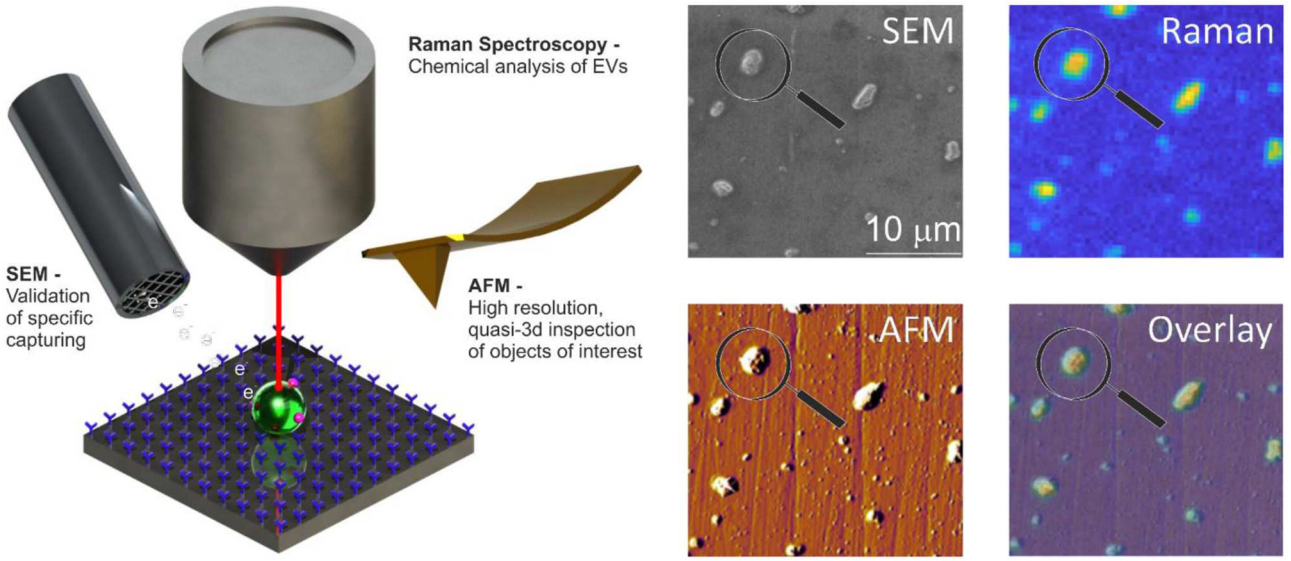

FIGURE 8 | Atomic force microscopy (AFM), scanning electron microscopy (SEM), and Raman spectroscopy of extracellular vesicle (EV) sample. Schematic representation of the system: antibody-functionalized stainless-steel substrate examined with SEM, AFM, and Raman for correlated multimodal analysis of individual EVs. Image adapted from Beekman et al. (15).

anti-EpCAM antibodies to the substrate (**Figure 8**) (55). EVs are incubated in poly(dimethylsiloxane) (PDMS) microchannels. The microchannels are washed to remove nonspecifically bound material. Next, EVs are incubated with paraformaldehyde in PBS for 15 min. The PDMS is removed by immersion in deionized water, 70% ethanol in water, and finally 100% ethanol for 5 min each step. Dehydration of tdEVs was followed by overnight drying. Alignment markers are embedded on the stainless-steel substrate by injecting patterned microfluidic channels with cyanoacrylate glue. The microscale alignment markers facilitate retracing individual EVs in the sample stages of the AFM (MFP-3D, Asylum Research, Wiesbaden, Germany), SEM (JEOL JSM-6610LA Analytical SEM, JEOL, Nieuw-Vennep, Netherlands), and Raman microspectroscopy]home-built system as described in Beekman et al. (15)]. SEM is used here to select regions of interest and confirm that the surface is successfully functionalized based on the attachment of EVs (15).

EV Definition

EVs are identified by SEM and a Raman spectrum with lipid-protein peaks (2,811–3,023 cm^{-1}) characteristic for EVs. The functionalization of the substrate ensures that the EVs are of epithelial cell origin permitting the determination of the mechanical characteristics, like deformability, of the tdEVs by AFM.

Value Added by Cancer-ID

The use of only one technique is often insufficient to identify and characterize EVs, as discussed in the previous sections (38). For example, both EVs and lipoproteins appear to be spherical by SEM. By combining SEM with AFM and Raman, we measure characteristics like size, chemical composition, and deformability to add certainty to the identification of tdEVs (15).

Relevance for Cancer Diagnostics

Using a combination of AFM, SEM, and Raman and the capture of tdEVs to a functionalized surface helps to distinguish EVs from non-EV particles and adds certainty to the origin of the EV.

In principle, this platform does not require distinguishing tdEVs from other species since enrichment is done by the functionalized surface (as assumed in **Table 1**). Since SEM measurements are faster than AFM or Raman, SEM was used for initial confirmation of tdEV presence on a chip; after enrichment, 1,000 tdEVs (of >100 nm) can be imaged in 1 h. Since AFM detects the more abundant much smaller particles (>30 nm) as compared to SEM (>100 nm), the fact that AFM is slower in terms of imaged square micrometer per unit time, is offset by a greater number of observed tdEV per imaged square micrometer, such that 1,000 tdEVs can be imaged in 2 h. For Raman, detection of 1,000 tdEVs would require about 100 measurements of 17 min each followed by several days of data processing.

ELECTROCHEMISTRY

Cancer-ID Specific Method and Operating Principle

Interdigitated nanoelectrodes (nIDEs), fabricated in the cleanroom of MESA+ Institute for Nanotechnology, are surface-modified with poly(ethylene glycol) diglycidyl ether to form an amine-reactive antifouling layer (**Figure 9A**) (56). Antibodies against EpCAM (VU1D9 clone) are covalently

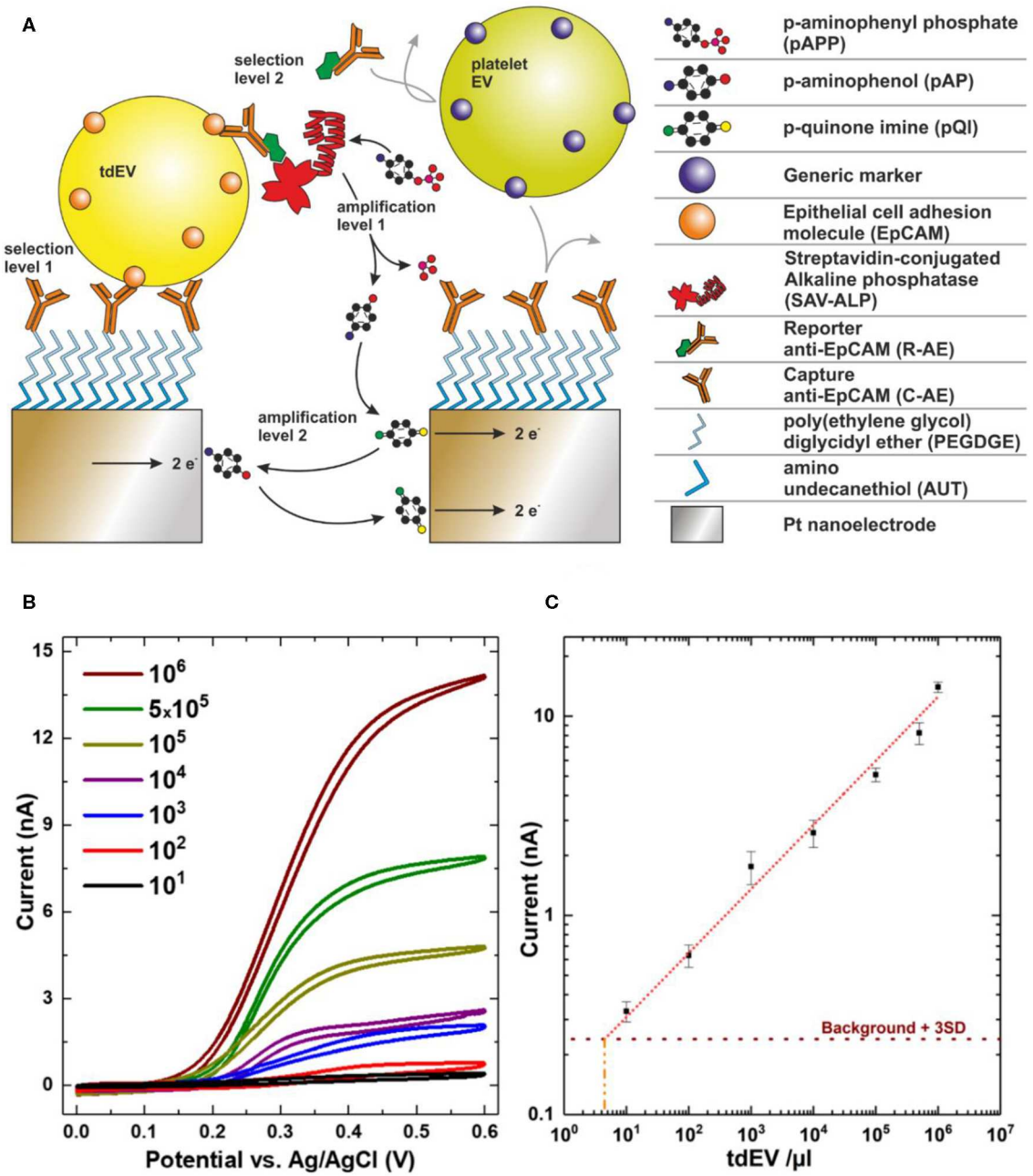

FIGURE 9 | Electrochemical detection of extracellular vesicle (EV) samples. **(A)** Scheme showing selective capture and *in-situ* labeling of EVs followed by enzymatic amplification of redox species and redox cycling. **(B)** Cyclic voltammograms recorded for a very wide range of EV concentrations. **(C)** Recorded current at 0.4 V for varying concentrations showing linear response over six orders of magnitude. Image adapted from Mathew et al. (19).

linked to this layer and the remainder of the surface blocked with bovine serum albumin (BSA). EV samples are introduced onto the device to allow binding to the electrodes. After incubation, a biotinylated reporter anti-EpCAM is introduced. The biotin moiety conjugates to streptavidin coupled to alkaline phosphatase (ALP). ALP, only present on EpCAM-positive particles, converts an electrochemically inert molecule (para-aminophenyl phosphate) into a redox-active species (para-aminophenol), to yield a first amplification phase. Next, the para-aminophenol undergoes redox cycling, providing a second amplification phase.

EV Definition

An increase in the redox current upon binding of particles to the nIDEs defines the presence of EVs. EVs from different species can be distinguished from each other by employing targeted

antibodies, yielding a very high selectivity. For example, the signal from platelet EVs did not vary from the background signal, whereas the introduction of LNCaP EVs markedly increased the signal (**Figure 9B**) (19).

Value Added by Cancer-ID

This new and sensitive technique was developed by Cancer-ID in collaboration with researchers from the NanoElectronics group at University of Twente, Netherlands. Several examples of sensitive integrated systems for (td)EV detection exist (57–60) (Lorencova). A unique feature of the technique discussed here is the ability to detect a low concentration of EVs with a low antigen expression. The linear response covers a broad range of concentrations, which largely overlaps with concentrations of tdEVs in patient blood.

Relevance for Cancer Diagnostics

Using electrochemistry, tdEVs can be discriminated from non-EV particles and EVs from other origin based on the expression of EpCAM. A dilution series of LNCaP EVs in PBS showed a linear response ranging from 5×10^3-10^9 tdEVs/ml (**Figure 9C**) (19), which overlaps with the expected tdEV concentration in plasma (10), showing that this technique is promising to identify, count, and characterize tdEVs in the range of clinical samples. Evaluation of the technique with plasma patient samples and association of the readout with clinical outcome remain to be tested.

The functionalized device is incubated with tdEV-containing sample and subsequently with reporter antibodies and redox mediator. In the experiments performed in the paper, these incubations were done over excessively long periods (2.5 h in total) to maximize the efficiency but, once optimized, can probably be performed several minutes to 1 h. The

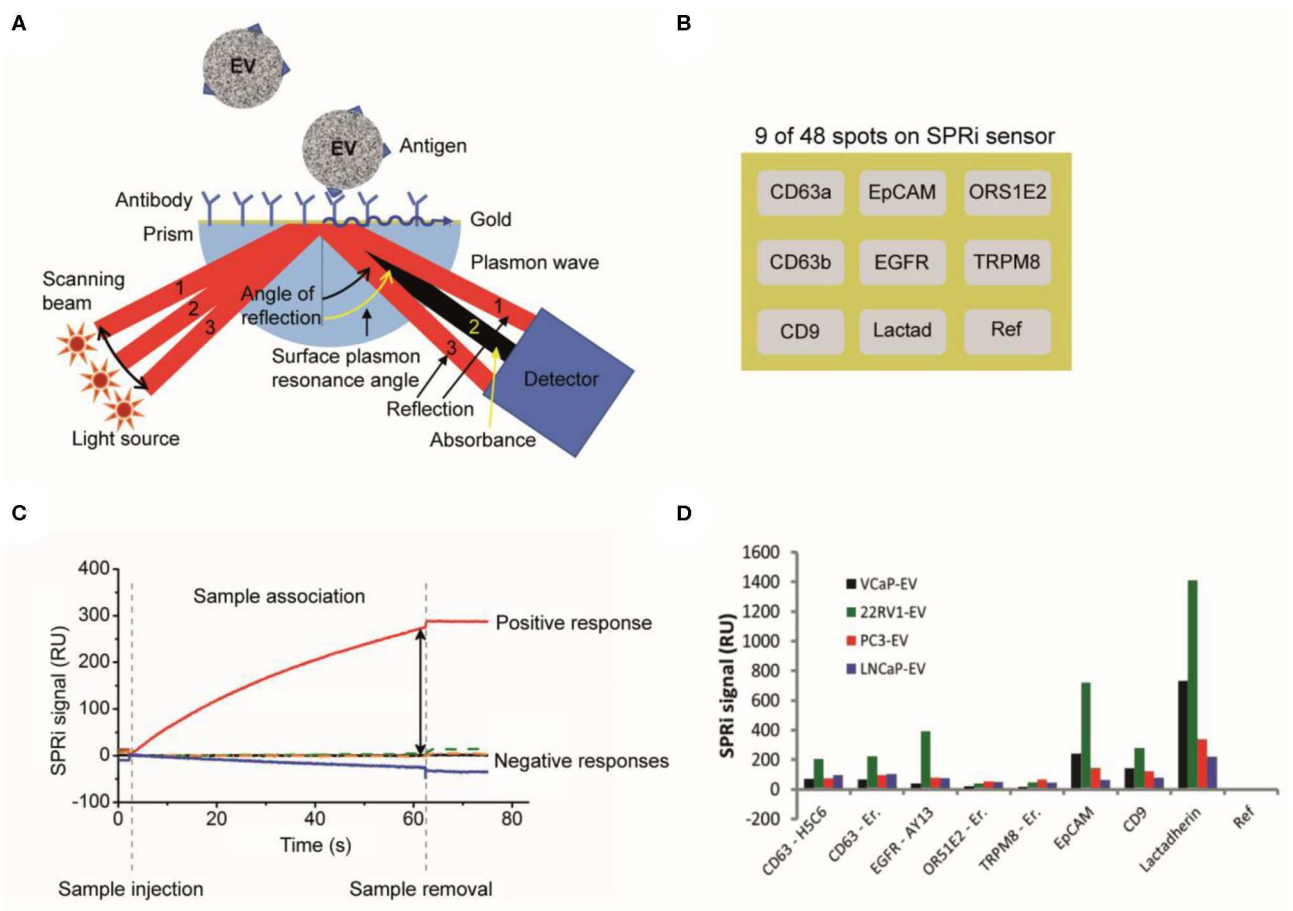

FIGURE 10 | Surface plasmon resonance imaging (SPRi) analysis of extracellular vesicles (EVs). **(A)** Schematic of a SPRi setup. A SPRi signal is generated when the sensor surface is illuminated at various angles with light and surface plasmons are excited (61). The resonance angle, specific angle (beam 2) where maximum plasmon excitation and minimal internal reflection occurs (62), depends on the refractive index contrast near the interface in the evanescent field. **(B)** The 48 spots on the SPRi sensor surface can be coated with different antibodies. In this example, only nine antibody-coated spots on the SPRi sensor surface are shown. **(C)** An EV sample is exposed to the SPRi sensor and measured for 60 min. The attachment of an ensemble of EVs to a specific antibody spot causes a change in the refractive index and generates a SPRi signal over time (16). **(D)** The SPRi signals after incubation with four prostate-cancer-derived EV samples are shown. The two CD63 clones show the same results for all samples. All samples are slightly positive for CD63, EGFR, and CD9. A higher positivity is seen for EpCAM and lactadherin. The SPRi signals for the 22RV1-EV sample are higher compared to the other samples (16).

cyclic voltammetry measurements were performed in 20 min, regardless of the concentration of tdEVs (5×10^3-10^9/ml of sample). Using patient plasma samples rather than cell culture medium may increase the background signal, thereby reducing the sensitivity of the technique. Nevertheless, compared to other techniques, electrochemical methods hold great promise to be applied in a clinical setting because of the high throughput.

SURFACE PLASMON RESONANCE IMAGING

Cancer-ID Specific Method and Operating Principle

The surface of a SPRi sensor is coated with a conductive gold layer and a 3D hydrogel-like layer to reduce nonspecific binding of non-EV particles to the surface (**Figure 10A**). Antibodies are printed on 48 spots on the sensor (**Figure 10B**), including isotype controls and a control (PBS) to correct for dissociation and nonspecific binding (16). Next, the surface is washed and deactivated by incubation with 2-amino ethanol followed by BSA. After an EV sample is exposed to the sensor, EVs bind to the antibody-coated sensor spot, which increases the refractive index near the sensor surface. This increase in refractive index is measured in time using the angle scanning principle of the IBIS MX96 instrument (IBIS Technologies, Enschede, Netherlands) and corresponds to the number of particles captured on the spot (**Figure 10C**).

EV Definition

With SPRi, EVs are identified based on their antigen exposure. EVs bind to antibodies printed on the sensor, e.g., anti-CD9, anti-CD63, antiepidermal growth factor receptor (anti-EGFR), anti-EpCAM, antiolfactory receptor 51E2 (anti-OR51E2), transient receptor potential cation channel subfamily M member 8

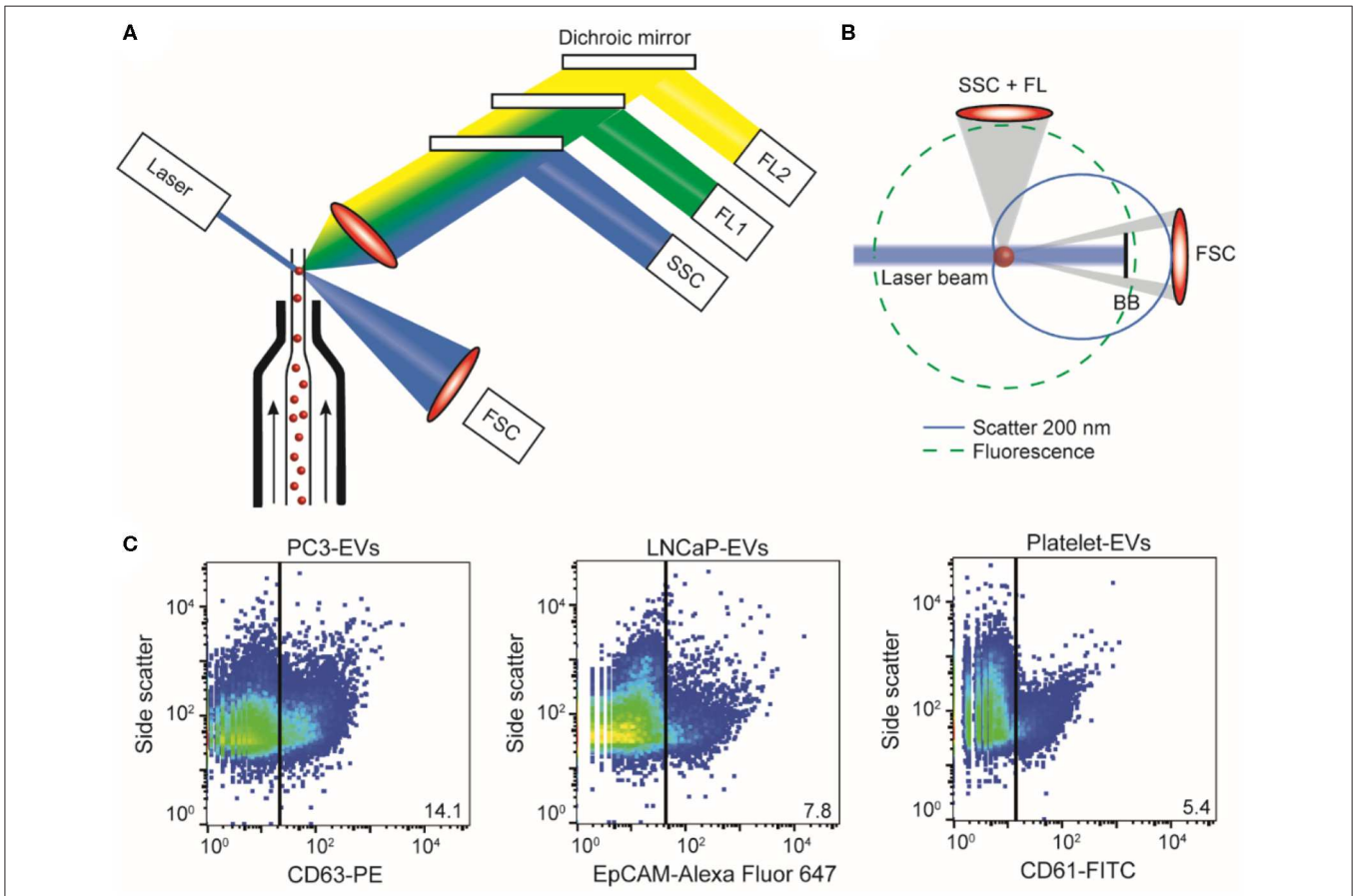

FIGURE 11 | Flow cytometry of extracellular vesicle (EV) samples. **(A)** In flow cytometry, a single particle suspension is hydrodynamically focused with sheath fluid (arrows) to intersect a laser. Light coming from the particle is collected by a forward scatter detector (FSC), a side scatter detector (SSC), and multiple fluorescence detectors (FL1, FL2, etc.). **(B)** Fluorescence (green dashed line) is isotropic and can be used to determine antigen expression and cellular origin. Scatter (blue solid line) has an angular distribution that depends on the size and refractive index of the particle (here, 200 nm polystyrene). Knowledge of the flow cytometer collection angles and Mie theory allows derivation of particle size and refractive index from the measured scatter signals (14, 20). **(C)** Scatter plots of side scatter vs. fluorescence for the PC3 EV sample stained with CD63-PE (left), the LNCaP EV sample stained with EpCAM-Alexa Fluor 647 (center), and the platelet EV sample stained with CD61-FITC (right). In PC3 EV sample, 14.1% was found to be positive for the EV marker CD63; in the LNCaP EV sample, 7.8% was found to be positive for cell surface epithelial marker EpCAM; and in the platelet EV sample, 5.4% of the particles was found to be positive for CD61. BB, blocker bar; FL, fluorescence.

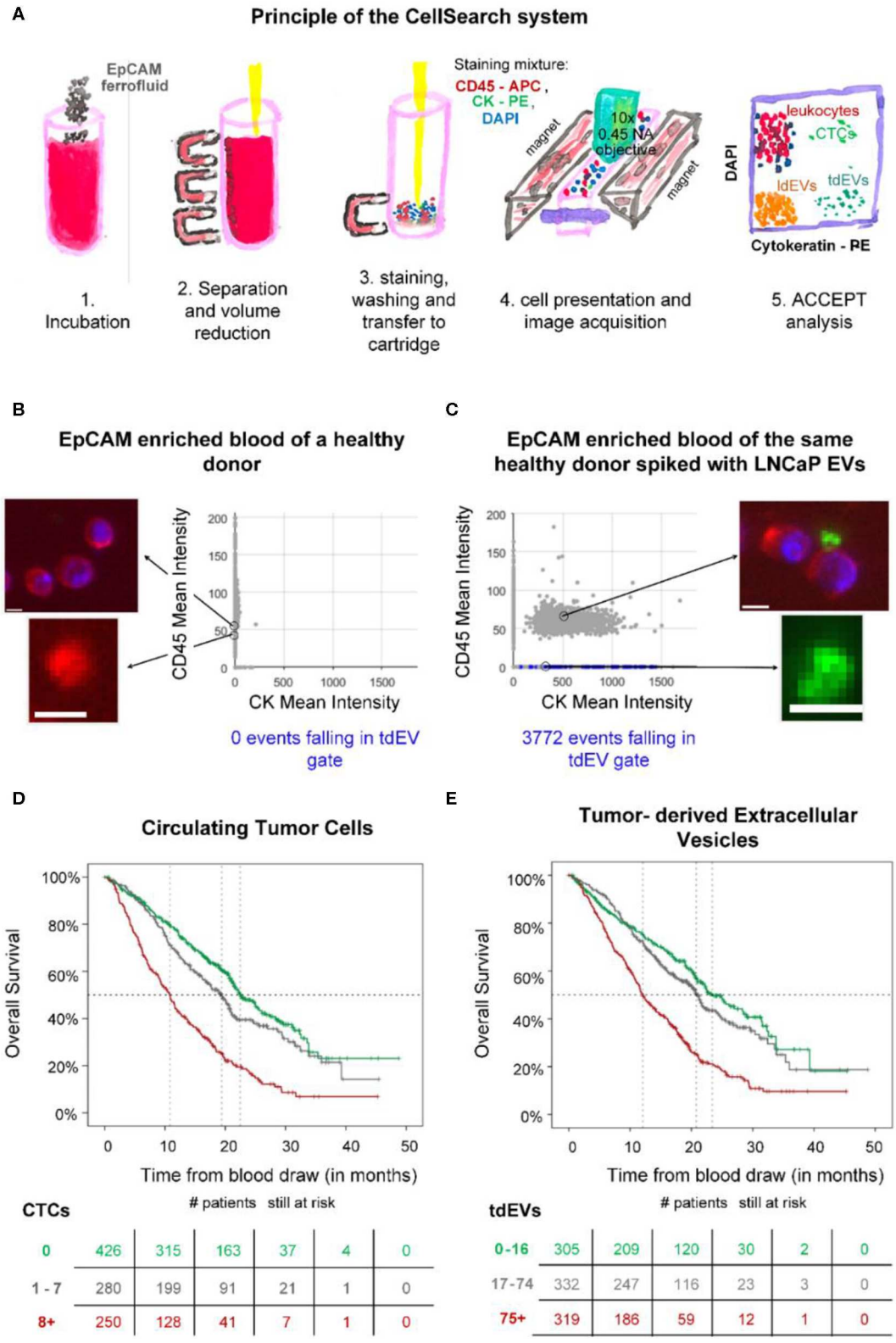

FIGURE 12 | Epithelial cell adhesion molecule (EpCAM) immunomagnetic enrichment and fluorescence microscopic (FM) detection of extracellular vesicle (EV) samples. **(A)** Principle of the CellSearch system. ACCEPT analysis of two CellSearch cartridges corresponding to EpCAM-enriched blood sample of a healthy donor

(Continued)

FIGURE 12 | (B) without and **(C)** with LNCaP EVs spiked. CD45 is depicted in red, CK in green, and 4′,6-diamidino-2-phenylindole (DAPI) in blue. The objects falling in the applied tdEV gate are depicted as blue dots in the scatter plots of CD45 mean intensity vs. CK mean intensity. The other particles are shown as gray dots. Thumbnail examples of four objects are shown. The $CD45^+$ and CK^+ particles are attached to the leukocytes, as illustrated. Scale bars indicate 6.4 μm. **(D,E)** show Kaplan Meier plots of overall survival of 956 metastatic colorectal, prostate, breast, and nonsmall cell lung cancer patients. Patients were grouped based on their **(D)** circulating tumor cells (CTC) or **(E)** tumor-derived EV (tdEV) counts demonstrating the equivalent prognostic power of CTCs and tdEVs (9).

(TRPM8), and lactadherin, see **Figure 10D**. SPRi detects a difference in response on the antibody spots between EV samples derived from different cell lines.

Value Added by Cancer-ID

Characterization of EVs by SPRi, using the IBIS MX96, revealed the ability to detect cell surface antigens present at relatively low antigen densities compared to cells, as their presence could not be detected by flow cytometry (16).

Relevance for Cancer Diagnostics

SPRi can be used to distinguish tdEVs from non-EV particles and EVs derived from other cells based on the antigen expression. The IBIS MX96 is able to detect antigens present at a low density on EVs compared to cells (16). SPRi has superior sensitivity when compared to flow cytometry (16) and ELISA (63). However, the required EV concentration to perform the herein reported measurements is high (2 × 108 EVs/mL), and not within the range of the expected tdEV frequency in plasma patient samples. A different configuration (nano-plasmonic exosome (nPLEX) assay) has been suggested by Im et al. to increase the throughput and make feasible the detection of tdEVs in ascites of ovarian cancer patient samples (63).

FLOW CYTOMETRY

Cancer-ID Specific Method and Operating Principle

EV samples are diluted in PBS (21-031-CV; Corning, Corning, NY) to prevent swarm detection (64) and stained with fluorescently labeled antibodies. Antibody aggregates are removed by centrifugation prior to use. The "antibody supernatant" is added to the EV sample followed by a 2-h incubation step, which is stopped by diluting the incubated sample with PBS.

In a flow cytometer, the sample is hydrodynamically focused with sheath fluid to intersect a laser beam (**Figure 11A**). Scattered light and fluorescence from the particle are collected by a forward scatter detector, a side scatter detector, and multiple fluorescence detectors (65) (**Figure 11B**). The measured scatter and fluorescent signals per particle can be represented and analyzed using scatter plots as shown in **Figure 11C**. In the works referenced here, samples were analyzed on an A60-Micro (Apogee, Hertfordshire, UK).

EV Definition

EV identification by FCM is commonly based on the expression of one or more antigens, which are detected using fluorescent immunostaining. Recently, we found that the refractive index of particles can be used as an additional parameter to distinguish EVs from lipoproteins (21). We therefore define an EV as a particle that expresses detectable levels of one or more antigens and has a refractive index <1.42.

Value Added by Cancer-ID

Within Cancer-ID, a technology to determine the size and refractive index of submicrometer particles was partly developed, evaluated, and used to find new applications. Based on refractive index, for example, EVs can be differentiated from lipoproteins without antibody labeling (21). Refractive index determination was used to show that generic EV dyes, which are commonly used to label EVs in FCM measurements, do not label all EVs and do label non-EV particles (17). The combination of antibody labeling and refractive index determination could be used to increase specificity of EV detection. Furthermore, the side scatter sensitivity of a conventional flow cytometer was improved 30-fold by systematically modifying the hardware, and a method was developed to quantify the scatter sensitivity of a flow cytometer.

Relevance for Cancer Diagnostics

FCM measures light scattering and fluorescence from thousands of individual particles per second. Although detection of the smallest single EVs is possible (66), only the most sensitive commercial flow cytometers are able to detect EVs with a diameter <200 nm (67). Based on the combination of an antibody and the refractive index, it is possible to discriminate tdEVs from lipoproteins and EVs from other origin. However, plasma samples are typically prediluted 10–100 times before measurements to prevent swarm detection (as assumed in **Table 1**). This dilution means that the detection of the few tdEVs that might be present in the plasma sample is impossible.

However, FCM provides information on the concentration, cellular origin and biochemical composition, size, and refractive index of single EVs (14, 20, 68).

IMMUNOMAGNETIC EPCAM ENRICHMENT FOLLOWED BY FLUORESCENCE MICROSCOPIC DETECTION

Cancer-ID Specific Method and Operating Principle

Blood of individuals is collected in CellSave blood collection tubes (Menarini, Huntingdon Valley, PA). After centrifugation of 7.5 mL of the blood for 10 min at 800 *g*, the sample is placed in the CellTracks Autoprep (Menarini, Huntingdon Valley, PA). The Autoprep aspirates and discards the plasma, whereas the blood cell fraction is incubated with anti-EpCAM (VU1D9 clone) ferrofluid (**Figure 12A**, step 1). The particles (cells and EVs)

bound to the ferrofluid are separated from the rest of the blood by the application of magnetic forces (step 2). Following the immunomagnetic isolation, EpCAM-enriched particles are stained with the nuclear dye 4′,6-diamidino-2-phenylindole (DAPI) and fluorophore-conjugated antibodies recognizing the epithelial specific cytokeratins 8, 18, and 19 (CK-PE) and the leukocyte-specific marker CD45 (CD45-APC) (step 3). The stained sample is loaded in a cartridge and placed between two magnets configured in such a way that all stained $EpCAM^+$-enriched particles homogeneously align on the glass slide on the surface of the cartridge (step 4). The cartridge is scanned using the CellTracks Analyzer II (Menarini, Huntingdon Valley, PA), a fluorescence microscope equipped with a 10× 0.45 NA objective (step 4). The images are analyzed using the open-source ACCEPT software to identify circulating tumor cells (CTCs), tdEVs, leukocytes, and leukocyte derived EVs (69) (step 5).

EV Definition

tdEVs are defined as EpCAM+, CK+, DAPI–, and CD45– particles. A gate for their automated enumeration from the CellSearch image data sets has previously been reported (8).

Value Added by Cancer-ID

In the frames of the Cancer-ID program, we reanalyzed digitally stored FM image data sets of retrospective clinical studies acquired after EpCAM enrichment. Our results suggest that large tdEVs (>1 μm), coisolated with CTCs, are negatively associated with the overall survival of metastatic prostate, colorectal, breast, and nonsmall cell lung cancer patients in a similar way as CTCs (**Figure 12**) (9) and could contribute in monitoring the disease and assessing therapeutic efficacy. However, the existing technique was developed for the detection of CTCs and eliminates the detection of smaller tdEVs or tdEVs with low antigen density even if they have been isolated by the anti-EpCAM ferrofluid.

To evaluate whether tdEVs from a model cancer cell line can be isolated using the CellSearch assay, two samples were used as a positive and negative control of the technique. Two blood samples of 7.5 ml, collected in CellSave tubes and drawn from an anonymous healthy individual, were provided by the TNW-ECTM-donor services (University of Twente, Enschede, Netherlands). Both samples were processed with the CellSearch system; however, the one sample remained intact without the addition of any EVs (negative control), whereas the other one was spiked with EVs produced from the $EpCAM^+$ LNCaP prostate cancer cell line (positive control). The application of a tdEV gate resulted in 0 events in the negative control and in 3,772 events in the positive control (**Figures 12B,C**).

This study was carried out in accordance with the recommendations of Dutch regulations. The protocol was approved by the Medical Ethical Assessment Committee Twente (METC Twente). The subject gave written informed consent in accordance with the Declaration of Helsinki.

Relevance for Cancer Diagnostics

The CellSearch system can be used to enrich CTCs and tdEVs based on their EpCAM expression, as EpCAM is not expected to be present on cells and EVs in blood of healthy individuals (70, 71). However, tdEVs isolated by the CellSearch system are limited to the larger EVs (>1 μm), as the technique was designed to isolate CTCs; therefore, the plasma (obtained after centrifugation at 800 *g*) containing the majority of EVs is discarded by default. As a consequence, more than 95% of the total tdEV population holding relevant clinical information is discarded. Nonetheless, the subset of isolated large $EpCAM^+$, CK^+ tdEVs from blood of cancer patients has a similar prognostic power to CTCs in metastatic prostate, breast, colorectal, and nonsmall cell lung cancer patients (**Figure 12**) and can complement CTCs in the CellSearch assay. Processing the plasma samples with the CellSearch assay and imaging of the enriched sample using a fluorescence microscope with a higher NA objective is expected to lead to increased tdEV detection with a higher offset when compared to the tdEV counts detected in the respective processed plasma samples of healthy individuals.

CANCER-ID INSIGHTS

Cancer-ID delivered new techniques and new insights to explore tdEV detection. Taken the complexity of blood into consideration, the necessity of enriching biological samples for tdEVs becomes obvious. EVs secreted from prostate cancer cell lines and EVs derived from red blood cells and platelets, resembling the expected background of EVs in plasma, were used to explore the utility of different techniques. The size distribution of EV samples was characterized by NTA; the EV size and/or morphology by TEM, SEM, and AFM; their biochemical composition by Raman spectroscopy; and their antigen expression profile by SPRi, FM, and FCM. The techniques were able to detect or image EVs present in culture supernatants from tumor cells. However, discrimination between EVs and non-EV particles becomes difficult in complex samples like plasma because non-EV particles outnumber EVs (**Figure 1**). Furthermore, most techniques cannot identify the cellular origin of single EVs and relate the measured signal or count to the concentration of tdEVs in plasma. The results of all individual techniques pointed out that a combination of more than one parameters or techniques will increase the certainty that tdEVs are being investigated, and immune affinity enrichment or detection is needed to cover the large size and density range of EVs.

EV isolation protocols have not been standardized within the EV field (72, 73). Size-based isolation techniques, such as size exclusion chromatography, can purify samples from contaminating lipoproteins and soluble protein of a size below 70 nm (29). Furthermore, centrifugation is often used to isolate biomarkers from whole blood. In the Cancer-ID program, we developed a model to predict the behavior of particles (cells and EVs) in solution during centrifugation and showed the coisolation of, for example, platelets and large EVs after centrifugation (73). Moreover, although the application of rate zonal centrifugation improved the separation of platelets from EVs, the aforementioned isolation techniques result in purification of EVs rather than enrichment of

tdEVs. Similarly, other techniques such as the asymmetric-flow field-flow fractionation can accurately separate exosomes and exomeres based on their size (74); however, for the characterization of EVs of interest, an additional pre-enrichment step will be required.

By the use of affinity-based techniques using antibodies directed to antigens expressed on tumor cells but not on blood cells, we demonstrated the enrichment of large (>1 μm) $EpCAM^+$ tdEVs from blood from metastatic cancer patients (8, 9). EVs from different origin were eliminated in the enriched sample. Efforts for the immunomagnetic enrichment of smaller (<1 μm) tdEVs from plasma samples based on EpCAM are ongoing. The frequency of small tdEV shown in **Figure 1** is based on an extrapolation from the frequency of the large tdEVs, and this surely will need to be validated. Moreover, whether the small tdEV have a similar relation with clinical outcome will need to be established. tdEV likely encompass different subclasses; for example, those responsible for communication with the environment and those involved in the process of apoptosis of cancer cells and as such relation with clinical outcome or its cargo being informative on the optimal treatment will likely be different between these subclasses. Here, only the EpCAM antigen was used to capture tdEVs; the use of different or a mixture of antibodies recognizing different cancer-specific antigens, such as VAR2CSA (75) and HsP70 (76, 77) could increase the capture efficacy and may identify different subclasses of tdEVs. Identification of tdEV among the EpCAM-enriched particles was obtained through identification of the presence of intracellular cytokeratins; the use of different components of the tdEV cargo might be important. Exploration of this cargo with label-free technologies such as Raman and SPRi identified some alternative avenues that can be explored. The onset of retrieving data from the molecular content of EVs has also been explored in the Cancer-ID program. A challenge is retrieving sufficient RNA to represent the messenger RNA (mRNA) and long noncoding RNA transcriptome. As a first step, various EV RNA isolation kits were tested, and of the isolation kits tested, the Norgen total RNA isolation protocol resulted in the highest amount of RNA as determined by reverse transcription quantitative PCR (RT-qPCR) of housekeeping and prostate-associated transcripts. Although this Norgen protocol will also extract non-EV RNA from urine, RNA yield and coverage by RNAseq are considered of higher priority than purity for our EV-based biomarker efforts.

State-of-the-art integrated systems developed in the Cancer ID Perspectief program come close to reliably detecting tdEVs at clinically relevant concentrations at high throughput. Small tdEVs (<1 μm) can be isolated using functionalized anti-EpCAM substrates and can be detected electrochemically in a label-free manner (19). Next, sorting of tdEV populations (as defined by fluorescence, by SPRi, electrochemically, or by Raman spectroscopy) can be used to perform downstream molecular analysis and reveal their genetic content that could play a critical role in identifying the best therapeutic strategy for cancer patients.

DATA AVAILABILITY STATEMENT

The datasets generated for this study are available on request to the corresponding author.

AUTHOR CONTRIBUTIONS

LR, PB, AE-M, AN, SL, CO, and LT drafted the manuscript. All other authors reviewed and improved on the draft.

FUNDING

This work was supported by the Netherlands Organization for Scientific Research—Domain Applied and Engineering Sciences (NWO-TTW), under research program Perspectief Cancer-ID (projects: 14190-14198) and research program VENI 15924.

REFERENCES

1. Conde-Vancells J, Rodriguez-Suarez E, Embade N, Gil D, Matthiesen R, Valle M, et al. Characterization and comprehensive proteome profiling of exosomes secreted by hepatocytes. *J Proteome Res.* (2008) 7:5157–66. doi: 10.1021/pr8004887
2. Verderio C, Muzio L, Turola E, Bergami A, Novellino L, Ruffini F, et al. Myeloid microvesicles are a marker and therapeutic target for neuroinflammation. *Ann Neurol.* (2012) 72:610–24. doi: 10.1002/ana.23627
3. Melo SA, Luecke LB, Kahlert C, Fernandez AF, Gammon ST, Kaye J, et al. Glypican-1 identifies cancer exosomes and detects early pancreatic cancer. *Nature.* (2015) 523:177–82. doi: 10.1038/nature14581
4. Meng Y, Sun J, Wang X, Hu T, Ma Y, Kong C, et al. Exosomes: a promising avenue for the diagnosis of breast cancer. *Technol Cancer Res Treat.* (2019) 18:1533033818821421. doi: 10.1177/1533033818821421
5. Kuchinskiene Z, Carlson LA. Composition, concentration, and size of low density lipoproteins and of subfractions of very low density lipoproteins from serum of normal men and women. *J Lipid Res.* (1982) 23:762–9.
6. Corash L, Costa JL, Shafer B, Donlon JA, Murphy D. Heterogeneity of human whole blood platelet subpopulations. *III Density-dependent differences in subcellular constituents. Blood.* (1984) 64:185–93. doi: 10.1182/blood.V64.1.185.185
7. Simonsen JB. What are we looking at? *Extracellular vesicles, lipoproteins, or both? Circ Res.* (2017) 121:920–2. doi: 10.1161/CIRCRESAHA.117.311767
8. Nanou A, Coumans FAW, Van Dalum G, Zeune LL, Dolling D, et al. Circulating tumor cells, tumor-derived extracellular vesicles and plasma cytokeratins in castration-resistant prostate cancer patients. *Oncotarget.* (2018) 9:19283–93. doi: 10.18632/oncotarget.25019
9. Nanou A, Miller MC, Zeune LL, De Wit S, Punt CJA, Groen HJM, et al. Tumour-derived extracellular vesicles in blood of metastatic cancer patients associate with overall survival. *Br J Cancer.* (2020) 122:801–11. doi: 10.1038/s41416-019-0726-9
10. Coumans F, Van Dalum G, Terstappen L. CTC Technologies and Tools. *Cytometry A.* (2018) 93:1197–201. doi: 10.1002/cyto.a.23684
11. Johnsen KB, Gudbergsson JM, Andresen TL, Simonsen JB. What is the blood concentration of extracellular vesicles? *Implications for the use of extracellular vesicles as blood-borne biomarkers of cancer. Biochim Biophys Acta Rev Cancer.* (2019) 1871:109–16. doi: 10.1016/j.bbcan.2018.11.006
12. Ricklefs FL, Maire CL, Reimer R, Duhrsen L, Kolbe K, Holz M, et al. Imaging flow cytometry facilitates multiparametric characterization of extracellular

vesicles in malignant brain tumours. *J Extracell Vesicles.* (2019) 8:1588555. doi: 10.1080/20013078.2019.1588555
13. Rikkert LG, Nieuwland R, Terstappen L, Coumans FAW. Quality of extracellular vesicle images by transmission electron microscopy is operator and protocol dependent. *J Extracell Vesicles.* (2019) 8:1555419. doi: 10.1080/20013078.2018.1555419
14. De Rond L, Coumans FAW, Nieuwland R, Van Leeuwen TG, Van Der Pol E. Deriving extracellular vesicle size from scatter intensities measured by flow cytometry. *Curr Protoc Cytom.* (2018) 86:e43. doi: 10.1002/cpcy.43
15. Beekman P, Enciso-Martinez A, Rho HS, Pujari SP, Lenferink A, Zuilhof H, et al. Immuno-capture of extracellular vesicles for individual multi-modal characterization using AFM, SEM and Raman spectroscopy. *Lab Chip.* (2019) 19:2526–36. doi: 10.1039/C9LC00081J
16. Gool EL, Stojanovic I, Schasfoort RBM, Sturk A, Van Leeuwen TG, Nieuwland R, et al. Surface plasmon resonance is an analytically sensitive method for antigen profiling of extracellular vesicles. *Clin Chem.* (2017) 63:1633–41. doi: 10.1373/clinchem.2016.271049
17. De Rond L, Van Der Pol E, Hau CM, Varga Z, Sturk A, Van Leeuwen TG, et al. Comparison of generic fluorescent markers for detection of extracellular vesicles by flow cytometry. *Clin Chem.* (2018) 64:680–9. doi: 10.1373/clinchem.2017.278978
18. Enciso-Martinez A, Van Der Pol E, Lenferink ATM, Terstappen LWMM, Van Leeuwen TG, Otto C. Synchronized Rayleigh and Raman scattering for the characterization of single optically trapped extracellular vesicles. *Nanomed Nanotechnol Biol Med.* (2019) 24:102109. doi: 10.1016/j.nano.2019.102109
19. Mathew D, Beekman P, Lemay SG, Zuilhof H, Le Gac S, Van Der Wiel WG. Electrochemical detection of tumor-derived extracellular vesicles on nano-interdigitated electrodes. *Nano Lett.* (2019) 20:820–8. doi: 10.1021/acs.nanolett.9b02741
20. Van Der Pol E, De Rond L, Coumans FAW, Gool EL, Boing AN, et al. Absolute sizing and label-free identification of extracellular vesicles by flow cytometry. *Nanomedicine.* (2018) 14:801–10. doi: 10.1016/j.nano.2017.12.012
21. De Rond L, Libregts S, Rikkert LG, Hau CM, Van Der Pol E, Nieuwland R, et al. Refractive index to evaluate staining specificity of extracellular vesicles by flow cytometry. *J Extracell Vesicles.* (2019) 8:1643671. doi: 10.1080/20013078.2019.1643671
22. Coumans FAW, Gool EL, Nieuwland R. Bulk immunoassays for analysis of extracellular vesicles. *Platelets.* (2017) 28:242–8. doi: 10.1080/09537104.2016.1265926
23. Van Der Pol E, Hoekstra AG, Sturk A, Otto C, Van Leeuwen TG, Nieuwland R. Optical and non-optical methods for detection and characterization of microparticles and exosomes. *J Thromb Haemost.* (2010) 8:2596–607. doi: 10.1111/j.1538-7836.2010.04074.x
24. Van Der Pol E, Coumans FAW, Grootemaat AE, Gardiner C, Sargent IL, et al. Particle size distribution of exosomes and microvesicles determined by transmission electron microscopy, flow cytometry, nanoparticle tracking analysis, and resistive pulse sensing. *J Thromb Haemost.* (2014) 12:1182–92. doi: 10.1111/jth.12602
25. Lee W, Nanou A, Rikkert L, Coumans FAW, Otto C, et al. Label-free prostate cancer detection by characterization of extracellular vesicles using raman spectroscopy. *Anal Chem.* (2018) 90:11290–6. doi: 10.1021/acs.analchem.8b01831
26. Van Der Pol E, Coumans FA, Sturk A, Nieuwland R, Van Leeuwen TG. Refractive index determination of nanoparticles in suspension using nanoparticle tracking analysis. *Nano Lett.* (2014) 14:6195–201. doi: 10.1021/nl503371p
27. Lötvall J, Hill AF, Hochberg F, Buzás EI, Di Vizio D, Gardiner C, et al. Minimal experimental requirements for definition of extracellular vesicles and their functions: a position statement from the International Society for Extracellular Vesicles. *J Extracell Vesicles.* (2014) 3:10.3402/jev.v3403.26913. doi: 10.3402/jev.v3.26913
28. Pisitkun T, Shen RF, Knepper MA. Identification and proteomic profiling of exosomes in human urine. *Proc Natl Acad Sci USA.* (2004) 101:13368–73. doi: 10.1073/pnas.0403453101
29. Boing AN, Van Der Pol E, Grootemaat AE, Coumans FA, Sturk A, Nieuwland R. Single-step isolation of extracellular vesicles by size-exclusion chromatography. *J Extracell Vesicles.* (2014) 3:10.3402/jev.v3403.23430. doi: 10.3402/jev.v3.23430
30. Keerthikumar S, Gangoda L, Liem M, Fonseka P, Atukorala I, Ozcitti C, et al. Proteogenomic analysis reveals exosomes are more oncogenic than ectosomes. *Oncotarget.* (2015) 6:15375–96. doi: 10.18632/oncotarget.3801
31. Atay S, Gercel-Taylor C, Kesimer M, Taylor DD. Morphologic and proteomic characterization of exosomes released by cultured extravillous trophoblast cells. *Exp Cell Res.* (2011) 317:1192–202. doi: 10.1016/j.yexcr.2011.01.014
32. Sahoo S, Klychko E, Thorne T, Misener S, Schultz KM, Millay M, et al. Exosomes from human CD34(+) stem cells mediate their proangiogenic paracrine activity. *Circ Res.* (2011) 109:724–35. doi: 10.1161/CIRCRESAHA.111.253286
33. Hong CS, Muller L, Boyiadzis M, Whiteside TL. Isolation and characterization of CD34+blast-derived exosomes in acute myeloid leukemia. *PLos ONE.* (2014) 9:e103310. doi: 10.1371/journal.pone.0103310
34. Cizmar P, Yuana Y. Detection and characterization of extracellular vesicles by transmission and cryo-transmission electron microscopy. *Methods Mol Biol.* (2017) 1660:221–32. doi: 10.1007/978-1-4939-7253-1_18
35. Gangalum RK, Atanasov IC, Zhou ZH, Bhat SP. alpha B-crystallin is found in detergent-resistant membrane microdomains and is secreted via exosomes from human retinal pigment epithelial cells. *J Biol Chem.* (2011) 286:3261–9. doi: 10.1074/jbc.M110.160135
36. Zhang H, Xie Y, Li W, Chibbar R, Xiong S, Xiang J. CD4(+) T cell-released exosomes inhibit CD8(+) cytotoxic T-lymphocyte responses and antitumor immunity. *Cell Mol Immunol.* (2011) 8:23–30. doi: 10.1038/cmi.2010.59
37. Xie Y, Zhang X, Zhao T, Li W, Xiang J. Natural CD8(+)25(+) regulatory T cell-secreted exosomes capable of suppressing cytotoxic T lymphocyte-mediated immunity against B16 melanoma. *Biochem Biophys Res Commun.* (2013) 438:152–5. doi: 10.1016/j.bbrc.2013.07.044
38. Thery C, Witwer KW, Aikawa E, Alcaraz MJ, Anderson JD, Andriantsitohaina R, et al. Minimal information for studies of extracellular vesicles 2018 (MISEV2018): a position statement of the International Society for Extracellular Vesicles and update of the MISEV2014 guidelines. *J Extracell Vesicles.* (2018) 7:1535750. doi: 10.1080/20013078.2018.1535750
39. Enciso-Martinez A, Timmermans FJ, Nanou A, Terstappen L, Otto C. SEM-Raman image cytometry of cells. *Analyst.* (2018) 143:4495–502. doi: 10.1039/C8AN00955D
40. Nanou A, Crespo M, Flohr P, De Bono JS, Terstappen L. Scanning electron microscopy of circulating tumor cells and tumor-derived extracellular vesicles. *Cancers.* (2018) 10:416. doi: 10.3390/cancers10110416
41. Vorselen D, Mackintosh FC, Roos WH, Wuite GJ. Competition between bending and internal pressure governs the mechanics of fluid nanovesicles. *ACS Nano.* (2017) 11:2628–36. doi: 10.1021/acsnano.6b07302
42. Sorkin R, Huisjes R, Boskovic F, Vorselen D, Pignatelli S, Ofir-Birin Y, et al. Nanomechanics of extracellular vesicles reveals vesiculation pathways. *Small.* (2018) 14:e1801650. doi: 10.1002/smll.201801650
43. Vorselen D, Marchetti M, Lopez-Iglesias C, Peters PJ, Roos WH, Wuite GJL. Multilamellar nanovesicles show distinct mechanical properties depending on their degree of lamellarity. *Nanoscale.* (2018) 10:5318–24. doi: 10.1039/C7NR09224E
44. Vorselen D, Van Dommelen SM, Sorkin R, Piontek MC, Schiller J, Dopp ST, et al. The fluid membrane determines mechanics of erythrocyte extracellular vesicles and is softened in hereditary spherocytosis. *Nat Commun.* (2018) 9:4960. doi: 10.1038/s41467-018-07445-x
45. Piontek MC, Roos WH. Atomic force microscopy: an introduction. *Methods Mol Biol.* (2018) 1665:243–58. doi: 10.1007/978-1-4939-7271-5_13
46. Enciso-Martinez A, Van Der Pol E, Hau CM, Nieuwland R, Van Leeuwen TG, Terstappen L, et al. Label-free identification and chemical characterisation of single extracellular vesicles and lipoproteins by synchronous Rayleigh and Raman scattering. *J Extracell Vesicles.* (2020). 9:1730134. doi: 10.1080/20013078.2020.1730134
47. Lee W, Offerhaus H. Classifying Raman spectra of extracellular vesicles using a convolutional neural network. In: *The 26th International Conference on Raman Spectroscopy 2018.* Jeju (2018).
48. Smith ZJ, Lee C, Rojalin T, Carney RP, Hazari S, Knudson A, et al. Single exosome study reveals subpopulations distributed among cell lines with

variability related to membrane content. *J Extracell Vesicles.* (2015) 4:28533. doi: 10.3402/jev.v4.28533
49. Carney RP, Hazari S, Colquhoun M, Tran D, Hwang B, Mulligan MS, et al. Multispectral optical tweezers for biochemical fingerprinting of CD9-positive exosome subpopulations. *Anal Chem.* (2017) 89:5357–63. doi: 10.1021/acs.analchem.7b00017
50. Krafft C, Wilhelm K, Eremin A, Nestel S, Von Bubnoff N, Schultze-Seemann W, et al. A specific spectral signature of serum and plasma-derived extracellular vesicles for cancer screening. *Nanomedicine.* (2017) 13:835–41. doi: 10.1016/j.nano.2016.11.016
51. Penders J, Pence IJ, Horgan CC, Bergholt MS, Wood CS, Najer A, et al. Single particle automated raman trapping analysis. *Nat Commun.* (2018) 9:4256. doi: 10.1038/s41467-018-06397-6
52. Kruglik SG, Royo F, Guigner JM, Palomo L, Seksek O, Turpin PY, et al. Raman tweezers microspectroscopy of circa 100 nm extracellular vesicles. *Nanoscale.* (2019) 11:1661–79. doi: 10.1039/C8NR04677H
53. Loozen GB, Karuna A, Fanood MMR, Schreuder E, Caro J. Integrated photonics multi-waveguide devices for optical trapping and Raman spectroscopy: design, fabrication and performance demonstration. *Beilstein J Nanotechnol.* (2020) 11:829–42. doi: 10.3762/bjnano.11.68
54. Lee W. *Raman Spectroscopy for Extracellular Vesicle Study* (PhD Dissertation). University of Twente, Enschede, Netherlands (2020).
55. Kosian M, Smulders MM, Zuilhof H. Structure and long-term stability of alkylphosphonic acid monolayers on SS316L stainless steel. *Langmuir.* (2016) 32:1047–57. doi: 10.1021/acs.langmuir.5b04217
56. Baggerman J, Smulders MMJ, Zuilhof H. Romantic surfaces: a systematic overview of stable, biospecific, and antifouling zwitterionic surfaces. *Langmuir.* (2019) 35:1072–84. doi: 10.1021/acs.langmuir.8b03360
57. Lorencova L, Bertok T, Bertokova A, Gajdosova V, Hroncekova S, Vikartovska A, et al. Exosomes as a source of cancer biomarkers: advances in electrochemical biosensing of exosomes. *ChemElectroChem.* doi: 10.1002/celc.202000075
58. Boriachek K, Masud MK, Palma C, Phan HP, Yamauchi Y, Hossain MSA, et al. Avoiding pre-isolation step in exosome analysis: direct isolation and sensitive detection of exosomes using gold-loaded nanoporous ferric oxide nanozymes. *Anal Chem.* (2019) 91:3827–34. doi: 10.1021/acs.analchem.8b03619
59. Huang R, He L, Xia Y, Xu H, Liu C, Xie H, et al. A Sensitive aptasensor based on a Hemin/G-quadruplex-assisted signal amplification strategy for electrochemical detection of gastric cancer exosomes. *Small.* (2019) 15:e1900735. doi: 10.1002/smll.201900735
60. Zhang P, Zhou X, He M, Shang Y, Tetlow AL, Godwin AK, et al. Ultrasensitive detection of circulating exosomes with a 3D-nanopatterned microfluidic chip. *Nat Biomed Eng.* (2019) 3:438–51. doi: 10.1038/s41551-019-0356-9
61. Kooyman RPH. Physics of surface plasmon resonance. In: Schasfoort RBM, Tudos AJ, editors. *Handbook for Surface Plasmon Resonance. Cambridge: The Royal Society of Chemistry.* (2008). 15–34 pp.
62. Ideta K, Arakawa T. Surface plasmon resonance study for the detection of some chemical species. *Sens Actuat B Chem.* (1993) 13:384–6. doi: 10.1016/0925-4005(93)85407-2
63. Im H, Shao H, Park YI, Peterson VM, Castro CM, Weissleder R, et al. Label-free detection and molecular profiling of exosomes with a nano-plasmonic sensor. *Nat Biotechnol.* (2014) 32:490–5. doi: 10.1038/nbt.2886
64. Van Der Pol E, Van Gemert MJ, Sturk A, Nieuwland R, Van Leeuwen TG. Single vs. swarm detection of microparticles and exosomes by flow cytometry. *J Thromb Haemost.* (2012) 10:919–30. doi: 10.1111/j.1538-7836.2012.04683.x
65. Brown M, Wittwer C. Flow cytometry: principles and clinical applications in hematology. *Clin Chem.* (2000) 46:1221–9. doi: 10.1093/clinchem/46.8.1221
66. Zhu S, Ma L, Wang S, Chen C, Zhang W, Yang L, et al. Light-scattering detection below the level of single fluorescent molecules for high-resolution characterization of functional nanoparticles. *ACS Nano.* (2014) 8:10998–1006. doi: 10.1021/nn505162u
67. Van Der Pol E, Sturk A, Van Leeuwen T, Nieuwland R, Coumans F, Group ISVW, et al. Standardization of extracellular vesicle measurements by flow cytometry through vesicle diameter approximation. *J Thromb Haemost.* (2018) 16:1236–45. doi: 10.1111/jth.14009
68. Coumans FAW, Brisson AR, Buzas EI, Dignat-George F, Drees EEE, et al. Methodological guidelines to study extracellular vesicles. *Circ Res.* (2017) 120:1632–48. doi: 10.1161/CIRCRESAHA.117.309417
69. Nanou A, Zeune LL, Terstappen L. Leukocyte-derived extracellular vesicles in blood with and without EpCAM enrichment. *Cells.* (2019) 8:937. doi: 10.3390/cells8080937
70. Allard WJ, Matera J, Miller MC, Repollet M, Connelly MC, Rao C, et al. Tumor cells circulate in the peripheral blood of all major carcinomas but not in healthy subjects or patients with nonmalignant diseases. *Clin Cancer Res.* (2004) 10:6897–904. doi: 10.1158/1078-0432.CCR-04-0378
71. Zhu L, Wang K, Cui J, Liu H, Bu X, Ma H, et al. Label-free quantitative detection of tumor-derived exosomes through surface plasmon resonance imaging. *Anal Chem.* (2014) 86:8857–64. doi: 10.1021/ac5023056
72. Van Der Pol E, Coumans F, Varga Z, Krumrey M, Nieuwland R. Innovation in detection of microparticles and exosomes. *J Thromb Haemost.* (2013) 11 (Suppl. 1):36–45. doi: 10.1111/jth.12254
73. Rikkert LG, Van Der Pol E, Van Leeuwen TG, Nieuwland R, Coumans FAW. Centrifugation affects the purity of liquid biopsy-based tumor biomarkers. *Cytometry A.* (2018) 93:1207–12. doi: 10.1002/cyto.a.23641
74. Zhang H, Lyden D. Asymmetric-flow field-flow fractionation technology for exomere and small extracellular vesicle separation and characterization. *Nat Protoc.* (2019) 14:1027–53. doi: 10.1038/s41596-019-0126-x
75. Agerbæk MØ, Bang-Christensen SR, Yang M-H, Clausen TM, Pereira MA, Sharma S, et al. The VAR2CSA malaria protein efficiently retrieves circulating tumor cells in an EpCAM-independent manner. *Nat Commun.* (2018) 9:3279. doi: 10.1038/s41467-018-05793-2
76. Sherman MY, Gabai VL. Hsp70 in cancer: back to the future. *Oncogene.* (2015) 34:4153–61. doi: 10.1038/onc.2014.349
77. Boudesco C, Cause S, Jego G, Garrido C. Hsp70: a cancer target inside and outside the cell. *Methods Mol Biol.* (2018) 1709:371–96. doi: 10.1007/978-1-4939-7477-1_27

Conflict of Interest: The authors declare that the research was conducted in the absence of any commercial or financial relationships that could be construed as a potential conflict of interest.

The handling Editor declared a past co-authorship with one of the authors LT.

frontiers in Oncology

REVIEW
published: 21 July 2020
doi: 10.3389/fonc.2020.01055

The Metastatic Cascade as the Basis for Liquid Biopsy Development

*Zahra Eslami-S†, Luis Enrique Cortés-Hernández† and Catherine Alix-Panabières**

Laboratory of Rare Human Circulating Cells (LCCRH), University Medical Centre of Montpellier, UPRES EA2415, Montpellier, France

The metastatic cascade describes the process whereby aggressive cancer cells leave the primary tumor, travel through the bloodstream, and eventually reach distant organs to develop one or several metastases. During the last decade, innovative technologies have exploited the recent biological knowledge to identify new circulating biomarkers for the screening and early detection of cancer, real-time monitoring of treatment response, assessment of tumor relapse risk (prognosis), identification of new therapeutic targets and resistance mechanisms, patient stratification, and therapeutic decision-making. These techniques are broadly described using the term of *Liquid Biopsy.* This field is in constant progression and is based on the detection of circulating tumor cells, circulating free nucleic acids (e.g., circulating tumor DNA), circulating tumor-derived extracellular vesicles, and tumor-educated platelets. The aim of this review is to describe the biological principles underlying the liquid biopsy concept and to discuss how functional studies can expand the clinical applications of these circulating biomarkers.

Keywords: metastatic cascade, liquid biopsy, circulating tumor cells, extracellular vesicles, circulating-tumor DNA, tumor educated platelets

OPEN ACCESS

Edited by:
Francesco Fabbri, Romagnolo Scientific Institute for the Study and Treatment of Tumors (IRCCS), Italy

Reviewed by:
Lasse Dahl Ejby Jensen, Linköping University, Sweden
Paul B. Fisher, Virginia Commonwealth University, United States

****Correspondence:***
Catherine Alix-Panabières
c-panabieres@chu-montpellier.fr

†These authors have contributed equally to this work

Specialty section:
This article was submitted to Cancer Molecular Targets and Therapeutics, a section of the journal Frontiers in Oncology

Received: *04 March 2020*
Accepted: *27 May 2020*
Published: *21 July 2020*

Citation:
Eslami-S Z, Cortés-Hernández LE and Alix-Panabières C (2020) The Metastatic Cascade as the Basis for Liquid Biopsy Development. Front. Oncol. 10:1055. doi: 10.3389/fonc.2020.01055

INTRODUCTION

In 1889, Stephen Paget proposed on the basis of postmortem data that cancer cells migrate to specific organs and that this could not be explained by chance or by the blood vessel distribution. He proposed that metastatic colonization could be achieved in the presence of a compatible and reciprocal communication between tumor cells and the organ *milieu*. Accordingly, this hypothesis was named "Seed and Soil" because certain organs, such as liver, seem more "fertile" to receive cancer cells (1). However, the mechanisms behind metastasis formation are not comprehensively understood yet.

To explain the process of cancer dissemination, Fidler et al. (2) proposed a model named the "metastatic cascade" based on experiments showing that the metastatic success of a cancer cell is minimal (3). This model recapitulates the progression of cancer cells and their spreading in the body through a series of organized steps. Failure to complete any of them stops the formation of a secondary cancerous lesion (4, 5).

Briefly, the metastatic cascade initiates with the transformation and progressive growth of cells. Then, it continues with the local invasion of the surrounding tissues by primary tumor

cells. This step provides a route for intravasation in already existing or new venules (after neo-angiogenesis induction) and capillaries. Subsequently, tumor cells circulate in the circulatory system (bloodstream and/or lymphatic vessels). If cancer cells manage to survive in this system, they will become trapped in the vascular walls of distant tissues where they can extravasate. Finally, if the microenvironment in these tissues offers the right conditions, cancer cells will proliferate, colonize, and form a metastatic tumor (4, 6).

Many biological factors are involved in the metastatic cascade. These factors or mechanisms are implicated in the final destination ("Soil") or in the behavior/survival of cancer cells ("Seed"), and they vary in function of the cancer type and the patient health status (or the animals used as model), although they share some features. These factors and mechanisms are often different from the normal physiological mechanisms, and they play a vital role in cancer dissemination and survival. Historically and currently, these differences have been used to diagnose and treat cancer, such as the higher cancer cell metabolism detected by positron emission tomography, the microscopical morphological changes associated with cell transformation, and the protein expression changes associated with specific cancer types. The development of molecular techniques allows exploiting cancer-specific genetic and genomic differences for diagnostic purposes. However, these approaches have been focused and applied predominantly in primary and metastatic tumors, while the majority of the intermediate steps of the metastatic cascade have been ignored.

Recently, more attention has been given to identify clinically useful cancer features using minimal invasive methods to detect analytes or biomarkers in blood. This approach has been named *liquid biopsy* (7). This is a broad term that includes the isolation, detection, and characterization of analytes released by or associated with cancer cells, such as circulating tumor cells (CTCs), circulating free nucleic acids (cfNA: circulating tumor DNA, ctDNA, and circulating free DNA, cfDNA), extracellular vesicles (EVs), and tumor-educated platelets (TEPs) (8). All of them have biological significance in the metastatic cascade and can provide clinical information that can be continuously evaluated during the natural course of the disease (**Figure 1**). The study of these analytes in the context of the metastatic cascade model might help to address the question formulated by Stephen Paget: "What is it that decides what organs shall suffer in a case of disseminated cancer?" (1), and more importantly, for people with cancer, "How this knowledge can help to prevent and cure cancer"?

The purpose of this review is to describe the metastatic steps with particular emphasis on the involvement of the analytes that can be tested by liquid biopsy.

PRIMARY TUMOR EXPANSION AND ANGIOGENESIS

The proliferation/expansion of cancer cells is promoted by the appearance of alterations in key genes related to cell fate, cell survival, and genome integrity maintenance. These so-called driver mutations confer a selective growth advantage to the cells that harbor them and lead to the formation of an aggressive tumor (9). Recently, it has been shown that 95% of cancers have at least one driver mutation (10). During tumor cell proliferation, the passive diffusion of oxygen and nutrients reach a threshold and cannot support the tumor growth rate any longer. Consequently, some cancer cells, which are poorly adapted to survive in hypoxic conditions, undergo necrosis or apoptosis (11). However, other cancer cells develop mechanisms of protection against these harsh conditions due to tumor cell heterogeneity. Moreover, cells in the tumor microenvironment, such as cancer-associated fibroblasts, will start to secrete factors that induce angiogenesis, thus supporting the tumor continuous growth. All these factors, actively and non-actively released in the blood circulation, can be used as analytes for liquid biopsy.

For example, tumor DNA might be released in the extracellular space by necrotic tumor cells, as a consequence of the tumoral high size growth rate (which limits the diffusion of oxygen and nutrients to the central regions of the tumor). Then, DNA can reach the circulation, after neo-angiogenesis, where it is described as ctDNA. This is just a fraction of the total cfDNA in blood, but this analyte can be analyzed to identify tumor driver mutations that can be therapeutically targeted, such as mutations in epidermal growth factor receptor (EGFR) in non-small cell lung cancer (NSCLC) that are currently used in the clinic (12). These cfNA (cfDNA and ctDNA) usually include fragments with a size similar to that of DNA surrounding nucleosomes, suggesting a nuclear origin after the disruption of the nuclear and cellular membranes (13–16). However, the mechanisms by which ctDNA originates are not clear. Indeed, some studies suggested that cfDNA is actively released by the cells (17). Moreover, most cfDNA normally originates from hematopoietic precursors in the bone marrow (18, 19). Also, somatic mutant clones can appear in healthy tissue cells during normal aging (20) and could be mistaken for ctDNA. Nonetheless, the total cfDNA amount is higher in patients with cancer patients, most likely due to an increase in the ctDNA fraction (15).

The presence of physiological cfDNA with somatic mutations might hamper the use of ctDNA and cfDNA for the diagnosis of early-stage cancer (21). However, a recent study showed that ctDNA can be used for NSCLC screening because ctDNA can be differentiated from hematopoietic cfDNA by correlating the DNA fragment size (shorter fragments were associated with ctDNA). The sensitivity and specificity of this method are lower than those of low-dose CT imaging (22), the currently used screening method, and similar to what was reported for chest X-rays (23). Nonetheless, ctDNA-based screening might be exploited as marker of tumor recurrence or for detection of driver mutations, for example, by identifying first the hematopoietic somatic mutations and then discarding them in order to focus only on ctDNA (24).

On the other hand, it has been also suggested that ctDNA is actively secreted inside tumoral EVs. These vesicles can protect it from degradation in the bloodstream. Exosomes, a small EV subtype of endocytic origin, are abundant in blood samples from patients with cancer (25) and contain dsDNA (26). Moreover,

A

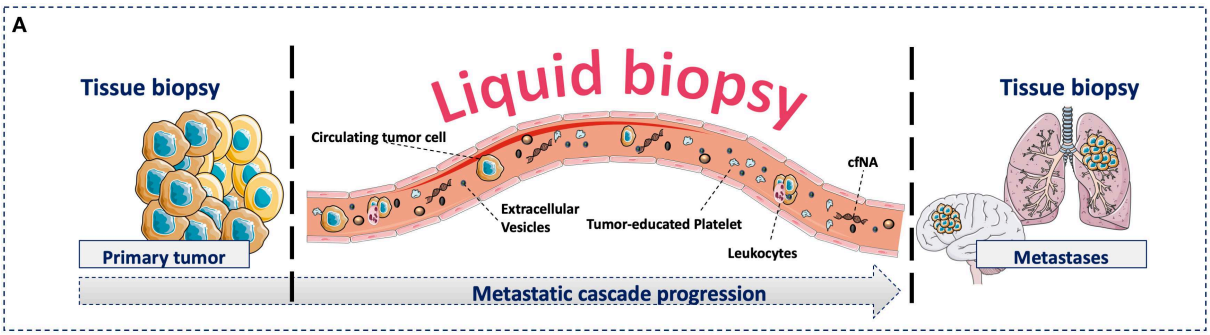

B

Features	Tissue biopsy	Liquid biopsy
Technique	Needle intra organ penetration	Venus blood samples
Accuracy	Limited to represent tumor heterogeneity, limited for localized cancer	On demand real-time repetition, continues overview of tumor heterogeneity, possible localized and metastasis cancers
Invasiveness	High	low
Disease monitoring	one-time assessment, not assess into tumor evolution	Multiple Real time insight for tumor evolution
Treatment monitoring	Not possible without re-biopsy	Real time monitoring for drug response
Cost	Moderate-high	Low-moderate
Timing	Time intensive procedure	Quick procedure
Prognostic and therapeutic prediction information	Dependent on one-time tissue assessment	Real time information available

FIGURE 1 | (A) Advantages of liquid biopsy vs. tissue biopsy during the metastatic cascade. **(A)** Compared with tissue biopsy (limitation for serial sampling and difficulty to access certain organs, such as brain and lung), liquid biopsy allows the real-time monitoring of cancer progression during the liquid phase of the metastatic cascade through the detection of different circulating analytes. These circulating analytes have specific biological functions and provide complementary information that can be continuously evaluated during cancer progression. **(B)** Comparison of tissue and liquid biopsies. Comparison of the relevant medical features of tissue biopsy and liquid biopsy.

it has been suggested that up to 93% of the ctDNA detected in blood is within exosomes (27). However, this was not confirmed by a recent study that used high-resolution methodologies to evaluate exosome isolation and molecular composition (17). In agreement, other studies reported that large EVs (e.g., apoptotic bodies) and not exosomes have the highest DNA cargo (28). The lack of standardized methods for EV isolation and of validated markers for their classification makes difficult to draw conclusions from most of the studies on EVs, and common guidelines have been published only recently (29). Therefore, more research is needed to address these issues.

In the context of liquid biopsy, the specific origin of cfDNA in blood is crucial because the current methods for cfDNA isolation and enrichment cannot efficiently distinguish ctDNA from other cfDNA fractions in blood. If ctDNA were associated with a specific EV type, it would be theoretically possible to isolate only the EVs containing all or most ctDNA.

The role of ctDNA or cfDNA in the metastatic cascade is unknown, and few studies have addressed this question. cfDNA might have different biological roles in function of the proteins it associated with. For example, cfDNA associated with histones can trigger a proinflammatory response related to toll-like receptors (TLR2/4), and cytotoxic effects in endothelial cells (31), whereas cfDNA released from apoptotic adipocytes induces an inflammatory reaction by increasing the accumulation of macrophages *via* TLR9 (32). However, evidence for this is still limited to *in vitro* studies, and the different methodologies used to isolate cfDNA and ctDNA make comparison among studies difficult.

More data are available on EV's role during the early steps of the metastatic cascade. During angiogenesis, exosomes facilitate the intravasation of the different liquid biopsy analytes into the bloodstream. Exosomes in the extracellular space have antiangiogenic and proangiogenic roles. For instance, *in vitro* studies have shown that miR-23a from tumor-associated exosomes secreted in hypoxic conditions has proangiogenic effects by increasing endothelial permeability and suppressing the expression of prolyl-hydroxylase 1 and 2. This leads to the accumulation of hypoxia-inducible factor 1 α (HIF-1 α) in endothelial cells (33). Accordingly, exosomes from colorectal cancer cell lines induce endothelial permeability *via* the cytoskeletal-associated RhoA/ROCK pathway (34). Moreover, in mouse models of oral cancer, microRNAs contained in EVs, such as miR-34a, miR21, and miR324, have been associated with adrenergic trans-differentiation of sensory nerves that innervate tumors upon loss of TP53 (35).

Other factors also are involved in the early steps of cancer cell dissemination, particularly several cytokines that are interesting therapeutic targets, for instance vascular endothelial growth factor (VEGF), tumor necrosis factor alpha and beta (TNF), and chemokine (C–C motif) ligand 2 (CCL2) (36). Moreover, different cancers can secrete different proteins. For

TABLE 1 | Comparison of "Classic" tumor markers and "New" liquid biopsy analytes.

Liquid biopsy field			
"Classic" tumor marker(s)		**"New" liquid biopsy analyte(s)**	
• **CA 27.29** • **CA 19-9** • **CA15-3** • **CA 125** • **PSA** • **NSE** • **CEA** • **AFP**	• **Strength** ✓High level with progressive disease ✓Decrease rate with remission ✓Simple procedure ✓Easily obtainable specimens ✓Minimal invasive ✓Currently using in clinic • **Limitation** ✓Lack of specificity and sensitivity ✓Detectable in benign and healthy conditions ✓Do not provide information related to the metastatic cascade ✓High level only in large tumor volumes	• **CTCs** • **ctDNA** • **TEPs** • **EVs**	• **Strength** ✓Cancer specific ✓Simple procedure ✓Easily obtainable specimens ✓Minimal invasive ✓Genome, transcriptome, proteome and secretome evaluation ✓Related with metastasis cascade ✓Informative for cancer heterogeneity ✓Monitoring drug response and resistance therapy ✓High specificity and sensitivity • **Limitation** ✓Not completely validate and/or utilize in clinic ✓Lack of standardize and integrated method for detection

Circulating analytes, such as CTCs, ctDNA, TEPs, and EVs, are already part of the liquid biopsy, and classical tumor markers also could be included. Indeed, they can be detected in serum, and the combination of classical tumor markers with circulating analytes (e.g., ctDNA) can be used to develop a multi-analyte blood test (30) as a screening method for early tumor detection.

**AFP, Alfa fetoprotein; CA, Carbohydrate antigen; CEA, Carcinoembryonic antigen; PSA, Prostate-specific antigen; NSE, Neuron specific enolase; CTC, Circulating tumor cells; CtDNA, Circulating tumor DNA; TEPs, tumor-educated platelets; EVs, Extracellular vesicles.*

example, prostate specific antigen (PSA), which is used as a blood cancer marker, is secreted by prostate cancer cells, and carcinoembryonic antigen (CEA) by colorectal cancer cells (37). These "classical" tumor markers are routinely tested in the framework of cancer management, but they often lack specificity or sensitivity. Cohen et al. (30) demonstrated that ctDNA can be combined with eight classical tumor markers in a multi-analyte liquid biopsy assay for cancer screening. This method shows promising results but needs to be validated for clinical applications (30). Therefore, these tumor markers should be considered in the liquid biopsy field (**Table 1**).

On their surface, cancer cells present peptides that are absent from the normal human genome and are called neoantigens. These peptides are generated by tumor-specific non-synonymous genetic alterations and are associated with the tumor mutation burden (TMB). Moreover, they are present at the cancer cell surface in association with the major histocompatibility complex (MHC). Therefore, neoantigens can trigger an immune reaction via activation of T cell receptors (TCRs) (38). Like for the previously described analytes, it has been proposed that neoantigens, TMB, and antitumoral T cells should be monitored by liquid biopsy. For instance, the detection of neoantigens on the surface of EVs or CTCs could be used as a treatment response as predictor for immune checkpoint therapies. Similarly, the TMB could be evaluated in ctDNA (39). Gros et al. (40) showed that neoantigen-specific T cells ($CD8^+$, $PD\text{-}1^+$) can be identified in blood samples from patients with melanoma. This might lead to the development of personalized therapies using these T cells (40).

All the aforementioned factors might be released in the hypoxic context of rapidly growing tumors and will facilitate the next step of the metastatic cascade related to cancer cell dissemination and therefore to CTC formation. Whether or not liquid biopsy analytes have a main role in the early steps of the metastatic cascade is still unknown, but the information that they bring might be valuable for clinical applications.

LOCAL INVASION, DETACHMENT, AND INTRAVASATION IN CIRCULATION

Tumor cell proliferation and neo-angiogenesis increase the chances that cancer cells reach the blood circulation. Epigenetic modifications play a major role in this step by altering the expression of genes related to cell migration, thus promoting the free movement of cells through the tissue (41). Then, some cancer cells break and cross the endothelial barrier to intravasate in the blood or lymphatic stream, thus becoming CTCs. Although this is a well-accepted idea, the exact mechanisms are not fully understood and might vary according to tumor type, anatomical location, patient health status, and cancer stage. Nevertheless, these mechanisms leave a signature in blood that can be assessed by liquid biopsy.

During local invasion, cancer cells secrete metalloproteinases that disrupt the basal membrane. Then, in order to detach from the tissue, they must acquire significant changes to survive in the harsh conditions of the bloodstream and the connective tissue (42). For instance, loss of cellular junctions

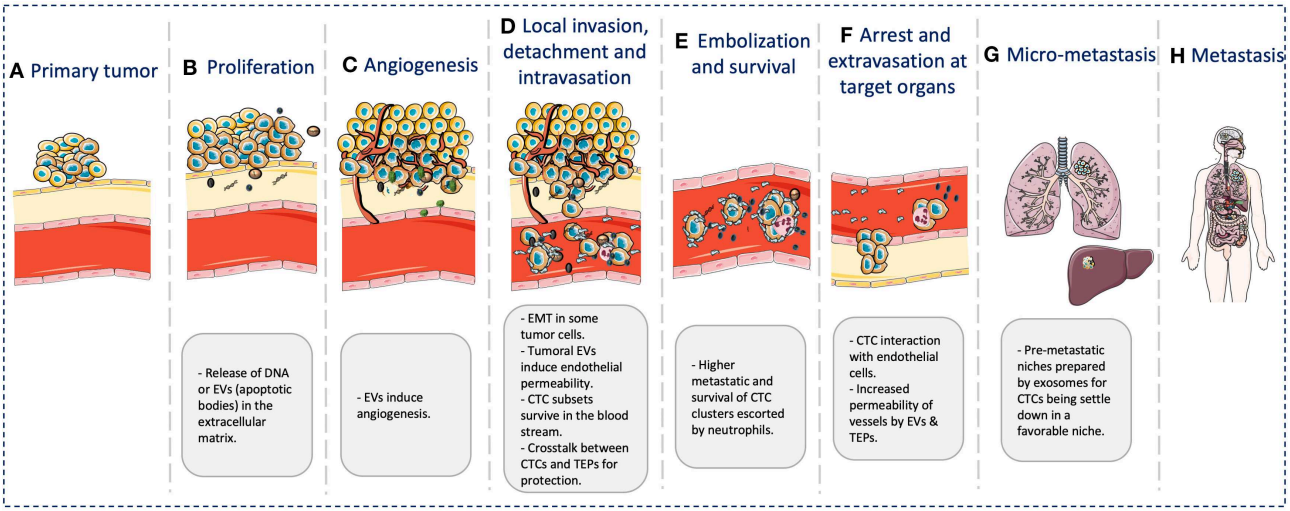

Metastasis steps	Liquid biopsy analyte involved
1- Proliferation	ctDNA, EVs
2- Angiogenesis	ctDNA, EVs
3- Local invasion, detachment and intravasation	CTCs, EVs
4- Embolization and survival	CTCs, TEPs

Metastasis steps	Liquid biopsy analyte involved
5- Arrest and extravasation at target organs	CTCs, EVs
6- Micro-metastasis	CTCs, EVs
7- Metastasis	CTCs

FIGURE 2 | Liquid biopsy and the metastatic cascade. During the metastatic cascade, different analytes are involved: **(A)** Primary tumor: tumor growth at the primary site. **(B)** Cancer cell proliferation: release of DNA from necrotic/apoptotic cells when due to the continuous cancer cell proliferation, passive diffusion of oxygen and nutrients is no longer enough to cover the cell requirement. **(C)** Angiogenesis: EVs are involved in neo-angiogenesis. **(D)** Local invasion, detachment, and intravasation: Cancer cells acquire significant changes to survive the physical interactions and mechanical forces in blood and tissues. Tumor cells also undergo epithelial-to-mesenchymal transition (EMT) to move within the connective tissue and then secrete exosomes that contribute to induce endothelial permeability for intravasation through endothelial cells. **(E)** Embolization and survival: CTCs can survive and adapt in the blood by forming CTC clusters/micro-emboli that display higher metastatic potential by increasing cancer cell survival and reducing apoptosis. Clustering with neutrophils can also promote cell-cycle progression and survival in CTCs, further promoting metastatic development. CTCs also gain physical and immune protection by interacting with platelets. **(F)** Arrest and extravasation in the target organ: CTCs interact with endothelial cells, mainly in capillaries where they become trapped. CTCs and platelets might release EVs that can modify the cytoskeleton of endothelial cells and increase the blood vessel permeability, thus allowing CTC extravasation. **(G)** Micro-metastases: CTCs need a favorable niche. Before CTC arrival, this niche is called pre-metastatic niche, and exosomes play a major role in its preparation. **(H)** Metastases: CTCs that arrive in distant organs, such as liver or lung, will form a metastatic lesion, thus concluding the metastatic cascade.

in normal epithelial cells induces apoptosis, a process called "anoikis" (43). To survive this process, it has been suggested that CTCs acquire mesenchymal features through the epithelial–mesenchymal transition (EMT) process. This mechanism is physiologically used by epithelial cells during embryogenesis or wound healing to acquire a mesenchymal phenotype, migrate to reach distant regions or cross connective tissues, and then to reacquire an epithelial phenotype. This process also allows cancer cells to detach from the main tumor, modify their cytoskeleton, move within the connective tissue, and intravasate through endothelial cells (41). As one of the key features of EMT is the switch from expression of the adherent junction protein E-cadherin to N-cadherin, this might limit the use of CTCs as liquid biopsy. In fact, most methods for CTC detection are based on epithelial markers, particularly epithelial cell adhesion molecule (EpCAM). This protein is expressed on the surface of epithelial cells and is used as an enrichment surface marker by the CellSearch® System (Menarini Silicon Biosystems©), the only method cleared by the US Food & Drug Administration (FDA) for CTC enumeration.

Intravasation might occur at early tumor stages, and it has been suggested that early-stage dissemination is a very common phenomenon (44). However, CTCs are a rare event in most patients, even those with advanced disease (7); therefore, the chance of capturing few CTCs is minimal in these early stages. However, their detection at early stages could represent an early marker of cancer or of recurrence after treatment.

On the other hand, during late dissemination, CTC enumeration has been clinically validated as a prognostic tool in many cancer types. For example, in metastatic breast cancer, detection of > 5 CTCs per 7.5 ml of blood is associated with shorter overall survival and lower progression-free survival (45). Ongoing clinical trials assess whether CTC enumeration might guide therapeutic decision-making, particularly as a sign of treatment failure, when the number of CTCs remains high. In addition, CTCs harbor therapeutic predictive markers that

in the current medical practice can only be analyzed in the tumor tissue. Some examples are PD-L1 in NSCLC (among many others) (46), HER2 in breast and stomach cancer (47), and androgen receptor variant 7 (AR-V7) in prostate cancer (48). As these markers have already shown their clinical utility when evaluated in tissue biopsy, their detection in CTCs could take the place of tissue biopsy in the future. However, not all patients have the same number of CTCs in blood. Therefore, it is crucial to determine the percentage of positive CTCs required for the correlation with the target therapy outcomes, based on the current diagnostic methods. CTC clinical implications have been extensively reviewed elsewhere (49, 50).

Nonetheless, the methods for detection, capture, and characterization of these rare cells must be improved to increase their clinical utility as liquid biopsy and possibly as a screening method in early-stage cancer.

EMBOLIZATION AND TUMOR CELL SURVIVAL

The next step of the metastatic cascade involves mainly CTCs and how these cells survive and adapt to the blood stream environment. This is the most critical part of the metastatic cascade, as indicated by the fact that < 0.1% of the cancer cells injected in animal models are viable after 24 h (2). Moreover, clinical studies showed that liver works as a filter against viable CTCs when cancer cells transit through the portal vein (51). This step is the least characterized because CTC study in blood is very challenging and only recent methodological approaches had allowed assessing the underlying mechanisms, with clear implications for the liquid biopsy field.

Cancer cells can reach the circulation as single cells or as clusters/micro-emboli. Recent studies found that CTC clusters are formed in the tumor. Such clusters display higher metastatic potential compared with single cells, because they increase cell survival and reduce apoptosis (52). CTC clustering also induce specific changes in DNA methylation that promote stemness properties and metastasis formation (53). Moreover, CTC clustering with neutrophils promote cell-cycle progression and survival, thus favoring metastasis developments (54). Unlike single CTCs, CTC clusters might not need to go through EMT. Indeed, Gkountela et al. (53) demonstrated a specific methylation pattern that promotes expression of stemness-related genes, when CTCs are clustered, but they did not find any change in the methylation profile of EMT-related genes. Other studies also suggested that EMT might not have a role in CTC clusters (55, 56).

Although CTC clusters might display higher metastatic potential, single CTCs are present in higher number, with a clear association with prognosis and overall survival (45, 57). This suggests that single CTCs might easily escape the physiological filters such as liver and that their higher number might increase the chance of producing a metastatic tumor, despite their low effectiveness. On the other hand, CTC clusters are less likely to escape these filters but are more efficient in metastasis formation. Different cancer types might use one or both ways to disseminate, in function of their stage or location (58).

It is important to note that there is neither standardized method nor criteria to characterize CTC clusters. Moreover, the current technologies might be biased toward the detection of single CTCs (smaller) or clusters (bigger), although both CTC types might be present in the blood of patients with cancer during the disease course. Therefore, the clinical meaning of CTC clusters is not clear yet. For clinical implications, it might be necessary to fully identify the different CTC subpopulations.

CTCs can also gain physical and immune protection by interacting with platelets that can form a kind of coat around CTCs (59) shortly after their release in the blood stream. Platelets' role in cancer metastases has been already highlighted (60), whereas their potential role as circulating biomarker (i.e., TEPs) is only emerging now (61). TEPs' role as biomarker is based on the cross talk between platelets and CTCs that affects tumor cell proliferation and dissemination (62). Indeed, TEPs promote CTC survival, escape from immune surveillance, tumor–endothelium interactions, and dissemination. Reciprocally, CTCs modify the RNA profile of blood platelets and "tumor-educate" them (61). This "education" process might occur during the formation of CTC-platelet clusters, possibly through the uptake of exosomes and/or thrombin from CTCs (63). Simultaneously, platelets release different growth factors from α-granules (64) that can induce tumor cell proliferation and angiogenesis and also EMT (65). TEP clinical applications require further validation and standardization.

Micro-emboli/cluster formation protects CTCs and increases their survival in the bloodstream (52, 66, 67). This occurs by interaction of tumor CD44 with platelet P-selectin and the fibrinogen receptor GPIIb-IIIa which are involved in CTC coating by platelets (68). Platelets enhance tissue factor and P2Y12 receptor activities that contribute to EMT (69, 70). Additionally, TGFβ secretion by platelets can induce the TGFβ/SMAD and NF-κB pathways, which are the main molecular pathways implicated in EMT induction, thus increasing CTC metastatic potential (71). In turn, EMT in CTCs increases their interaction with platelets through the expression of heat shock protein 47 (HSP47), a chaperone implicated in collagen secretion and deposition that might enhance the formation of CTC clusters associated with platelets. Finally, HSP47 amplification in CTCs has been associated with a higher metastatic rate (72, 73).

ESTABLISHMENT OF THE TUMOR MICROENVIRONMENT, ARREST, AND EXTRAVASATION IN A TARGET ORGAN

In the last step of the metastatic cascade, CTCs must interact with endothelial cells, mainly in capillaries where cancer cells get trapped. After their arrival in the endothelium, CTCs increase the permeability of the endothelial barrier, allowing their extravasation in a tissue/organ. Once in the tissue, cancer cells

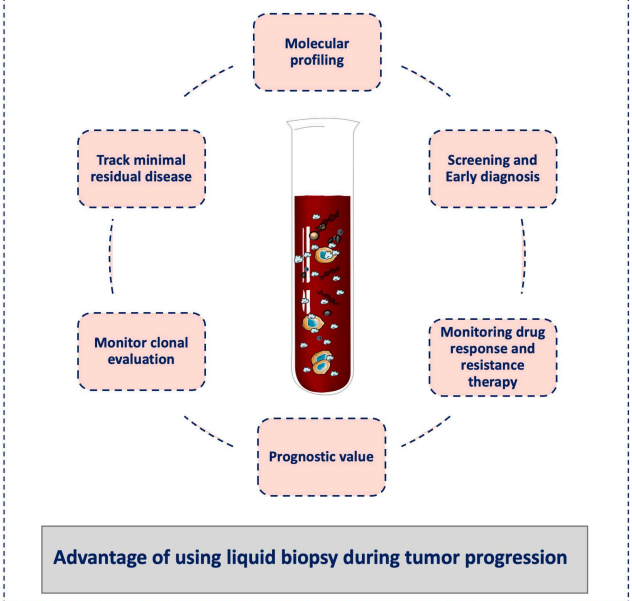

FIGURE 3 | Advantages of liquid biopsy to monitor tumor progression. Liquid biopsy has broad potential applications for cancer diagnosis and treatment, including screening for early diagnosis, study of tumor heterogeneity, and clonal evolution, and detection of minimal residual disease. During cancer progression, liquid biopsy might help clinicians to stratify patients for treatment personalization and to monitor the treatment response and the development of resistance. It can also be used for the tumor molecular characterization, and its minimally invasive nature allows repeat sampling to monitor changes over time without the need for a tissue biopsy.

will grow if the local microenvironment conditions are favorable for their survival and proliferation (i.e., "fertile soil").

Many proteins are involved in CTC arrest at the surface of endothelial cells. *In vivo* experiments in zebrafish cancer models have shown that CTC arrest occurs in two steps: first by weak interactions *via* CD44 and the integrin αVβ3 and then by stronger attachment *via* the integrin α5β1 (74). Hydrodynamic forces also influence CTC arrest. For instance, the brain supratentorial regions are more susceptible to metastases due to the local low perfusion and low flow pressure (75). Nevertheless, the involved mechanisms might vary according to the cancer type and the target organ. Moreover, CTC clusters might get trapped in arterioles or venules due to their larger size, and this might play a bigger role than protein interactions in their arrest at the surface of endothelial cells.

Then, blocked CTCs must extravasate to the tissue. As observed during intravasation, CTCs might release EVs that modify the cytoskeleton of endothelial cells and increase their permeability, thus allowing the crossing of the endothelial barrier (34, 76). Platelets also might be involved in this process. Indeed, CD97-expressing CTCs activate platelets to release their granules that might first increase coagulation around the cells and then promote endothelial permeabilization through secretion of ATP that mediates endothelial cell junction dynamics (77).

Finally, CTCs must arrive in a favorable niche, known as pre-metastatic niche. Exosomes are crucial for the induction of the pre-metastatic niche. Hoshino et al. (78) showed that tumor-associated exosomes present cancer-specific integrin profiles that are associated with formation of the pre-metastatic niche in specific organs, for instance integrin αvβ5 and liver, or α6β4, and α6β1 and lung (i.e., cancer cell organotropism) (79). Uptake by target cells in these organs stimulates the expression of genes that promote migration and inflammation in Küpfer cells and lung fibroblasts, or cell migration-inducing and hyaluronan-binding protein (CEMIP) in the brain (80), thus finalizing the metastatic cascade. However, a favorable pre-metastatic niche is not enough to maintain cancer cell proliferation. Therefore, CTCs must have additional features to sustain their growth, like stem cells (81). For instance, the expression of aldehyde dehydrogenase (a tumor-initiating stem cell marker) together with other surface markers can suggest which CTCs is competent for brain metastasis (82). Detection of these exosome- and CTC-related markers by liquid biopsy might allow predicting specific metastatic sites or even developing target therapies.

CONCLUSION

In this review, we highlighted the role of different liquid biopsy analytes to understand the biology of the metastatic cascade (**Figure 2**). Although their role is fundamental in most of the steps of this process, other factors are involved as well. However, clinical decision-making based on the metastatic cascade biology must be the final goal of liquid biopsy. The increasing knowledge of the whole metastatic process (cellular and molecular) will allow the identification of new biomarkers and analytes that can be detected during the entire disease course, by taking advantage of the fact the cancer cells disseminate mainly through the blood. Therefore, it is humanly and technically possible to monitor in real time cancer progression in a patient.

There are many more factors than those described in this review that can be used as liquid biopsy. For instance, leukocytes might provide crucial information on how the immune system is reacting against the cancer. This is becoming very important due to the development of immune therapy. This is just an example of how the metastatic cascade model can help to predict new biomarkers in the liquid biopsy field and to offer possible alternative solutions in case of technical limitations. Additionally, the identification of new biomarkers will promote the development of targeted therapies against the metastatic process and not just against the primary tumor.

Finally, a liquid biopsy test should not be seen as a method to detect just one specific biomarker or analyte but as a comprehensive approach for the selection and combination of different biological clues during cancer progression. Similar to tissue biopsy, these tests should not be understood only as "positive or negative" tests, but they should be chosen and analyzed in the clinical context of each single patient in order to provide a real-time personalized medicine approach. In this

way, liquid biopsy can become the tool to monitor the entire metastatic cascade avoiding the limitations of tissue biopsy sampling of single tumors, which might not be representative of the whole evolution of the cancer disease (**Figure 3**).

AUTHOR CONTRIBUTIONS

All authors contributed in the design and wrote of this manuscript.

FUNDING

This project has received funding from the European Union Horizon 2020 Research and Innovation program under the Marie Skłodowska-Curie grant agreement no. 765492. CA-P also received funding from The National Institute of Cancer, SIRIC Montpellier Cancer Grant INCa_Inserm_DGOS_12553 and The ERA-NET TRANSCAN 2 JTC 2016 PROLIPSY.

ACKNOWLEDGMENTS

We thank Dr. Elisabetta Andermarcher for assistance with her comments and proofreading which greatly improved the manuscript. The figures were designed with the assistance of and modification to the images provided by the Servier Medical Art database (http://smart.servier.com/). Further information pertaining to the license and disclaimer notices can be found here: https://creativecommons.org/licenses/by/3.0/.

REFERENCES

1. Paget S. The distribution of secondary growths in cancer of the breast. *Lancet.* (1889) 133:571–3. doi: 10.1016/S0140-6736(00)49915-0
2. Fidler IJ. Metastasis: quantitative analysis of distribution and fate of tumor emboli labeled with 125 I-5-iodo-2'-deoxyuridine. *J Natl Cancer Inst.* (1970) 45:773–82.
3. Chambers AF, Naumov GN, Vantyghem SA, Tuck AB. Molecular biology of breast cancer metastasis. Clinical implications of experimental studies on metastatic inefficiency. *Breast Cancer Res.* (2000) 2:400–7. doi: 10.1186/bcr86
4. Fidler IJ. The pathogenesis of cancer metastasis: the "seed and soil" hypothesis revisited. *Nat Rev Cancer.* (2003) 3:453–8. doi: 10.1038/nrc1098
5. Poste G, Fidler IJ. The pathogenesis of cancer metastasis. *Nature.* (1980) 283:139–46. doi: 10.1038/283139a0
6. Lambert AW, Pattabiraman DR, Weinberg RA. Emerging biological principles of metastasis. *Cell.* (2017) 168:670–91. doi: 10.1016/j.cell.2016.11.037
7. Pantel K, Alix-Panabières C. Liquid biopsy and minimal residual disease — latest advances and implications for cure. *Nat Rev Clin Oncol.* (2019) 16:409–24. doi: 10.1038/s41571-019-0187-3
8. Eslami-S Z, Cortes-Hernandez LE, Cayrefourcq L, Alix-Panabieres C. The different facets of liquid biopsy: a Kaleidoscopic view. *Cold Spring Harb Perspect Med.* (2019) 10:a037333. doi: 10.1101/cshperspect.a037333
9. Vogelstein B, Papadopoulos N, Velculescu VE, Zhou S, Diaz LAJ, Kinzler KW. Cancer genome landscapes. *Science.* (2013) 339:1546–58. doi: 10.1126/science.1235122
10. Campbell P, Getz G, Korbel J, Joshua M, Jennings J, Stein L, et al. Pan-cancer analysis of whole genomes. *Nature.* (2020) 578:82–93. doi: 10.1038/s41586-020-1969-6
11. Al Tameemi W, Dale TP, Al-Jumaily RMK, Forsyth NR. Hypoxia-modified cancer cell metabolism. *Front cell Dev Biol.* (2019) 7:4. doi: 10.3389/fcell.2019.00004
12. Merker JD, Oxnard GR, Compton C, Diehn M, Hurley P, Lazar AJ, et al. Circulating tumor DNA analysis in patients with cancer: American society of clinical oncology and college of American pathologists joint review. *J Clin Oncol.* (2018) 36:1631–41. doi: 10.1200/JCO.2017.76.8671
13. Lo YMD, Chan KCA, Sun H, Chen EZ, Jiang P, Lun FMF, et al. Maternal plasma DNA sequencing reveals the genome-wide genetic and mutational profile of the fetus. *Sci Transl Med.* (2010) 2:61ra91 LP. doi: 10.1126/scitranslmed.3001720
14. Thierry AR, Mouliere F, Gongora C, Ollier J, Robert B, Ychou M, et al. Origin and quantification of circulating DNA in mice with human colorectal cancer xenografts. *Nucleic Acids Res.* (2010) 38:6159–75. doi: 10.1093/nar/gkq421
15. Kustanovich A, Schwartz R, Peretz T, Grinshpun A. Life and death of circulating cell-free DNA. *Cancer Biol Ther.* (2019) 20:1057–67. doi: 10.1080/15384047.2019.1598759
16. Lampignano R, Neumann MHD, Weber S, Kloten V, Herdean A, Voss T, et al. Multicenter evaluation of circulating cell-free DNA extraction and downstream analyses for the development of standardized (pre)analytical work flows. *Clin Chem.* (2019) 66:clinchem.2019.306837. doi: 10.1373/clinchem.2019.306837
17. Jeppesen DK, Fenix AM, Franklin JL, Higginbotham JN, Zhang Q, Zimmerman LJ, et al. Reassessment of exosome composition. *Cell.* (2019) 177:428–45.e18. doi: 10.1016/j.cell.2019.02.029
18. Sun K, Jiang P, Chan KCA, Wong J, Cheng YKY, Liang RHS, et al. Plasma DNA tissue mapping by genome-wide methylation sequencing for noninvasive prenatal, cancer, and transplantation assessments. *Proc Natl Acad Sci USA.* (2015) 112:E5503–12. doi: 10.1073/pnas.1508736112
19. Razavi P, Li BT, Brown DN, Jung B, Hubbell E, Shen R, et al. High-intensity sequencing reveals the sources of plasma circulating cell-free DNA variants. *Nat Med.* (2019) 25:1928–37. doi: 10.1038/s41591-019-0652-7
20. Martincorena I, Fowler JC, Wabik A, Lawson ARJ, Abascal F, Hall MWJ, et al. Somatic mutant clones colonize the human esophagus with age. *Science.* (2018) 362:911–7. doi: 10.1126/science.aau3879
21. Mattox AK, Bettegowda C, Zhou S, Papadopoulos N, Kinzler KW, Vogelstein B. Applications of liquid biopsies for cancer. *Sci Transl Med.* (2019) 11:eaay1984. doi: 10.1126/scitranslmed.aay1984
22. Chabon JJ, Hamilton EG, Kurtz DM, Esfahani MS, Moding EJ, Stehr H, et al. Integrating genomic features for non-invasive early lung cancer detection. *Nature.* (2020) 580:245–51. doi: 10.1038/s41586-020-2140-0
23. Gavelli G, Giampalma E. Sensitivity and specificity of chest X-ray screening for lung cancer: review article. *Cancer.* (2000) 89(Suppl. 11):2453–6. doi: 10.1002/1097-01422000120189:112453::aid-cncr213.3.co;2-d
24. Leal A, van Grieken NCT, Palsgrove DN, Phallen J, Medina JE, Hruban C, et al. White blood cell and cell-free DNA analyses for detection of residual disease in gastric cancer. *Nat Commun.* (2020) 11:525. doi: 10.1038/s41467-020-14310-3
25. Kalluri R, LeBleu VS. The biology, function, and biomedical applications of exosomes. *Science.* (2020) 367:eaau6977. doi: 10.1126/science.aau6977
26. Thakur BK, Zhang H, Becker A, Matei I, Huang Y, Costa-Silva B, et al. Double-stranded DNA in exosomes: a novel biomarker in cancer detection. *Cell Res.* (2014) 24:766–9. doi: 10.1038/cr.2014.44
27. Fernando MR, Jiang C, Krzyzanowski GD, Ryan WL. New evidence that a large proportion of human blood plasma cell-free DNA is localized in exosomes. *PLoS ONE.* (2017) 12:e0183915. doi: 10.1371/journal.pone.0183915
28. Vagner T, Spinelli C, Minciacchi VR, Balaj L, Zandian M, Conley A, et al. Large extracellular vesicles carry most of the tumour DNA circulating in prostate cancer patient plasma. *J Extracell Vesicles.* (2018) 7:1505403. doi: 10.1080/20013078.2018.1505403
29. Thery C, Witwer KW, Aikawa E, Alcaraz MJ, Anderson JD, Andriantsitohaina R, et al. Minimal information for studies of extracellular vesicles 2018 (MISEV2018): a position statement of the International society for extracellular vesicles and update of the MISEV2014 guidelines. *J Extracell Vesicles.* (2018) **7**:1535750. doi: 10.1080/20013078.2018.1461450
30. Cohen JD, Li L, Wang Y, Thoburn C, Afsari B, Danilova L, et al. Detection and localization of surgically resectable cancers with a multi-analyte blood test. *Science.* (2018) 359:926–30. doi: 10.1126/science.aar3247

31. Xu J, Zhang X, Pelayo R, Monestier M, Ammollo CT, Semeraro F, et al. Extracellular histones are major mediators of death in sepsis. *Nat Med.* (2009) 15:1318–21. doi: 10.1038/nm.2053
32. Nishimoto S, Fukuda D, Higashikuni Y, Tanaka K, Hirata Y, Murata C, et al. Obesity-induced DNA released from adipocytes stimulates chronic adipose tissue inflammation and insulin resistance. *Sci Adv.* (2016) 2:e1501332. doi: 10.1126/sciadv.1501332
33. Hsu YL, Hung JY, Chang WA, Lin YS, Pan YC, Tsai PH, et al. Hypoxic lung cancer-secreted exosomal miR-23a increased angiogenesis and vascular permeability by targeting prolyl hydroxylase and tight junction protein ZO-1. *Oncogene.* (2017) 36:4929–42. doi: 10.1038/onc.2017.105
34. Schillaci O, Fontana S, Monteleone F, Taverna S, Di Bella MA, Di Vizio D, et al. Exosomes from metastatic cancer cells transfer amoeboid phenotype to non-metastatic cells and increase endothelial permeability: their emerging role in tumor heterogeneity. *Sci Rep.* (2017) 7:4711. doi: 10.1038/s41598-017-05002-y
35. Amit M, Takahashi H, Dragomir MP, Lindemann A, Gleber-Netto FO, Pickering CR, et al. Loss of p53 drives neuron reprogramming in head and neck cancer. *Nature.* (2020) 578:449–54. doi: 10.1038/s41586-020-1996-3
36. Maru Y. Premetastasis. *Cold Spring Harb Perspect Med.* (2019) a036897. doi: 10.1101/cshperspect.a036897. [Epub ahead of print].
37. Holdenrieder S, Pagliaro L, Morgenstern D, Dayyani F. Clinically meaningful use of blood tumor markers in oncology. *Biomed Res Int.* (2016) 2016:9795269. doi: 10.1155/2016/9795269
38. Jiang T, Shi T, Zhang H, Hu J, Song Y, Wei J, et al. Tumor neoantigens: from basic research to clinical applications. *J Hematol Oncol.* (2019) 12:93. doi: 10.1186/s13045-019-0787-5
39. Hofman P, Heeke S, Alix-Panabières C, Pantel K. Liquid biopsy in the era of immuno-oncology: is it ready for prime-time use for cancer patients? *Ann Oncol.* (2019) 30:1448–59. doi: 10.1093/annonc/mdz196
40. Gros A, Parkhurst MR, Tran E, Pasetto A, Robbins PF, Ilyas S, et al. Prospective identification of neoantigen-specific lymphocytes in the peripheral blood of melanoma patients. *Nat Med.* (2016) 22:433–8. doi: 10.1038/nm.4051
41. Dongre A, Weinberg RA. New insights into the mechanisms of epithelial-mesenchymal transition and implications for cancer. *Nat Rev Mol Cell Biol.* (2019) 20:69–84. doi: 10.1038/s41580-018-0080-4
42. Wirtz D, Konstantopoulos K, Searson PC. The physics of cancer: the role of physical interactions and mechanical forces in metastasis. *Nat Rev Cancer.* (2011) 11:512–22. doi: 10.1038/nrc3080
43. Gilmore AP. Anoikis. *Cell Death Differ.* (2005) 12:1473–7. doi: 10.1038/sj.cdd.4401723
44. Hu Z, Ding J, Ma Z, Sun R, Seoane JA, Scott Shaffer J, et al. Quantitative evidence for early metastatic seeding in colorectal cancer. *Nat Genet.* (2019) 51:1113–22. doi: 10.1038/s41588-019-0423-x
45. Bidard F-C, Peeters DJ, Fehm T, Nolé F, Gisbert-Criado R, Mavroudis D, et al. Clinical validity of circulating tumour cells in patients with metastatic breast cancer: a pooled analysis of individual patient data. *Lancet Oncol.* (2014) 15:406–14. doi: 10.1016/S1470-2045(14)70069-5
46. Mazel M, Jacot W, Pantel K, Bartkowiak K, Topart D, Cayrefourcq L, et al. Frequent expression of PD-L1 on circulating breast cancer cells. *Mol Oncol.* (2015) 9:1773–82. doi: 10.1016/j.molonc.2015.05.009
47. Riethdorf S, Müller V, Zhang L, Rau T, Loibl S, Komor M, et al. Detection and HER2 expression of circulating tumor cells: prospective monitoring in breast cancer patients treated in the neoadjuvant GeparQuattro trial. *Clin Cancer Res.* (2010) 16:2634–45. doi: 10.1158/1078-0432.CCR-09-2042
48. Scher HI, Lu D, Schreiber NA, Louw J, Graf RP, Vargas HA, et al. Association of AR-V7 on circulating tumor cells as a treatment-specific biomarker with outcomes and survival in castration-resistant prostate Cancer. *JAMA Oncol.* (2016) 2:1441–9. doi: 10.1001/jamaoncol.2016.1828
49. Eslami-S Z, Cortés-Hernández LE, Alix-Panabières C. Circulating tumor cells: moving forward into clinical applications. *Precis Cancer Med March.* (2020) 3:4. doi: 10.21037/pcm.2019.11.07
50. Cortés-Hernández LE, Eslami-SZ, Pantel K, Alix-Panabières C. Molecular and functional characterization of circulating tumor cells: from discovery to clinical application. *Clin Chem.* (2019) 66:303586. doi: 10.1373/clinchem.2019.303586
51. Denève E, Riethdorf S, Ramos J, Nocca D, Coffy A, Daurès JP, et al. Capture of viable circulating tumor cells in the liver of colorectal cancer patients. *Clin Chem.* (2013) 59:1384–92. doi: 10.1373/clinchem.2013.202846
52. Aceto N, Bardia A, Miyamoto DT, Donaldson MC, Wittner BS, Spencer JA, et al. Circulating tumor cell clusters are oligoclonal precursors of breast cancer metastasis. *Cell.* (2014) 158:1110–22. doi: 10.1016/j.cell.2014.07.013
53. Gkountela S, Castro-Giner F, Szczerba BM, Vetter M, Landin J, Scherrer R, et al. Circulating tumor cell clustering shapes DNA methylation to enable metastasis seeding. *Cell.* (2019) 176:98–112.e14. doi: 10.1016/j.cell.2018.11.046
54. Szczerba BM, Castro-Giner F, Vetter M, Krol I, Gkountela S, Landin J, et al. Neutrophils escort circulating tumour cells to enable cell cycle progression. *Nature.* (2019) 566:553–7.doi: 10.1038/s41586-019-0915-y
55. Hong SM, Jung D, Kiemen A, Gaida MM, Yoshizawa T, Braxton AM, et al. Three-dimensional visualization of cleared human pancreas cancer reveals that sustained epithelial-to-mesenchymal transition is not required for venous invasion. *Mod Pathol.* (2019) 33:639–47. doi: 10.1038/s41379-019-0409-3
56. Padmanaban V, Krol I, Suhail Y, Szczerba BM, Aceto N, Bader JS, et al. E-cadherin is required for metastasis in multiple models of breast cancer. *Nature.* (2019) 573:439–44. doi: 10.1038/s41586-019-1526-3
57. Cabel L, Proudhon C, Gortais H, Loirat D, Coussy F, Pierga JY, et al. Circulating tumor cells: clinical validity and utility. *Int J Clin Oncol.* (2017) 22:421–30. doi: 10.1007/s10147-017-1105-2
58. Tissot T, Massol F, Ujvari B, Alix-Panabieres C, Loeuille N, Thomas F. Metastasis and the evolution of dispersal. *Proc Biol Sci.* (2019) 286:20192186. doi: 10.1098/rspb.2019.2186
59. Jiang X, Wong KHK, Khankhel AH, Zeinali M, Reategui E, Phillips MJ, et al. Microfluidic isolation of platelet-covered circulating tumor cells. *Lab Chip.* (2017) 17:3498–503. doi: 10.1039/C7LC00654C
60. Gasic GJ, Gasic TB, Galanti N, Johnson T, Murphy S. Platelet-tumor-cell interactions in mice. The role of platelets in the spread of malignant disease. *Int J cancer.* (1973) 11:704–18. doi: 10.1002/ijc.2910110322
61. Best MG, Sol N, Kooi I, Tannous J, Westerman BA, Rustenburg F, et al. RNA-Seq of tumor-educated platelets enables blood-based pan-cancer, multiclass, and molecular pathway cancer diagnostics. *Cancer Cell.* (2015) 28:666–76. doi: 10.1016/j.ccell.2015.09.018
62. Kuznetsov HS, Marsh T, Markens BA, Castano Z, Greene-Colozzi A, Hay SA, et al. Identification of luminal breast cancers that establish a tumor-supportive macroenvironment defined by proangiogenic platelets and bone marrow-derived cells. *Cancer Discov.* (2012) 2:1150–65. doi: 10.1158/2159-8290.CD-12-0216
63. Heeke S, Mograbi B, Alix-Panabières C, Hofman P. Never travel alone: the crosstalk of circulating tumor cells and the blood microenvironment. *Cells.* (2019) 8:714. doi: 10.3390/cells8070714
64. Menter DG, Tucker SC, Kopetz S, Sood AK, Crissman JD, Honn K V. Platelets and cancer: a casual or causal relationship: revisited. *Cancer Metastasis Rev.* (2014) 33:231–69. doi: 10.1007/s10555-014-9498-0
65. McAllister SS, Weinberg RA. The tumour-induced systemic environment as a critical regulator of cancer progression and metastasis. *Nat Cell Biol.* (2014) 16:717–27. doi: 10.1038/ncb3015
66. Hou JM, Krebs MG, Lancashire L, Sloane R, Backen A, Swain RK, et al. Clinical significance and molecular characteristics of circulating tumor cells and circulating tumor microemboli in patients with small-cell lung cancer. *J Clin Oncol.* (2012) 30:525–32. doi: 10.1200/JCO.2010.33.3716
67. Giuliano M, Shaikh A, Lo HC, Arpino G, De Placido S, Zhang XH, et al. Perspective on circulating tumor cell clusters: why it takes a village to metastasize. *Cancer Res.* (2018) 78:845–52. doi: 10.1158/0008-5472.CAN-17-2748
68. Gay LJ, Felding-Habermann B. Contribution of platelets to tumour metastasis. *Nat Rev Cancer.* (2011) 11:123–34. doi: 10.1038/nrc3004
69. Wang Y, Sun Y, Li D, Zhang L, Wang K, Zuo Y, et al. Platelet P2Y12 is involved in murine pulmonary metastasis. *PLoS ONE.* (2013) 8:e80780. doi: 10.1371/journal.pone.0080780
70. Orellana R, Kato S, Erices R, Bravo ML, Gonzalez P, Oliva B, et al. Platelets enhance tissue factor protein and metastasis initiating cell markers, and act as chemoattractants increasing the migration of ovarian cancer cells. *BMC Cancer.* (2015) 15:290. doi: 10.1186/s12885-015-1304-z

71. Labelle M, Begum S, Hynes RO. Direct signaling between platelets and cancer cells induces an epithelial-mesenchymal-like transition and promotes metastasis. *Cancer Cell.* (2011) 20:576–90. doi: 10.1016/j.ccr.2011.09.009
72. Xiong G, Chen J, Zhang G, Wang S, Kawasaki K, Zhu J, et al. Hsp47 promotes cancer metastasis by enhancing collagen-dependent cancer cell-platelet interaction. *Proc Natl Acad Sci USA.* (2020) 117:3748–58. doi: 10.1073/pnas.1911951117
73. Zhu J, Xiong G, Fu H, Evers BM, Zhou BP, Xu R. Chaperone Hsp47 drives malignant growth and invasion by modulating an ECM gene network. *Cancer Res.* (2015) 75:1580–91. doi: 10.1158/0008-5472.CAN-14-1027
74. Osmani N, Follain G, García León MJ, Lefebvre O, Busnelli I, Larnicol A, et al. Metastatic tumor cells exploit their adhesion repertoire to counteract shear forces during intravascular arrest. *Cell Rep.* (2019) 28:2491–500.e5. doi: 10.1016/j.celrep.2019.07.102
75. Follain G, Osmani N, Azevedo AS, Allio G, Mercier L, Karreman MA, et al. Hemodynamic forces tune the arrest, adhesion, and extravasation of circulating tumor cells. *Dev Cell.* (2018) 45:33–52.e12. doi: 10.1016/j.devcel.2018.02.015
76. Peinado H, Alečković M, Lavotshkin S, Matei I, Costa-Silva B, Moreno-Bueno G, et al. Melanoma exosomes educate bone marrow progenitor cells toward a pro-metastatic phenotype through MET. *Nat Med.* (2012) 18:883–91. doi: 10.1038/nm.2753
77. Ward Y, Lake R, Faraji F, Sperger J, Martin P, Gilliard C, et al. Platelets promote metastasis via binding tumor CD97 leading to bidirectional signaling that coordinates transendothelial migration. *Cell Rep.* (2018) 23:808–22. doi: 10.1016/j.celrep.2018.03.092
78. Hoshino A, Costa-Silva B, Shen TL, Rodrigues G, Hashimoto A, Tesic Mark M, et al. Tumour exosome integrins determine organotropic metastasis. *Nature.* (2015) 527:329–35. doi: 10.1038/nature15756
79. Costa-Silva B, Aiello NM, Ocean AJ, Singh S, Zhang H, Thakur BK, et al. Pancreatic cancer exosomes initiate pre-metastatic niche formation in the liver. *Nat Cell Biol.* (2015) 17:816–26. doi: 10.1038/ncb3169
80. Rodrigues G, Hoshino A, Kenific CM, Matei IR, Steiner L, Freitas D, et al. Tumour exosomal CEMIP protein promotes cancer cell colonization in brain metastasis. *Nat Cell Biol.* (2019) 21:1403–12. doi: 10.1038/s41556-019-0404-4
81. Agnoletto C, Corrà F, Minotti L, Baldassari F, Crudele F, Cook JW, et al. Heterogeneity in circulating tumor cells: the relevance of the stem-cell subset. *Cancers.* (2019) 11:483. doi: 10.3390/cancers11040483
82. Zhang L, Ridgway LD, Wetzel MD, Ngo J, Yin W, Kumar D, et al. The identification and characterization of breast cancer CTCs competent for brain metastasis. *Sci Transl Med.* (2013) 5:180ra48. doi: 10.1126/scitranslmed.3005109

Conflict of Interest: CA-P is one of the patent holders (US Patent Number 16,093,934) for detecting and/or characterizing circulating tumor cells.

The remaining authors declare that the research was conducted in the absence of any commercial or financial relationships that could be construed as a potential conflict of interest.

frontiers in Oncology

ORIGINAL RESEARCH
published: 30 July 2020
doi: 10.3389/fonc.2020.01220

Circulating Tumor DNA as a Potential Marker to Detect Minimal Residual Disease and Predict Recurrence in Pancreatic Cancer

Jiahong Jiang[1†], Song Ye[2†], Yaping Xu[3†], Lianpeng Chang[3], Xiaoge Hu[1], Guoqing Ru[4], Yang Guo[1], Xin Yi[3], Liu Yang[1] and Dongsheng Huang[1*]*

[1] Key Laboratory of Tumor Molecular Diagnosis and Individualized Medicine of Zhejiang Province, Department of Medical Oncology, Zhejiang Provincial People's Hospital, People's Hospital of Hangzhou Medical College, Hangzhou, China, [2] Division of Hepatobiliary and Pancreatic Surgery, Department of Surgery, The Second Affiliated Hospital, School of Medicine, Zhejiang University, Hangzhou, China, [3] Department of Translational Medicine, Geneplus-Beijing Institute, Beijing, China, [4] Department of Pathology, Zhejiang Provincial People's Hospital, People's Hospital of Hangzhou Medical College, Hangzhou, China

OPEN ACCESS

Edited by:
Elisabetta Rossi,
University of Padova, Italy

Reviewed by:
Kevin Xueying Sun,
Harbin Medical University, China
Justin Vareecal Joseph,
Aarhus University, Denmark

***Correspondence:**
Liu Yang
yangliu@hmc.edu.cn
Dongsheng Huang
dshuang@zju.edu.cn

[†]These authors have contributed equally to this work

Specialty section:
This article was submitted to Cancer Molecular Targets and Therapeutics, a section of the journal Frontiers in Oncology

Received: 18 January 2020
Accepted: 15 June 2020
Published: 30 July 2020

Citation:
Jiang J, Ye S, Xu Y, Chang L, Hu X, Ru G, Guo Y, Yi X, Yang L and Huang D (2020) Circulating Tumor DNA as a Potential Marker to Detect Minimal Residual Disease and Predict Recurrence in Pancreatic Cancer. Front. Oncol. 10:1220. doi: 10.3389/fonc.2020.01220

Pancreatic ductal adenocarcinoma (PDAC) is one of the leading causes of cancer death, partly due to the high recurrence rates for patients with PDAC. Current postoperative surveillance methods, including monitoring of clinical symptoms, tumor markers, and CT imaging, lack sensitivity and specificity for minimal residual disease (MRD). We investigated whether the detection of circulating tumor DNA (ctDNA) could identify MRD and predict relapse in postoperative patients with PDAC. In this study, we performed panel-captured sequencing to detect somatic mutations. Matched tissue samples were obtained to verify mutation. A total of 27 patients and 65 plasma samples were included. Among the somatic mutations, KRAS and TP53 were the most recurrent genes in both tissue and plasma samples. The detectable rate of ctDNA increased with the stage of PDAC. The maximal variant allele fraction (VAF) of ctDNA had a positive correlation with tumor largest diameter ($p = 0.0101$). Patients with ctDNA-positive status postoperatively had a markedly reduced disease-free survival (DFS) compared to those with ctDNA-negative status (HR, 5.20; $p = 0.019$). Positive vascular invasion significantly influenced disease-free survival (DFS) ($p = 0.036$), and positive postoperative ctDNA status was an independent prognostic factor for DFS (HR = 3.60; 95% CI, 1.15–11.28; $p = 0.028$). Postoperative ctDNA detection provides strong evidence of MRD and identifies patients with a high risk of relapse. ctDNA detection is a promising approach for personalized patient management during postoperative follow-up.

Keywords: pancreatic cancer, minimal residual disease, circulating tumor DNA, disease recurrence, KRAS

INTRODUCTION

Pancreatic ductal adenocarcinoma (PDAC) is the seventh leading cause of cancer deaths in China, with ∼90.1 new cancer cases and 79.4 cancer deaths (per 100,000) projected to occur every year (1). Surgical resection is a potentially curative treatment that could improve the overall 5-years survival rate from 8 to 25% in PDAC (2, 3). Unfortunately, disease recurrence severely influences the outcomes of postoperative patients with PDAC.

The current criterion to evaluate disease recurrence is based on the serum tumor marker cancer antigen 19-9 (CA19-9) and computed tomography. However, the standard biomarker CA19-9 has limited sensitivity and specificity in PDAC and is even negative in Lewis (-) individuals (4). Only macroscopic disease recurrence can be detected through CT surveillance, and identification is usually uncertain due to normal tissue changes after surgery. Recurrence risk was associated with some clinical and pathological features, such as poorly differentiated histology, maximum tumor size, and positive lymph node status. Nevertheless, only these factors were inadequate to assess recurrence risk accurately (5). Indeed, more than 70% of postoperative patients with PDAC will die from recurrent disease (6); thus, a reliable approach is urgently needed to identify minimal residual disease (MRD) and predict the recurrence risk for PDAC.

Liquid biopsy is a promising approach for disease surveillance in solid tumors (7). Emerging evidence has shown that circulating tumor DNA (ctDNA) analysis can identify MRD shortly after surgery in patients with non-metastatic colon cancer and breast cancer (8, 9). These studies indicated that ctDNA detection can predict cancer recurrence with high sensitivity. Meanwhile, ctDNA detection is a promising approach for personalized patient management during postoperative follow-up due to its non-invasive, real-time, and dynamic features.

In this study, we aimed to determine whether ctDNA analysis can reliably identify MRD in postoperative patients with PDAC and compare dynamic changes in ctDNA with ordinary tumor surveillance during treatment.

MATERIALS AND METHODS

Patients and Samples

Between July 2016 and September 2018, a total of 27 patients diagnosed with PDAC were enrolled at Zhejiang Provincial People's Hospital. Plasma samples were collected at these time nodes: preoperation, postoperation (7-days after surgery), and each follow-up visits (1 or 3 months after operation) (**Table S1**). Surgical tumor tissue samples were obtained from formalin-fixed paraffin-embedded tissues. According to the Response Evaluation Criteria in Solid Tumors (RECIST) version 1.1, a computed tomography scan and cancer antigen 19-9 (CA 19-9) are used to assess treatment effectiveness and monitor tumor progression every 1–3 months. This study was approved by the ethical committee at Zhejiang Provincial People's Hospital (No. 2016KY129). All participants provided written informed consent before any study-related operation was performed.

Genomic DNA Extraction

In each eligible patient, at least 10 ml of peripheral blood was collected to isolate plasma and lymphocytes. All samples were stored at −80°C prior to DNA extraction. QIAamp DNA Blood Mini Kits and QIAamp DNA Mini Kits (Qiagen, Hilden, Germany) were used to extract genomic DNA from plasma lymphocytes (germline DNA) and tumor tissue (tumor DNA), respectively. Circulating cell-free DNA (cfDNA) was extracted from plasma using the QIAamp Circulating Nucleic Acid Kit (Qiagen, Hilden, Germany). cfDNA released by tumor cells was termed as ctDNA, which carries tumor-specific genetic mutations, including somatic single nucleotide variations (SNVs) and somatic insertions/deletions (Indels). DNA concentrations were quantified using a Qubit fluorometer (Invitrogen, Carlsbad, CA, USA). The length of cfDNA fragments was assessed using the Agilent 2100 BioAnalyzer (Agilent Technologies, Santa Clara, CA, USA).

Library Preparation, Hybridization Capture, and Sequencing

Germline and tumor DNA was fragmented into 200–250 bp segments using a Covaris S2 instrument (Woburn, MA, USA). After an end repair and A-tailing reaction, adapters with unique base sequences (unique identifiers, UIDs) were ligated to both ends of the double-stranded molecules, and then fragment amplification was performed using PCR. Indexed Illumina NGS libraries were prepared for germline DNA, tumor DNA, and cfDNA using the NEB DNA Library Preparation Kit (NEB, MA, USA). Subsequently, constructed libraries were hybridized to custom-designed biotinylated oligonucleotide probes (IDT, Coralville, IA, USA) covering 1,017 cancer susceptibility genes (**Table S2**). DNA sequencing was performed on a HiSeq2000 System (Illumina, CA, USA). The sequencing protocol was executed as previously described (10).

Raw Data Processing

Adapter sequences from the raw data and reads with a high *N* rate (>50%) or low-quality bases (>50%, Q < 5) were filtered out to obtain clean data. The clean reads were aligned to the hg19 human genome using the Burrows-Wheel Aligner (BWA, http://bio-bwa.sourceforge.net/) program. Subsequently, duplicate reads were identified using Picard's Mark Duplicates tool (https://software.broadinstitute.org/gatk/documentation/tooldocs/4.0.3.0/picard_sam_markduplicates_MarkDuplicates.php). Base quality recalibration and local realignment were performed using The Gene Analysis Toolkit (GATK, https://www.broadinstitute.org/gatk/).

Mutation Identification

SNVs and somatic Indels were identified using GATK and MuTect2 (https://software.broadinstitute.org/gatk/documentation/tooldocs/3.8-0/org_broadinstitute_gatk_tools_walkers_cancer_m2_MuTect2.php) and filtered by the sequencing results of peripheral blood lymphocytes. All variants underwent further filtration with the following criteria: 1) variants with <5 high-quality reads were removed (mapping quality ≥ 30, base quality ≥ 30); 2) variants included in the false positive database were removed; 3) variants with <0.1% mutant frequency that were included in several single nucleotide polymorphism databases (dbsnp, https://www.ncbi.nlm.nih.gov/projects/SNP/; 1000G, https://www.1000genomes.org/; ESP6500, https://evs.gs.washington.edu/; ExAC, http://exac.broadinstitute.org/) were retained; and 4) exonic or splicing variants were retained while synonymous variants were removed. The retained variants following this filtration were denoted as high-confidence somatic variants.

TABLE 1 | Clinical characteristics of enrolled patients.

Characteristics	Total ($n = 27$)
Age (years)	
Median (range)	62 (43–82)
Sex, no. (%)	
Male	17 (62.97)
Female	10 (37.04)
Stage, no. (%)	
I	13 (48.15)
II	9 (33.34)
IV	5 (18.52)
Lymph nodes metastasis, no. (%)	
Positive	7 (25.93)
Negative	20 (74.07)
Nerve invasion, no. (%)	
Positive	17 (62.96)
Negative	10 (37.04)
Vascular invasion, no. (%)	
Positive	10 (37.04)
Negative	17 (62.96)
Differentiation, no. (%)	
Moderately-poor	15 (55.56)
High	12 (44.44)
Tumor size, no. (%)	
>4 cm	12 (44.44)
≤4 cm	15 (55.56)

Statistical Analysis

The relationship of maximal variant allele fraction (VAF), CEA, CA19-9 and tumor largest diameter (TLD) was assessed using linear analysis. Categorical time-to-event analyses of disease-free survival were conducted using the Kaplan–Meier method with log-rank test to estimate *p*-values, and the Cox exp (beta) method was used to estimate hazard ratios. Univariate and Multivariate Cox analyses for risk factors for relapse were performed using SPSS 22.0 (IBM, Armonk, NY, USA). A $p < 0.05$ was considered significant.

RESULTS

Patient Characteristics

In this study, we profiled 65 plasma and 27 tissue samples from 27 eligible patients with PDAC. The clinical characteristics of all patients are summarized in **Table 1**. All patients were treated with surgical resection. As of 14 November 2018, the median follow-up was 18.6 months (range 12.4–28.9 months), and 14 patients experienced relapse.

ctDNA was successfully extracted from all plasma samples with an average concentration of 28.38 ng/ml (range, 5.57–119.10 ng/ml). The average coverage depths for sequenced tumor DNA and ctDNA were 864.64 × (range, 371×-1590.80×) and 1323.18× (range, 719.92×-2423×), respectively, and the fractions of target region coverage were all above 99%.

Mutant Prevalence of Plasma and Tissue Samples

The mutant prevalence of tissue samples and plasma samples collected before surgery is shown in **Figure 1A**. In total, 153 somatic mutations were identified in tissue samples from 27 patients, including 123 missense mutations (80.39%), 8 non-sense mutations (5.23%), 16 frameshift mutations (10.46%), 1 deletion of a small fragment (0.65%), and 1 insertion of a small fragment (0.65%) in the coding sequence. In addition, we also identified one mutation in 3' splice sites (0.65%) and three mutations in 5' splice sites (1.96%). TP53 (24/27, 88.89%), KRAS (23/27, 85.19%), and SMAD4 (9/27, 33.34%) were the most frequent mutant genes in the tissue samples. Interestingly, co-mutants TP53/KRAS, TP53/SMAD4, and KRAS/SMAD4 occurred in 20 (74.04%), 9 (33.34%), and 7 patients (25.93%), respectively. Mutant TP53, KRAS, and SMAD4 were co-expressed in seven patients (25.93%). In contrast, ctDNA was detected in 18 of 27 preoperative plasma samples including 65 somatic mutations. Frequencies of KRAS and TP53 reached 50.00% (9/18) and 44.45% (8/18) in preoperative ctDNA positive patients, respectively. Mutant KRAS and TP53 co-occurred in four patients (14.81%). To confirm the validity of the sequencing results, we compared the prevalence of mutations detected in our analysis to those detected in publicly available PDAC tissue datasets (QCMG, TCGA, and ICGC) (11–13). The top 5 mutant genes in our study and public datasets were listed in **Figure 1B**. The gene mutation rates of tumor tissue in our cohort were generally higher than those in public datasets except KRAS, possibly due to the low depth of whole exon sequencing and racial difference. We also assessed the correlation between the prevalence of mutations in tumor DNA and ctDNA in our cohort. The mutation rates of the top 10 genes in ctDNA were significantly correlated with those in tumor DNA ($R^2 = 0.875$; $p < 0.0001$) (**Figure 1C**). There were also some differences between tumor DNA and ctDNA, such as the lower frequency of TP53 in ctDNA (**Figure 1B**).

ctDNA Detection and Clinical Feature Analysis

ctDNA was detected in 18 of 27 preoperative plasma samples, resulting in a detectable rate of 66.67%. The majority of patients were stage I ($n = 13$, 48.15%) and stage II ($n = 9$, 33.34%), while only five patients were stage IV ($n = 5$, 18.52%) in this cohort. The detectable rate increased with the stage of PDAC (from 53.8 to 66.7%, reaching 100% for stage IV) (**Figure 1D**). To determine whether the ctDNA burden is associated with tumor size, the maximal VAF of 18 ctDNA detectable patients, CEA and CA19-9 were assessed preoperatively to identify the correlation between TLDs. Linear analysis revealed a positive correlation between the maximal VAF (ranged from 0.05 to 13.64%) in plasma and the TLD ($p = 0.0101$), while CEA and CA19-9 showed no distinct relevance ($p = 0.1114$, $p = 0.4242$) (**Figure 2A**). After 7 days of surgical resection, the status of ctDNA was changed in 19 patients, in which one turned positive and 10 turned negative completely. We compared the changes of maximal VAF between preoperative (ranged from 0.00 to 13.64%) and postoperative

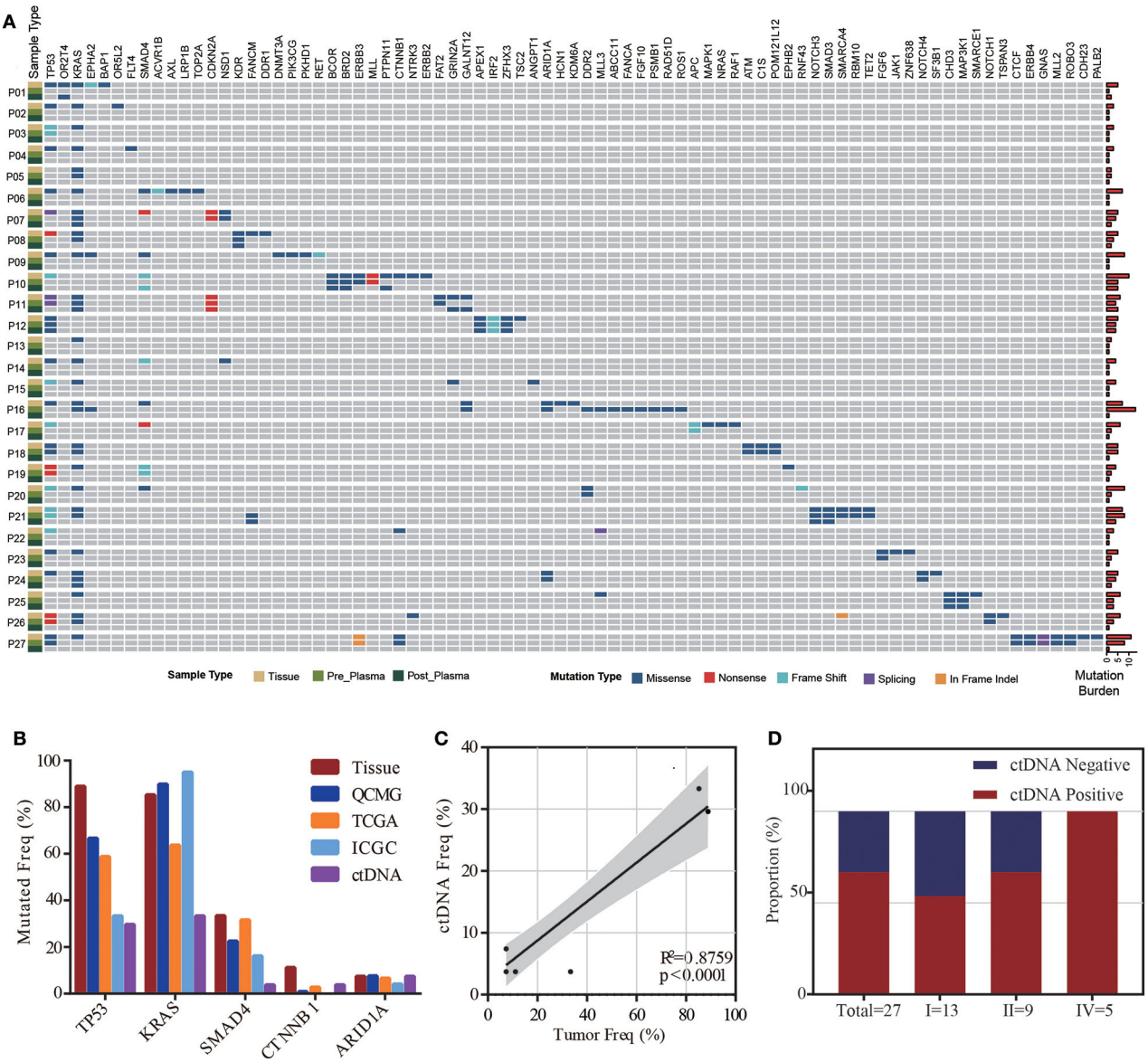

FIGURE 1 | ctDNA and tissue mutational landscape in patients with pancreatic ductal adenocarcinoma (PDAC). **(A)** Heatmap illustrating tissue, preoperative and postoperative ctDNA mutations identified in this study. Right bars indicate the mutation burden of each sample. **(B)** Comparison of mutation frequencies in our study (tissue and preoperative ctDNA) and public tissue databases (QCMG, TCGA, and ICGC). **(C)** Correlation between mutation rates in preoperative ctDNA and tumor DNA. **(D)** The detectable rate of different clinical stages in preoperative plasma samples from 27 PDAC patients.

(ranged from 0.00 to 0.38%) plasma, the maximal VAF level was significantly decreased when compared to the preoperative levels in most patients ($p = 0.036$). However, only slight changes appeared in CEA ($p = 0.346$) and CA19-9 levels ($p = 0.196$), suggesting a better sensitivity of ctDNA for detecting dynamic tumor changes (**Figure 2B**).

Landmark Analysis of Prognosis for Postoperative Patients

To investigate serial ctDNA analysis for disease surveillance during follow-up, we performed postoperative monitoring of 27 patients with ctDNA analysis, tumor biomarkers, and CT scans. Postoperative ctDNA was positive in nine patients, and eight of these patients ultimately recurred. Patients with ctDNA-positive status postoperatively had a markedly reduced disease-free survival (DFS) compared to those with ctDNA-negative status (HR, 5.20; $p = 0.019$) (**Figure 3B**). However, preoperative ctDNA status showed no significant effect on DFS (HR, 1.20; $p = 0.759$) (**Figure 3A**).

We also explored the correlation between DFS and clinical risk factors to help predict patient prognosis. Survival analysis demonstrated that localized or metastatic clinical stage had

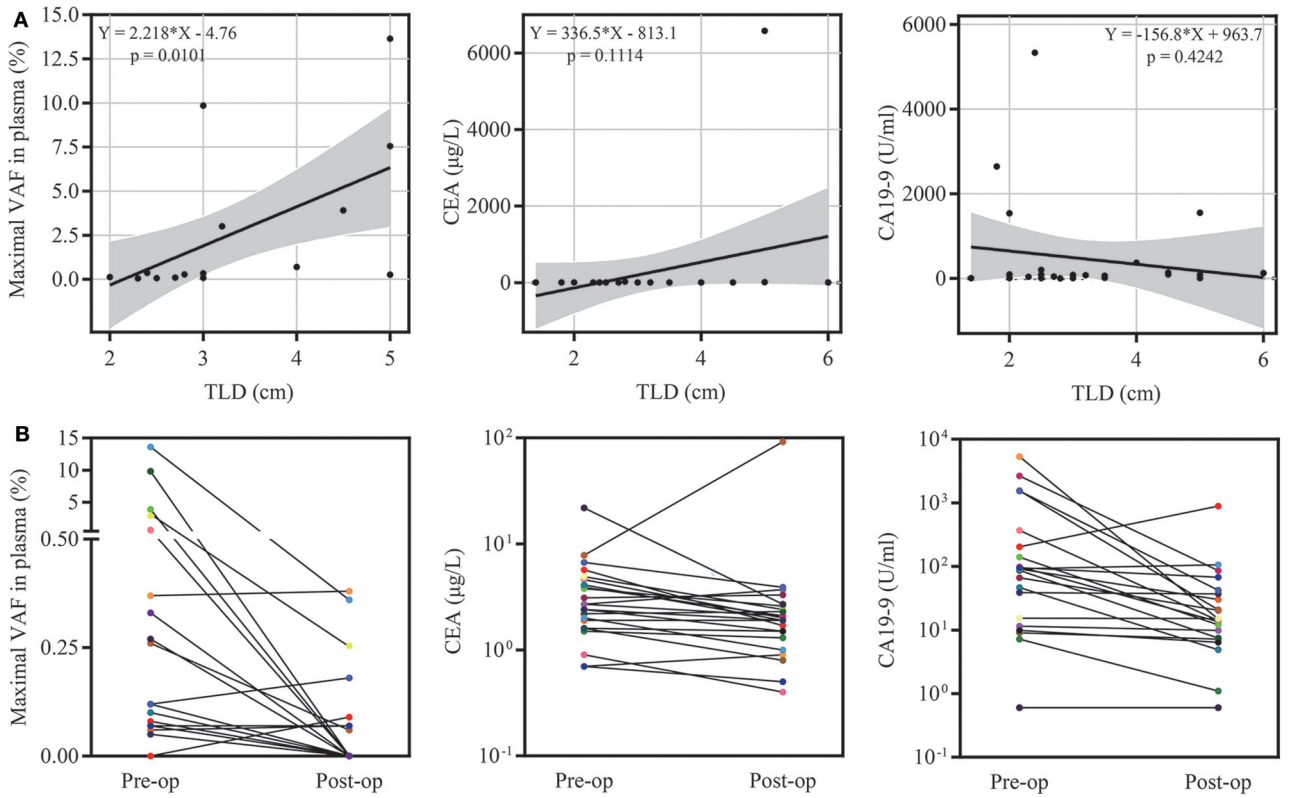

FIGURE 2 | ctDNA burden and clinical feature analysis. **(A)** The relationship of the maximal variant allele fraction (VAF), CEA, CA19-9 and tumor largest diameter (TLD). **(B)** Dynamic changes in the maximal VAF, CEA and CA19-9 7 days after surgery.

no difference on patient DFS ($p = 0.917$) (**Figure 3C**). Other risk factors, including larger tumor size (>4 cm), positive lymph node metastasis, positive nerve invasion, moderate-poor differentiation, and postoperative CA19-9 level, also showed the same results ($p > 0.05$) (**Figures 3D–F,H,I**). However, patients with positive vascular invasion had significantly lower freedom from progression than those without vascular invasion ($p = 0.036$) (**Figure 3G**). To further validate the correlation of postoperative ctDNA status and disease recurrence, we performed a Cox analysis for the aforementioned risk factors and postoperative ctDNA status. The results of the univariate analysis were consistent with those of the survival analysis, in which only vascular invasion (HR, 3.16; 95% CI, 0.93–10.79; $p = 0.036$) and postoperative ctDNA status (HR, 3.55; 95% CI, 0.90–13.89; $p = 0.019$) were associated with disease relapse. Several risk factors, such as differentiation, nerve invasion, and postoperative CA19-9 levels, also showed a tendency to affect disease recurrence but failed to obtain positive results due to the small sample size. Subsequently, multivariate analysis was performed to adjust for the potential effects of differentiation, lymph node metastasis, nerve invasion, and vascular invasion. With these adjustments, postoperative ctDNA detection still affected disease recurrence in patients with PDAC (HR, 3.60; 95% CI, 1.15–11.28; $p = 0.028$) (**Table 2**).

DISCUSSION

Pancreatic ductal adenocarcinoma is one of the most lethal diseases and has a poor prognosis, which may be correlated with disease recurrence and the lack of effective monitoring methods. Recently, several studies have demonstrated that ctDNA profiling is associated with tumor burden and can predict tumor recurrence in patients with colon cancer and breast cancer (8, 9); however, research that focuses on PDAC and NGS based ctDNA analysis is still scarce. We collected tumor tissue and blood specimens from 27 PDAC patients and performed panel-based NGS of all samples. We then evaluated the concordance between our plasma samples, matched tumor samples and public tissue datasets. The correlation of MRD, ctDNA status, and risk factors for relapse will also be discussed.

In our study, most mutant genes in tumor DNA showed higher mutation frequencies than those reported in public datasets, which may be partly due to low depth of whole exon sequencing or racial differences in public datasets. Notably, mutant genes detected in ctDNA had a lower frequency than those detected in matched tumor tissue. Given the biological features such as abundant extracellular matrix, the shedding into peripheral blood is usually poor for ctDNA in PDAC patients. Besides, PDAC is genomic heterogeneous and different mutations in the same tumor may yield distinct allele frequencies

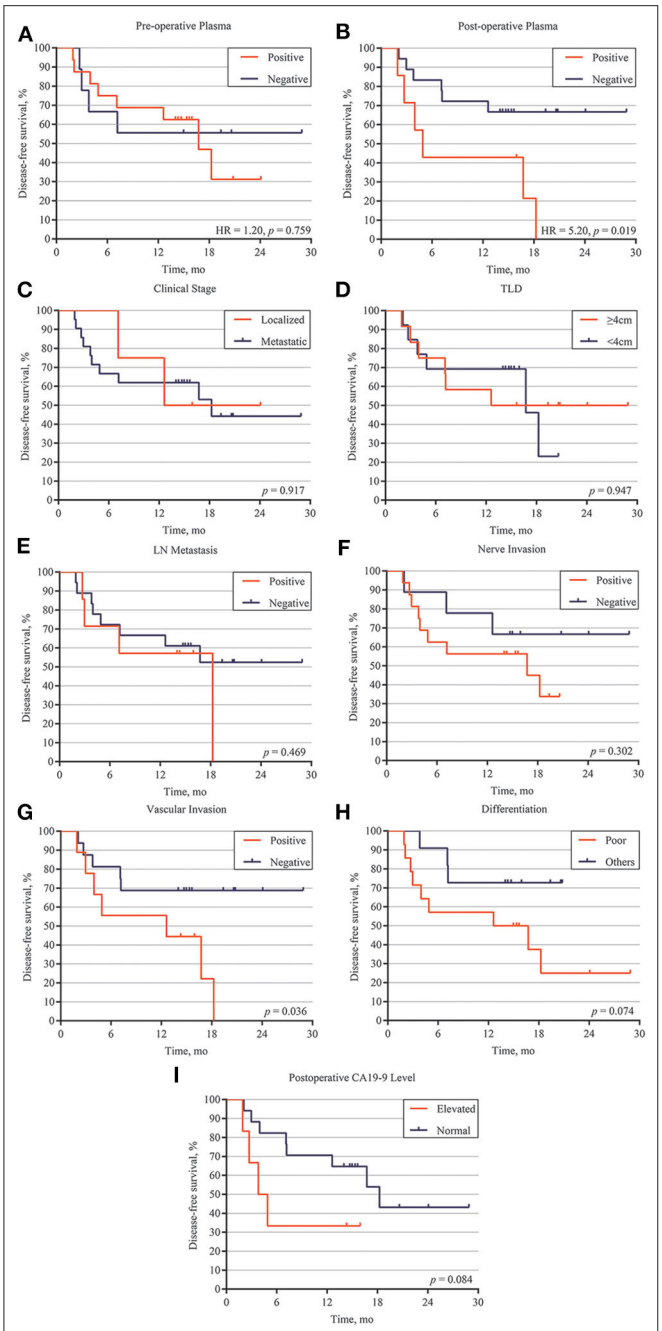

FIGURE 3 | Correlation between ctDNA, clinical high-risk factors and disease relapse. **(A)** Disease-free survival analysis of preoperative ctDNA detection patients with PDAC. **(B)** Disease-free survival analysis of postoperative ctDNA detection patients with PDAC. Disease-free survival analysis of 27 patients with different clinical features, including localized /metastatic clinical stage **(C)**, tumor largest size **(D)**, lymph node (LM) metastasis **(E)**, nerve invasion **(F)**, vascular invasion **(G)**, differentiation **(H)**, and postoperative CA19-9 level **(I)**.

(AFs), and those with relatively low AFs may not yet reach limit of detection and thus are deemed as undetected. Thus, it's difficult to reflect the entire mutational landscape via ctDNA profiling for individual PDAC patient. However, we revealed the significant correlation between the prevalence of mutation in tumor DNA and ctDNA based on cohort level, indicating that current platform is eligible to detected tumor-derived mutations in plasma ctDNA. Actually, several studies about the utility of ctDNA in MRD identification have been reported, and usually the presence of one or two tumor-derived mutations in plasma ctDNA is associated with post-operative survival (14, 15). In these cases, the mutational spectrum of tumor tissue provides prior knowledge for mutation tracing in ctDNA, and the circulating tumor burden reflected by mutational AFs can serve as an indicator for tumor surveillance. The most frequently mutated genes were TP53 and KRAS in both the tissue and plasma samples, and these genes play an important role in tumor proliferation and recurrence (16, 17).

After further filtration, at least one tumor-specific mutation was detected in ctDNA from 27 patients, and nearly 60% of tumor-derived mutations were detected in matched ctDNA, indicating that ctDNA profiling is a reliable and non-invasive source of molecular characteristics for PDAC. A previous study demonstrated that the detectable rate of mutations in ctDNA was significantly increased in patients with late-stage tumors compared with those with early-stage tumors (18). In this study, the detectable rate of mutations in ctDNA increased with tumor stage and finally reached 100% for stage IV, which was consistent with previous findings.

CA19-9 is considered the most common biomarker in PDAC diagnosis, treatment monitoring, and survival prediction. However, the level of CA19-9 is also increased in many benign conditions, such as biliary disease, liver disease, and pancreatitis, and only applicable in Lewis (+) patients (4, 19). Compared to CA19-9, CEA shows lower sensitivity and specificity in PDAC (20). In this condition, the postoperative ctDNA analysis revealed a positive relationship between the maximal VAF and dynamic tumor burden changes and proved to be efficient for detecting relapse compared to CA19-9 and CEA. Besides, consistent with other studies, ∼90% recurrence patients were postoperative ctDNA-positive before the time of radiologic relapse, indicating that postoperative ctDNA analysis may be more sensitive than CT imaging in MRD identification (21, 22).

The presence of postoperative ctDNA appeared to be a prognostic factor for poor DFS and OS. Pietrasz et al. demonstrated that patients with postoperatively undetectable ctDNA had a longer DFS (17.6 vs. 4.6 months) and OS (32.2 vs. 19.3 months) than those with detectable ctDNA (14). Hadano et al. reported that patients with positive ctDNA had only half the median OS duration of those without detectable ctDNA (13.6 vs. 27.6 months) (15). Our work also reveals that ctDNA analysis indicates MRD after surgery and predicts recurrence in patients with PDAC. Additionally, survival analysis and univariate analysis demonstrated that only positive vascular invasion could affect DFS, while other clinical risk factors showed no significant results. The small sample size may have caused the negative results of some risk factors. The multivariate analysis provided further proof for the detection of postoperative ctDNA as an independent prognostic factor for patients with PDAC. Two key limitations of our study are the small cohort

TABLE 2 | Univariate and multivariate cox analysis for risk factors of relapse.

Variable	Univariate analysis		Multivariate analysis	
	HR (95% CI)	*p*	HR (95% CI)	*p*
Clinical stage, Metastatic vs. Localized	0.92 (0.21–4.05)	0.917	-	-
Tumor size, ≥4 vs. <4 cm	0.96 (0.31–2.99)	0.947	-	-
Differentiation, Poor vs. Other	3.08 (0.99–9.56)	0.074	2.30 (0.51–10.45)	0.279
Lymph node metastasis, Positive vs. Negative	1.55 (0.41–5.77)	0.469	1.14 (0.29–4.50)	0.850
Nerve invasion, Positive vs. Negative	1.96 (0.62–6.24)	0.302	1.51 (0.35–6.43)	0.578
Vascular invasion, Positive vs. Negative	3.16 (0.93–10.79)	0.036*	1.50 (0.23–9.82)	0.673
Postoperative CA19-9 level, Elevated vs. Normal	2.69 (0.57–12.75)	0.084	-	-
Preoperative ctDNA status, Positive vs. Negative	0.65 (0.20–2.05)	0.453		
Postoperative ctDNA status, Positive vs. Negative	3.55 (0.90–13.89)	0.019*	3.60 (1.15–11.28)	0.028*[a]

**Statistical significance.*

[a]Multivariate analysis was performed to adjust for the potential effects of differentiation, lymph node metastasis, nerve invasion, and vascular invasion.

and the lack of follow-up blood sample. However, these two limitations may not influence the accuracy and sensitivity of ctDNA detection.

In conclusion, this study revealed the utility of ctDNA detection as a prognostic biomarker in patients with PDAC. Highly precise ctDNA detection has the potential to transform clinical practice via non-invasive monitoring of solid tumor malignancies and identification of MRD at earlier time points than standard clinical surveillance.

DATA AVAILABILITY STATEMENT

The datasets presented in this study can be found in online repositories. The names of the repository/repositories and accession number(s) can be found below: the National Center for Biotechnology Information (http://www.ncbi.nlm.nih.gov/) GenBank database as individual BioProjects PRJNA634169.

ETHICS STATEMENT

The studies involving human participants were reviewed and approved by the Ethical Committee of Zhejiang Provincial People's Hospital. The patients/participants provided their written informed consent to participate in this study.

AUTHOR CONTRIBUTIONS

LY and DH contributed to the conception of the study. JJ, SY, and YX contributed to experimental technology and experimental design. LC, YG, and GR provided molecular biology experimental technical support. JJ, SY, and XH performed the data analysis. XY helped perform the analysis with constructive discussions and paper modification. JJ, LY, and DH wrote the manuscript. All authors contributed to the article and approved the submitted version.

FUNDING

This work was supported by the Key Foundation of Science Technology Department of Zhejiang Province (No. 2015C03030), the National Natural Science Foundation of China (No. 81772575), Medical and Health Science Technology Project of Zhejiang Province (No. 2019RC105), and the Foundation of Science Technology Department of Zhejiang Province (No. 2017C33116).

SUPPLEMENTARY MATERIAL

The Supplementary Material for this article can be found online at: https://www.frontiersin.org/articles/10.3389/fonc.2020.01220/full#supplementary-material

REFERENCES

1. Chen W, Zheng R, Baade PD, Zhang S, Zeng H, Bray F, et al. Cancer statistics in China, 2015. *CA Cancer J Clin.* (2016) 66:115–32. doi: 10.3322/caac.21338
2. Bilimoria KY, Bentrem DJ, Ko CY, Stewart AK, Winchester DP, Talamonti MS. National failure to operate on early stage pancreatic cancer. *Ann Surg.* (2007) 246:173–80. doi: 10.1097/SLA.0b013e3180691579
3. Ryan DP, Hong TS, Bardeesy N. Pancreatic adenocarcinoma. *N Eng J Med.* (2014) 371:2140–1. doi: 10.1056/NEJMra1404198
4. Luo G, Liu C, Guo M, Long J, Liu Z, Xiao Z, et al. CA19-9-Low&Lewis (+) pancreatic cancer: a unique subtype. *Cancer Lett.* (2017) 385:46–50. doi: 10.1016/j.canlet.2016.10.046
5. Ghaneh P, Kleeff J, Halloran CM, Raraty M, Jackson R, Melling J, et al. The impact of positive resection margins on survival and recurrence following resection and adjuvant chemotherapy for pancreatic ductal adenocarcinoma. *Ann Surg.* (2019) 269:520–9. doi: 10.1097/SLA.0000000000002557
6. Spanknebel K, Conlon KC. Advances in the surgical management of pancreatic cancer. *Cancer J.* (2001) 7:312–23.

7. Diaz LA Jr, Bardelli A. Liquid biopsies: genotyping circulating tumor DNA. *J Clin Oncol.* (2014) 32:579–86. doi: 10.1200/JCO.2012.45.2011
8. Tie J, Wang Y, Tomasetti C, Li L, Springer S, Kinde I, et al. Circulating tumor DNA analysis detects minimal residual disease and predicts recurrence in patients with stage II colon cancer. *Sci Transl Med.* (2016) 8:346ra92. doi: 10.1126/scitranslmed.aaf6219
9. Garcia-Murillas I, Schiavon G, Weigelt B, Ng C, Hrebien S, Cutts RJ, et al. Mutation tracking in circulating tumor DNA predicts relapse in early breast cancer. *Sci Transl Med.* (2015) 7:302ra133. doi: 10.1126/scitranslmed.aab0021
10. Yang L, Wang G, Zhao X, Ye S, Shen P, Wang W, et al. A novel WRN frameshift mutation identified by multiplex genetic testing in a family with multiple cases of cancer. *PloS ONE.* (2015) 10:e0133020. doi: 10.1371/journal.pone.0133020
11. Bailey P, Chang DK, Nones K, Johns AL, Patch AM, Gingras MC, et al. Genomic analyses identify molecular subtypes of pancreatic cancer. *Nature.* (2016) 531:47–52. doi: 10.1038/nature16965
12. Waddell N, Pajic M, Patch AM, Chang DK, Kassahn KS, Bailey P, et al. Whole genomes redefine the mutational landscape of pancreatic cancer. *Nature.* (2015) 518:495–501. doi: 10.1038/nature14169
13. Cancer Genome Atlas Research Network. Electronic address, Cancer Genome Atlas Research N. Integrated genomic characterization of pancreatic ductal adenocarcinoma. *Cancer Cell.* (2017) 32:185–203.e13. doi: 10.1016/j.ccell.2017.07.007
14. Pietrasz D, Pecuchet N, Garlan F, Didelot A, Dubreuil O, Doat S, et al. Plasma circulating tumor DNA in pancreatic cancer patients is a prognostic marker. *Clin Cancer Res.* (2017) 23:116–23. doi: 10.1158/1078-0432.CCR-16-0806
15. Hadano N, Murakami Y, Uemura K, Hashimoto Y, Kondo N, Nakagawa N, et al. Prognostic value of circulating tumour DNA in patients undergoing curative resection for pancreatic cancer. *Br J Cancer.* (2016) 115:59–65. doi: 10.1038/bjc.2016.175
16. Kim H, Park CY, Lee JH, Kim JC, Cho CK, Kim HJ. Ki-67 and p53 expression as a predictive marker for early postoperative recurrence in pancreatic head cancer. *Ann Surg Treat Res.* (2015) 88:200–7. doi: 10.4174/astr.2015.88.4.200
17. Eser S, Schnieke A, Schneider G, Saur D. Oncogenic KRAS signalling in pancreatic cancer. *Br J Cancer.* (2014) 111:817–22. doi: 10.1038/bjc.2014.215
18. Bettegowda C, Sausen M, Leary RJ, Kinde I, Wang Y, Agrawal N, et al. Detection of circulating tumor DNA in early- and late-stage human malignancies. *Sci Transl Med.* (2014) 6:224ra24. doi: 10.1126/scitranslmed.3007094
19. Poruk KE, Gay DZ, Brown K, Mulvihill JD, Boucher KM, Scaife CL, et al. The clinical utility of CA 19-9 in pancreatic adenocarcinoma: diagnostic and prognostic updates. *Curr Mol Med.* (2013) 13:340–51. doi: 10.2174/1566524011313030003
20. Brody JR, Witkiewicz AK, Yeo CJ. The past, present, and future of biomarkers: a need for molecular beacons for the clinical management of pancreatic cancer. *Adv Surg.* (2011) 45:301–21. doi: 10.1016/j.yasu.2011.04.002
21. Scholer LV, Reinert T, Orntoft MW, Kassentoft CG, Arnadottir SS, Vang S, et al. Clinical implications of monitoring circulating tumor DNA in patients with colorectal cancer. *Clin Cancer Res.* (2017) 23:5437–45. doi: 10.1158/1078-0432.CCR-17-0510
22. Wang JSZ, Sausen M, Parpart-Li S, Murphy DM, Velculescu VE, Wood LD, et al. Circulating tumor DNA (ctDNA) as a prognostic marker for recurrence in resected pancreas cancer. *J Clin Oncol.* (2015) 33:16971. doi: 10.1200/jco.2015.33.15_suppl.11025

Conflict of Interest: YX, LC, and XY were employed by the company Geneplus-Beijing Institute.

The remaining authors declare that the research was conducted in the absence of any commercial or financial relationships that could be construed as a potential conflict of interest.

frontiers in Oncology

ORIGINAL RESEARCH
published: 28 August 2020
doi: 10.3389/fonc.2020.01320

Allelic Imbalance Analysis in Liquid Biopsy to Monitor Locally Advanced Esophageal Cancer Patients During Treatment

Elisa Boldrin[1*†], *Matteo Curtarello*[1†], *Matteo Fassan*[2], *Massimo Rugge*[2], *Stefano Realdon*[3], *Rita Alfieri*[4], *Alberto Amadori*[1,5] *and Daniela Saggioro*[1]

[1] Immunology and Molecular Oncology, Veneto Institute of Oncology IOV-IRCCS, Padova, Italy, [2] Department of Medicine (DIMED), Surgical Pathology and Cytopathology, University of Padova, Padova, Italy, [3] Endoscopy Unit, Veneto Institute of Oncology IOV-IRCCS, Padova, Italy, [4] Oncological Surgery, Veneto Institute of Oncology IOV-IRCCS, Padova, Italy, [5] Department of Surgical Sciences, Oncology and Gastroenterology, University of Padova, Padova, Italy

OPEN ACCESS

Edited by:
Matteo Bocci,
Lund University, Sweden

Reviewed by:
David Stephen Guttery,
University of Leicester,
United Kingdom
Dawn Sijin Nin,
National University
of Singapore, Singapore

***Correspondence:**
Elisa Boldrin
elisa.boldrin@iov.veneto.it

[†] These authors have contributed equally to this work

Specialty section:
This article was submitted to Cancer Molecular Targets and Therapeutics, a section of the journal Frontiers in Oncology

Received: 07 May 2020
Accepted: 24 June 2020
Published: 28 August 2020

Citation:
Boldrin E, Curtarello M, Fassan M, Rugge M, Realdon S, Alfieri R, Amadori A and Saggioro D (2020) Allelic Imbalance Analysis in Liquid Biopsy to Monitor Locally Advanced Esophageal Cancer Patients During Treatment. Front. Oncol. 10:1320. doi: 10.3389/fonc.2020.01320

Esophageal cancer (EC) is a highly aggressive tumor, and the current monitoring procedures are partially inadequate to evaluate treatment efficacy. The aim of this study was to investigate whether allelic imbalance analysis in liquid biopsy could be used as an additional tool to monitor tumor burden in EC patients. For this purpose, circulating cell-free DNA (cfDNA) from 52 patients with a locally advanced EC, which underwent neoadjuvant treatment and resection, was analyzed. Data from four representative longitudinally followed patients are also reported. Furthermore, 17 DNAs from formalin-fixed paraffin-embedded (FFPE) tumor samples were analyzed and compared to time-matched cfDNAs. To look for allelic imbalance, which is the main genetic alteration in both EC histotypes, we used a panel of five microsatellites (MSs) and three single-nucleotide polymorphisms (SNPs) near genes described as frequently altered. The Fisher exact and Mann-Whitney *U* tests were used to analyze categorical and continuous data, respectively. The correlation coefficient between cfDNA and FFPE-DNA was calculated with the Pearson's correlation test. We found that the selected tumor-related alterations are present in cfDNA of both adenocarcinoma (EADC) and squamous cell carcinoma (ESCC) with similar frequencies. The only exception were the MSs, one downstream and one upstream, of *SMAD4* of which the loss was only observed in EADC (26 vs. 0%, $P = 0.018$). More interestingly, longitudinal studies disclosed that in patients with disease progression, tumor-related alterations were present in cfDNA before overt clinical or instrumental signs of relapse. In conclusion, our data indicate that the evaluation of tumor-related gene allelic imbalance in cfDNA might be a useful tool to complement the current monitoring procedures for EC patients and to guide their management.

Keywords: esophageal cancer, esophageal adenocarcinoma (EADC), esophageal squamous cell carcinoma (ESCC), circulating cell free DNA (cfDNA), liquid biopsy, longitudinal studies, loss of heterozygosis (LOH), allelic imbalance

INTRODUCTION

Esophageal cancer (EC) is a highly aggressive tumor, and the majority of patients die of recurrent disease within 2 years from diagnosis; this happens even after a putative radical esophagectomy (1, 2). EC presents two main histotypes, which occur in distinct esophageal districts: adenocarcinoma (EADC) and squamous cell carcinoma (ESCC). EADC develops in the lower esophagus, near the gastroesophageal junction, while ESCC arises in the mid upper esophagus. The incidence of EADC is rising in the Western countries where it now represents the most diffuse histotype; ESCC instead remains the most common EC throughout Asia (1).

From the genetic point of view, both EC subtypes are mainly dominated by allelic imbalance, with frequent tumor suppressor gene mutations and losses and oncogene amplifications, as reported in the Cancer Genome Atlas study (3). Moreover, EADC and ESCC show differences at the molecular level. EADC is more similar to the chromosomal unstable (CIN) gastric adenocarcinoma subtype, while ESCC is molecularly closer to head and neck tumors (4). EADCs present frequent amplifications of *ERBB2* (32%), *VEGFA* (28%), *GATA6* (21%) and *GATA4* (21%), and deletion of *SMAD4* (24%), while ESCCs exhibit the prevalent amplification of *CCDN1* (57%), *TP63* (48%), and *EGFR* (19%). Both histotypes have high frequencies of *TP53* (73 vs. 92%) and *CDKN2A* (76 vs. 76%) inactivation and *MYC* amplification (32 vs. 23%) (3, 5).

In recent years, with the increasing knowledge of esophageal tumor genetics, clinical trials of targeted therapy have been conducted, especially using anti-HER2 and anti-VEGF drugs for EADC and anti-EGFR for ESCC; immunotherapy trials are still at an early stage (6–10). However, despite the introduction of these new options, the outcome of EC patients did not improve, and the standard of care for locally advanced tumors remains preoperative treatment with common chemotherapeutic drugs (platinum derivatives, 5-Fluorouracil, taxane, antracyclines), flanked by radiation, and followed by surgery (11, 12). No clear data on the benefit of adjuvant treatment exist (13, 14). For this reason, when a R0 resection is achieved, adjuvant treatment is provided at disease recurrence [i.e., Italian Association of Medical Oncology (AIOM) 2018 guidelines for esophageal cancer treatment].

The poor outcome of EC patients is usually ascribable to diagnosis at an advanced stage, but it is also related to the inadequacy of the current monitoring practices that are not always able to evaluate the effectiveness of treatment or to assess the likelihood of relapse, causing a delay in the administration of efficient therapies.

Recently, circulating cell-free DNA (cfDNA) emerged as a promising tool to diagnose and to monitor tumor behavior in terms of response to treatment, detection of minimal residual disease, and recurrence (15). Moreover, it has been suggested that cfDNA could represent, more efficiently than traditional biopsies, the real status of the tumor by overcoming the challenge of the intra-tumor heterogeneity (16–19).

In this pilot study, we explored the possibility of using liquid biopsy (cfDNA) as a possible additional strategy to follow EC patients during their therapeutic iter. cfDNAs of EC patients, together with DNAs of longitudinally collected samples and time-matched tumor specimens, were analyzed for the presence of tumor-related allelic imbalance events, such as the loss of heterozygosity (LOH) of tumor suppressor genes and the amplification of oncogenes, using a panel of 5 microsatellites (MSs) and 3 single-nucleotide polymorphisms (SNPs). Mutational analysis is currently the most common approach to test the presence of cancer-related alterations in cfDNA. However, we chose allelic imbalance analysis since we believe that this approach allows a more accurate detection of tumor-related alterations, usually present at low frequency in cfDNA. Indeed, LOH that involves the loss of the wild-type allele is needed to unmask somatic mutations occurring in tumor suppressor genes (20). Consequently, at a given locus, the frequency of LOH is generally similar to the frequency of a mutation in a hot-spot region. Conversely, when at a given locus we are faced with different low-frequency mutations, the LOH occurrence is usually higher than that of the single mutation; in this case, the loss of the wild-type allele includes more than one mutation (20).

MATERIALS AND METHODS

Patients

For this pilot study, 52 consecutive EC patients were selected among those who were referred to the Veneto Institute of Oncology IOV-IRCCS between 2013 and 2017. Inclusion criteria consisted of a T3-T4 classification at the time of primary staging or at reevaluation after neoadjuvant chemotherapy, and the availability of clinicopathological data and plasma. Patients with previous neoplasia at other sites or affected by major comorbidities were excluded. Among 10 EC patients for which samples were consecutively collected, four were chosen for longitudinal study on the basis of their clinical history and availability of clinical data. To evaluate the concordance between cfDNA and tumor DNA, 17 time-matched formalin-fixed, paraffin-embedded (FFPE) EADC specimens were also analyzed.

DNA Extraction

Venous blood samples were collected in EDTA tubes and processed within 2 h. Plasma was isolated from corpuscular components of the blood by centrifugation at 2,000×*g*; plasma was centrifuged a second time at 16,000×*g* to remove cellular debris, and then stored at −80°C until cfDNA extraction. One aliquot of whole blood was also stored for future germline DNA extraction. cfDNA was extracted from 1 ml of plasma using the QIAamp Circulating Nucleic Acid Kit (Qiagen, Milan, Italy); the amount of cfDNA ranged between 500 and 750 ng/ml plasma. Germline DNA was isolated from 250 µl of peripheral blood with the MagNA Pure Compact Nucleic Acid Isolation Kit I using the automated extractor MagNA Pure Compact Instrument (Roche, Milan, Italy), following the manufacturer's recommendations. FFPE tumor DNA was isolated from eight consecutive 10-µm-thick sections using QIAamp Mini Kit (Qiagen, Milan, Italy). A neoplastic component ≥70% was considered adequate for tumor DNA analysis; when necessary, samples were enriched

TABLE 1 | Markers used in genetic analysis.

Microsatellite or SNP	Heterozygosity (%)	Gene	Distance from gene	PCR Conditions	Size	Primers
rs28673064 (3q28)	53	*TP63*	5′UTR	35 cycles: 95°C 1 min, 56°C 1 min, 72°C 1 min; final extension: 72°C 45 min	180 bp	Fw: TGAAGGAGAGAAGTGCCTAAAC Rw: GTGGCACACCGTGAAGT
rs9344 (11q13.3)	56	*CCND1*	exon 4	33 cycles: 95°C 1 min, 57°C 1 min, 72°C 1 min; final extension: 72°C 45 min	177 bp	Fw: CCAACAACTTCCTGTCCTACT Rw: CCCAACCTTGTCACCCTT
D9S171 (9p21.3)	71	*CDKN2A/2B*	2.5 Mb downstream	32 cycles: 94°C 1 min, 58°C 1 min, 72°C 50 s; final extension: 72°C 45 min	158–177 bp	Fw: [6FAM]AGCTAAGTGAACCTCATCTCTCTGTCT Rw: ACCCTAGCACTGATGGTATAGTCT
D17S796 (17p13.2)	77	*TP53*	1.3 Mb upstream	30 cycles: 94°C 1 min, 58°C 1 min, 72°C 1 min; final extension: 72°C 45 min	144–174 bp	Fw: [HEX]CAATGGAACCAAATGTGGTC Rw: AGTCCGATAATGCCAGGATG
D17S578 (17p13.1)	69	*TP53*	0.75 Mb upstream	32 cycles: 94°C 1 min, 58°C 1 min, 72°C 1 min; final extension: 72°C 45 min	134–174 bp	Fw: [6FAM]CTATCAATAAGCATTGGCCT Rw: CTGGAGTTGAGACTAGCCT
rs11078663 (17p13.1)	60	*TP53*	0.63 Mb upstream	35 cycles: 94°C 1 min, 58°C 1 min e 30 s, 72°C 1 min; final extension: 72°C 45 min	198 bp	Fw: TGTAGCTCAGGCTCCCA Rw: CCATTCCACTTACCTGAGAGAG
D18S363 (18q21.2)	85	*SMAD4*	0.27 Mb upstream	30 cycles: 94°C 1 min, 56°C 1 min, 72°C 1 min; final extension: 72°C 45 min	177–247 bp	Fw: [6FAM]GAAGATTTGGCTCTGTTGA Rw: TGTCTTACTGCTATAGCTTTCATAA
D18S474 (18q21.2)	82	*SMAD4*	0.08 Mb downstream	35 cycles: 94°C 1 min, 61°C 1 min, 72°C 1 min; final extension: 72°C 45 min	119–139 bp	Fw: [HEX]TGGGGTGTTTACCAGCATC Rw: TGGCTTTCAATGTCAGAAGG

by manual macro-dissection. DNA quantity and quality were assessed with the NanoDrop 1000 spectrophotometer (Thermo Fisher Scientific, Monza, Italy). The cfDNA quality of samples selected at random was further evaluated by means of the Agilent 2100 Bioanalyzer using the High Sensitivity DNA kit (Agilent Technologies, Milan, Italy).

Genetic Analysis

As a marker of LOH, we used the following MSs: D9S171 in chr. 9p21.3, at 2.5 Mb downstream of *CDKN2A/2B*; D17S796 in chr.17p13.2 and D17S578 in chr.17p13.1 at 1.3 and 0.75 Mb upstream of *TP53*, respectively; D18S363 and D18S474 in chr.18q21.2 at 0.27 Mb upstream and 0.08 Mb downstream of *SMAD4*, respectively. The following SNPs were used as markers of allelic imbalance: rs28673064 located in the 5'UTR of *TP63* (chr.3q28), rs9344 in chr.11q13.3 within the exon 4 of *CCND1*, and rs11078663 in 17p13.1 at 0.63 Mb upstream of *TP53* (**Table 1**). These markers were selected based on their good frequency of heterozygosity (informativeness) in the Caucasian population (range 56–85%) and chromosomal position proximate to or within tumor suppressor genes and oncogenes known to be frequently altered in EC (3, 21). A small size of the amplification products was another requirement to successfully amplify cfDNA. Primer sequences, obtained from the UCSC Genome Browser (GRCh38/hg38 Assembly), and PCR conditions are reported in **Table 1**. All selected markers have an appropriate size range to amplify cfDNA fragments, with the exception of rs11078663 and D18S363 that have a suboptimal size (**Table 1**). However, we decided to include also these two markers since they map in regions covered by other more appropriate markers, making us more confident about the results. For PCR amplification, we used 20–30 ng of DNA.

The informativeness of each marker was evaluated in the constitutive DNA, and the analysis was only carried out in the cfDNA of heterozygous individuals. All samples were tested in duplicate to assess data reproducibility. Fragment analysis for the evaluation of LOH events and sequencing analysis for the detection of allelic imbalance were carried out by capillary electrophoresis using the 3730XL DNA analyzer (Life Technologies, Monza, Italy). LOH was calculated by dividing the allele ratio in cfDNA by the allele ratio in germline DNA. Considering the different tumor DNA concentration, LOH positivity was set at $\geq$35% reduction in one allele for cfDNA and at $\geq$40% for FFPE-DNA samples. Since Sanger sequencing is not quantitative, the SNP imbalance was arbitrarily defined as a reduction in the peak of at least 50% compared to the germline reference DNA. The global alterations index was calculated by dividing the number of positive loci by the number of informative loci and was defined as Fractional Alteration (FA) index.

Statistics

Categorical and continuous data were analyzed using Fisher's exact test and Mann-Whitney *U* test, respectively. Pearson's correlation test was applied to calculate the correlation coefficient between cfDNA and FFPE-DNA. All statistical tests were two-sided; a P-value < 0.05 was considered significant.

RESULTS

Clinicopathological Characteristics of Patients

In this study, we analyzed the cfDNA of 52 patients with EC. The cohort included 33 EADC and 19 ESCC patients, 48 males and 4 females, and the median age at diagnosis was 66 years

TABLE 2 | Clinicopathological characteristics of EC patients.

Patients	Total
	N (%)
	52 (100)
Age	
Median (IQR)	66 (57–73)
(Range)	(42–79)
Gender	
Male	48 (92)
Female	4 (8)
Histotype	
EADC	33 (63)
ESCC	19 (37)
TNM	
T	
3	51 (98)
4	1 (2)
N	
0	9 (17)
1+	43 (83)
M	
0	51 (98)
1	1 (2)

IQR, interquartile range; EADC, Esophageal adenocarcinoma; ESCC, Esophageal squamous cell carcinoma.

(**Table 2**). The fraction of tumor DNA present in the total cfDNA is generally considered proportional to tumor burden (22). Thus, to have more favorable conditions to detect cell free tumor DNA, we enrolled only patients with a T3–T4 neoplasia at diagnosis or at restaging after neoadjuvant therapy. The majority of patients (83%) had at least one positive lymph node (**Table 2**). All patients had surgical resection after neoadjuvant chemo-radiotherapy; only one patient underwent surgery directly due to frailty. Four patients were also analyzed longitudinally.

Genetic Alterations Analysis in cfDNA

All cfDNA samples were tested for the presence of tumor-related genetic alterations using as markers a custom panel of 5 MSs and 3 SNPs. The chosen markers map within or near suppressor genes or oncogenes reported to be altered or lost with a high frequency in EC (3, 5). Results showed that, according to our markers and to their fractional alteration (FA) index, EADC patients could be stratified into three subgroups (**Figure 1A**). Group 1 showed a highly altered profile (median FA index 0.40, range 1–0.30), group 2 had an intermediate profile (median FA index 0.20, range 0.29–0.12), while group 3 was characterized by the absence of any alterations in the considered markers (FA index 0). ESCC patients could also be divided into subgroups: one (group 1/2) with a high/intermediate number of alterations (median FA index 0.20, range 0.40–0.14) and another (group 3) with no detectable alterations (FA index 0) (**Figure 1B**). In both histotypes the FA index of each subgroup was statistically different (*P* value ranging from

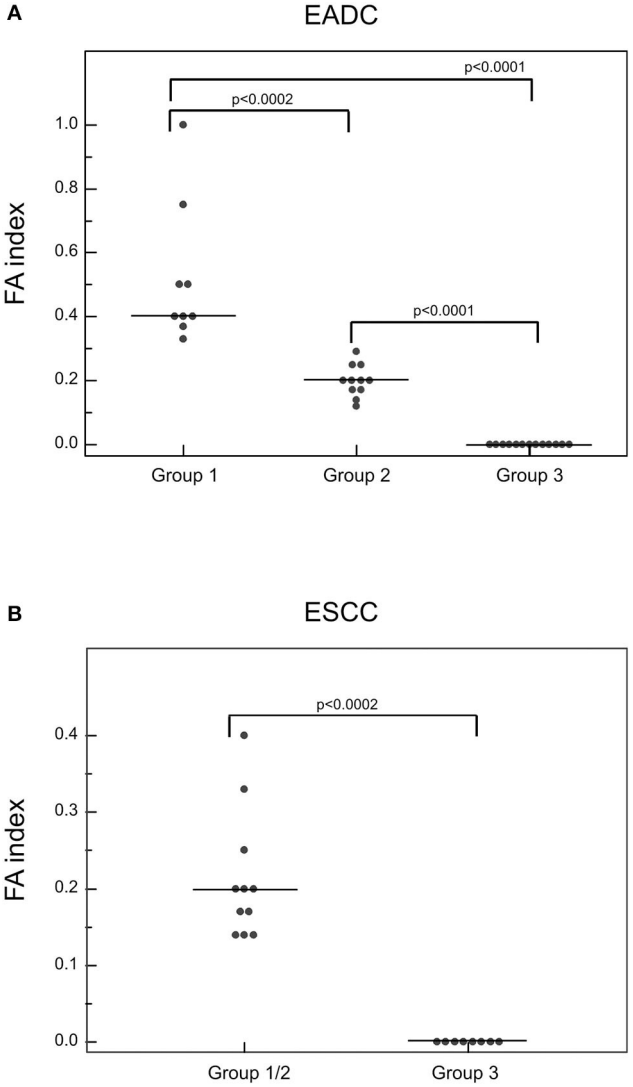

FIGURE 1 | Detection of genetic alterations in cfDNA of EADC **(A)** and ESCC **(B)** patients. The plotted values correspond to the FA index obtained from dividing the number of positive markers by the total number of informative loci. *P*-values were calculated using the Mann-Whitney *U* test. Group 1 represents the highly altered profile group; group 2, the intermediate altered profile group; and group 3, the not altered profile group.

<0.0002 to <0.0001). In order to verify whether the absence of any detectable alteration was due to a low quantity or a bad quality of cfDNA, we performed capillary electrophoretic runs of a few randomly selected marker-negative (group 3) samples; as a control, cfDNA of a few randomly chosen marker-positive (group 1 or 2) samples were included in the runs. The resulting quality and quantity of cfDNA were quite similar between the two groups (**Figure 2**), indicating that the non-detectability of the selected tumor-related alterations was not ascribable to technical problems.

When we considered the alterations in their totality, we found that EADC and ESCC had a comparable number of

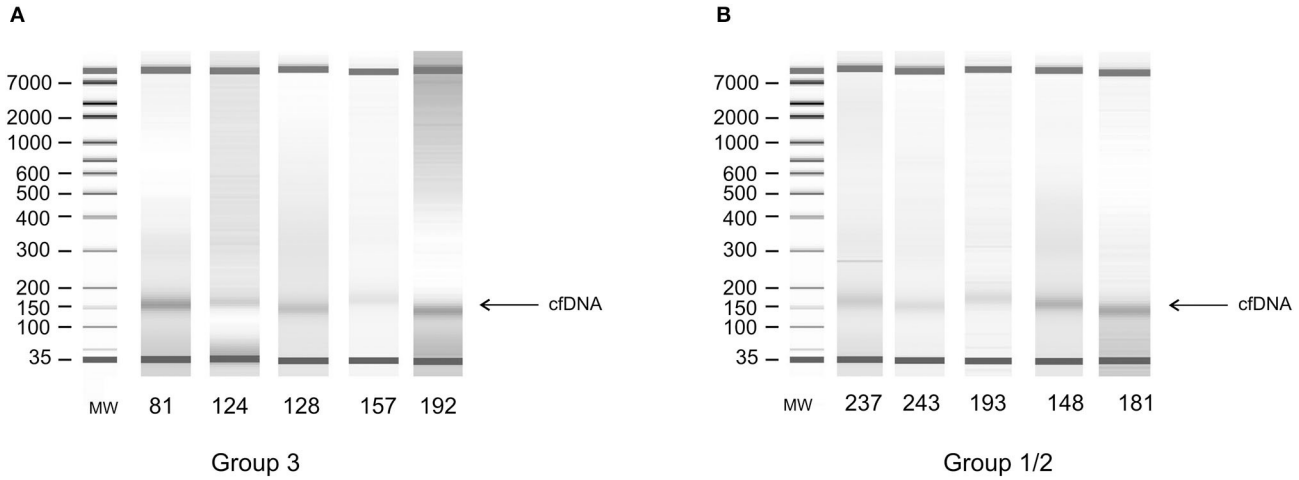

FIGURE 2 | Electrophoretic runs of DNA extracted from plasma. **(A)** Random selected samples from alteration-negative (group 3) cfDNA. **(B)** Random selected samples from alteration-positive (group 1 or 2) cfDNA.

TABLE 3 | Alteration frequencies at single marker or locus level.

		Single marker			Locus*		
Marker ID	**Involved gene**	**EADC**	**ESCC**	***p*-value**	**EADC**	**ESCC**	***p*-value**
rs28673064	*TP63*	12%	10%	1			
rs9344	*CCND1*	19%	13%	1			
D17S796	*TP53*	12%	0%	0.28	48%	47%	1
D17S578		41%	28%	0.50			
rs11078663		22%	38%	0.43			
D9S171	*CDKN2A*	25%	15%	0.68			
D18S363	*SMAD4*	15%	0%	0.13	26%	0%	0.018
D18S474		19%	0%	0.14			

**When determining alterations at a locus mapped by more than one marker, an alteration was considered present if it appeared in at least one of the markers; only one alteration per locus has been counted.*

alterations (median FA index: 0.17 vs. 0.14). The locus of tumor suppressor *TP53* was the most altered in both EC histotypes (48% in EADC vs. 47% in ESCC; **Table 3**), although MS D17S796, the most distal to *TP53*, was not altered in ESCC. Similar frequencies of imbalance were also observed for the markers mapping *TP63* (12 vs. 10%) and *CCND1* (19 vs. 13%), while losses at the *CDKN2A/B* locus were higher in EADCs (25 vs. 15%), although not statistically relevant ($P = 0.68$). On the contrary, LOH at the *SMAD4* locus was a peculiarity of EADCs. Indeed, considering D18S363 and D18S474, located, respectively, upstream and downstream of *SMAD4*, we found a LOH frequency of 26% in EADC vs. 0% in ESCC samples ($P = 0.018$) (**Table 3**).

Analysis of Concordance Between cfDNA and Tumor DNA

To verify whether the alterations detected in cfDNA were representative of those present in tumor tissue, we analyzed tumor DNA isolated from 17 time-matched EADC FFPE specimens. Considering all the markers together, we found that the average of the overall concordance between tumor DNA and cfDNA was 68% with a 32% discrepancy divided into 19% positivity only in tumor DNA and 13% only in cfDNA (**Figure 3A**). The concordance was quite variable from individual to individual with three patients having a 100% concordance; four, a concordance $\geq$80%; five, a concordance $>$50%; and the remaining five patients, a concordance ranging from 50 to 33% (**Figure 3B**). When we estimated the concordance at the level of individual markers, we observed that, among the eight analyzed markers, some had a better match than others. As reported in **Figure 3C**, rs28673064 (*TP63*), rs9344 (*CCND1*), and rs11078663 (*TP53*) exhibited an individual concordance $>$70%. MS D18S474 (*SMAD4*) was even better, showing a concordance of 93% with a few discrepant samples being positive only in cfDNA. This last result might reflect the capability of cfDNA to better represent tumor heterogeneity rather than a false outcome. Altogether, the eight markers exhibited a 0.84 correlation coefficient with a significance of $P = 0.009$ (**Figure 3D**).

Analysis of Longitudinal Cases

cfDNA analysis, among its many potentialities, has been indicated as a possible method for tumor detection in patients without clinical evidence of the disease (15, 16). Thus, we studied a few EC patients longitudinally to see whether the search for tumor markers in cfDNA could be useful for monitoring the patients during their therapeutic journey. Here, we reported data regarding four representative patients.

Patient 157. Figure 4A The patient presented an adenocarcinoma (cT3N2M0) at diagnosis. Both cfDNA and FFPE-DNA resulted negative for our genetic markers as well as the cfDNA obtained at surgery. However, 3 months after resection, although no clinical signs of recurrence were

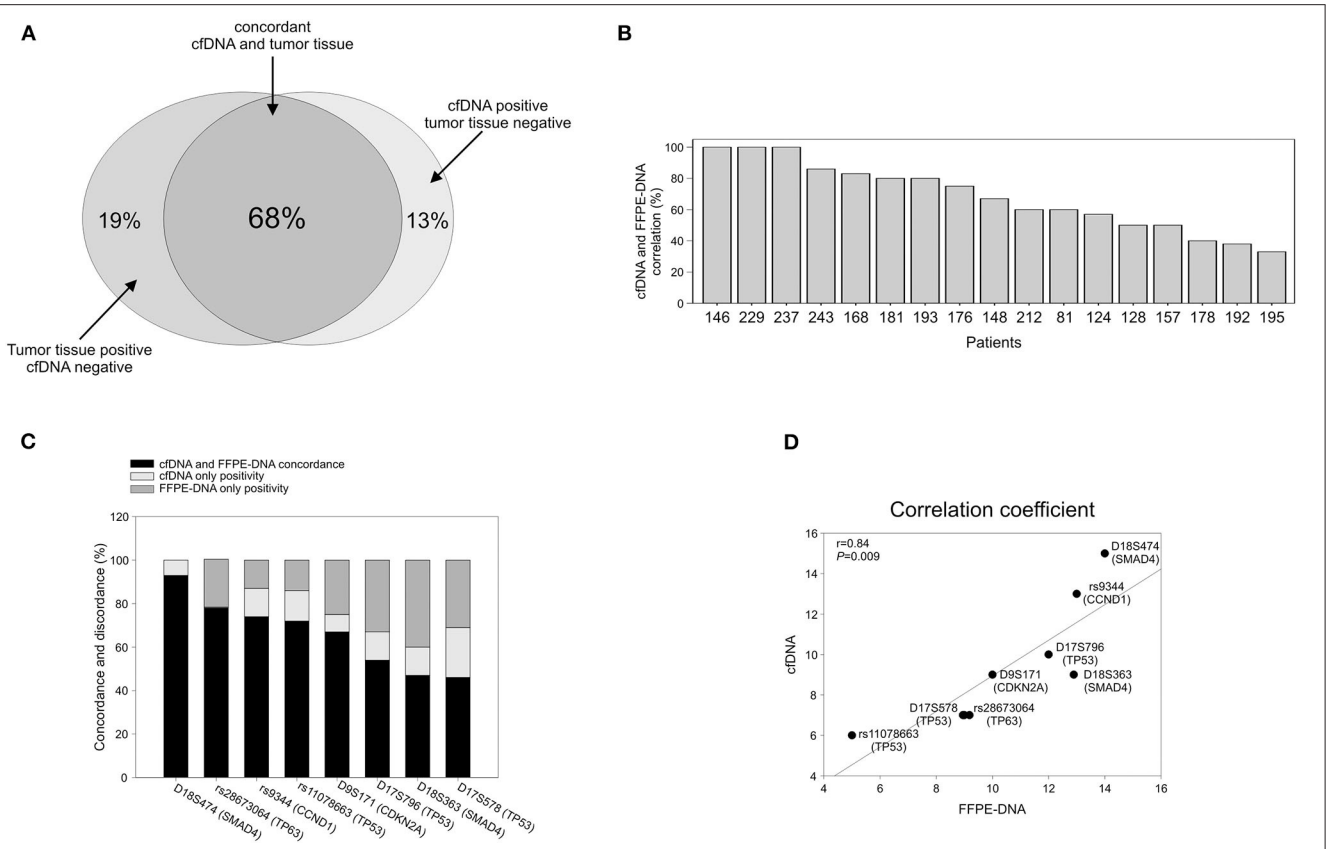

FIGURE 3 | Correlation between cfDNA and time-matched tumor DNA. **(A)** Global concordance. **(B)** Concordance at the single patient level. **(C)** Concordance at the single marker level. **(D)** Graphic representation of the Pearson's correlation coefficient.

present and the tumor soluble markers S-CEA and S-Ca 19.9 remained below the threshold of positivity, the FA index became highly positive (0.33). At the next follow-up, 3 months later, the FA index increased further (0.50); at this time, a suspicion of a lung nodule was advanced. However, the lump was not confirmed at radiological examination 3 months later; soluble tumor markers continued to be negative. One year later, the patient presented pleural effusion and the lung metastasis was confirmed. S-CEA and S-Ca 19.9 were still negative.

Patient 95. Figure 4B Blood samples were collected at the diagnosis of adenocarcinoma (T3N1M0) at restaging after neoadjuvant treatment and at 6 months after surgery. At the time of diagnosis, it was possible to detect tumor-related alterations in the cfDNA sample (FA index: 0.17), and the tumor soluble markers S-CEA and S-Ca 19.9 were highly positive. After neoadjuvant therapy, S-CEA and S-Ca 19.9 dropped but remained above the threshold of positivity; on the contrary, FA index did not change. Surgical resection was not curative and a cycle of adjuvant therapy was scheduled. The tumor did not respond to treatment and progressed; FA index doubled and reached the value of 0.33.

Patient 229. Figure 4C At the diagnosis of adenocarcinoma (T3N0M0), genetic alterations were found in cfDNA (FA index 0.37), but not in the time-matched FFPE-DNA; the patient was also positive for soluble tumor markers. Because of the poor state of general health, the patient underwent surgery without neoadjuvant therapy. Interestingly, the DNA isolated from the FFPE surgical specimen resulted positive for alterations with a 75% concordance with the alterations found in cfDNA collected at diagnosis. At follow-up performed 3 months after surgery, the patient did not present clinical signs of relapse; S-CEA became negative; and S-Ca 19.9, although still positive, was far below the initial value. On the contrary, the FA index remained high after tumor resection. Four months later, the patient presented cutaneous metastasis.

Patient 125. Figure 4D At diagnosis of squamous cell carcinoma (T3N1M0), the patient was negative for the tumor soluble markers S-CEA and S-Ca 19.9. By contrast, genetic alterations were detected in cfDNA (FA index 0.17). The patient had a complete response to neoadjuvant therapy (ypTisN0M0). At surgery, cfDNA resulted negative for the presence of tumor-related alterations and remained negative 5 months later. The patient did not show clinical signs of relapse during a 30-month follow-up.

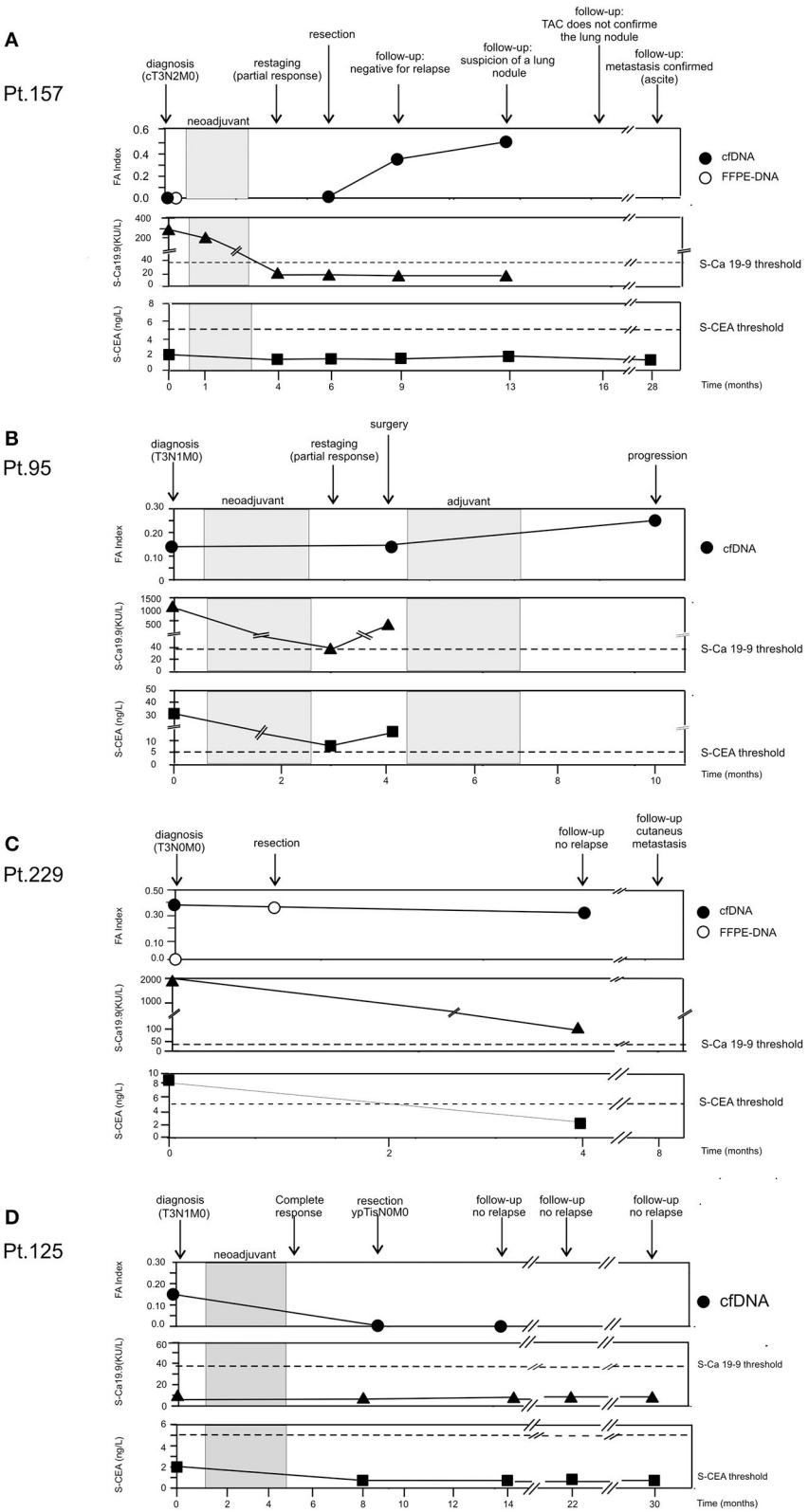

FIGURE 4 | Longitudinal analysis. cfDNA was isolated from serial plasma. CEA and Ca 19.9 values were obtained from patient's clinical record. **(A)** Patient 157. **(B)** Patient 95. **(C)** Patient 229. **(D)** Patient 125.

DISCUSSION

EC is a highly aggressive tumor of which the survival rate remains low despite the application of multimodal therapeutic protocols (23). In addition, current monitoring procedures sometimes do not adequately account for the efficacy of treatments or the risk of relapse. For this reason, we investigated whether liquid biopsy could be used, alongside current methods, for the monitoring of locally advanced EC patients.

ECs are characterized by high mutational frequencies and recurrent losses/gains of tumor suppressor genes or oncogenes. Using a panel of 5 MSs and 3 SNPs that map near loci highly altered in EC (3, 5, 21), we were able to find tumor-related alterations in cfDNA of EC patients and follow the disease longitudinally.

No statistical differences were observed between EADC and ESCC when the alterations were globally considered. Also, at the level of a single genetic marker, the frequency of alterations was quite similar, and in line with the genetic alteration landscape of EC, we observed a high proportion of deletions at the *TP53* locus in both histotypes. Interestingly, ESCCs did not have LOH at the MS most distal to *TP53* (D17S796), suggesting that the LOH event at the *TP53* locus is probably wider in EADC.

In line with the literature data (3, 24, 25), EADC exhibited loss of the *SMAD4* locus with a good frequency; this event was peculiar to EADC since ESCC did not exhibit any loss at this locus ($P = 0.018$). In addition, the frequency of *TP63* and *CCND1* loci in EADC were similar to previous reported data (12 vs. 11% for *TP63* and 19 vs. 15% for *CCND1*) (3). On the contrary, the frequency of these loci was lower than expected in ESCC samples. This discrepancy might be due to the small number of informative samples for these markers in ESCC cohort.

Moreover, not all the studied patients exhibited alterations in at least one of the eight chosen markers. Indeed, almost 1/3 did not show any change, although the quality and quantity of their cfDNA were comparable to those of positive samples. These data are in line with the 64–70% mutation positivity in driver genes found using next-generation sequencing (NGS) in larger cohorts of lung cancer patients (26, 27). In our cohort, this negativity was also observed in a few time-matched tumor DNA (i.e., Pt. 157; **Figure 4A** and data not shown), suggesting that these samples are most likely characterized by other genetic events. Despite the limited number of analyzed cases, these findings suggest that both EADC and ESCC can be stratified into subgroups that differ in the number and, perhaps, in the type of alterations. No correlation between the FA index and tumor progression was observed, indicating that alterations at the analyzed markers or their number are not linked to a more aggressive disease. Nonetheless, the recognition of subgroups that differ for the number of molecular alterations could be relevant for therapy stratification of EC patients. Indeed, patients with a high FA index could be putatively eligible for an immunotherapeutic approach.

When we compared the alterations detectable in cfDNA and those present in the time-matched tumor DNA, we found a global correlation of 68% with, among the discordant samples, 13% alteration-positive only in the cfDNA. This finding could be ascribable to the hypothesized greater representativeness of cfDNA of tumor heterogeneity with respect to a single tissue biopsy (16, 28, 29). This hypothesis is also sustained by the results obtained in Pt. 229 (**Figure 4C**). Indeed, while the cfDNA obtained at diagnosis and the matched tissue biopsy-DNA were discordant (i.e., alterations vs. no alterations, respectively), the tumor DNA obtained from the specimen at surgery had 75% concordance with the cfDNA gathered at diagnosis.

Data from longitudinal cases indicate that cfDNA analysis can be useful to follow EC patient response to neoadjuvant treatment or to determine whether surgical resection was curative. In some cases, the resulting FA index was more reliable than traditional soluble tumor markers such as S-CEA and S-Ca 19.9 to indicate tumor progression. Indeed, tumors that were also positive for S-CEA or S-Ca 19.9 at diagnosis sometimes did not retain their positivity during progression. On the contrary, FA index never became negative during progression.

The limitations of this study are its retrospective nature and the relatively low number of patients enrolled, which renders it an exploratory and hypothesis-driven study that needs further prospective confirmatory trials. Nevertheless, our work is in line with previous studies that, using next-generation sequencing technology (NGS), highlighted the relevance of cfDNA analysis to follow EC patient behavior (30–32). The Kato et al. (30) and Maron et al. (32) studies have cohorts that include mainly gastric and junction adenocarcinomas. More similar to our study is the paper of Azad et al. (31), which includes a cohort of 45 EADC and ESCC patients. This data concordance highlights our findings and technical approach.

Thus, despite its limitations, our study indicates the validity of our approach that is easy to perform and economically sustainable. Furthermore, we confirmed the capacity of liquid biopsy to assess response to neoadjuvant therapy and to detect a putative residual disease before instrumental examination, as suggested by longitudinal studies. Although further confirmatory studies are required, we believe that in the near future, liquid biopsy could be used alongside the current EC patient monitoring strategies to guide and improve patient management.

DATA AVAILABILITY STATEMENT

The raw data will be made available upon motivated request.

ETHICS STATEMENT

The studies involving human participants were reviewed and approved by Comitato Etico per la Sperimentazione Clinica (CESC) of the Veneto Institute of Oncology. The

patients/participants provided their written informed consent to participate in this study.

AUTHOR CONTRIBUTIONS

EB, MC, and DS: conception and design, analysis and data collection, interpretation of data, and manuscript preparation. MF, MR, SR, and RA: sample collection. EB, MC, DS, MF, and AA: critical revision of manuscript. AA: funding acquisition. All authors contributed to the article and approved the submitted version.

FUNDING

This work was supported by grant from Associazione Italiana per la Ricerca sul Cancro (AIRC) (IG2013-14032) and Institutional funding from the Veneto Institute of Oncology IOV-IRCCS.

ACKNOWLEDGMENTS

We are grateful to the patients for their participation and collaboration.

REFERENCES

1. Smyth EC, Lagergren J, Fitzgerald RC, Lordick F, Shah MA, Lagergren P, et al. Oesophageal cancer. *Nat Rev Dis Primers.* (2017) 3:17048. doi: 10.1038/nrdp.2017.48
2. Krug S, Michl P. Esophageal cancer: new insights into a heterogenous disease. *Digestion.* (2017) 95:253–61. doi: 10.1159/000464130
3. Cancer Genome Atlas Research Network, Analysis Working Group: Asan University, BC Cancer Agency, Brigham and Women's Hospital, Broad Institute; Brown University, Case Western Reserve University, et al. Integrated genomic characterization of oesophageal carcinoma. *Nature.* (2017) 541:169–75. doi: 10.1038/nature20805
4. Peyser ND, Grandis JR. Cancer genomics: spot the difference. *Nature.* (2017) 541:162–3. doi: 10.1038/nature21112
5. Agrawal N, Jiao Y, Bettegowda C, Hutfless SM, Wang Y, David S, et al. Comparative genomic analysis of esophageal adenocarcinoma and squamous cell carcinoma. *Cancer Discov.* (2012) 2:899–905. doi: 10.1158/2159-8290.CD-12-0189
6. Abdo J, Agrawal DK, Mittal SK. "Targeted" chemotherapy for esophageal cancer. *Front Oncol.* (2017) 7:63. doi: 10.3389/fonc.2017.00063
7. Abdo J, Agrawal DK, Mittal SK. Basis for molecular diagnostics and immunotherapy for esophageal cancer. *Exp Rev Anticancer Ther.* (2017) 17:33–45. doi: 10.1080/14737140.2017.1260449
8. Lyons T, Ku GY. Systemic therapy for esophagogastric cancer: immune checkpoint inhibition. *Chin Clin Oncol.* (2017) 6:53. doi: 10.21037/cco.2017.09.03
9. Young K, Chau I. Targeted therapies for advanced oesophagogastric cancer: recent progress and future directions. *Drugs.* (2016) 76:13–26. doi: 10.1007/s40265-015-0510-y
10. van den Ende T, Smyth E, Hulshof MCCM, van Laarhoven HWM. Chemotherapy and novel targeted therapies for operable esophageal and gastroesophageal junctional cancer. *Best Pract Res Clin Gastroenterol.* (2018) 36–37:45–52. doi: 10.1016/j.bpg.2018.11.005
11. van Hagen P, Hulshof MC, van Lanschot JJ, Steyerberg EW, van Berge Henegouwen MI, Wijnhoven BP. Preoperative chemoradiotherapy for esophageal or junctional cancer. *N Engl J Med.* (2012) 366:2074–84. doi: 10.1056/NEJMoa1112088
12. Deng J, Wang C, Xiang M, Liu F, Liu Y, Zhao K. Meta-analysis of postoperative efficacy in patients receiving chemoradiotherapy followed by surgery for resectable esophageal carcinoma. *Diagn Pathol.* (2014) 9:151. doi: 10.1186/1746-1596-9-151
13. Atay SM, Blum M, Sepesi B. Adjuvant chemotherapy following trimodality therapy for esophageal carcinoma-Is the evidence sufficient? *J Thorac Dis.* (2017) 9:3626–9. doi: 10.21037/jtd.2017.09.68
14. Saeed NA, Mellon EA, Meredith KL, Hoffe SE, Shridhar R, Frakes J, et al. Adjuvant chemotherapy and outcomes in esophageal carcinoma. *J Gastrointest Oncol.* (2017) 8:816–24. doi: 10.21037/jgo.2017.07.10
15. Pantel K, Alix-Panabières C. Liquid biopsy and minimal residual disease - latest advances and implications for cure. *Nat Rev Clin Oncol.* (2019) 16:409–24. doi: 10.1038/s41571-019-0187-3
16. Corcoran RB, Chabner BA. Application of cell-free DNA analysis to cancer treatment. *N Engl J Med.* (2018) 379:1754–65. doi: 10.1056/NEJMra1706174
17. Bettegowda C, Sausen M, Leary RJ, Kinde I, Wang Y, Agrawal N, et al. Detection of circulating tumor DNA in early- and late-stage human malignancies. *Sci Transl Med.* (2014) 6:224ra24. doi: 10.1126/scitranslmed.3007094
18. Siravegna G, Marsoni S, Siena S, Bardelli A. Integrating liquid biopsies into the management of cancer. *Nat Rev Clin Oncol.* (2017) 14:531–48. doi: 10.1038/nrclinonc.2017.14
19. Volckmar AL, Sültmann H, Riediger A, Fioretos T, Schirmacher P, Endris V, et al. A field guide for cancer diagnostics using cell-free DNA: from principles to practice and clinical applications. *Genes Chromosomes Cancer.* (2018) 57:123–39. doi: 10.1002/gcc.22517
20. Ryland GL, Doyle MA, Goode D, Boyle SE, Choong DY, Rowley SM, et al. Loss of heterozygosity: what is it good for? *BMC Med Genomics.* (2015) 8:45. doi: 10.1186/s12920-015-0123-z
21. Rumiato E, Boldrin E, Malacrida S, Realdon S, Fassan M, Morbin T et al. Detection of genetic alterations in cfDNA as a possible strategy to monitor the neoplastic progression of Barrett's esophagus. *Transl Res.* (2017) 190:16–24.e1. doi: 10.1016/j.trsl.2017.09.004
22. Diaz LA, Bardelli A. Liquid biopsies: genotyping circulating tumor DNA. *J Clin Oncol.* (2014) 32:579–86. doi: 10.1200/JCO.2012.45.2011
23. Sohda M, Kuwano H. Current status and future prospects for esophageal cancer treatment. *Ann Thorac Cardiovasc Surg.* (2017) 23:1–11. doi: 10.5761/atcs.ra.16-00162
24. Weaver JMJ, Ross-Innes CS, Shannon N, Lynch AG, Forshew T, Barbera M, et al. Ordering of mutations in preinvasive disease stages of esophageal carcinogenesis. *Nat Genet.* (2014) 46:837–43. doi: 10.1038/ng.3013
25. Gregson EM, Bornschein J, Fitzgerald RC. Genetic progression of Barrett's oesophagus to oesophageal adenocarcinoma. *Br J Cancer.* (2016) 115:403–10. doi: 10.1038/bjc.2016.219
26. Sabari JK, Offin M, Stephens D, Ni A, Lee A, Pavlakis N, et al. A prospective study of circulating tumor DNA to guide matched targeted therapy in lung cancers. *J Natl Cancer Inst.* (2018) 111:575–83. doi: 10.1093/jnci/djy156
27. Li BT, Janku F, Jung B, Hou C, Madwani K, Alden R, et al. Ultra-deep next-generation sequencing of plasma cell-free DNA in patients with advanced lung cancers: results from the Actionable Genome Consortium. *Ann Oncol.* (2019) 30:597–603. doi: 10.1093/annonc/mdz046
28. Gao J, Wang H, Zang W, Li B, Rao G, Li L, et al. Circulating tumor DNA functions as an alternative for tissue to overcome tumor heterogeneity in advanced gastric cancer. *Cancer Sci.* (2017) 108:1881–7. doi: 10.1111/cas.13314
29. Bardelli A, Pantel K. Liquid biopsies, what we do not know (yet). *Cancer Cell.* (2017) 31:172–9. doi: 10.1016/j.ccell.2017.01.002
30. Kato S, Okamura R, Baumgartner JM, Patel H, Leichman L, Kelly K, et al. Analysis of circulating tumor DNA and clinical correlates in patients with esophageal, gastroesophageal junction, and gastric adenocarcinoma.

Clin Cancer Res. (2018) 24:6248–56. doi: 10.1158/1078-0432.CCR-18-1128

31. Azad TD, Chaudhuri AA, Fang P, Qiao Y, Esfahani MS, Chabon JJ, et al. Circulating tumor DNA analysis for detection of minimal residual disease after chemoradiotherapy for localized esophageal cancer. *Gastroenterology*. (2020) 158:494–505.e6. doi: 10.1053/j.gastro.2019.10.039
32. Maron SB, Chase LM, Lomnicki S, Kochanny S, Moore KL, Joshi SS, et al. Circulating tumor DNA sequencing analysis of gastroesophageal adenocarcinoma. *Clin Cancer Res.* (2019) 25:7098–112. doi: 10.1158/1078-0432.CCR-19-1704

Conflict of Interest: The authors declare that the research was conducted in the absence of any commercial or financial relationships that could be construed as a potential conflict of interest.

frontiers in Oncology

ORIGINAL RESEARCH
published: 03 September 2020
doi: 10.3389/fonc.2020.01658

Circulating Tumor Cells Expressing the Prostate Specific Membrane Antigen (PSMA) Indicate Worse Outcome in Primary, Non-Metastatic Triple-Negative Breast Cancer

Sabine Kasimir-Bauer[1]†, Corinna Keup[1†], Oliver Hoffmann[1], Siegfried Hauch[2], Rainer Kimmig[1] and Ann-Kathrin Bittner[1]*

[1] Department of Gynecology and Obstetrics, University Hospital of Essen, Essen, Germany, [2] QIAGEN GmbH, Hilden, Germany

OPEN ACCESS

Edited by:
Rui P. L. Neves,
University Hospital
Düsseldorf, Germany

Reviewed by:
Carrie D. House,
San Diego State University,
United States
Michal Mego,
Campus Bio-Medico University, Italy
Vassilis Georgoulias,
University of Crete, Greece

***Correspondence:**
Sabine Kasimir-Bauer
sabine.kasimir-bauer@uk-essen.de

[†] These authors have contributed equally to this work

Specialty section:
This article was submitted to Cancer Molecular Targets and Therapeutics, a section of the journal Frontiers in Oncology

Received: 20 May 2020
Accepted: 28 July 2020
Published: 03 September 2020

Citation:
Kasimir-Bauer S, Keup C, Hoffmann O, Hauch S, Kimmig R and Bittner A-K (2020) Circulating Tumor Cells Expressing the Prostate Specific Membrane Antigen (PSMA) Indicate Worse Outcome in Primary, Non-Metastatic Triple-Negative Breast Cancer. Front. Oncol. 10:1658. doi: 10.3389/fonc.2020.01658

Background: We analyzed mRNA profiles of prostate cancer related genes in circulating tumor cells (CTCs) of primary, non-metastatic triple-negative breast cancer (TNBC) patients (pts) before and after neoadjuvant chemotherapy to elucidate the potential of prostate cancer targets in this BC subgroup.

Method: Blood from 41 TNBC pts ($n = 41$ before / 26 after therapy) was analyzed for CTCs applying the AdnaTest EMT-2/Stem Cell Select. Multimarker RT-qPCR allowed the detection of the prostate specific antigen *PSA*, the prostate specific membrane antigen *PSMA*, full-length androgen receptor (*AR-FL*), and AR splice-variant seven (*AR-V7*).

Results: Before therapy, at least one prostate cancer related gene was detected in 15/41 pts (37%). Notably, in 73% of *AR-FL* positive cases, *AR-V7* was co-expressed. After therapy, CTCs of only one patient harbored prostate cancer related genes. *AR-V7*+ and *PSMA*+ CTCs significantly correlated with early relapse ($p = 0.041$; $p = 0.00039$) whereas *PSMA*+ CTCs also associated with a reduced OS ($p = 0.0059$). This correlation was confirmed for *PSMA*+ CTCs in univariate (PFS $p = 0.002$; OS $p = 0.015$), but not multivariate analysis.

Conclusion: Although CTCs that expressed prostate cancer related genes were eliminated by the given therapy, *PSMA*+ CTCs significantly identified pts at high risk for relapse. Furthermore, AR inhibition, often discussed for this BC subgroup, might not be successful in the primary setting of the disease since we identified *AR-FL*+ CTCs together with *AR-V7*+ CTCs, associated with therapeutic failure.

Keywords: triple-negative breast cancer, circulating tumor cells, PSMA, androgen receptor, androgen receptor splice variant seven

INTRODUCTION

Triple-negative breast cancer (TNBC), accounting for 15–20% of all breast cancers (BC), has an destructive behavior which is associated with poor prognosis (1, 2). Neoadjuvant chemotherapy (NACT) is the standard of care (3, 4) and combination therapy containing carboplatin improved the pathological complete response (pCR) rate (5), as well as progression free survival (PFS) and overall survival (OS) in some clinical trials (6, 7). However, treatment options are limited since TNBC remains a biologically variable disease with different subtypes defined and thus, a target or signal transduction pathway for therapy is difficult to identify (8). Currently, immunotherapy is under investigation in this patient subset and has already shown a significantly improved pCR adding the checkpoint inhibitor anti-PD-1, pembrolizumab, to NACT in early TNBC with a trend seen for a prolonged event free survival (9).

Looking for new predictive biomarkers, prostate cancer related markers have been evaluated in TNBC for additional treatment options. In this context, based on findings in prostate cancer (PCA), the prostate specific membrane antigen (PSMA) has become an attractive molecular target for oncological imaging and radionuclide therapy using PSMA PET/CT in TNBC (10, 11). In addition, among the different subtypes defined (12), the luminal androgen receptor (LAR) subtype was found to be enriched in mRNA expression of androgen receptor (AR) and several downstream AR targets, resulting in enhanced sensitivity to the AR antagonist bicalutamide (13) which qualifies AR as a suitable target in LAR TNBC. In this context, ongoing clinical trials are testing the effectiveness of other AR inhibitors in TNBC, including abiraterone and enzalutamide, commonly prescribed in PCA (14–17). AR, overexpressed in 10–35% of TNBC, shows some similarities with the hormonal-receptors (HR) estrogen- (ER) and progesterone- (PR) receptor. AR is a member of the steroid-hormone-receptor family and functions after activation by binding of androgens as nuclear transcription factor. Similar to observations in ER-positive (+) BC, its expression has been associated with improved PFS and OS (8, 18, 19). In another retrospective trial, low AR expression was correlated with higher risk of distant metastasis, whereas high AR expression was correlated with prolonged survival. In addition, AR status was an independent predictor for better outcome regardless of tumor size, grade, and nodal stage (20). Further studies revealed that AR+ tumors were associated with small tumor size, lower histologic grade and stage (21). Interestingly, in the prospective German GeparTrio trial, pCR in TNBC after NACT was lower in AR+ compared with AR-negative disease. However, in accordance with other studies, AR+ tumors had a significant better PFS and OS as compared to tumors not expressing AR in the intention to treat population but stratified by subgroups these findings could only be shown for the TNBC patients. AR positivity selected a group with significant better PFS and OS in the non-pCR group, however, no difference with regard to AR expression was shown for the pCR group (22). In contrast, some other studies could not confirm these observations and have shown either no difference or worse outcomes for AR-positive (+) vs. AR-negative disease (23–27).

Comparable with data for HR, concordance of AR expression status between primary BC tissue and metastatic lesions was shown to be 15–35% (28). Consequently, AR expression on tissue samples might not be appropriate to select BC patients for AR-targeting drugs.

Therefore, a few metastatic BC studies have analyzed AR expression on circulating tumor cells (CTCs) in blood as a minimal invasive approach to assess the real time AR status (29–33). Most of these studies were performed in HR+/HER2- BC, but AR+ CTCs could be detected in 13% of metastatic TNBC cases applying mRNA expression profiling for CellSearch enriched CTCs (32) and in 91% of metastatic TNBC cases using the Maintrac Assay (30). Performing comprehensive molecular CTC characterization in early TNBC patients after immunomagnetic CTC-selection, we recently demonstrated that TNBC-derived CTCs appeared to upregulate most of the analyzed 17 transcripts or kept their expression frequency on a high level after therapy except for *AR* which was detected in 33% of the patients before but rarely after therapy (34). However, several studies on AR expression in patients with castration-resistant PCA demonstrated that not the AR full length (*AR-FL*) wildtype itself but AR splice variants, and in particular AR variant seven (*AR-V7*), have been linked to resistance toward anti-AR drugs like enzalutamide and abiraterone (35). In this context, *AR-V7*+ CTCs before AR blockade correlated with decreased PFS, decreased time on therapy and shorter OS as compared to patients without *AR-V7*+ CTCs (36, 37). In BC, the *AR-V7* variant was shown to be commonly expressed in primary BC tumor tissue and BC cancer cell lines, providing evidence to promote growth and mediate resistance to AR inhibitory treatment (38).

Based on the current findings, the complex interplay of AR and the prostate specific antigen (PSA) and PSMA (39) and the growing interest of the application of AR-targeted therapies in TNBC, we here analyzed mRNA profiles of CTCs for the expression of *AR-FL*, *AR-V7*, *PSA*, and *PSMA* in blood samples of 41 TNBC patients before and 26 TNBC patients after therapy to elucidate their prognostic value and their potential as therapeutic targets.

Abbreviations: AR, androgen receptor; AR-FL, AR-full length; HGNC ID:644; AR-V7, androgen receptor variant seven; BC, breast cancer; CTCs, circulating tumor cells; ER, estrogen receptor; HR, hormonal receptors; LAR, luminal androgen receptor; NACT, neoadjuvant chemotherapy; OS, overall survival; PCA, prostate cancer; pCR, pathological complete response; PFS, progression free survival; pPR, pathological partial response; PR, progesterone receptor; PSA, prostate specific antigen; HGNC: KLK3, ID:6364; PSMA, prostate specific membrane antigen; HGNC: FOLH1; ID:3788; pts, patients; TNBC, triple-negative breast cancer.

RESULTS

Clinical Characteristics

The clinical characteristics of all patients evaluated before and after therapy are shown in **Table 1**. More than 50% of the patients were postmenopausal, the predominant histological subtype was ductal carcinoma and most of the patients had an aggressive

tumor biology with a grade 3 tumor. The majority of the patients showed a Ki67 above 30% and presented with T1 and T2 tumors. At the time of primary diagnosis, two third of the patients were node-negative and except for two patients, all patients received NACT. The therapeutic regimens are shown in **Table S1**. Overall, response to therapy resulted in a ratio of 92% (46% pCR, 46% pPR) of responders and 8% of non-responders.

Gene Expression Profiles in CTCs Before and After Therapy

In total, 41 primary, non-metastatic TNBC patients were analyzed for CTCs. Matched samples of these 41 patients were available after therapy in 26 cases resulting in 26 paired samples (before and after therapy). Using immunomagnetic selection *via* EpCAM, HER2, and EGFR, a patient was defined as CTC+ if overexpression of one of the four prostate cancer related genes was detected. Before therapy, at least one prostate cancer related gene was detected in 15/41 pts (37%). The expression of *AR-FL* was documented in 11/41 patients (27%), *AR-V7* in 8/41 patients (20%), *PSMA* in 6/41 patients (15%), and *PSA* in 5/41 patients (12%), respectively. Notably, as apparent from **Figure 1B**, in 8/11 patients (73%) of *AR-FL*+ cases before therapy, *AR-V7* was co-expressed. In 26 of the in total 41 patients analyzed before therapy, we were able to perform CTC analysis also after therapy. In only one of these 26 patients after therapy, we found CTCs with an overexpression of prostate cancer related genes (*AR-FL*, *AR-V7*, and *PSMA*, **Figure 1A**). In addition, this patient showed a persistence of *AR-FL* and *AR-V7* expressing CTCs and the presence of *PSMA*+ CTCs after therapy. In all the other 25/26 patients analyzed after therapy, no CTCs expressing prostate cancer related genes were detected.

Before therapy, *PSMA*+ CTCs were more often found in patients experiencing no pCR, as compared to those achieving one. Although these findings were not significant (two-tailed Fishers exact test: $p = 0.19$; **Figure S2**), the only patient harboring *PSMA*+ CTCs before therapy and achieving a pCR was the only patient in the pCR subgroup who deceased within the follow-up time.

Survival Analysis

Thirteen relapses were documented after a median follow-up time of 16 months (range: 3–34 months). 8/41 (20%) of the patients died, eight of them BC specific, after a median survival time of 25 months (range: 3–38 months).

PSMA+ CTCs (**Figure 2A**) and *AR-V7*+ CTCs (**Figure 2C**) before therapy significantly correlated with early relapse ($p = 0.00039$; $p = 0.041$). *PSMA*+ CTCs (**Figure 2B**) also associated with a reduced OS ($p = 0.0059$) while *AR-V7*+ CTCs (**Figure 2D**) reached borderline significance ($p = 0.051$). While half of the pts showing *PSMA*+ CTCs relapsed within 19 months after first diagnosis, more than half of the pts with *PSMA*- CTCs did not experience a relapse within the period of follow-up (**Figure 2A**).

Figures 3A,B as well as **Table S3** are showing survival analysis using Cox univariate and multivariate proportional

TABLE 1 | Patient characteristics.

	Total (% of all applicable)
Total	41
Median Age (IQR) at diagnosis [years]	52 (15)
<50 years old	17/41 (41)
≥50 years old	24/41 (59)
Menopausal Status	
Premenopausal	8/41(20)
Perimenopausal	8/41 (20)
Postmenopausal	25/41 (60)
Histology	
Ductal	30/39 (77)
Lobular	1/39 (3)
Others	8/39 (20)
Not known	2/41
Tumor Grading	
I	0/41 (0)
II	11/41 (27)
III	30/41 (73)
Not known	0/41
Ki 67	
0–10%	2/37 (5)
11–30%	4/37 (11)
>30%	31/37 (84)
Not known	4/41
Tumor Size at First Diagnosis (c/T)	
T1a-c	16/41 (39)
T2	22/41 (54)
T3	3/41 (7)
T4	0/41 (0)
Tumor Size After NACT (ypT)	
ypT0	17/39 (44)
ypT1	12/39 (31)
ypT2	9/39 (23)
ypT3-4	1/39 (3)
Not applicable	2/41
Nodal Status at First Diagnosis (c/pN)	
Node negative	27/41 (66)
Node positive	13/41 (32)
N1	10/41 (24)
N2	1/41 (2)
N3	3/41 (7)
Nodal Status After NACT (ypN)	
Node negative	2/3 (66)
Node positive	1/3 (33)
ypN1	0/3 (0)
ypN2	1/3 (33)
ypN3	0/3 (0)
Not applicable	38/41
Pathological Response	
Complete response	18/39 (46)
Partial response	18/39 (46)
No response	3/39 (8)
Not applicable	2/41
Chemotherapy	
Yes	41/41 (100)
Neoadjuvant	39/41 (95)
Adjuvant	2/41 (5)

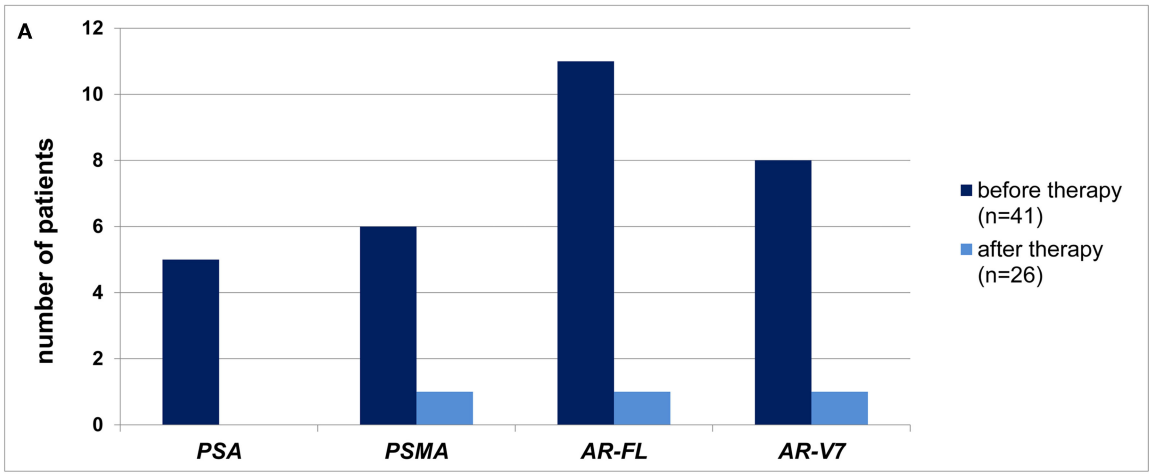

[n]	PSA	PSMA	AR-FL	AR-V7
before therapy (n=41)	5	6	11	8
after therapy (n=26)	0	1	1	1

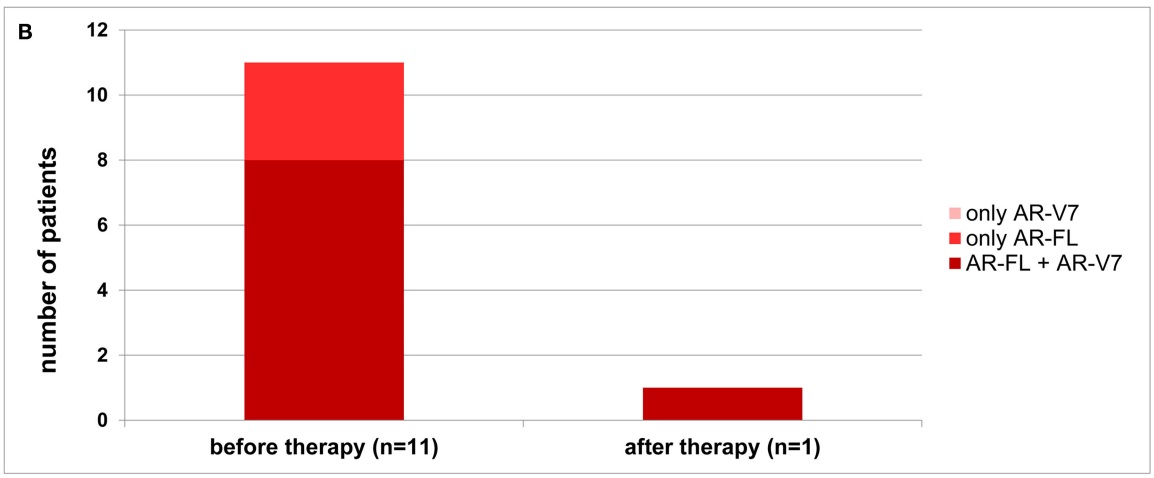

[n]	AR-FL + AR-V7	only AR-FL	only AR-V7
before therapy (n=11)	8	3	0
after therapy (n=1)	1	0	0

FIGURE 1 | Prevalence of primary TNBC patients with prostate cancer related transcripts detected in CTCs. **(A)** In 41 TNBC patients before therapy (dark blue) and 26 TNBC patients after neoadjuvant therapy (light blue) *PSA*, *PSMA*, *AR-FL*, and *AR-V7* RNA profiles were examined. **(B)** Co-expression of *AR-FL* and *AR-V7* (dark red) was detected in the majority of *AR-FL*+ CTCs. Some patients displayed only *AR-FL*+ CTCs (red), but no patient was examined to have only *AR-V7*+ CTCs (light red).

hazard analysis with the standard staging parameters tumor size and lymph node involvement before and after therapy. In univariate analysis, *PSMA*+ CTCs turned out as a significant unfavorable predictor for PFS (**Figure 3A**; $p = 0.002$) and OS (**Figure 3B**; $p = 0.015$), respectively. Using multivariate Cox proportional hazard analysis, neither *PSMA*+ CTCs nor *AR-V7*+ CTCs, independently associated with a significant shorter PFS (**Figure 3A**) nor with OS (**Figure 3B**). With regard to clinical parameters, univariate analysis identified tumor size before and after therapy ($p = 0.044$; $p = 0.0097$) as well as lymph node involvement before therapy ($p = 0.028$) and non-pCR ($p = 0.01$) as unfavorable variables for PFS which was confirmed in multivariate analysis for non-pCR ($p = 0.041$) and lymph nodes before therapy ($p = 0.008$). For OS, univariate analysis identified tumor size before ($p = 0.034$), after therapy ($p = 0.041$) and non-pCR ($p = 0.041$) to associate with shorter OS.

Combining the CTC results obtained here with our already published results for comprehensive CTC-analysis in this subgroup (34), Cox multivariate proportional hazard analysis additionally identified DNA excision repair protein *ERCC1*+ CTCs, associated with resistance, as an unfavorable factor for PFS ($p = 0.026$) and OS ($p = 0.017$) (**Figure S1**).

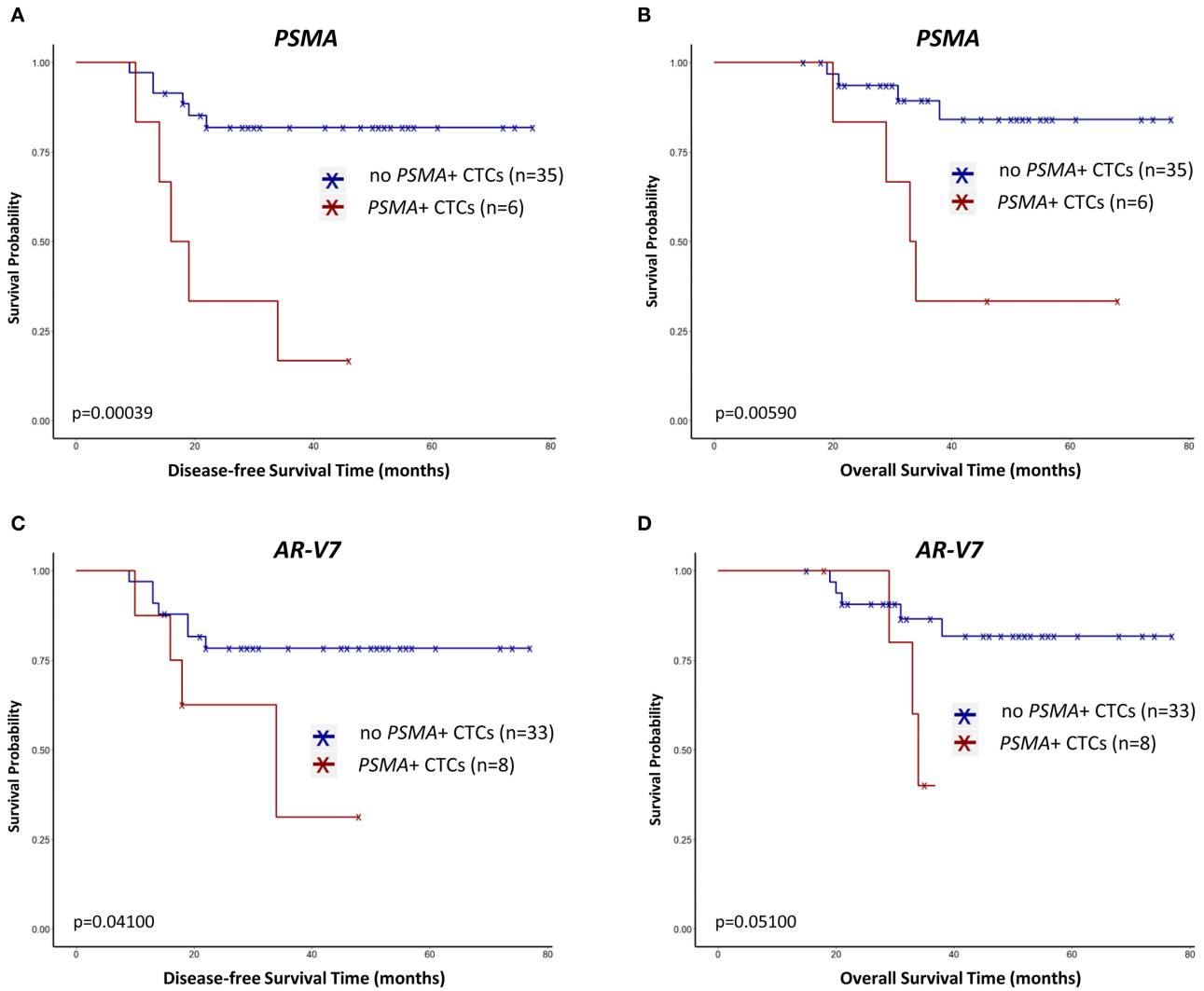

FIGURE 2 | Survival curves regarding *PSMA*+ CTCs **(A,B)** and *AR-V7*+ CTCs **(C,B)** in primary TNBC patients before neoadjuvant treatment. Survival intervals were screened from the time of first diagnosis until the date of recurrence [here disease-free survival; (**A,C**)] or death [overall survival; (**B,D**)] and calculated with Kaplan-Meier estimator (Log-rank test).

DISCUSSION

TNBC remains a subtype with a very aggressive behavior and worse outcome (1, 2). Thus, predictive biomarkers are urgently needed to stratify patients for further therapeutic options. In this context, we recently published a comprehensive CTC-analysis in three different BC subtypes before and after neoadjuvant treatment (34). Using a multi-marker gene panel including 17 different genes that target different pathways associated with stemness, EMT, resistance and survival of tumor cells, we recently demonstrated the heterogeneity of CTCs before and after therapy in these TNBC patients as compared to non-TNBC patients (34). For the group of TNBC patients, the most interesting and most important finding was the fact that ERBB2+/ERBB3+CTCs were found before and after therapy in about 20% of cases. Furthermore, EGFR+/ERBB2+/ERBB3+CTCs before and ERBB2+/ERBB3+CTCs after therapy significantly correlated with a shorter PFS ($p = 0.01$ and $p = 0.02$). Consequently, comprehensive analysis of CTCs could probably direct physicians to stratify TNBC patients for additional treatment options. The same holds true for prostate cancer related genes, especially AR, which has frequently been discussed to be a target for treatment of TNBC patients.

We here demonstrated that prostate cancer related genes expressed on CTCs in primary, non-metastatic TNBC patients were mainly found before but rarely after therapy, thus, were eliminated by the given therapy. However, *PSMA*+ CTCs before therapy significantly identified patients with worse outcome. In the context of AR inhibition, often discussed for the TNBC subgroup, this therapeutic approach might not be successful in

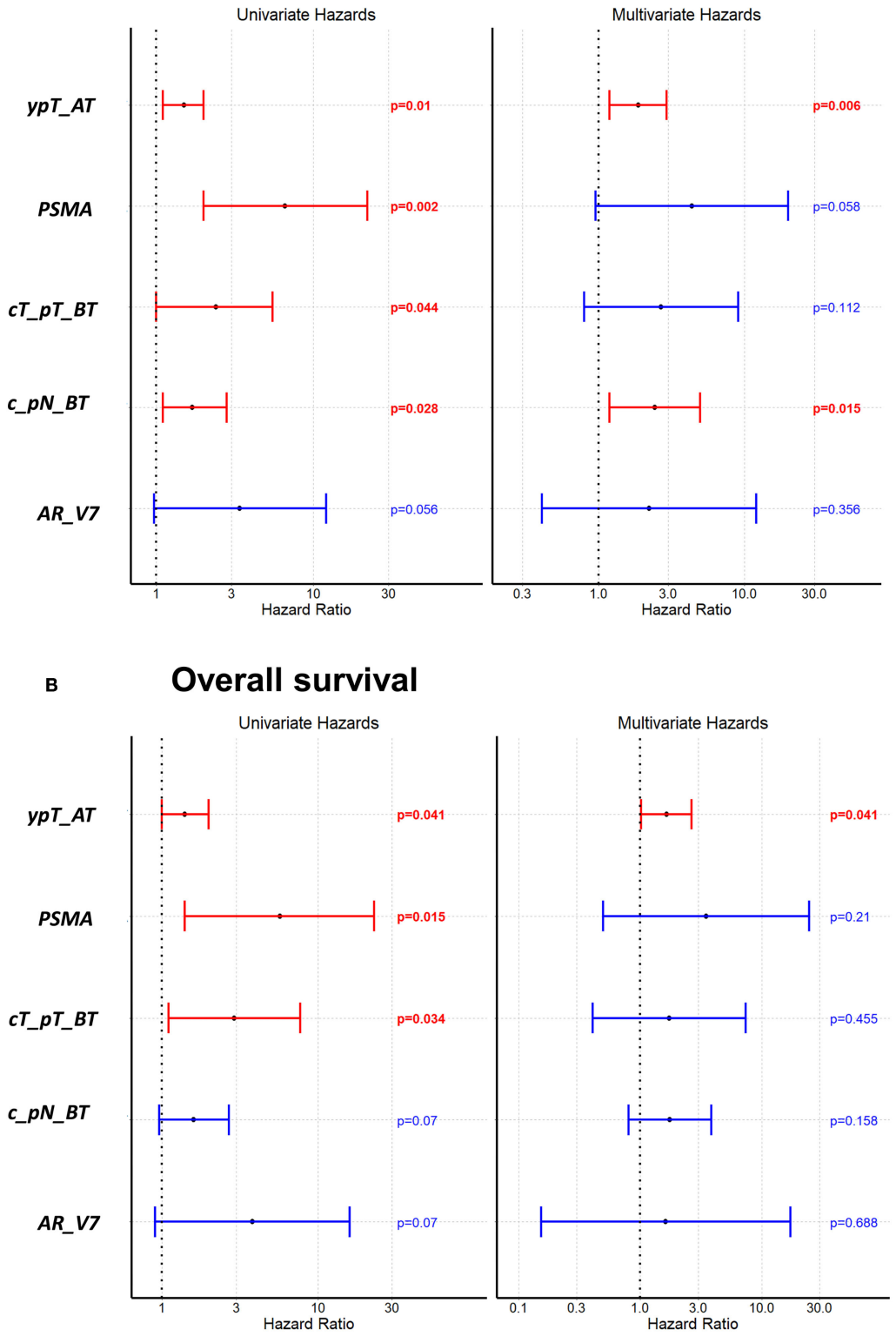

FIGURE 3 | Univariate and multivariate Cox proportional hazard analysis regarding PFS **(A)** and OS **(B)**. Univariate analysis shows the prognostic value of *PSMA*+ CTCs for PFS and OS. ypT_AT: tumor size after therapy, cT_pT_BT: tumor size before therapy, c_pN_BT: lymph node status before therapy.

the primary setting since we detected *AR-FL*+ CTCs together with *AR-V7*+ CTCs, associated with therapeutic failure.

AR expression in BC has mainly been studied on tissue samples resulting in a positivity rate of 10–35% (8, 19). Using immunohistochemistry for the evaluation of AR in 164 primary tumors and 83 corresponding metastases, a concordance between primary tumor and metastasis of >60% was proven (28). Consequently, the authors concluded that, if a new biopsy is performed and used for therapy selection, AR evaluation should be repeated. In another publication, this group further demonstrated that AR expression was not useful to predict the efficacy of endocrine treatment in advanced BC (40). Since metastatic biopsies are often not feasible and very invasive, CTCs as a so-called liquid biopsy have received considerable attention as a non-invasive alternative to the biopsy of metastasis and there is data suggesting that the characteristics of CTCs represent those of the metastasis better than the primary tumor (41–45). Consequently, CTCs might be more appropriate to select BC patients for AR-targeting drugs. Up to now, only very few groups have addressed the expression of prostate cancer related genes on CTCs in BC (29–33, 46). Most of these studies analyzed CTCs of metastatic HR+/HER2- BC patients for the expression of AR with a detection rate ranging from 20 to 43%, respectively (29, 31–33). Krujiff et al., further compared AR expression in primary tumor tissues and matched CTCs and observed switches from AR+ to AR-negative and *vice versa* with an overall disconcordance of 58% (32). In abiraterone/prednisone-treated postmenopausal ER+ advanced BC patients neither the analysis of biomarkers in serum, CTCs nor tumor tissue identified a subgroup a patients with significantly improved PFS, although dual expression of AR and ER in baseline CTCs were supposed to have an association with improved PFS (47). Nevertheless, these results highlight the role for AR in BC bone metastasis and suggest that inhibitory AR treatment could be successful in that subset of patients. In the mentioned studies, only AR itself but neither its splice variant nor other prostate cancer related genes were evaluated. In addition, no data were published with regard to primary BC, especially TNBC. Consequently, we can only discuss our findings with results obtained for PCA patients where CTCs have been intensively analyzed, mostly in later stages of the disease (35, 48, 49). In this regard, from the technical point of view, El-Heliebi et al., published the feasibility and utility of *in situ* padlock probe technology for the analysis of *AR-V7*, *AR-FL*, and *PSA* expression in combination with immunostaining (panCK and CD45) in CTCs from PCA patients (50). Furthermore, using the CellSearch system for enrichment, followed by the detection of *AR-V7* transcripts applying qPCR, adapted from the original Antonarakis et al. publication in 2014, allowed the detection of *AR-V7* and *keratin 19* (*K19*) transcripts from as low as a single *AR-V7*+/*K19*+ cell (36, 51). In the context of clinical studies, patients with CTCs expressing *AR-V7* showed worst outcome when compared to those patients harboring *AR-V7*-negative CTCs or no CTCs (52). Very recently, it was demonstrated that men with metastatic PCA who were tested positive for nuclear-localized AR-V7 protein in CTCs were likely to live longer if taxane based chemotherapy was used (53). In the PROPHECY Trial, a multicenter, prospective-blinded study of men with high-risk metastatic castration resistant PCA starting abiraterone acetate or enzalutamide treatment, the detection of *AR-V7* in CTCs by two assays was independently associated with shorter PFS and OS, concluding that such men should be offered alternative treatments (54). Based on the findings in PCA that not the AR itself but AR-V7 has been linked to resistance toward anti-AR drugs and thus, therapeutic failure, we can only speculate that AR inhibitory treatment might not be successful in non-metastatic TNBC since in two thirds of our patients with *AR*+ CTCs, *AR-V7* was also expressed. Nevertheless, although not analyzing CTCs, our findings are supported by Hickey et al., who showed that *AR-V7* protein was highly expressed in tumor tissues of a subgroup of HR-negative BCs. Moreover, they observed enzalutamide to induce *AR* and also *AR-V7* transcript expression in MDA-MB-453 cells and primary BCs. This group finally raised caution when exploring AR inhibitory treatment in women with BC and proposed the potential of AR-V7 as a predictive biomarker of anti-AR therapy response (38). We rarely found CTC-positive patients with regard to prostate cancer related genes after therapy. Thus, a decrease in CTC-positivity after therapy might also be explained by a reduction of CTC numbers under the given therapy. Due to the molecular approach used for this study, we cannot show CTC counts before and after therapy. However, we have already demonstrated that neoadjuvant therapy was able to eliminate most of the CTCs present before therapy in locally advanced BC. Interestingly, most of the residual CTCs after therapy displayed mesenchymal and/or stem cell like features (55).

Several phase II studies evaluated the effect of AR-targeting drugs in metastatic BC, especially TNBC (14, 16, 17, 56). Applying bicalutamide in AR+ but HR-negative advanced BC patients resulted in a clinical benefit rate of 19% (14) and in a multicenter single-arm trial in women with AR+, metastatic or inoperable locally advanced TNBC, the combination of abiraterone acetate plus prednisone was only beneficial for some patients with molecular apocrine tumors (16). Evaluating locally advanced or metastatic AR+ TNBC patients, enzalutamide demonstrated clinical activity and was well-tolerated, however, response rates were 25% in the intention to treat population, showing an activity in only a subset of patients (17). These preliminary studies are encouraging and understanding the AR signaling pathway harbors clinical relevance to unravel its role in TNBC pathogenesis. In this regard, AR inhibition was observed to have promising effect in preclinical studies and clinical trials with combinational approaches of AR blockade plus CDK4/6 inhibitors, PI3K inhibition, chemotherapy, and immunotherapy are currently ongoing (56).

One of our key findings was the significant correlation of *PSMA*+ CTCs with early relapse and reduced OS. Interestingly, using the same method for the detection of *PSMA*+ CTCs, *PSMA* transcript declines appeared to be associated with concurrent decreases in serum PSA, thus, sequential CTC sampling was proposed to provide a non-invasive response assessment to systemic treatment for metastatic castration-resistant PCA (57).

PSMA expression was detected in endothelial cells of the neovasculature, but not in adjacent normal endothelium, thus,

its expression has already been studied in a variety of cancer tissues, including TNBC. In this context, Morgenroth et al. recently identified PSMA as potential target for radio-ligand therapy in TNBC MDA-MB231 cells (11). Kasoha et al., observed PSMA to be expressed in the neovasculature of breast tumors and its distant metastases. Interestingly, the ^{68}Ga-PSMA tracer was strongly uptaken in the bone metastases of a metastatic BC patients, elucidating PSMA as a therapeutic vascular target (10). In the management of PCA, PSMA has already become an attractive target for oncological imaging and radionuclide therapy since its expression persisted in a high percentage of these patients, confirmed by positron emission tomography/computer tomography (58). These findings supported the use of imaging for diagnostic purposes as compared to the assessment of blood-based PSA values (59–63). For PCA, radioligand therapy using 177Lu-PSMA-617 was shown to be safe with a low toxicity profile and PSMA-11-derived dual-labeled PSMA inhibitors for preoperative imaging and guided surgery were feasible to detect PSMA-specific PCA lesions (64, 65).

Conclusion and Limitation of the Study

To validate the feasibility of our blood-based approach, a comparison of blood and tissue would have been necessary. However, before therapy, at least three tissue biopsies are taken for diagnostic purposes while the remaining tissue is kept as a so-called "back-up" for repeating analysis or additional analyses in case of relapse. After therapy, the same holds true since neoadjuvant chemotherapy results in tumor shrinkage in most cases, reducing the chance of tissue analysis for other purposes than diagnostics. In addition, a comparison of CTC characteristics on the mRNA level and CTC characteristics on the protein level would have been interesting. However, the CTC isolation method used in this study is not suitable for protein expression analysis, making a direct comparison of matched CTC samples for RNA and protein analysis not feasible. It is to mention that all currently available CTC isolation methods, including the one used for the current study, do not capture the entirety of CTCs. However, using positive immunomagnetic selection targeting EpCAM, HER2, and EGFR improved and optimized the enrichment of tumor stem cell and EMT like CTC compared to cell capturing with anti-EpCAM alone in different tumor entities (66–68).

Nevertheless, to the best of our knowledge, this is the first study, comprehensively analyzing some prostate cancer related genes in CTCs of a defined primary, non-metastatic TNBC subgroup before and after therapy. Although expressed in a minority of patients, *PSMA*+ CTCs significantly identified patients with worse outcome and could serve as a new predictive marker in this BC subgroup, probably in combination with 68Ga-PSMA imaging or even as target for treatment. Furthermore, in the context of AR inhibition, our findings demonstrate that this treatment option might not be successful in the primary setting of TNBC since we identified *AR-FL*+ CTCs together with *AR-V7*+ CTCs, associated with therapeutic failure. However, these findings carefully have to be evaluated in further clinical studies.

MATERIALS AND METHODS

Patient Characteristics

The study was conducted at the Department of Gynecology and Obstetrics, at the University Hospital of Essen, in Germany. In total, 41 early TNBC patients (before therapy: $n = 41$, matched samples after therapy $n = 26$), diagnosed between January 2013 and August 2018, were enrolled. All patients presented with first diagnosis of TNBC in our clinic, were non-metastatic and had not been treated before. Blood was obtained after written informed consent from all subjects using protocols approved by the clinical ethic committee of the University Hospital Essen (05/2856). Patient characteristics are documented in **Table 1**.

Eligibility Criteria and Response Criteria

The eligibility criteria were as follows: histologically proven BC, no severe uncontrolled comorbidities or medical conditions, and no further malignancies at present or in the patient history. Blood was drawn at primary diagnosis and after NACT. Completion of NACT ($n = 39$) or adjuvant treatment ($n = 2$) (anthracyclines, taxanes, cyclophosphamide, carbo- and cisplatin, gemcitabine; **Table S1**) were applied according to current guidelines as well as radiotherapy (3). Two patients received the PARP-inhibitor Olaparib in a clinical trial (GeparOla). For each of the 41 patients, the tumor type, TNM-staging, grading and Ki67 were assessed in the Institute of Pathology, at the University Hospital Essen as part of the West German Comprehensive Cancer Center. Pathological response to therapy was defined according to the grading system of Sinn et al., 1994 (69): 0 = no effect; 1 = resorption and tumor sclerosis; 2 = minimal residual invasive tumor (<0.5 cm); 3 = residual non-invasive tumor only, ductal carcinoma *in situ* (DCIS); 4 = no tumor detectable. pCR was defined as regression 4 according to Sinn, no evidence of residual invasive cancer and DCIS, both, in breast and axilla; pathological partial response (pPR) was defined as regression 1–3 according to Sinn (69).

Sampling of Blood

2 x 5 ml EDTA blood were collected for CTC isolation in S-Monovettes® (Sarstedt AG & Co., Germany). Samples were stored at 4°C and processed not later than 4 h after blood withdrawal.

Enrichment of Circulating Tumor Cells, mRNA Isolation, and Reverse Transcription

Positive immunomagnetic selection targeting EpCAM, EGFR, and HER2 (AdnaTest EMT-2/StemCell Select^{TM}, QIAGEN GmbH, Hilden, Germany) was employed for CTC isolation from 2 × 5 ml blood. The method has been described in detail elsewhere (70). mRNA was isolated by oligo(dT)$_{25}$-beads and was reverse transcribed (AdnaTest *EMT-2*/StemCell Detect^{TM}, QIAGEN GmbH, Hilden, Germany). The final reaction volume of 40 µl cDNA was stored at −20°C.

Quantitative PCR

The multimarker RT-qPCR AdnaTest *ProstateCancerPanel AR-V7* detecting *CD45 (PTPRC), PSA (KLK3), PSMA (FOLH1), full-length AR (AR-FL), AR splice variant seven* (*AR-V7),* and *GAPDH* (QIAGEN GmbH, Hilden, Germany) has been described in detail recently (71–73). The primer set to detect *AR-FL* does not detect the *AR-V7* transcript. The method requires transcript-specific pre-amplification of 6.25 µl cDNA using the 2xMultiplex PCR Master Mix (QIAGEN GmbH, Hilden, Germany) with 18 PCR cycles. PCR was performed as follows: denaturation for 5 min at 95°C, followed by 18 cycles of 30 s at 95°C, 90 s at 60°C, and 90 s at 72°C. Preamplified cDNA (3 µl; 1:10 diluted) was analyzed in duplicates for one of the six transcripts in a reaction volume with miRCURY SYBR Green MasterMix (QIAGEN GmbH, Hilden, Germany) and ROX Reference Dye (0.75 µl; QIAGEN GmbH, Hilden, Germany) of in total 15 µl. RT-qPCR was performed with the StepOnePlus™ (Thermo Fisher Scientific, Waltham, USA) real-time system as follows: PCR activation for 10 min at 95°C, followed by 35 cycles 10 s at 95°C, 10 s at 60°C, and 10 s at 78°C. In addition to fluorescence readout at 78°C in each cycle, melting curves were obtained.

Data Evaluation

CTC isolation was conducted in duplicate from 2 × 5 ml blood for each patient sample. cDNA was analyzed separately from these duplicates. The fluorescence threshold of 0.48 was employed for all transcripts (programmed with StepOne Software v2.3) and defined the PCR cycle used for transcript quantification. CTC expression data was normalized to data of healthy donor controls ($n = 14$) using individual cut off values for each gene (raw data shown in **Table S2**). *GAPDH* not exclusively expressed in CTCs but also in the 100–200 contaminating leukocytes was normalized to the leukocyte-specific transcript *PTPRC* ($\Delta\Delta$Cq = [Cutoff(gene)-Sample Cq(gene)]-[Cutoff(*PTPRC*)-Sample Cq(*PTPRC*)]. The transcripts *PSA, PSMA, AR-FL, AR-V7* were independent of a growing number of leukocytes, thus, the ΔCq value was calculated as follows: ΔCq = [Cutoff(gene)-Sample Cq(gene)]. Only positive $\Delta(\Delta)$Cq values were considered as evaluable signals and signals were analyzed binary to be interpreted as overexpression yes/no results. Results of primer that showed Cq values below 35 in the negative control and results of amplicons with the wrong melt temperature [ΔTm (positive control – sample) >2°C] and [Tm <76.6°C] were excluded. We evaluated a sample to be positive for one transcript, if at least one of the two sample duplicates showed a Cq value below the cut-off. Cq values of all patient samples and healthy donors are listed in **Table S2**.

Statistical Analysis

Statistical analysis was performed using R (version 3.6.1) with R packages shiny, hmisc, ggplot2, survival, broom, and dplyr. Survival intervals were screened from the time of first diagnosis until the date of recurrence (PFS) or death (OS) and calculated with Kaplan-Meier estimator (Log-rank test). In this cohort, recurrence was supposed in all deceased patients ($n = 2$) who had no documented BC associated death. In addition, a univariate and multivariate Cox proportional hazard analysis was conducted to confirm the Kaplan Meier findings and to identify factor dependencies. $P < 0.05$ were considered to indicate a statistically significant difference. Diagrams were computed with the R script mentioned or with Microsoft Excel (Microsoft Corporation, Redmond, WA, USA).

DATA AVAILABILITY STATEMENT

All datasets presented in this study are included in the article/**Supplementary Material**.

ETHICS STATEMENT

The studies involving human participants were reviewed and approved by clinical ethic committee of the University Hospital Essen (05/2856). The patients/participants provided their written informed consent to participate in this study.

AUTHOR CONTRIBUTIONS

SK-B and RK supervised the study. SK-B developed the concept and design of the study. SH established and developed the method. CK established, validated the method in the Department of Gynecology and Obstetrics, University Hospital Essen, and wrote sections of the manuscript. OH and A-KB recruited the patients. SK-B, CK, OH, and A-KB collected the experimental and clinical data. SK-B, CK, and SH evaluated, analyzed the data, reviewed, and edited the manuscript. CK and SH performed the statistical analysis and visualized the results. SK-B and A-KB wrote the first draft of the manuscript. All authors contributed to manuscript revision, read, and approved the submitted version.

FUNDING

The APC was funded by the Open Access Publication Fund of the University of Duisburg-Essen.

ACKNOWLEDGMENTS

We thank Ute Kirsch for excellent technical assistance.

SUPPLEMENTARY MATERIAL

The Supplementary Material for this article can be found online at: https://www.frontiersin.org/articles/10.3389/fonc.2020.01658/full#supplementary-material

REFERENCES

1. Sharma P. Update on the treatment of early-stage triple-negative breast cancer. *Curr Treat Options Oncol.* (2018) 19:22. doi: 10.1007/s11864-018-0539-8
2. Schneeweiss A, Denkert C, Fasching PA, Fremd C, Gluz O, Kolberg-Liedtke C, et al. Diagnosis and Therapy of Triple-Negative Breast Cancer (TNBC)–recommendations for daily routine practice. *Geburtshilfe Frauenheilkd.* (2019) 79:605–17. doi: 10.1055/a-0887-0285
3. AGO Breast Committee. *Diagnosis and Treatment of Patients With Primary and Metastatic Breast Cancer: Recommendations 2020*. (2020) Available online at: https://www.ago-online.de/fileadmin/ago-online/downloads/_leitlinien/kommission_mamma/2020/Alle_aktuellen_Empfehlungen_2020.pdf (accessed 30 Mar, 2020).
4. Isakoff SJ. Triple-negative breast cancer: role of specific chemotherapy agents. *Cancer J.* (2010) 16:53–61. doi: 10.1097/PPO.0b013e3181d24ff7
5. Sikov WM, Berry DA, Perou CM, Singh B, Cirrincione CT, Tolaney SM, et al. Impact of the addition of carboplatin and/or bevacizumab to neoadjuvant once-per-week paclitaxel followed by dose-dense doxorubicin and cyclophosphamide on pathologic complete response rates in stage II to III triple-negative breast cancer: CALGB 40603 (Alliance). *J Clin Oncol.* (2015) 33:13–21. doi: 10.1200/JCO.2014.57.0572
6. Minckwitz G von, Schneeweiss A, Loibl S, Salat C, Denkert C, Rezai M, et al. Neoadjuvant carboplatin in patients with triple-negative and HER2-positive early breast cancer (GeparSixto; GBG 66): a randomised phase 2 trial. *Lancet Oncol.* (2014) 15:747–56. doi: 10.1016/S1470-2045(14)70160-3
7. Castrellon AB, Pidhorecky I, Valero V, Raez LE. The role of carboplatin in the neoadjuvant chemotherapy treatment of triple negative breast cancer. *Oncol Rev.* (2017) 11:324. doi: 10.4081/oncol.2017.324
8. Rahim B, O'Regan R. AR signaling in breast cancer. *Cancers.* (2017) 9:30021. doi: 10.3390/cancers9030021
9. Schmid P, Cortes J, Pusztai L, McArthur H, Kümmel S, Bergh J, et al. Pembrolizumab for early triple-negative breast cancer. *N Engl J Med.* (2020) 382:810–21. doi: 10.1056/NEJMoa1910549
10. Kasoha M, Unger C, Solomayer E-F, Bohle RM, Zaharia C, Khreich F, et al. Prostate-specific membrane antigen (PSMA) expression in breast cancer and its metastases. *Clin Exp Metastasis.* (2017) 34:479–90. doi: 10.1007/s10585-018-9878-x
11. Morgenroth A, Tinkir E, Vogg AT, Sankaranarayanan RA, Baazaoui F, Mottaghy FM. Targeting of prostate-specific membrane antigen for radioligand therapy of triple-negative breast cancer. *Breast Cancer Res.* (2019) 21:116. doi: 10.1186/s13058-019-1205-1
12. Lehmann BD, Jovanović B, Chen X, Estrada MV, Johnson KN, Shyr Y, et al. Refinement of triple-negative breast cancer molecular subtypes: implications for neoadjuvant chemotherapy selection. *PLoS ONE.* (2016) 11:e0157368. doi: 10.1371/journal.pone.0157368
13. Lehmann BD, Bauer JA, Chen X, Sanders ME, Chakravarthy AB, Shyr Y, et al. Identification of human triple-negative breast cancer subtypes and preclinical models for selection of targeted therapies. *J Clin Invest.* (2011) 121:2750–67. doi: 10.1172/JCI45014
14. Gucalp A, Tolaney S, Isakoff SJ, Ingle JN, Liu MC, Carey LA, et al. Phase II trial of bicalutamide in patients with androgen receptor-positive, estrogen receptor-negative metastatic Breast Cancer. *Clin Cancer Res.* (2013) 19:5505–12. doi: 10.1158/1078-0432.CCR-12-3327
15. Chia K, O'Brien M, Brown M, Lim E. Targeting the androgen receptor in breast cancer. *Curr Oncol Rep.* (2015) 17:4. doi: 10.1007/s11912-014-0427-8
16. Bonnefoi H, Grellety T, Tredan O, Saghatchian M, Dalenc F, Mailliez A, et al. A phase II trial of abiraterone acetate plus prednisone in patients with triple-negative androgen receptor positive locally advanced or metastatic breast cancer (UCBG 12-1). *Ann Oncol.* (2016) 27:812–8. doi: 10.1093/annonc/mdw067
17. Traina TA, Miller K, Yardley DA, Eakle J, Schwartzberg LS, O'Shaughnessy J, et al. Enzalutamide for the treatment of androgen receptor-expressing triple-negative breast cancer. *J Clin Oncol.* (2018) 36:884–90. doi: 10.1200/JCO.2016.71.3495
18. Vera-Badillo FE, Templeton AJ, Gouveia P de, Diaz-Padilla I, Bedard PL, Al-Mubarak M, et al. Androgen receptor expression and outcomes in early breast cancer: a systematic review and meta-analysis. *J Natl Cancer Inst.* (2014) 106:djt319. doi: 10.1093/jnci/djt319
19. Kono M, Fujii T, Lim B, Karuturi MS, Tripathy D, Ueno NT. Androgen receptor function and androgen receptor-targeted therapies in breast cancer: a review. *JAMA Oncol.* (2017) 3:1266–73. doi: 10.1001/jamaoncol.2016.4975
20. Aleskandarany MA, Abduljabbar R, Ashankyty I, Elmouna A, Jerjees D, Ali S, et al. Prognostic significance of androgen receptor expression in invasive breast cancer: transcriptomic and protein expression analysis. *Breast Cancer Res Treat.* (2016) 159:215–27. doi: 10.1007/s10549-016-3934-5
21. Hu R, Dawood S, Holmes MD, Collins LC, Schnitt SJ, Cole K, et al. Androgen receptor expression and breast cancer survival in postmenopausal women. *Clin Cancer Res.* (2011) 17:1867–74. doi: 10.1158/1078-0432.CCR-10-2021
22. Loibl S, Müller BM, Minckwitz G von, Schwabe M, Roller M, Darb-Esfahani S, et al. Androgen receptor expression in primary breast cancer and its predictive and prognostic value in patients treated with neoadjuvant chemotherapy. *Breast Cancer Res Treat.* (2011) 130:477–87. doi: 10.1007/s10549-011-1715-8
23. Rakha EA, El-Sayed ME, Green AR, Lee AH, Robertson JF, Ellis IO. Prognostic markers in triple-negative breast cancer. *Cancer.* (2007) 109:25–32. doi: 10.1002/cncr.22381
24. Sutton LM, Cao D, Sarode V, Molberg KH, Torgbe K, Haley B, et al. Decreased androgen receptor expression is associated with distant metastases in patients with androgen receptor-expressing triple-negative breast carcinoma. *Am J Clin Pathol.* (2012) 138:511–6. doi: 10.1309/AJCP8AVF8FDPTZLH
25. Mrklić I, Pogorelić Z, Capkun V, Tomić S. Expression of androgen receptors in triple negative breast carcinomas. *Acta Histochem.* (2013) 115:344–8. doi: 10.1016/j.acthis.2012.09.006
26. McGhan LJ, McCullough AE, Protheroe CA, Dueck AC, Lee JJ, Nunez-Nateras R, et al. Androgen receptor-positive triple negative breast cancer: a unique breast cancer subtype. *Ann Surg Oncol.* (2014) 21:361–7. doi: 10.1245/s10434-013-3260-7
27. Pistelli M, Caramanti M, Biscotti T, Santinelli A, Pagliacci A, Lisa M de, et al. Androgen receptor expression in early triple-negative breast cancer: clinical significance and prognostic associations. *Cancers.* (2014) 6:1351–62. doi: 10.3390/cancers6031351
28. Bronte G, Bravaccini S, Ravaioli S, Puccetti M, Scarpi E, Andreis D, et al. Androgen receptor expression in breast cancer: what differences between primary tumor and metastases? *Transl Oncol.* (2018) 11:950–6. doi: 10.1016/j.tranon.2018.05.006
29. Fujii T, Reuben JM, Huo L, Espinosa Fernandez JR, Gong Y, Krupa R, et al. Androgen receptor expression on circulating tumor cells in metastatic breast cancer. *PLoS ONE.* (2017) 12:e0185231. doi: 10.1371/journal.pone.0185231
30. Pizon M, Lux D, Pachmann U, Pachmann K, Schott D. Influence of endocrine therapy on the ratio of androgen receptor (AR) to estrogen receptor (ER) positive circulating epithelial tumor cells (CETCs) in breast cancer. *J Transl Med.* (2018) 16:356. doi: 10.1186/s12967-018-1724-z
31. Keup C, Mach P, Aktas B, Tewes M, Kolberg H-C, Hauch S, et al. RNA profiles of circulating tumor cells and extracellular vesicles for therapy stratification of metastatic breast cancer patients. *Clin Chem.* (2018) 64:1054–62. doi: 10.1158/1538-7445.AM2017-3777
32. Kruijff IE de, Sieuwerts AM, Onstenk W, Jager A, Hamberg P, Jongh FE de, et al. Androgen receptor expression in circulating tumor cells of patients with metastatic breast cancer. *Int J Cancer.* (2019) 145:1083–9. doi: 10.1002/ijc.32209
33. Krawczyk N, Neubacher M, Meier-Stiegen F, Neubauer H, Niederacher D, Ruckhäberle E, et al. Determination of the androgen receptor status of circulating tumour cells in metastatic breast cancer patients. *BMC Cancer.* (2019) 19:1101. doi: 10.1186/s12885-019-6323-8
34. Bittner A-K, Keup C, Hoffmann O, Hauch S, Kimmig R, Kasimir-Bauer S. Molecular characterization of circulating tumour cells identifies predictive markers for outcome in primary, triple-negative breast cancer patients. *J Cell Mol Med.* (2020) 24:8405–16. doi: 10.1111/jcmm.15349
35. Pantel K, Hille C, Scher HI. Circulating tumor cells in prostate cancer: from discovery to clinical utility. *Clin Chem.* (2019) 65:87–99. doi: 10.1373/clinchem.2018.287102
36. Antonarakis ES, Lu C, Wang H, Luber B, Nakazawa M, Roeser JC, et al. AR-V7 and resistance to enzalutamide and abiraterone in prostate cancer. *N Engl J Med.* (2014) 371:1028–38. doi: 10.1056/NEJMoa1315815

37. Scher HI, Lu D, Schreiber NA, Louw J, Graf RP, Vargas HA, et al. Association of AR-V7 on circulating tumor cells as a treatment-specific biomarker with outcomes and survival in castration-resistant prostate cancer. *JAMA Oncol.* (2016) 2:1441–9. doi: 10.1001/jamaoncol.2016.1828
38. Hickey TE, Irvine CM, Dvinge H, Tarulli GA, Hanson AR, Ryan NK, et al. Expression of androgen receptor splice variants in clinical breast cancers. *Oncotarget*. (2015) 6:44728–44. doi: 10.18632/oncotarget.6296
39. Asangani IA, Dommeti VL, Wang X, Malik R, Cieslik M, Yang R, et al. Therapeutic targeting of BET bromodomain proteins in castration-resistant prostate cancer. *Nature*. (2014) 510:278–82. doi: 10.1038/nature13229
40. Bronte G, Rocca A, Ravaioli S, Puccetti M, Tumedei MM, Scarpi E, et al. Androgen receptor in advanced breast cancer: is it useful to predict the efficacy of anti-estrogen therapy? *BMC Cancer*. (2018) 18:348. doi: 10.1186/s12885-018-4239-3
41. Aktas B, Kasimir-Bauer S, Müller V, Janni W, Fehm T, Wallwiener D, et al. Comparison of the HER2, estrogen and progesterone receptor expression profile of primary tumor, metastases and circulating tumor cells in metastatic breast cancer patients. *BMC Cancer*. (2016) 16:522. doi: 10.1186/s12885-016-2587-4
42. Onstenk W, Sieuwerts AM, Mostert B, Lalmahomed Z, Bolt-de Vries JB, van Galen A, et al. Molecular characteristics of circulating tumor cells resemble the liver metastasis more closely than the primary tumor in metastatic colorectal cancer. *Oncotarget*. (2016) 7:59058–69. doi: 10.18632/oncotarget.10175
43. Lianidou E, Pantel K. Liquid biopsies. *Genes Chromosomes Cancer*. (2018) doi: 10.1002/gcc.22695
44. Maheswaran S, Haber DA. *Ex vivo* culture of CTCs: an emerging resource to guide cancer therapy. *Cancer Res.* (2015) 75:2411–5. doi: 10.1158/0008-5472.CAN-15-0145
45. Micalizzi DS, Maheswaran S, Haber DA. A conduit to metastasis: circulating tumor cell biology. *Genes Dev.* (2017) 31:1827–40. doi: 10.1101/gad.305805.117
46. Abreu M, Cabezas-Sainz P, Pereira-Veiga T, Falo C, Abalo A, Morilla I, et al. Looking for a better characterization of triple-negative breast cancer by means of circulating tumor cells. *J Clin Med.* (2020) 9:20353. doi: 10.3390/jcm9020353
47. Li W, O'Shaughnessy J, Hayes D, Campone M, Bondarenko I, Zbarskaya I, et al. Biomarker associations with efficacy of abiraterone acetate and exemestane in postmenopausal patients with estrogen receptor-positive metastatic breast cancer. *Clin Cancer Res.* (2016) 22:6002–9. doi: 10.1158/1078-0432.CCR-15-2452
48. Miyamoto DT, Zheng Y, Wittner BS, Lee RJ, Zhu H, Broderick KT, et al. RNA-Seq of single prostate CTCs implicates noncanonical Wnt signaling in antiandrogen resistance. *Science*. (2015) 349:1351–6. doi: 10.1126/science.aab0917
49. Miyamoto DT, Lee RJ, Stott SL, Ting DT, Wittner BS, Ulman M, et al. Androgen receptor signaling in circulating tumor cells as a marker of hormonally responsive prostate cancer. *Cancer Discov*. (2012) 2:995–1003. doi: 10.1158/2159-8290.CD-12-0222
50. El-Heliebi A, Hille C, Laxman N, Svedlund J, Haudum C, Ercan E, et al. *In situ* detection and quantification of AR-V7, AR-FL, PSA, and KRAS point mutations in circulating tumor cells. *Clin Chem*. (2018) 64:536–46. doi: 10.1373/clinchem.2017.281295
51. Hille C, Gorges TM, Riethdorf S, Mazel M, Steuber T, Amsberg G von, et al. Detection of Androgen Receptor Variant 7 (ARV7) mRNA levels in EpCAM-enriched CTC fractions for monitoring response to androgen targeting therapies in prostate cancer. *Cells*. (2019) 8:91067. doi: 10.3390/cells8091067
52. Antonarakis ES, Lu C, Luber B, Wang H, Chen Y, Zhu Y, et al. Clinical significance of androgen receptor splice variant-7 mRNA detection in circulating tumor cells of men with metastatic castration-resistant prostate cancer treated with first- and second-line abiraterone and enzalutamide. *J Clin Oncol*. (2017) 35:2149–56. doi: 10.1200/JCO.2016.70.1961
53. Graf RP, Hullings M, Barnett ES, Carbone E, Dittamore R, Scher HI. Clinical utility of the nuclear-localized AR-V7 biomarker in circulating tumor cells in improving physician treatment choice in castration-resistant prostate cancer. *Eur Urol*. (2020) 77:170–7. doi: 10.1016/j.eururo.2019.08.020
54. Armstrong AJ, Halabi S, Luo J, Nanus DM, Giannakakou P, Szmulewitz RZ, et al. Prospective multicenter validation of androgen receptor splice variant 7 and hormone therapy resistance in high-risk castration-resistant prostate cancer: the PROPHECY study. *J Clin Oncol*. (2019) 37:1120–9. doi: 10.1200/JCO.18.01731
55. Kasimir-Bauer S, Bittner A-K, König L, Reiter K, Keller T, Kimmig R, et al. Does primary neoadjuvant systemic therapy eradicate minimal residual disease? Analysis of disseminated and circulating tumor cells before and after therapy. *Breast Cancer Res*. (2016) 18:20. doi: 10.1186/s13058-016-0679-3
56. Shi Y, Yang F, Huang D, Guan X. Androgen blockade based clinical trials landscape in triple negative breast cancer. *Biochim Biophys Acta Rev Cancer*. (2018) 1870:283–90. doi: 10.1016/j.bbcan.2018.05.004
57. Paller CJ, Piana D, Eshleman JR, Riel S, Denmeade SR, Isaacsson Velho P, et al. A pilot study of prostate-specific membrane antigen (PSMA) dynamics in men undergoing treatment for advanced prostate cancer. *Prostate*. (2019) 79:1597–603. doi: 10.1002/pros.23883
58. Ruigrok EA, van Weerden WM, Nonnekens J, Jong M de. The future of PSMA-targeted radionuclide therapy: an overview of recent preclinical research. *Pharmaceutics*. (2019) 11:110560. doi: 10.3390/pharmaceutics11110560
59. Osborne JR, Akhtar NH, Vallabhajosula S, Anand A, Deh K, Tagawa ST. Prostate-specific membrane antigen-based imaging. *Urol Oncol*. (2013) 31:144–54. doi: 10.1016/j.urolonc.2012.04.016
60. Jadvar H. PSMA PET in prostate cancer. *J Nucl Med*. (2015) 56:1131–2. doi: 10.2967/jnumed.115.157339
61. Ceci F, Uprimny C, Nilica B, Geraldo L, Kendler D, Kroiss A, et al. 68Ga-PSMA PET/CT for restaging recurrent prostate cancer: which factors are associated with PET/CT detection rate? *Eur J Nucl Med Mol Imaging*. (2015) 42:1284–94. doi: 10.1007/s00259-015-3078-6
62. Tagawa ST, Milowsky MI, Morris M, Vallabhajosula S, Christos P, Akhtar NH, et al. Phase II study of Lutetium-177-labeled anti-prostate-specific membrane antigen monoclonal antibody J591 for metastatic castration-resistant prostate cancer. *Clin Cancer Res*. (2013) 19:5182–91. doi: 10.1158/1078-0432.CCR-13-0231
63. Weineisen M, Schottelius M, Simecek J, Baum RP, Yildiz A, Beykan S, et al. 68Ga- and 177Lu-Labeled PSMA I&T: optimization of a PSMA-targeted theranostic concept and first proof-of-concept human studies. *J Nucl Med*. (2015) 56:1169–76. doi: 10.2967/jnumed.115.158550
64. Ahmadzadehfar H, Zimbelmann S, Yordanova A, Fimmers R, Kürpig S, Eppard E, et al. Radioligand therapy of metastatic prostate cancer using 177Lu-PSMA-617 after radiation exposure to 223Ra-dichloride. *Oncotarget*. (2017) 8:55567–74. doi: 10.18632/oncotarget.15698
65. Baranski A-C, Schäfer M, Bauder-Wüst U, Roscher M, Schmidt J, Stenau E, et al. PSMA-11-derived dual-labeled PSMA inhibitors for preoperative PET imaging and precise fluorescence-guided surgery of prostate cancer. *J Nucl Med*. (2018) 59:639–45. doi: 10.2967/jnumed.117.201293
66. Bredemeier M, Edimiris P, Mach P, Kubista M, Sjöback R, Rohlova E, et al. Gene expression signatures in circulating tumor cells correlate with response to therapy in metastatic breast cancer. *Clin Chem*. (2017) 63:1585–93. doi: 10.1373/clinchem.2016.269605
67. Hanssen A, Wagner J, Gorges TM, Taenzer A, Uzunoglu FG, Driemel C, et al. Characterization of different CTC subpopulations in non-small cell lung cancer. *Sci Rep*. (2016) 6:28010. doi: 10.1038/srep28010
68. Todenhöfer T, Hennenlotter J, Dorner N, Kühs U, Aufderklamm S, Rausch S, et al. Transcripts of circulating tumor cells detected by a breast cancer-specific platform correlate with clinical stage in bladder cancer patients. *J Cancer Res Clin Oncol*. (2016) 142:1013–20. doi: 10.1007/s00432-016-2129-0
69. Sinn HP, Schmid H, Junkermann H, Huober J, Leppien G, Kaufmann M, et al. Histologische Regression des Mammakarzinoms nach primärer (neoadjuvanter) Chemotherapie. *Geburtshilfe Frauenheilkd*. (1994) 54:552–8. doi: 10.1055/s-2007-1022338
70. Bredemeier M, Edimiris P, Tewes M, Mach P, Aktas B, Schellbach D, et al. Establishment of a multimarker qPCR panel for the molecular characterization of circulating tumor cells in blood samples of metastatic breast cancer patients during the course of palliative treatment. *Oncotarget*. (2016) 7:41677–90. doi: 10.18632/oncotarget.9528

71. Maillet D, Allioli N, Peron J, Plesa A, Decaussin-Petrucci M, Tartas S, et al. Improved androgen receptor splice variant 7 detection using a highly sensitive assay to predict resistance to abiraterone or enzalutamide in metastatic prostate cancer patients. *Eur Urol Oncol.* (2019). doi: 10.1016/j.euo.2019.08.010
72. Cattrini C, Rubagotti A, Zinoli L, Cerbone L, Zanardi E, Capaia M, et al. Role of Circulating Tumor Cells (CTC), Androgen Receptor Full Length (AR-FL) and Androgen Receptor Splice Variant 7 (AR-V7) in a prospective cohort of castration-resistant metastatic prostate cancer patients. *Cancers.* (2019) 11:91365. doi: 10.3390/cancers11091365
73. Hench IB, Cathomas R, Costa L, Fischer N, Gillessen S, Hench J, et al. Analysis of AR/ARV7 expression in isolated circulating tumor cells of patients with metastatic castration-resistant prostate cancer (SAKK 08/14 IMPROVE Trial). *Cancers.* (2019) 11:81099. doi: 10.3390/cancers110 81099

Conflict of Interest: SK-B is a consultant for QIAGEN and has received honoraria from Novartis. CK received support for travel expenses from QIAGEN. OH received honoraria from Roche, Amgen, Pfizer, MSD, and Novartis. SH is an employee at QIAGEN. RK has received honoraria/is part of the advisory board from/at Tesaro, Astra-Zeneca, Medtronic in the last 3 years, and council of IGCS, president of SERGS and proctored and presented for Intuitive Surgical. A-KB received honoraria from Roche.

frontiers in Oncology

ORIGINAL RESEARCH
published: 24 September 2020
doi: 10.3389/fonc.2020.567809

Plasma *AR* Copy Number Changes and Outcome to Abiraterone and Enzalutamide

Giorgia Gurioli[1]*, *Vincenza Conteduca*[2], *Cristian Lolli*[2], *Giuseppe Schepisi*[2], *Stefania Gargiulo*[1], *Amelia Altavilla*[2], *Chiara Casadei*[2], *Emanuela Scarpi*[3] and *Ugo De Giorgi*[2]

[1] Biosciences Laboratory, Istituto Scientifico Romagnolo per lo Studio e la Cura dei Tumori (IRST) IRCCS, Meldola, Italy, [2] Department of Medical Oncology, Istituto Scientifico Romagnolo per lo Studio e la Cura dei Tumori (IRST) IRCCS, Meldola, Italy, [3] Unit of Biostatistics and Clinical Trials, Istituto Scientifico Romagnolo per lo Studio e la Cura dei Tumori (IRST) IRCCS, Meldola, Italy

OPEN ACCESS

Edited by:
Elisabetta Rossi,
University of Padua, Italy

Reviewed by:
Victor C. Kok,
Asia University, Taiwan
Francesco Massari,
Integrated University Hospital Verona, Italy

***Correspondence:**
Giorgia Gurioli
giorgia.gurioli@irst.emr.it

Specialty section:
This article was submitted to Cancer Molecular Targets and Therapeutics, a section of the journal Frontiers in Oncology

Received: 30 May 2020
Accepted: 13 August 2020
Published: 24 September 2020

Citation:
Gurioli G, Conteduca V, Lolli C, Schepisi G, Gargiulo S, Altavilla A, Casadei C, Scarpi E and De Giorgi U (2020) Plasma AR Copy Number Changes and Outcome to Abiraterone and Enzalutamide. Front. Oncol. 10:567809. doi: 10.3389/fonc.2020.567809

Introduction: Plasma androgen receptor (*AR*) copy number (CN) status identifies castration-resistant prostate cancer (CRPC) patients with worse outcome on abiraterone/enzalutamide. However, the impact of *AR* CN changes on clinical outcome in CRPC is unknown.

Materials and Methods: Plasma samples from 73 patients treated with abiraterone or enzalutamide were collected at baseline and at the time of progression disease (PD). Droplet digital polymerase chain reaction was used to assess *AR* CN status.

Results: We showed that 11 patients (15.1%) changed *AR* CN status from baseline to PD (9 patients from normal to gain, 2 from gain to normal). Patients changing *AR* CN status from normal at baseline to gain at PD had intermediate median overall survival (OS) of 20.5 months (95% CI = 8.0–44.2) between those who remained *AR* CN normal from baseline to PD (27.3 months [95% CI = 21.9–34.4]) and those who remained *AR* CN gain from baseline to PD (9.1 months [95% CI = 3.8–14.5], $p < 0.0001$). Patients changing *AR* CN from normal at baseline to gain at PD had a median progression-free survival (PFS) of 9.2 months (95% CI = 2.0–14.7), patients who remained *AR* CN normal had a median PFS of 9.1 months (95% CI = 7.2–10.1), and patients who remained *AR* CN gain had a median PFS of 5.4 (95% CI = 3.6–6.5, $p = 0.0005$). Both OS and PFS were not significantly different between patients with *AR* CN that changes from normal to gain and patients with stable *AR* CN normal.

Conclusions: We showed that CRPC patients changing *AR* CN status from baseline to progression time point had intermediate OS and we suggested that *AR* CN evaluation at baseline could be the most informative for clinical outcome of CRPC patients treated with abiraterone or enzalutamide. Larger prospective studies are warranted.

Keywords: cell free DNA, androgen receptor, copy number changes, abiraterone acetate, enzalutamide, clinical outcome

INTRODUCTION

Abiraterone acetate and enzalutamide belong to therapies introduced in the past years for patients with metastatic castration-resistant prostate cancer (CRPC), improving patient survival and quality of life (1–4). During therapy, the fractions of DNA alterations may vary under treatment selection, giving rise to alterations originally present in a very small number of cancer cells (5). Moreover, currently there is not yet a validated sequence of therapies and patient selection strategies, so there is now an urgent need to identify noninvasive biomarkers able to guide treatment selection for CRPC personalized medicine. Cell free DNA (cfDNA) has emerged as a minimally invasive and good source of biomarkers deriving from multiple metastases, suggesting its role in monitoring clinical outcome and tumor heterogeneity (6–8). Literature data reported that changes in cfDNA concentration correlate with radiological progression-free survival (PFS) and overall survival (OS) and may be used as independent prognostic biomarker of response to taxanes (9).

Androgen receptor (AR) has a key role in prostate cancer development and progression (10, 11). Copy number (CN) of *AR* has been well-investigated and is considered to be one of the main mechanisms of hormone-sensitive to hormone-resistant transition (12). Plasma *AR* CN at baseline of abiraterone and enzalutamide was associated with resistance to these therapies, both in pre- and post-chemotherapy with docetaxel (13). In this study, we evaluate the role of plasma *AR* CN changes on clinical outcome in CRPC patients treated with abiraterone or enzalutamide.

MATERIALS AND METHODS

Patients

From August 2012 to June 2016, CRPC patients with histologically confirmed diagnosis of prostate adenocarcinoma were enrolled. Patients were treated with abiraterone or enzalutamide in pre- or post-chemotherapy settings. Treatment was continued until evidence of disease progression or unacceptable toxicity. The choice of therapy was at the discretion of the treating physician.

Serum prostate-specific antigen (PSA), alkaline phosphatase (ALP), serum lactate dehydrogenase (LDH), cell blood count to determine neutrophil to lymphocyte ratio were measured within 1 week of starting therapy and once per month thereafter. Radiographic disease was assessed with computed tomography (CT) and bone scans at the time of screening and once every 12 weeks during treatment. ^{18}F-fluorocholine positron emission tomography/computed tomography (FCH-PET/CT) was performed after 12 ± 4 weeks of treatment.

Progression disease (PD) was assessed considering radiographic evidence of new lesions by bone scintigraphy and/or new or enlarging soft tissue lesions by CT or magnetic resonance imaging, per the Prostate Cancer Clinical Trials Working Group 3 guidelines (14). The study was approved by the Local Ethics Committee and informed consent was obtained from each patient for their biological material to be used for research purposes (CEIIAV IRSTB048).

Molecular Analysis

Peripheral blood samples were collected before initiating therapy with abiraterone or enzalutamide and at the time of PD. The blood was drawn into 10 ml ethylene diamine tetra-acetic acid (EDTA) tubes, maintained at room temperature, processed within 30 min and stored at −80°C. Circulating DNA was extracted from 1 or 2 ml of plasma using QIAamp Circulating Nucleic Acid Kit (Qiagen). Total extracted DNA was quantified with the Quant-iT high sensitivity PicoGreen double-stranded DNA Assay Kit (Invitrogen). We performed plasma *AR* CN analysis with a multiplex digital droplet polymerase chain reaction (Biorad) assay using three reference genes: *NSUN3*, *ElF2C1*, and *AP3B1* and *ZXDB* at Xp11.21 as a control gene not involving the whole arm of the chromosome, as previously described (15).

Statistical Analyses

PFS was defined as the time elapsed between the date of start of therapy and the date of radiological/clinical or biochemical progression or last tumor evaluation. OS was defined as the time elapsed between the date of start of therapy and the date of death from any cause or the date of last follow-up. PFS and OS were estimated using Kaplan–Meier method and compared using logrank test. *P*-values were two-sided and a $p < 0.05$ was considered as statistically significant. Statistical analyses were performed with SAS statistical software, version 9.4 (SAS Institute, Cary, NC, USA).

RESULTS

This study evaluated 73 patients with sufficient plasma DNA for *AR* CN detection in both baseline and progression samples. Of these, 35 (48%) and 38 (52%) received abiraterone or enzalutamide pre- and post- chemotherapy, respectively. When comparing the baseline patient characteristics according to therapy, post-chemotherapy setting displayed a higher Gleason score, a greater incidence of bone and visceral metastases as well as higher levels of ALP and LDH (as shown in **Table 1**). We found that 84% (49) of 58 patients with *AR* CN normal and 87% (13) of 15 with *AR* CN gain at baseline showed no changes in *AR* CN status in their PD sample (**Figure 1A**), observing a 15.1% conversion rate of *AR* CN status from baseline to PD time point. Clinical outcome in terms of OS (**Figure 1B**) and PFS (**Figure 1C**) was evaluated. In univariate analyses, we found that patients who were *AR* CN normal at baseline, then converted to *AR* CN gain at PD, had intermediate OS between those who were *AR* CN normal at baseline and remained normal at PD and those who were *AR* CN gain at baseline and remained gain. Patients changing *AR* CN from gain to normal were not included in the analyses because the group is only represented by two

Abbreviations: AR, androgen receptor; CN, copy number; CRPC, castration-resistant prostate cancer; PD, progression disease; OS, overall survival; PFS, progression-free survival; cfDNA, Cell free DNA; PSA, prostate-specific antigen; ALP, alkaline phosphatase; LDH, lactate dehydrogenase; CT, computed tomography; AR-V7, AR splice variant 7; CTC, circulating tumor cells; ctDNA, circulating tumor DNA.

TABLE 1 | Patient characteristics.

	Abi/Enza pre-docetaxel (*n* = 35)	Abi/Enza post-docetaxel (*n* = 38)	
	***N* (%)**	***N* (%)**	***p***
Age, years: median value (IQR)	72 (68–80)	75 (72–77)	0.557
Gleason score			
6–7	18 (52.9)	8 (25.8)	
8–10	16 (47.1)	23 (74.2)	0.027
Unknown/missing	1	7	
Metastastic sites			
Bone	18 (51.4)	34 (89.5)	0.0004
Visceral	2 (5.7)	12 (31.6)	0.005
Liver	1 (2.9)	3 (9.4)	0.342
Nodal	16 (45.7)	17 (44.7)	0.934
Previous abi or enza treatment			
No	35 (100)	28 (73.7)	
Yes	0	10 (26.3)	–
Previous cabazitaxel treatment			
No	35 (100)	35 (92.1)	
Yes	0	3 (7.9)	0.241
***AR* copy number**			
Normal	29 (82.9)	29 (76.3)	
Gain	6 (17.1)	9 (23.7)	0.492
Baseline ALP, U/L: median value (IQR)	88 (67–121)	109 (79–196)	0.129
<129	28 (80.0)	22 (57.9)	
≥129	7 (20.0)	16 (42.1)	0.044
Baseline LDH, U/L: median value (IQR)	163 (143–190)	179 (115–968)	0.047
<225	32 (91.4)	32 (84.2)	
≥225	3 (8.6)	6 (15.8)	0.482
Baseline NLR: median value (IQR)	2.49 (2.04–3.31)	2.41 (1.86–4.16)	0.904
<3	22 (62.9)	21 (55.3)	
≥3	13 (37.1)	17 (44.7)	0.513
Baseline Neutrophil: median value (IQR)	3,560 (3,090–5,090)	3,590 (2,850–4,960)	0.904
Baseline Lymphocyte: median value (IQR)	1,540 (1,090–1,761)	1,310 (1,050–1,740)	0.202
Baseline PSA, ng/mL: median value (IQR)	32.13 (6.80–68.38)	65.06 (19.76–182.10)	0.129

IQR, interquartile range; abi, abiraterone; enza, enzalutamide; AR, androgen receptor; ALP, alkaline phosphatase; LDH, lactate dehydrogenase; NLR, neutrophil to lymphocyte ratio; PSA, prostate specific antigen.

men. Particularly, we showed that patients changing *AR* CN from normal to gain had an intermediate median OS of 20.5 months (95% CI = 8.0–44.2) between patients with stable *AR* CN normal that presented a median OS of 27.3 months (95% CI = 21.9–34.4) and patients with stable *AR* CN gain with a median OS of 9.1 (95% CI = 3.8–14.5, $p < 0.0001$). The two patients changing *AR* CN from gain to normal presented an OS of 8.5 and 17.4 months, respectively. No significantly worse OS was observed for patients changing *AR* CN from normal to gain compared to patients with stable *AR* CN normal ($p = 0.318$, **Figure 1B**).

Patients changing *AR* CN from normal to gain status had a median PFS of 9.2 months (95% CI = 2.0–14.7), patients with stable *AR* CN normal presented a median PFS of 9.1 months (95% CI = 7.2–10.1) and patients with stable *AR* CN gain had a median PFS of 5.4 (95% CI = 3.6–6.5, $p = 0.0005$). The two patients changing *AR* CN from gain to normal presented a PFS of 8.5 and 3.8 months, respectively. No significantly worse PFS was observed for patients changing *AR* CN from normal to gain compared to patients with stable *AR* CN normal ($p = 0.551$) (**Figure 1C**).

Correlation analysis between *AR* CN changes and PSA change was performed and we did not found a statistically significant correlation, as shown in **Supplementary Table 1**. PSA change was defined as a PSA decline >50% from baseline at first radiological evaluation (after about 3 months from starting therapy) according to the Prostate Cancer Clinical Trials Working Group 3 guidelines. PSA decline was available for 66 patients and we did not consider the two patients changing *AR* CN from gain to normal. Interestingly, we found that all patients changing *AR* CN status from normal to gain (8) did not show PSA decline.

DISCUSSION

This study represents the first evidence of the impact of plasma *AR* CN changes from baseline to progression time point on clinical outcome of CRPC patients. We identified a low conversion rate of *AR* CN status, suggesting that, for most of patients, *AR* CN does not change under the pressure of abiraterone and enzalutamide. These results confirm those found by Romanel et al. (13) that showed that *AR* CN status in individual metastases does not noticeably change with treatment, but the impact on clinical outcome was not investigated.

We hypothesized that this could be challenging for physicians in helping treatment decision and possibly substituting therapy if *AR* CN change occurs during treatment, minimizing overtreatment. Our results showed that patients changing *AR* CN from normal to gain had intermediate median OS between patients with stable *AR* CN normal and patients with stable *AR* CN gain. This trend of intermediate prognosis was not observed for PFS, probably because *AR* CN was analyzed at the time of disease progression, impeding to impact on PFS itself. However, since the number of patients changing *AR* CN from normal to gain (9) was very low, additional validation is needed. Similarly, only 2 of the 15 *AR* CN gain patients became normal at PD, so it does not allow to identify the role of *AR* CN conversion in this setting of patients. Moreover, since both PFS and OS were not significantly different between patients with *AR* CN that changes from normal to gain and patients with stable *AR* CN normal, we hypothesized that the difference on clinical outcome depends on *AR* CN status at baseline. For this reason, we suggested that baseline assessment could be the most relevant time point to consider for *AR* CN status in therapeutic decision making.

Clinical utility of cfDNA biomarkers has emerged because of the impracticality of sampling bone metastatic tissue in CRPC patients. Circulating DNA is easy to obtain for serial

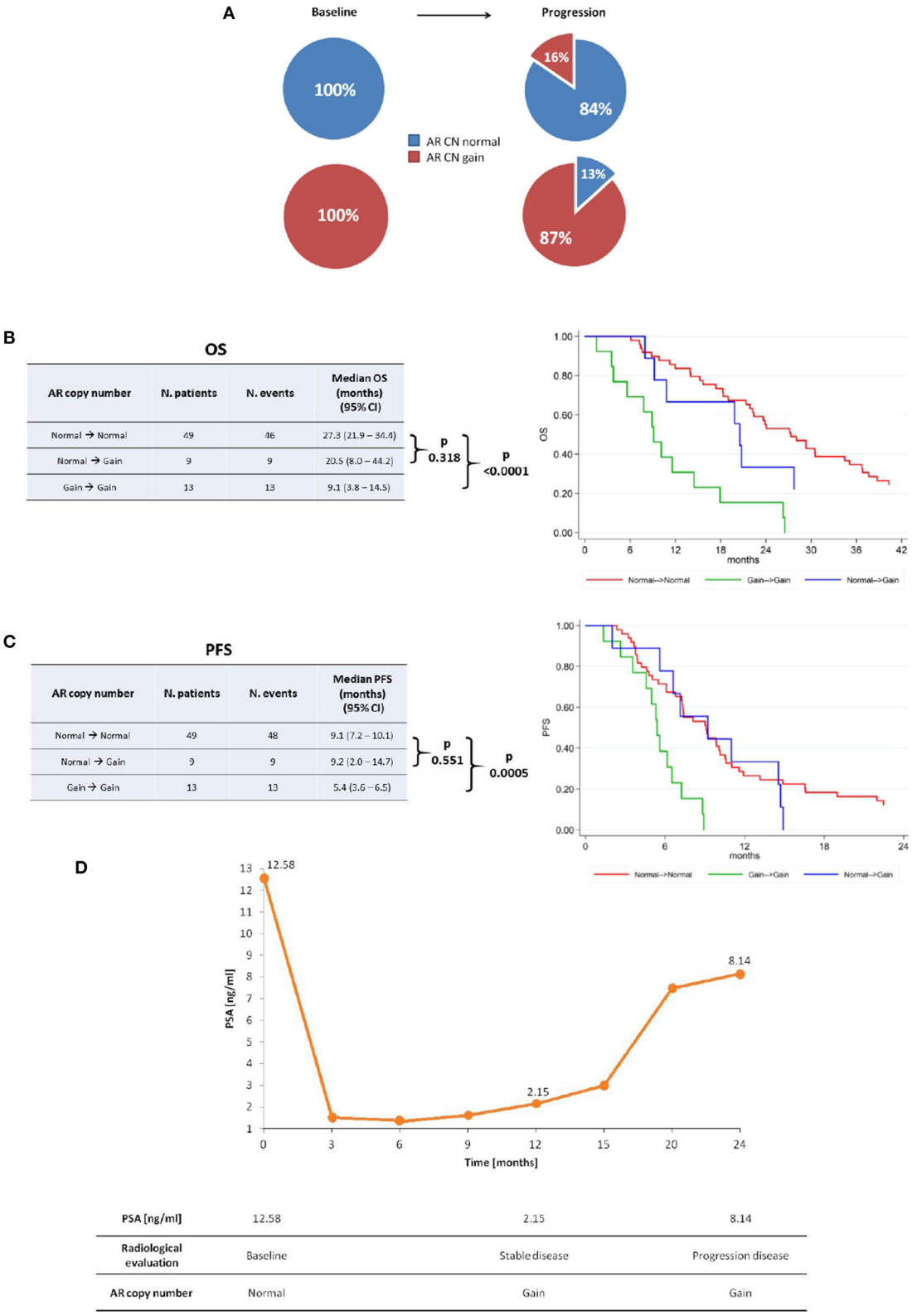

FIGURE 1 | *AR* copy number changes. **(A)** *AR* copy number changes from baseline to progression time point. Median OS **(B)** and PFS **(C)** of stable *AR* CN normal, *AR* CN changing from normal to gain, and stable *AR* CN gain patients with the corresponding Kaplan–Meier curves. **(D)** Representative case that changed *AR* CN from normal to gain at stable disease and remained gain at disease progression, even though PSA response occurred.

monitoring of tumor dynamics, allowing the recognition of tumor heterogeneity (15). Primary and acquired resistance to AR-targeted therapies has been associated with mutations or amplification of *AR* gene (8, 16–18) and the expression of AR splice variants (i.e., AR-V7) in circulating tumor cells (CTC) or in metastatic tissues (19, 20). Hörnberg et al. (20) found that high levels expression of AR-V7 in prostate cancer bone metastases correlates with particularly poor prognosis. Antonarakis et al. (21) showed that 14% of patients AR-V7 negative at their baseline CTC samples converted to AR-V7 positive during the course of treatment with abiraterone/enzalutamide or at the time of PD and demonstrated that these patients had intermediate clinical outcomes (PSA response rates, PFS) between AR-V7 negative patients that remained negative and AR-V7 positive patients who remained all positive (21). Changes in AR-V7 status (i.e., conversion from AR-V7 negative to positive during AR-targeted therapies and reversion from AR-V7 positive to negative during taxanes) highlight the potential role of AR-V7 as a dynamic marker (22). However, large cohorts studies are needed to better clarify the predictive ability of AR-V7, standardize sensitive, and cost-sustainable clinical laboratory assays for the measurement of patients AR variants (23).

Actually, it is unclear whether lethal phenotype derives from multiple foci with different genomic patterns that metastasize or it depends on a single clone that maintains dominance during the course of the disease. These mechanisms could select specific clones, shedding light on the biological processes underlying the conversion of *AR* CN status (from normal to gain or from gain to normal) during therapies (5).

In treatment-naïve patients, intra-tumoral heterogeneity increases as the tumor burden increases, and individual metastatic lesions are affected by their local microenvironment. CRPC cells modify themselves because of the presence of distinct clones selected by therapies, that could be a basis of treatment resistance (7, 24). Abiraterone acetate and enzalutamide were introduced into clinical practice to overcome AR signaling reactivation after androgen deprivation therapies (25, 26). Since treatment resistance mechanisms occurs, there is an urgent need to identify the predictive and prognostic biomarkers for treatment selection in CRPC.

The present study represents the first evidence of the impact of plasma *AR* CN changes during abiraterone and enzalutamide treatments. We showed that conversion rate of *AR* CN was low and that CRPC patients changing *AR* CN status from baseline to progression time point had intermediate OS. Moreover, we suggested that *AR* CN evaluation at baseline could be the most informative for clinical outcome of CRPC patients treated with abiraterone or enzalutamide. The major limitations of the study included the relatively small number of patients enrolled and the retrospective nature of the study. Moreover, we evaluated *AR* CN status at baseline and progression time points, but *AR* CN at first radiological evaluation after 3 months of therapy is needed, as it represents the most clinically significant time point, according to Prostate Cancer Clinical Trials Working Group 3 guidelines. Finally, we did not distinguished circulating tumor DNA (ctDNA) from normal DNA present in cfDNA that potentially affects the detection of *AR* gain in patients with a low proportion of ctDNA. Larger prospective biomarkers study is warranted.

DATA AVAILABILITY STATEMENT

The raw data supporting the conclusions of this article will be made available by the authors, without undue reservation.

ETHICS STATEMENT

The studies involving human participants were reviewed and approved by COMITATO ETICO della Romagna. The patients/participants provided their written informed consent to participate in this study.

AUTHOR CONTRIBUTIONS

Conceptualization: GG and VC. Methodology, writing—original draft preparation, and writing—review and editing: GG. Software: SG. Validation: UD, VC, and ES. Formal analysis: ES. Investigation: CL. Resources: GS. Data curation: AA. Visualization: CC. Supervision: UD. Project administration: VC. All authors have read and agreed to the published version of the manuscript.

ACKNOWLEDGMENTS

The authors would like to thank Alessia Filograna at Istituto Scientifico Romagnolo per lo Studio e la Cura dei Tumori for her nursing support.

SUPPLEMENTARY MATERIAL

The Supplementary Material for this article can be found online at: https://www.frontiersin.org/articles/10.3389/fonc.2020.567809/full#supplementary-material

REFERENCES

1. de Bono JS, Logothetis CJ, Molina A, Fizazi K, North S, Chu L, et al. Abiraterone and increased survival in metastatic prostate cancer. *N Engl J Med.* (2011) 364:1995–2005. doi: 10.1056/NEJMoa1014618
2. Ryan CJ, Smith MR, de Bono JS, Molina A, Logothetis CJ, de Souza P, et al. Abiraterone in metastatic prostate cancer without previous chemotherapy. *N Engl J Med.* (2013) 368:138–48. doi: 10.1056/NEJMx130004
3. Beer TM, Armstrong AJ, Rathkopf DE, Loriot Y, Sternberg CN, Higano CS, et al. Enzalutamide in metastatic prostate cancer before chemotherapy. *N Engl J Med.* (2014) 371:424–33. doi: 10.1056/NEJMoa1405095
4. Scher HI, Fizazi K, Saad F, Taplin ME, Sternberg CN, Miller K, et al. Increased survival with enzalutamide in prostate cancer after chemotherapy. *N Engl J Med.* (2012) 367:1187–97. doi: 10.1056/NEJMoa1207506
5. Diehl F, Li M, Dressman D, He Y, Shen D, Szabo S, et al. Detection and quantification of mutations in the plasma of patients with colorectal tumors. *Proc Natl Acad Sci U S A.* (2005) 102:16368–73. doi: 10.1073/pnas.0507904102

6. Diaz LA Jr, Bardelli A. Liquid biopsies: genotyping circulating tumor DNA. *J Clin Oncol.* (2014) 32:579–86. doi: 10.1200/JCO.2012.45.2011
7. Gundem G, Van Loo P, Kremeyer B, Alexandrov LB, Tubio JMC, Papaemmanuil E1, et al. The evolutionary history of lethal metastatic prostate cancer. *Nature.* (2015) 520:353–7. doi: 10.1038/nature14347
8. Wyatt AW, Azad AA, Volik SV, Annala M, Beja K, McConeghy B, et al. Genomic alterations in cell-free DNA and enzalutamide resistance in castration-resistant prostate cancer. *JAMA Oncol.* (2016) 2:1598–606. doi: 10.1001/jamaoncol.2016.0494
9. Mehra N, Dolling D, Sumanasuriya S, Christova R, Pope L, Carreira S, et al. Plasma cell-free DNA concentration and outcomes from taxane therapy in metastatic castration-resistant prostate cancer from two phase III trials (FIRSTANA and PROSELICA). *Eur Urol.* (2018) 74:283–91. doi: 10.1016/j.eururo.2018.02.013
10. Scher HI, Sawyers CL. Biology of progressive, castration-resistant prostate cancer: directed therapies targeting the androgen-receptor signaling axis. *J Clin Oncol.* (2005) 23:8253–61. doi: 10.1200/JCO.2005.03.4777
11. Dai C, Heemers H, Sharifi N. Androgen signaling in prostate cancer. *Cold Spring Harb Perspect Med.* (2017) 7:a030452. doi: 10.1101/cshperspect.a030452
12. Attard G, Parker C, Eeles RA, Schröder F, Tomlins SA, Tannock I, et al. Prostate cancer. *Lancet.* (2016) 387:70–82. doi: 10.1016/S0140-6736(14)61947-4
13. Romanel A, Gasi Tandefelt D, Conteduca V, Jayaram A, Casiraghi N, Wetterskog D, et al. Plasma AR and abiraterone-resistant prostate cancer. *Sci Transl Med.* (2015) 7:312re10. doi: 10.1126/scitranslmed.aac9511
14. Scher HI, Morris MJ, Stadler WM, Higano C, Basch E, Fizazi K, et al. Trial design and objectives for castration-resistant prostate cancer: updated recommendations from the prostate cancer clinical trials working group 3. *J Clin Oncol.* (2016) 34:1402–18. doi: 10.1200/JCO.2015.64.2702
15. Conteduca V, Wetterskog D, Scarpi E, Romanel A, Gurioli G, Jayaram A, et al. Plasma tumour DNA as an early indicator of treatment response in metastatic castration-resistant prostate cancer. *Br J Cancer.* (2020). doi: 10.1038/s41416-020-0969-5. [Epub ahead of print].
16. Conteduca V, Wetterskog D, Sharabiani MTA, Grande E, Fernandez-Perez MP, Jayaram A, et al. Androgen receptor gene status in plasma DNA associates with worse outcome on enzalutamide or abiraterone for castration-resistant prostate cancer: a multi-institution correlative biomarker study. *Ann Oncol.* (2017) 28:1508–16. doi: 10.1093/annonc/mdx155
17. Ulz P, Belic J, Graf R, Auer M, Lafer I, Fischereder K, et al. Whole-genome plasma sequencing reveals focal amplifications as a driving force in metastatic prostate cancer. *Nat Commun.* (2016) 7:12008. doi: 10.1038/ncomms12008
18. Azad AA, Volik SV, Wyatt AW, Haegert A, Le Bihan S, Bell RH, et al. Androgen receptor gene aberrations in circulating cell-free DNA: biomarkers of therapeutic resistance in castration-resistant prostate cancer. *Clin Cancer Res.* (2015) 21:2315–24. doi: 10.1158/1078-0432.CCR-14-2666
19. Scher HI, Lu D, Schreiber NA, Louw J, Graf RP, Vargas HA, et al. Association of AR-V7 on circulating tumor cells as a treatment specific biomarker with outcomes and survival in castration-resistant prostate cancer. *JAMA Oncol.* (2016) 2:1441–9. doi: 10.1001/jamaoncol.2016.1828
20. Hörnberg E, Ylitalo EB, Crnalic S, Antti H, Stattin P, Widmark A, et al. Expression of androgen receptor splice variants in prostate cancer bone metastases is associated with castration-resistance and short survival. *PLoS One.* (2011) 6:e19059. doi: 10.1371/journal.pone.0019059
21. Antonarakis ES, Lu C, Wang H, Luber B, Nakazawa M, Roeser JC, et al. AR-V7 and resistance to enzalutamide and abiraterone in prostate cancer. *N Engl J Med.* (2014) 371:1028–38. doi: 10.1056/NEJMoa1315815
22. Nakazawa M, Lu C, Chen Y, Paller CJ, Carducci MA, Eisenberger MA, et al. Serial blood-based analysis of AR-V7 in men with advanced prostate cancer. *Ann Oncol.* (2015) 26:1859–65. doi: 10.1093/annonc/mdv282
23. Ciccarese C, Santoni M, Brunelli M, Buti S, Modena A, Nabissi M, et al. AR-V7 and prostate cancer: the watershed for treatment selection? *Cancer Treat Rev.* (2016) 43:27–35. doi: 10.1016/j.ctrv.2015.12.003
24. Carreira S, Romanel A, Goodall J, Grist E, Ferraldeschi R, Miranda S, et al. Tumor clone dynamics in lethal prostate cancer. *Sci Transl Med.* (2014) 6:254ra125. doi: 10.1126/scitranslmed.3009448
25. Tran C, Ouk S, Clegg NJ, Chen Y, Watson PA, Arora V, et al. Development of a second-generation antiandrogen for treatment of advanced prostate cancer. *Science.* (2009) 324:787–90. doi: 10.1126/science.1168175
26. Attard G, Belldegrun AS, de Bono JS. Selective blockade of androgenic steroid synthesis by novel lyase inhibitors as a therapeutic strategy for treating metastatic prostate cancer. *BJU Int.* (2005) 96:1241–6. doi: 10.1111/j.1464-410X.2005.05821.x

Conflict of Interest: GG has received travel support from Sanofi. VC has received speaker honoraria or travel support from Astellas, Janssen-Cilag, and Sanofi-Aventis, and has received consulting fee from Bayer. CL has received honoraria for consulting (advisory board) from Bristol-Myers Squibb and Janssen-Cilag. UD has served as consultant/advisory board member for Astellas, Bayer, BMS, Ipsen, Janssen, Merck, Pfizer, Sanofi, and has received travel support from BMS, Ipsen, Janssen, Pfizer, and has received research funding from AstraZeneca, Roche, Sanofi (Inst).

The remaining authors declare that the research was conducted in the absence of any commercial or financial relationships that could be construed as a potential conflict of interest.

The reviewer FM declared past co-authorships with the authors to the handling editor.

frontiers in Oncology

ORIGINAL RESEARCH
published: 08 October 2020
doi: 10.3389/fonc.2020.572895

Detection of EGFR Mutations in cfDNA and CTCs, and Comparison to Tumor Tissue in Non-Small-Cell-Lung-Cancer (NSCLC) Patients

*Haiyan E. Liu[1†], Meghah Vuppalapaty[1†], Charles Wilkerson[1], Corinne Renier[1], Michael Chiu[1], Clementine Lemaire[1], James Che[1], Melissa Matsumoto[2], James Carroll[3], Steve Crouse[1], Violet R. Hanft[4], Stefanie S. Jeffrey[4], Dino Di Carlo[2,5,6], Edward B. Garon[3,6], Jonathan Goldman[3,6] and Elodie Sollier[1]**

[1] Vortex Biosciences, Inc., Pleasanton, CA, United States, [2] Department of Bioengineering, University of California, Los Angeles, Los Angeles, CA, United States, [3] Department of Medicine, David Geffen School of Medicine at UCLA, Los Angeles, CA, United States, [4] Department of Surgery, Stanford University School of Medicine, Stanford, CA, United States, [5] California NanoSystems Institute, Los Angeles, CA, United States, [6] UCLA Jonsson Comprehensive Cancer Center, Los Angeles, CA, United States

Lung cancer is the leading cause of cancer-related mortality worldwide. Epidermal growth factor receptor (EGFR) tyrosine kinase inhibitor (TKI) therapies, based on the evaluation of *EGFR* mutations, have shown dramatic clinical benefits. *EGFR* mutation assays are mainly performed on tumor biopsies, which carry risks, are not always successful and give results relevant to the timepoint of the assay. To detect secondary *EGFR* mutations, which cause resistance to 1st and 2nd generation TKIs and lead to the administration of a 3rd generation drug, effective and non-invasive monitoring of *EGFR* mutation status is needed. Liquid biopsy analytes, such as circulating tumor cells (CTCs) and circulating tumor DNA (cfDNA), allow such monitoring over the course of the therapy. The aim of this study was to develop and optimize a workflow for the evaluation of cfDNA and CTCs in NSCLC patients all from one blood sample. Using Vortex technology and EntroGen ctEGFR assay, *EGFR* mutations were identified at 0.5 ng of DNA (∼83 cells), with a sensitivity ranging from 0.1 to 2.0% for a total DNA varying from 25 ng (∼4 CTCs among 4000 white blood cells, WBCs) to 1 ng (∼4 CTCs among 200 WBCs). The processing of plasma-depleted-blood provided comparable capture recovery as whole blood, confirming the possibility of a multimodality liquid biopsy analysis (cfDNA and CTC DNA) from a single tube of blood. Different anticoagulants were evaluated and compared in terms of respective performance. Blood samples from 24 NSCLC patients and 6 age-matched healthy donors were analyzed with this combined workflow to minimize blood volume needed and sample-to-sample bias, and the *EGFR* mutation profile detected from CTCs and cfDNA was compared to matched tumor

OPEN ACCESS

Edited by:
Elisabetta Rossi, University of Padua, Italy

Reviewed by:
Hanqing Liu, Jiangsu University, China
Azhar Ali, National University of Singapore, Singapore

***Correspondence:**
Elodie Sollier
elodie@vortexbiosciences.com

† These authors have contributed equally to this work

Specialty section:
This article was submitted to Cancer Molecular Targets and Therapeutics, a section of the journal Frontiers in Oncology

Received: *15 June 2020*
Accepted: *02 September 2020*
Published: *08 October 2020*

Citation:
Liu HE, Vuppalapaty M, Wilkerson C, Renier C, Chiu M, Lemaire C, Che J, Matsumoto M, Carroll J, Crouse S, Hanft VR, Jeffrey SS, Di Carlo D, Garon EB, Goldman J and Sollier E (2020) Detection of EGFR Mutations in cfDNA and CTCs, and Comparison to Tumor Tissue in Non-Small-Cell-Lung-Cancer (NSCLC) Patients. Front. Oncol. 10:572895. doi: 10.3389/fonc.2020.572895

tissues. Despite the limited size of the patient cohort, results from this non-invasive *EGFR* mutation analysis are encouraging and this combined workflow represents a valuable means for informing therapy selection and for monitoring treatment of patients with NSCLC.

Keywords: Vortex technology, circulating tumor cell, total liquid biopsy, epidermal grow factor receptor, EGFR mutation analysis, Non-small cell carcinoma, circulating tumor biomarkers, circulating free DNA (cfDNA)

INTRODUCTION

Lung cancer is the leading cause of cancer deaths in the United States, among both men and women. An estimated 135,270 deaths from lung cancer occurred in 2019 (1). Non-Small Cell Lung Cancers (NSCLC), which include adenocarcinoma, squamous cell carcinoma, large cell carcinoma and large cell neuroendocrine tumors, account for ∼85% of primary lung cancers (2). Most NSCLC patients present with advanced or metastatic disease at diagnosis. With recent evidence showing that 10–30% of the NSCLC patients present "actionable" mutations of Epidermal Growth Factor Receptor (*EGFR*) (3), tremendous advances have been made in the treatment of these patients in recent years, by directly targeting these specific mutations (4).

Following the approval of the first *EGFR* tyrosine kinase inhibitor (TKI) gefitinib in 2003, other TKIs such as afatinib, erlotinib, dacomitinib, and osimertinib have been approved, from which many patients have benefited (**Figure 1**). Some of these drugs are now used as the first-line therapy for specific advanced NSCLCs. *EGFR* is a cellular transmembrane glycoprotein, consisting of (i) an extracellular epidermal growth factor (EGF)-binding-domain, and (ii) an intracellular tyrosine kinase domain, which when activated, triggers several signal transduction cascades that ultimately control cellular growth and proliferation (5). Several studies have shown that distinct mutation patterns in *EGFR*, including exon 19 deletion and exon 21 L858R substitution, were associated with positive treatment outcomes following first-line TKI therapy with afatinib, erlotinib, gefitinib and dacomitinib. These drugs can be administrated alone or, for a better overall survival, in combination with other treatment options. For example, the RELAY trial has demonstrated that a dual blockade of the *EGFR* and VEGF pathways (i.e., ramucirumab plus erlotinib) in *EGFR*-mutated untreated metastatic NSCLC patients provided superior progression-free survival compared to blocking the *EGFR* pathway only (placebo plus erlotinib) (6). In other studies, *EGFR* combined with cytotoxic chemotherapy (gefitinib plus carboplatin and pemetrexed) was identified as more effective than the *EGFR* TKI alone (7, 8). However, most patients eventually develop *EGFR*-TKI acquired resistance after a few months, due, partly, to the emergence of a new mutation known as *EGFR* T790M. Osimertinib (Tagrisso) is a second-line TKI that has demonstrated selectivity for T790M-resistant mutation in patients with advanced NSCLC and disease progression after prior *EGFR*-TKI therapy (**Figure 1**). Osimertinib can even be used as a frontline TKI, as demonstrated by the FLAURA trial (9). Therefore, the monitoring of these actionable mutations throughout the patient care is fundamental for the selection of suitable TKI treatment.

For most of clinical cases, tumor biopsies are used to evaluate the *EGFR* mutations and guide the patient treatment. However, lung tissue biopsies through needle biopsy or bronchoscopies may be painful, expensive, potentially risky for the patients, and not always successful (10). Sometimes, mutation profiling can be inaccurate due to inter or intra-tumoral heterogeneity. In some cases, re-biopsy may be required to obtain additional molecular information on the patient tumor. For monitoring the mutations over the course of the treatment, some patients with recurrence and poor overall status are not fit enough to have multiple biopsies. Thus, the capture of tumoral genomic content in bodily fluids such as blood, has been evaluated as an alternative for tissue biopsy (11). These so-called "liquid biopsies," i.e., cell-free circulating tumor DNA (cfDNA) and circulating tumor cells (CTCs) are the main sources of tumor genomic material present in the blood and have been investigated for non-invasive detection and monitoring of tumors (12). Both liquid biopsies provide non-invasive ways to repeatedly sample cancer tumor(s) and set-up an *EGFR* mutation profiling to adjust treatment as the cancer evolves. Multiple studies have also reported the use of cfDNA or CTCs to assess the prognosis and to guide the treatment of NSCLC patients (13–15). Altogether, non-invasive liquid biopsies enable an ongoing evaluation of the NSCLC (16), to assess the cancer spread, to monitor the effects of the treatment (17, 18) and forewarn the physicians for possible recurrences (19), while also providing clues on the reasons for treatment inefficiency and cancer resistance (10).

VTX-1 Liquid Biopsy System (Vortex Biosciences) is a microfluidic label-free CTC isolation system, capturing CTCs based on their physical characteristics such as size and deformability instead of their surface markers (20–22). VTX-1 provides intact CTCs with high recovery and purity, alongside with a simple and fully automated process. This technology was described elsewhere in detail (20) and applied to various cancer types such as metastatic colorectal, breast, prostate and non-small-cell lung cancer (23–26). The blood sample can be depleted of its plasma first and further processed with the VTX-1 to recover the CTCs, thereby enabling the analysis of *EGFR* gene mutations in both CTCs and cfDNA from a single tube of blood.

The purpose of this study was to develop and characterize an integrated workflow for the profiling of *EGFR* mutations in NSCLC patients from cfDNA and CTCs from a single tube of blood. Different blood collection tubes were assessed in view of blood sample transportation and shipping to guarantee an optimal CTC recovery and DNA preservation. Finally, this workflow was applied to lung cancer patient blood samples as

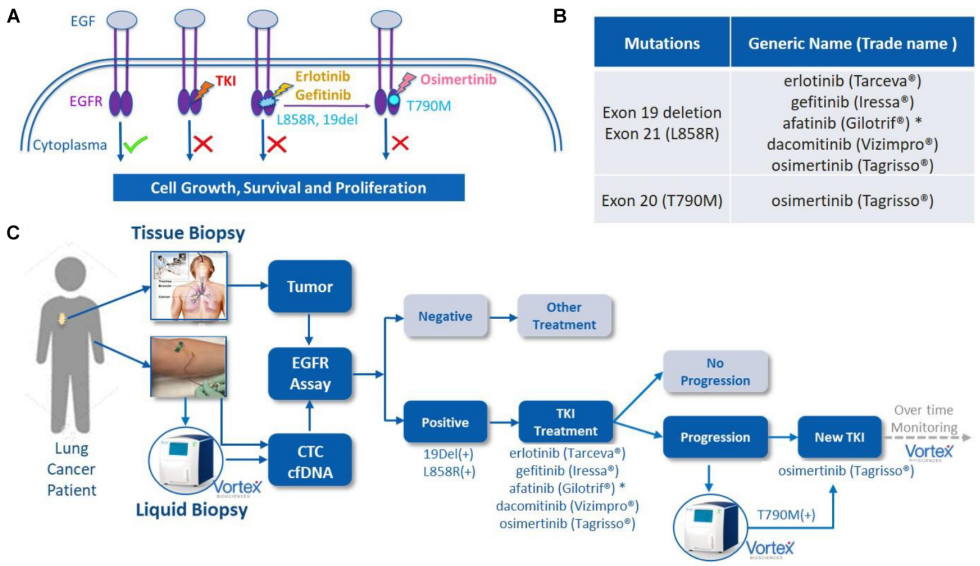

FIGURE 1 | *EGFR* mutations, *EGFR* tyrosine kinase inhibitor (TKI) treatment and liquid biopsies. **(A)** EGF/*EGFR*, *EGFR* mutations and TKIs. When EGF binds to the extracellular binding domain of *EGFR*, the intracellular tyrosine kinase triggers several signal transduction cascades to regulate the cellular growth and proliferation. This effect can be blocked by TKIs, such as afatinib or erlotinib among others, when mutations of 19 Del or L858R are present in this kinase domain. A resistance often occurs due to the development of T790M mutation, which can then be blocked by second line TKI osimertinib. Original figure. **(B)** List of currently FDA approved TKIs. **(C)** The potential role of VTX-1 Liquid Biopsy System in the monitoring and treatment of lung cancer. By providing CTCs with high recovery, high purity, and with a simple and fully automated process, the VTX-1 enables an ongoing and non-invasive monitoring of *EGFR* mutations throughout the disease. * afatinib is approved in some rarer *EGFR* mutations as well. The pictures of Vortex instrument and the blood draw have been provided by Vortex Biosciences with the appropriate permissions. The picture of the thoracic biopsy has been revised from https://www.semanticscholar.org/paper/Chapter-2-Review-on-Image-Guided-Lung-Biopsy-Rizqie-Yusof/41e9a8569c1a3c89d4331f766215e4d8299e34cd.

a preliminary validation. Ultimately, we compared the results of this combined liquid biopsy to the tumor tissue biopsy when available, in order to further investigate the feasibility of using non-invasive *EGFR* mutation analysis as a potential tool for monitoring treatment and medication guidance of NSCLC patients (**Figure 1**).

MATERIALS AND METHODS

Cell Lines

Human NSCLC cell lines A549 (ATCC® CCL-185™, *EGFR* wild type), H1975 (ATCC® CRL-5908™, *EGFR* exon 20 T790M, and L858R exon 21 L858R mutations) and HCC827 (ATCC® CRL-2868™, *EGFR* exon 19 deletion), as well as MCF7 breast cancer cell line (ATCC® HTB22™) were used in this study. The cells were grown at 37°C and 5% CO2, in RPMI 1640 (H1975 and HCC827 cells), F-12K (A549 cells) or RPMI1640 + GlutaMax (MCF7 cells) medium (Gibco®), respectively, supplemented with 10% fetal bovine serum (HyClone) and 1% Penicillin-Streptomycin (Corning) and 0.01 mg/ml Human Recombinant Insulin for MCF7 cells.

Direct Sanger Sequencing was performed to confirm the mutation status of each lung cancer cell line (**Supplementary Figure 1**). To do so, DNA was extracted from the cells using the QIAamp DNA Micro Kit (Qiagen). The extracted DNA was quantified by Qubit Fluorometer (Thermo Fisher Scientific) and then subjected to PCR directly using primers against the *EGFR* exons 19, 20, and 21, covering hotspot regions of 19 deletion, T790M and L858R mutations (**Supplementary Figure 2**). After a control step with E-Gel Electrophoresis (Thermo Fisher Scientific) and Qubit for both PCR specificity and PCR product quantity, the PCR products were purified using the QIAquick PCR Purification Kit (Qiagen) and Sanger sequenced on a 3730XL DNA Analyzer (Elim Biopharmaceuticals). ABI chromatogram files were analyzed using the BioEdit sequence alignment editor.

Donor Recruitment and Blood Collection

(i) For assay development and characterization using spiked cell lines, healthy volunteers were recruited according to a protocol with informed consent, as approved by the Institutional Review Board (protocol #5630) from Stanford University School of Medicine or through the Stanford Blood Center. Depending on the experiment, peripheral blood was collected into different blood collection tubes (BCTs): EDTA tube (BD Vacutainer®), CellSave Preservation Tubes (Janssen diagnostics LLC.), Streck Cell-Free DNA (Streck Inc.) or LBgard (Biomatrica). Immediately after the draw, the blood tubes were gently inverted 10 times, transported at room temperature (RT), and processed with Vortex technology.

(ii) For EGFR assay validation with patient samples, blood samples from 24 NSCLC patients and six age-matched healthy donors were recruited at David Geffen School of Medicine,

University of California, Los Angeles (UCLA), according to the clinical study protocol UCLA IRB #11-001798. Before being enrolled into the study, all donors provided a written informed consent. All blood samples were deidentified to the persons doing the blood processing and *EGFR* assays. Donors' age, diagnosis, disease stage and treatment history are summarized in the **Table 1**. Blood was collected in LBgard tubes, gently inverted 10 times immediately after the draw, and shipped in an insulated box (Saf-T-Pak #STP-302) with gel packs at room temperature (RT) from UCLA to Vortex headquarters, where they were processed within 1 h of reception.

Blood Sample Processing and Workflow

For assay validation with patient samples, blood was processed following the workflow described in **Figure 2**. In general, two tubes of blood were collected from each donor (healthy donors and patients), which corresponds to 16 mL of blood at the most, depending on the blood collection tube, the nurse, the donor veins, and the drawing event itself. From the two tubes of blood, the plasma was separated to isolate cfDNA. The plasma-depleted blood (PDB) was processed through Vortex technology to isolate CTCs. Plasma cfDNA and CTCs were analyzed for *EGFR* mutations.

Plasma Separation

To separate the plasma, the blood tube was centrifuged at 1900 *g*, RT for 10 min with no brake. The plasma layer (top) was gently aspirated without disturbing the buffy coat and RBC layers underneath and transferred to a 15mL-Falcon tube. The plasma was further centrifuged at 3700 *g*, 4°C, for 15 min with slow deceleration and then transferred to a new tube and stored at −80°C until cfDNA extraction. The plasma-depleted-blood was resuspended to the original blood sample volume with 1X PBS (Gibco #20012043) and processed for CTC enrichment.

Cancer Cell Enrichment From Blood Samples

(i) For spiking experiments, 2 to 4 mL of healthy whole blood or plasma-depleted blood (depending on the experiments) were diluted 10× with PBS. About 500 cells were spiked per run for "high spiking" experiments, while 50–200 cells were spiked per run for "low spiking" experiments. Cancer cells were isolated with Vortex technology, using either a manual platform described previously (23), or the VTX-1 Liquid Biopsy System (Vortex Biosciences) (20).

(ii) For patient samples, Isolated cells were collected into an 8-well strip for downstream fixation, immunofluorescence staining, imaging and enumeration, followed by DNA extraction and *EGFR* mutation profiling.

Immunofluorescence Staining and Cell Enumeration

Cells enriched with Vortex technology were collected in either untreated 96 well plates (Greiner CELLSTAR® #655180) or 96 Well (1 × 8 Strip Well) Clear Flat Bottom Polystyrene TC-Treated Microplates (Corning #9102). After a centrifugation (600 *g*, 1 min, RT) and aspiration of the supernatant, cells were fixed with 2% PFA (Electron Microscopy Sciences #157-4) for 10 min, permeabilized with 0.2% volume/volume Triton X-100 (Research Products International Corp) and 5% Goat Serum (Invitrogen) for 7 min, blocked with 10% Goat Serum for 30 min, and immunostained.

(i) For the experiments assessing the different blood collection tubes, immunostaining was performed using antibodies directed against cytokeratins (CK) (FITC, Clone CAM 5.2, BD Biosciences #347653; Clone CK3-6H5 Miltenyi Biotec #130080101), against CD45 (PE, Clone HI30, BD Pharmingen #555483) and counterstained with DAPI (Molecular Probes #D3571).

(ii) For all EGFR spiking experiments and patient samples, cells were stained with anti-CK FITC (Clone CAM 5.2, BD Biosciences, #347653; Clone CK3-6H5, MACS Miltenyi, #130-080-101; Clone AE1/AE3, eBioscience, #53-9003-82), anti-Vimentin AF647 (Clone V9, Abcam, #195878), anti-N-Cadherin AF647 (Clone EPR1791-4, Abcam, #195186) and anti-CD45 PE (Clone HI30, BD Biosciences, #555483) and counterstained with DAPI. H1975 cells and human WBCs were used as staining controls for all staining experiments.

The cells were imaged at 10× magnification (Axio Observer Z1, Zeiss) and enumerated using the Zen2 software (Zeiss). (i) For spike-in experiments, DAPI + /CK + /CD45- cells were identified as cancer cells while DAPI + /CK-/CD45 + cells were counted as WBCs. Capture efficiency was calculated as the number of cancer cells recovered over the total number of cancer cells spiked into the blood. Capture purity was calculated as the number of cancer cells isolated over the total number of cells collected, i.e., cancer cells and WBCs. (ii) For patient samples, putative CTCs were identified using the criteria described previously (21). Basically, potential CTCs were identified as nucleated cells (DAPI +) that are CD45- and either CK + /Vim-/ NCad-, CK + /Vim + /NCad + or CK-/Vim + /NCad + . WBCs were identified as nucleated cells (DAPI +) that are CK- and CD45 + . Cell populations were documented and the number of CTCs/mL of whole blood calculated.

For complimentary analysis, the level of cell debris can be evaluated. Following cell immunofluorescence staining, collection wells are entirely imaged with 10X magnification, both with the adequate fluorescent channels and brightfield channels. The debris are then very clearly recognizable: a qualitative and visual debris assessment can thus be defined while scanning through the wells.

DNA Extraction and Quantification

(i) cfDNA from plasma was extracted using the QIAamp Circulating Nucleic Acid Kit (Qiagen #55114). Thawed plasma was lysed using buffer ACL and Proteinase K at 60°C for 30 min and then mixed with buffer ACB to enable cfDNA binding onto the column. The column was then washed and cfDNA was eluted in 50-100 μL water.

(ii) DNA from fixed and stained cells was extracted using QIAamp DNA Micro kit (Qiagen) with a modified protocol as described previously (27). Briefly, the well-plates were centrifuged at 250 *g* for 2 min and the supernatant from each well was carefully removed, leaving behind ∼50 μL per well. Tissue

TABLE 1 | Clinical samples information.

Donor ID	Age	Histology	Stage	Treatment (years)
PA01	60–65	Adenocarcinoma	IV	afatinib (2016); erlotinib (2017 to time of blood collection)
PA02	75–80	Adenocarcinoma	IIIB	erlotinib (2010; 2014; 2016)
PA03.1	55–60	Adenocarcinoma	IV	Anti-PD1 (2016); Chemo (2017)
PA03.2				
PA03.3				
PA04.1	30–35	Squamous	IV	Anti-PD1 (2017)
PA04.2				
PA05.1	70–75	Adenocarcinoma	IV	Anti-PD1 and thoracentesis (2016)
PA05.2				
PA06.1	60–65	Adenocarcinoma	IV	erlotinib (2015); osimertinib (2016)
PA06.2				
PA07	65–70	Adenocarcinoma	IV	N/A
PA08	55–60	Adenocarcinoma	IA	erlotinib (2011–2015); rociletinib (2015); osimertinib (2015–2017); Chemo (2017)
PA09	60–65	Adenocarcinoma	IV	No treatment started at the time of blood collection
PA10	90–95	Adenocarcinoma	IV	No treatment started at the time of blood collection
PA11	55–60	Adenocarcinoma	IV	erlotinib and ramucirumab (2016–2017)
PA12	75–80	Adenocarcinoma	IV	erlotinib (2015–2016); osimertinib (2016–2017); Chemo (2017)
PA13	60–65	Adenocarcinoma	IV	No treatment started at the time of blood collection
PA14	80–85	Adenocarcinoma	IV	taxotere/carboplatin/avastin (2015); nivolumab (2016); abraxane (2016); PD (2017)
PA15	70–75	Adenocarcinoma	IV	erlotinib (2014); rociletinib (2015–2016); osimertinib (2016–2017); rucaparib (2017); pembrolizumab (time of blood collection)
PA16	45–50	Adenocarcinoma	IV	erlotinib (2018); osimertinib (2018 to time of blood collection)
PA17	45–50	Adenocarcinoma	IIIB–IV	Untreated
PA18	65–70	Adenocarcinoma	IV	erlotinib (2012–2013); rociletinib (2013–2016); osimertinib (2016–2018); PD (2018)
PA19	60–65	Adenocarcinoma	IV	pembrolizumab (2014 to time of blood collection)
PA20	70–75	Adenocarcinoma	IV	erlotinib (2017); osimertinib (2017 to time of blood collection)
PA21	55–60	Adenocarcinoma	IV	osimertinib (2016–2017); carboplatin/pemetrexed/pembrolizumab (2017); osimertinib (2017-time of blood collection), PD (2018)
PA22	50–55	Adenocarcinoma	IV	carbo/alimta (2015); erlotinib (2015–2017); osimertinib (2017); Avastin (2017); erlotinib (2017); osimertinib (2018 to time of blood collection)
PA23	80–85	Adenocarcinoma	IV	Astellas SOLAR trial (2017); erlotinib (2017)
PA24	65–70	Mixed	IV	carbo/taxol (2017); durvalumab (2017); prednisone (2018)
HD01	35–40	Healthy		
HD02	65–70	Healthy		
HD03	40–45	Healthy		
HD04	45–50	Healthy		
HD05	35–40	Healthy		

For EGFR assay validation, blood samples were collected from NSCLC patients (PA) and healthy donors (HD) and blinded for the user before processing. A total of 35 samples were collected, including 29 samples from 24 unique patients and 6 healthy donor samples. Patients PA03, PA04, PA05, and PA06 had serial blood draws, as indicated by the numbering.

lysis buffer ATL and proteinase K were added and incubated overnight at 60°C. Then, the lysate was transferred from the well-plate to microcentrifuge tubes. Lysis buffer AL was added to help the binding of the DNA in the lysate onto the QiaAmp column. The loaded column was then washed with buffers AW1 and AW2, the bound DNA was eluted in 25 μL of water.

(iii) DNA Quantification. When the DNA yield was expected to be high, such as for the DNA extracted from cell lines, DNA was quantified using Qubit™ 3.0 Fluorometer (Thermo Fisher) and Qubit® dsDNA HS Assay Kit (Thermo Fisher). To quantify the DNA extracted from a low number of cells, a more sensitive and accurate method was needed. Therefore, an absolute quantitative PCR was performed using 7500 Fast Real-Time PCR system (Applied Biosystems®) and human long interspersed nuclear element-1 (hLINE-1) as the targeted gene (Forward primer: 5′-TCACTCAAAGCCGCTCAACTAC-3′ and Reverse primer: 5′-TCTGCCTTCATTTCGTTATGTACC-3′) (28). Serial dilutions of normal human genomic reference DNA (Roche Diagnostics Corporation) were used as standards.

Multiplex qPCR-based *EGFR* Mutation Detection

EGFR mutation profiling was performed on cfDNA and CTC DNA samples using an ultra-sensitive multiplex qPCR-based ctEGFR kit (EntroGen), which detects L858R mutation in Exon 21, T790M mutation in Exon 20, and 48 different deletions in Exon 19. This commercial kit has been designed and validated

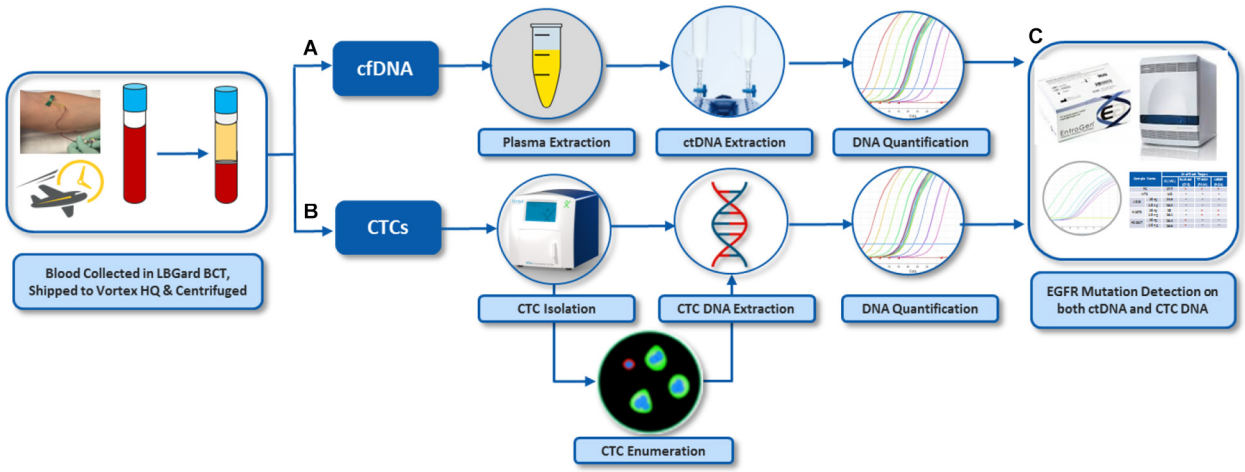

FIGURE 2 | Overall workflow for *EGFR* assay on both cfDNA and CTCs from the same blood samples. **(A)** Plasma was separated from whole blood by centrifugation. cfDNA was extracted from the plasma. **(B)** CTCs were isolated from plasma-depleted blood (PDB) by VTX-1, immunostained and enumerated. DNA was also extracted from these CTCs. **(C)** *EGFR* mutation assay was performed on DNA from CTCs and plasma cfDNA. The pictures of Vortex instrument and the blood draw have been provided by Vortex Biosciences with the appropriate permission. The pictures of Qiagen reagents have been obtained from Qiagen website with the appropriate permission. Other pictures are original.

for cfDNA with a limit of detection (LOD) of 0.4% for Ex19del (Cy5), 0.4% for T790M (FAM) and 2.5% for L858R (ROX), when using 5 ng of cfDNA as starting material. The assay was optimized in terms of sample input and assay sensitivity to be compatible with CTCs: For each sample, the 3 targeted mutations and an internal control were multiplexed in a single PCR reaction using Cy5, FAM, ROX, and VIC fluorescent probes, at a threshold set as 30,000/Cy5; 50,000/FAM; 100,000/ROX; and 20,000/VIC, with the baseline set to 3 for the first cycle and 22 for the last cycle following the manual. A positive mutation result was then determined based on the Ct criteria recommended by EntroGen.

RESULTS

ctEGFR Assay Characterization for Rare Cancer Cells

ctEGFR kit from EntroGen is designed for cfDNA for 0.4% LOD in 5 ng of DNA input. To evaluate this assay for CTCs, 3 NSCLC cell lines (A549, H1975, HCC827) with representative *EGFR* mutations (**Supplementary Figure 1**) were used as surrogate to characterize the CTC workflow. *In terms of DNA input,* the corresponding *EGFR* mutation was successfully detected for each cell line for DNA quantities as low as 0.2 ng, which corresponds to approximately 33 cells (**Figure 3A**). *To assess the assay sensitivity,* DNA from cancer cells and WBCs were mixed at different ratios mimicking a typical Vortex output, i.e., from 1 to 25 ng of total DNA with as low as 4 CTCs among 180 to 5000 WBCs, corresponding to a purity ranging from 0.1 to 10% (**Figure 3B**). All *EGFR* mutations tested were successfully detected at 0.1% purity with 25 ng DNA as starting material (∼5 CTCs among 5000 WBCs) and at 2% purity with 1 ng DNA input (∼4 CTCs among 200 WBCs).

Characterization of the cfDNA – CTC DNA Workflow

(i) On one hand, to validate the cfDNA workflow, HCC827 DNA was spiked into EDTA whole blood at 0.5 ng per 2 mL of blood (Experiment ①, **Figure 4**). cfDNA was extracted from the plasma and tested for *EGFR* mutations. 19Del was successfully detected as expected.

(ii) On the other hand, to validate the cell workflow and evaluate the impact of plasma depletion on cell recovery, H1975 cells were spiked in whole blood at 250 cells/mL of blood and processed through VTX-1, either from the whole blood or from the plasma-depleted blood (PDB) (Experiment ②, **Figure 4**). Capture efficiency was similar between the whole blood (an average recovery of 70%) and the PDB (an average recovery of 66%) for $N = 2$ (**Figure 4B**). T790M and L858R mutations were successfully detected for both conditions, confirming that PDB can be used as an input sample for CTC isolation.

(iii) Finally, to assess the combined workflow, H1975 cells and HCC827 DNA were simultaneously spiked in the whole blood at the same spiking ratio (Experiment ③, **Figure 4**). Plasma was extracted from the blood and the PDB was processed through VTX-1 for cancer cell enrichment. *EGFR* mutations were evaluated from both the plasma cfDNA and the DNA from the cells isolated. All expected *EGFR* mutations were successfully detected, which confirmed the possibility with VTX-1 to assess both the cfDNA and the CTC DNA from the same tube of blood.

Assessment of Blood Collection Tubes for 24 h and 48 h RT Storage

Blood was collected in 4 different blood collection tubes (BCT): EDTA, CellSave, Streck ctDNA and LBgard. Around 600 H1975 cells along with 1.5 ng of HCC827 cell DNA were spiked in 12 mL of whole blood from each type of

A

DNA input (ng)		Ex19del	T790M	L858R
NTC		-	-	-
LPC		+	+	+
A549	2	-	-	-
	0.5	-	-	-
	0.2	-	-	-
H1975	2	-	+	+
	1	-	+	+
	0.5	-	+	+
	0.2	-	+	+
HCC827	2	+	-	-
	1	+	-	-
	0.5	+	-	-
	0.2	+	-	-

B

Purity (%)		Cell #		HCC827			H1975		
		CTCs	WBCs	Ex19del	T790M	L858R	Ex19del	T790M	L858R
NTC		N/A	N/A	-	-	-	-	-	-
LPC		N/A	N/A	+	+	+	+	+	+
1 ng	10%	20	180	+	-	-	-	+	+
	5%	10	190	+	-	-	-	+	+
	2%	4	196	+	-	-	-	+	+
2 ng	5%	20	380	+	-	-	-	+	+
	2%	8	392	+	-	-	-	+	+
	1%	4	396	+	-	-	-	+	+/-
25 ng	0.5%	25	4975	+	-	-	-	+	+
	0.2%	10	4990	+	-	-		+	+
	0.1%	5	4995	+	-	-	-	+	+

FIGURE 3 | Characterization of an assay for both DNA input and sensitivity (purity) using cancer cell samples. **(A)** ctEGFR kit was tested with pure cell line DNA. Mutant DNA amount was identified for as low as 0.2 ng. **(B)** The assay sensitivity (LOD) was assessed for a range of purity varying from 0.1 to 2% for a total DNA amount varying from 25 to 1 ng. NTC, No Template Control. LPC, Low Positive Control. Expected mutations are Ex19del for HCC827; T790M and L858R for H1975.

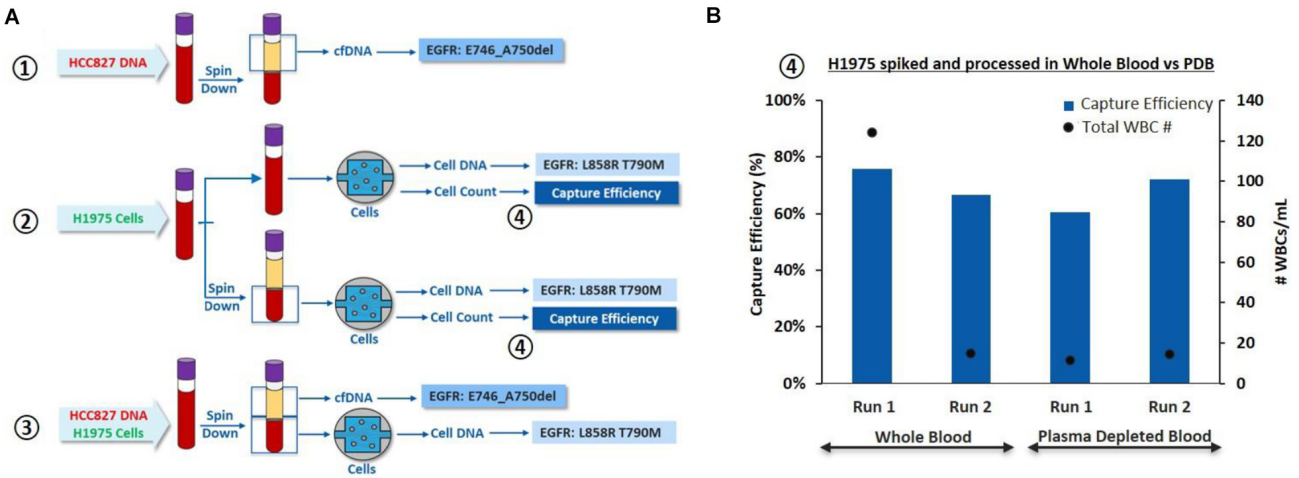

C

Exp. #	Experiment	Input	# Cells	HCC827 DNA	EGFR Assay	
					Cells	cfDNA
①	Cancer cell DNA: Spiking in Plasma	Blood	N/A	Yes	N/A	19Del+
②	Cancer cells: (high) Spiking in Blood vs PDB	Blood	250/mL	No	T790M+; L858R+	N/A
		PDB	250/mL	No	T790M+; L858R+	N/A
③	Cancer cells (low) and cancer cell DNA: Spiking in Blood vs PDB	Blood	50/mL	Yes	T790M+; L858R+	19Del+
		PDB	50/mL	Yes	T790M+; L858R+	19Del+

FIGURE 4 | Characterization of the overall workflow with cancer cells spiked in whole blood and plasma depleted blood. **(A)** Schematic of the experiments performed: ①HCC827 DNA is spiked into whole blood (0.5 ng/2 mL of blood), cfDNA is tested for *EGFR* mutations. ②H1975 cells are spiked in whole blood (250 cells/mL of blood) and processed through VTX-1, from the whole blood or PDB. Capture efficiency and *EGFR* mutations are assessed. ③H1975 cells and HCC827 DNA are spiked in whole blood. *EGFR* mutations are evaluated on the "cfDNA" fraction and on DNA extracted from the isolated cells. **(B)** Comparison of capture performance, i.e., capture efficiency and capture purity (through WBC count), for H1975 cells spiked into whole blood and processed through VTX-1, as whole blood or as plasma depleted blood (④) ($N = 2$). **(C)** Side by side comparison of the *EGFR* mutation results obtained from experiments ①, ②, and ③. All pictures are original and courtesy of Vortex Biosciences.

BCT, in order to have a final concentration of 100 cells and 250 pg DNA per 2 mL blood, respectively. The spiked blood from each BCT was then processed as indicated in the combined workflow described above, on Day 0 (i.e., immediately after spiking), Day 1 (24 h post-spiking) and Day 2 (48 h post-spiking). Initial blood cell viability, cell capture efficiency and purity after VTX-1 processing, debris in the VTX-1 output sample, cfDNA yield, CTC DNA yield and *EGFR* mutations were all evaluated for each of these conditions and recapitulated in **Figure 5A**.

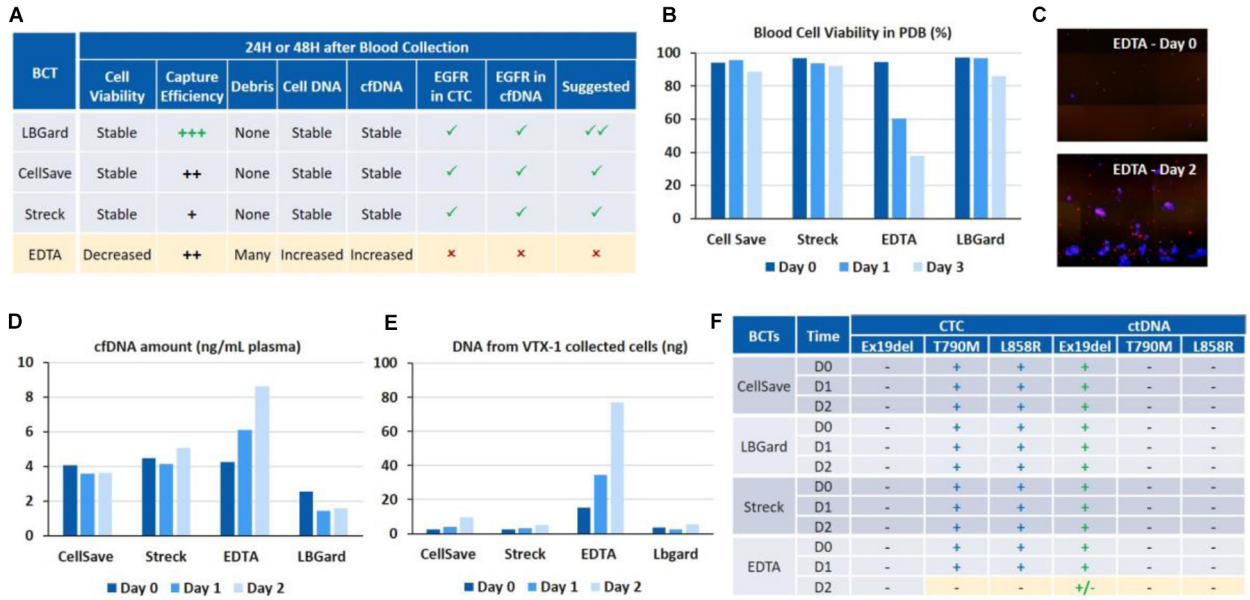

FIGURE 5 | Assessment of different blood collection tubes for *EGFR* assays on cfDNA and CTC DNA after 24 and 48 h of blood storage. **(A)** Overall performance of the different BCTs. LBgard is identified as the preferred BCT as opposed to EDTA, which performance significantly worsens over the storage duration. **(B)** Initial blood cell viability in the plasma-depleted blood sample, before VTX-1 processing. **(C)** Presence of numerous DAPI + debris, i.e., nucleus from dead cells, in the VTX-1 output from EDTA BCTs after 48 h. **(D)** cfDNA yield from the plasma workflow. **(E)** Cell DNA yield from the cell workflow after VTX-1 processing. **(F)** *EGFR* mutation detection for cfDNA and CTC DNA, at Day 0, 1, and 2. All pictures are original.

Initial Blood Cell Viability

Blood cell viability of the plasma depleted blood was estimated for each BCT and at each time point before VTX-1 processing (**Figure 5B**). Cell viability (>80%) remained stable over 48 h of storage for CellSave, Streck, and LBgard. For EDTA, however, cell viability dropped significantly from 94% (Day 0) to 60% (Day 1), and to as low as 37% (Day 2).

VTX-1 Performance and Debris

Capture efficiency for the 4 BCTs (data not shown) spiked with MCF7 breast cancer cells indicated a worse recovery for EDTA at Day 1 and Day 2, while Streck was lower (data not available). LBGard, however, had the best capture efficiency over time, slightly higher than CellSave. Images from the VTX-1 output indicated the presence of numerous DAPI + debris enriched from the EDTA blood after a long storage time, and this phenomenon became worse over time (**Figure 5C**).

DNA Yield

cfDNA extraction yields (**Figure 5D**) were consistent between CellSave, Streck and LBgard BCTs for the 3 timepoints, ranging from 2 to 5 ng/mL of plasma, with LBgard showing the lowest cfDNA yield. The cfDNA yield for EDTA was the same as the 3 others BCTs at Day 0 but increased with the storage duration, from 4.25 ng/mL at Day 0 to 6.1 ng/mL at Day 1 and 8.63 ng/mL at Day 2, indicating the significant presence of non-specific DNA, probably coming from the numerous debris observed from cell lysis, usually due to WBC lysis. For the CTC DNA yield (**Figure 5E**), CellSave, Streck and LBgard again showed similar and stable results for Day 0 and Day 1, with a slight increase at Day 3. For EDTA, the quantity of DNA extracted from the cellular output of VTX-1 was much higher than for the other BCTs at Day 0 and, again, increased further at Day 1 and Day 2, confirming the impact of debris presence.

EGFR Assay Validation

The expected *EGFR* mutations could be detected from all four BCTs, from both cfDNA and CTC DNA, at Day 0 and Day 1 (**Figure 5F**). At Day 2, however, the mutations were missed from EDTA tubes due to the higher background of debris DNA, while they were successfully detected from CellSave, Streck, and LBgard BCTs.

Overall, LBGard tubes demonstrated the best performance in terms of DNA yield and cell recovery, answering all the needs for this combined assay and was selected for the patient samples.

EGFR Mutation Profiling on Patient Samples

CTC vs. cfDNA

Blood samples from 24 metastatic NSCLC patients and six age-matched healthy donors were analyzed for *EGFR* mutations on both cfDNA and CTC DNA (**Table 2**). No *EGFR* mutation was detected in the cohort of healthy donors, neither in cfDNA nor in cell DNA. Among 24 patients, *EGFR* mutations were detected in 11 patients (45.8%), from either cfDNA or from CTCs. For 3/11 patients, the same mutation was identified from both cfDNA and CTCs. For 7/11 patients, the mutation was detected from cfDNA but not from CTCs, and conversely 1 sample showed an exon 19

TABLE 2 | EGFR assay comparison.

	EGFR Assay – Vortex			EGFR Assay – UCLA		Concordance to Tissue – UCLA	Concordance to cfDNA – UCLA
ID	**CTCs**	**cfDNA**	**CTCs + cfDNA**	**Tissue**	**cfDNA**		
PA01	ND	Exon 19 del	Exon 19 del	Exon 19 del (Lung; 2015)		Yes	N/A
PA02	ND	ND	ND	Exon 19 del (Lung; 2010) T790M (Lung; 2017)		No (missed)	N/A
PA03.1	Exon 19 del	ND	Exon 19 del	ND (Lung; 2016)		No (extra)	N/A
PA03.2	Exon 19 del	ND	Exon 19 del				
PA03.3	ND	ND	ND				
PA04.1	ND	ND	ND	ND (Lung; 2016)		Yes	N/A
PA04.2	ND	ND	ND				
PA05.1	ND	Exon 19 del	Exon 19 del		Exon 19 del (Guardant360; 2016)	N/A	Yes
PA05.2	ND	Exon 19 del	Exon 19 del				
PA06.1	ND	L858R	L858R	L858R (LN; 2017)	L858R + T790M (Guardant360; 2016)	Yes	Yes
PA06.2	ND	L858R	L858R				
PA07	ND	ND	ND	Exon 19 del (Lung; 2016)	ND (Guardant360; 2017)	No (missed)	Yes
PA08	Exon 19 del	Exon 19 del	Exon 19 del	Exon 19 del (Lung; 2010) T790M (Lung; 2015) ND (Pleural Fluid; 2017);	ND (Guardant360; 2017)	Yes / No	No (extra)
PA09	ND	L858R	L858R	L858R(LN; 2017)		Yes	N/A
PA10	ND	ND	ND	L858R (Lung; 2017)		No (missed)	N/A
PA11	ND	L858R	L858R	L858R (Lung; 2016)		Yes	N/A
PA12	L858R + T790M	L858R + T790M	L858R + T790M	L858R (LN; 2015)	L858R + T790M (Biocept; 2015)	Yes	Yes
PA13	ND	L858R	L858R	L858R (Lung)		Yes	N/A N/A
PA14	ND	ND	ND	ND(LN;2016)		Yes	
PA15	ND	ND	ND	L858R + T790M(LN;2014)		No (missed)	N/A N/A
PA16	ND	ND	ND	Exon 19 del (Lung; 2017)		No (missed)	
PA17	ND	ND	ND	ND (Lung; 2017)		Yes	N/A
PA18	ND	Exon 19 del	Exon 19 del	Exon 19 del (Lung; 2012)	Exon 19 del + T790M (Guardant; 2016); Exon 19 del (Guardant; 2017)	Yes	Yes
PA19	ND	ND	ND	L858R (Lung; 2017)	No (missed)	N/A	
PA20	ND	ND	ND	L858R (Lung; 2017); L858R + T790M (Pleural Fluid; 2017)	L858R (Guardant360; 2017);	No (missed)	No (missed)
PA21	T790M	L858R + T790M	L858R + T790M	L858R + T790M (Lung; 2016);	L858R + T790M (Guardant360; 2017)	Yes	Yes
PA22	ND	ND	ND	Exon 19 del + T790M (Lung; 2018)	Exon 19 del + T790M (Guardant360; 2018)	No (missed)	No (missed)
PA23	ND	ND	ND	L858R (LN; 2017)		No (missed)	N/A
PA24	ND	ND	ND	ND (Lung; 2017)		Yes	N/A
HDOI HD02 HD03 HD04 HD05 HD06		ND		N/A	N/A	N/A	

Analysis of 36 samples from NSCLC patients (PA) and healthy donors (HD). Side-by-side comparison of EGFR results from assays performed at UCLA and Vortex Biosciences. ND, non detected. N/A, not available. LN, Lymph Nodes.

deletion mutation only in CTCs but not in cfDNA. To confirm this last result, two additional blood samples were collected from this patient at 1 month and 5 months follow-ups, after the initial blood draw. This same exon 19 deletion was detected in CTCs after 1 month but was not detected again after 5 months.

CTC and cfDNA vs. Tumor Tissue

Out of 24 patients, 13 had a concordant mutation status between tissue and combined CTC and cfDNA liquid biopsies, 10 had discordance between tissue and liquid biopsies, with one patient having more mutations detected in the liquid biopsy than in the tissue. For most of the patients, however, the tumor biopsies were analyzed up to 7 years before the blood sampling (>1 year for 12/24 patients), which might explain the discrepancy observed. Tissue biopsy was not available for 1/24 patients.

CTCs and cfDNA vs. UCLA Standard cfDNA Assay

Among these 24 patients, 9 had a cfDNA *EGFR* mutation analysis performed previously at a UCLA clinic (the assay used for these 9 patients is described in **Table 2**). Of those, 6 returned the same mutation profile as the Vortex-EntroGen combined workflow. For the 3 discordant patient samples, 1 had more mutations detected by the combined Vortex workflow.

CTC Immunostaining and Enumeration

For 20 patient samples, extra blood volume was processed specifically for immunostaining and enumeration, as defined in the Methods section. Representative images of CTCs are presented in **Figure 6A**, while the enumeration results are plotted in **Figure 6B**. Patients had from 0 to 7.4 CTCs/mL of blood processed (average: 1.1 CTCs/mL, median: 0.5 CTCs/mL), with 35 to 932 WBCs/mL (average: 360.9 WBCs/mL, median: 339.8 WBCs/mL). The patient sample with the most CTCs corresponds to the first draw of Patient PA03, for which Exon 19 deletion mutation was detected only in the CTCs. No CTC enumeration was performed on healthy donor's blood in this current study but in others (21, 25).

DISCUSSION

The discovery of oncogenic driver mutations of the *EGFR* gene and the approval of *EGFR* inhibitors have revolutionized the targeted individualized treatment approach in non-small-cell lung cancer (NSCLC) (29). Patients with *EGFR* exon 19 deletions or exon 21 L858R mutations are eligible for treatment with gefitinib, afatinib, erlotinib, dacomitinib and osimertinib. Patients who later develop *EGFR* T790M mutation and whose disease is progressing on or after erlotinib, gefitinib, afatinib or dacomitinib can benefit from treatment with osimertinib. *EGFR* mutation profiling and corresponding *EGFR* inhibitors have already significantly prolonged many patients' lives. Most of the FDA approved *EGFR* mutation detection tests rely on tissue biopsies. In parallel, some plasma-based assays, such as the cobas®*EGFR* Mutation Test from Roche, offer a non-invasive alternative for those patients not eligible for a tissue biopsy. Liquid biopsies allow the clinicians to monitor treatment effectiveness and disease progression over time. While cfDNA *EGFR* mutation tests are widely adopted for selecting the appropriate *EGFR* inhibitor for a given patient, CTCs are less popular and not used in the clinic. No FDA approved *EGFR* mutation test is approved for CTCs. This can be explained by two reasons: First, CTCs are rare, and retrieving CTCs from a blood sample with millions of WBCs and billions of RBCs in the background is not as straightforward as separating the plasma from the blood. Second, it also requires a very good CTC enrichment system that can recover sufficient CTCs with few normal blood cells to satisfy the requirements of the downstream *EGFR* assay in terms of sensitivity and specificity.

We examined the performance of the kits available for cfDNA and selected the ones that could be compatible with CTCs as well[1]. qPCR-based assays were favored over Next-Generation Sequencing methods as they require less input DNA (e.g., as low as 2 ng) and are more sensitive (with limit of detection/LOD as low as 0.4%). Among these qPCR-based kits, the Roche cobas® *EGFR* real-time PCR test targets a panel of 42 mutations in exons 18, 19, 20, and 21 but requires an amount of starting material that cannot be obtained from CTC samples (50 ng of DNA per reaction in 8 reactions[2]). Among all the *EGFR* mutations considered, only a few are clinically actionable; with the most famous examples being *EGFR* exon 19 deletions, L858R and T790M. Therefore, the ctEGFR Mutation Detection Kit from EntroGen was selected owing to its ability to simultaneously detect these 3 key *EGFR* mutations in plasma cfDNA through FAM, VIC, ROX, and CY5 fluorescent probes with very high sensitivity. This assay requires as little as 2 μg of DNA, for a LOD that can reach 0.4%. This kit was validated with cell lines mimicking a typical CTC sample in terms of DNA input and purity. Interestingly, during our research, we found a SNP c.2361 G > A (p.Q878Q) in the three cancer cell lines considered, 8 nucleotides upstream of c. 2369 C > T (p.T790M) (**Supplementary Figure 1**). This was not considered in the kit we started with and might affect the probes/primers and overall performance. This information was reported to EntroGen; the commercial kits revised accordingly and used for the next steps of our studies for both plasma and CTC samples. Also, the C797 mutations, osimertinib emergent, were not considered by this combined assay and could be considered later on.

Among the CTC isolation platforms currently available, some rely on different cell surface markers expressed by the cells at their surface, such as EpCAM or CK. Such platforms may not capture the CTCs lacking the markers targeted (30–32). Other platforms rely on the cell dimensions, using filtering features either in a paper filter or in a microfluidic chip. Such platforms often leave CTCs trapped on a filter or inside a chip, making their intact retrieval a challenge (33). Vortex has developed a microfluidic label-free and automated CTC isolation system, which captures cells using vortices and inertial forces (20, 22). Cells are collected in suspension in the container of choice and remain intact, which guarantees the integrity of CTC DNA or RNA signatures, for an ideal compatibility with downstream gene mutation or gene expression assays (25, 27, 34). More importantly for this study, the very little number of WBCs collected (<100 WBCs/mL blood) advantageously provides a CTC sample with a very

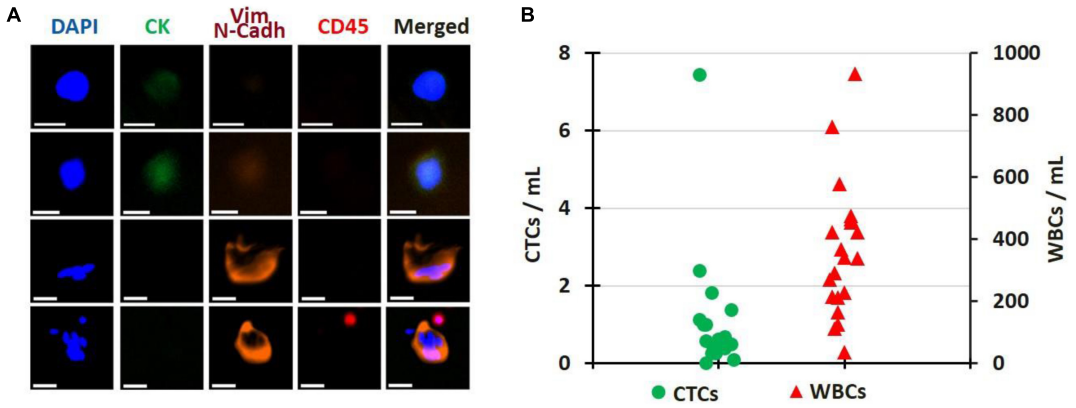

FIGURE 6 | CTC Enumeration. **(A)** Gallery of CTCs, single or clustered, isolated from patient samples. Scale bar: 20 μm. **(B)** Cell enumeration per mL of blood processed for 20 patient samples; CTCs (green circles) and WBCs (red triangles). All pictures are original.

high purity that can be then directly used for *EGFR* mutation detection (23).

One purpose of the study was to evaluate the feasibility to process and isolate CTCs from plasma depleted blood with Vortex technology. Indeed, the possibility to use the same blood sample to isolate and analyze cfDNA, extracellular vesicles, and CTCs would ensure no genomic and transcriptomic information is missed, yielding a total liquid biopsy. Collecting multiple blood samples from metastatic patients can prove difficult at times, because of the patient's poor general condition and the blood drawn at a given clinic appointment is generally split over numerous tests. Achieving one integrated workflow to minimize the blood volume needed and sample-to-sample bias while getting the complete transcriptomic and genomic information would be both beneficial to the patient and informative to the clinician. As confirmed in our results, the capture efficiency from the whole blood and the plasma-depleted blood were similar, demonstrating that Vortex technology could work on both whole blood and plasma depleted blood. Beyond *EGFR* mutation profiling, this gives researchers the opportunity to perform more assays with one tube of blood, for example to look at exosome plasma RNA versus CTC RNA. Even more, besides plasma vs. cellular phase, future studies will consider assays on both CTCs and leukocytes, as leukocytes can be collected intact from VTX-1 waste streams.

More generally, we are targeting assays that could be used by multiple sites, i.e., assuming patient samples need to be shipped from a sampling site to a processing lab, which potentially can take up to 48 h. In this purpose, different blood collection tubes were considered and compared to the classic BD vacutainer K_2 EDTA tube (without any preservative added) over 2 days, considering all the key steps of the combined workflow: blood viability, cfDNA amount, cell recovery, cell DNA amount, and *EGFR* mutations. We selected blood collection tubes commercially available and marketed for cfDNA and/or CTCs, such as CellSave (recommended for CTCs analysis by CellSearch), Streck cfDNA (recommended for cfDNA and CTCs), and LBgard (recommended for cfDNA and CTCs). Other blood collection tubes may have been launched on the market since, which would be interesting to consider as well moving forward. The results demonstrated that while collecting blood in classic BD vacutainer K_2 EDTA tubes works fine for same day processing and analysis of both cfDNA and CTCs, performance was affected as soon as 24 h post draw: after processing, lots of debris was present in the blood, increasing dramatically the overall contaminating background thus the cfDNA and cell DNA amount. CellSave, Streck and LBgard tubes showed better performance, with LBgard significantly better for all the parameters evaluated. This study highlights the crucial impact of pre-analytical variables; the blood collection method and storage duration for this specific assay, which can actually apply to all liquid biopsy related assays. Ideally, even if time and resource consuming, such side-by-side assessment should be commonly performed as early as possible in the development process, considering also the storage temperature and the shipping technique.

Our results indicate that *EGFR* mutations were identified in 11 out of 24 (45.8%) patient samples tested. Among the 11 patients with *EGFR* mutations; seven mutations were identified in the cfDNA but not in the CTCs, 1 exon 19 deletion was found only in the CTCs and not in the cfDNA, while three harbored the same mutations in both cfDNA and CTC fractions. No *EGFR* mutations were detected in the healthy donor samples using our integrated workflow. Despite the relatively small patient cohort, these results provide a preliminary indication of the efficiency and specificity of our "Total Liquid Biopsy" workflow. Mutational profiles from cfDNA and gDNA from CTCs differ significantly and together may give a more comprehensive picture. These results show that the combination of cfDNA and CTCs may be more useful than either test alone. The patient who had positive CTCs but negative cfDNA had 2 subsequent blood draws within 5 months; the same exon 19 deletion was detected in the second blood draw but not in the 3rd one. Even if rare, such occurrence could still give some useful information as a complement to cfDNA alone. The overall performance of cfDNA is superior than CTCs for this DNA based assay. This might be explained by

several reasons: 1/Most of the patients in this small cohort had already received chemotherapy or *EGFR* inhibitors at the time of the blood collection. A portion of CTCs might have died during the treatments, which is also indicated by the number of CTCs that is lower than in other studies (21). 2/In the case of CTC apoptosis, CTCs die and more ctDNA is released into the plasma, which increases the ctDNA portion in the cfDNA and results in better performance for ctDNA than CTCs. However, this explanation implies that new mutations would be first detected in the CTCs while cfDNA would provide a snapshot of dying cancer cells instead. Combining *EGFR* mutation analysis of both cfDNA and CTC DNA would thus be of special interest to detect earlier a new mutation and adjust accordingly the treatment regimen of NSCLC patients, for example to switch a patient to Osimertinib if T790M mutation is being detected on erlotinib, gefitinib, afatinib or dacomitinib. This point has been further described elsewhere and emphasizes the clinical importance of CTCs as a point of access to intact cancer DNA, RNA or proteins (35–37). In the study from Sundaresan et al., cfDNA or CTC analysis alone had less sensitivity vs. combining both, with a genotyping of 70 and 80% for CTCs and cfDNA, respectively, but 100% when combined (35).

In parallel, we compared the mutational profiles from cfDNA and gDNA from CTCs to the ones obtained from tissue biopsies (tumor or LN). Still, 13 out of 24 patient samples had the same mutation results for tissue vs. combined CTC + cfDNA, for more than 50% concordance. Yet, the comparison with tissue biopsies is to be taken cautiously, with an expected discrepancy, as some biopsies were analyzed up to 7 years before the blood sampling, and the patient cohort is limited. This also emphasizes the change of mutations over the course of the disease and treatment regimens, and the crucial relevance of liquid biopsies to monitor patient progression. We envision a larger study, considering a larger patient cohort with more stringent patient selection criteria, to further assess the accuracy of the assay and to enable a comparison between total liquid biopsy and tissue biopsy results.

Lastly, when we compare the Vortex combined *EGFR* cfDNA CTC workflow with some commercial assays (Guardant Health or Ion Torrent) performed at UCLA on nine cfDNA samples; there was concordance for six samples (66.7%). For two samples, commercial assays detected more mutations. For one sample, our combined workflow found more comprehensive results. These differences could be explained by different blood collection timepoints, the small patient cohort and a different sensitivity for each assay. As there is no gold standard assay, this remains unclear which is correct for each of the samples.

CONCLUSION

Although the present study is limited by the small patient cohort considered, and the time gap between the tissue biopsy and the blood collection, these preliminary results present, characterize and validate a combined workflow for *EGFR* mutation analysis on cfDNA and CTCs from a single tube of blood. DNA mutation detection of a small targeted panel using qPCR is easier from cfDNA, but combining and comparing cfDNA with CTC DNA is possible with a streamlined workflow. cfDNA being potentially indicative of dying cells after therapy while CTCs living after therapy may have more valuable information, a combined workflow could provide complementary indication on the patient resistance as a "total liquid biopsy." An extended study should be considered on a larger patient cohort, using isolated CTCs to detect *EGFR* mutations alongside with a potent heterogeneity analysis of somatic copy number alterations and mutations.

DATA AVAILABILITY STATEMENT

All datasets presented in this study are included in the article/**Supplementary Material**. The authors can be contacted for further information.

ETHICS STATEMENT

The studies involving human participants were reviewed and approved by UCLA IRB 11-001798 and STANFORD IRB 5630. The patients/participants provided their written informed consent to participate in this study.

AUTHOR CONTRIBUTIONS

HL, MV, CW, CR, MC, CL, JCh, and ES designed the experiments. HL, MV, CW, CR, MC, and CL performed the experiments. MM, JCa, VH, SSJ, EG, and JG identified the donors and/or obtained the blood samples. HL, MV, CW, CR, JCh, and ES analyzed the results. HL, MV, CR, and ES wrote the manuscript with assistance from all authors. All authors have read and approved this manuscript.

FUNDING

HL, MV, CW, CR, MC, CL, JCh, SC, DDC, and ES have financial interests in Vortex Biosciences. JCh, DDC, and ES have interests in the intellectual property described herein for Vortex Biosciences technology. UCLA acknowledges research funding support from Vortex Biosciences (MM, JCa, and DDC). SSJ is on the Scientific Advisory Board of Ravel Biotechnology and Quantumcyte.

ACKNOWLEDGMENTS

The authors thank all the study participants and members of the clinical team for their contributions to blood sample collection. Specifically, they also thank Juan Avalos from UCLA who did the majority of the healthy blood collection.

SUPPLEMENTARY MATERIAL

The Supplementary Material for this article can be found online at: https://www.frontiersin.org/articles/10.3389/fonc.2020.572895/full#supplementary-material

Supplementary Figure S1 | NSCLC cell line characterization. **(A)** 3 human NSCLC cell lines with known *EGFR* mutations – A549 (ATCC® CCL-185™, wild type), H1975 (ATCC® CRL-5908™, T790M and L858R mutations), and HCC827 (ATCC® CRL-2868™, 19 deletion) – were used to characterize the CTC workflow. For each cell line, cell mutations were confirmed by Sanger sequencing. **(B)** The amplified PCR products corresponding to the *EGFR* exons 19, 20, 21 covering 19 deletion, T790M and L858R mutations were verified by E-Gel Electrophoresis and subjected to Sanger sequencing. **(C)** The sequencing results demonstrate the presence of the expected mutations in the corresponding cell lines. All the pictures are original.

Supplementary Figure S2 | Primer sequences. The primers were specifically designed to amplify the regions of the *EGFR* exons 19, 20, and 21 covering 19 deletion, T790M and L858R mutations. For all spiking experiments, cells at a confluency of 40–60% were dissociated using TrypLE express (Gibco). The concentration of live cells, cell viability and average cell diameter were measured using an automated cell counter (Cellometer K2, Nexcelom) after staining with Acridine Orange and Propidium Iodide (AOPI) dyes. Stock cell suspensions were serially diluted in complete medium to obtain the desired final concentrations before spiking in blood.

REFERENCES

1. Siegel RL, Miller KD, Jemal A. Cancer statistics. *CA Cancer J Clin.* (2020) 70:7–30. doi: 10.3322/caac.21590
2. Crinò L, Weder W, van Meerbeeck J, Felip E, ESMO Guidelines Working Group Early stage and locally advanced (non-metastatic) non-small-cell lung cancer: ESMO clinical practice guidelines for diagnosis, treatment and follow-up. *Ann Oncol Suppl.* (2010) 5:v103–15. doi: 10.1093/annonc/mdq207
3. Midha A, Dearden S, McCormack R. EGFR mutation incidence in non-small-cell lung cancer of adenocarcinoma histology: a systematic review and global map by ethnicity (mutMapII). *Am J Cancer Res.* (2015) 5:2892–911.
4. Gelatti ACZ, Drilon A, Santini FC. Optimizing the sequencing of tyrosine kinase inhibitors (TKIs) in epidermal growth factor receptor (EGFR) mutation-positive non-small cell lung cancer (NSCLC). *Lung Cancer.* (2019) 137:113–122. doi: 10.1016/j.lungcan.2019.09.017
5. Bethune G, Bethune D, Ridgway N, Xu Z. Epidermal growth factor receptor (EGFR) in lung cancer: an overview and update. *J Thorac Dis.* (2010) 2:48–51.
6. Nakagawa K, Garon EB, Seto T, Nishio M, Ponce Aix S, Paz-Ares L, et al. Ramucirumab plus erlotinib in patients with untreated, EGFR-mutated, advanced non-small-cell lung cancer (RELAY): a randomised, double-blind, placebo-controlled, phase 3 trial. *Lancet Oncol.* (2019) 20:1655–69. doi: 10.1016/S1470-2045(19)30634-5
7. Hosomi Y, Morita S, Sugawara S, Kato T, Fukuhara T, Gemma A, et al. Gefitinib alone versus Gefitinib plus chemotherapy for non–small-cell lung cancer with mutated epidermal growth factor receptor: NEJ009 study. *J Clin Oncol.* (2020) 38:115–23. doi: 10.1200/JCO.19.0148
8. Noronha V, Maruti Patil V, Joshi A, Menon N, Chougule A, Mahajan A, et al. Gefitinib versus Gefitinib plus pemetrexed and carboplatin chemotherapy in EGFR-mutated lung cancer. *J Clin Oncol.* (2020) 38:124–36. doi: 10.1200/JCO.19.01154
9. Ramalingam SS, Vansteenkiste J, Planchard D, Cho BC, Gray JE, Ohe Y, et al. Overall survival with Osimertinib in untreated, EGFR-mutated advanced NSCLC. *N Engl J Med.* (2020) 382:41–50. doi: 10.1056/NEJMoa1913662
10. Marrugo-Ramírez J, Mir M, Samitier J. Blood-based cancer biomarkers in liquid biopsy: a promising non-invasive alternative to tissue biopsy. *Int J Mol Sci.* (2018) 19:2877. doi: 10.3390/ijms19102877
11. Arneth B. Update on the types and usage of liquid biopsies in the clinical setting: a systematic review. *BMC Cancer.* (2018) 18:527. doi: 10.1186/s12885-018-4433-3
12. Calabuig-Fariñas S, Jantus-Lewintre E, Herreros-Pomares A, Camps C. Circulating tumor cells versus circulating tumor DNA in lung cancer—which one will win? *Transl Lung Cancer Res.* (2016) 5:466–82. doi: 10.21037/tlcr.2016.10.02
13. Singh AP, Li S, Cheng H. Circulating DNA in EGFR-mutated lung cancer. *Ann Transl Med.* (2017) 5:379. doi: 10.21037/atm.2017.07.10
14. Mason J, Blyth B, MacManus MP, Martin OA. Treatment for non-small-cell lung cancer and circulating tumor cells. *Lung Cancer Manag.* (2018) 6:129–39. doi: 10.2217/lmt-2017-0019
15. Kapeleris J, Kulasinghe A, Warkiani ME, Vela I, Kenny L, O'Byrne K, et al. The prognostic role of circulating tumor cells (CTCs) in lung cancer. *Front Oncol.* (2018) 8:311. doi: 10.3389/fonc.2018.00311
16. Santarpia M, Liguori A, D'Aveni A, Karachaliou N, Gonzalez-Cao M, Daffinà MG, et al. Liquid biopsy for lung cancer early detection. *J Thorac Dis.* (2018) 10(Suppl. 7):S882–97. doi: 10.21037/jtd.2018.03.81
17. Phallen J, Leal A, Woodward BD, Forde PM, Naidoo J, Marrone KA, et al. Early noninvasive detection of response to targeted therapy in non-small cell lung cancer. *Cancer Res.* (2019) 79:1204–13. doi: 10.1158/0008-5472.CAN-18-1082
18. Anagnostou V, Forde PM, White JR, Niknafs N, Hruban C, Naidoo J, et al. Dynamics of tumor and immune responses during immune checkpoint blockade in non-small cell lung cancer. *Cancer Res.* (2019) 79:1214–25. doi: 10.1158/0008-5472.CAN-18-1127
19. Liang H, Huang J, Wang B, Liu Z, He J, Liang W. The role of liquid biopsy in predicting post-operative recurrence of non-small cell lung cancer. *J Thorac Dis.* (2018) 10(Suppl. 7):S838–45. doi: 10.21037/jtd.2018.04.08
20. Lemaire CA, Liu SZ, Wilkerson CL, Ramani VC, Barzanian NA, Huang KW, et al. Fast and label-free isolation of circulating tumor cells from blood: from a research microfluidic platform to an automated fluidic instrument, VTX-1 liquid biopsy system. *SLAS Technol.* (2018) 23:16–29. doi: 10.1177/2472630317738698
21. Che J, Yu V, Dhar M, Renier C, Matsumoto M, Heirich K, et al. Classification of large circulating tumor cells isolated with ultra-high throughput microfluidic Vortex technology. *Oncotarget.* (2016) 7:12748–60. doi: 10.18632/oncotarget.7220
22. Sollier E, Go DE, Che J, Gossett DR, O'Byrne S, Weaver WM, et al. Size-selective collection of circulating tumor cells using Vortex technology. *Lab Chip.* (2014) 14:63–77. doi: 10.1039/C3LC50689D
23. Kidess-Sigal E, Liu HE, Triboulet MM, Che J, Ramani VC, Visser BC, et al. Enumeration and targeted analysis of KRAS, BRAF and PIK3CA mutations in CTCs captured by a label-free platform: comparison to cfDNA and tissue in metastatic colorectal cancer. *Oncotarget.* (2016) 7:85349–64. doi: 10.18632/oncotarget.13350
24. Sinkala E, Sollier-Christen E, Renier C, Rosàs-Canyelles E, Che J, Heirich K, et al. Profiling protein expression in circulating tumour cells using microfluidic western blotting. *Nat Commun.* (2017) 8:14622. doi: 10.1038/ncomms14622
25. Renier C, Pao E, Che J, Liu HE, Lemaire CA, Matsumoto M, et al. Label-free isolation of prostate circulating tumor cells using Vortex microfluidic technology. *NPJ Precis Oncol.* (2017) 2017:15.
26. Dhar M, Wong J, Che J, Matsumoto M, Grogan T, Elashoff D, et al. Evaluation of PD-L1 expression on vortex-isolated circulating tumor cells in metastatic lung cancer. *Sci Rep.* (2018) 8:2592. doi: 10.1038/s41598-018-19245-w
27. Liu HE, Triboulet M, Zia A, Vuppalapaty M, Kidess-Sigal E, Coller J, et al. Workflow optimization of whole genome amplification and targeted panel sequencing for CTC mutation detection. *NPJ Genom Med.* (2017) 2:34.
28. Rago C, Huso DL, Diehl F, Karim B, Liu G, Papadopoulos N, et al. Serial assessment of human tumor burdens in mice by the analysis of circulating DNA. *Cancer Res.* (2007) 67:9364–70. doi: 10.1158/0008-5472.CAN-07-0605
29. Singh N, Bal A, Aggarwal AN, Das A, Behera D. Clinical outcomes in non-small-cell lung cancer in relation to expression of predictive and prognostic biomarkers. *Future Oncol.* (2010) 6:741–67. doi: 10.2217/fon.10.30
30. Ramalingam N, Jeffrey SS. Future of liquid biopsies with growing technological and bioinformatics studies: opportunities and challenges in discovering tumor heterogeneity with single-cell level analysis. *Cancer J.* (2018) 24:104–108. doi: 10.1097/PPO.0000000000000308
31. Murlidhar V, Rivera-Báez L, Nagrath S. Affinity versus label-free isolation of circulating tumor cells: who wins? *Small.* (2016) 12:4450–4463. doi: 10.1002/smll.201601394
32. Lampignano R, Schneck H, Neumann M, Fehm T, Neubauer H. Enrichment, isolation and molecular characterization of EpCAM-negative circulating

tumor cells. *Adv Exp Med Biol.* (2017) 994:181–203. doi: 10.1007/978-3-319-55947-6_10

33. Mu Z, Benali-Furet N, Uzan G, Znaty A, Ye Z, Paolillo C, et al. Detection and characterization of circulating tumor associated cells in metastatic breast cancer. *Int J Mol Sci.* (2016) 17:1665. doi: 10.3390/ijms17101665
34. Ju JA, Lee CJ, Thompson KN, Ory EC, Lee RM, Mathias TJ, et al. Partial thermal imidization of polyelectrolyte multilayer cell tethering surfaces (TetherChip) enables efficient cell capture and microtentacle fixation for circulating tumor cell analysis. *Lab Chip.* (2020) 20:2872–88.
35. Sundaresan TK, Sequist LV, Heymach JV, Riely GJ, Jänne PA, Koch WH, et al. Detection of T790M, the acquired resistance EGFR mutation, by tumor biopsy versus noninvasive blood-based analyses. *Clin Cancer Res.* (2016) 22:1103–10. doi: 10.1158/1078-0432.CCR-15-1031
36. Keup C, Storbeck M, Hauch S, Hahn P, Sprenger-Haussels M, Tewes M, et al. Cell-free DNA variant sequencing using CTC-depleted blood for comprehensive liquid biopsy testing in metastatic breast cancer. *Cancers (Basel).* (2019) 11:238. doi: 10.3390/cancers11020238
37. Keup C, Storbeck M, Hauch S, Hahn P, Sprenger-Haussels M, Hoffmann O, et al. Multimodal targeted deep sequencing of circulating tumor cells and matched cell-free DNA provides a more comprehensive tool to identify therapeutic targets in metastatic breast cancer patients. *Cancers (Basel).* (2020) 12:1084. doi: 10.3390/cancers12051084

Conflict of Interest: HL, MV, CW, CR, MC, CL, JCh, SC, DDC, and ES have financial interests in Vortex Biosciences. JCh, DDC, and ES have interests in the intellectual property described herein for Vortex Biosciences technology. UCLA acknowledges research funding support from Vortex Biosciences (MM, JCa, and DDC).

The remaining authors declare that the research was conducted in the absence of any commercial or financial relationships that could be construed as a potential conflict of interest.

frontiers in Oncology

REVIEW
published: 14 October 2020
doi: 10.3389/fonc.2020.565666

Circulating Extracellular Vesicles in Gynecological Tumors: Realities and Challenges

Carolina Herrero[1,2], *Miguel Abal*[1,2,3] *and Laura Muinelo-Romay*[3,4]*

[1] Translational Medical Oncology Group (Oncomet), Health Research Institute of Santiago de Compostela (IDIS), University Hospital of Santiago de Compostela (SERGAS), Santiago de Compostela, Spain, [2] Nasasbiotech, S.L., A Coruña, Spain, [3] Instituto de Salud Carlos III, Centro de Investigación Biomédica en Red de Cáncer (CIBERONC), Madrid, Spain, [4] Liquid Biopsy Analysis Unit, Translational Medical Oncology (Oncomet), Health Research Institute of Santiago de Compostela (IDIS), Santiago de Compostela, Spain

Although liquid biopsy can be considered a reality for the clinical management of some cancers, such as lung or colorectal cancer, it remains a promising field in gynecological tumors. In particular, circulating extracellular vesicles (cEVs) secreted by tumor cells represent a scarcely explored type of liquid biopsy in gynecological tumors. Importantly, these vesicles are responsible for key steps in tumor development and dissemination and are recognized as major players in cell-to-cell communication between the tumor and the microenvironment. However, limited work has been reported about the biologic effects and clinical value of EVs in gynecological tumors. Therefore, here we review the promising but already relatively limited data on the role of circulating EVs in promoting gynecological tumor spread and also their value as non-invasive biomarkers to improve the management of these type of tumors.

Keywords: ovarian cancer (OC), endometrial cancer (EC), circulating extracellular vesicles (cEVs), biomarkers, liquid biopsy

OPEN ACCESS

Edited by:
Francesco Fabbri, Romagnolo Scientific Institute for the Study and Treatment of Tumors (IRCCS), Italy

Reviewed by:
Stefano Fais, National Institute of Health (ISS), Italy
Christine Fillmore Brainson, University of Kentucky, United States
Tanner DuCote, University of Kentucky, United States, in collaboration with reviewer CB

***Correspondence:**
Laura Muinelo-Romay
laura.muinelo.romay@sergas.es

Specialty section:
This article was submitted to Cancer Molecular Targets and Therapeutics, a section of the journal Frontiers in Oncology

Received: *25 May 2020*
Accepted: *13 August 2020*
Published: *14 October 2020*

Citation:
Herrero C, Abal M and Muinelo-Romay L (2020) Circulating Extracellular Vesicles in Gynecological Tumors: Realities and Challenges. Front. Oncol. 10:565666. doi: 10.3389/fonc.2020.565666

INTRODUCTION

Precision oncology has emerged with the aim of achieving more accurate and active treatments for individual patients on the basis of the molecular characteristics of the tumor. This personalized oncology is intimately associated with the discovery of molecular biomarkers useful in predicting tumor prognosis and therapy response, and attaining accurate disease monitoring. In this context, circulating biomarkers and liquid biopsies are key elements for implementing personalized oncology as an ideal complement to tissue biopsies and radiologic analyses. The use of circulating biomarkers clearly improves the assessment of tumor spatial and temporal heterogeneity and evolution. Therefore, together with immunotherapy applications, the use of liquid biopsies to characterize tumors has marked a revolution in oncology (1).

Presently, liquid biopsy strategies are mainly based on the characterization of circulating tumor DNA (ctDNA), circulating tumor cells (CTCs), and circulating extracellular vesicles (cEVs) as sources of proteomic and genetic information. In fact, the determination of *EGFR* mutations in non-small cell lung cancer (NSCLC) through ctDNA analyses is been used to identify candidate patients for TKI based therapy (2). Besides, accumulating scientific evidence indicates the utility of ctDNA analyses to detect other clinically relevant alterations in different genes, such as *RAS*, *BRAF*, or *PI3KCA* in colorectal, melanoma, or breast tumors (3–5). In addition, during the past 20 years, the study of tumor cells released into the circulation, the CTC population, has provided broad information

about the molecular mechanisms favoring tumor spread and dissemination (6, 7). However, their clinical use remains anecdotal, and their application is mainly focused on translational research, owing to the difficulty of their isolation and their high heterogeneity; therefore, their analysis remains a challenge in many tumor types and clinical contexts (8, 9).

The last of the three pillars of circulating biomarker research is circulating extracellular vesicles (cEVs), a complex population of cell-derived membranous structures secreted by numerous cell types and generated by different cellular mechanisms (described in detail in **Figure 1**) (10, 11). Importantly, EVs refer to three main entities: exosomes, ranging from 30 to 100 nm; microvesicles, which are large membrane vesicles of 50–2,000 nm; and apoptotic bodies, which are typically 500–4,000 nm. These structures have a pivotal role in cancer, interacting with stromal cells, favoring tumor cell growth and proliferation, and enhancing the invasiveness and metastatic ability of target cells (12). Specially, EVs are key players in the establishment of the premetastatic niches required for cancer cell dissemination and engrafting at distal sites. Premetastatic niches comprise a specialized and favorable microenvironment that facilitates colonization and promotes the survival and outgrowth of disseminated tumor cells (13). Of note, hypoxia and microenvironmental acidity are key factors influencing cell fate within the tumor microenvironment as well as the secretion of EVs (14–16), independently of tumor histology (17). These data reinforce the value of assessing EV levels as a common biomarker in cancer (18). For example, high levels of cEVs are present in the plasma of patients with glioblastoma and change over the disease course (19).

Among the cancer related mechanisms mediated by EVs, angiogenesis appears to be important for maintaining tumor growth and dissemination. In fact, EVs secreted by different tumor cells have been shown to be relevant mediators of angiogenesis (20). In addition, several studies have shown that EVs modulate drug resistance through different mechanisms. For example, HER2-positive EVs secreted by breast cancer cells bind Trastuzumab and inhibit its anti-proliferative activity (21). In addition, the release of P-glycoprotein (P-gp) via EVs has been described as another mechanism of drug resistance in breast (22) and prostate cancer patients (23). Alternative mechanisms mediated by EVs have been found to be responsible for resistance to Temozolamide in glioblastoma (24), Gefitinib in esophageal squamous cell carcinoma (25), or Tamoxifen in breast cancer (26).

In addition to the important roles of EVs in tumor promotion and their interest as therapeutic targets, as we previously described, EVs have emerged as promising cancer biomarkers because they increase in different biological fluids as a consequence of the disease (12) and have high stability in circulation, protecting their molecular cargo (proteins, mRNAs, non-coding RNAs, and single-stranded or double-stranded DNAs) from the environment. Therefore, the analysis of cEVs is a promising tool for improving the clinical management of cancer patients but is currently far from being clinically validated. For example, increased exosomal PSA levels have been shown to be a valuable biomarker for both screening and secondary prevention of prostate cancer in a clinical study (27). Rodríguez-Zorrilla et al. have shown, in a pilot study, that CAV-1 positive exosomes increase after surgery, whereas low peri-surgical levels of plasmatic exosomes correlate with better survival in patients with oral squamous cell carcinoma (28).

Other studies aiming to characterize and validate EVs as a clinical tool have focused on PC. Melo et al. have identified glypican-1-associated EVs as a potential non-invasive diagnostic tool to detect early stages of pancreatic cancer (PC) (29). Opposite, other study has described low levels of miR-let7a and high levels of exosomal miR-10b, miR-21, miR-30c, and miR-181a, differentiating better PC from healthy control and chronic disease, compared plasma CA 19-9 levels or with exosomal glypican-1 (30). Several works have demonstrated that EV miRNAs may be useful as diagnostic biomarkers in different tumor types. Ogata-Kawata et al. have identified higher levels of seven serum exosomal miRNAs (let-7a, miR-1229, miR-1246, miR-150, miR-21, miR-223, and miR-23a) in patients with primary CRC than in healthy people (31). In the same line, a recent study has described exosomal miR-19b and miR-21 as independent diagnostic factors with higher sensitivity and specificity than the routinely used clinical biomarker CEA (32). Liu et al. have shown that elevated levels of exosomal miR-23b-3p, miR-10b-5p, and miR-21-5p are independently associated with poor overall survival in patients with NSCLC (33), whereas downregulation of the exosomal miRNA let-7a-5p leads to elevated expression of the target gene BCL2L1 and poor survival of patients with lung cancer (34). More recently, a combination of miR-375, miR-655-3p, miR-548b-5p, and miR-24-2-5p has been postulated to be a good diagnostic tool to detect early breast cancer (35).

Overall, all these data evidence the major roles of EVs in cancer as an indicator of tumor complexity, and a promising diagnostic and therapeutic tool. However, as we previously highlighted, the field of EVs is now far from clinical applicability in all tumor types, particularly gynecologic cancers. Therefore, the present review aims to summarize the knowledge on the pathological functions of EVs in endometrial and ovarian cancer as well as on the clinical potential involving the analysis of their protein and miRNA cargo.

CIRCULATING EVs IN ENDOMETRIAL CANCER

Endometrial cancer (EC) is the most prevalent gynecological cancer in developed countries. Most cases are diagnosed at a localized stage with a 5-year relative survival of 95%. However, this rate decreases to 69% when regional spread exists and to 16% when distant metastasis occurs (36). Although most cases are diagnosed at early stages, 2–15% of cases develop recurrent disease, and this proportion can reach 50% in women with advanced stage EC (37). EC treatment usually consists of surgery and adjuvant radiotherapy for patients with a high risk of recurrence. Chemotherapy is administrated in patients with metastatic/recurrent disease and high-grade tumors (38), but traditional chemotherapy is less active than in other cancers

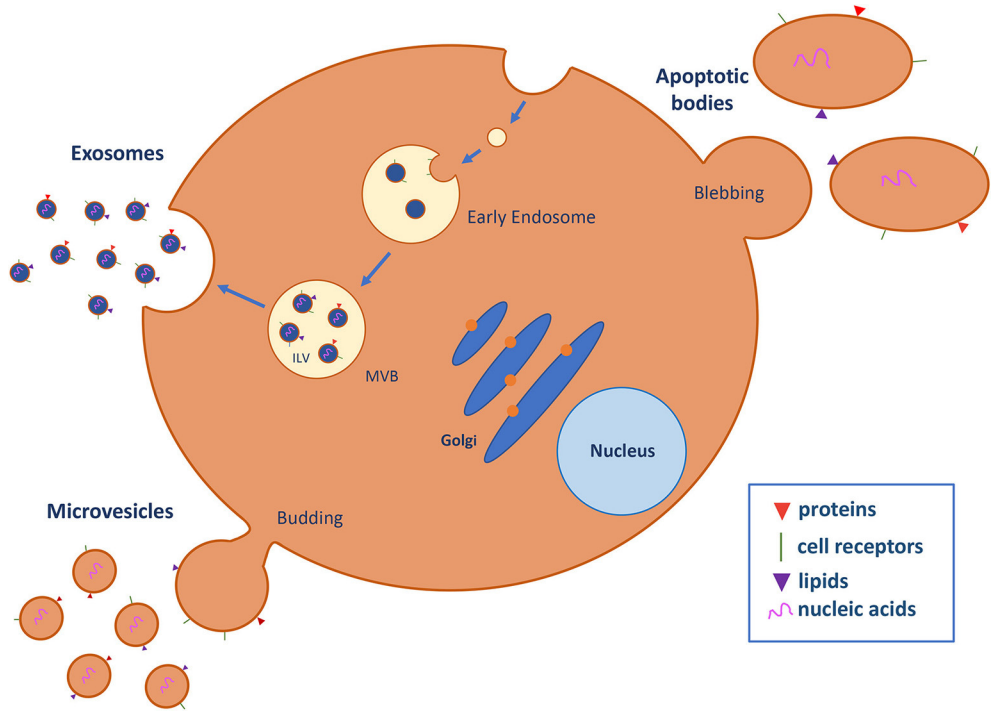

FIGURE 1 | Extracellular vesicle (EV) biogenesis and secretion. EVs are classified into three major subtypes on the basis of biogenic and morphological properties: exosomes, microvesicles (MVs), and apoptotic bodies. Exosomes are nanostructures of approximately 30–100 nm in diameter that originate as intraluminal vesicles (ILV) in multivesicle endosomes (MVB), which are intermediates in the endosomal system and can fuse with the plasma membrane and secrete their contents in exosomes into the extracellular space. Microvesicles (50–2,000 nm) are generated by direct budding and fission of the plasma membrane into the extracellular space. Apoptotic bodies (500–4,000 nm) are released by the blebbing process during programmed cell death. EVs contain several cell-specific components, such as proteins, lipids, and nucleic acids (DNA, mRNA, miRNA, and lncRNA) that are transferred to target cells (10, 11).

because of acquired resistance and the absence of targeted therapies (39). In this regard, efforts to improve EC management have mainly focused on the discovery of new therapeutic targets, and prognostic and predictive biomarkers to better define the risk of recurrence and the response to therapy.

Several biomarkers with prognostic and predictive value have been studied in EC tissue samples, such as L1CAM, a prognostic factor for FIGO stage I tumors, and ANXA2, identified as a predictor of recurrent disease in EC (40, 41). However, none of these biomarkers have been implemented in clinical practice, because of their limited sensitivity and/or specificity. Moreover, although the potential of liquid biopsies in EC has scarcely been explored, some studies have demonstrated the feasibility of detecting both CTCs and ctDNA in blood samples from patients with different stages of the disease, mainly with high-risk or metastatic cases (42–44). These promising preclinical results support the need for exploring the clinical benefit of circulating biomarkers to stratify patients with EC and identify alternative therapies. For this purpose, cEVs present in blood, urine, or uterine aspirates constitute a valuable alternative for improving the analytical sensitivity of protein and genetic biomarkers (43). Importantly, in this regard, the eventual effects of EVs on the uterine microenvironment have been explored in the context of embryo implantation, with the transfer of the miRNA content of exosomes and microvesicles between endometrial epithelial cells and trophectodermal cells of the blastocyst (45) and in endometriosis (46), but not in the context of the endometrial carcinoma environment (47), where their role is unknown.

In searching for new clinical EV-associated biomarkers, our group has recently studied ANXA2 levels in complete plasma and the cEV fraction. We observed that ANXA2 protein is present mainly in isolated cEVs but not as a soluble protein in the plasma. Importantly, in this work, we identified higher levels of ANXA2 in cEVs isolated from plasma samples of patients with EC than healthy controls. Furthermore, the analysis of ANXA2 in plasma EVs had favorable specificity and sensitivity as an EC biomarker (AUROC = 0.74) and was correlated with tumors with high risk of recurrence and non-endometrioid histology, thus indicating the potential of cEV-based ANXA2 levels as a promising diagnostic and prognostic liquid biomarker in EC (48).

In recent years, the study of miRNAs as potential biomarkers has increased. In patients with EC, miRNAs are associated with regulation of gene expression, epigenetic dysfunction, and carcinogenesis (49). Circulating free miRNAs have also been described as potential biomarkers for early EC diagnostic and detection of tumor progression (50, 51). Of note, several studies have identified miRNAs in EVs from different body

fluids. Srivastava et al. have evaluated the potential of miRNAs from urine-derived exosomes as a diagnostic biomarker for EC, showing an enrichment of miR-200c-3p in urine exosomes from patients (52). Roman-Canal et al. studied the miRNA profile in EVs from peritoneal lavage in EC. The authors found 114 miRNAs significantly altered in EVs from patients with EC. Among these, miR-383-5p, miR-10b-5p, miR-34c-3p, miR-449b-5p, miR-34c-5p, miR-200b-3p, miR-2110, and miR-34b-3p were downregulated in patients with EC and have been found to have predictive performance (AUC $\sim$ 0.90) (53). Another study by Li et al. has explored the roles of miR-302a-enriched EVs derived from human umbilical cord mesenchymal stem cell (hUCMSC) in EC cell growth and mobility. The authors suggest that these miR-302a-loaded EVs impair cell proliferation and migration by downregulating cyclin D1 and suppressing AKT signaling, thus suggesting that EVs rich in miR-302a may be a potential therapeutic strategy in EC (54). In addition, exosomal miR-93 and miR-205 have been found to increase in serum from patients with EC, and high miR-205 levels were associated with poor tumor evolution (55). Although all these data, the application of miRNAs in EVs from EC patients is still underdeveloped, being necessary more studies to explore all their potential.

CIRCULATING EVs IN OVARIAN CANCER

Ovarian cancer (OC) is the second most frequent tumor in Western countries after cervical cancer. There are no specific symptoms or screening tests for OC. Moreover, most OCs are high grade tumors that affect one or both ovaries, and have a high dissemination capacity (56). Survival rates in patients with OC have not substantially improved in recent years, because of the lack of effective targeted therapies (57). After surgical intervention, patients with advanced OC are treated with adjuvant chemotherapy, mainly based on platinum. However, most of these cancers recur, thus representing another important challenge to improving OC survival and achieving early diagnosis of the disease (58). The most common histological subtype is high grade serous OC, which is characterized by the presence of *P53* mutations and deficiency in homologous recombination. Since the DNA repair mechanisms are often altered in high grade serous OC, they are normally highly sensitive to platinum regimens but often acquire resistance mechanisms (59). In this context, only CA-125 levels are being used as a surrogate circulating biomarker to manage the disease (60). Therefore, in OC, as with EC, there is a need for accurate non-invasive biomarkers with clinical value for improving OC diagnosis and predict patient outcomes after surgery, to facilitate more precise follow-up and therapy selection. In this sense, the study of EVs as a non-invasive liquid biopsy tool sheds light on the discovery of new diagnostic and prognostic biomarkers together with therapeutic targets for OC.

EVs optimize the microenvironment for OC colonization, promoting angiogenesis, stromal remodeling, and immunosuppression in the premetastatic niche (61). Exosomes released into ascitic fluid might result in biophysical and functional changes in fibroblasts that promote the development of a malignant tumor microenvironment in OC (62). Likewise, the crosstalk between OC cells and endothelial cells modulating tumor angiogenesis may implicate exosomes and their miRNA content (63). Exosomes released in the hypoxic tumor microenvironment may also contribute to metastasis and chemotherapy resistance in OC, thus representing an opportunity to improve treatment success (64). In fact, our group has identified roles of exosomes derived from ascites in the communication between tumor cells and their environment. We found that exosomes obtained from ascites from patients with OC promote adhesion of SKOV3 cells. We took the advantage of this finding to develop a novel tumor cell capture system (M-Trap) comprising exosomes with an adhesive capacity to capture tumor cells and to impair the generalized peritoneal spreading in OC. In a murine model of OC spread generated by intraperitoneal injection of SKOV3 cells, when the M-Trap was implanted at the peritoneum, the dissemination of SKOV3 cells became markedly different, such that the metastasis localized on the M-Trap. Thus, M-trap technology is able to remodel metastatic patterns, transforming a systemic disease into a focal disease and offering a new therapeutic approach (65).

EVs also carry several factors that suppress the immune system and are responsible for the differentiation and activation of immune suppressor cells, modulating antigen presentation, or inducing T-cell apoptosis (66). In this sense, Peng et al. have detected FasL and TRAIL in EVs isolated from ascites of patients with OC; these proteins are associated with the apoptosis of immune cells and tumor escape from the immune response (67). Another study by Czystowska-Kuzmicz et al. has identified ARG1 in OC-derived EVs as a suppressor of peripheral T-cells that promotes tumor growth and evasion of the immune system (68).

There is more literature regarding the value of EVs as biomarkers in OC than in other gynecological tumors, such as EC. Thus, different protein cargos derived from EVs have been described as potential clinical biomarkers in OC. Li et al. have observed an enrichment in Claudin 4 in plasma exosomes from patients with OC, thus indicating its value as potential biomarker in OC (69). EVs isolated from OC ascites have been also described to contain L1CAM, CD24, ADAM10, and EMMPRIN, which favor tumor progression (70). Peng et al. have identified eight proteins normally expressed in OC (CLIC4, AKT1, EMAPII, SNX3, FAM49B, FERMT3, TUBB3, and lactotransferrin) in circulating exosomes and have suggested their utility in early diagnosis (71). In addition, CD9/HER2-positive EVs were found higher in the serum from patients with OC than in healthy controls and patients with non-malignant disease (72). More recently, the presence of GSN, FGG, FGA, and LBP proteins in OC derived exosomes has been described and associated with the promotion of the coagulation dysfunction that frequently occurs in OC (73). Besides, EV proteins also have important roles in tumor staging and as biomarkers for treatment response in patients with OC. In this regard, Szajnik et al. have reported that plasma from patients with OC is characterized by higher levels of exosomal proteins than those in plasma from controls (benign disease and healthy donors), and these levels are correlated with tumor stage (74).

Beyond EV associated proteins, mRNAs or miRNAs have been also related to OC carcinogenesis and aggressiveness. Yokoi et al. have found that cEVs containing MMP1 mRNA in ascites from patients with OC induce apoptosis in mesothelial cells, thereby promoting peritoneal dissemination (75). Taylor et al. have described an EVs miRNA signature of tumor derived-exosomes that are of interest as diagnostic markers. This signature includes miR-21, miR-200a, miR-200b, miR-141, miR-200c, miR-205, miR-214, and miR-203. Furthermore, the authors have found that the exosomal miRNA profiles from the serum of patients with OC are similar and significantly distinct from the profiles observed in benign disease (76). In addition, in the serum, exosome miR-222-3p is higher in patients with OC than healthy controls, and this elevation is associated with the interactions between ovarian tumor cells and macrophages (77). Meng et al. have found that exosomal miR-373, miR-200a, miR-200b, and miR-200c are significantly higher in serum samples from patients with epithelial OC than from healthy women. Moreover, miR-200b and miR-200c are associated with poor overall survival and tumor progression (78). Xu et al. have identified an alteration in miR101 levels in tissue samples and serum exosomes from patients with OC. Their results indicate that a decrease in miR101 in serum exosomes may serve as potential diagnostic biomarker in OC (79). In addition, high levels of EV-associated miR-99a-5p have been detected in serum from patients with OC and correlated with the promotion of invasion by regulating human peritoneal mesothelial cells (HPMCs) through vitronectin and fibronectin (80). In an analysis of plasma EVs in OC and healthy controls, Zhang et al. have found that miR-106a-5p, hsa-let-7d-5p, and miR-93-5p are significantly higher in OC, whereas miR-185-5p, miR-122-5p, and miR-99b-5p are lower. The authors suggest that these differentially expressed EV-associated miRNAs may be potential diagnostic and prognostic targets for OC treatment (81). Pan et al. have also focused on the influence of exosomal miRNAs on the pathogenesis of epithelial OC. They have found significantly higher miR-21, miR-100, miR-200b, and miR-320, and lower miR-16, miR-93, miR-126, and miR-223 in exosomes from the plasma of 106 patients with epithelial OC compared with 29 healthy women. Of note, the levels of miR-200b correlate with the tumor marker CA125 and overall patient survival (82). There is also evidence of a role of EV-associated miRNAs in therapy response of OC. Kuhlmann et al. have analyzed a set of EV-associated miRNAs in plasma samples from patients with OC and different response to platinum-based regimens. This panel is differentially abundant in platinum resistant vs. platinum sensitive OC, thus suggesting their potential as biomarkers predictors for platinum resistance (83).

Other body fluids have also been explored in OC for EV associated miRNA analyses. Thus, Vaksman et al. have identified an increase in miR-21, miR-23b, and miR-29a in exosomes derived from OC effusion supernatants. These miRNAs are associated with poor progression-free survival, and high expression of miR-21 correlates with poor overall survival (84). In contrast, global miRNA characterization has shown that miR-30a-5p is up-regulated in urine samples from patients with OC compared with healthy controls. This study suggests that the increased levels of this miRNA in urine samples may be due to the secretion of exosomes from OC cells; therefore, miR-30a-5p has been proposed as a new diagnostic marker in OC (85).

All these studies show that EVs are a potential source of diagnostic and prognostic biomarkers for OC. However, many challenges must be addressed before clinical utilization of EVs in detection and treatment of OC will be possible.

CHALLENGES IN THE CLINICAL APPLICATION OF cEVs IN GYNECOLOGICAL TUMORS

EVs play an important role in cell interaction by modulating the activity of target cells through either the action of surface proteins or trafficking with molecules between cells. This role is common among tumor types. As we previously described, EVs activity is a key element in multiple pathophysiological procedures, such as inflammatory responses, immunoregulation, carcinogenesis, tumor invasion, and metastasis. In fact, tumor-derived EVs have emerged as a new source of circulating cancer biomarkers, because they are present in all body fluids and have different molecular cargos from those of non-tumor EVs. Notably, in comparison with other circulating elements such as ctDNA or CTCs, cEVs are found in body fluids in higher concentrations, and, more importantly, they protect and stabilize their molecular cargo. Therefore, cEVs have great promise as biomarkers for different tumor types, including endometrial cancer and OC. Despite this potential, generalized implementation of EV-based biomarkers in clinical contexts remains far from reality.

One of the main challenges to improving EV applications for treatment of cancer, particularly gynecological tumors, is the limited performance of methods for the isolation and characterization of EVs. There is no technical standardization, and evidence of high specificity and sensitivity for routine clinical implementation is lacking. The need for standardized protocols includes sample collection and processing, EV isolation, and numerous strategies to analyze EV molecular cargo, thus making comparison of the results obtained in different studies difficult. In particular, EV isolation strategies are normally grouped into five isolation techniques: ultracentrifugation, polymer-based precipitation, immune-selection, density-gradient separation, and microfluidic isolation. All these strategies can be combined and applied to different body fluids. However, all these methods have some limitations. Ultracentrifugation is the most commonly used method for isolating EVs; however, it is time consuming, requires high sample volumes, and provides low recovery of EVs. An ideal method for isolation of EVs in a clinical context should enable simple use without a need for complex equipment, and should be fast and compatible with many samples. Currently, there are easily used technologies for EV isolation from liquid biopsies, which have been successfully applied in gynecological tumors; these include ExoQuick, ExoSpin, and ExoGAG (48, 84). The results obtained with these technologies are promising; however, most of the studies on endometrial and ovarian tumors have been performed in limited cohorts of patients (**Table 1**). Therefore, there is a clear need for large scale clinical studies using robust technologies to answer relevant questions about

TABLE 1 | EVs as non-invasive biomarkers in gynecological tumors.

EV source	Isolation method	Type of molecule (protein/miRNA)	Cohort (n)	Clinical application	References
Plasma	ExoGAG (Nasas Biotech)	ANXA2 and L1CAM	41 patients with EC vs. 20 healthy controls	Diagnosis/ prognosis	(48)
Urine	UC	miR-200c-3p	22 patients with EC vs. 5 symptomatic controls	Diagnosis/prognosis	(52)
Peritoneal lavage	UC	miR-383-5p, miR-10b-5p, miR-34c-3p, miR-449b-5p, miR-34c-5p, miR-200b-3p, miR-2110, and miR-34b-3p	25 patients with EC vs. 25 healthy controls	Diagnosis	(53)
Serum	miRCURY (Qiagen)	miR-93 and miR-205	100 patients with EC vs. 100 healthy controls	Diagnosis/prognosis	(55)
Plasma/ serum	UC	TGF-beta and MAGE3/6	22 patients with OC vs. 10 patients with serous cysts vs. 10 healthy controls	Diagnosis	(74)
Plasma	UC	Claudin 4	63 patients with OC vs. 50 healthy controls	Diagnosis	(69)
Ascites	UC	FasL and TRAIL, TCR, CD20, HLA-DR, B7-2, HER2/neu, CA125 and histone H2A	35 patients with OC	Immune system regulation	(67)
Serum	UC	CLIC4, PK1, AIMP1, SNX3, protein FAM49B, FERMT3, TUBB3 and lactotransferrin	10 patients with OC vs. 10 healthy women	Diagnosis	(71)
Serum	Immune isolation and nano/optical detection ExoCounter	CD9/HER2	50 patients with OC vs. 63 healthy controls	Diagnosis	(72)
Plasma	Precipitation ExoEasy Maxi kit (Qiagen)	GSN, FGG, FGA and LBP	40 patients with OC vs. 40 healthy women	Diagnosis/prognosis/ therapeutic target	(73)
Ascites	UC	MMP1	48 patients with OC vs. 12 benign disease	Prognosis	(75)
Serum	EpCAM based immunoisolation	miR-21, miR-141, miR- 200a, miR-200c, miR-200b, miR-203, miR-205 and miR-214	50 patients with OC vs. 10 patients with adenomas vs. 10 healthy women	Diagnosis	(76)
Serum	Precipitation Total Exosome Isolation Reagent (Invitrogen)	miR-200b and miR-200c	163 patients with OC, 20 patients with benign ovarian diseases and 32 healthy women	Diagnosis/prognosis	(78)
Serum	Precipitation ExoQuick (System Bioscience)	miR-100	20 patients with OC and 20 healthy women	Diagnosis	(79)
Serum	Precipitation Total Exosome Isolation Reagent (Invitrogen)	miR-222-3p	6 patients with OC vs. 6 healthy controls	Diagnosis/therapeutic target	(77)
Serum	UC	miR-99a-5p	62 patients with OC vs. 26 patients with benign ovarian tumors vs. 20 healthy volunteers	Diagnosis/therapeutic target	(80)
Plasma	UC	Up: miR-106a-5p, hsa-let-7d-5p, and miR-93-5p Down: miR-185-5p, miR-122-5p, and miR-99b-5p	30 patients with OC vs. 30 healthy volunteers	Diagnosis	(81)
Plasma	Precipitation ExoQuick (SystemBioscience)	Up: miR-21, miR-100, miR-200b, and miR-320 Down: miR-16, miR-93, miR-126, and miR-223	106 patients with OC vs. 8 patients with ovarian cystadenoma vs. 29 healthy women	Diagnosis /prognosis	(82)
Plasma	Precipitation ExoQuick (System Bioscience)	miR-181a, miR-1908, miR-21, miR-486 and miR-223	30 patients with OC (15 platinum resistant vs. 15 platinum sensible)	Therapy prediction	(83)
Pleural and peritoneal effusions	Precipitation ExoQuick (System Bioscience)	miRNAs 21, miRNA23b and 29a	86 patients with OC	Prognosis	(84)

(Continued)

TABLE 1 | Continued

EV source	Isolation method	Type of molecule (protein/miRNA)	Cohort (n)	Clinical application	References
Urine	UC	miR-30a-5p	39 patients with OC vs. 26 patients with benign gynecological disease vs. 30 healthy controls vs. 40 patients with gastric/colon cancer	Diagnosis/ therapeutic target	(85)

UC, ultracentrifugation.

gynecological tumors. For OC, the key clinical need is the validation of biomarkers for early diagnostic and screening, in addition to markers of prognostic and therapeutic value. In EC, clinicians require new accurate biomarkers to stratify patients who have a higher risk of recurrence after surgery and new markers to guide therapy selection in metastatic settings. The improvement of cEV isolation technologies, together with the application of multi-omics strategies to characterize their molecular cargo, and the selection of larger and well defined cohorts of patients for studies, will be critical in the near future to enable clinical translation of circulating EVs in the management of gynecologic tumors.

Other challenging line of work includes validation of EVs for drug delivery (86). This possibility is supported by evidence of the tissue tropism of EVs, mediated by surface molecules that might eventually be translated to specific tumor targeting and subsequent drug delivery. Liposomes are the most illustrative example of versatile clinically available drug delivery vehicles (87). Both the lipid membrane and interior space are tunable for loading of hydrophobic and hydrophilic drugs, respectively. Likewise, functionalization of EVs is a promising alternative for the development of diagnostic tests predicting organ-specific metastasis and for more efficient therapies impairing metastasis. For example, exosomal integrins have been shown to direct organ-specific colonization by fusing with target cells in a tissue-specific fashion (88). Efficient functionalization of EVs, control of the yield and stability of the therapeutic cargo, purification and production scaling methods, sustained delivery during extended periods compatible with clinical timings, and appropriate and specific preclinical study designs are major challenges in the translation of these technologies into clinical practice for many tumor types, including gynecologic tumors.

For effective translation of EV-based analysis into clinical practice, substantial scientific effort will be required, involving both basic-science researchers and clinicians. In addition, this work should follow the recommendations of the International Society for Extracellular Vesicles (ISEV) and various working groups supporting the harmonization of protocols to improve the reproducibility of procedures and kits for EV analyses (89, 90), and to address relevant clinical questions in adequate clinical cohorts.

CONCLUSIONS

Herein, we have reviewed the potential of cEVs in the development of gynecologic cancer biomarkers and therapies. Liquid biopsy approaches are minimally invasive and provide a comprehensive picture of tumors, thus providing a new opportunity for the application of personalized oncology. In particular, cEVs present in blood, ascites, or urine have shown great potential as biomarkers in the clinical management of gynecologic tumors. Both protein and miRNA EV cargo have shown promise in preclinical studies as biomarkers for early detection, prognosis, and prediction of the response to therapy and the acquisition of resistances in endometrial or ovarian tumors. However, this field is in its infancy, and many challenges must be met before clinical utilization of EVs can be achieved for detection, monitoring, and therapy selection for gynecologic tumors.

AUTHOR CONTRIBUTIONS

All authors have contributed to the bibliographic review and manuscript preparation.

FUNDING

This research was funded by CIBERONC (CB16/12/00328), Instituto de Salud Carlos III, grant PI17/01919, co-financed by the European Regional Development Fund (FEDER) and the AECC (Grupos Estables de Investigacion 2018-AECC). LM-R was supported by AECC.

ACKNOWLEDGMENTS

We would like to thank AECC and ISCIII for supporting our research focused on endometrial cancer.

REFERENCES

1. Pantel K, Alix-Panabières C. Liquid biopsy: potential and challenges. *Mol Oncol.* (2016) 10:371–3. doi: 10.1016/j.molonc.2016.01.009

2. Karlovich C, Goldman JW, Sun J-M, Mann E, Sequist LV, Konopa K, et al. Assessment of EGFR mutation status in matched plasma and tumor tissue of NSCLC patients from a Phase I study of rociletinib (CO-1686). *Clin Cancer Res.* (2016) 22:2386–95. doi: 10.1158/1078-0432.CCR-15-1260

3. Garcia-Murillas I, Schiavon G, Weigelt B, Ng C, Hrebien S, Cutts RJ, et al. Mutation tracking in circulating tumor DNA predicts relapse in early breast cancer. *Sci Transl Med.* (2015) 7:302ra133. doi: 10.1126/scitranslmed.aab0021
4. Tie J, Wang Y, Tomasetti C, Li L, Springer S, Kinde I, et al. Circulating tumor DNA analysis detects minimal residual disease and predicts recurrence in patients with stage II colon cancer. *Sci Transl Med.* (2016) 8:346ra92. doi: 10.1126/scitranslmed.aaf6219
5. Rowe SP, Luber B, Makell M, Brothers P, Santmyer J, Schollenberger MD, et al. From validity to clinical utility: the influence of circulating tumor DNA on melanoma patient management in a real-world setting. *Mol Oncol.* (2018) 12:1661–72. doi: 10.1002/1878-0261.12373
6. Pantel K, Speicher MR. The biology of circulating tumor cells. *Oncogene.* (2016) 35:1216–24. doi: 10.1038/onc.2015.192
7. Dianat-Moghadam H, Azizi M, Eslami-S Z, Cortés-Hernández LE, Heidarifard M, Nouri M. The role of circulating tumor cells in the metastatic cascade: biology, technical challenges, and clinical relevance. *Cancers.* (2020) 12:867. doi: 10.3390/cancers12040867
8. Cabel L, Proudhon C, Gortais H, Loirat D, Coussy F, Pierga J-Y, et al. Circulating tumor cells: clinical validity and utility. *Int J Clin Oncol.* (2017) 22:421–30. doi: 10.1007/s10147-017-1105-2
9. Siravegna G, Marsoni S, Siena S, Bardelli A. Integrating liquid biopsies into the management of cancer. *Nat Rev Clin Oncol.* (2017) 14:531–48. doi: 10.1038/nrclinonc.2017.14
10. Akers JC, Gonda D, Kim R, Carter BS, Chen CC. Biogenesis of extracellular vesicles (EV): exosomes, microvesicles, retrovirus-like vesicles, and apoptotic bodies. *J Neurooncol.* (2013) 113:1–11. doi: 10.1007/s11060-013-1084-8
11. van Niel G, D'Angelo G, Raposo G. Shedding light on the cell biology of extracellular vesicles. *Nat Rev Mol Cell Biol.* (2018) 19:213–28. doi: 10.1038/nrm.2017.125
12. Becker A, Thakur BK, Weiss JM, Kim HS, Peinado H, Lyden D. Extracellular vesicles in cancer: cell-to-cell mediators of metastasis. *Cancer Cell.* (2016) 30:836–48. doi: 10.1016/j.ccell.2016.10.009
13. Nogués L, Benito-Martin A, Hergueta-Redondo M, Peinado H. The influence of tumor-derived extracellular vesicles on local and distal metastatic dissemination. *Mol Aspects Med.* (2018) 60:15–26. doi: 10.1016/j.mam.2017.11.012
14. Gillies RJ, Pilot C, Marunaka Y, Fais S. Targeting acidity in cancer and diabetes. *Biochim Biophys Acta Rev Cancer.* (2019) 1871:273–80. doi: 10.1016/j.bbcan.2019.01.003
15. Logozzi M, Spugnini E, Mizzoni D, Di Raimo R, Fais S. Extracellular acidity and increased exosome release as key phenotypes of malignant tumors. *Cancer Metastasis Rev.* (2019) 38:93–101. doi: 10.1007/s10555-019-09783-8
16. Pillai SR, Damaghi M, Marunaka Y, Spugnini EP, Fais S, Gillies RJ. Causes, consequences, and therapy of tumors acidosis. *Cancer Metastasis Rev.* (2019) 38:205–22. doi: 10.1007/s10555-019-09792-7
17. Logozzi M, Mizzoni D, Angelini DF, Di Raimo R, Falchi M, Battistini L, et al. Microenvironmental pH and exosome levels interplay in human cancer cell lines of different histotypes. *Cancers.* (2018) 10:370. doi: 10.3390/cancers10100370
18. Cappello F, Logozzi M, Campanella C, Bavisotto CC, Marcilla A, Properzi F, et al. Exosome levels in human body fluids: a tumor marker by themselves? *Eur J Pharm Sci.* (2017) 96:93–8. doi: 10.1016/j.ejps.2016.09.010
19. Osti D, Del Bene M, Rappa G, Santos M, Matafora V, Richichi C, et al. Clinical significance of extracellular vesicles in plasma from glioblastoma patients. *Clin Cancer Res.* (2019) 25:266–76. doi: 10.1158/1078-0432.CCR-18-1941
20. Todorova D, Simoncini S, Lacroix R, Sabatier F, Dignat-George F. Extracellular vesicles in angiogenesis. *Circ Res.* (2017) 120:1658–73. doi: 10.1161/CIRCRESAHA.117.309681
21. Ciravolo V, Huber V, Ghedini GC, Venturelli E, Bianchi F, Campiglio M, et al. Potential role of HER2-overexpressing exosomes in countering trastuzumab-based therapy. *J Cell Physiol.* (2012) 227:658–67. doi: 10.1002/jcp.22773
22. Lv M, Zhu X, Chen W, Zhong S, Hu Q, Ma T, et al. Exosomes mediate drug resistance transfer in MCF-7 breast cancer cells and a probable mechanism is delivery of P-glycoprotein. *Tumor Biol.* (2014) 35:10773–9. doi: 10.1007/s13277-014-2377-z
23. Kato T, Mizutani K, Kameyama K, Kawakami K, Fujita Y, Nakane K, et al. Serum exosomal P-glycoprotein is a potential marker to diagnose docetaxel resistance and select a taxoid for patients with prostate cancer. *Urol Oncol Semin Orig Investig.* (2015) 33:385.e15–20. doi: 10.1016/j.urolonc.2015.04.019
24. Zhang Z, Yin J, Lu C, Wei Y, Zeng A, You Y. Exosomal transfer of long non-coding RNA SBF2-AS1 enhances chemoresistance to temozolomide in glioblastoma. *J Exp Clin Cancer Res.* (2019) 38:166. doi: 10.1186/s13046-019-1139-6
25. Kang M, Ren M, Li Y, Fu Y, Deng M, Li C. Exosome-mediated transfer of lncRNA PART1 induces gefitinib resistance in esophageal squamous cell carcinoma via functioning as a competing endogenous RNA. *J Exp Clin Cancer Res.* (2018) 37:171. doi: 10.1186/s13046-018-0845-9
26. Wei Y, Lai X, Yu S, Chen S, Ma Y, Zhang Y, et al. Exosomal miR-221/222 enhances tamoxifen resistance in recipient ER-positive breast cancer cells. *Breast Cancer Res Treat.* (2014) 147:423–31. doi: 10.1007/s10549-014-3037-0
27. Logozzi M, Angelini DF, Giuliani A, Mizzoni D, Di Raimo R, Maggi M, et al. Increased plasmatic levels of PSA-expressing exosomes distinguish prostate cancer patients from benign prostatic hyperplasia: a prospective study. *Cancers.* (2019) 11:1449. doi: 10.3390/cancers11101449
28. Rodríguez Zorrilla S, Pérez-Sayans M, Fais S, Logozzi M, Gallas Torreira M, García García A. A pilot clinical study on the prognostic relevance of plasmatic exosomes levels in oral squamous cell carcinoma patients. *Cancers.* (2019) 11:429. doi: 10.3390/cancers11030429
29. Melo SA, Luecke LB, Kahlert C, Fernandez AF, Gammon ST, Kaye J, et al. Glypican-1 identifies cancer exosomes and detects early pancreatic cancer. *Nature.* (2015) 523:177–82. doi: 10.1038/nature14581
30. Lai X, Wang M, McElyea SD, Sherman S, House M, Korc M. A microRNA signature in circulating exosomes is superior to exosomal glypican-1 levels for diagnosing pancreatic cancer. *Cancer Lett.* (2017) 393:86–93. doi: 10.1016/j.canlet.2017.02.019
31. Ogata-Kawata H, Izumiya M, Kurioka D, Honma Y, Yamada Y, Furuta K, et al. Circulating exosomal microRNAs as biomarkers of colon cancer. *PLoS ONE.* (2014) 9:e92921. doi: 10.1371/journal.pone.0092921
32. de Miguel Pérez D, Rodriguez Martínez A, Ortigosa Palomo A, Delgado Ureña M, Garcia Puche JL, Robles Remacho A, et al. Extracellular vesicle-miRNAs as liquid biopsy biomarkers for disease identification and prognosis in metastatic colorectal cancer patients. *Sci Rep.* (2020) 10:3974. doi: 10.1038/s41598-020-60212-1
33. Liu Q, Yu Z, Yuan S, Xie W, Li C, Hu Z, et al. Circulating exosomal microRNAs as prognostic biomarkers for non-small-cell lung cancer. *Oncotarget.* (2017) 8:13048–58. doi: 10.18632/oncotarget.14369
34. Zhang L, Hao C, Zhai R, Wang D, Zhang J, Bao L, et al. Downregulation of exosomal let-7a-5p in dust exposed- workers contributes to lung cancer development. *Respir Res.* (2018) 19:235. doi: 10.1186/s12931-018-0949-y
35. Yan C, Hu J, Yang Y, Hu H, Zhou D, Ma M, et al. Plasma extracellular vesicle-packaged microRNAs as candidate diagnostic biomarkers for early-stage breast cancer. *Mol Med Rep.* (2019) 20:3991–4002. doi: 10.3892/mmr.2019.10669
36. Siegel RL, Miller KD, Jemal A. Cancer statistics, 2020. *CA Cancer J Clin.* (2020) 70:7–30. doi: 10.3322/caac.21590
37. Felix AS, Brasky TM, Cohn DE, Mutch DG, Creasman WT, Thaker PH, et al. Endometrial carcinoma recurrence according to race and ethnicity: an NRG oncology/gynecologic oncology group 210 study. *Int J Cancer.* (2018) 142:1102–15. doi: 10.1002/ijc.31127
38. Colombo N, Creutzberg C, Amant F, Bosse T, González-Martín A, Ledermann J, et al. ESMO-ESGO-ESTRO Consensus conference on endometrial cancer. *Int J Gynecol Cancer.* (2016) 26:2–30. doi: 10.1097/IGC.0000000000000609
39. Brasseur K, Gévry N, Asselin E. Chemoresistance and targeted therapies in ovarian and endometrial cancers. *Oncotarget.* (2017) 8:4008–42. doi: 10.18632/oncotarget.14021
40. Zeimet AG, Reimer D, Huszar M, Winterhoff B, Puistola U, Abdel Azim S, et al. L1CAM in early-stage type I endometrial cancer: results of a large multicenter evaluation. *JNCI J Natl Cancer Inst.* (2013) 105:1142–50. doi: 10.1093/jnci/djt144
41. Alonso-Alconada L, Santacana M, Garcia-Sanz P, Muinelo-Romay L, Colas E, Mirantes C, et al. Annexin-A2 as predictor biomarker of recurrent disease in endometrial cancer. *Int J Cancer.* (2015) 136:1863–73. doi: 10.1002/ijc.29213
42. Alonso-Alconada L, Muinelo-Romay L, Madissoo K, Diaz-Lopez A, Krakstad C, Trovik J, et al. Molecular profiling of circulating tumor cells links plasticity

to the metastatic process in endometrial cancer. *Mol Cancer.* (2014) 13:223. doi: 10.1186/1476-4598-13-223
43. Muinelo-Romay L, Casas-Arozamena C, Abal M. Liquid biopsy in endometrial cancer: new opportunities for personalized oncology. *Int J Mol Sci.* (2018) 19:2311. doi: 10.3390/ijms19082311
44. Casas-Arozamena C, Díaz E, Moiola CP, Alonso-Alconada L, Ferreiros A, Abalo A, et al. Genomic profiling of uterine aspirates and cfDNA as an integrative liquid biopsy strategy in endometrial cancer. *J Clin Med.* (2020) 9:585. doi: 10.3390/jcm9020585
45. Ng YH, Rome S, Jalabert A, Forterre A, Singh H, Hincks CL, et al. Endometrial exosomes/microvesicles in the uterine microenvironment: a new paradigm for embryo-endometrial cross talk at implantation. *PLoS ONE.* (2013) 8:e58502. doi: 10.1371/journal.pone.0058502
46. Chen M, Zhou Y, Xu H, Hill C, Ewing RM, He D, et al. Bioinformatic analysis reveals the importance of epithelial-mesenchymal transition in the development of endometriosis. *Sci Rep.* (2020) 10:8442. doi: 10.1038/s41598-020-65606-9
47. Nguyen HPT, Simpson RJ, Salamonsen LA, Greening DW. Extracellular vesicles in the intrauterine environment: challenges and potential functions. *Biol Reprod.* (2016) 95:109. doi: 10.1095/biolreprod.116.143503
48. Herrero C, de la Fuente A, Casas-Arozamena C, Sebastian V, Prieto M, Arruebo M, et al. Extracellular vesicles-based biomarkers represent a promising liquid biopsy in endometrial cancer. *Cancers.* (2019) 11:2000. doi: 10.3390/cancers11122000
49. Banno K, Yanokura M, Kisu I, Yamagami W, Susumu N, Aoki D. MicroRNAs in endometrial cancer. *Int J Clin Oncol.* (2013) 18:186–92. doi: 10.1007/s10147-013-0526-9
50. Torres A, Torres K, Pesci A, Ceccaroni M, Paszkowski T, Cassandrini P, et al. Deregulation of miR-100, miR-99a and miR-199b in tissues and plasma coexists with increased expression of mTOR kinase in endometrioid endometrial carcinoma. *BMC Cancer.* (2012) 12:369. doi: 10.1186/1471-2407-12-369
51. Tsukamoto O, Miura K, Mishima H, Abe S, Kaneuchi M, Higashijima A, et al. Identification of endometrioid endometrial carcinoma-associated microRNAs in tissue and plasma. *Gynecol Oncol.* (2014) 132:715–21. doi: 10.1016/j.ygyno.2014.01.029
52. Srivastava A, Moxley K, Ruskin R, Dhanasekaran DN, Zhao YD, Ramesh R. A non-invasive liquid biopsy screening of urine-derived exosomes for miRNAs as biomarkers in endometrial cancer patients. *AAPS J.* (2018) 20:82. doi: 10.1208/s12248-018-0220-y
53. Roman-Canal B, Moiola CP, Gatius S, Bonnin S, Ruiz-Miró M, González E, et al. EV-associated miRNAs from peritoneal lavage are a source of biomarkers in endometrial cancer. *Cancers.* (2019) 11:839. doi: 10.3390/cancers11060839
54. Li X, Wang K, Ai H. Human umbilical cord mesenchymal stem cell-derived extracellular vesicles inhibit endometrial cancer cell proliferation and migration through delivery of exogenous miR-302a. *Stem Cells Int.* (2019) 2019:1–11. doi: 10.1155/2019/8108576
55. Zheng W, Yang J, Wang Y, Liu X. Exosomal miRNA-93 and miRNA-205 expression in endometrial cancer. *J King Saud Univ Sci.* (2020) 32:1111–5. doi: 10.1016/j.jksus,.2019.10.006
56. Brett MR, Jennifer BP, Thomas AS. Epidemiology of ovarian cancer: a review. *Cancer Biol Med.* (2017) 14:9–32. doi: 10.20892/j.issn.2095-3941.2016.0084
57. Torre LA, Trabert B, DeSantis CE, Miller KD, Samimi G, Runowicz CD, et al. Ovarian cancer statistics, 2018. *CA Cancer J Clin.* (2018) 68:284–96. doi: 10.3322/caac.21456
58. Corrado G, Salutari V, Palluzzi E, Distefano MG, Scambia G, Ferrandina G. Optimizing treatment in recurrent epithelial ovarian cancer. *Expert Rev Anticancer Ther.* (2017) 17:1147–58. doi: 10.1080/14737140.2017.1398088
59. Cortez AJ, Tudrej P, Kujawa KA, Lisowska KM. Advances in ovarian cancer therapy. *Cancer Chemother Pharmacol.* (2018) 81:17–38. doi: 10.1007/s00280-017-3501-8
60. Dochez V, Caillon H, Vaucel E, Dimet J, Winer N, Ducarme G. Biomarkers and algorithms for diagnosis of ovarian cancer: CA125, HE4, RMI and ROMA, a review. *J Ovarian Res.* (2019) 12:28. doi: 10.1186/s13048-019-0503-7
61. Feng W, Dean DC, Hornicek FJ, Shi H, Duan Z. Exosomes promote pre-metastatic niche formation in ovarian cancer. *Mol Cancer.* (2019) 18:124. doi: 10.1186/s12943-019-1049-4
62. Lee AH, Ghosh D, Quach N, Schroeder D, Dawson MR. Ovarian cancer exosomes trigger differential biophysical response in tumor-derived fibroblasts. *Sci Rep.* (2020) 10:8686. doi: 10.1038/s41598-020-65628-3
63. He L, Zhu W, Chen Q, Yuan Y, Wang Y, Wang J, et al. Ovarian cancer cell-secreted exosomal miR-205 promotes metastasis by inducing angiogenesis. *Theranostics.* (2019) 9:8206–20. doi: 10.7150/thno.37455
64. Dorayappan KDP, Wanner R, Wallbillich JJ, Saini U, Zingarelli R, Suarez AA, et al. Hypoxia-induced exosomes contribute to a more aggressive and chemoresistant ovarian cancer phenotype: a novel mechanism linking STAT3/Rab proteins. *Oncogene.* (2018) 37:3806–21. doi: 10.1038/s41388-018-0189-0
65. de la Fuente A, Alonso-Alconada L, Costa C, Cueva J, Garcia-Caballero T, Lopez-Lopez R, et al. M-Trap: exosome-based capture of tumor cells as a new technology in peritoneal metastasis. *J Natl Cancer Inst.* (2015) 107:djv184. doi: 10.1093/jnci/djv184
66. Czernek L, Düchler M. Functions of cancer-derived extracellular vesicles in immunosuppression. *Arch Immunol Ther Exp.* (2017) 65:311–23. doi: 10.1007/s00005-016-0453-3
67. Peng P, Yan Y, Keng S. Exosomes in the ascites of ovarian cancer patients: origin and effects on anti-tumor immunity. *Oncol Rep.* (2011) 25:749–62. doi: 10.3892/or.2010.1119
68. Czystowska-Kuzmicz M, Sosnowska A, Nowis D, Ramji K, Szajnik M, Chlebowska-Tuz J, et al. Small extracellular vesicles containing arginase-1 suppress T-cell responses and promote tumor growth in ovarian carcinoma. *Nat Commun.* (2019) 10:3000. doi: 10.1038/s41467-019-10979-3
69. Li J, Sherman-Baust CA, Tsai-Turton M, Bristow RE, Roden RB, Morin PJ. Claudin-containing exosomes in the peripheral circulation of women with ovarian cancer. *BMC Cancer.* (2009) 9:244. doi: 10.1186/1471-2407-9-244
70. Keller S, König A-K, Marmé F, Runz S, Wolterink S, Koensgen D, et al. Systemic presence and tumor-growth promoting effect of ovarian carcinoma released exosomes. *Cancer Lett.* (2009) 278:73–81. doi: 10.1016/j.canlet.2008.12.028
71. Peng P, Zhang W, Cao D, Yang J, Shen K. The proteomic comparison of peripheral circulation-derived exosomes from the epithelial ovarian carcinoma (EOC) patients and non-EOC subjects. *Transl Cancer Res.* (2019) 8:452–65. doi: 10.21037/tcr.2019.03.06
72. Kabe Y, Suematsu M, Sakamoto S, Hirai M, Koike I, Hishiki T, et al. Development of a highly sensitive device for counting the number of disease-specific exosomes in human sera. *Clin Chem.* (2018) 64:1463–73. doi: 10.1373/clinchem.2018.291963
73. Zhang W, Ou X, Wu X. Proteomics profiling of plasma exosomes in epithelial ovarian cancer: a potential role in the coagulation cascade, diagnosis and prognosis. *Int J Oncol.* (2019) 54:1719–33. doi: 10.3892/ijo.2019.4742
74. Szajnik M, Derbis M, Lach M, Patalas P, Michalak M, Drzewiecka H, et al. Exosomes in plasma of patients with ovarian carcinoma: potential biomarkers of tumor progression and response to therapy. *Gynecol Obstet.* (2013) Suppl. 4:3. doi: 10.4172/2161-0932.S4-003
75. Yokoi A, Yoshioka Y, Yamamoto Y, Ishikawa M, Ikeda S, Kato T, et al. Malignant extracellular vesicles carrying MMP1 mRNA facilitate peritoneal dissemination in ovarian cancer. *Nat Commun.* (2017) 8:14470. doi: 10.1038/ncomms14470
76. Taylor DD, Gercel-Taylor C. MicroRNA signatures of tumor-derived exosomes as diagnostic biomarkers of ovarian cancer. *Gynecol Oncol.* (2008) 110:13–21. doi: 10.1016/j.ygyno.2008.04.033
77. Ying X, Wu Q, Wu X, Zhu Q, Wang X, Jiang L, et al. Epithelial ovarian cancer-secreted exosomal miR-222-3p induces polarization of tumor-associated macrophages. *Oncotarget.* (2016) 7:43076–87. doi: 10.18632/oncotarget.9246
78. Meng X, Müller V, Milde-Langosch K, Trillsch F, Pantel K, Schwarzenbach H. Diagnostic and prognostic relevance of circulating exosomal miR-373, miR-200a, miR-200b and miR-200c in patients with epithelial ovarian cancer. *Oncotarget.* (2016) 7:16923–35. doi: 10.18632/oncotarget.7850
79. Xu Y, Xu L, Zheng J, Geng L, Zhao S. MiR-101 inhibits ovarian carcinogenesis by repressing the expression of brain-derived neurotrophic factor. *FEBS Open Bio.* (2017) 7:1258–66. doi: 10.1002/2211-5463.12257
80. Yoshimura A, Sawada K, Nakamura K, Kinose Y, Nakatsuka E, Kobayashi M, et al. Exosomal miR-99a-5p is elevated in sera of ovarian cancer patients and promotes cancer cell invasion by increasing fibronectin and vitronectin expression in neighboring peritoneal

mesothelial cells. *BMC Cancer*. (2018) 18:1065. doi: 10.1186/s12885-018-4974-5
81. Zhang H, Xu S, Liu X. MicroRNA profiling of plasma exosomes from patients with ovarian cancer using high-throughput sequencing. *Oncol Lett.* (2019) 17:5601–7. doi: 10.3892/ol.2019.10220
82. Pan C, Stevic I, Müller V, Ni Q, Oliveira-Ferrer L, Pantel K, et al. Exosomal microRNAs as tumor markers in epithelial ovarian cancer. *Mol Oncol.* (2018) 12:1935–48. doi: 10.1002/1878-0261.12371
83. Kuhlmann JD, Chebouti I, Kimmig R, Buderath P, Reuter M, Puppel S-H, et al. Extracellular vesicle-associated miRNAs in ovarian cancer – design of an integrated NGS-based workflow for the identification of blood-based biomarkers for platinum-resistance. *Clin Chem Lab Med.* (2019) 57:1053–62. doi: 10.1515/cclm-2018-1048
84. Vaksman O, Tropé C, Davidson B, Reich R. Exosome-derived miRNAs and ovarian carcinoma progression. *Carcinogenesis.* (2014) 35:2113–20. doi: 10.1093/carcin/bgu130
85. Zhou J, Gong G, Tan H, Dai F, Zhu X, Chen Y, et al. Urinary microRNA-30a-5p is a potential biomarker for ovarian serous adenocarcinoma. *Oncol Rep.* (2015) 33:2915–23. doi: 10.3892/or.2015.3937
86. Wang Y, Zhang Y, Cai G, Li Q. Exosomes as actively targeted nanocarriers for cancer therapy. *Int J Nanomed.* (2020) 15:4257–73. doi: 10.2147/IJN.S239548
87. Massing U, Fuxius S. Liposomal formulations of anticancer drugs: selectivity and effectiveness. *Drug Resist Updat.* (2000) 3:171–7. doi: 10.1054/drup.2000.0138
88. Hoshino A, Costa-Silva B, Shen T-L, Rodrigues G, Hashimoto A, Tesic Mark M, et al. Tumor exosome integrins determine organotropic metastasis. *Nature.* (2015) 527:329–35. doi: 10.1038/nature15756
89. Lener T, Gimona M, Aigner L, Börger V, Buzas E, Camussi G, et al. Applying extracellular vesicles based therapeutics in clinical trials - an ISEV position paper. *J Extracell Vesicles.* (2015) 4:30087. doi: 10.3402/jev.v4.30087
90. Fais S, O'Driscoll L, Borras FE, Buzas E, Camussi G, Cappello F, et al. Evidence-based clinical use of nanoscale extracellular vesicles in nanomedicine. *ACS Nano.* (2016) 10:3886–99. doi: 10.1021/acsnano.5b08015

Conflict of Interest: MA has ownership in Nasasbiotech. This company commercializes ExoGAG. CH was employed by Nasasbiotech, S.L.

The remaining author declares that the research was conducted in the absence of any commercial or financial relationships that could be construed as a potential conflict of interest.

frontiers in Oncology

ORIGINAL RESEARCH
published: 15 October 2020
doi: 10.3389/fonc.2020.583228

Tryptophan Catabolism and Response to Therapy in Locally Advanced Rectal Cancer (LARC) Patients

Sara Crotti[1]*, *Alessandra Fraccaro*[2], *Chiara Bedin*[1], *Antonella Bertazzo*[3], *Valerio Di Marco*[2], *Salvatore Pucciarelli*[4] and *Marco Agostini*[1,4]*

[1] Nano-Inspired Biomedicine Laboratory, Institute of Paediatric Research—Città della Speranza, Padua, Italy, [2] Department of Chemical Sciences, University of Padua, Padua, Italy, [3] Department of Pharmaceutical and Pharmacological Sciences, University of Padua, Padua, Italy, [4] First Surgical Clinic Section, Department of Surgical, Oncological and Gastroenterological Sciences, University of Padua, Padua, Italy

In locally advanced rectal cancer patients (LARC), preoperative chemoradiation improves local control and sphincter preservation. The response rate to treatment varies substantially between 20 and 30%, and it is an important prognostic factor. Indeed, nonresponsive patients are subjected to higher rates of local and distant metastases, and worse survival compared to patients with complete response. In the search of predictive biomarkers for response prediction to therapy in LARC patients, we found increased plasma tryptophan levels in nonresponsive patients. On the basis of plasma levels of 5-hydroxy-tryptophan and kynurenine, the activities of tryptophan 5-hydroxylase 1 (TPH1) and indoleamine-2,3-dioxygenases 1 (IDO1)/tryptophan-2,3-dioxygenase (TDO2) have been obtained and data have been correlated with gene expression profiles. We demonstrated that TDO2 overexpression in nonresponsive patients correlates with kynurenine plasma levels. Finally, through the gene expression and targeted metabolomic analysis in paired healthy mucosa-rectal cancer tumor samples, we evaluated the impact of tryptophan catabolism at tissue level in responsive and nonresponsive patients.

Keywords: tryptophan, rectal cancer, IDO1, TDO2, TPH1, kynurenine pathway, serotonin pathway

OPEN ACCESS

Edited by:
Matteo Bocci,
Lund University, Sweden

Reviewed by:
Namkyu Kim,
Yonsei University, South Korea
Min Hee Kang,
Texas Tech University Health Sciences Center, United States

***Correspondence:**
Sara Crotti
s.crotti@irpcds.org
Marco Agostini
m.agostini@unipd.it

Specialty section:
This article was submitted to Cancer Molecular Targets and Therapeutics, a section of the journal Frontiers in Oncology

Received: *14 July 2020*
Accepted: *25 August 2020*
Published: *15 October 2020*

Citation:
Crotti S, Fraccaro A, Bedin C, Bertazzo A, Di Marco V, Pucciarelli S and Agostini M (2020) Tryptophan Catabolism and Response to Therapy in Locally Advanced Rectal Cancer (LARC) Patients. Front. Oncol. 10:583228. doi: 10.3389/fonc.2020.583228

INTRODUCTION

Cancer is a major cause of death in industrialized countries, and colorectal cancer (CRC) is one of the most common tumors in both male and female (1). About 30% of CRC cases concern the rectal tract of the large intestine, approximately the last 15 cm of the intestinal tract. In the most advanced stages of the disease, the tumor delocalizes and begins its proliferation in areas of the body different from the one in which it arose. Due to the different blood and lymph node ducts to which they are connected, colon cancer mainly develops liver metastases while rectal cancer develops, in addition to the liver ones, also thoracic metastases. Prevention and diagnosis strategies for rectal and colon cancer are mostly the same; the planned therapy, however, is shared only for some traits.

Preoperative chemoradiotherapy (pCRT) is worldwide accepted as a standard treatment for locally advanced rectal cancer (LARC) with stage II and III aiming at improving local tumor control, and inducing tumor downsizing and downstaging (2). Standard treatment includes

administration of ionizing radiation for 45–50.4 Gy associated with 5-fluorouracil administration during radiation therapy and few modifications (e.g., adding Oxaliplatin) are introduced to ameliorate primary tumor response and, consequently, patients' outcome. Typically, complete pathologic response rate to pCRT is between 20 and 30% (3). It follows that patients with *a priori* resistant tumor should not be included in the treatment, which is associated with substantial adverse effects and higher rates of local and distant metastases. The search of predictive biomarkers for response prediction to therapy in rectal cancer would improve the patients' management. In this frame, in adjunction to clinical features (4, 5), the potentiality of liquid biopsy has been extensively employed to identify circulating predictive biomarkers (6, 7). Indeed, a number of putative biomarkers including proteins (8, 9), circulating peptides (10), and circulating tumor cells or nucleic acids (11–13) have been proposed. However, recently an increased focus on the tumor microenvironment offered further opportunities to understand the tumor response biology and the relations between pCRT and the radiation-induced response (14, 15), together with tumor-specific immune response (16).

Physiologically, several pro-inflammatory mediators and T cells cytotoxic activity are modulated by tryptophan (TRP) and its metabolites, as an adaptation mechanism to restrict excessive acute immune response in tissues (17). Tryptophan is the precursor of several active compounds, collectively named TRYCATs (**Figure 1**). At the tumor microenvironment, TRP catabolism is promoted by indoleamine 2,3-dioxygenase (IDO1) overexpression under pro-inflammatory conditions, and it plays an important role in modulating antitumor immune response

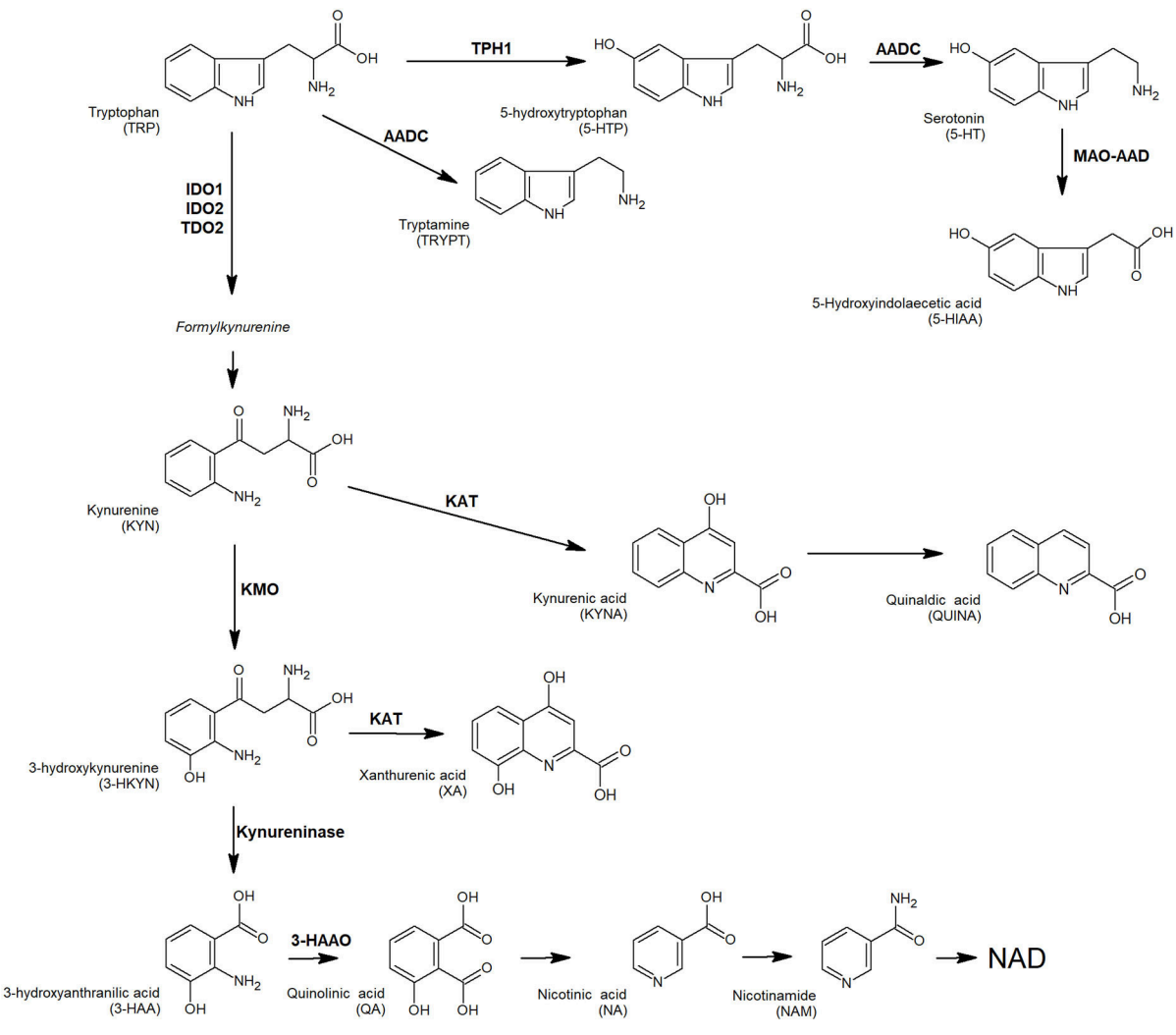

FIGURE 1 | TRP and its key catabolites (TRYCATs) produced via three biochemical pathways: the kynurenine pathway, tryptamine pathway, and serotonin pathway. Enzymes involved: AADC, aromatic L-amino acid decarboxylase; AD, aldehyde dehydrogenase; 3-HAAO, 3-hydroxyanthranilate 3,4-dioxygenase; IDO1, indoleamine-2,3-dioxygenases 1; IDO2, indoleamine-2,3-dioxygenases 2; KAT, L-kynurenine aminotransferase; KMO, kynurenine monooxygenase; MAO-A, monoamine oxidase A; TDO, tryptophan-2,3-dioxygenase; TPH1, tryptophan hydroxylase 1.

(18–20). In CRC, IDO1 expression at the tumor invasion front correlates with disease progression and worse clinical outcome (21) and is associated with the frequency of liver metastases (22). As observed in other tumors, local TRP depletion in CRC plays an important role in either antitumor immune response suppression or cancer cell proliferation/survival support (23–25). Beside IDO1, a second enzyme involved in TRP metabolism, tryptophan-2,3-dioxygenase (TDO2) is expressed in a significant proportion of human tumors and is involved in proliferation, migration, invasion, and immunoresistance (26–28). A valuable way to measure local catabolism is represented by plasma or blood quantification of TRP and its main metabolites, i.e., 5-hydroxy-tryptophan (5-HTP), kynurenine (KYN), and serotonin (5-HT). Consequently, circulating levels of TRP can be used as a "proxy" for tumor microenvironment metabolism.

In this frame, we highlighted that CRC-associated inflammation is capable of modulating circulating levels of TRP and its metabolites along the adenoma–carcinoma sequence. Indeed, decreased TRP concentration and increased IDO1 and tryptophan hydroxylase 1 (TPH1) enzymatic activities were detectable in plasma samples concomitant to precancerous lesion (high grade-adenomas) or in association to risk factors (inflammatory bowel diseases) (29). Moreover, we defined the TRP catabolism as a possible source of prognostic marker for familial adenomatous polyposis patients, based on IDO1 and TPH1 activity with high sensitivities and specificities (up to 92%) (30). Agostini et al. have firstly suggested the link between IDO1 and chemoresistance of rectal cancer patients in a *de novo* meta-analysis on rectal tumor tissues (31). IDO1 and other two genes involved in the immune system pathway (AKR1C3 and CXCL10) have been identified as a gene set associated with pCRT response and survival. Consistently with these results, we focused our attention on TRP metabolism as a hallmark of immune host response modulation in LARC. In this study, both at circulating and at tissue level, we investigated metabolic and genetic markers of the TRP catabolism before pCRT in LARC patients in order to find out new predictive biomarkers measuring the response to therapy.

MATERIALS AND METHODS

Chemicals

Isotopically labeled internal standards d_5-tryptophan (TRPd, 98.8%), d_4-serotonin (5HTd, 98.7%), and d_5-kynurenic acid (KINAd, 99.2%) were purchased from CDN isotopes (Quebec, Canada) while $^{13}C_6$-nicotinamide (NAmC, 99.4%) was purchased from Sigma Aldrich (Milan, Italy). Analytical standards for tryptophan (TRP), kynurenine (KYN), 5-hydroxy-tryptophan (5-HTP), serotonin (5-HT), tryptamine (Tryp), kynurenic acid (KYNA), quinaldic acid (QA), xanthurenic acid (XA), 3-hydroxyanthranilic acid (3-HAA), 5-hydroxyindoleacetic acid (5-HIAA), nicotinic acid (NA), quinolinic acid (QuiA), and nicotinamide (NAm) have been purchased from Sigma Aldrich (Milan, Italy). LC-MS-grade solvents (acetonitrile, methanol, chloroform, isopropanol), and suprapure trifluoroacetic acid (TFA) were purchased from Romil. TRIzol™ reagent was obtained from Thermo Fisher Scientific.

TABLE 1 | Clinical and demographic characteristics of all LARC patients.

Characteristic		*N*	%
Age	Median (range yrs.)	66 (31–79)	
Sex	Male	52	63%
	Female	30	37%
Tumor distance from anal verge	≤7 cm	26	32%
	>7 cm	39	48%
	Not available	17	20%
TRG	1–2	37	45%
	3–5	45	55%
Specimens	Plasma	45	
	Tissues	69	
Paired samples	Plasma–tumor samples	32	
	Healthy mucosa–tumor samples	13	

Tumor regression grade (TRG) is calculated according to Mandard et al. (32). TRG 1–2, responders; TRG 3–5, nonresponders.

LC-MS/MS and LC-UV/FLD Analyses

Mass spectrometry measurements were performed by using an API 4000 triple quadrupole mass spectrometer (AB SCIEX, MA, USA) coupled to an Ultimate 3000 UPLC system (Thermo Fisher). Analyzed metabolites were TRP, KYN, 5-HTP, 5-HT, Tryp, KYNA, QA, XA, 3-HAA, 5-HIAA, NA, QuiA, and NAm. Scheduled MRM transitions, instrumental parameters, and chromatographic conditions were reported in **Supplementary Material S1**.

HPLC-UV/FLD analyses of plasma samples to detect and quantify TRP, KYN, 5-HTP, and 5-HT were performed as previously reported (29).

Sample Collection

This study was conducted according to the principles expressed in the Declaration of Helsinki. Biological specimens (de-personalized plasma and tissue biopsies) were obtained from the Tissue Biobank of the First Surgical Clinic of Padua Hospital (Italy). The protocol was approved by the ethics committee of the institution (Comitato Etico del Centro Oncologico Regionale, Approved Protocol Number: P448). Selected samples were obtained from rectal cancer patients before preoperative chemoradiotherapy (pCRT) which consisted of external-beam radiotherapy (>6 MV) using a conventional fractionation (>50 Gy in 28 fractions, 1.8 Gy per day, 5 sessions per week) and 5-fluorouracil administered as neoadjuvant chemotherapy drug by bolus or continuous venous infusion. Elective surgery was performed after 7 weeks (median value) to completion of preoperative chemoradiotherapy (interquartile range 6–8 weeks), and patients' response to pCRT was evaluated after histological evaluation of surgical resection as the tumor regression grade (TRG) according to Mandard et al. (32). All demographic and clinical data are presented in **Table 1**.

TABLE 2 | Tryptophan (TRP), kynurenine (KYN), 5-hydroxy-tryptophan (5-HTP), serotonin (5-HT) plasma levels and tumor tissue expression of enzymes involved in TRP metabolism.

Plasma metabolite levels					
	TRG 1–2 ($n = 17$)		TRG 3–5 ($n = 28$)		*p*-value
	Median	Q1, Q3	Median	Q1, Q3	
TRP μg/mL	8.43	7.06, 10.71	10.24	8.37, 11.93	<0.05
KYN μg/mL	0.31	0.24, 0.46	0.41	0.30, 0.53	
5HTP μg/mL	0.06	0.05, 0.07	0.05	0.04, 0.06	
5HT μg/mL	0.01	0.005,0.01	0.01	0.001, 0.02	
Gene expression of involved enzymes					
	TRG 1–2 ($n = 25$)		TRG 3–5 ($n = 27$)		*p*-value
	Median	Q1, Q3	Median	Q1, Q3	
IDO1 (RQ)	66.87	23.08, 138.6	57.46	25.73, 98.07	
TDO2 (RQ)	67.21	40.12, 148.7	185.8	57.74, 250.0	<0.05
TPH1 (RQ)	1.68	0.66, 6.44	2.97	0.82, 12.0	

RQ, relative quantitation.

Sample Preparation

Healthy rectum mucosa and tumor pre-therapy biopsies were processed to isolate total RNA by TRIzol™ reagent following the manufacturer's protocol. After chloroform addition, the aqueous upper layer was transferred for the subsequent gene expression analysis while the lower organic phase containing the interphase layer was stored at −20°C for metabolite quantification. RNA concentration and purity were estimated as the ratio 260/280 nm by the NanoDrop 2000 spectrophotometer (Thermo Scientific, USA). Only samples with a ratio between 1.7 and 2.1 were considered suitable for downstream analysis. Reverse transcription and quantitative real-time PCR (qPCR) were performed as described in **Supplementary Material S2**.

TRP and its metabolites were extracted from the lower organic phase obtained during the RNA isolation by adding an equal volume of acidified cold water (0.05% TFA) containing known amounts of the following internal standards: TRPd, 5HTd, KINAd, and NAmC. The mixture was centrifuged at 4°C for 5 min (12,000 rpm) using a Heraeus Fresco 21 centrifuge (Thermo Electron Corp.). Extracted analytes were transferred into a new tube and dried under vacuum. The residual organic layer, containing the interphase, was treated with ethanol (300 μL) to eliminate DNA, and residual protein pellet was extracted according to TRIzol™ manufacturer's instructions. Total protein amount was finally quantified by the Pierce BCA Protein Assay Kit (Thermo Fisher).

Statistical Analysis

Statistical analysis was performed with GraphPad Prism, version 5.00, 2007 (La Jolla, CA, USA). Normality of data was evaluated using the D'Agostino-Pearson omnibus normality test, and parametric (or nonparametric) statistical analyses were completed accordingly. Spearman rank test was used to determine the strength and direction of the relationship between variables.

RESULTS AND DISCUSSION

Circulating TRP Metabolite Levels and Response to Therapy

TRP catabolism in 45 LARC patients was assessed through plasma level quantification of TRP and its major metabolites (KYN, 5-HTP, and 5-HT) by means of HPLC-UV-VIS/FLD analysis. Usually, TRP plasma levels are physiologically regulated by the hepatic TDO2 enzyme. However, under non-physiological conditions (e.g., in presence of inflammation or cancer), overexpression of IDO1/TDO2 enzymes can actively contribute to TRP catabolism. The median TRP concentration was 9.01 μg/mL (8.68–10.01, 95% CI) which is—as expected—very close to the TRP concentration we observed in our previous investigation for control (i.e., healthy subjects) plasma samples (29). Indeed, we already demonstrated that TRP catabolism increases more in people affected by colon cancer than those affected by rectal cancer. Differently, in the present study, the cohort of rectal cancer patients was collected to check for differences between TRG 1–2 and TRG 3–5 patients and not for diagnostic evaluation (i.e., comparison with healthy subjects). Data reported in **Table 2** suggest that a statistically significant increase of TRP in TRG 3–5 patients is present, together with an increasing trend of KYN levels. No difference is present between 5-HTP and 5-HT plasma levels. When IDO1/TDO2 and TPH1 enzymatic activities are estimated from these data, following the usual approach (29), a lower TPH1 enzymatic activity ($p < 0.01$) resulted for TRG 3–5 patients (**Figure 2A**, box-plots). This decrease underlines a possible involvement of serotonin pathway in tumor response, while the IDO1/TDO2 activity, which is an

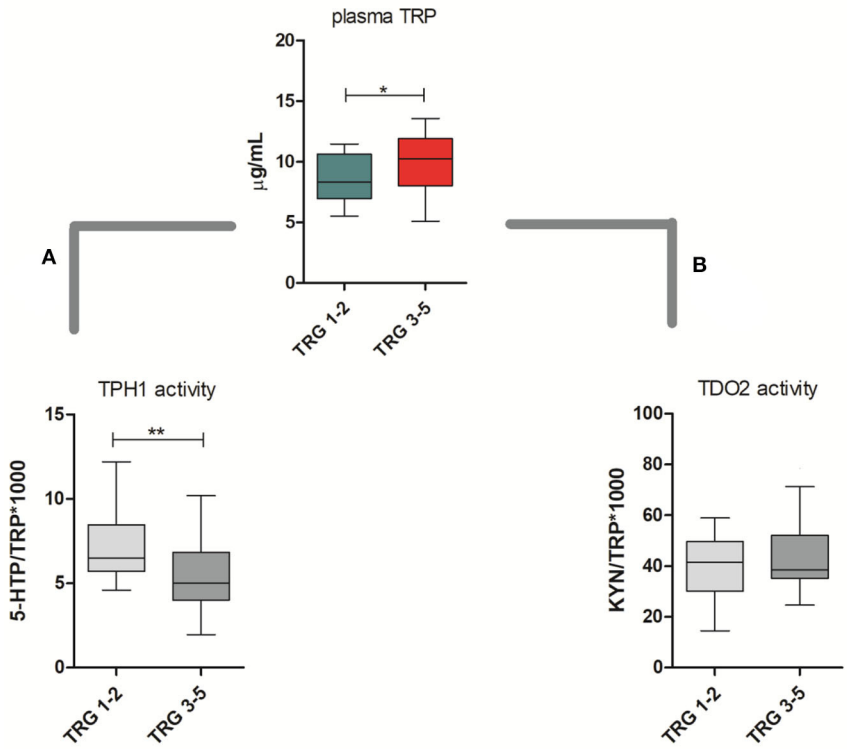

FIGURE 2 | Circulating plasma levels of tryptophan (TRP) in responsive (TRG 1–2) and nonresponsive (TRG 3–5) rectal cancer patients. Calculated TPH1 activity **(A)** and IDO1/TDO2 **(B)** activities are reported. Mann–Whitney, * = $p < 0.05$, ** = $p < 0.01$.

estimation of kynurenine pathway, shows only a nonstatistically significant increasing trend (**Figure 2B**, box-plots).

To evaluate this hypothesis, we decided to perform a gene expression analysis of IDO1, TDO2, and TPH1 in order to clarify whether in TRG 3–5 patients the decrease in TPH1 systemic activity actually means a downregulation of TPH1 gene expression. However, as underlined by gene expression data reported in **Table 2**, there is no difference for TPH1 and IDO1 between TRG 1–2 and TRG 3–5 patients. On the contrary, TDO2 shows instead a statistically significant increase in TRG 3–5 patients ($p < 0.05$). Even after data normalization to healthy rectal mucosa ($n = 17$ samples, not paired), TDO2 was still overexpressed in TRG 3–5 patients only (tumor/healthy mucosa average ratio: 1.035 for TRG 1–2 and 2.230 for TRG 3–5), while TPH1 was equally downregulated in both patients' groups (tumor/healthy mucosa average ratio: 0.015 for TRG 1–2 and 0.022 for TRG 3–5). To further verify whether these metabolic and gene expression alterations may be consistent, Spearman's rank correlation test was employed to analyze the results from only the paired plasma-tumor samples ($n = 32$). Plasma levels of detected metabolites (both precursors TRP and its products KYN, 5-HTP, and 5-HT) and the calculated enzymatic activities of IDO1, TDO2, and TPH1 have been compared against their quantified genes expression. Obtained results indicated that in rectal cancer patients, KYN plasma levels are strongly correlated with TDO2 gene expression ($r = 0.6026$, $p < 0.001$, $n = 32$) and, after patients' stratification according to their response to therapy, only those having TRG 3–5 still showed a positive correlation between KYN and TDO2 ($r = 0.556$, $p < 0.05$, $n = 17$).

Following the same procedure, we found that neither IDO1 nor TPH1 gene expressions were correlated with their metabolites or calculated activities in rectal cancer patients. Other authors previously showed this discrepancy for IDO1 (33). To explain this behavior, it should be noted that that enzymatic process coordination depends upon temporal regulation of both substrates and enzymes. Moreover, changes in mRNA levels of IDO1 and TPH1 just indicate cell metabolic changes and may moderately correlate with changes in enzymes activity. Consequently, as for most of proteins, disparity between mRNA levels and protein abundance make it difficult to predict real activity for these enzymes (34).

Local Quantification of TRP Metabolites Better Reflects Gene Expression

To clarify whether it is possible to correlate the amount of TRP and its metabolites to enzyme activity and their gene expression in LARC patients, we developed and validated an analytical method for the simultaneous evaluation of TRP catabolism at both metabolic and genetic levels. By this method, metabolite

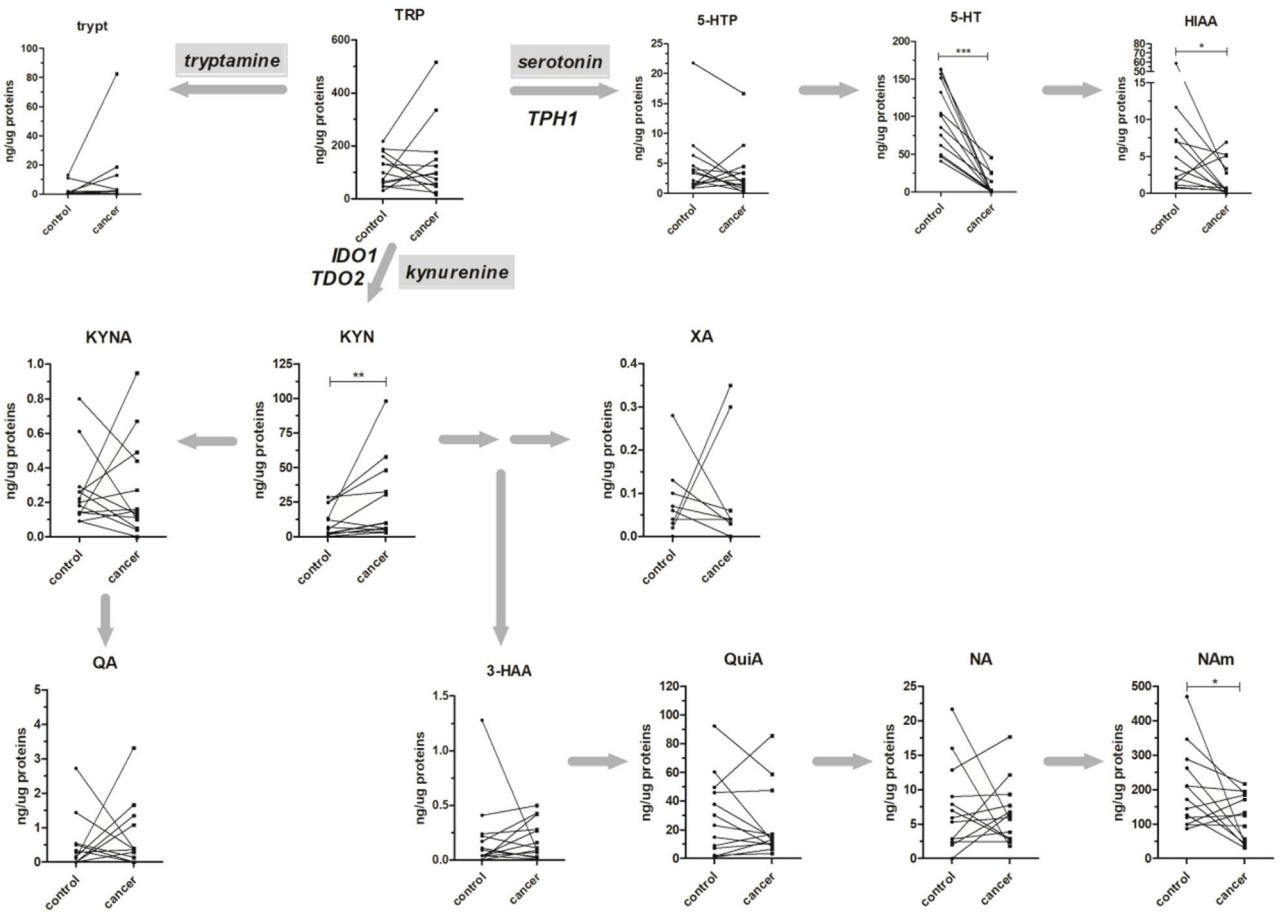

FIGURE 3 | Absolute amounts (presented as ng of metabolite per μg of total proteins) of TRP along the kynurenine and serotonin pathways in 13 healthy mucosa (control) and rectal cancer (cancer) paired samples. The tryptamine metabolic pathway is presented for completeness. Matched samples are connected together. Results from Wilcoxon signed rank test are reported (*$p < 0.05$; **$p < 0.01$; ***$p < 0.001$).

quantification and gene expression analysis were obtained in the same tissue samples, by means of a sequential extraction procedure. In brief, paired biopsies (healthy mucosa and rectal cancer counterpart) have been extracted with TRIzol™ following the manufacturers' protocol. The resultant upper aqueous phase was used for quantitative real-time PCR of IDO1, TDO2, and TPH1 genes, while the lower organic phase was added by the four internal standards (TRPd, 5HTd, KINAd, and NAmC) before metabolite extraction (see Sample Preparation section for details).

A total of 13 metabolites have been quantified by a single scheduled LC-MRM analysis. These metabolites were tryptophan (TRP), kynurenine (KYN), 5-hydroxy-tryptophan (5-HTP), serotonin (5-HT), tryptamine (Tryp), kynurenic acid (KYNA), quinaldic acid (QA), xanthurenic acid (XA), 3-hydroxyanthranilic acid (3-HAA), 5-hydroxyindoleacetic acid (5-HIAA), nicotinic acid (NA), quinolinic acid (QuiA), and nicotinamide (NAm). Instrumental parameters and scheduled transitions employed to quantify and qualify metabolites are resumed in **Supplementary Material S3**. Good performances in terms of LLOQ, LOD, CV %, and accuracy % for all metabolites have been obtained, with exception to Tryp and 3-HAA (**Supplementary Material S3**). For these two metabolites, the present method was not able to provide enough reproducibility and then quantitative results should be considered as approximate.

The method was applied to the analysis of 13 paired healthy mucosa/rectal cancer samples, and obtained results are reported in **Figure 3**. All the major metabolites along the kynurenine and serotonin pathways have been quantified; in addition, Tryp has been included in the present study for completeness, even if tryptamine pathway accounts only for the <1% of TRP catabolism (35). For both types of samples, no difference was present in the TRP tissue level (average values: 97.98 and 95.06 ng/μg of proteins, for healthy mucosa and rectal cancer, respectively). However, in cancer tissues a trend of decrease along the serotonin pathway was observable for 5-HTP and further confirmed by the statistically significant decrease of 5-HT ($p < 0.001$, Wilcoxon signed-rank test) and its final catabolite 5-HIAA ($p < 0.05$, Wilcoxon signed-rank test). This strong decrease in serotonin level is reasonably due to the lack of enterochromaffin cells, which are normally present in

TABLE 3 | Normalized (tumor/healthy mucosa) gene expression (*nRQ*) for all paired samples.

	All samples ($n = 13$ pairs)				
	Mean	**Min, Max**	**Trend in tumor**	**Correlation with metabolites**	***p*-value**
IDO1 (nRQ)	0.71	0.10, 2.41	=	NAm ($r = 0.424$)	<0.05
TDO2 (nRQ)	1.56	0.09, 10.04	↑		
Calculated activity	230 (111)	8.6, 636 (2.19, 441)	↑	KYN ($r = 0.803$) TRP ($r = -0.461$)	<0.0001 <0.05
TPH1 (nRQ)	0.43	0.001, 3.65	↓	5-HT ($r = 0.810$)	<0.0001
Calculated activity	36.3 (40.7)	1.2, 148 (8.6, 115.7)	=	5-HTP ($r = 0.680$)	<0.0001

Data are presented as mean fold change and minimum and maximum (Min, Max) values. Enzymatic activity is reported as calculated mean value for rectal cancer samples (healthy mucosa) and relative minimum, maximum. "Trend in tumor" column highlights fold changes at least >1.5 (or <0.67). Correlation between gene expression and TRP metabolites was evaluated using Spearman's rank test and only significant results are reported.

healthy rectal mucosa but not in cancer tissue. These cells are a specialized subset of enteroendocrine cells and the largest producer of 5-HT in the body (∼95%), which is critical to gastrointestinal motility (36). On the contrary, KYN increased significantly in rectal cancer tissues ($p < 0.01$, Wilcoxon signed-rank test). This increase could be the result of a diminished TRP consumption along the serotonin pathway and could explain, at least theoretically, the unaltered total TRP levels in rectal cancer tissues. Increased KYN levels in colon cancer tissues and human colon cancer cells have been recently correlated with the tumor proliferation through the activation of the aryl hydrocarbon receptor (AHR) (37). KYN exerts also immunomodulating effects at the tumor microenvironment (38) and is the precursor of quinaldic acid (QA), xanthurenic acid (XA), and nicotinamide (NAm) (**Figure 3**). QA and XA levels were comparable between healthy mucosa and rectal cancer samples. On the contrary, NAm, which is the precursor for redox cofactor NAD^+, was decreased in rectal cancer samples ($p < 0.05$, Wilcoxon signed-rank test). NAm decrease may be a hallmark of increased energetic demand in tumor; indeed, cancer cells are able to reprogram their metabolism (nutrient uptake, intracellular metabolism, and gene expression) for sustaining survival, growth, and metastasis. In particular, to satisfy their NAD^+ demand, tumors can overcome the limitation of a *de novo* synthesis from TRP and adopt a salvage pathway, which "recycles" existing NA and NAm (39).

The gene expression of rate-limiting step enzymes IDO1, TDO2, and TPH1 and their calculated activity were finally obtained for each sample (**Table 3**). For all the three enzymes, the mean of normalized RQ (cancer/healthy mucosa) was calculated and presented as fold change (F.C.). Obtained data revealed that in rectal cancer samples the kynurenine pathway was characterized by TDO2 overexpression, while IDO1 expression remained practically unchanged (using a 1.5-fold ratio criterion). These data are consistent with others reported in literature, in which TDO2 expression in several human tumor cell lines and tissues has been demonstrated (26, 28, 40–42). Similarly, a rise in the calculated enzymatic activity (KYN/TRP*1,000) in rectal cancer tissues compared to mucosa was detected (mean activity: 111 and 230 for healthy mucosa and rectal cancer, respectively; $p < 0.05$, Wilcoxon signed-rank test). This increase positively correlated with KYN produced and negatively correlated with the enzyme substrate TRP (**Table 3**) suggesting that, in rectal cancer, TDO2 may be responsible for increased KYN levels.

Most importantly, the THP1 downregulation observed for this group of rectal cancer is consistent with that previously observed in the plasma–tissue correlation (actual fold change: 0.43). Differently to the previous observation, however, actual 5-HT tissue levels strongly correlated with THP1 expression and the calculated THP1 activity positively correlated with 5-HTP production (**Table 3**). Collectively, these results indicated that local quantification of TRP metabolites better reflects gene expression and enzymatic activity.

Preliminary Correlation Between TRP Metabolism and Response Prediction

In our first analysis on paired plasma–tissue samples, we suggested that a decreased THP1 activity together with TDO2 overexpression was a common hallmark of lack of response to therapy in rectal cancer patients (**Figure 2** and **Table 2**). In our second analysis on 13 paired control/cancer samples, we aimed at verifying these results and at correlating them to metabolite production at the tissue level. Again, we found that, after stratification of gene expression data, IDO1 was substantially unchanged in TRG 1–2 and TRG 3–5 patients, while TDO2 overexpression was peculiar of nonresponsive patients only (**Table 4**). Consistently to TDO2 overexpression, an increase in the calculated enzymatic activity along the kynurenine pathway has been detected in these patients (136 vs. 311, for TRG 1–2 and TRG 3–5, respectively). TPH1-normalized gene expression decreased in both TRG 1–2 patients (nRQ = 0.19) and TRG 3–5 patients (nRQ = 0.66), even if in the latter the decrease was less consistent. Conversely, calculated THP1 activity showed an opposite trend (43 vs. 29, for TRG 1–2 and TRG 3–5, respectively).

Metabolic data have been finally stratified according to patients' TRG, and obtained results are reported in **Figure 4**. For both kynurenine and serotonin pathways, no statistical differences have been observed, probably due to the low sample size ($n = 6$ and $n = 7$ for TRG 1–2 and TRG 3–5, respectively). Even if a trend of decrease in 5-HT and HIAA tissue levels of TRG 3–5 patients can be inferred from the data, this trend is not supported by gene expression data (**Table 4**).

TABLE 4 | Normalized (tumor/healthy mucosa) gene expression (*nRQ*) after patients' stratification according to their TRG (responders: TRG 1–2; nonresponders: TRG 3–5).

	TRG 1–2 (n = 6 pairs)		TRG 3–5 (n = 7 pairs)		
	Mean	**Min, max**	**Mean**	**Min, max**	**Trend in TRG 3–5**
IDO1 (nRQ)	0.66	0.13, 2.00	0.789	0.10, 2.41	=
TDO2 (nRQ)	0.88	0.40, 1.99	2.13	0.09, 10.04	↑
Calculated activity	136	8.6, 292.5	311	11.6, 636.6	↑
TPH1 (nRQ)	0.19	0.002, 0.44	0.66	0.001, 3.65	↑
Calculated activity	43	1.2, 149	29	2.6, 94.7	=

Data are presented as mean fold change and minimum and maximum (Min, Max) values. "Trend in tumor" column highlights fold changes at least >1.5 (or <0.67). Enzymatic activity is reported as calculated mean value for rectal cancer samples (healthy mucosa) and relative minimum and maximum.

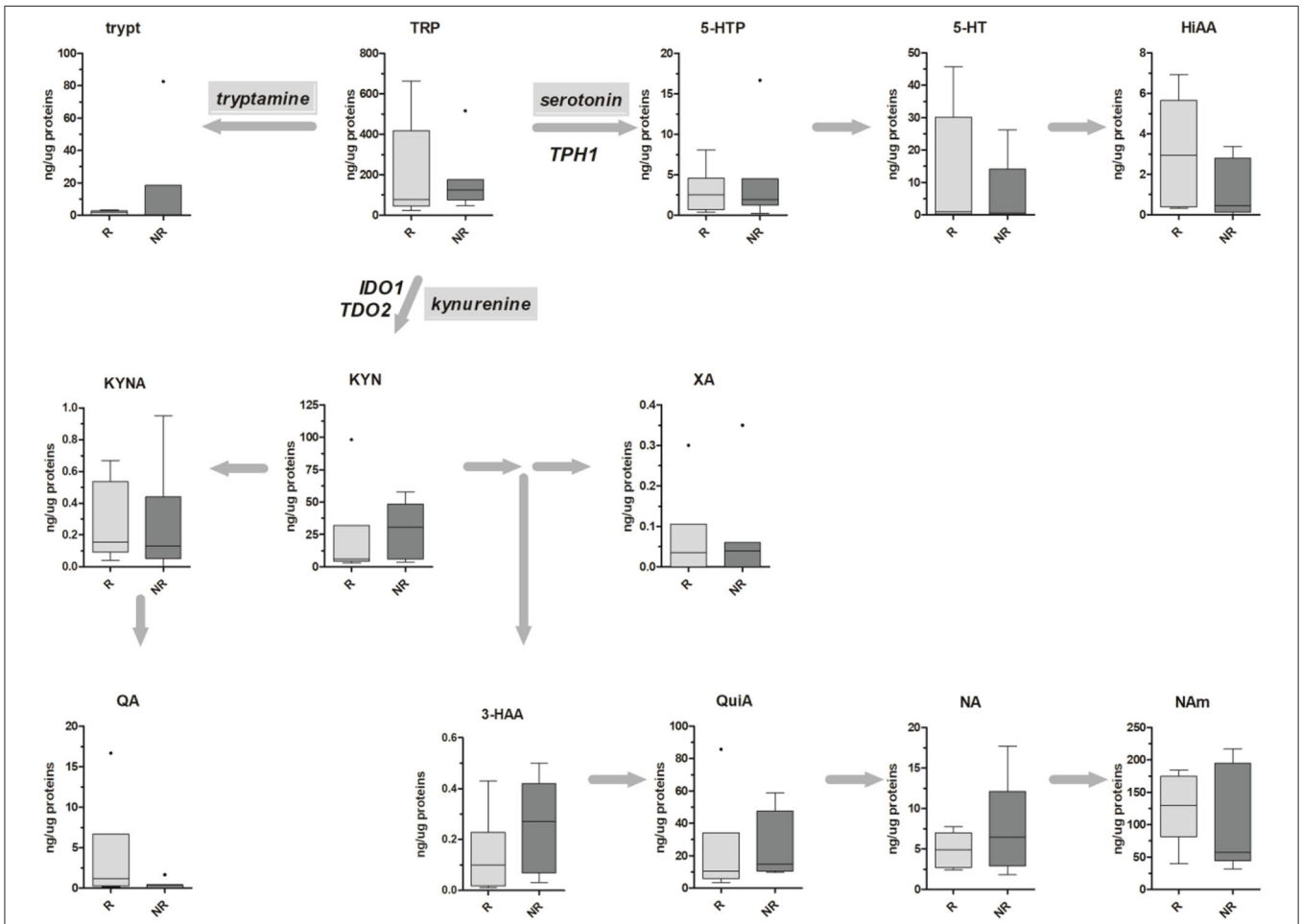

FIGURE 4 | Box-plots representing the absolute amounts (presented as ng of metabolite per μg of total proteins) of TRP along the kynurenine and serotonin pathways in six TRG 1–2 (responders, R) and seven TRG 3–5 (nonresponders, NR) rectal cancer patients. Outliers are also reported.

CONCLUSION

In this work, metabolic and genetic markers of the TRP catabolism before pCRT in LARC patients have been investigated in plasma and tissue samples. In plasma, changes in TRP levels firstly evidenced the difference between responsive (TRG 1–2) and nonresponsive (TRG 3–5) patients. Moreover, TRG 3–5 patients revealed an increased activity along the kynurenine pathway, which correlates with TDO2 overexpression. However, discordant results were obtained from the analysis of the serotonin pathway. Indeed, the decrease in THP1 activity calculated both in plasma and in tissues showed opposite results with respect to the tissue expression. This probably suggests the presence of a posttranscriptional regulation in THP1 protein

abundance, which in turn affects its activity in TRG 3–5 patients. Of note, the THP1 posttranscriptional regulation and the diurnal variation of TPH1 activity in the central nervous system have been demonstrated (43–45), but none seems to be reported about cancer. Collectively, these results indicate that mechanisms regulating TRP catabolism may be different between responsive and nonresponsive LARC patients. To confirm these data, further analyses should be performed to increase the sample size and to better investigate the mechanisms involved in tumor response to therapy.

DATA AVAILABILITY STATEMENT

The original contributions presented in the study are included in the article/**Supplementary Material**, further inquiries can be directed to the corresponding author/s.

ETHICS STATEMENT

The studies involving human participants were reviewed and approved by Comitato Etico del Centro Oncologico Regionale, Approved Protocol Number: P448. The patients/participants provided their written informed consent to participate in this study.

AUTHOR CONTRIBUTIONS

SC: conceptualization and writing - original draft. AF: investigation. CB and AB: investigation and writing - review and editing. VM: writing - review and editing. SP: clinical data management. MA: project supervision. All authors contributed to the article and approved the submitted version.

FUNDING

The research leading to these results has received funding from AIRC under IG 2016 - ID. 19104 project – P.I. Agostini Marco.

SUPPLEMENTARY MATERIAL

The Supplementary Material for this article can be found online at: https://www.frontiersin.org/articles/10.3389/fonc.2020.583228/full#supplementary-material

REFERENCES

1. Rawla P, Sunkara T, Barsouk A. Epidemiology of colorectal cancer: incidence, mortality, survival, and risk factors. *Przeglad Gastroenterol*. (2019) 14:89–103. doi: 10.5114/pg.2018.81072
2. Bosset JF, Collette L, Calais G, Mineur L, Maingon P, Radosevic-Jelic L, et al. Chemotherapy with preoperative radiotherapy in rectal cancer. *N Engl J Med*. (2006) 355:1114–23. doi: 10.1056/NEJMoa060829
3. Brown CL, Ternent CA, Thorson AG, Christensen MA, Blatchford GJ, Shashidharan M, et al. Response to preoperative chemoradiation in stage II and III rectal cancer. *Dis Colon Rectum*. (2003) 46:1189–93. doi: 10.1007/s10350-004-6714-y
4. Pucciarelli S, Toppan P, Friso ML, Russo V, Pasetto L, Urso E, et al. Complete pathologic response following preoperative chemoradiation therapy for middle to lower rectal cancer is not a prognostic factor for a better outcome. *Dis Colon Rectum*. (2004) 47:1798–807. doi: 10.1007/s10350-004-0681-1
5. Das P, Skibber JM, Rodriguez-Bigas MA, Feig BW, Chang GJ, Wolff RA, et al. Predictors of tumor response and downstaging in patients who receive preoperative chemoradiation for rectal cancer. *Cancer*. (2007) 109:1750–5. doi: 10.1002/cncr.22625
6. Agostini M, Crotti S, Bedin C, Cecchin E, Maretto I, D'Angelo E, et al. Predictive response biomarkers in rectal cancer neoadjuvant treatment. *Front Biosci*. (2014) 6:110–9. doi: 10.2741/S418
7. Bedin C, Crotti S, D'Angelo E, D'Aronco S, Pucciarelli S, Agostini M. Circulating biomarkers for response prediction of rectal cancer to neoadjuvant chemoradiotherapy. *Curr Med Chem*. (2019) 27:1–21. doi: 10.2174/0929867326666190507084839
8. Helgason HH, Engwegen JYMN, Zapatka M, Vincent A, Cats A, Boot H, et al. Identification of serum proteins as prognostic and predictive markers of colorectal cancer using surface enhanced laser desorption ionization-time of flight mass spectrometry. *Oncol Rep*. (2010) 24:57–64. doi: 10.3892/or_00000828
9. Repetto O, De Re V, De Paoli A, Belluco C, Alessandrini L, Canzonieri V, et al. Identification of protein clusters predictive of tumor response in rectal cancer patients receiving neoadjuvant chemo-radiotherapy. *Oncotarget*. (2017) 8:28328–41. doi: 10.18632/oncotarget.16053
10. Crotti S, Enzo MV, Bedin C, Pucciarelli S, Maretto I, Del Bianco P, et al. Clinical predictive circulating peptides in rectal cancer patients treated with neoadjuvant chemoradiotherapy. *J Cell Physiol*. (2015) 230:1822–8. doi: 10.1002/jcp.24894
11. Magni E, Botteri E, Ravenda PS, Cassatella MC, Bertani E, Chiappa A, et al. Detection of circulating tumor cells in patients with locally advanced rectal cancer undergoing neoadjuvant therapy followed by curative surgery. *Int J Colorectal Dis*. (2014) 29:1053–9. doi: 10.1007/s00384-014-1958-z
12. Azizian A, Kramer F, Jo P, Wolff HA, Beissbarth T, Skarupke R, et al. Preoperative prediction of lymph node status by circulating Mir-18b and Mir-20a during chemoradiotherapy in patients with rectal cancer. *World J Surg*. (2015) 39:2329–35. doi: 10.1007/s00268-015-3083-8
13. D'Angelo E, Fassan M, Maretto I, Pucciarelli S, Zanon C, Digito M, et al. Serum miR-125b is a non-invasive predictive biomarker of the pre-operative chemoradiotherapy responsiveness in patients with rectal adenocarcinoma. *Oncotarget*. (2016) 7:28647–57. doi: 10.18632/oncotarget.8725
14. Park JH, Richards CH, McMillan DC, Horgan PG, Roxburgh CSD. The relationship between tumour stroma percentage, the tumour microenvironment and survival in patients with primary operable colorectal cancer. *Ann Oncol*. (2014) 25:644–51. doi: 10.1093/annonc/mdt593
15. Trumpi K, Ubink I, Trinh A, Djafarihamedani M, Jongen JM, Govaert KM, et al. Neoadjuvant chemotherapy affects molecular classification of colorectal tumors. *Oncogenesis*. (2017) 6:e357. doi: 10.1038/oncsis.2017.48
16. Matsutani S, Shibutani M, Maeda K, Nagahara H, Fukuoka T, Nakao S, et al. Significance of tumor-infiltrating lymphocytes before and after neoadjuvant therapy for rectal cancer. *Cancer Sci*. (2018) 109:966–79. doi: 10.1111/cas.13542
17. Comai S, Bertazzo A, Brughera M, Crotti S. Tryptophan in health and disease. *Adv Clin Chem*. (2020) 95:165–218. doi: 10.1016/bs.acc.2019.08.005
18. Theate I, van Baren N, Pilotte L, Moulin P, Larrieu P, Renauld JC, et al. Extensive profiling of the expression of the indoleamine 2,3-dioxygenase 1 protein in normal and tumoral human tissues. *Cancer Immunol Res*. (2015) 3:161–72. doi: 10.1158/2326-6066.CIR-14-0137
19. Amobi A, Qian F, Lugade AA, Odunsi K. Tryptophan catabolism and cancer immunotherapy targeting IDO mediated immune suppression. *Adv Exp Med Biol*. (2017) 1036:129–44. doi: 10.1007/978-3-319-67577-0_9
20. Schramme F, Crosignani S, Frederix K, Hoffmann D, Pilotte L, Stroobant V, et al. Inhibition of tryptophan-dioxygenase activity increases the antitumor efficacy of immune checkpoint inhibitors. *Cancer Immunol Res*. (2020) 8:32–45. doi: 10.1158/2326-6066.CIR-19-0041

21. Ferdinande L, Decaestecker C, Verset L, Mathieu A, Moles Lopez X, Negulescu AM, et al. Clinicopathological significance of indoleamine 2,3-dioxygenase 1 expression in colorectal cancer. *Br J Cancer*. (2012) 106:141–7. doi: 10.1038/bjc.2011.513
22. Brandacher G, Perathoner A, Ladurner R, Schneeberger S, Obrist P, Winkler C, et al. Prognostic value of indoleamine 2,3-dioxygenase expression in colorectal cancer: effect on tumor-infiltrating T cells. *Clin Cancer Res*. (2006) 12:1144–51. doi: 10.1158/1078-0432.CCR-05-1966
23. Fallarino F, Grohmann U, You S, McGrath BC, Cavener DR, Vacca C, et al. The combined effects of tryptophan starvation and tryptophan catabolites down-regulate T cell receptor zeta-chain and induce a regulatory phenotype in naive T cells. *J Immunol*. (2006) 176:6752–61. doi: 10.4049/jimmunol.176.11.6752
24. Thaker AI, Rao MS, Bishnupuri KS, Kerr TA, Foster L, Marinshaw JM, et al. IDO1 metabolites activate beta-catenin signaling to promote cancer cell proliferation and colon tumorigenesis in mice. *Gastroenterology*. (2013) 145:416–25 e411–4. doi: 10.1053/j.gastro.2013.05.002
25. Pflugler S, Svinka J, Scharf I, Crncec I, Filipits M, Charoentong P, et al. IDO1(+) Paneth cells promote immune escape of colorectal cancer. *Commun Biol*. (2020) 3:252. doi: 10.1038/s42003-020-0989-y
26. D'Amato NC, Rogers TJ, Gordon MA, Greene LI, Cochrane DR, Spoelstra NS, et al. A TDO2-AhR signaling axis facilitates anoikis resistance and metastasis in triple-negative breast cancer. *Cancer Res*. (2015) 75:4651–64. doi: 10.1158/0008-5472.CAN-15-2011
27. van Baren N, Van den Eynde BJ. Tryptophan-degrading enzymes in tumoral immune resistance. *Front Immunol*. (2015) 6:34. doi: 10.3389/fimmu.2015.00034
28. Pham QT, Oue N, Sekino Y, Yamamoto Y, Shigematsu Y, Sakamoto N, et al. TDO2 overexpression is associated with cancer stem cells and poor prognosis in esophageal squamous cell carcinoma. *Oncology*. (2018) 95:297–308. doi: 10.1159/000490725
29. Crotti S, D'Angelo E, Bedin C, Fassan M, Pucciarelli S, Nitti D, et al. Tryptophan metabolism along the kynurenine and serotonin pathways reveals substantial differences in colon and rectal cancer. *Metabolomics*. (2017) 13:148. doi: 10.1007/s11306-017-1288-6
30. Crotti S, Bedin C, Bertazzo A, Digito M, Zuin M, Urso ED, et al. Tryptophan metabolism as source of new prognostic biomarkers for FAP patients. *Int J Tryptophan Res*. (2019) 12:1178646919890293. doi: 10.1177/1178646919890293
31. Agostini M, Janssen KP, Kim IJ, D'Angelo E, Pizzini S, Zangrando A, et al. An integrative approach for the identification of prognostic and predictive biomarkers in rectal cancer. *Oncotarget*. (2015) 6:32561–74. doi: 10.18632/oncotarget.4935
32. Mandard AM, Dalibard F, Mandard JC, Marnay J, Henry-Amar M, Petiot JF, et al. Pathologic assessment of tumor regression after preoperative chemoradiotherapy of esophageal carcinoma. Clinicopathologic correlations. *Cancer*. (1994) 73:2680–6. doi: 10.1002/1097-0142(19940601)73:11<2680::AID-CNCR2820731105>3.0.CO;2-C
33. Puccetti P, Fallarino F, Italiano A, Soubeyran I, MacGrogan G, Debled M, et al. Accumulation of an endogenous tryptophan-derived metabolite in colorectal and breast cancers. *PLoS ONE*. (2015) 10:e0122046. doi: 10.1371/journal.pone.0122046
34. Tian Q, Stepaniants SB, Mao M, Weng L, Feetham MC, Doyle MJ, et al. Integrated genomic and proteomic analyses of gene expression in Mammalian cells. *Mol Cell Proteomics*. (2004) 3:960–9. doi: 10.1074/mcp.M400055-MCP200
35. Stavrum AK, Heiland I, Schuster S, Puntervoll P, Ziegler M. Model of tryptophan metabolism, readily scalable using tissue-specific gene expression data. *J Biol Chem*. (2013) 288:34555–66. doi: 10.1074/jbc.M113.474908
36. Terry N, Margolis KG. Serotonergic mechanisms regulating the GI tract: experimental evidence and therapeutic relevance. *Handb Exp Pharmacol*. (2017) 239:319–42. doi: 10.1007/164_2016_103
37. Venkateswaran N, Lafita-Navarro MC, Hao YH, Kilgore JA, Perez-Castro L, Braverman J, et al. MYC promotes tryptophan uptake and metabolism by the kynurenine pathway in colon cancer. *Genes Dev*. (2019) 33:1236–51. doi: 10.1101/gad.327056.119
38. Opitz CA, Litzenburger UM, Sahm F, Ott M, Tritschler I, Trump S, et al. An endogenous tumour-promoting ligand of the human aryl hydrocarbon receptor. *Nature*. (2011) 478:197–203. doi: 10.1038/nature10491
39. Houtkooper RH, Canto C, Wanders RJ, Auwerx J. The secret life of NAD+: an old metabolite controlling new metabolic signaling pathways. *Endocr Rev*. (2010) 31:194–223. doi: 10.1210/er.2009-0026
40. Pilotte L, Larrieu P, Stroobant V, Colau D, Dolusic E, Frederick R, et al. Reversal of tumoral immune resistance by inhibition of tryptophan 2,3-dioxygenase. *Proc Natl Acad Sci USA*. (2012) 109:2497–502. doi: 10.1073/pnas.1113873109
41. Hsu YL, Hung JY, Chiang SY, Jian SF, Wu CY, Lin YS, et al. Lung cancer-derived galectin-1 contributes to cancer associated fibroblast-mediated cancer progression and immune suppression through TDO2/kynurenine axis. *Oncotarget*. (2016) 7:27584–98. doi: 10.18632/oncotarget.8488
42. Tina E, Prosen S, Lennholm S, Gasparyan G, Lindberg M, Gothlin Eremo A. Expression profile of the amino acid transporters SLC7A5, SLC7A7, SLC7A8 and the enzyme TDO2 in basal cell carcinoma. *Br J Dermatol*. (2019) 180:130–40. doi: 10.1111/bjd.16905
43. Sitaram BR, Lees GJ. Diurnal rhythm and turnover of tryptophan hydroxylase in the pineal gland of the rat. *J Neurochem*. (1978) 31:1021–6. doi: 10.1111/j.1471-4159.1978.tb00142.x
44. Sugden D, Grady R Jr, Mefford IN. Measurement of tryptophan hydroxylase activity in rat pineal glands and pinealocytes using an HPLC assay with electrochemical detection. *J Pineal Res*. (1989) 6:285–92. doi: 10.1111/j.1600-079X.1989.tb00424.x
45. Huang Z, Liu T, Chattoraj A, Ahmed S, Wang MM, Deng J, et al. Posttranslational regulation of TPH1 is responsible for the nightly surge of 5-HT output in the rat pineal gland. *J Pineal Res*. (2008) 45:506–14. doi: 10.1111/j.1600-079X.2008.00627.x

Conflict of Interest: The authors declare that the research was conducted in the absence of any commercial or financial relationships that could be construed as a potential conflict of interest.

frontiers in Oncology

MINI REVIEW
published: 28 October 2020
doi: 10.3389/fonc.2020.582843

Liquid Biopsies in Renal Cell Carcinoma—Recent Advances and Promising New Technologies for the Early Detection of Metastatic Disease

Harini Lakshminarayanan, Dorothea Rutishauser, Peter Schraml, Holger Moch and Hella A. Bolck**

Department of Pathology and Molecular Pathology, University of Zurich and University Hospital Zurich, Zurich, Switzerland

OPEN ACCESS

Edited by:
Francesco Fabbri, Romagnolo Scientific Institute for the Study and Treatment of Tumors (IRCCS), Italy

Reviewed by:
Alfredo Berruti, University of Brescia, Italy
Lasse Dahl Ejby Jensen, Linköping University, Sweden

***Correspondence:**
Hella A. Bolck
Hella.Bolck@usz.ch
Holger Moch
Holger.Moch@usz.ch

Specialty section:
This article was submitted to Cancer Molecular Targets and Therapeutics, a section of the journal Frontiers in Oncology

Received: *13 July 2020*
Accepted: *29 September 2020*
Published: *28 October 2020*

Citation:
Lakshminarayanan H, Rutishauser D, Schraml P, Moch H and Bolck HA (2020) Liquid Biopsies in Renal Cell Carcinoma—Recent Advances and Promising New Technologies for the Early Detection of Metastatic Disease. Front. Oncol. 10:582843. doi: 10.3389/fonc.2020.582843

Clear cell renal cell carcinoma (ccRCC) displays a highly varying clinical progression, from slow growing localized tumors to very aggressive metastatic disease (mRCC). Almost a third of all patients with ccRCC show metastatic dissemination at presentation while another third develop metastasis during the course of the disease. Survival rates of mRCC patients remain low despite the development of novel targeted treatment regimens. Biomarkers indicating disease progression could help to define its aggressive potential and thus guide patient management. However, molecular markers that can reliably assess metastatic dissemination and disease recurrence in ccRCC have not been recommended for clinical practice to date. Liquid biopsies could provide an attractive and non-invasive method to determine the risk of recurrence or metastatic dissemination during follow-up and thus assist the search for surveillance biomarkers in ccRCC tumors. A wide spectrum of circulating molecules have already shown considerable potential for ccRCC diagnosis and prognostication. In this review, we outline state of the art of the key circulating analytes such as cfDNA, cfRNA, proteins, and exosomes that may serve as biomarkers for the longitudinal monitoring of ccRCC progression to metastasis. Moreover, we address some of the prevailing limitations in the past approaches and present promising adoptable technologies that could help to pursue the implementation of liquid biopsies as a prognostic tool for mRCC.

Keywords: liquid biopsy, prognostic markers, renal cell carcinoma (RCC), translational research, tumor biomarkers

INTRODUCTION

Kidney cancer is the seventh most frequent cancer worldwide and is responsible for nearly 100,000 deaths each year. Clear cell renal cell carcinoma (ccRCC), the most common subtype of RCC, accounts for almost 75% of detected cases and is therefore far more frequently studied than the rarer histologies (1). One of the landmark events in its tumorigenesis is loss of the short arm of chromosome 3p on which the *VHL* tumor suppressor is encoded. This is often concurrent with a

gain of chromosome 5q resulting in the generation of a small population of tumor-initiating cells (2). Consequently, the inactivation of the second copy of the VHL gene heralds the development of clinically aggressive ccRCC (2). Genetically, ccRCC is characterized by high intra-tumor heterogeneity (3, 4). Recurrent somatic mutations found in ccRCCs occur in the epigenetic regulators *PBRM1*, *SETD2* and *BAP1*, all of which are also located on chromosome 3p and are therefore prone to inactivation similar to *VHL* (5). These specific genetic changes are reflected at the RNA and protein levels, for instance, by activation of the HIF-pathway and a corresponding increase in expression of angiogenesis-related mRNA signatures and hypoxic signaling, which are direct consequences of VHL inactivation (6). Extensive metabolic reprogramming is another result of the genetic changes that occur during ccRCC initiation and progression and this is increasingly recognized to correlate with aggressive disease (7). This is exemplified by the inactivation of the pyruvate dehydrogenase complex (PDC) which in turn impairs the Krebs cycle and oxidative phosphorylation resulting in a metabolic shift toward glycolysis (8). Importantly, metabolic rewiring in ccRCC has been shown to induce HIF-signaling independent of VHL through signaling pathways that involve for example mTOR and MET. This metabolic distortion could influence epigenetic changes and chromatin dysregulation, contributing to the aggressiveness of the tumor (9).

In contrast to primary ccRCCs, which often show a high number of subclonal drivers, metastatically progressed disease sites have a more homogenous molecular landscape. They contain fewer somatic mutations indicating the excerption of only those clones that are metastatically competent. Conserved trajectories have been identified to lead to metastasis, with PBRM1 mutations often predicating dissemination (10). Other hallmark genomic alterations that lead to metastasis are the loss of chromosome 9p and 14q. Interestingly, microRNA (miRNA) signatures are also disparate between the primary and metastatic sites, with several miRNAs associating with worse patient outcomes (11). A prominent example is miR-30c, which showed decreased expression in metastatic disease corresponding to lower progression-free survival (PFS). This finding is in line with its observed function in cell adhesion and invasion (12).

Importantly, the clinical diagnosis of ccRCC is most often incidental. Almost 30% of ccRCC patients already present with metastatic disease while another 30% develop metastasis later during the course of the disease (1). The prognosis for metastatic RCC (mRCC) is still relatively dismal with a variable spectrum of overall survival (OS) times ranging from less than 6 months to more than 5 years (13). It is therefore clear that accurate prognostic and risk identification strategies that enable the early prediction of recurrences could impact ccRCC clinical management (**Figure 1**). In fact, the likelihood of a favorable response to treatment is superior with limited metastatic burden (14). However, no specific molecular marker has been recommended for this clinical use to date (15). Liquid biopsies are emerging as a minimally invasive, rapid, and cost-effective tool to determine cancer markers in biological liquids such as blood or urine (**Figure 1**) (16, 17). The source for these potential

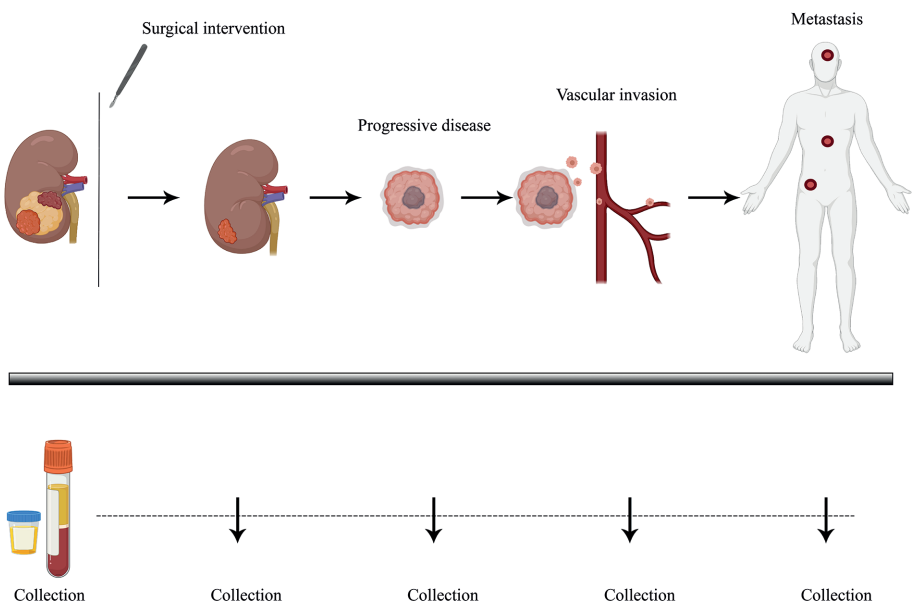

FIGURE 1 | Longitudinal monitoring of disease progression *via* liquid biopsy. Liquid biopsy presents as a minimally invasive prognostic technique, allowing the surveying of disease burden and progression in patients through biological liquid samples such as blood and urine. ccRCC patients, who tend to show high variability in disease progression, could benefit from better therapeutic response and PFS (Progression-free survival) with continuous follow-up of tumor molecular profiling through analyzing tumor-specific circulating biomarkers over time. Plasma and urine samples could be collected over several time points and profiled *via* ultra-sensitive analytical techniques, helping guide clinical management strategies.

biomarkers is the "circulome", which refers to the molecules released into circulation from all tissue, including the tumor tissue. Therefore, liquid biopsies may contain tumor-specific information in the form of circulating tumor cells (CTCs), circulating tumor DNA (ctDNA), circulating tumor RNA (ctRNA), secreted proteins, extracellular vesicles, metabolites, and tumor-educated platelets. Currently, a small number of non-invasive blood tests that detect ctDNA are used as companion diagnostic tool for cancers such as non-small cell lung carcinoma (NSCLC), prostate and colorectal carcinoma. These tests are mainly used as rationales for treatment decisions, for example to detect activating mutations in the Epidermal Growth Factor Receptor (EGFR) that can be treated by administering Osimertinib in patient with NSCLC (18). Alongside, several liquid biopsy tests are under investigation in clinical trials as reviewed by Heidrich et al. (19). Among the putative markers with prognostic relevance in mRCC, ctDNA, ctRNA, proteins and exosomes are currently under heavy examination. In this review, we will provide a brief overview of the recent developments in the identification of circulating biomarkers that are indicative of a metastatic lesion and which allow the identification of disease recurrence in ccRCC patients. Moreover, we present several novel and promising technologies that could overcome some of the current limitations of liquid biopsy analysis that have been roadblocks to implementing them as a prognostic tool with clinical utility (**Figure 2**).

CIRCULATING TUMOR DNA

The highly aggressive and vascularized nature of ccRCC prompted the intuitive expectation that tumor material, such as DNA, could be shed into circulation constituting a powerful tool to profile the tumor genome bypassing the need for a tissue biopsy. We have identified a number of studies, using the search terms "Renal cell carcinoma" and "Circulating tumor DNA" from public databases, that have investigated such possibilities (**Table 1**). Early reports paved the way by demonstrating the feasibility of genetic analysis from liquid biopsies, initially proposing the use of cell-free DNA (cfDNA) concentration and fragmentation as a guide for predicting and following the progression toward mRCC. Repeatedly, cfDNA concentrations were shown to be significantly higher in patients with advanced or metastatic disease compared to healthy individuals and patients with localized tumors (**Table 1**). Interestingly, analysis of the housekeeping gene *ACTB* as a surrogate measure of cfDNA concentration showed a consistent and significant elevation in RCC patients compared to healthy controls (21). Additionally, Wan et al. reported that the average plasma cfDNA level was significantly higher in metastatic tumors than in localized disease indicating that they could even be reflective of ccRCC progression (22). Even though these observations are noteworthy, both studies reported only moderate sensitivity and specificity for the alterations and thus further validation is required to clarify the clinical benefit of cfDNA concentrations as a circulating biomarker.

Fragmentation of cfDNA has also been studied as a diagnostic and prognostic marker in RCC patients (28, 30). Several groups performed these analyses using marker DNA fragments from genes like *ACTB*, *GAPDH* and *APP* as well as Alu short interspersed nucleotide elements and the mitochondrial DNA fragments Mito-1 and Mito-2 (20, 21, 24). Lu et al. could correlate shorter cfDNA fragments of the gene amyloid beta (A4) precursor protein (*APP*) with prognostic factors for recurrence-free and OS in patients with ccRCC and the cfDNA

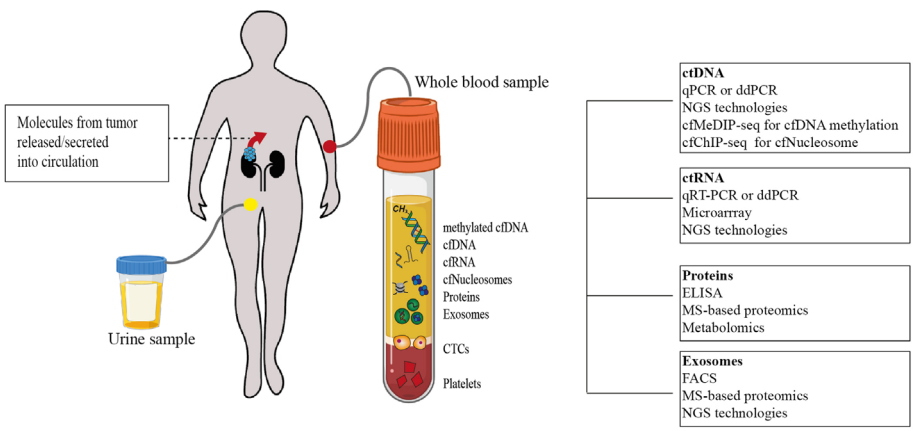

FIGURE 2 | Tumor-specific circulome and technologies used for their analysis. Tumor-specific circulating biomarkers can include several molecules involved in tumorigenesis and tumor progression. Analytes that have been studied as potential biomarkers so far are depicted. Using a variety of techniques, their quantification at a single time point may allow disease staging and prognostication (cfDNA. cell-free DNA; cfRNA. cell-free RNA; cfNucleosomes. cell-free nucleosomes; CTCs, circulating tumor cells; ctDNA, circulating tumor DNA; qPCR, quantitative polymerase chain reaction; ddPCR, droplet digital polymerase chain reaction; NGS, next-generation sequencing; cfMeDIP-seq, cell-free methylated DNA immunoprecipitation sequencing; cfChIP-seq, cell-free chromatin immunoprecipitation sequencing; ctRNA, circulating tumor RNA; ELISA, enzyme-linked immunosorbent assay; MS, Mass spectrometry; FACS, fluorescence-activated cell sorting).

TABLE 1 | Circulating Tumor DNA.

Reference	Evaluation method	No of Patient samples	Results
Gang et al. (20)	qPCR	Serum of 36 ccRCC patients and 42 healthy controls	• Significant association between cfDNA integrity and tumor size and stage • A significant difference in cfDNA fragmentation between pre and post-nephrectomy samples was observed
Hauser et al. (21)	qPCR	Serum of 35 RCC patients (29 ccRCC patients) and 54 healthy controls	• Amplified *ACTB*^{384} and *ACTB*^{106} fragments were significantly higher in RCC group compared to healthy controls (ACTB-384: 1.77 vs. 0.61 ng/ml, p = 0.0003; ACTB-106:.31 ng/ml vs. 0.77 ng/ml p = 0.003). • cfDNA threshold levels to distinguish between RCC patients and healthy individuals were 1.03 ng/ml for ACTB-106 (68.6% sensitivity and 70.4% specificity) and 1.70 ng/ml for ACTB-384 (57.1%, sensitivity and 81.5% specificity) • The significant higher level of ACTB^{384} in RCC patients indicates that cell-free serum DNA is fragmented to a higher degree in cancer patients. Cell-free DNA levels of ACTB^{384}, ACTB^{106} and DNA integrity did not correlate with clinical parameters such as tumor stage and grade
Wan et al. (22)	qPCR	Plasma of 92 ccRCC patients, 44 healthy controls	• Decrease in cfDNA concentration in plasma samples following nephrectomy. • Higher cfDNA levels in patients with metastatic disease (6.04ng/ml ± 0.72) when compared to patients with localized disease (5.29 ± 0.53, p = 0.017) or healthy controls (0.65 ± 0.29, p < 0.001) • Increased cfDNA levels were associated with shorter recurrence-free survival • Pre-treatment level of plasma cfDNA could predict recurrence with a sensitivity of 70.6% at specificity of 71.2%
Bettegowda et al. (23)	NGS	Plasma of 5 mRCC patients	• <50% patients had detectable ctDNA
Lu et al. (24)	qPCR	Plasma of healthy individuals (n = 40), non-metastatic (n = 145), and metastatic (n = 84) ccRCC patients	• The mitochondrial cfDNAs *Mito-1* and *Mito-2* were higher in metastatic than in non-metastatic patients and controls. • *Mito-1* and *Mito-2* fragment concentration significantly correlated with Fuhrman grade (r_s = 0.209 and 0.206, p = 0.0121 and 0.014, respectively) • *APP-3* fragment concentration decreased in both ccRCC groups • The cfDNA integrity decreased from controls to metastatic patients.
Corrò et al. (25)	NGS	Plasma and serum samples of 9 ccRCC patients	• It was not possible to identify genetic alterations such as the *VHL* mutation in ccRCC plasma without prior knowledge of patient-specific mutation profiles from primary tumor tissue
Maia et al. (26)	NGS- Gaurdant360 panel	Plasma from 34 RCC patients (26 ccRCC patients)	• ctDNA was detected in 18 late-stage or mRCC patients (53%) with a median of 2 GAs per patient. *VHL* (n = 5) and *TP53* (n = 7) were the most frequent GAs. • Patients with detectable ctDNA had significantly higher tumor size (8.81 vs. 4.49 cm; *P* = 0.04)
Pal et al. (27)	NGS - Guardant360	Plasma from 220 mRCC patients	• Using an approach with great sensitivity to mutant cfDNA fragments at below 1%, GAs were detected in 79% patients. Most frequent GAs were TP53 (35%), VHL (23%), EGFR (17%), NF1 (16%), and ARID1A (12%). • Mutations from non-RCC related somatic expansions like CHIP were not excluded • 55% of variants were of unknown significance • 45% of SNVs and indels were characterized with known significance. Distribution of GAs amongst patients were as follows: TP53- 30% VHL-32%, NF1-22%, EGFR-13%, and ARID1A-18%
Yamamoto et al. (28)	qPCR	Plasma from 92 ccRCC patients and 41 healthy controls	• cfDNA concentration significantly higher in ccRCC group vs. healthy control (3803 vs. 2242 copies/ml, p < 0.001) and increased with TNM staging. • Median cfDNA fragment size in ccRCC group significantly shorter vs. healthy control and negatively associated with PFS • cfDNA showed 63% sensitivity and 78.1% specificity as diagnostic marker in ROC curve analysis
Smith et al. (29)	Whole genome/ exome sequencing	MonRec study (43 metastatic RCC patients treated with multiple systemic therapies and longitudinal follow-up) and 90 patients from DIAMOND study (samples taken either prior to surgery or during progressive disease)	• RCC is a ctDNA low malignancy, detection rates of ctDNA in patient plasma are ~30% using an untargeted sequencing strategy • A sensitive personalized approach which is based on prior knowledge of individual tumor-specific mutations from matched tumor tissue could detect plasma ctDNA in ~50% of patients, • ctDNA detection in plasma was more frequent amongst patients with larger tumors and in those patients with venous tumor thrombus
Yamamoto et al. (30)	NGS - RCC-specific gene panel (48 genes)	Plasma of 53 ccRCC patients	• Targeted sequencing was carried out using plasma cfDNA and ctDNA • In 30% patients, somatic mutations were detected in cfDNA. Most frequently detected mutations included TP53 (n = 6), BAP1 (n = 5), VHL (n = 5), TSC1 (n = 4), and SETD2 (n = 3. • ccRCC patients with detectable ctDNA showed shorter fragment sizes of cfDNA.

(Continued)

TABLE 1 | Continued

Reference	Evaluation method	No of Patient samples	Results
			• cfDNA fragments with *SETD2*, *BAP1*, and *NF2* mutations were significantly shorter than wild type cfDNA fragments. • Detectable ctDNA and cfDNA size associated with poor PFS and CSS (long vs. short, P = .004, P = .011 and high vs. low, P = .317, P = .127, respectively)
Bacon et al. (31)	NGS - Roche SeqCap EZ Human Oncology Panel	Plasma from 55 mRCC patients	• 33.3% of patients showed evidence for the presence of ctDNA, exhibiting a somatic mutation in ≥1 established RCC gene. The estimated ctDNA fraction was 3.9% and median VAF = 3.6%. • Most commonly mutated genes include *VHL* (41%), *BAP1* (29%), and *PBRM1* (17%). Mutation profiles were highly concordant between ctDNA and corresponding tissue (77% of mutations were shared) • 11 patients were identified harbouring non-RCC specific cfDNA somatic mutations and lower VAF = 1.5%, arising from CHIP • 22 CHIP-related mutations in all patient samples, median VAF = 2.15%. ctDNA positive patients had lower PFS and OS • Evidence of somatic expansions unrelated to RCC, such as CHIP were detected in 43% of patients.

List of original articles cited in this section, with the main results summarized. The classification in RCC subtypes was not unequivocally done in all studies. Since ccRCC accounts for the majority of RCC cases, reports that did not state specifically which histological subtype was analyzed were also included. BRT, Benign renal tumors; cfDNA, Cell-free DNA; CHIP, clonal hematopoiesis of intermediate potential; ctDNA, Circulating tumor DNA; CSS, Cause-specific survival; GA, Genomic alterations; NGS, Next-generation sequencing; qPCR, Quantitative real-time polymerase chain reaction; PFS, Progression-free survival; VAF, Variant allele frequency; OS, Overall survival.

integrity index calculated based on the ratio of these fragment concentrations showed a decreased trend from controls to mRCC patients (24). Similarly, mitochondrial and Alu elements showed increased fragmentation and lower cfDNA integrity in RCC patients. However, when analyzing DNA integrity using *ACTB* and *GAPDH* as markers, cfDNA fragmentation was increased in RCC compared to controls (20, 21). While it has been shown that cfDNA fragmentation could be a valuable biomarker, further work needs to clarify which genetic elements have to be selected to ensure a complete visualization of the cfDNA fragment landscape and its diagnostic and prognostic potential (24). ctDNA has been identified in renal cancer patients of all stages but the probability of detection increased with the tumor size indicating that advanced disease stages may be better reflected in liquid biopsies (29). However, a number of studies reported ctDNA to be much less abundant in liquid biopsy samples from RCC patients compared with those from other cancers and several groups showed that ccRCC-specific ctDNA could be detected in only about 30%–50% patients (23, 25, 26, 29, 31). In a recent study, Bacon et al. used the Roche SeqCap EZ Human Oncology Panel to analyze the coding regions of 981 cancer-related genes in plasma cfDNA of 55 mRCC patients (31). Even this comprehensive analysis could only detect evidence for RCC-derived ctDNA, such as a somatic mutation in more than one established RCC genes, in a third of the patients. It is noteworthy that this was the first study that accounted for non-RCC specific somatic clones in liquid biopsies which can stem from clonal hematopoiesis of indeterminate potential (CHIP) by analysis of patient-matched leukocyte DNA. This could have decreased the sensitivity toward cfDNA mutations while increasing the sensitivity to RCC-derived ctDNA mutations. In addition, this study reveals that the blood-borne ctDNA fraction was as low as 3.9%, which is considerably less than in metastatic breast or lung cancer (32, 33).

Two other recent studies have reported higher numbers of ctDNA-positive patients. One of the largest studies by Pal et al., which included 220 mRCC patients, promisingly reported RCC-specific alterations in genes such as *VHL*, *TP53*, *EGFR*, *NF1*, and *ARID1A* in almost 80% of the patients when using a driver gene deep sequencing approach, with great sensitivity to mutant cfDNA fragments (<1%) (27). This apparent discrepancy in detecting tumor-specific mutations in the aforementioned study could be due to two factors: Although Pal et al. analyzed a larger cohort, only 56% of the samples were histologically characterized, of which 70% were classified as ccRCC. In comparison, the cohort used by Bacon et al. was completely histologically classified and contained 85% ccRCC patients. Moreover, Pal et al. did not account for non-RCC specific somatic clones which may be a rather large contributor to the genetic alterations observed in RCC liquid biopsies.

A second recent and sophisticated pipeline to detect cell-free tumor DNA in RCC patients' plasma and urine samples was introduced by Smith et al. and was termed as a "personalized method" of ctDNA sequencing. Similar to other studies, sequencing of plasma cfDNA alone could identify ctDNA in a third of the RCC patients, including those with mRCC. However, when the personalized method that was based on prior sequencing of the primary tumor tissue and subsequent assessment of the known mutations in corresponding liquid biopsies was applied ctDNA detection rates improved to ~50% (29). In addition, in a small cohort of patients, the authors could show the prognostic value of ctDNA analysis by revealing that longitudinal plasma sampling could track disease progression. Another important finding from this study is that plasma ctDNA represented 90% of the disparate mutations found in multiple biopsy regions from individual tumors of two well characterized ccRCC patients and thus indicated that ctDNA could be used to circumvent tumor sampling bias that might be present in

conventional tissue biopsies. This is an attractive approach to overcome the well-established tumor heterogeneity present in ccRCCs (34).

Taken together, a number of studies indicate RCC as a ctDNA-low malignancy by showing that only 30%–50% of patients benefitted from characterization of ccRCC-specific ctDNA using the currently available profiling technologies (23, 25, 26, 29, 31). Despite these drawbacks, ctDNA was detected more frequently in plasma amongst patients with larger tumors and hence longitudinal sampling could be used to monitor the course of the disease at least in a subset of advanced patients. Even though cfDNA analysis does not seem to enable straightforward surveillance at the moment, novel technologies could significantly improve this situation in the future.

PROTEINS AND ONCOMETABOLITES

Liquid biopsies could help to further investigate the proteomic landscape reflecting the changes triggered, for example, by extravasation of the ccRCC into circulation. Blood, abundant with proteins, is an inviting medium for exploring disease-related markers but it is technically challenging to mine tumor-specific signatures amidst highly abundant plasma proteins and other soluble factors. Studies identified with a keyword search for "renal cell carcinoma", "liquid biopsy or plasma", "protein or proteome" were further selected based on their diagnostic and prognostic value and are discussed in this section. A number of these studied utilized different experimental approaches in order to identify proteins with differential abundance in RCC plasma or serum relative to controls (**Table 2**; Please refer to Clark and Zhang Clin Proteom 2020 (52) for a comprehensive review). Historically, one of the most extensively studied proteins in this context is the Kidney Injury Molecule 1 (KIM1). KIM1 levels were found to be significantly increased in RCC patients (36). In fact, high grade ccRCCs showed an almost 7-fold increase in KIM1 abundance and mRCC patients displayed particularly high KIM1 levels in their plasma (47, 49). Despite the rather widespread expression of KIM1 in several renal diseases (53), circulating KIM1 showed 83% specificity in detecting early stage tumors with an increase to 97% specificity in later stages (47). While this makes it a promising biomarker, further studies need to validate the clinical utility of KIM1 as a ccRCC-specific circulating protein. Acknowledging the involvement of *VHL* mutations in ccRCC tumorigenesis, proteins downstream of the hypoxia-pathway represent a class of interesting soluble markers. For instance HIG2, a hypoxia inducible protein, was elevated approximately 3-fold in the plasma of RCC patients in an ELISA-based study and its abundance decreased drastically after nephrectomy (38). CAIX, one of the most prominent targets of the VHL-HIF-pathway, also emerged as a potential biomarker showing increased protein concentrations and activity in the plasma of ccRCC patients compared controls (45). Similarly, high IMP3 levels have been observed in RCC patients and correlated with the development of distant metastasis (48). Additionally, high levels of soluble CD27 were detected in sera of ccRCC patients and *in vitro* analyses suggested that this was triggered by the high expression of the HIF-target gene CD70 (43). These examples illustrate how the knowledge of ccRCC-specific cellular aberrations can be leveraged in the search for candidate biomarkers. Nevertheless, looking beyond the VHL-HIF-pathway, the TNF-related apoptosis-inducing ligand (TRAIL) was identified as a potential biomarker showing a 2-fold decrease in RCC patient sera and being highly predictive of venous invasion and metastasis (41).

Despite their initial promise, none of these circulating protein markers were clinically approved. Subsequently, large-scale proteomic technologies were utilized in order to provide a deeper characterization of ccRCC-specific protein assisting the search for candidate liquid biomarkers (**Figure 2**). An earlier study could distinguish RCC patients from non-RCC and healthy controls by using SELDI-TOF and applying pattern analysis based on five proteins with masses in the range of 3,900–5,900 Da (35). Similar studies have identified other peaks at 4,151 and 8,968 m/z that significantly differed between RCC and healthy controls and had an overall specificity of 80% (37). These even provided evidence for the utility of individual proteins including factor XIIIB, complement C3, misato homolog 1, hemopexin, alpha-1-B-glycoprotein (39) and HSC71 (44) as RCC-specific soluble biomarkers. Moreover, using MALDI-TOF, RNA-binding protein 6 (RBP6), tubulin beta chain (TUBB), and zinc finger protein 3 (ZFP3) were found to reduce following surgical intervention (40). Taken together, these findings underscore the opportunity to use the plasma proteome for longitudinal disease monitoring.

Much like it has been utilized with ctDNA, linking liquid biopsy protein profiles to those of the primary RCC could provide important complimentary data for the search of candidate biomarkers. In an interesting discovery study, White et al. used LC-MS/MS analysis to identify differentially expressed proteins in ccRCC compared to normal kidney tissue (42). From this analysis, heat shock protein beta-1 (HSPB1/Hsp27) emerged as a promising candidate and consequently the utility of Hsp27 as a useful non-invasive marker was confirmed in patient sera. Besides being elevated in serum and urine of ccRCC patients, Hsp27 was also associated with high grade (Grade 3–4) tumors.

Finally, it makes intuitive sense that the assessment of soluble immune-checkpoint proteins could have the added benefit of predicting immunotherapy responses besides their diagnostic or prognostic potential alone. Soluble factors such as sLAG3, sPD-L2, sBTLA, and sTIM3 were observed in higher concentrations in ccRCC patients and were significantly correlated with survival, death-risk and recurrence (50). Moreover, these proteins have already been developed as biomarkers for immune therapy prediction in several other cancer types (54). Apart from the proteome, other oncometabolites originating from metabolic processes such as amino acid metabolism, hormone synthesis and lipid transport including leucine, N-lactoyl-leucine, N-acetly-phenylalanine, hydroxylprolyl-valine, cortolone, and testosterone have been nominated as potential liquid biomarkers in RCC patients (46, 51). A panel consisting of the

TABLE 2 | Proteins and oncometabolites.

Reference	Evaluation method	No of Patient samples	Results
Won et al. (35)	SELDI-TOF MS/MS	Serum of 15 RCC patients, 15 patients with other urological malignancies and 6 healthy controls	• 119 mass peaks were identified from all samples. Bioinformatics analysis using a predictive classifier (decision tree) was constructed with 5 distinct masses (3,900, 4,107, 4,153, 5,352, and 5,987 kDa) • Decision tree correctly predicted the diagnosis of 85.7% of test samples (Sensitivity = 87%, specificity = 85%)
Han et al. (36)	Western blot and ELISA	Urine of 42 RCC patients	• KIM1 was elevated in RCC urine samples • Upon examining association between KIM1 levels and RCC, Urinary KIM1 of concentrations higher than 0.1 ng/ml was associated with a >36-fold risk of RCC, 82% sensitivity, and 90% specificity • Urinary KIM1 levels decrease after surgical removal of the tumor
Hara Tomohiko et al. (37)	SELDI-TOF MS/MS	Serum from 40 RCC samples, 44 healthy controls and 5 patients with pyelonephritis	• Significantly prominent mass peaks of 4,151 and 8,968 m/z were found in RCC samples • Simultaneous recognition of both peaks discriminated RCC samples from controls at 89.5% sensitivity and 80% specificity • Stage I RCC could be discrimination from healthy or later stage at 88.9% sensitivity using both mass peaks.
Togashi et al. (38)	ELISA	Plasma of 32 RCC patients, 20 healthy controls and 10 chronic glomerulonephritis patients	• Higher plasma HIG2 in RCC (~2.5-fold increase) • Decreased HIG2 post-surgery in stage I and stage II
Xu et al. (39)	2D gel electrophoresis, MALDI-TOF MS/MS	Serum of 20 RCC patients and 20 healthy controls	• Analysis of serum from diseased and healthy patients identified 19 differentially expressed proteins • Finally, 6 proteins were identified with a significant Mascot score (>66): factor XIII B, complement C3, complement C3 precursor, hemopexin, and alpha-1-B-glycoprotein.
Yang et al. (40)	ELISA	Plasma samples from 68 RCC patients and 39 healthy controls	• Plasma VEGF levels were significantly higher in RCC patients. • VEGF levels associated with lymph node invasion and/or metastases
Toiyama et al. (41)	ELISA	Serum of 84 RCC patients and 52 healthy controls	• TRAIL levels were lower in RCC patients (55.9 vs. 103.1 pg/ml; P = 0.019) • Decreased TRAIL expression associated with lymph node metastasis, distant metastasis and venous invasion
White et al. (42)	LC-MS/MS, western blotting	Serum of 54 RCC patients and 36 normal individuals; urine of 21 RCC patients and 9 normal individuals	• Using proteomic analysis, 55 proteins were identified to be significantly dysregulated in ccRCC compared to normal kidney tissue • Heat shock protein beta-1 (HSPB1/Hsp27) was confirmed in two independent sets of patients by western blot and immunohistochemistry • Hsp27 was elevated in the urine and serum from RCC patients • Higher tumor grades (grade III-IV) were associated with higher Hsp27 expression in patient serum (p = 0.013)
Ruf et al. (43)	ELISA	Serum of 54 ccRCC patients and 17 healthy controls	• High levels of soluble CD27 in patients with CD70-expressing ccRCC cells and $CD27^+$ Tumor infiltrating lymphocytes • CD70 expression levels in tissue were not reflected in sera (n = 31)
Zhang et al. (44)	Western blot, ELISA and iTRAQ-labelled MS/MS	Serum of 40 RCC patients, 10 healthy controls and 20 patients with other urological malignancies	• 16 proteins increased >1.5-fold and 14 proteins decreased <0.67-fold in RCC patients compared to controls. • Quantification by western blot showed that HSC71 was significantly upregulated in RCC sera (P = 0.0037) • HSC71 was elevated in RCC sera when measured with ELISA (P = 0.0028 vs. control, P = 0.0008 vs. non-RCC) and showed diagnostic value (AUC = 0.86 and 87% sensitivity at 80% specificity)
Lucarini et al. (45)	Western blot, ELISA and enzyme activity assay	Plasma of 8 ccRCC patients, 8 BRT and 8 controls	• Plasma CAIX levels were significantly higher in ccRCC patients ($p \leq 0.005$) • CA IX activity was lower in healthy controls compared to ccRCC or BRT (kcat $5.57 \times 10^4\ s^{-1}$ vs. kcat $1.62 \times 10^6\ s^{-1}$ or $1.46 \times 10^4\ s^{-1}$)
Knott et al. (46)	UPLC-MS/MS	Serum samples from 5 ccRCC patients and 5 healthy controls	• Renal carcinoma cell lines were used to define a panel of 21 tumor-specific metabolic features and these were assessed in human serum samples. • 9 of these features were present in serum samples. A PCA model based on these 9 feature panel provided showed diagnostic value, utilizing 2PCs at a total variance of 70.87%
Kushlinskii et al. (47)	ELISA	Plasma of 99 ccRCC patients, 14 BRT and 29 healthy controls	• KIM-1 levels are elevated in ccRCC patients and BRT • KIM-1 levels could discriminate ccRCC at all stages: Stage I: 81% sensitivity; Stage II-IV: 97% sensitivity • KIM-1 levels correlated with tumor stage (stage 1/2 vs. stage 3/4)
Tschirdewahn et al. (48)	ELSIA	Plasma of 98 RCC patients and 20 healthy controls	• Plasma IMP3 was elevated in RCC samples (20 ng/ml vs. 10 ng/ml median, p = 0.015)

(Continued)

TABLE 2 | Continued

Reference	Evaluation method	No of Patient samples	Results
			• IMP3 levels were higher in plasma from metastatic patients • High IMP3 plasma levels were associated with OS and CSS
Scelo et al. (49)	ELISA	Plasma from 190 RCC patients and 190 healthy controls	• KIM-1 detected in 93% RCC samples and 70% controls • Incident rate ratio for doubling of KIM-1 levels was 1.71 • 5-year risk of RCC increased with increased KIM-1 levels (low vs. high: 0.2% vs. 1.0%)
Wang et al. (50)	Multiplex Luminex assay	Plasma samples from 182 ccRCC patients	• High levels of soluble LAG3 were associated with an increased risk of advanced disease (OR = 3.36, P = 0.002) • High soluble PD-L2 concentration correlated with an increased risk of disease recurrence (HR = 2.51, P = 9.33×10^{-4}) • Patients with high soluble BTLA and high soluble TIM3 showed an increased risk of tumor-related death (6-fold increase) and decreased OS (log-rank P = 9.81×10^{-8} and log-rank P = 6.29×10^{-5}, respectively)
Zhang et al. (51)	LC-M/MS	Urine samples from 39 RCC patients, 22 BRTs and 68 healthy controls	• 79 metabolites with differential abundance were identified. • Pathway analysis showed disturbance in amino acid metabolism, including phenylalanine metabolism, lysine degradation, lysine biosynthesis and histidine metabolism in renal tumors • 16 metabolites showed good diagnostic clinical value. Cortolone, testosterone and l-2-aminoadipate adenylate levels could distinguish malignant from benign tumors. • A logistic regression model based on this panel of metabolites could discriminate RCC patients from controls with a specificity of 100% and a sensitivity 75% in the test cohort (n = 68). • In an independent validation cohort, both sensitivity and specificity were 80% (n = 49) • 56 metabolites were differentially expressed between RCC and normal in this validation cohort. Finally, a panel with aminoadipic acid, 2-(formamido)-N1-(5-phospho-d-ribosyl) acetamidine and alpha-N-phenylacetyl-l-glutamine could predict RCC specificity of 75% at 93% sensitivity (AUC = 0.885)

List of original articles cited in this section, with the main results summarized. The classification in RCC subtypes was not unequivocally done in all studies. Since ccRCC accounts for the majority of RCC cases, reports that did not state specifically which histological subtype was analyzed were also included. AUC, Area under curve; BRT, Benign renal tumors; CSS, Cause-specific survival; ELISA, Enzyme linked immunosorbent assay; iTRAQ, Isobaric tag for relative and absolute quantitation; HR, Hazards ratio; LC, Liquid chromatography; MALDI, Matrix-assisted laser desorption/ionization; MS, Mass spectrometry; OR, Odds ratios; OS, Overall survival; PCA, Principal component analysis; TOF, Time of flight; SELDI, Surface-enhanced laser desorption/ionization; UPLC, Ultra-performance liquid chromatography.

metabolites cortolone, testosterone and l-2-aminoadipate adenylate was able to distinguish RCC patients from benign renal tumors with 100% specificity at 75% sensitivity, indicating an increased effectiveness in discrimination when combining groups of biomarkers that are involved in disturbed metabolic pathways (51).

Taken together, several studies have already investigated RCC-specific metabolites and in particular proteins but a large proportion of these have only examined patient samples in comparison to healthy controls in order to delineate aberrant expression patterns specific for RCC diagnosis. Even though interesting markers have been nominated, information on the prognostic value of many of these candidates is still lacking. In addition, large-scale deep proteomic characterization has revealed various potential biomarkers but due to the lack of validation in clinical cohorts, very little can be used conclusively to define a panel of markers for ccRCC monitoring. Novel mass spectrometry and multi-marker based approaches are awaited to provide more comprehensive insights and a deeper understanding of potential secretory protein markers and their prognostic value in ccRCC.

CIRCULATING RNA AND EXOSOMES

Cell-free RNA either enters the blood through active release from cells in extracellular vesicles like exosomes or conjugated to proteins (55–57). Coding RNA such as messenger RNA (mRNA) as well as small non-coding RNAs like miRNA and lncRNA have presented themselves as potential liquid biopsy biomarkers (**Figure 2**). Search terms "renal cell carcinoma", "Circulating RNA or mRNA or miRNA or lncRNA" yielded studies that were pruned to select a smaller collection with relevant clinical value for ccRCC prognosis. So far, miRNAs remain the most frequently studied class of RNA molecules probably owing to the shorter half-life of mRNA and the relative novelty of lncRNA (**Table 3**). Several miRNAs which have previously been studied in the context of cancer progression and development, have also been proposed as liquid biomarkers in ccRCC. One of the most interesting examples is *miR-210*, which is known to be regulated by the VHL/HIF-pathway (58) and has emerged as a novel indicator for ccRCC tumor burden. Elevated levels of circulating *miR-210* have been reported in patient sera and following nephrectomy they were observed to

TABLE 3 | Circulating RNA and exosomes.

Reference	Evaluation methods	No of Patient samples	Results
Zhao et al. (58)	qPCR	Serum of 68 ccRCC patients and 42 healthy controls	• miR-210 showed high expression in ccRCC serum and could differentiate ccRCC patients from healthy controls; 81% sensitivity, and 79.4% specificity • miR-210 levels correlated with ccRCC stage and were reduced after nephrectomy.
Teixeira et al. (59)	qPCR	Plasma of 77 RCC patients	• miR-221 and miR-222 were more abundant in RCC plasma ($2^{-\Delta\Delta Ct}$ = 2.8, P = 0.028; $2^{-\Delta\Delta Ct}$ = 2.2, P = 0.044, respectively). • miR-221 levels were higher in plasma of metastatic patients than patients with no metastasis ($2^{-\Delta\Delta Ct}$=10.9, P = 0.001) and high expression correlated with lower OS (48 vs. 116 months, respectively; P = 0.024)
Wu et al. (60)	qPCR	Serum of 71 ccRCC patients, 8 BRT, 62 healthy controls	• lncRNAs showed differential abundance: 13 lncRNAs were down-regulated and 1 lncRNAs was up-regulated in ccRCC serum. The signature of lncRNA-LET, PVT1, PANDAR, PTENP1 and linc00963 was highly specific and sensitive in discriminating between ccRCC and controls • This 5-lncRNA signature was also correlated with all pathological stages of ccRCC (AUC = 0.85 and 0.8 for stage I and II-IV, respectively)
Li et al. (61)	qPCR	Urine of 75 ccRCC and 45 healthy controls	• Urinary miR-210 was significantly elevated in ccRCC samples and discriminated ccRCC from healthy controls, 57.8% sensitivity, and 80% specificity. • miR-210 levels decreased after surgical removal of the tumor
Petrozza et al. (62)	qPCR	Urine of 38 ccRCC patients	• miR-210 was upregulated in ccRCC samples and levels significantly decreased after nephrectomy
Heinemann et al. (63)	NGS- Small RNA sequencing	Serum of 86 ccRCC, 55 BRT, 28 controls	• 2588 miRNAs were detected from which 29 miRNAs were differentially expressed between healthy and disease samples: 17 miRNAs were up-regulated and 12 miRNAs were down-regulated in the tumor samples. • Serum miR-122-5p and miR-206 (log2 fold change – 1.55; p = 0.002 and log2 fold change – 1.56; p < 0.001, respectively) were down-regulated in ccRCC sera. miR-122-5p and miR-206 could discriminate ccRCC from controls • miR-122-5p significantly increased in mRCC • Elevated serum miR-122-5p and miR-206 correlated with shorter PFS, CSS and OS
Liu et al. (64)	qPCR	Serum of 10 ccRCC patients, 10 healthy controls	• miR– 141–3p and miR– 508–3p were down-regulated while miR– 885–5p and miR– 592 were up-regulated in ccRCC samples. All 4 miRNAs could discriminate RCC samples from healthy donors (AUC = 0.73, 0.86, 0.91, and 0.78, respectively) • The combinations of miR– 508–3p and miR– 885–5p analysis improved the discriminative power between healthy and diseased samples (AUC = 0.9)
Simonovic et al. (65)	qPCR	Plasma from 10 mRCC and 6 ccRCC patients, 7 healthy controls.	• CDK18 and CCND1 mRNAs were less abundant in the plasma of ccRCC patients (2.1 fold change, p = 0.001 and 1.55 fold change, p = 0.039, respectively)
			Exosomes
Raimondo et al. (66)	LC-MS/MS	Urine of 29 RCC patients and 23 healthy controls	• Proteomic analysis was performed on 9 urinary exosome pooled samples and led to the identification of 261 proteins from control samples and 186 from RCC patient samples. • Most of the identified proteins are membrane associated or cytoplasmic • A panel of 10 proteins (CD10, CP, DPEP1, MMP9, EMMPRIN, CAIX, Syntenin 1, PODXL, AQP1, DKK4) that were differently abundant in tumor and normal EVs were validated by immunoblotting
Butz et al. (67)	qPCR	109 ccRCC patients, 24 BRT and 33 healthy controls	• The combination of miR-126-3p and miR-449a or miR-24b-5p could distinguish ccRCC from controls
Qu et al. (68)	qPCR	Plasma of 71 RCC patients	• The non-coding transcript lncASR was increased in RCC patients • lncASR levels decreased after nephrectomy and increased again upon relapse
Du et al. (69)	qPCR	109 RCC patients	• miR-190b, miR 26a-1-3p, miR-let-7i-5p, miR-145-3p, miR-200-3p, and miR-9-5p associated with OS in an initial test cohort (n = 44) • In an additional validation cohort, association with OS was verified for miR-let-7i-5p, miR-26a-1-3p, and miR-615-3p.
Jingushi et al. (70)	LC/MS, Western blotting	Serum of 19 ccRCC patients and 10 healthy controls	• Extracellular vesicles (EVs) directly isolated from surgically resected ccRCC tissues and adjacent normal renal tissues were analyzed with quantitative LC/MS. This analysis identified 3,871 tissue-exudative EV proteins, among which azurocidin (AZU1) was highly enriched in tumor EVs (fold-change = 31.59). • AZU1 content in EVs was significantly higher in ccRCC patients compared to those from healthy donors. • Subsequent functional analyses indicated that EV-AZU1 could be engaged with vesicle-mediated hematogenous metastasis of RCC.
Zhang et al. (71)	qPCR	82 ccRCC patients, 80 healthy controls	• Exosomal miR-210 and miR-1233 significantly higher in ccRCC, and higher in each stage compared to normal • miR-210 and miR-1233 significantly lower post-surgery • miR-1233 had higher discriminatory capability with higher specificity and sensitivity than miR-210.

List of original articles cited in this section, with the main results summarized. AUC, Area under curve; CSS, Cause-specific survival; LC, Liquid chromatography; MS, Mass spectrometry; NGS, Next-generation sequencing; OS, Overall survival; PFS, Progression-free survival; qPCR, Quantitative real-time polymerase chain reaction.

decrease in the urine of disease-free patients during follow-up (61, 62). Several other miRNAs still remain to be explored as biomarkers in circulation. Studies in primary ccRCC tissue have identified 65 miRNAs, including *miR-215*, which were significantly different between patients with mRCC and localized ccRCCs (72). Whether these miRNAs can indicate metastatic dissemination of the primary tumor in liquid biopsies has not been not investigated to date. Circulating miRNAs that have already been implicated in predicting mRCC include *miR-122-5p*, *miR-206* (63), and *miR-221*. Importantly, out of these *miR-221* has also been shown to significantly correlate with lower survival (59). In addition, the combination of serum *miR-508-3p* and *miR-885-5p* could differentiate ccRCC patients, and these miRNAs have been implicated in the positive regulation of metabolic processes such as inositol phosphate metabolism and in the Hippo and Wnt signaling pathways that have been implicated in ccRCC tumorigenesis (64). Studying these miRNAs in metastatic patients and establishing their regulatory roles in ccRCC would likely improve their value as a circulating biomarker.

Messenger RNA is a crucial intermediate in relaying genetic changes to the protein level and may therefore reflect mutational and regulatory changes in the tumor. However, technical difficulties in detecting tumor-specific mRNA in patients' blood has limited its development as a biomarker for disease monitoring. Recently, novel sequencing technologies have provided impetus to further investigate the potential of circulating mRNA and consequently CDK18 and CCND1 messengers were shown to be downregulated in blood of ccRCC patients (65) (**Table 2**). Similarly, an increase in lysyl oxidase (*LOX*) expression marked metastatic samples from the same cohort (65). In addition, circulating lncRNA (73), one of the newer players in the field of small non-coding RNAs, also showed promise as a RCC-specific biomarker. A signature of 5 lncRNAs (*lncRNA-LET*, *PVT1*, *PANDAR*, *PTENP1*, and *linc00963*) could distinguish RCC samples from controls with a specificity of 91% at 67% sensitivity in a training set independent of stage classification. An increase to 76% sensitivity was observed when the training set was limited to controls and stage I ccRCC patients, indicating good discrimination even for less advanced patients (60).

Exosomes are nanoscale secreted membrane-bound vesicles that play a role in cellular communication by transferring signaling molecules as packaged cargo. One of the most frequent cargo is miRNA, while several other molecules including DNA, proteins and other classes of RNAs are transported in exosomes as well (74). Studied far more in urine than in blood, these vesicles are observed to contain molecules that are capable of differentiating and identifying ccRCC and mRCC. Comparable to circulating *miR-210*, exosomal *miR-210* was elevated in ccRCC patient sera and could distinguish ccRCC patients from healthy individuals, albeit only with a specificity of 62% (71). Considering that circulating levels of miR-210 have been described as relevant biomarkers in the context of cell-free analytes and as exosomal cargo, this is nevertheless one of the more promising molecules warranting further studies to assess its diagnostic and prognostic potential as a liquid biomarker for the clinical routine. Several other exosomal miRNAs or their combinations such as enumerated in **Table 2** were also able to differentiate RCC patients from healthy controls and supported the proposed use of exosomal cargo as potential biomarkers in ccRCC (67, 69). Additionally the non-coding transcript *lncARSR* (activated in RCC with Sunitinib Resistance) that is transmitted *via* exosomes, showed increased levels in the serum of RCC patients, decreased after tumor resection and subsequently increased again during tumor relapse making it an interesting candidate for non-invasive disease monitoring (68). A small number of studies have investigated the potential of exosomal protein markers (66, 70) giving first insights into their differential abundance between healthy and tumor patients. Interestingly, comprehensive protein cargo analysis by LC/MS revealed that azurocidin (AZU1) was significantly enriched in tumor-derived exosomes and these may even play a functional role in driving metastatic dissemination (70).

Despite the initial reports, neither lncRNA nor exosomal miRNAs or proteins have been thoroughly investigated as potential biomarkers for the metastatic disease yet. Large sample volumes and complicated and expensive processing set-ups appear as major roadblocks in this search. Therefore, technical advances are needed to improve the current approaches and pave the way to further investigate and translate RNA- or exosome-based cancer detection in the clinical setting.

FUTURE AVENUES IN LIQUID BIOPSY

Evidently, the field of liquid biopsy analysis is quickly evolving and has shown considerable promise for anticipating cancer progression, for example in lung, breast and colorectal cancer (75–77). However, currently there is still insufficient evidence for the clinical utility of majority of the circulating molecules in many advanced cancers as well as in ccRCC (78). Several approaches are under heavy investigation and their successful implementation could provide further rationales for using liquid biopsies as a tool for ccRCC patient management (**Figure 2**). However, one of the most important aspects for consideration in any further developments is the need to validate the emergence of potential liquid biomarkers in larger patient cohorts in order to consider them as specific and sensitive non-invasive markers of clinical utility. Currently, many interesting studies have sought to assess differential features between samples from healthy and diseased individuals. Significantly more work will be required to obtain a deeper understanding of the prognostic potential of the candidate markers as they should not only be prioritized based on their discriminatory benefit but also for their value in disease monitoring, e.g., to indicate metastatic dissemination.

One of the rather unexpected obstacles in developing a clinically applicable liquid biopsy analysis platform was the low ctDNA abundance that has so far hindered ctDNA from becoming a simple alternative to tissue biopsy in diagnosing and tracking

mRCC (23, 25, 26, 29, 31, 79). Nevertheless, mutant fragments derived from RCC cells have been identified in patients' plasma and the mutations closely mirrored the known landscape of the primary tumors (31). Several studies indicated that there are opportunities for liquid biopsies in the longitudinal follow-up of ccRCC patients provided additional improvements will be made in isolation and detection approaches. Among the main challenges is the concomitant presence of mutant fragments from non-RCC somatic clones stemming, for example, from CHIP which was identified as a main cause for the discordance between plasma and tissue RCC samples (31, 79). Incorporating appropriate controls such as white blood cell DNA could prove to be essential to eliminate variants arising from such unrelated somatic expansions. Combining personalized mutations identified from archival tumor tissue is another attractive strategy that was proposed to improve the sensitivity of ctDNA detection in mRCC (25, 29, 79). Conversely, most recently, a novel approach that is based on genome-wide mutational signal integration has challenged the paradigm of increasing the sequencing depth of a limited set of target genes for reliable ctDNA detection (80). By placing the emphasis on broadening the mutational landscape, this genome-wide single-nucleotide variant (SNV) detection platform showed evidence for allowing ultra-sensitive detection even at low-sequencing depths as well as enabling quantitative dynamic monitoring of disease burden. Thus, this approach could prove to be an attractive alternative to overcome the low ccRCC-specific ctDNA abundance and significantly increase detection sensitivity in the future.

Epigenetic regulation presents a wide avenue to explore ccRCC specific patterns, particularly since chromatin remodelers are among the most frequently altered factors. Based on the principle that tumor cells acquire aberrant DNA methylation, cell-free methylated DNA immunoprecipitation sequencing (cfMeDIP Seq) was able to markedly improve sensitivity for detecting patients with mRCC. The assessment of top differentially methylated regions of the cell-free methylome could also distinguish ccRCC and control samples (81). Since blood cfDNA is derived from fragmented chromatin, it often remains associated with histones that may contain evidence of the epigenetic landscape of the cells they originate from (82, 83). Thus, circulating cell-free nucleosomes could become interesting targets for observing mRCC-specific changes in expression programs that are often imposed by alteration in *SETD2*, *PBRM1*, or *BAP1*. Chromatin immunoprecipitation sequencing of cell-free nucleosomes (cfChIP-seq) has emerged capable of identifying cell-of-origin expression marks as well as changes in gene activity and transcription in gastrointestinal cancers (82). Extrapolating this to ccRCC could open a new window to provide detailed information about the state of the disease from liquid biopsy analysis.

Novel proteomic technologies will also bolster the development of circulating biomarkers. To aid the acquisition of ccRCC-specific peptides, pre-fractionation with the aim to either remove high-abundance proteins or enrich certain proteins could be employed. In addition, novel MS-based proteomic approaches such as Microflow LC-MS/MS (84) and Trapped Ion Mobility Spectroscopy (TIMS) (85) constitute valuable technologies for biomarker discovery. These, combined with higher throughput, will likely help to identify mRCC-specific proteins in liquid biopsies. A promising impetus for further studies in this domain was provided with the identification of several proteins differing in abundance with the infiltration of ccRCC into the renal vasculature using nano-scale liquid chromatographic tandem electrospray ionization mass spectrometry (nLC-ESI-MS/MS) for the proteomic analysis of urine and plasma (86).

Circulating RNAs (circRNA) represent a newly discovered class of small non-coding RNAs that have recently come into light as potential biomarkers for kidney diseases. Studies leveraging primary tissue collections have identified several combinations of these circRNA that are capable of identifying ccRCC (87, 88) and also correlated with tumor grade (80). Importantly, circRNAs have already been discovered as exosomal cargo in urine and plasma from patients with Idiopathic Membranous Nephropathy (89), raising the interesting possibility that these molecules could also be studied as indicators of renal cancer. Exosomes show high potential as a useful vehicle for tracking disease progression and dissemination by virtue of their aiding intercellular communication. Due to their small size and low density, recovery from plasma or urine remains the limiting step towards straightforward isolation, detection, and quantification (90). A novel chemical affinity-based capture method has been developed for extracellular vesicle isolation (EVtrap) from plasma, which showed a 7-fold increase in capture compared to ultracentrifugation and can potentially ameliorate this problem. In a promising proof-of-concept study, phosphoproteomic analysis of RCC plasma samples revealed several proteins capable of distinguishing five RCC patients from five healthy controls (91) indicating that EVtrap could be exploited to develop additional markers for disease monitoring.

It is also becoming increasingly apparent that the best definition of tumor status and prognosis may arise from the simultaneous study of various complimentary constituents of the circulome and thus, a multi-marker based approach may prove to be useful toward developing reliable biomarkers for disease surveillance (92). Harnessing the indicative potential of several of the molecules described in this review together may in fact be key to achieving prognostic utility in ccRCC liquid biopsy profiling.

CONCLUSION

Liquid biopsy analysis offers a range of complementary information through the circulome and has the potential to cause a major breakthrough in clinical oncology. In contrast to conventional tissue biopsy, it may even be able to capture a larger amount of the molecular heterogeneity described for ccRCCs and inform about aggressive clones that have disseminated toward the metastatic niche. Before this potential can be realized, a number of hurdles remain but given the rapid pace of technological development there

is an air of optimism regarding its utility, especially for monitoring the metastatic progression in ccRCC patients.

AUTHOR CONTRIBUTIONS

HL and HB contributed to the conception of the review article. HL, HB, and DR drafted the manuscript. PS and HM critically revised the manuscript. All authors contributed to the article and approved the submitted version.

FUNDING

This work was supported by the Swiss National Science Foundation (SNSF grant number 310030_166391).

ACKNOWLEDGMENTS

Figures in the review were created with www.Biorender.com.

REFERENCES

1. Hsieh JJ, Purdue MP, Signoretti S, Swanton C, Albiges L, Schmidinger M, et al. Renal cell carcinoma. *Nat Rev Dis Primers* (2017) 3:17009. doi: 10.1038/nrdp.2017.9
2. Mitchell TJ, Turajlic S, Rowan A, Nicol D, Farmery JHR, O'Brien T, et al. Timing the Landmark Events in the Evolution of Clear Cell Renal Cell Cancer: TRACERx Renal. *Cell* (2018) 173(3):611–623.e17. doi: 10.1016/j.cell.2018.02.020
3. Gerlinger M, Rowan AJ, Horswell S, Math M, Larkin J, Endesfelder D, et al. Intratumor Heterogeneity and Branched Evolution Revealed by Multiregion Sequencing. *N Engl J Med* (2012) 366(10):883–92. doi: 10.1056/NEJMoa1113205
4. Bolck HA, Corrò C, Kahraman A, von Teichman A, Toussaint NC, Kuipers J, et al. Tracing Clonal Dynamics Reveals that Two- and Three-dimensional Patient-derived Cell Models Capture Tumor Heterogeneity of Clear Cell Renal Cell Carcinoma. *Eur Urol Focus* (2019) 11. doi: 10.1016/j.euf.2019.06.009
5. Bihr S, Ohashi R, Moore AL, Rüschoff JH, Beisel C, Hermanns T, et al. Expression and Mutation Patterns of PBRM1, BAP1 and SETD2 Mirror Specific Evolutionary Subtypes in Clear Cell Renal Cell Carcinoma. *Neoplasia* (2019) 21(2):247–56. doi: 10.1016/j.neo.2018.12.006
6. Beuselinck B, Verbiest A, Couchy G, Job S, de Reynies A, Meiller C, et al. Pro-angiogenic gene expression is associated with better outcome on sunitinib in metastatic clear-cell renal cell carcinoma. *Acta Oncol* (2018) 57(4):498–508. doi: 10.1080/0284186X.2017.1388927
7. The Cancer Genome Atlas Research Network. Comprehensive molecular characterization of clear cell renal cell carcinoma. *Nature* (2013) 499 (7456):43–9. doi: 10.1038/nature12222
8. Ricketts CJ, Cubas AAD, Fan H, Smith CC, Lang M, Reznik E, et al. The Cancer Genome Atlas Comprehensive Molecular Characterization of Renal Cell Carcinoma. *Cell Rep* (2018) 23(1):313–326.e5. doi: 10.1016/j.celrep.2018.03.075
9. Jones PA, Baylin SB. The epigenomics of cancer. *Cell* (2007) 128(4):683–92. doi: 10.1016/j.cell.2007.01.029
10. Turajlic S, Xu H, Litchfield K, Rowan A, Chambers T, Lopez JI, et al. Tracking Cancer Evolution Reveals Constrained Routes to Metastases: TRACERx Renal. *Cell* (2018) 173(3):581–594.e12. doi: 10.1016/j.cell.2018.03.057
11. Lukamowicz-Rajska M, Mittmann C, Prummer M, Zhong Q, Bedke J, Hennenlotter J, et al. MiR-99b-5p expression and response to tyrosine kinase inhibitor treatment in clear cell renal cell carcinoma patients. *Oncotarget* (2016) 7(48):78433–47. doi: 10.18632/oncotarget.12618
12. Heinzelmann J, Unrein A, Wickmann U, Baumgart S, Stapf M, Szendroi A, et al. MicroRNAs with Prognostic Potential for Metastasis in Clear Cell Renal Cell Carcinoma: A Comparison of Primary Tumors and Distant Metastases. *Ann Surg Oncol* (2014) 21(3):1046–54. doi: 10.1245/s10434-013-3361-3
13. Assi HI, Patenaude F, Toumishey E, Ross L, Abdelsalam M, Reiman T. A simple prognostic model for overall survival in metastatic renal cell carcinoma. *Can Urol Assoc J* (2016) 10(3–4):113–9. doi: 10.5489/cuaj.3351
14. Antonelli A, Cozzoli A, Zani D, Zanotelli T, Nicolai M, Cunico SC, et al. The follow-up management of non-metastatic renal cell carcinoma: definition of a surveillance protocol. *BJU Int* (2007) 99(2):296–300. doi: 10.1111/j.1464-410X.2006.06616.x
15. Escudier B, Porta C, Schmidinger M, Rioux-Leclercq N, Bex A, Khoo V, et al. Renal cell carcinoma: ESMO Clinical Practice Guidelines for diagnosis, treatment and follow-up. *Ann Oncol* (2019) 30(5):706–20. doi: 10.1093/annonc/mdz056
16. Kwapisz D. The first liquid biopsy test approved. Is it a new era of mutation testing for non-small cell lung cancer? *Ann Transl Med* (2017) 5(3):46. doi: 10.21037/atm.2017.01.32
17. Mattox AK, Bettegowda C, Zhou S, Papadopoulos N, Kinzler KW, Vogelstein B. Applications of liquid biopsies for cancer. *Sci Trans Med* (2019) 11(507):3. doi: 10.1126/scitranslmed.aay1984
18. Rijavec E, Coco S, Genova C, Rossi G, Longo L, Grossi F. Liquid Biopsy in Non-Small Cell Lung Cancer: Highlights and Challenges. *Cancers (Basel)* (2019) 12(1):17. doi: 10.3390/cancers12010017
19. Heidrich I, Ačkar L, Mossahebi Mohammadi P, Pantel K. Liquid biopsies: Potential and challenges. *Int J Cancer* (2020). ijc.33217. doi: 10.1002/ijc.33217
20. Gang F, Guorong L, An Z, Anne G-P, Christian G, Jacques T. Prediction of Clear Cell Renal Cell Carcinoma by Integrity of Cell-free DNA in Serum. *Urology* (2010) 75(2):262–5. doi: 10.1016/j.urology.2009.06.048
21. Hauser S, Zahalka T, Ellinger J, Fechner G, Heukamp LC, Ruecker AV, et al. Cell-free Circulating DNA: Diagnostic Value in Patients with Renal Cell Cancer. *Anticancer Res* (2010) 5.
22. Wan J, Zhu L, Jiang Z, Cheng K. Monitoring of Plasma Cell-Free DNA in Predicting Postoperative Recurrence of Clear Cell Renal Cell Carcinoma. *UIN* (2013) 91(3):273–8. doi: 10.1159/000351409
23. Bettegowda C, Sausen M, Leary RJ, Kinde I, Wang Y, Agrawal N, et al. Detection of Circulating Tumor DNA in Early- and Late-Stage Human Malignancies. *Sci Transl Med* (2014) 6(224):224ra24. doi: 10.1158/1538-7445.AM2014-5606
24. Lu H, Busch J, Jung M, Rabenhorst S, Ralla B, Kilic E, et al. Diagnostic and prognostic potential of circulating cell-free genomic and mitochondrial DNA fragments in clear cell renal cell carcinoma patients. *Clin Chim Acta* (2016) 452:109–19. doi: 10.1016/j.cca.2015.11.009
25. Corrò C, Hejhal T, Poyet C, Sulser T, Hermanns T, Winder T, et al. Detecting circulating tumor DNA in renal cancer: An open challenge. *Exp Mol Pathol* (2017) 102(2):255–61. doi: 10.1016/j.yexmp.2017.02.009
26. Maia MC, Bergerot PG, Dizman N, Hsu J, Jones J, Lanman RB, et al. Association of Circulating Tumor DNA (ctDNA) Detection in Metastatic Renal Cell Carcinoma (mRCC) with Tumor Burden. *Kidney Cancer* (2017) 1 (1):65–70. doi: 10.3233/KCA-170007
27. Pal SK, Sonpavde G, Agarwal N, Vogelzang NJ, Srinivas S, Haas NB, et al. Evolution of Circulating Tumor DNA Profile from First-line to Subsequent Therapy in Metastatic Renal Cell Carcinoma. *Eur Urol* (2017) 72(4):557–64. doi: 10.1016/j.eururo.2017.03.046
28. Yamamoto Y, Uemura M, Nakano K, Hayashi Y, Wang C, Ishizuya Y, et al. Increased level and fragmentation of plasma circulating cell-free DNA are diagnostic and prognostic markers for renal cell carcinoma. *Oncotarget* (2018) 9(29):20467–75. doi: 10.18632/oncotarget.24943
29. Smith CG, Moser T, Mouliere F, Field-Rayner J, Eldridge M, Riediger AL, et al. Comprehensive characterization of cell-free tumor DNA in plasma and urine of patients with renal tumors. *Genome Med* (2020) 12(1):23. doi: 10.1186/s13073-020-00723-8
30. Yamamoto Y, Uemura M, Fujita M, Maejima K, Koh Y, Matsushita M, et al. Clinical significance of the mutational landscape and fragmentation of circulating tumor DNA in renal cell carcinoma. *Cancer Sci* (2019) 110 (2):617–28. doi: 10.1111/cas.13906

31. Bacon JVW, Annala M, Soleimani M, Lavoie J-M, So A, Gleave ME, et al. Plasma Circulating Tumor DNA and Clonal Hematopoiesis in Metastatic Renal Cell Carcinoma. *Clin Genitourinary Cancer* (2020) 18(4):322–331.e2. doi: 10.1016/j.clgc.2019.12.018
32. Hu Z-Y, Xie N, Tian C, Yang X, Liu L, Li J, et al. Identifying Circulating Tumor DNA Mutation Profiles in Metastatic Breast Cancer Patients with Multiline Resistance. *EBioMedicine* (2018) 32:111–8. doi: 10.1016/j.ebiom.2018.05.015
33. Reckamp KL, Melnikova VO, Karlovich C, Sequist LV, Camidge DR, Wakelee H, et al. A Highly Sensitive and Quantitative Test Platform for Detection of NSCLC EGFR Mutations in Urine and Plasma. *J Thorac Oncol* (2016) 11 (10):1690–700. doi: 10.1016/j.jtho.2016.05.035
34. Turajlic S, Xu H, Litchfield K, Rowan A, Horswell S, Chambers T, et al. Deterministic Evolutionary Trajectories Influence Primary Tumor Growth: TRACERx Renal. *Cell* (2018) 173(3):595–610.e11. doi: 10.1016/j.cell.2018.03.043
35. Won Y, Song H-J, Kang TW, Kim J-J, Han B-D, Lee S. Pattern analysis of serum proteome distinguishes renal cell carcinoma from other urologic diseases and healthy persons. *Proteomics* (2003) 3(12):2310–6. doi: 10.1002/pmic.200300590
36. Han WK, Alinani A, Wu C-L, Michaelson D, Loda M, McGovern FJ, et al. Human Kidney Injury Molecule-1 Is a Tissue and Urinary Tumor Marker of Renal Cell Carcinoma. *JASN* (2005) 16(4):1126–34. doi: 10.1681/ASN.2004070530
37. Hara T, Honda K, Ono M, Naito K, Hirohashi S, Yamada T. Identification of 2 serum biomarkers of renal cell carcinoma by surface enhanced laser desorption/ionization mass spectrometry. *J Urol* (2005) 174(4 Part 1):1213–7. doi: 10.1097/01.ju.0000173915.83164.87
38. Togashi A, Katagiri T, Ashida S, Fujioka T, Maruyama O, Wakumoto Y, et al. Hypoxia-Inducible Protein 2 (HIG2), a Novel Diagnostic Marker for Renal Cell Carcinoma and Potential Target for Molecular Therapy. *Cancer Res* (2005) 65(11):4817–26. doi: 10.1158/0008-5472.CAN-05-0120
39. Xu G, Hou C-R, Jiang H-W, Xiang C-Q, Shi N, Yuan H-C, et al. Serum protein profiling to identify biomarkers for small renal cell carcinoma. *Indian J Biochem Biophys* (2010) 47(4):211–8.
40. Yang J, Yang J, Gao Y, Zhao L, Liu L, Qin Y, et al. Identification of Potential Serum Proteomic Biomarkers for Clear Cell Renal Cell Carcinoma. *PloS One* (2014) 9(11):e111364 doi: 10.1371/journal.pone.0111364
41. Toiyama D, Takaha N, Shinnoh M, Ueda T, Kimura Y, Nakamura T, et al. Significance of serum tumor necrosis factor-related apoptosis-inducing ligand as a prognostic biomarker for renal cell carcinoma. *Mol Clin Oncol* (2013) 1 (1):69–74. doi: 10.3892/mco.2012.35
42. White NMA, Masui O, DeSouza LV, Krakovska-Yutz O, Metias S, Romaschin AD, et al. Quantitative proteomic analysis reveals potential diagnostic markers and pathways involved in pathogenesis of renal cell carcinoma. *Oncotarget* (2014) 5(2):506–18. doi: 10.18632/oncotarget.1529
43. Ruf M, Mittmann C, Nowicka AM, Hartmann A, Hermanns T, Poyet C, et al. pVHL/HIF-Regulated CD70 Expression Is Associated with Infiltration of CD27+ Lymphocytes and Increased Serum Levels of Soluble CD27 in Clear Cell Renal Cell Carcinoma. *Clin Cancer Res* (2015) 21(4):889–98. doi: 10.1158/1078-0432.CCR-14-1425
44. Zhang Y, Cai Y, Yu H, Li H. iTRAQ-Based Quantitative Proteomic Analysis Identified HSC71 as a Novel Serum Biomarker for Renal Cell Carcinoma. *Bio Med Res Int* (2015) 2015:210–9. doi: 10.1155/2015/802153
45. Lucarini L, Magnelli L, Schiavone N, Crisci A, Innocenti A, Puccetti L, et al. Plasmatic carbonic anhydrase IX as a diagnostic marker for clear cell renal cell carcinoma. *J Enzyme Inhib Med Chem* (2017) 33(1):234–40. doi: 10.1080/14756366.2017.1411350
46. Knott ME, Manzi M, Zabalegui N, Salazar MO, Puricelli LI, Monge ME. Metabolic Footprinting of a Clear Cell Renal Cell Carcinoma in Vitro Model for Human Kidney Cancer Detection. *J Proteome Res* (2018) 17(11):3877–88. doi: 10.1021/acs.jproteome.8b00538
47. Kushlinskii NE, Gershtein ES, Naberezhnov DS, Taipov MA, Bezhanova SD, Pushkar' D, et al. Kidney Injury Molecule-1 (KIM-1) in Blood Plasma of Patients with Clear-Cell Carcinoma. *Bull Exp Biol Med* (2019) 167(3):388–92. doi: 10.1007/s10517-019-04533-w
48. Tschirdewahn S, Panic A, Püllen L, Harke NN, Hadaschik B, Riesz P, et al. Circulating and tissue IMP3 levels are correlated with poor survival in renal cell carcinoma. *Int J Cancer* (2019) 145(2):531–9. doi: 10.1002/ijc.32124
49. Scelo G, Muller DC, Riboli E, Johansson M, Cross AJ, Vineis P, et al. KIM-1 as a blood-based marker for early detection of kidney cancer: a prospective nested case-control study. *Clin Cancer Res* (2018) 24(22):5594–601. doi: 10.1158/1078-0432.CCR-18-1496
50. Wang Q, Zhang J, Tu H, Liang D, Chang DW, Ye Y, et al. Soluble immune checkpoint-related proteins as predictors of tumor recurrence, survival, and T cell phenotypes in clear cell renal cell carcinoma patients. *J Immunother Cancer* (2019) 7:9. doi: 10.1186/s40425-019-0810-y
51. Zhang M, Liu X, Liu X, Li H, Sun W, Zhang Y. A pilot investigation of a urinary metabolic biomarker discovery in renal cell carcinoma. *Int Urol Nephrol* (2020) 52(3):437–46. doi: 10.1007/s11255-019-02332-w
52. Clark DJ, Zhang H. Proteomic approaches for characterizing renal cell carcinoma. *Clin Proteom* (2020) 17(1):28. doi: 10.1186/s12014-020-09291-w
53. Song J, Yu J, Prayogo GW, Cao W, Wu Y, Jia Z, et al. Understanding kidney injury molecule 1: a novel immune factor in kidney pathophysiology. *Am J Transl Res* (2019) 11(3):1219–29.
54. Nixon AB, Schalper KA, Jacobs I, Potluri S, Wang I-M, Fleener C. Peripheral immune-based biomarkers in cancer immunotherapy: can we realize their predictive potential? *J Immuno Ther Cancer* (2019) 7(1):325. doi: 10.1186/s40425-019-0799-2
55. Arroyo JD, Chevillet JR, Kroh EM, Ruf IK, Pritchard CC, Gibson DF, et al. Argonaute2 complexes carry a population of circulating microRNAs independent of vesicles in human plasma. *Proc Natl Acad Sci USA* (2011) 108(12):5003–8. doi: 10.1073/pnas.1019055108
56. Vickers KC, Palmisano BT, Shoucri BM, Shamburek RD, Remaley AT. MicroRNAs are transported in plasma and delivered to recipient cells by high-density lipoproteins. *Nat Cell Biol* (2011) 13(4):423–33. doi: 10.1038/ncb2210
57. Wang K, Zhang S, Weber J, Baxter D, Galas DJ. Export of microRNAs and microRNA-protective protein by mammalian cells. *Nucleic Acids Res* (2010) 38(20):7248–59. doi: 10.1093/nar/gkq601
58. Zhao A, Li G, Péoc'h M, Genin C, Gigante M. Serum miR-210 as a novel biomarker for molecular diagnosis of clear cell renal cell carcinoma. *Exp Mol Pathol* (2013) 94(1):115–20. doi: 10.1016/j.yexmp.2012.10.005
59. Teixeira AL, Ferreira M, Silva J, Gomes M, Dias F, Santos JI, et al. Higher circulating expression levels of miR-221 associated with poor overall survival in renal cell carcinoma patients. *Tumor Biol* (2014) 35(5):4057–66. doi: 10.1007/s13277-013-1531-3
60. Wu Y, Wang Y-Q, Weng W-W, Zhang Q-Y, Yang X-Q, Gan H-L, et al. A serum-circulating long noncoding RNA signature can discriminate between patients with clear cell renal cell carcinoma and healthy controls. *Oncogenesis* (2016) 5(2):e192. doi: 10.1038/oncsis.2015.48
61. Li G, Zhao A, Péoch M, Cottier M, Mottet N. Detection of urinary cell-free miR-210 as a potential tool of liquid biopsy for clear cell renal cell carcinoma. *Urol Oncol: Semin Orig Invest* (2017) 35(5):294–9. doi: 10.1016/j.urolonc.2016.12.007
62. Petrozza V, Pastore AL, Palleschi G, Tito C, Porta N, Ricci S, et al. Secreted miR-210-3p as non-invasive biomarker in clear cell renal cell carcinoma. *Oncotarget* (2017) 8(41):69551–8. doi: 10.18632/oncotarget.18449
63. Heinemann FG, Tolkach Y, Deng M, Schmidt D, Perner S, Kristiansen G, et al. Serum miR-122-5p and miR-206 expression: non-invasive prognostic biomarkers for renal cell carcinoma. *Clin Epigenet* (2018) 10:11. doi: 10.1186/s13148-018-0444-9
64. Liu S, Deng X, Zhang J. Identification of dysregulated serum miR-508-3p and miR-885-5p as potential diagnostic biomarkers of clear cell renal carcinoma. *Mol Med Rep* (2019) 20(6):5075–83. doi: 10.3892/mmr.2019.10762
65. Simonovic S, Hinze C, Schmidt-Ott KM, Busch J, Jung M, Jung K, et al. Limited utility of qPCR-based detection of tumor-specific circulating mRNAs in whole blood from clear cell renal cell carcinoma patients. *BMC Urol* (2020) 20:7. doi: 10.1186/s12894-019-0542-9
66. Raimondo F, Morosi L, Corbetta S, Chinello C, Brambilla P, Mina PD, et al. Differential protein profiling of renal cell carcinoma urinary exosomes. *Mol Biosyst* (2013) 9(6):1220–33. doi: 10.1039/c3mb25582d
67. Butz H, Nofech-Mozes R, Ding Q, Khella HWZ, Szabó PM, Jewett M, et al. Exosomal MicroRNAs Are Diagnostic Biomarkers and Can Mediate Cell–Cell Communication in Renal Cell Carcinoma. *Eur Urol Focus* (2016) 2(2):210–8. doi: 10.1016/j.euf.2015.11.006
68. Qu L, Ding J, Chen C, Wu Z-J, Liu B, Gao Y, et al. Exosome-Transmitted lncARSR Promotes Sunitinib Resistance in Renal Cancer by Acting as a

Competing Endogenous RNA. *Cancer Cell* (2016) 29(5):653–68. doi: 10.1016/j.ccell.2016.03.004
69. Du M, Giridhar KV, Tian Y, Tschannen MR, Zhu J, Huang C-C, et al. Plasma exosomal miRNAs-based prognosis in metastatic kidney cancer. *Oncotarget* (2017) 8(38):63703–14. doi: 10.18632/oncotarget.19476
70. Jingushi K, Uemura M, Ohnishi N, Nakata W, Fujita K, Naito T, et al. Extracellular vesicles isolated from human renal cell carcinoma tissues disrupt vascular endothelial cell morphology via azurocidin. *Int J Cancer* (2018) 142 (3):607–17. doi: 10.1002/ijc.31080
71. Zhang W, Ni M, Su Y, Wang H, Zhu S, Zhao A, et al. MicroRNAs in Serum Exosomes as Potential Biomarkers in Clear-cell Renal Cell Carcinoma. *Eur Urol Focus* (2018) 4(3):412–9. doi: 10.1016/j.euf.2016.09.007
72. White NMA, Khella HWZ, Grigull J, Adzovic S, Youssef YM, Honey RJ, et al. miRNA profiling in metastatic renal cell carcinoma reveals a tumour-suppressor effect for miR-215. *Br J Cancer* (2011) 105(11):1741–9. doi: 10.1038/bjc.2011.401
73. Hsiao K-Y, Sun HS, Tsai S-J. Circular RNA - New member of noncoding RNA with novel functions. *Exp Biol Med (Maywood)* (2017) 242(11):1136–41. doi: 10.1177/1535370217708978
74. Miranda KC, Bond DT, Levin JZ, Adiconis X, Sivachenko A, Russ C, et al. Massively parallel sequencing of human urinary exosome/microvesicle RNA reveals a predominance of non-coding RNA. *PloS One* (2014) 9(5):e96094. doi: 10.1371/journal.pone.0096094
75. Alimirzaie S, Bagherzadeh M, Akbari MR. Liquid biopsy in breast cancer: A comprehensive review. *Clin Genet* (2019) 95(6):643–60. doi: 10.1111/cge.13514
76. Norcic G. Liquid Biopsy in Colorectal Cancer-Current Status and Potential Clinical Applications. *Micromachines (Basel)* (2018) 9(6):300. doi: 10.3390/mi9060300
77. Santarpia M, Liguori A, D'Aveni A, Karachaliou N, Gonzalez-Cao M, Daffinà MG, et al. Liquid biopsy for lung cancer early detection. *J Thorac Dis* (2018) 10 (Suppl 7):S882–97. doi: 10.21037/jtd.2018.03.81
78. Merker JD, Oxnard GR, Compton C, Diehn M, Hurley P, Lazar AJ, et al. Circulating Tumor DNA Analysis in Patients With Cancer: American Society of Clinical Oncology and College of American Pathologists Joint Review. *JCO* (2018) 36(16):1631–41. doi: 10.1200/JCO.2017.76.8671
79. Lasseter K, Nassar AH, Hamieh L, Berchuck JE, Nuzzo PV, Korthauer K, et al. Plasma cell-free DNA variant analysis compared with methylated DNA analysis in renal cell carcinoma. *Genet Med* (2020) 22:1366–73. doi: 10.1038/s41436-020-0801-x
80. Zviran A, Schulman RC, Shah M, Hill STK, Deochand S, Khamnei CC, et al. Genome-wide cell-free DNA mutational integration enables ultra-sensitive cancer monitoring. *Nat Med* (2020) 26:1114–24. doi: 10.1038/s41591-020-0915-3
81. Nuzzo PV, Berchuck JE, Spisak S, Korthauer K, Nassar A, Abou Alaiwi S, et al. Sensitive detection of renal cell carcinoma using plasma and urine cell-free DNA methylomes. *JCO* (2020) 38(6_suppl):728–8. doi: 10.1200/JCO.2020.38.6_suppl.728
82. Sadeh R, Fialkoff G, Sharkia I, Rahat A, Nitzan M, Fox-Fisher I, et al. ChIP-seq of plasma cell-free nucleosomes identifies cell-of-origin gene expression programs. *Mol Biol* (2019) doi: 10.1101/638643
83. Snyder MW, Kircher M, Hill AJ, Daza RM, Shendure J. Cell-free DNA comprises an in vivo nucleosome footprint that informs its tissues-of-origin. *Cell* (2016) 164(0):57–68. doi: 10.1016/j.cell.2015.11.050
84. Bache N, Geyer PE, Bekker-Jensen DB, Hoerning O, Falkenby L, Treit PV, et al. A Novel LC System Embeds Analytes in Pre-formed Gradients for Rapid, Ultra-robust Proteomics. *Mol Cell Proteom* (2018) 17(11):2284–96. doi: 10.1074/mcp.TIR118.000853
85. Bruderer R, Muntel J, Müller S, Bernhardt OM, Gandhi T, Cominetti O, et al. Analysis of 1508 Plasma Samples by Capillary-Flow Data-Independent Acquisition Profiles Proteomics of Weight Loss and Maintenance. *Mol Cell Proteom* (2019) 18(6):1242–54. doi: 10.1074/mcp.RA118.001288
86. Chinello C, Stella M, Piga I, Smith AJ, Bovo G, Varallo M, et al. Proteomics of liquid biopsies: Depicting RCC infiltration into the renal vein by MS analysis of urine and plasma. *J Proteom* (2019) 191:29–37. doi: 10.1016/j.jprot.2018.04.029
87. Franz A, Ralla B, Weickmann S, Jung M, Rochow H, Stephan C, et al. Circular RNAs in Clear Cell Renal Cell Carcinoma: Their Microarray-Based Identification, Analytical Validation, and Potential Use in a Clinico-Genomic Model to Improve Prognostic Accuracy. *Cancers (Basel)* (2019) 11 (10):1473. doi: 10.3390/cancers11101473
88. Wang K, Sun Y, Tao W, Fei X, Chang C. Androgen receptor (AR) promotes clear cell renal cell carcinoma (ccRCC) migration and invasion via altering the circHIAT1/miR-195-5p/29a-3p/29c-3p/CDC42 signals. *Cancer Lett* (2017) 394:1–12. doi: 10.1016/j.canlet.2017.03.039
89. Ma H, Xu Y, Zhang R, Guo B, Zhang S, Zhang X. Differential expression study of circular RNAs in exosomes from serum and urine in patients with idiopathic membranous nephropathy. *Arch Med Sci* (2019) 15(3):738–53. doi: 10.5114/aoms.2019.84690
90. Stranska R, Gysbrechts L, Wouters J, Vermeersch P, Bloch K, Dierickx D, et al. Comparison of membrane affinity-based method with size-exclusion chromatography for isolation of exosome-like vesicles from human plasma. *J Transl Med* (2018) 16:1–9. doi: 10.1186/s12967-017-1374-6
91. Iliuk A, Wu X, Li L, Sun J, Hadisurya M, Boris RS, et al. Plasma-derived EV Phosphoproteomics through Chemical Affinity Purification. *J Proteome Res* (2020) 19(7):2563–74. doi: 10.1021/acs.jproteome.0c00151
92. Qiu J, Xu J, Zhang K, Gu W, Nie L, Wang G, et al. Refining Cancer Management Using Integrated Liquid Biopsy. *Theranostics* (2020) 10 (5):2374–84. doi: 10.7150/thno.40677

Conflict of Interest: The authors declare that the research was conducted in the absence of any commercial or financial relationships that could be construed as a potential conflict of interest.

frontiers in Oncology

ORIGINAL RESEARCH
published: 15 January 2021
doi: 10.3389/fonc.2020.607840

Detection of Low-Frequency *KRAS* Mutations in cfDNA From *EGFR*-Mutated NSCLC Patients After First-Line EGFR Tyrosine Kinase Inhibitors

Giorgia Nardo[1], *Jessica Carlet*[2], *Ludovica Marra*[2], *Laura Bonanno*[2], *Alice Boscolo*[3], *Alessandro Dal Maso*[3], *Andrea Boscolo Bragadin*[3], *Stefano Indraccolo*[1*†] *and Elisabetta Zulato*[1†]

[1] Immunology and Molecular Oncology Unit, Istituto Oncologico Veneto IOV - IRCCS, Padova, Italy, [2] Medical Oncology 2, Istituto Oncologico Veneto IOV - IRCCS, Padova, Italy, [3] Department of Surgery, Oncology and Gastroenterology, University of Padua, Padova, Italy

OPEN ACCESS

Edited by:
Francesco Fabbri,
Romagnolo Scientific Institute for the Study and Treatment of Tumors (IRCCS), Italy

Reviewed by:
Vienna Ludovini,
Hospital of Santa Maria della Misericordia in Perugia, Italy
Marcello Tiseo,
University Hospital of Parma, Italy

***Correspondence:**
Stefano Indraccolo
stefano.indraccolo@unipd.it

†These authors have contributed equally to this work

Specialty section:
This article was submitted to Cancer Molecular Targets and Therapeutics, a section of the journal Frontiers in Oncology

Received: 18 September 2020
Accepted: 30 November 2020
Published: 15 January 2021

Citation:
Nardo G, Carlet J, Marra L, Bonanno L, Boscolo A, Dal Maso A, Boscolo Bragadin A, Indraccolo S and Zulato E (2021) Detection of Low-Frequency KRAS Mutations in cfDNA From EGFR-Mutated NSCLC Patients After First-Line EGFR Tyrosine Kinase Inhibitors. Front. Oncol. 10:607840. doi: 10.3389/fonc.2020.607840

Background: Molecular profiling of advanced *EGFR* mutated NSCLC has recently demonstrated the co-existence of multiple genetic alterations. Specifically, co-existing *KRAS*-mutations in *EGFR* NSCLCs have been described, despite their prevalence at progression and their role in the response to *EGFR* tyrosine kinase inhibitors (TKIs) remain marginally explored. Aim of our study was to investigate the prevalence of co-existing *KRAS* mutations at the time of progressive disease and explore their impact on clinical outcome.

Materials and Methods: We retrospectively analyzed by digital droplet PCR prevalence of *KRAS* co-mutations in 106 plasma samples of *EGFR* mutated NSCLC patients, in progressive disease after *EGFR* TKI treatment as first-line therapy.

Results: *KRAS* co-mutations (codon 12 and 13) were identified in 3 patients (2.8% of analyzed samples), with low allelic frequency (<0.2%), and had a negative impact on clinical outcome to first-line *EGFR* TKI.

Conclusion: Detection of *KRAS* mutations in cell-free DNA of *EGFR* mutant NSCLC patients at progression after first or second generation *EGFR* TKI is a rare event. Due to their low abundance, the negative impact of *KRAS* mutations on the response to *EGFR* TKI remains to be confirmed in larger studies.

Keywords: *KRAS*, *EGFR*, liquid biopsy, non-small-cell lung cancer, cell free DNA, tyrosine kinase inhibitors

INTRODUCTION

Non-small-cell lung cancer (NSCLC) is the leading cause of cancer-related mortality worldwide with five-year survival rate less than 10% among patients with advanced disease (1). Activating mutations in the epidermal growth factor receptor (*EGFR*) gene occur as early cancer-driving clonal event (2) in a subset of NSCLC patients (approximately 15% of Caucasian patients) and predict sensitivity to *EGFR* tyrosine kinase inhibitors (TKIs) (3). Improvement in clinical outcome, in terms of objective response rate (ORR), progression-free survival (PFS) and overall survival (OS),

compared with upfront platinum doublet chemotherapy, made TKIs standard of care for advanced stage *EGFR* mutant NSCLC (4–8). However, resistance invariably develops, with EGFR T790M mutation accounting for approximately 50–60% of the mechanisms of acquired resistance to first- or second-generation *EGFR*-TKI therapy (3). Other less common *EGFR*- independent mechanisms of resistance include activation of bypassing pathways and histologic transformation to small-cell lung cancer (10–15% of cases) (9–11). In addition, 20–30% of patients do not show response on *EGFR* TKI treatment, probably due to intrinsic mechanisms of resistance (12).

Recently, comprehensive molecular-pathological profiling of advanced *EGFR* mutated NSCLC prior to therapy demonstrated co-existence of multiple genetic alterations (13). Consequently, the question arises as to whether co-occurring genetic alterations cooperate with the primary driver *EGFR* gene in promoting tumor progression and limiting efficacy of target therapy. Recent studies showed that co-mutations in the *TP53* gene are a negative predictive factor of response to *EGFR*-TKI and an independent prognostic factor of shorter survival in advanced *EGFR* mutant NSCLC (14–17). Moreover, co-existing *KRAS*-mutations in *EGFR* NSCLCs have been reported by several studies (18–23). However, their prevalence at progression and their role in the response to TKIs treatment has been investigated only in one study including a small number of patients (n=33) (24).

Here, we performed a retrospective analysis of *KRAS* co-genetic alterations in 106 *EGFR* mutated NSCLC patients with progressive disease after *EGFR* TKI first-line therapy. We quantitated *KRAS* mutation in plasma samples by droplet digital PCR (ddPCR), with the aim to investigate the prevalence of co-existing *KRAS* mutations at the time of progression and explore their impact on clinical outcome.

MATERIAL AND METHODS

Study Design and Patient Population

The primary aim of this study was to assess the prevalence of *KRAS* co-mutations in *EGFR* mutated NSCLC patients, in progressive disease after *EGFR* TKI treatment as first-line therapy. For this purpose, we retrospectively selected 122 consecutive patients with *EGFR*-mutated NSCLC with progressive disease after first-line TKI treatment, referring to our Institution from 2016 to 2019. Eligibility criteria were confirmed histological diagnosis of advanced NSCLC, presence of an *EGFR* exon 18 to 21 mutation at diagnosis, progression to front line systemic treatment with first- or second-generation *EGFR* TKIs (erlotinib, gefitinib, or afatinib), and available liquid biopsy material collected at progressive disease, and clinical follow-up. Patients who did not progress to first-line *EGFR* TKIs, or without available liquid biopsy material after progression were excluded.

At the time of diagnosis, tissue molecular analyses of *EGFR* gene exons 18 to 21 were performed according to standard clinical practice, and *KRAS* mutational status was not routinely examined because mutually exclusive with activating *EGFR* mutations in this patient population.

At progressive disease, plasma samples were collected for liquid biopsy to assess the T790M mutational status in cell-free (cf)-DNA. Molecular analyses were performed according to standard lab practice, using the CE IVD cobas® EGFR Mutation Test v2.

The studies involving human participants were reviewed and approved by IOV Institutional Review Board and Ethics Committee (CESC IOV 2020/57), and were performed in accordance with the declaration of Helsinki. The patients/participants provided their written informed consent to participate in this study. For patients who were dead or lost to follow-up at the time of study enrolment, we used the Italian Data Protection Authority Authorisation 9/2016 on "privacy protective rules for recording clinical data for research and study purposes".

Cell Free DNA (cfDNA) Extraction and Analysis

Residual plasma collected at the time of progression for routine diagnostic activity was used: cfDNA was extracted from 1–2 ml of plasma using the Maxwell® RSC ccfDNA Plasma Kit (Promega, Madison, Wisconsin, USA), and eluted into 60 µl of buffer, according to manufacturer's instructions. cfDNA was quantified using the QuBit dsDNA HS Assay kit with QuBit 3.0 fluorimeter (Thermo Fisher Scientific, San Jose, CA), and stored at −20°C before use.

Detection of *KRAS* mutations in codons 12 and 13 in cfDNA was performed by droplet digital PCR (ddPCR), as previously described (25). The ddPCR assay was purchased from Bio-Rad (the ddPCR *KRAS* G12/G13 Screening Kit #186-3506), and it does not enable to distinguish among different mutations in *KRAS* codon G12/G13 (G12A, G12C, G12D, G12R, G12S, G12V, G13D). Each sample was analyzed in triplicate and in each test at least three control wells with a negative *KRAS* cfDNA, one negative control well without DNA and one positive control were included. In line with our previous study (25) and as reported in the manufacturer's instructions, a cut-off of three droplets was used to call a sample mutant, according to the Poisson's law of small numbers. The sensitivity of our assay to detect *KRAS* mutation in plasma samples was 48% (25).

Data Analysis

Progression free survival (PFS) was calculated as the time between the first day of treatment and the radiologic and/or clinical evidence of progression; time to treatment failure (TTF) was defined as the time from the first day of *EGFR*-TKI administration to the date of treatment failure; overall survival (OS) was measured as the time elapsed from diagnosis to death for any cause. Patients who did not develop an event during the study period were censored at the date of last observation. Median PFS, TTF and OS were estimated using the Kaplan–Meier method.

Chi-square test was used to evaluate whether the frequency of cases with single or double *KRAS* positive droplets differ among *EGFR* mutant and *EGFR* wild-type cfDNA samples.

RESULTS

Patients

Study layout is summarized in **Figure 1**. From 2016 to 2019, 122 patients with advanced *EGFR* mutated NSCLC referring to our Institution received treatment with a first- or second -*EGFR*-TKI as first-line therapy and underwent cfDNA genotyping for assessment of *EGFR* mutations at progression. Residual plasma samples were available for 106 patients. Clinical characteristics of patients matching the eligibility criteria are shown in **Table 1**. At the time of diagnosis, median age was 68 years. Most patients were females (59%), with *EGFR* mutant stage III–IV lung adenocarcinoma (90.5%) and without smoking history (62%). Patients presented in an optimal or good Eastern Cooperative Oncology Group (ECOG) performance status (PS), with 46 (43%) and 55 (52%) having ECOG 0 and 1, respectively. *EGFR* exon 19 deletion was carried by 64 out of 106 patients (60%); 35 patients (33%) had an EGFR p.L858R point mutation and 7 (7%) had different *EGFR* mutations. The majority of patients (n=54) received gefitinib as first-line TKI treatment (51%), 26 out of 106 (24.5%) patients received erlotinib, and 26 (24.5%) afatinib (**Table 1**). Median Progression Free Survival (PFS) was 24.30 months (95%, CI: 19.29–29.31).

At the time of progressive disease, *EGFR* sensitizing mutations were detected by liquid biopsy in 68 out of 106 plasma samples tested (64%), whereas the remaining 38 plasma samples (36%) did not bear *EGFR* mutations (**Table 2**). The T790M-resistance mutation was found in 35 out of 106 samples (33%), or 35 out of 68 plasma samples bearing *EGFR* sensitizing mutations (50.7%) (**Table 2**).

TABLE 1 | Clinical features of patients at time of diagnosis.

Age at diagnosis (years)	Median (Q1–Q3)	68 (35–85)
Gender	Male	43 (41%)
	Female	63 (59%)
Smoking	No	66 (62%)
	Yes	7 (7%)
	Ex	28 (26%)
	nd	5 (5%)
PS	0	46 (43%)
	1	55 (52%)
	2	3 (3%)
	nd	2 (2)
Stage at diagnosis	I–II	10 (9.5%)
	III–IV	90 (90.5%)
Baseline EGFR mutation status	Exon 19 deletion	64 (60%)
	Ex 21 mutations (L858R)	35 (33%)
	Others	7 (7%)
Type of treatment	Gefitinib	54 (51%)
	Erlotinib	26 (24.5%)
	Afatinib	26 (24.5%)
Best response to TKI	CR	1 (1%)
	PR	71 (67%)
	SD	18 (17%)
	PD	11 (10%)
	nd	5 (5%)
T790M status at progressive disease	T790M positive	35 (33%)
	T790M negative	71 (67%)
PFS (months)	Mean (CI 95%)	24.30 (19.29–29.31)
TTF (months)	Mean (CI 95%)	41.44 (29.45–53.39)
OS (months)	Mean (CI 95%)	67.98 (51.07–84.89)
Total		**106**

nd, no determined.

Prevalence of *KRAS* Co-Mutations at Progressive Disease

Among 106 patients with plasma samples available, 104 were successfully screened by ddPCR for the presence of concomitant *KRAS* mutation in codon 12 and 13, whereas 2 samples were not evaluable (**Figure 1**).

Considering the standard cut-off value of three droplets, as detailed in the *Materials and Methods* section, *KRAS* mutations were detected in 3 patients (2.8%) (**Figure 1**). Tumor tissue collected at diagnosis was available only for one (ID#88) out of 3 *KRAS* positive patients, and its analysis confirmed the

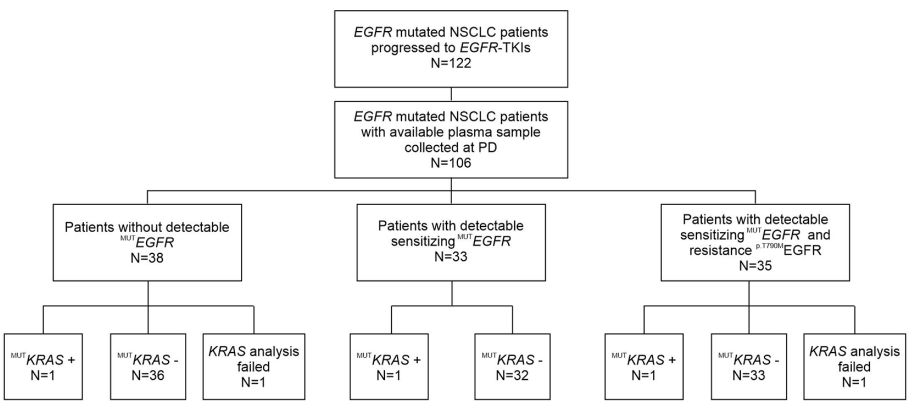

FIGURE 1 | Flow chart of patients enrolled in this study, who progressed after front-line first- or second-generation *EGFR*-TKI treatment and underwent liquid biopsy to assess the T790M mutational status.

co-existence of *EGFR* and *KRAS* mutations (*KRAS* allelic frequency 13.8%). In all 3 positive cases, the allelic frequency of the *KRAS* mutations in the liquid biopsy samples was low (<0.2%) (**Table 3**). All *KRAS* positive patients (n=3) had poor clinical outcome to first-line *EGFR* TKI, in terms of TTF, PFS and OS (**Figure 2; Table 3**). Interestingly, these patients were current or former smoker and one of them had squamous cell carcinoma histology. At diagnosis they all presented with extra-thoracic disease, but they did not show any specific clinical negative prognostic marker (i.e. worse performance status; see **Table 3**). Two of them did not respond to first line *EGFR* TKI, while one of them achieved partial response with a PFS of about six months. At progression to first line TKI, only one of them carried T790M mutation (ID#39), but he did not respond to osimertinib.

Interestingly, one or two positive droplets for *KRAS* mutations were detected in additional 28 plasma samples out of 104 analyzed (27%), with allelic frequency of the *KRAS* variant very low (mean 0.15%; median 0.12%) and ranging between 0.016 and 0.32% (**Table 4**). These single or double *KRAS* positive droplets were similarly distributed among *EGFR* mutant and *EGFR* wild-type cfDNA samples (15 out of 68 *EGFR* mutant versus 13 out of 38 *EGFR* wild-type samples, respectively. Chi-square test, P=0.21). With regard to clinical correlates, patients with borderline *KRAS* positivity (n=28) behave similarly to *KRAS* negative patients (n=73) in terms of TTF, PFS, and OS (**Figure 2**). Details about median TTF, PFS and OS in *KRAS* positive, borderline and negative patients are reported in **Table 5**.

We conclude that frank positivity for codon 12 and 13 *KRAS* mutations in cfDNA of *EGFR* mutant NSCLC at progression after first or second generation *EGFR* TKI treatment is a rare event.

DISCUSSION

We report a retrospective evaluation of the prevalence of codon 12 and 13 *KRAS* co-mutations in *EGFR* mutated NSCLC patients in progressive disease after *EGFR* TKI treatment as first-line therapy, with the aim to establish their prevalence and explore their impact on clinical outcome. Mutations in *EGFR* and *KRAS* are considered mutually exclusive in NSCLC (26) and this is also remarked by epidemiologic data, being *KRAS* mutations associated with smoke and *EGFR* mutations more common in non-smokers, respectively. On the other hand, genetic studies involving multi-region sequencing of tumors have clearly shown that genetic heterogeneity exists in lung adenocarcinoma and *EGFR* mutations generally occur in the genetic trunk of the tumor and are hence clonal, whereas *KRAS* mutations are often sub-clonal (2). This genetic model is also supported by studies which investigated *EGFR* and *KRAS* mutations in matched primary tumor and metastasis from the same patients and reported the occasional presence of *KRAS* mutations in metastatic lesions from *EGFR* mutant primary tumors (27). Moreover, up to 8–15% NSCLC are diagnosed with multiple lung nodules and can disclose extensive inter-tumor genetic variation in the same patient (28, 29).

In line with these arguments, previous studies investigated and found pathogenic *KRAS* mutations in *EGFR* mutant NSCLC at diagnosis (18–23, 30–32). Percentages of *KRAS* mutation vary widely among studies (range 1.2–10.5%), depending on the broadly different size of the study population (ranging from 58 to 6637 samples), the various analytical sensitivity of the techniques utilized (Sanger, RT-PCR, NGS, ddPCR) and the type of sample analyzed (tissue or cfDNA). Concomitant *KRAS* mutations often involve canonical codon 12 and 13 mutational

TABLE 2 | *EGFR* mutational status.

Diagnosis*	n° (%)	Progressive Disease**	n° (%)
Exon 19 deletion	64 (60 %)	No detectable mutations	19 (29.7 %)
		Exon 19 deletion +	19 (29.7 %)
		Exon 19 deletion + and T790M +	26 (40.6 %)
Exon 21 mutation (L858R)	35 (33 %)	No detectable mutations	13 (37.1 %)
		Exon 21 mutation +	13 (37.1 %)
		Exon 21 mutation + and T790M +	9 (25.8 %)
Other mutations	7 (7 %)	No detectable mutations	6 (85.7 %)
		EGFR-sensitizing mutation +	1 (14.3 %)
		Mutation + and T790M +	0 (0 %)

**Tissue (FFPE); **cfDNA.*

TABLE 3 | *EGFR* and *KRAS* co-mutated cases.

Patients ID	Diagnosis - Sensitizing ^{MUT}*EGFR*	Progression Disease - ^{MUT}*EGFR* in liquid biopsy	*KRAS* n° of positive droplets (MAFA)	Age at diagnosis (years)	Smoking	PS	Stage at Diagnosis	PFS (months)	TTF (months)	OS (months)
88	L858R	no mutation	4 (0.11%)	77	yes	1	IV	2	4	4
13	ex19 del	ex19 del	3 (0.11%)	65	ex	1	IV	5	6	18
39	ex19 del	ex19del-T790M	3 (0.036%)	71	yes	0	IV	5	5	6

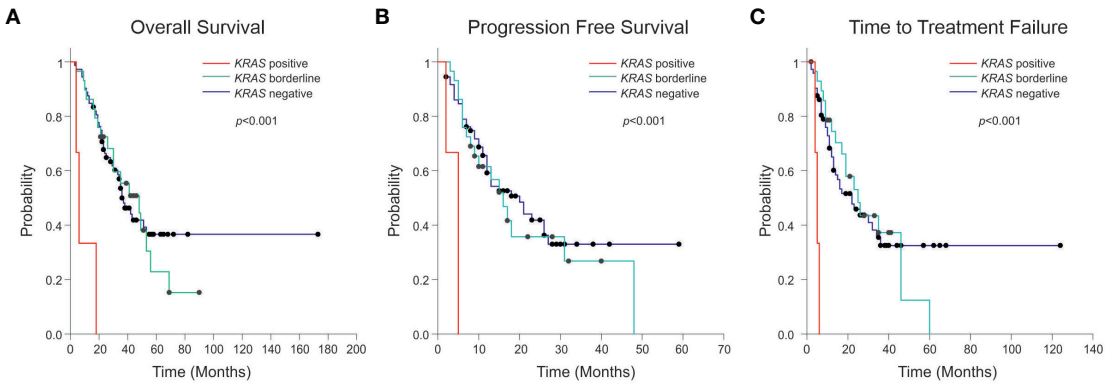

FIGURE 2 | Kaplan-Meier curves showing Overall Survival (OS) **(A)**, Progression Free Survival (PFS) **(B)** and Time to Treatment Failure (TTF) **(C)** according to the presence, the absence, or borderline positivity (1–2 positive droplets) of *KRAS* mutation. The *p*-value related to the presence or the absence of *KRAS* mutation is reported in figure.

TABLE 4 | *KRAS* borderline samples with one or two positive droplets in cfDNA.

Patient ID	Diagnosis-Sensitizing ^{MUT}*EGFR*	Progression Disease - ^{MUT}*EGFR* in liquid biopsy	*KRAS* n° of positive droplets (MAFA)	Age at diagnosis (years)	Smoking	PS	Stage at Diagnosis	PFS (months)	TTF (months)	OS (months)
16	L858R	no mutation	1 (0.12%)	72	no	1	IV	11	21	21
20	ex19 del	no mutation	2 (0.32%)	73	no	0	IV	28	33	39
54	ex19 del	no mutation	1 (0.10%)	85	\	1	IVb	48	60	69
56	L858R	no mutation	1 (0.10%)	49	no	0	IVb	3	9	9
57	G719	no mutation	1 (0.30%)	63	ex	0	Ib	10	19	53
78	ex19 del	no mutation	1 (0.19%)	71	\	0	IVa	31	46	48
81	ex19 del	no mutation	1 (0.22%)	72	no	0	IVa	13	35	49
92	ex19 del	no mutation	1 (0.30%)	75	ex	0	IV	40	41	51
3	ex19 del	ex19 del	1 (0.24%)	80	no	1	IV	32	40	46
9	ex19 del	ex19 del	2 (0.06%)	67	ex	2	IV	5	8	10
23	ex19 del	ex19 del	1 (0.25%)	60	no	0	IV	8	11	23
29	ex19 del	ex19 del	1 (0.07%)	63	ex	0	IV	9	14	19
33	ex19 del	ex19 del	1 (0.31%)	56	no	1	IV	4	4	4
45	ex19 del	ex19 del	1 (0.07%)	64	no	1	IV	15	17	21
52	ex19 del	ex19 del	1 (0.11%)	67	no	1	IVb	5	5	11
91	ex19 del	ex19 del	1 (0.15%)	55	\	0	Ia	16	46	56
102	ex19 del	ex19 del	1 (0.18%)	68	no	1	IV	9	10	22
48	L858R	L858R	1 (0.29%)	79	no	1	IV	17	25	26
76	L858R	L858R	2 (0.07%)	54	no	1	IIIb	18	19	30
44	L858R	L858R - S768I	1 (0.016%)	44	no	0	Ib	7	9	17
19	ex19 del	ex19 del - T790M	1 (0.03%)	68	yes	0	Iib	10	10	42
27	ex19 del	ex19 del - T790M	1 (0.12%)	37	no	0	IV	10	35	90
30	ex19 del	ex19 del - T790M	1 (0.22%)	51	no		IV	6	23	35
41	ex19 del	ex19 del - T790M	2 (0.24%)	64	ex	0	IV	15	2	44
43	ex19 del	ex19 del - T790M	1 (0.07%)	66	no	1	IV	8	12	30
49	ex19 del	ex19 del - T790M	1 (0.21%)	82	ex	0	IV	22	28	69
60	ex19 del	ex19 del - T790M	1 (0.20%)	60	no	1	IIIa	6	26	41
36	L858R	L858R - T790M	1 (0.16%)	71	no	1	IV	6	7	16

TABLE 5 | Overall Survival (OS), Progression Free Survival (PFS) and Time to Treatment Failure (TTF) in *KRAS* negative, borderline and positive patients at Progressive Disease (PD).

KRAS	**N°**	**mOS (m)**	**CI95% (m)**	**P-value**
Negative	75	36	28.5-43.5	
Borderline	28	48	23.2-72.8	<0.001
Positive	3	6	2.8-9-2	
KRAS	**N°**	**mPFS (m)**	**CI95% (m)**	**P-value**
Negative	75	20	12-6-27-4	
Borderline	28	16	10-2-21-8	<0.001
Positive	3	5	5-0-5-0	
KRAS	**N°**	**mTTF (m)**	**CI95% (m)**	**P-value**
Negative	75	22	11-5-32-5	
Borderline	28	25	14-9-35-1	<0.001
Positive	3	5	3.4-6.6	

mOS, median Overall Survival; mPFS, median Progression Free Survival.
mTTF, median Time To Failure treatment; m, months.

hotspots and are well known pathogenic mutations which constitutively activate KRAS firing. These mutations could theoretically impact on the response to EGFR inhibitors, due to bypassing the inhibition of EGFR by TKIs. Consequences on clinical responses to *EGFR* TKIs have been investigated in some studies with variable results. In early studies, Takeda et al. and Pao et al. found that *KRAS* mutation is a negative predictor of response to *EGFR*-TKIs in *EGFR* mutation-positive NSCLC patients (33, 34). On the other hand, Benesoma et al. described 3 NSCLC patients with coexistence of *EGFR* and *KRAS* mutations uncoupled from negative response to *EGFR* TKIs (23). More recently, Hong et al. genotyped 58 *EGFR* mutant NSCLC patients before TKI treatment and found that concomitant *KRAS* mutations in cfDNA associated with shorter duration of PFS and OS (18). However, conclusions from these studies were based on small cohorts of patients and other groups reported overlapping clinical outcome in *EGFR* mutant NSCLC patients with or without concomitant *KRAS* mutations (32). These contrasting results could, among other factors, depend on the sub-clonal nature of *KRAS* mutations and their different abundance in the studied patients' cohorts.

A field relatively less investigated so far involves the prevalence of *KRAS* mutations following treatment and onset of clinical resistance to *EGFR* TKI. Del Re et al. found that 16 out of 33 (48.5%) NSCLC samples studied at progression after *EGFR* TKI had concomitant codon 12 *KRAS* mutations in cfDNA, with percentages of mutated allele ranging from 1–98% (24). However, in this study it was not stated which cut-off has been used for interpretation of ddPCR results. Moreover, accurate assessment of the percentage of *KRAS* mutation in this patient population could be challenging, due to the small number of samples analyzed and the value reported (48.5%) was much greater than previously found by others (18–22, 30–32). In our study by using stringent criteria for interpretation of ddPCR data and analysing a large population of samples (n=104), *KRAS* mutations were rarely found in cfDNA from these patients (2.8%) and had a negative impact on response to TKI and clinical outcome (TTF, PFS, OS) (**Figure 2**). *KRAS* positivity was confirmed in one available matched tumor tissue biopsy at diagnosis. Although this is limited to one patient, results are in-line with a recent study suggesting that *EGFR*-mutated NSCLC patients with *KRAS* mutations detected in tumor before the start of treatment do not benefit from *EGFR* TKIs (22).

It is important to stress that technicalities, such as the cut-off values used to interpret ddPCR results are key to determine the result. In fact, if we lowered the cut-off and considered as *KRAS* mutant even samples with 1–2 positive droplets in cfDNA (n=28), the percentage of *KRAS* mutated samples was much higher (29%). In any case it should be considered that the abundance of *KRAS* mutations was very low, as indicated by the low MAFA values (mean 0.15%, median 0.12%, range 0.016–0.32%), compared with those found in cfDNA from NSCLC patients bearing *KRAS* mutant tumors (mean 8.87%, median 3%, range 0.46–53.7 %) (25). Of regard, we found no prognostic association of borderline *KRAS* mutations in cfDNA with PFS, nor with OS (**Figure 2**).

The main limitation of this study is the relatively limited number of frankly *KRAS* positive patients (n=3), compared with *KRAS* negative patients (n=73). However, our data suggest a potential negative prognostic impact, and confirmed recent reports indicating that *EGFR*-mutated NSCLC patients with additional driver alterations show reduced sensitivity to TKIs. Clearly, our findings should be confirmed in larger series to investigate the impact of *KRAS* mutation detection on clinical decisions, with particular regard to selection of patients for combination treatments, currently under investigation in lung cancer, such as EGFR inhibitor plus chemotherapy or plus antiangiogenic treatment (35).

On the other hand, 36% of plasma samples analyzed at progressive disease were negative for *EGFR* mutation, indicating the possible lack of circulating tumor DNA (ctDNA). This aspect could determine an underestimation of the patients with co-occurring *KRAS* mutations, even though the low presence of ctDNA could be associated with lower tumor burden and better prognosis (36).

Another limitation is represented by the fact that our study did not include systematic analysis of baseline *KRAS* mutation either in plasma or in tissue, which could unravel the multi-clonal character

of the tumours. Therefore, we could not draw definitive conclusions on the role of sub-clones in the response to *EGFR* TKI.

We conclude that detection of *KRAS* mutations in cfDNA is rare in *EGFR* mutant patients treated with TKI and these mutations are more likely to be detected in smokers, possibly underlying broader genetic heterogeneity of these tumors compared with those on non-smokers.

DATA AVAILABILITY STATEMENT

The raw data supporting the conclusions of this article will be made available by the authors, without undue reservation.

ETHICS STATEMENT

The studies involving human participants were reviewed and approved by IOV Institutional Review Board and Ethics Committee (CESC IOV 2020/57). The patients/participants provided their written informed consent to participate in this study.

AUTHOR CONTRIBUTIONS

GN contributed to the design of the study, performed the analysis, and wrote sections of the manuscript. JC, LM, and ABB processed the samples and performed the experiments. EZ analyzed the data, and wrote the manuscript. LB, AB, and AM recruited patients, collected, and analyzed clinical data and performed statistical analysis. SI contributed conception and design of the study, wrote the advanced draft of the manuscript revising it critically for intellectual content, and provided approval for publication of the content. All authors contributed to the article and approved the submitted version.

FUNDING

This work was funded by IOV intramural research grant 2017 – SINERGIA (to SI and LB). The QX200 ddPCR system (Bio-Rad Laboratories) was purchased through a grant provided by Università degli Studi di Padova, Padova, Italy (2015).

REFERENCES

1. Cheng TY, Cramb SM, Baade PD, Youlden DR, Nwogu C, Reid ME. The International Epidemiology of Lung Cancer: Latest Trends, Disparities, and Tumor Characteristics. *J Thorac Oncol* (2016) 11(10):1653–71. doi: 10.1016/j.jtho.2016.05.021
2. Jamal-Hanjani M, Wilson GA, McGranahan N, Birkbak NJ, Watkins TBK, Veeriah S, et al. Tracking the Evolution of Non-Small-Cell Lung Cancer. *N Engl J Med* (2017) 376(22):2109–21. doi: 10.1056/NEJMoa1616288
3. Piotrowska Z, Sequist LV. Epidermal Growth Factor Receptor-Mutant Lung Cancer: New Drugs, New Resistance Mechanisms, and Future Treatment Options. *Cancer J* (2015) 21(5):371–7. doi: 10.1097/PPO.0000000000000147
4. Maemondo M, Inoue A, Kobayashi K, Sugawara S, Oizumi S, Isobe H, et al. Gefitinib or chemotherapy for non-small-cell lung cancer with mutated EGFR. *N Engl J Med* (2010) 362(25):2380–8. doi: 10.1056/NEJMoa0909530
5. Mok TS, Wu YL, Thongprasert S, Yang CH, Chu DT, Saijo N, et al. Gefitinib or carboplatin-paclitaxel in pulmonary adenocarcinoma. *N Engl J Med* (2009) 361(10):947–57. doi: 10.1056/NEJMoa0810699
6. Rosell R, Carcereny E, Gervais R, Vergnenegre A, Massuti B, Felip E, et al. Erlotinib versus standard chemotherapy as first-line treatment for European patients with advanced EGFR mutation-positive non-small-cell lung cancer (EURTAC): a multicentre, open-label, randomised phase 3 trial. *Lancet Oncol* (2012) 13(3):239–46. doi: 10.1016/S1470-2045(11)70393-X
7. Sequist LV, Yang JC, Yamamoto N, O'Byrne K, Hirsh V, Mok T, et al. Phase III study of afatinib or cisplatin plus pemetrexed in patients with metastatic lung adenocarcinoma with EGFR mutations. *J Clin Oncol* (2013) 31(27):3327–34. doi: 10.1200/JCO.2012.44.2806
8. Soria JC, Ohe Y, Vansteenkiste J, Reungwetwattana T, Chewaskulyong B, Lee KH, et al. Osimertinib in Untreated EGFR-Mutated Advanced Non-Small-Cell Lung Cancer. *N Engl J Med* (2018) 378(2):113–25. doi: 10.1056/NEJMoa1713137
9. Marcoux N, Gettinger SN, O'Kane G, Arbour KC, Neal JW, Husain H, et al. EGFR-Mutant Adenocarcinomas That Transform to Small-Cell Lung Cancer and Other Neuroendocrine Carcinomas: Clinical Outcomes. *J Clin Oncol* (2019) 37(4):278–85. doi: 10.1200/JCO.18.01585
10. Van Der Steen N, Giovannetti E, Carbone D, Leonetti A, Rolfo CD, Peters GJ. Resistance to epidermal growth factor receptor inhibition in non-small cell lung cancer. *Cancer Drug Resistance* (2018) 1(4):230–49. doi: 10.20517/cdr.2018.13
11. Leonetti A, Sharma S, Minari R, Perego P, Giovannetti E, Tiseo M. Resistance mechanisms to osimertinib in EGFR-mutated non-small cell lung cancer. *Br J Cancer* (2019) 121(9):725–37. doi: 10.1038/s41416-019-0573-8
12. Santoni-Rugiu E, Melchior LC, Urbanska EM, Jakobsen JN, de Stricker K, Grauslund M, et al. Intrinsic resistance to EGFR-Tyrosine Kinase Inhibitors in EGFR-Mutant Non-Small Cell Lung Cancer: Differences and Similarities with Acquired Resistance. *Cancers* (2019) 11(7):923. doi: 10.3390/cancers11070923
13. Blakely CM, Watkins TBK, Wu W, Gini B, Chabon JJ, McCoach CE, et al. Evolution and clinical impact of co-occurring genetic alterations in advanced-stage EGFR-mutant lung cancers. *Nat Genet* (2017) 49(12):1693–704. doi: 10.1038/ng.3990
14. Bria E, Pilotto S, Amato E, Fassan M, Novello S, Peretti U, et al. Molecular heterogeneity assessment by next-generation sequencing and response to gefitinib of EGFR mutant advanced lung adenocarcinoma. *Oncotarget* (2015) 6(14):12783–95. doi: 10.18632/oncotarget.3727
15. Canale M, Petracci E, Delmonte A, Chiadini E, Dazzi C, Papi M, et al. Impact of TP53 Mutations on Outcome in EGFR-Mutated Patients Treated with First-Line Tyrosine Kinase Inhibitors. *Clin Cancer Res* (2017) 23(9):2195–202. doi: 10.1158/1078-0432.CCR-16-0966
16. Labbe C, Cabanero M, Korpanty GJ, Tomasini P, Doherty MK, Mascaux C, et al. Prognostic and predictive effects of TP53 co-mutation in patients with EGFR-mutated non-small cell lung cancer (NSCLC). *Lung Cancer* (2017) 111:23–9. doi: 10.1016/j.lungcan.2017.06.014
17. Molina-Vila MA, Bertran-Alamillo J, Gasco A, Mayo-de-las-Casas C, Sanchez-Ronco M, Pujantell-Pastor L, et al. Nondisruptive p53 mutations are associated with shorter survival in patients with advanced non-small cell lung cancer. *Clin Cancer Res* (2014) 20(17):4647–59. doi: 10.1158/1078-0432.CCR-13-2391
18. Hong S, Gao F, Fu S, Wang Y, Fang W, Huang Y, et al. Concomitant Genetic Alterations With Response to Treatment and Epidermal Growth Factor Receptor Tyrosine Kinase Inhibitors in Patients With EGFR-Mutant Advanced Non-Small Cell Lung Cancer. *JAMA Oncol* (2018) 4(5):739–42. doi: 10.1001/jamaoncol.2018.0049
19. Hu W, Liu Y, Chen J. Concurrent gene alterations with EGFR mutation and treatment efficacy of EGFR-TKIs in Chinese patients with non-small cell lung cancer. *Oncotarget* (2017) 8(15):25046–54. doi: 10.18632/oncotarget.15337
20. Jakobsen JN, Santoni-Rugiu E, Grauslund M, Melchior L, Sorensen JB. Concomitant driver mutations in advanced EGFR-mutated non-small-cell lung cancer and their impact on erlotinib treatment. *Oncotarget* (2018) 9(40):26195–208. doi: 10.18632/oncotarget.25490

21. Lee T, Lee B, Choi YL, Han J, Ahn MJ, Um SW. Non-small Cell Lung Cancer with Concomitant EGFR, KRAS, and ALK Mutation: Clinicopathologic Features of 12 Cases. *J Pathol Transl Med* (2016) 50(3):197–203. doi: 10.4132/jptm.2016.03.09
22. Rachiglio AM, Fenizia F, Piccirillo MC, Galetta D, Crino L, Vincenzi B, et al. The Presence of Concomitant Mutations Affects the Activity of EGFR Tyrosine Kinase Inhibitors in EGFR-Mutant Non-Small Cell Lung Cancer (NSCLC) Patients. *Cancers (Basel)* (2019) 11(3):341. doi: 10.3390/cancers11030341
23. Benesova L, Minarik M, Jancarikova D, Belsanova B, Pese M. Multiplicity of EGFR and KRAS mutations in non-small cell lung cancer (NSCLC) patients treated with tyrosine kinase inhibitors. *Anticancer Res* (2010) 30(5):1667–71.
24. Del Re M, Tiseo M, Bordi P, D'Incecco A, Camerini A, Petrini I, et al. Contribution of KRAS mutations and c.2369C > T (p.T790M) EGFR to acquired resistance to EGFR-TKIs in EGFR mutant NSCLC: a study on circulating tumor DNA. *Oncotarget* (2017) 8(8):13611–9. doi: 10.18632/oncotarget.6957
25. Zulato E, Attili I, Pavan A, Nardo G, Del Bianco P, Boscolo Bragadin A, et al. Early assessment of KRAS mutation in cfDNA correlates with risk of progression and death in advanced non-small-cell lung cancer. *Br J Cancer* (2020) 123(1):81–91. doi: 10.1038/s41416-020-0833-7
26. Sholl LM, Aisner DL, Varella-Garcia M, Berry LD, Dias-Santagata D, Wistuba II, et al. Multi-institutional Oncogenic Driver Mutation Analysis in Lung Adenocarcinoma: The Lung Cancer Mutation Consortium Experience. *J Thorac Oncol* (2015) 10(5):768–77. doi: 10.1097/JTO.0000000000000516
27. Sun L, Zhang Q, Luan H, Zhan Z, Wang C, Sun B. Comparison of KRAS and EGFR gene status between primary non-small cell lung cancer and local lymph node metastases: implications for clinical practice. *J Exp Clin Cancer Res* (2011) 30:30. doi: 10.1186/1756-9966-30-30
28. Mansuet-Lupo A, Barritault M, Alifano M, Janet-Vendroux A, Zarmaev M, Biton J, et al. Proposal for a Combined Histomolecular Algorithm to Distinguish Multiple Primary Adenocarcinomas from Intrapulmonary Metastasis in Patients with Multiple Lung Tumors. *J Thorac Oncol* (2019) 14(5):844–56. doi: 10.1016/j.jtho.2019.01.017
29. Roepman P, Ten Heuvel A, Scheidel KC, Sprong T, Heideman DAM, Seldenrijk KA, et al. Added Value of 50-Gene Panel Sequencing to Distinguish Multiple Primary Lung Cancers from Pulmonary Metastases: A Systematic Investigation. *J Mol Diagn* (2018) 20(4):436–45. doi: 10.1016/j.jmoldx.2018.02.007
30. Li S, Li L, Zhu Y, Huang C, Qin Y, Liu H, et al. Coexistence of EGFR with KRAS, or BRAF, or PIK3CA somatic mutations in lung cancer: a comprehensive mutation profiling from 5125 Chinese cohorts. *Br J Cancer* (2014) 110(11):2812–20. doi: 10.1038/bjc.2014.210
31. Scheffler M, Ihle MA, Hein R, Merkelbach-Bruse S, Scheel AH, Siemanowski J, et al. K-ras Mutation Subtypes in NSCLC and Associated Co-occuring Mutations in Other Oncogenic Pathways. *J Thorac Oncol* (2019) 14(4):606–16. doi: 10.1016/j.jtho.2018.12.013
32. Zhuang X, Zhao C, Li J, Su C, Chen X, Ren S, et al. Clinical features and therapeutic options in non-small cell lung cancer patients with concomitant mutations of EGFR, ALK, ROS1, KRAS or BRAF. *Cancer Med* (2019) 8(6):2858–66. doi: 10.1002/cam4.2183
33. Pao W, Wang TY, Riely GJ, Miller VA, Pan Q, Ladanyi M, et al. KRAS mutations and primary resistance of lung adenocarcinomas to gefitinib or erlotinib. *PloS Med* (2005) 2(1):e17. doi: 10.1371/journal.pmed.0020017
34. Takeda M, Okamoto I, Fujita Y, Arao T, Ito H, Fukuoka M, et al. De novo resistance to epidermal growth factor receptor-tyrosine kinase inhibitors in EGFR mutation-positive patients with non-small cell lung cancer. *J Thorac Oncol* (2010) 5(3):399–400. doi: 10.1097/JTO.0b013e3181cee47e
35. Tam Z. Combination Strategies Using EGFR-TKi in NSCLC Therapy: Learning from the Gap between Pre-Clinical Results and Clinical Outcomes. *Int J Biol Sci* (2018) 14(2):204–16. doi: 10.7150/ijbs.22955
36. Luis A, Diaz J. Liquid Biopsies: Genotyping Circulating Tumor DNA. *J Clin Oncol* (2014) 32(6):579–86. doi: 10.1200/JCO.2012.45.2011

Conflict of Interest: The authors declare that the research was conducted in the absence of any commercial or financial relationships that could be construed as a potential conflict of interest.

frontiers in Oncology

ORIGINAL RESEARCH
published: 09 February 2021
doi: 10.3389/fonc.2020.597486

A Urine-Based Liquid Biopsy Method for Detection of Upper Tract Urinary Carcinoma

Yansheng Xu[1,2†], Xin Ma[1†], Xing Ai[3†], Jiangping Gao[4†], Yiming Liang[5†], Qin Zhang[5], Tonghui Ma[5], Kaisheng Mao[5], Qiaosong Zheng[5], Sizhen Wang[5], Yuchen Jiao[6], Xu Zhang[1] and Hongzhao Li[1*]*

[1] Department of Urology, The First Medical Center of Chinese PLA General Hospital, Beijing, China, [2] Department of Urology, The Sixth Medical Center of Chinese PLA General Hospital, Beijing, China, [3] Department of Urology, The Seventh Medical Center of Chinese PLA General Hospital, Beijing, China, [4] Department of Urology, The Fourth Medical Center of Chinese PLA General Hospital, Beijing, China, [5] Genetron Health (Beijing) Technology, Co. Ltd., Beijing, China, [6] State Key Lab of Molecular Oncology, National Cancer Center/National Clinical Research Center for Cancer/Cancer Hospital, Chinese Academy of Medical Sciences and Peking Union Medical College, Beijing, China

OPEN ACCESS

Edited by:
Francesco Fabbri,
Romagnolo Scientific Institute for the Study and Treatment of Tumors (IRCCS), Italy

Reviewed by:
Fabio Tavora,
Federal University of Ceara, Brazil
Giovanni Porta,
University of Insubria, Italy

***Correspondence:**
Xu Zhang
xzhang@tjh.tjmu.edu.cn
Hongzhao Li
urolancet@126.com

[†]These authors share first authorship

Specialty section:
This article was submitted to Cancer Molecular Targets and Therapeutics, a section of the journal Frontiers in Oncology

Received: 21 August 2020
Accepted: 16 November 2020
Published: 09 February 2021

Citation:
Xu Y, Ma X, Ai X, Gao J, Liang Y, Zhang Q, Ma T, Mao K, Zheng Q, Wang S, Jiao Y, Zhang X and Li H (2021) A Urine-Based Liquid Biopsy Method for Detection of Upper Tract Urinary Carcinoma. Front. Oncol. 10:597486. doi: 10.3389/fonc.2020.597486

Background: Conventional clinical detection methods such as CT, urine cytology, and ureteroscopy display low sensitivity and/or are invasive in the diagnosis of upper tract urinary carcinoma (UTUC), a factor precluding their use. Previous studies on urine biopsy have not shown satisfactory sensitivity and specificity in the application of both gene mutation or gene methylation panels. Therefore, these unfavorable factors call for an urgent need for a sensitive and non-invasive method for the diagnosis of UTUC.

Methods: In this study, a total of 161 hematuria patients were enrolled with (n = 69) or without (n = 92) UTUC. High-throughput sequencing of 17 genes and methylation analysis for *ONECUT2* CpG sites were combined as a liquid biopsy test panel. Further, a logistic regression prediction model that contained several significant features was used to evaluate the risk of UTUC in these patients.

Results: In total, 86 UTUC– and 64 UTUC+ case samples were enrolled for the analysis. A logistic regression analysis of significant features including age, the mutation status of *TERT* promoter, and *ONECUT2* methylation level resulted in an optimal model with a sensitivity of 94.0%, a specificity of 93.1%, the positive predictive value of 92.2% and a negative predictive value of 94.7%. Notably, the area under the curve (AUC) was 0.957 in the training dataset while internal validation produced an AUC of 0.962. It is worth noting that during follow-up, a patient diagnosed with ureteral inflammation at the time of diagnosis exhibiting both positive mutation and methylation test results was diagnosed with ureteral carcinoma 17 months after his enrollment.

Conclusion: This work utilized the epigenetic biomarker *ONECUT2* for the first time in the detection of UTUC and discovered its superior performance. To improve its sensitivity, we combined the biomarker with high-throughput sequencing of 17 genes test. It was found that the selected logistic regression model diagnosed with ureteral cancer can evaluate upper tract urinary carcinoma risk of patients with hematuria and outperform other existing

panels in providing clinical recommendations for the diagnosis of UTUC. Moreover, its high negative predictive value is conducive to rule to exclude patients without UTUC.

Keywords: hematuria, liquid biopsy, next-generation sequencing, methylation, upper tract urinary carcinoma, logistic regression model

INTRODUCTION

Upper tract urinary carcinoma (UTUC) including renal pelvic cancer and ureteral cancer accounts for approximately 5% of urothelial carcinomas (1, 2). During its diagnosis, patients are subjected to extensive examinations, including endoscopy, imaging of the urinary tract, and cytology or FISH testing. However, a few cases still cannot be accurately diagnosed. Before surgery, ureteroscopy is the only standard method applied to acquire the pathological status of the samples (3, 4). This method, nevertheless, is an invasive procedure that can only be performed in the hospital by experienced doctors. Besides causing discomfort and pain, it causes complications such as severe infections, i.e., 4%~25% as documented and even prophylactic use of antibiotics (5). Besides, the risk of implantation and dissemination of tumor cells might be encountered during the procedure (6). As diagnostic tools, cytology, and FISH are non-invasive yet display low sensitivity (7). Generally, an effective diagnostic method is imperative for the appropriate treatment of UTUC.

With the advent of next-generation sequencing in the last decade, biomarker searching became much easier, and multiple driver gene variations have been identified in urinary carcinoma. Of note, high rates of activating mutations in the upstream promoter of the *TERT* gene were found in the majority of upper tract urinary carcinomas and bladder cancers (BCs) (8–10). Additionally, important oncogene mutations by *FGFR3*, *HRAS*, *KRAS*, and *PIK3CA* occur at high frequency in non-muscle-invasive BCs (11–13). While mutations by *TP53*, *CDKN2A*, *MLL*, and *ERBB2* genes are frequently found in muscle-invasive BCs and UTUC (14–16). Unlike in UTUC research, molecular diagnostic methods have performed effectively in BC research. For instance, the diagnostic sensitivity of the UroSEEK method detecting mutations by 11 genes in UTUC was only 75%, much lower than 95% in BC (17).

DNA methylation, which is associated with the loss of gene expression occurs prevalently in patients diagnosed with urothelial cancer. In a previous study conducted in China, the methylation status of 10 selected genes among them, *ABCC6*, *BRCA1*, *CDH1*, *GDF15*, *HSPA2*, *RASSF1A*, *SALL3*, *THBS1*, *TMEFF2*, and *VIM* was tested during the detection of BC and UTUC. Results suggested a sensitivity and specificity of 0.82 and 0.68, respectively, among the UTUC cohort, which was insufficient for clinical application (18).

Based on the findings reported above, a more reliable biomarker is needed to advance the diagnosis of UTUC. Herein, we evaluated the performance of the *ONECUT2* methylation test in the detection of UTUC. To further improve the sensitivity of this tool, commonly occurring mutations of 17 genes in urothelial cancer were added into our test panel.

MATERIALS AND METHODS

Patients and Samples

This double-blind and prospective clinical trial was started in 2017. Between October 2017 and May 2018, all urine samples were collected from patients without a history of any malignant disease in recent 5 years and with microscopic or macroscopic hematuria from three hospitals (The First, the Fourth and The Seventh Medical Center of Chinese PLA Navy General Hospital). Informed written consent was obtained from patients at PLA General Hospital and the study was approved by the Committee on Clinical Research Ethics of the Chinese PLA General Hospital. A total of 69 hematuria patients diagnosed with malignant UTUC (UTUC+) while the other 92 hematuria patients that were diagnosed with non-malignant UTUC (UTUC−) were enrolled respectively. All the enrolled patients were examined by endoscopy, abdomen ultrasound, CT scan, and MRI of abdomen and pelvis. Using these clinical standard diagnostic methods, no malignant tumor was found in UTUC− patients. At the same time, considering the slight limitation of the sensitivity of these methods, we followed up the UTUC− group for about 2 years to exclude undetected tumors. Correspondingly, all 69 malignant patients' diagnosis results had been confirmed by histopathological methods after surgical treatments.

In total, 50-ml first-void Urine sample was processed within 12 h after collection. The samples were centrifuged at 2000g for 10 min, then the pellet was once washed with phosphate-buffered saline, and stored at −80°C until DNA extraction. Twelve tissue samples were effectively collected for validation, immersed in an RNA later solution (Thermo Fisher, Cat. No. AM7022) and stored following the manufacturer's instruction until DNA extraction. The tests were blinded to the clinical data of the patients.

Next-Generation Sequencing Analysis

Amplicon-Based Sequencing Design

The panel of Genetron-health 17 genes (**Supplementary File 1**) was designed to maximize the number of unique driver gene variants of UTUC by a limited number of amplicons. The regions were selected in reference to the results of previous research (17, 19, 20). In total, 38 pairs of primers were selected using a customized procedure to balance coverage, Tm, dimmer potential, and predicted specificity with the human genome (Cancer Gene Considerable Cover algorithm).

Multiplex PCR-Based Next-Generation Sequencing

Primers for several segments of the 17 genes in the first and second enrichments were designed separately. They were synthesized by Sangon Biotech and dissolved to 100 μmol/L

with low TE buffer. Sequencing libraries were generated using multiplex PCR methods (primers and reaction conditions are described in **Supplementary File 1**). Subsequently, 20ul pooled amplicons were sequenced on the Ion Proton system (Thermo Fisher Scientific).

Data Analysis and Workflow

Local alignments of reads to the hg19 genome were performed using bowtie2 (version 2.2.4) in paired-end mode. SAM alignment files were converted to BAM files, sorted and indexed using Samtools (version 0.1.19). BAM files were processed with bam-read count and the outputs were processed with a custom-written Perl script. Normal SNP variant mutation frequency is usually at around 50%, here, the frequency was set at >0.5% and supporting unduplicated reads at ≧20 as an abnormal cutoff to distinguish the variants appeared in the detection.

Methylation Analysis

This assay was designed to detect CpG-sites on the *ONECUT2* gene, it was performed using EZ DNA Methylation-Lightning™ Kit (Zymo Research Corporation, Irvine, California, USA), according to the manufacturer's protocol. Briefly, bisulfite-specific real-time PCR was designed for 20-ng bisulfite transformed DNA. Ct values representing the relative quantity of methylated and unmethylated parts were separately measured by FAM and VIC signals, and the delta ct values were calculated as methylation score.

Statistical Analysis and Logistic Regression Model

Statistical analysis was performed using Python (Version 3.6) with scipy (1.1.0) and scikit-learn (0.19.2) module. P-values at $P < 0.05$ were considered statistically significant. Univariate logistic regression analysis was used to calculate the association between UTUC and the diagnostic variables.

A logistic regression model was constructed from the training cohort of 115 samples by random sampling. The model performance was evaluated both on the training and validation data sets, by the area under the curve (AUC) statistics. The sensitivity and specificity of the model were also determined using an optimized cutoff value which was applied using Youden's index. Cross-validated coefficients for each feature using logistic regression have been given. The model was initiated in R package 'glmnet' (R version 3.5.1), and the penalty parameter alpha was optimized with 10-fold cross-validation within the training data set and the optimized value was 0.

RESULTS

Patient Demographics

In total, 150 (93.2%) of the urine samples and 11 (91.7%) of tissue samples passed the quality control for further testing (**Figure 1**). Overall, 107 males and 43 females were enrolled as subjects, with a median age of 60 (range from 18 to 88) years. Patients and tumor characteristics are described in **Table 1**. In 64 cases, UTUC was confirmed as a cause of hematuria while the cause of the remaining 86 patients was found to be non-malignant. Patients diagnosed with UTUC were significantly older compared to non-malignant patients ($p < 0.01$, **Table 2**). FISH tests were only performed on 80% (n = 51) of UTUC+ and 9% (n = 8) of UTUC– patients. The sensitivity and specificity of FISH were 51% (26/51) and 100% (0/8) respectively.

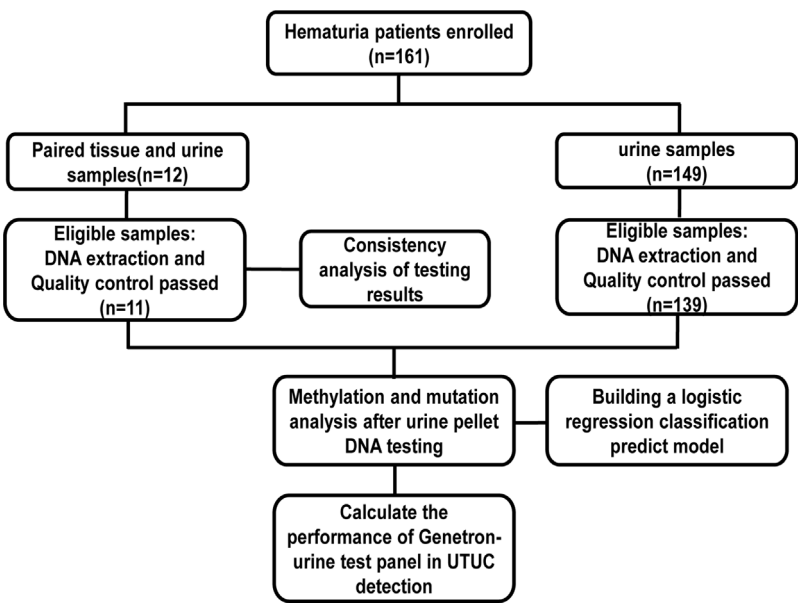

FIGURE 1 | Sample and data processing work-flow.

TABLE 1 | Clinical and histopathological characteristics of enrolled cases.

Characteristic	Number of UTUC+ patients (N = 64)	Number of UTUC– patients (N = 86)
Age, y		
Median (range)	67(26~88)	56(18~82)
Gender, n (%)		
Male	40(62.5)	67(77.9)
Female	24(37.5)	19(22.1)
FISH, n (%)		
Positive	26(40.6)	0(0.0)
Negative	25(39.1)	8(9.3)
Grade, n (%)		
Low grade	17(26.6)	-
High grade	47(73.4)	-
Type, n (%)		
NMIUC	22(34.4)	–
MIUC	39(60.9)	–

FISH, Fluorescence in situ hybridization; NMIUC, Non-muscle-invasive urothelial carcinoma; MIUC, Muscle-invasive urothelial carcinoma.

The Concordance Profiling Between Urine ctDNA and Matched Tumor Tissues

The consistency of mutations in urine samples and the corresponding tissue samples were evaluated to confirm the sources of these variants. As a result, a total of 12 matched tissue samples were effectively collected and 11 qualified DNA samples were identified. As shown in **Figure 2**, 14 variants from 5 genes were detected from 9 UTUC+ samples where 13 of them were positive in both types of samples. In the case of RG180, *AKT* mutation was shown from urine other than tissue samples indicating the effectiveness of urine samples as a supplement for genetic analysis of UTUC tissue samples in instances where genetic heterogeneity is considered as an issue. In addition, no mutations were detected in the urine and tissue samples of the two UTUC– patients. In summary, the concordance rate of variant detection between urine and tissue samples was 93% (13/14).

TABLE 2 | Univariable logistic regression analysis including significant features.

Variables	OR*	95% CI	P value
Gender			
male	0.47	0.23~0.97	0.04 (<0.05)
Age, y	1.08	1.04~1.12	<0.01
>50			
Mutations			
FGFR3	28.33	3.64~220.31	<0.01
TERT	37.06	8.39~163.74	<0.01
PIK3CA	7.2	0.82~63.25	0.075
TP53	8.47	2.33~30.73	<0.01
Methylation			
ONECUT2(△ct<7.93)	131.91	39.87~436.49	<0.01
Panel			
≥1 gene mutated or the *ONECUT2*gene methylated	133.17	40.26~440.45	<0.01

**OR was defined as UTUC risk of each feature.*

Univariate Logistic Regression of Significant Features

Univariate analysis was performed for each of these variants as well as clinical factors to assess the strength of these factors in evaluating UTUC risk by calculating the odds ratios (**Table 2**). Mutated or methylated Gene including *FGFR3*, *TERT*, *TP53*, *ONECUT2*, and age older than 50 showed a significant impact in evaluating UTUC risks (P-value < 0.01). And the superiority of the panel was witnessed in the integration of all these markers (≥1 of 17 genes mutated or *ONECUT2* CpG methylated).

Gene Mutations Results of Urine Samples Were Consistent With Characteristics of Previous UTUC Mutation and Provided New Clinical Potential Applications

To better understand how each variant contributes to this panel, a heatmap was drawn in **Figure 3**. Despite this panel covering hotspots mutations of 17 genes, only variants from nine genes showed positive mutations. *TERT* C228T, *FGFR3* c.746C>G, c.1118A>G, and *TERT* C250T were on the top 4 of the list with a long tail of several other mutations from *ERBB2*, *HRAS*, *KRAS*, *PIK3CA*, *TP53*, *U2AF1*, and *AKT1* (**Supplementary Table 1**). This distribution pattern of driver genes corroborates with previous research in the sense that *TERT*, *FGFR3*, *TP53*, *PIK3CA*, and *RAS* genes exhibited high frequencies in the UTUC mutation landscape. FISH test results were shown along with the panel, notably, the sensitivity of the FISH

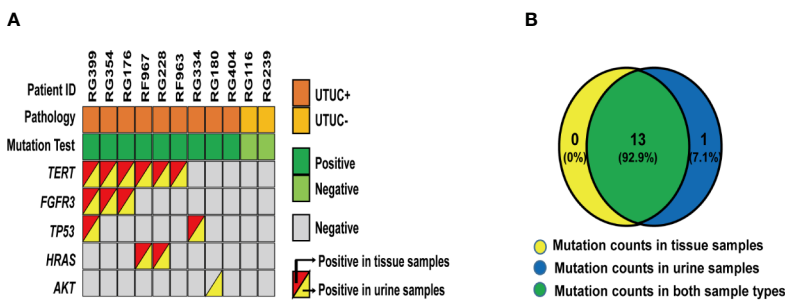

FIGURE 2 | Variants detected in 12 paired urine and tissue samples: **(A)** A heatmap shows variants detected in 12 paired urine and tissue samples. **(B)** A Venn diagram shows the relationship of these 26 variants from each set of different types of samples.

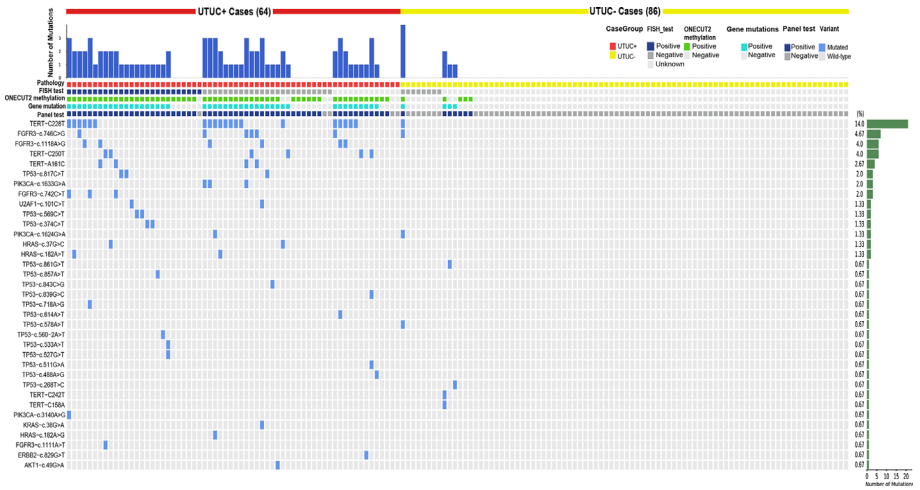

FIGURE 3 | Heatmap of all variations in urine samples: it demonstrates the variants detected in each case's urine sample.

test was low [about 51% (26/51)], but with perfect specificity and no false-positive found from the 8 tested UTUC− samples (**Table 1**). With the mutation test, the sensitivity and specificity were 71.9% and 91.4% respectively (**Table 3**), which was close to the sensitivity of 75% in the UTUC diagnostic cohort in a previous study that solely used mutant genes panel (19). Therefore, these data confirm the limitation of sensitivity when gene mutation detection was used solely in the diagnosis of UTUC.

When the mutation detection results were analyzed solely, there was a significant difference between the muscle-invasive group and the non-muscle-invasive group (**Supplementary Table 2**, p value = 0.037). Additionally, a significantly higher frequency of *TP53* mutations in high versus low-grade samples (31.9% vs. 0%; p = 0.0065, Fisher's Exact Test) was observed, and conversely, found disproportionately more *FGFR3* mutations (47.1% vs. 17.0%; p = 0.0223, Fisher's Exact Test) and *PIK3CA* mutations (23.5% vs. 2.1%; p = 0.0155, Fisher's Exact Test) in low versus high-grade cases (**Figure 4A**). Likewise, a significantly higher frequency of *TERT* promoter mutations (72.7% vs. 25.6%; p = 0.0005, Fisher's Exact Test) and *HRAS* mutations (0% vs. 18.2%; p = 0.014, Fisher's Exact Test) was evident in non-muscle-invasive versus muscle-invasive samples for the first time in UTUC cohort (**Figure 4B**). This thus reflected the significance of adding detection of gene mutation to our test panel, which could provide evidence for the classification of UTUC+ patients.

ONECUT2 Methylation Exhibited a Satisfactory Performance as a Diagnostic Biomarker of UTUC

The analysis was performed to confirm the best cutoff of *ONECUT2* methylation status (**Figure 5**). The Δct value of *ONECUT2* in all urine samples is shown in **Figure 5A**. With a cutoff of 7.93, the *ONECUT2* methylation detection ability was the largest, displaying the AUC of 0.93 (**Figure 5B**). With the singly use of the *ONECUT2* methylation test in this cutoff value, genetic abnormalities in 89.1% (57/64) urine of UTUC+ patients and 5.8% (5/86) of UTUC− group were detected resulting in a sensitivity of 89.1% (57/64), and a specificity of 94.2% (81/86) (**Table 3**). This performance of the *ONECUT2* methylation test was better than the one reported previously (sensitivity of 82% and specificity of 62% with a panel of *VIM*, *RASSF1A*, *GDF15*, and *TMEFF2* methylation in UTUC group) (18).

The Performance of the Test Panel in UTUC Detection Showed Higher Sensitivity and NPV

By combining *ONECUT2* methylation and gene mutation results as a UTUC diagnostic test panel (≥1 of 17 genes mutated or *ONECUT2* CpG methylated showed a positive result), the performance of the test improved, the sensitivity of this test

TABLE 3 | Comparison of detection performance when using gene mutations solely, *ONECUT2* methylation solely and panel test.

	Test performance			
	Sensitivity(95%CI)	**Specificity(95%CI)**	**PPV(95%CI)**	**NPV(95%CI)**
**ONECUT2* methylation	89.1%(79.1%~94.6%)	94.2%(87.1%~97.5%)	91.9%(82.5%~96.5%)	92.0%(84.5%~96.1%)
**Gene Mutations	71.9%(59.9%~81.4%)	95.4%(88.6%~98.2%)	92.0%(81.2%~96.9%)	82.0%(73.3%~83.3%)
***Panel	92.2% (83.0%~96.6%)	91.9%(84.1%~96.0%)	89.4%(79.7%~94.8%)	94.1% (86.8%~97.4%)

**ONECUT2 methylation positive: ΔCt value is smaller than the cutoff value(7.93).*

***Mutation positive: ≥1 of 17 genes are mutated.*

****Panel positive: At least one of ONECUT2 methylation test and mutation test is positive.*

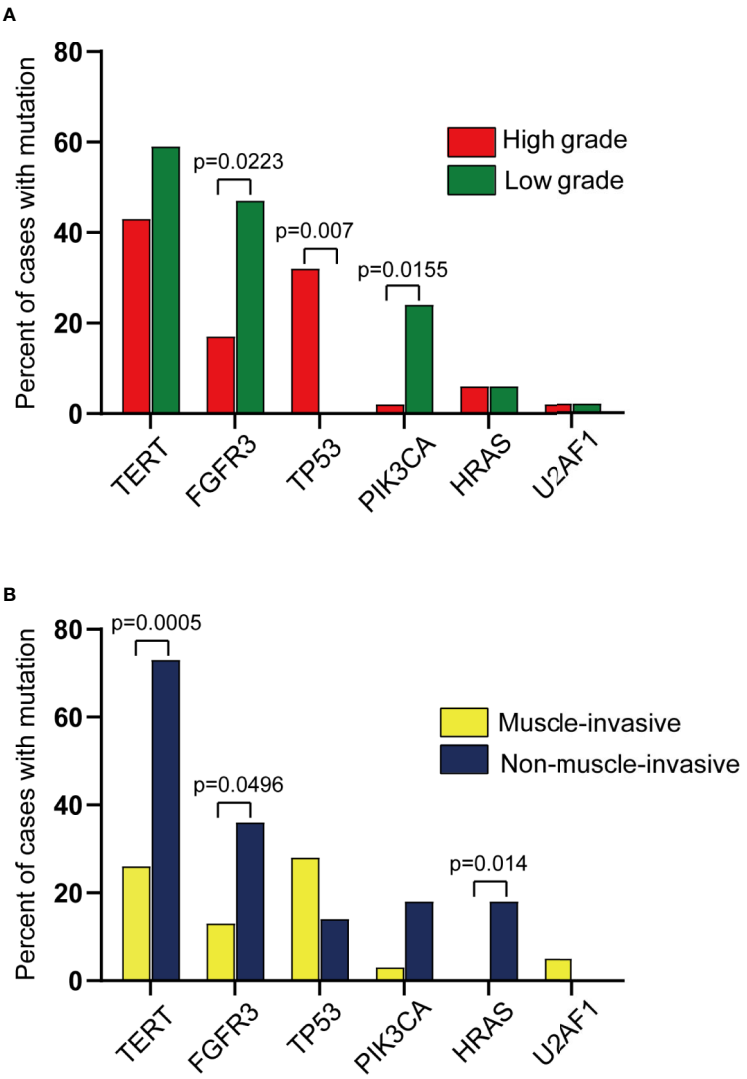

FIGURE 4 | Comparison of mutations across different groups profiled in this study. (Pairwise comparison results from Fisher's exact test). **(A)** Comparison of mutations across high vs. low grade UTUC. **(B)** Comparison of mutations across muscle-invasive vs. non-muscle-invasive UTUC.

panel rose to 92.2% (59/64), and the specificity was 91.9% (79/86). Simultaneously, the panel demonstrated a positive predictive value of 89.4% and a negative predictive value of 94.1% (**Table 3**). Moreover, by combining the detection results of gene mutations with *ONECUT2* methylation, the sensitivity was further improved. It was worth noting that the double-positive result (≥1 of 17 genes mutated and *ONECUT2* CpG methylated) potentially reveal a higher risk of UTUC. By the time the article was being written, almost all patients enrolled had completed a two-year follow-up, and two patients named RH645 and RG342 (**Supplementary Table 1**) with double-positive test results in UTUC– cohort were focused. It was found that patient RG342 was diagnosed with ureteral cancer in May 2019. Notably, a close follow-up of patient RH645 was still ongoing.

Comparison of Multivariate Logistic Regression Models Prompted the Direction of Panel Optimization

Out of the 150 samples, 108 were randomly selected as the training set, and the remaining 42 samples were the validation set. Based on the results of Univariate logistic regression, significant features were combined to construct 4 logistic regression models. From the ROC curve shown in **Figure 6**, the model constructed with the features of age and the mutation status of *TERT* promoter (mutation of at least one hotspot on *TERT* g.1295228C>T and g.1295250C>T) and *ONECUT2* methylation level (Model D) had the largest AUC of 0.957, whereas the AUC of other three models were 0.947 (age and panel test results, Model C), 0.953 (age and *ONECUT2*

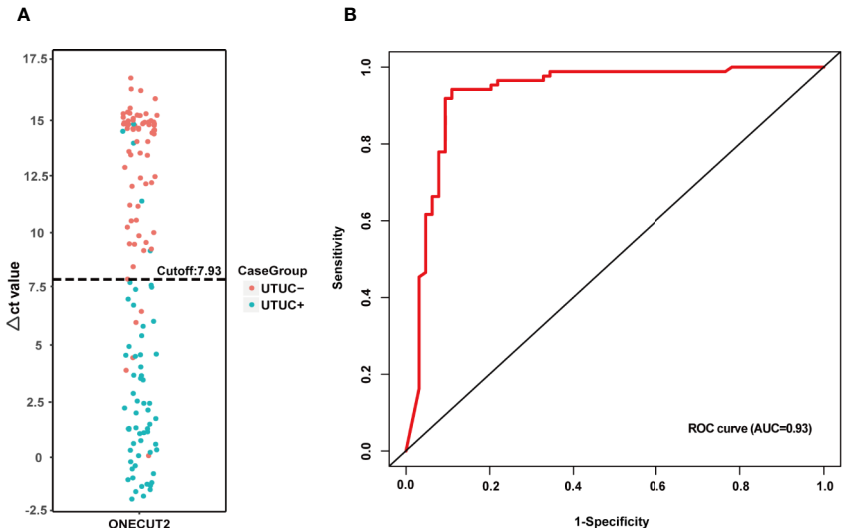

FIGURE 5 | Performance analysis of *ONECUT2* methylation: **(A)** The *ONECUT2* methylation Δct-value distribution of different types of samples. **(B)** ROC curve of the *ONECUT2* methylation (AUC = 0.92) also indicating the optimized Δct value cutoff is at 7.93 in this study.

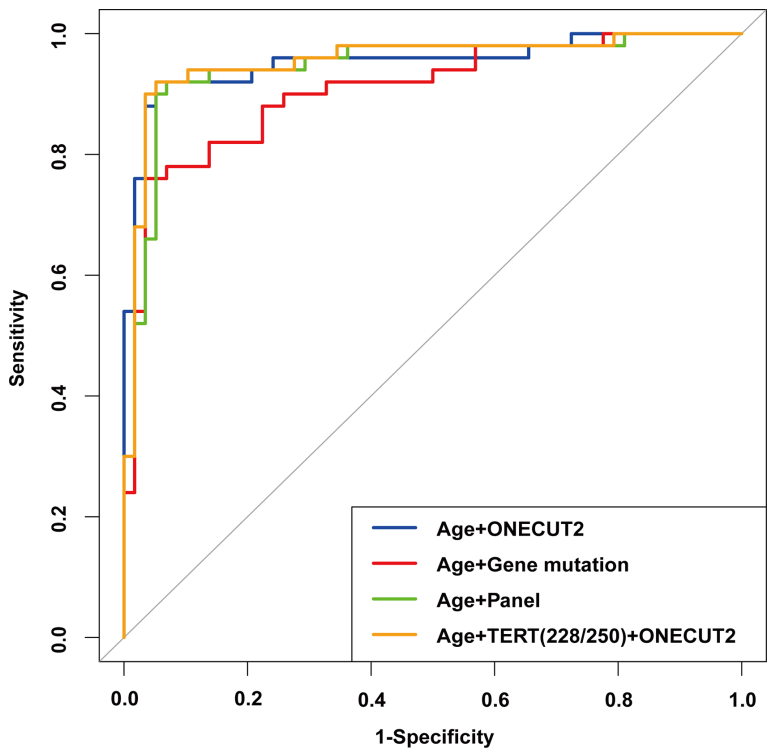

FIGURE 6 | ROC of the multivariable logistic regression models with different features in the training set.

methylation, Model A), and 0.903 (age and 17 genes mutation test result, Model B). By selecting the optimal cutoff according to the highest Youden index in each of the four models, the model with age, mutation status of *TERT* promoter and *ONECUT2* methylation level showed an optimal performance with a sensitivity of 94.0%, a specificity of 93.1%, a PPV of 92.2% and an NPV of 94.7% (**Table 4**). This model maximized sensitivity without a major reduction in specificity hence was considered

TABLE 4 | Effect on sensitivity, specificity, PPV and NPV at the respective cutoff of different models.

Variables of models	Models with different features			
	Model A	**Model B**	**Model C**	**Model D**
AUC of training set	0.953(0.911~0.996)	0.903(0.844~0.962)	0.947(0.901~0.992)	0.957(0.916~0.999)
Cutoff	0.408	0.497	0.498	0.412
Sensitivity(%)	92.0(81.2~96.9)	76.0(62.6~85.7)	92.0(81.2~96.9)	94.0(83.8~97.9)
Specificity(%)	94.8(85.9~98.2)	96.6(88.3~99.1)	93.1(83.6~97.3)	93.1(83.6~97.3)
PPV (%)	93.9(83.5~97.9)	95.0(84.5~98.6)	92.0(81.2~96.9)	92.2(81.5~96.9)
NPV (%)	93.2(83.8~97.3)	82.4(71.6~89.6)	93.1(83.6~97.3)	94.7(85.6~98.2)

Features in different models as follows:
Model A: age+ Onecut2 methylation.
Model B: age+ gene mutations.
Model C: age+ panel test.
Model D: age+ TERT C228T/C250T+ Onecut2 methylation.
PPV, Positive predictive value; NPV, Negative predictive value.
95% CI values were showed in brackets.

optimal. And in the validation set, a prediction using the above features were completed and obtained an AUC of 0.962 (**Supplementary Figure 1**).

DISCUSSION

The accurate distinction between benign and malignant tumors in the diagnosis of UTUC from a large number of hematuria patients remains a clinically challenging issue. Herein, we evaluated the performance of *ONECUT2* methylation detection in the UTUC diagnostic cohort for the first time, with mutations of 17 genes being combined into the test panel. Surprisingly, this is the first time that the superiority of this epigenetic biomarker *ONECUT2* has been demonstrated in UTUC diagnostic studies, and reported a high potential for clinical application compared to other methylation related methods. A logistic regression prediction model based on liquid biopsy of gene variants and clinical factors was screened for the accurate diagnosis of UTUC patients presenting microscopic or macroscopic hematuria. This will enable urologists to adjust the examination or treatment plan of the patient according to the risk, thereby reducing the discomfort and minimizing the cost incurred by the patient. In the current study, the test panel demonstrates high sensitivity and NPV for detecting patients with a high risk of UTUC as well as accurately excluding patients with benign hematuria. Specifically, the performance of our test panel shows a comprehensive improvement compared to previous studies which were based on either gene mutation panel or genes methylation panel.

So far, numerous studies have focused on the use of molecular tests in the diagnosis of urinary carcinoma in patients presenting hematuria, and a handful of these assays have already been approved by FDA (21–25). However, the effectiveness of cytology and imunocytology highly depends on the skills and experience of the pathologist and not the efficacy of the method (26). Generally, the FISH tests from previous research have usually been reporting a sensitivity of about 70%~80% in detecting urothelial cell carcinoma (8), nevertheless, the FISH test in our study was unable to obtain sensitivity in nearly half of UTUC+ cases (25/51). This explains its limitation in clinical practice, however, for a reliable conclusion, more experiments with larger sample sizes are necessary. On the other hand, we noted a single case of FISH positive UTUC+ with a negative panel test (RH350), this test result implies that our panel design can be improved by adding more content of chromosome structure variation or gene copy number variation detection.

After further analysis, an inference emerged that multiple gene mutations detected in a few patients with false-negative test results potentially indicate the need for close follow-up. After a lower ureterectomy, a patient with hematuria in our cohort was clinically diagnosed with ureteral inflammation in December 2017 through pathology testing. Furthermore, it was found that his *TERT*, *FGFR3*, *TP53*, and *PIK3CA* genes were mutated respectively and the *ONECUT2* methylation result was positive. As a consequence, regular follow-up on this patient was performed and diagnosed him with ureteral carcinoma in May 2019, suggesting that the changes in urine genomics potentially precede the changes in imaging and can detect minimal tumor existence beyond the surgical site. Therefore, patients with a double-positive result in testing needed regular follow-ups.

In tumor grade analysis, the proportion of patients with *TERT* promoter mutations was higher in low-grade UTUC than that in high-grade ones, which was in agreement with the results of the previous UTUC cohort studies (17). And *TERT* promoter mutations status showed a significant difference in muscle-invasive and non-muscle-invasive UTUC samples. However, this is a newly discovered conclusion that needs to be validated by large-scale research. Meanwhile, genes such as *TP53* and *FGFR3* also showed their roles in predicting the grade of UTUC, which further reflected the value of our gene mutation testing. Also, it is worth noting that a non-invasive urine biopsy test has shown its potential ability in predicting tumor grade and the risk of UTUC.

TERT promoter mutations that had been previously reported to be closely related to UTUC were indeed significant factors in our cohort. For instance, an optimized model that only combined *TERT* promoter mutation with *ONECUT2* methylation and age yielded a satisfactory performance in the prediction of the samples. This suggests that reducing the genes to be tested in the optimized product significantly reduces the cost and time for testing as well as maintaining high accuracy. Nevertheless, this optimization of testing panel calls for validation in a larger cohort.

Again, since the relationship between age and cancer has been observed, cutoffs based on age stratification should be considered in further studies. Besides, the majority of BC share similar histogenesis as UTUC, therefore we propose that this panel test should be externally validated in a larger prospective patient cohort which includes more patients with benign and malignant bladder disease.

Furthermore, this cohort excluded information on follow-ups in a few of the enrolled patients, particularly the ones diagnosed benignly in their first testing. This attempts to answer these questions: (1) can this panel be also utilized in clinical follow-up visits to minimize the times of unnecessary invasive operations for postoperative patients or reveal the recurrence in a much more convenient way; and (2) which of these frequently mutated genes or variants can be biomarkers for prognosis prediction or even indicators of different treatment choices.

CONCLUSION

In conclusion, we utilized the epigenetic biomarker *ONECUT2* for the first time in the detection of UTUC and discovered its superior performance. As a result, we developed an accurate testing panel combined with mutation of significant genes. Results suggested that this panel might result in a less extensive examination of low-risk patients and due to its high NPV, it reduces costs and discomfort among patients. Therefore, this panel provides clinicians with important predictions in addition to imaging and routine urine cytology analysis to significantly advance the diagnostic precision of UTUC. Meanwhile, a more precise disease management plan should be set up upon the discovery of a high-risk UTUC. Further validation in a large prospective cohort of a broad population is vital to confirm the true clinical value of this newly developed method.

DATA AVAILABILITY STATEMENT

The original contributions presented in the study are publicly available. This data can be found here: https://www.biosino.org/node/, accession number OEP001778.

ETHICS STATEMENT

The studies involving human participants were reviewed and approved by Medical Ethics Committee of PLA General Hospital. The patients provided their written informed consent to participate in this study. Written informed consent was obtained from the individuals for the publication of any potentially identifiable images or data included in this article.

AUTHOR CONTRIBUTIONS

HL and XZ designed and supervised the study. YX and YL searched the literatures. YX, XM, XA, JG, YL, TM, SW, and YJ participated in data acquisition. YX, XA, JG, YL, and KM did the data analysis and interpretation. YX, YL, TM, and JG drafted the manuscript. YX, YL, and YJ did statistical analysis. YX and YL gave critical revision of the manuscript for important intellectual content. All authors contributed to the article and approved the submitted version.

ACKNOWLEDGMENTS

We are grateful to the physicians at the Department of Urology, the First Medical Center of Chinese PLA General Hospital who contributed patient material.

SUPPLEMENTARY MATERIAL

The Supplementary Material for this article can be found online at: https://www.frontiersin.org/articles/10.3389/fonc.2020.597486/full#supplementary-material

SUPPLEMENTARY FIGURE 1 | ROC of the optimal model with the features of age and panel test results in the validation set.

REFERENCES

1. Siegel RL, Miller KD, Jemal A. Cancer statistics, 2018. *CA Cancer J Clin* (2018) 68(1):7–30. doi: 10.3322/caac.21442
2. Roupret M, Babjuk M, Comperat E, Zigeuner R, Sylvester RJ, Burger M, et al. European Association of Urology Guidelines on Upper Urinary Tract Urothelial Carcinoma: 2017 Update. *Eur Urol* (2018) 73(1):111–22. doi: 10.1016/j.eururo.2017.07.036
3. Chow LC, Kwan SW, Olcott EW, Sommer G. Split-bolus MDCT urography with synchronous nephrographic and excretory phase enhancement. *AJR Am J Roentgenol* (2007) 189:314–22. doi: 10.2214/AJR.07.2288
4. Jinzaki M, Matsumoto K, Kikuchi E, Sato K, Horiguchi Y, Nishiwaki Y, et al. Comparison of CT urography and excretory urography in the detection and localization of urothelial carcinoma of the upper urinary tract. *AJR Am J Roentgenol* (2011) 196(5):1102–9. doi: 10.2214/AJR.10.5249
5. Streem SB, Pontes JE, Novick AC, Montie JE. Ureteropyeloscopy in the Evaluation of Upper Tract Filling Defects. *J Urol* (1986) 136(2):383–5. doi: 10.1016/S0022-5347(17)44875-0
6. Blute ML, Segura JW, Patterson DE, Benson RCJr, Zincke H. Impact of Endourology on Diagnosis and Management of Upper Urinary Tract Urothelial Cancer. *J Urol* (1989) 141:1298–301. doi: 10.1016/S0022-5347(17)41286-9
7. Harmon WJ, Sershon PD, Blute ML, Patterson DE, Segura JW. Ureteroscopy: Current Practice and Long-Term Complications. *J Urol* (1997) 157:28–32. doi: 10.1016/S0022-5347(01)65272-8
8. Schmitz-Dräger BJ, Droller M, Lokeshwar VB, Lotan Y, Hudson MA, van Rhijn BW, et al. Molecular Markers for Bladder Cancer Screening, Early Diagnosis, and Surveillance: The WHO/ICUD Consensus. *Urol Int* (2015) 94:1–24. doi: 10.1159/000369357
9. Killela PJ, Reitman ZJ, Jiao Y, Bettegowda C, Agrawal N, Diaz LA, et al. *TERT* Promoter Mutations Occur Frequently in Gliomas and a Subset of Tumors Derived from Cells with Low Rates of Self-Renewal. *Proc Natl Acad Sci* (2013) 110:6021–6. doi: 10.1073/pnas.1303607110
10. Huang DS, Wang Z, He XJ, Diplas BH, Yang R , Killela PJ, et al. Recurrent *TERT* Promoter Mutations Identified in a Large-Scale Study of Multiple Tumour Types Are Associated with Increased *TERT* Expression and Telomerase Activation. *Eur J Cancer* (2015) 51:969–76. doi: 10.1016/j.ejca.2015.03.010

11. Rodriguez Pena MDC, Tregnago AC, Eich ML, Springer S, Wang YX, Taheri D, et al. Spectrum of Genetic Mutations in de Novo PUNLMP of the Urinary Bladder. *Virchows Arch* (2017) 471:761–7. doi: 10.1007/s00428-017-2164-5
12. Netto GJ. Molecular Biomarkers in Urothelial Carcinoma of the Bladder: Are We There Yet? *Nat Rev Urol* (2012) 9:41–51. doi: 10.1038/nrurol.2011.193
13. The Cancer Genome Atlas Research Network. Comprehensive Molecular Characterization of Urothelial Bladder Carcinoma. *Nature* (2014) 507:315–22. doi: 10.1038/nature12965
14. Lee JY, Kim K, Sung HH, Jeon HG, Jeong BC, Seo S, et al. Molecular Characterization of Urothelial Carcinoma of the Bladder and Upper Urinary Tract. *Transl Oncol* (2018) 11:37–42. doi: 10.1016/j.tranon.2017.10.008
15. Moss TJ, Qi Y, Xi L, Peng B, Kim TB, Ezzedine NE, et al. Comprehensive Genomic Characterization of Upper Tract Urothelial Carcinoma. *Eur Urol* (2017) 72:641–9. doi: 10.1016/j.eururo.2017.05.048
16. Togneri FS, Ward DG, Foster JM, Devall AJ, Wojtowicz P, Alyas S, et al. Genomic Complexity of Urothelial Bladder Cancer Revealed in Urinary cfDNA. *Eur J Hum Genet* (2016) 24:1167–74. doi: 10.1038/ejhg.2015.281
17. Springer SU, Chen CH, Pena MDCR, Li L, Douville C, Wang YX, et al. Non-invasive detection of urothelial cancer through the analysis of driver gene mutations and aneuploidy. *Elife* (2018) 7:e32143. doi: 10.7554/eLife.32143
18. Guo RQ, Xiong GY, Yang KW, Zhang L, He SM, Gong YQ, et al. Detection of urothelial carcinoma, upper tract urothelial carcinoma, bladder carcinoma, and urothelial carcinoma with gross hematuria using selected urine-DNA methylation biomarkers: A prospective, single-center study. *Urol Onco Semin Ori* (2018) 7:313–48. doi: 10.1016/j.urolonc.2018.04.001
19. Yuan X, Liu C, Wang K, Liu L, Liu TT, Ge N, et al. The Genetic Difference between Western and Chinese Urothelial Cell Carcinomas: Infrequent *FGFR3* Mutation in Han Chinese Patients. *Oncotarget* (2016) 7:25826–35. doi: 10.18632/oncotarget.8404
20. Christensen E, Birkenkamp-Demtröder K, Nordentoft I, Hoyer S, van der Keur K, van Kessel K, et al. Liquid Biopsy Analysis of *FGFR3* and *PIK3CA* Hotspot Mutations for Disease Surveillance in Bladder Cancer. *Eur Urol* (2017) 71:961–9. doi: 10.1016/j.eururo.2016.12.016
21. van Kessel KE, Van Neste L, Lurkin I, Zwarthoff EC, Van Criekinge W. Evaluation of an Epigenetic Profile for the Detection of Bladder Cancer in Patients with Hematuria. *J Urol* (2016) 195:601–7. doi: 10.1016/j.juro.2015.08.085
22. Beukers W, Kandimalla R, van Houwelingen D, Kovacic H, Chin JF, Lingsma HF, et al. The Use of Molecular Analyses in Voided Urine for the Assessment of Patients with Hematuria. *PloS One* (2013) 8:e77657. doi: 10.1371/journal.pone.0077657
23. O'Sullivan P, Sharples K, Dalphin M, Davidson P, Gilling P, Cambridge L, et al. A Multigene Urine Test for the Detection and Stratification of Bladder Cancer in Patients Presenting with Hematuria. *J Urol* (2012) 188:741–7. doi: 10.1016/j.juro.2012.05.003
24. Sarosdy MF, Kahn PR, Ziffer MD, Love WR, Barkin J, Abara EO, et al. Use of a Multitarget Fluorescence In Situ Hybridization Assay to Diagnose Bladder Cancer in Patients With Hematuria. *J Urol* (2006) 176:44–7. doi: 10.1016/S0022-5347(06)00576-3
25. Roobol MJ, Bangma CH, El Bouazzaoui S, Franken-Raab CG, Zwarthoff EC. Feasibility Study of Screening for Bladder Cancer with Urinary Molecular Markers (the BLU-P Project). *Urol Oncol* (2010) 28:686–90. doi: 10.1016/j.urolonc.2009.12.002
26. Karakiewicz PI, Benayoun S, Zippe C, Ludecke G, Boman H, Sanchez-Carbayo M, et al. Institutional Variability in the Accuracy of Urinary Cytology for Predicting Recurrence of Transitional Cell Carcinoma of the Bladder. *BJU Int* (2006) 97:997–1001. doi: 10.1111/j.1464-410X.2006.06036.x

Conflict of Interest: YL, QZ, TM, KM, QZ, and SW were employed by the company Genetron Health (Beijing) Technology, Co. Ltd.

The remaining authors declare that the research was conducted in the absence of any commercial or financial relationships that could be construed as a potential conflict of interest.

frontiers in Oncology

ORIGINAL RESEARCH
published: 16 March 2021
doi: 10.3389/fonc.2021.626104

Prognostic Stratification of Metastatic Prostate Cancer Patients Treated With Abiraterone and Enzalutamide Through an Integrated Analysis of Circulating Free microRNAs and Clinical Parameters

Evgeniya Sharova[1†], Marco Maruzzo[2†], Paola Del Bianco[3], Ilaria Cavallari[1], Francesco Pierantoni[2], Umberto Basso[2‡], Vincenzo Ciminale[1,4*‡] and Vittorina Zagonel[2‡]*

[1] Immunology and Molecular Oncology Unit, Veneto Institute of Oncology IOV – IRCCS, Padua, Italy, [2] Oncology 1 Unit, Department of Oncology, Veneto Institute of Oncology IOV – IRCCS, Padua, Italy, [3] Clinical Research Unit, Veneto Institute of Oncology IOV – IRCCS, Padua, Italy, [4] Department of Surgery, Oncology and Gastroenterology, University of Padua, Padua, Italy

Androgen Receptor-Targeted Agents (ARTA) have dramatically changed the therapeutic landscape of metastatic Castration-Resistant Prostate Cancer (mCRPC), but 20–40% of these patients progress early after start of ARTA treatment. The present study investigated the potential utility of plasma cell-free microRNAs (cfmiRNAs) as prognostic markers by analyzing a prospective cohort of 31 mCRCP patients treated with abiraterone ($N = 10$) or enzalutamide ($N = 21$). Additional potential prognostic factors were extracted from clinical records and outcome was evaluated as overall survival (OS) and progression-free survival (PFS). cfmiRNAs were measured in plasma samples using quantitative real-time RT-PCR. Linear correlation among clinical factors and cfmiRNAs was assessed using the Spearman's rank correlation coefficient. The association with survival was studied using univariate and multivariate Cox proportional hazards models. Continuous variables were dichotomized with the cut points corresponding to the most significant relation with the outcome. Univariate analysis indicated that plasma levels of miR-21-5p, miR-141-3p and miR-223-3p, time to development of castration-resistance (tCRPC), and blood hemoglobin (Hb) levels strongly correlated with both PFS and OS. Multivariate analysis revealed that low plasma levels of miR-21, shorter tCRPC, and lower Hb values were independent factors predicting reduced PFS and OS. These findings suggest that the integrated analysis of cfmiRNAs, tCRPC, and Hb may provide a promising, non-invasive tool for the prognostic stratification of mCRPC patients treated with ARTA.

Keywords: mCRPC, cfmiRNA, abiraterone, enzalutamide, OS, PFS, prognostic biomarkers

OPEN ACCESS

Edited by:
Rui P. L. Neves, University Hospital Düsseldorf, Germany

Reviewed by:
Mario Eisenberger, Johns Hopkins Medicine, United States
Lucia Nappi, The Vancouver Prostate Centre, Canada

***Correspondence:**
Umberto Basso
umberto.basso@iov.veneto.it
Vincenzo Ciminale
v.ciminale@unipd.it

[†] These authors share first authorship

[‡] These authors share senior authorship

Specialty section:
This article was submitted to Cancer Molecular Targets and Therapeutics, a section of the journal Frontiers in Oncology

Received: *04 November 2020*
Accepted: *19 February 2021*
Published: *16 March 2021*

Citation:
Sharova E, Maruzzo M, Del Bianco P, Cavallari I, Pierantoni F, Basso U, Ciminale V and Zagonel V (2021) Prognostic Stratification of Metastatic Prostate Cancer Patients Treated With Abiraterone and Enzalutamide Through an Integrated Analysis of Circulating Free microRNAs and Clinical Parameters. Front. Oncol. 11:626104. doi: 10.3389/fonc.2021.626104

INTRODUCTION

The fact that tumor cells from metastatic castration-resistant prostate cancer (mCRPC) patients are still somewhat addicted to androgen signaling (1) posed the rational base for the design of next-generation Androgen Receptor-Targeted Agents (ARTA) that achieve profound inhibition of androgen signaling in these patients. These compounds include abiraterone, a CYP17A1 inhibitor that blocks the synthesis of androgenic precursors, and enzalutamide, which antagonizes AR activation and nuclear translocation (2). The introduction of ARTA has considerably improved the overall survival (OS) of mCRPC patients from 12–18 months to approximately 3 years in docetaxel-naïve patients (3–5). However, the evaluation of response to ARTA is challenging. A decline in the levels of Prostate Specific Antigen (PSA) blood levels in the first 4 weeks of treatment with ARTA was demonstrated to be correlated with OS in large retrospective trials (6). However, a reduction in PSA cannot be considered as a predictive factor "*per se*" in all cases since paradoxical PSA surges have been described in patients treated with ARTA (7). Therefore, there is a pressing need for additional biomarkers for the early identification of relapse and to guide the choice of the best treatment for the individual patient.

Several studies have highlighted the role of microRNAs (miRNAs) in the pathogenesis of PCa (8); among these, miR-21 and miR-141 play key regulatory roles in activation of the epithelial-mesenchymal transition (EMT) program, and their expression in cancer cells is correlated with patients' prognosis and response to therapy (8, 9). Circulating free miRNAs (cfmiRNAs) released by cancer cells as well as by cells of the tumor microenvironment are emerging as promising markers of disease, as they are resistant to degradation and are readily quantifiable. Our pilot study was aimed at investigating the possible relationship between cfmiRNAs and the clinical outcome of mCRPC patients treated with ARTA.

MATERIALS AND METHODS

Study Design and Patients

This exploratory prospective observational study was performed on a cohort of 31 mCRPC patients treated with abiraterone (10 patients) or enzalutamide (21 patients); ARTA was administered either as first-line therapy (26 patients) or after treatment with docetaxel (five patients). All consecutive patients who were candidates to receive ARTA and were eligible according to the study criteria were enrolled between September 2016 and October 2017 at the Veneto Institute of Oncology. The study was conducted according to the Declaration of Helsinki and approved by the local Ethics Committee; all patients signed an informed consent form prior to their inclusion.

Patients were selected according to the following inclusion criteria: (i) histological diagnosis of prostate cancer; (ii) metastatic disease at any site; (iii) mCRPC according to the Prostate Cancer Working Group 3 (PCWG3) definition (10); (iv) at least 6 months of life expectancy; (v) patients receiving bisphosphonates or antiresorptive drugs were included in the study if these treatments started before enrolment or after the first disease assessment. Patients with known cerebral lesions or impending spinal cord compression were excluded from study, as well as subjects with severe cardiovascular or metabolic diseases or swallowing problems contraindicating the administration of ARTA. Patients with previous exposure to second-line chemotherapy (cabazitaxel) or other second-line treatment were also excluded from the study.

At the start of ARTA treatment blood samples were collected for the miRNA analyses. All the patients were then treated as per clinical practice, according to the drugs' current label authorization and international guidelines for the treatment of mCRPC. ARTA therapy was administered until progression and clinical need to start another therapy, or when the patient experienced unacceptable toxicity or decided to withdraw from treatment. Disease progression was defined according to the PCWG3 criteria. No change in patients' management was introduced based on the results of the biomarker analysis. Comorbidities and contraindications to steroids guided the choice between abiraterone and enzalutamide. Adverse events were documented and treated in line with the best clinical practice.

Clinical examination and assessment of hematological and biochemical parameters were performed on a monthly basis during treatment. Disease restaging was performed every 3 to 4 months with serum PSA quantification and contrast-enhanced CT scan of the thorax, abdomen and pelvis plus bone scan, or with a total body CT/PET scan with ^{18}F-choline. Plasma samples for miRNA analysis were obtained within 1 day before the start of ARTA. After disease progression, all the patients were followed up for survival, and received further lines of therapy or only best supportive care (BSC) according to their performance status and fitness to treatment, as indicated by the national and international guidelines for mCRPC.

Sample Processing and miRNA Quantification

Blood samples were collected in EDTA-containing tubes at room temperature and processed for plasma isolation within 2 h as described by Cavallari et al. (11). Plasma samples were assayed for haemolysis (the presence of free hemoglobin corrected for lipoproteins) by measuring absorbance at 385 nm and 414 nm with a NanoDrop® ND-1000 UV-Vis spectrophotometer (Thermo Fisher Scientific) as described elsewhere (12) (**Supplementary Table 1**). Plasma samples were aliquoted and stored at −80°C. Total RNA (<1,000 nt/bp size range) was extracted from 300 μl of plasma with the Nucleo Spin miRNA plasma kit (Macherey-Nagel) following the manufacturer's instructions and eluted in 30 μl of RNAse-free water. Samples were analyzed for miRNA expression using specific TaqMan stem-loop reverse-transcription and PCR primer/probe assays (Thermo Fisher Scientific) in a Roche Light Cycler 480 thermal cycler as described by Sharova et al. (13). The following miRNAs were examined: hsa-miR-141-3p (Assay ID 000463), hsa-miR-223-3p (Assay ID 002295), and hsa-miR-21-5p (Assay ID 000397), chosen because of their reported relevance to mCRPC (14). Ct values obtained for the miRNAs

TABLE 1 | Patients' characteristics before the start of ARTA.

		Abiraterone Acetate (*N*=10)	Enzalutamide (*N*=21)	Total (*N* = 31)	*P*-value
Age, years	Median (Q1–Q3)	69.5 (66.5;73.2)	78 (73;82)	75 (69.5;80.5)	*0.031‡*
PSA, ng/ml	Median (Q1–Q3)	33.3 (8.2;65.7)	19.2 (9.4;53.4)	19.2 (8.4;58.6)	*0.767‡*
Time to CRCP, months	Median (Q1–Q3)	36.5 (19.5;48.9)	38.1 (19.2;56.4)	38.1 (19.1;53.1)	*0.800‡*
N, 10^9/L	Median (Q1-Q3)	4.1 (2.7;5.1)	3.7 (2.7;5.0)	3.7 (2.7;5.0)	*0.767‡*
Ly, 10^9/L	Median (Q1-Q3)	1.6 (1.1;2.1)	1.8 (1.4;2.4)	1.7 (1.3;2.3)	*0.228‡*
N/L	Median (Q1–Q3)	2.3 (1.4;4.3)	1.7 (1.4;2.4)	1.9 (1.4;3.0)	*0.375‡*
Hb, g/L	Median (Q1–Q3)	134.5 (129.2;135.0)	131.0 (122.0;135.0)	132.0 (124.5;135.0)	*0.421‡*
Site of metastasis	Lymph node	2 (20.0%)	5 (23.8%)	7 (22.6%)	*1.00°*
	Bone	5 (50.0%)	9 (42.8%)	14 (45.2%)	
	Lymph node, bone	3 (30.0%)	6 (28.6%)	9 (29.0%)	
	Visceral	0	1 (4.8%)	1 (3.2%)	
ECOG PS	0	6 (60.0%)	4 (19.0%)	10 (32.3%)	*0.040°*
	1–2	4 (40.0%)	17 (81.0%)	21 (67.7%)	
Gleason score	<=7 (5–7)	3 (30.0%)	4 (22.2%)	7 (25.0%)	*0.674°*
	>7 (8–10)	7 (70.0%)	14 (77.8%)	21 (75.0%)	
	Missing		3	3	

PSA, prostate-specific antigen; Time to CRPC, time to development of castration-resistance; N, neutrophils; Ly, lymphocytes; N/L, neutrophil-lymphocyte ratio; HB, hemoglobin; ECOG PS, Eastern Cooperative Oncology Group Performance Status. Data are expressed as median (interquartile range) for continuous data and n (percentage) for categorical data. ‡ Kruskal-Wallis test; °Fisher's Exact Test.

of interest were normalized against the Ct values measured for hsa-miR-1228-3p (Assay ID 002919) using the formula $2^{-\Delta Ct} = 2^{-(\text{CtmiRx}-\text{CtmiR1228})}$. miR-1228 was chosen as the normalizer based on its prior use as a normalizer in studies of prostate cancer patients (15, 16). Our assays confirmed the low variability of miR-1228 levels in the plasma samples studied here (**Supplementary Table 1**).

Statistical Analysis

Clinical variables to be tested as prognostic factors were PSA, type of ARTA, performance status, time to CRPC, neutrophil/lymphocyte ratio, hemoglobin and Gleason score. Quantitative variables were described as median and interquartile range, categorical variables were summarized as counts and percentages. The median follow-up time was based on the reverse Kaplan-Meier estimator. The association of patients' characteristics with the treatment received was assessed using the $\chi 2$ or Fisher exact test as appropriate. The linear correlation between continuous clinical variables and cfmiRNAs was assessed using the Spearman's rank correlation coefficient.

OS was defined as the time from the start of treatment with ARTA to death, and progression-free survival (PFS) was calculated from the start of treatment with ARTA to the date of radiological/clinical disease progression, or death. Patients who did not develop an event during the study period were censored at the date of the last observation. The cfmiRNAs were dichotomized with cut points corresponding to the most significant relation with the outcome, estimated from maximally selected log-rank statistic for values between the 10 and 90% quantiles using the upper bound of the *p*-value by Hothorn and Lausen (17).

Survival curves were estimated with the non-parametric Kaplan-Meier method and comparisons among strata were performed using the log-rank test. The 95% confidence interval (CI) for the median survival was calculated according to Brookmeyer and Crowley. Hazard ratios (HR) and 95% CI for each group were estimated using univariate Cox proportional hazards models with Efron's method of tie handling. No deviation from the proportional hazards assumption was found by the test statistic of Grambsch and Therneau (18). To assess the False-Discovery-Rate, *p*-values were adjusted by applying the Benjamini-Hochberg correction (19).

The independent role of each covariate in predicting survival was verified in a multivariable model considering all characteristics significantly associated with the outcome in the univariate analyses. All statistical tests were two-sided and a *p*-value <0.05 was considered statistically significant. Statistical analyses were performed using RStudio (RStudio: Integrated Development for R. RStudio Inc., Boston, MA, U.S.A.).

RESULTS

Characteristics of the Patient Cohort

Thirty-one mCRPC patients were enrolled in the present study, 10 of whom were treated with abiraterone acetate and 21 with enzalutamide (**Table 1**). The median age was 75 years (range 69.5–80.5). Thirteen patients had stage IV disease at diagnosis of prostate cancer. All patients had been treated with ADT using Luteinizing Hormone Releasing Hormone (LHRH) analogs or antagonists after evidence of metastatic disease. The median time from start of ADT to castration resistance was 38.1 months. Five patients were previously exposed to docetaxel. Docetaxel-treated

patients did not show a significant difference in the levels of the cfmiRNAs examined (miR-21, miR-141 and miR-223) compared to chemonaïve patients. 75% of all patients had a Gleason score greater than 8 at diagnosis. At the study's conclusion, 26 patients had progressed and 13 died. The median PFS was 19.3 months (95%CI 11.7–29.6) (**Supplementary Table 2**). The median OS was not reached (**Supplementary Table 3**). The median follow-up time was 36.6 months (95%CI: 35.4–39.3). Upon development of disease progression, 14 patients received only BSC, 10 were treated with docetaxel, 2 with cabazitaxel, 3 with Radium^{223}, 1 with a second ARTA (abiraterone) and 1 with oral cyclophosphamide.

Plasma Levels of miR-21 and tCRPC Predict PFS of mCRPC Patients

A series of statistical analyses was performed to interrogate the possible prognostic value of plasma levels of miR-21, miR-141, and miR-223 (all normalized against miR-1228) measured for mCRPC patients at the start of ARTA treatment (see section Materials and Methods).

Univariate analysis indicated a significant association between plasma levels of miR-21, miR-141, miR-223 and PFS (**Figure 1A** and **Supplementary Figure 1**). Low plasma levels of miR-21 ($2^{-\Delta Ct} \leq 2.69$) and miR-223 ($2^{-\Delta Ct} \leq 4.35$) and high plasma miR-141 values ($2^{-\Delta Ct} > 0.20$) were significantly associated with shorter PFS in all patients. In addition, shorter tCRPC (≤15.2 months) and low blood hemoglobin (≤127 g/L) were also significantly correlated with reduced PFS. N/L, PSA values, and the Gleason score at the start of ARTA treatment were not related to clinical outcome in our cohort.

Figure 1B shows results of multivariable Cox regression analysis, indicating that only normalized plasma miR-21 levels and tCRPC were independent predictors of PFS.

The median PFS was 2.1 months for patients with shorter tCRPC and low miR-21 values (95%CI: 2.1-NE), 11.7 months for patients with one risk factor (shorter tCRPC or low miR-21 values) (95%CI: 8.7-NE) and 29.3 months for patients with longer tCRPC and high miR-21 values (95%CI: 20.1_NE) (**Figure 3A**).

Plasma Levels of miR-21, Anemia and tCRPC Are Independent Predictors of OS for mCRPC Patients

In univariate analysis, OS was correlated with the plasma levels of miR-21, miR-141, and miR-223, and with tCRPC and Hb (**Figure 2A**). **Figure 2B** shows the results of the multivariate Cox regression model revealing three independent factors predicting OS: plasma levels of miR-21, blood Hb and tCRPC.

The median OS was not reached for patients with longer tCRPC, high hemoglobin concentration and high plasma miR-21 values (i.e., no risk factors). The median OS was 36.0 months (95%CI: 12.3-NE) for patients with one risk factor, 18.7 months (95%CI: 8.4-NE) for patients with two risk factors, and 4.6 months (95%CI: 3.4-NE) for patients with shorter tCRPC, low Hb concentration and low plasma miR-21 values (**Figure 3B**).

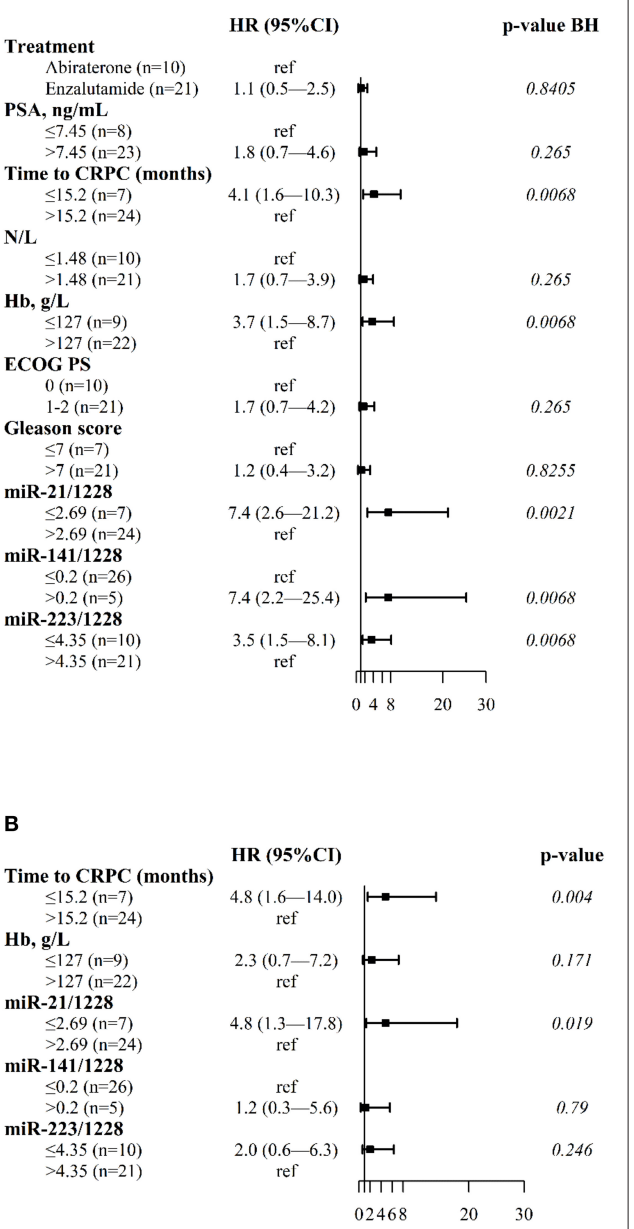

FIGURE 1 | Forest plots of clinical variables and cfmiRNAs associated with PFS. **(A)** Univariate Cox regression model; **(B)** Multivariable Cox regression model. Indicated are the hazard ratios (HR) and 95% confidence intervals (CI) and corresponding *p*-values; *p*-value BH indicates the *p*-values determined using the Benjamini-Hochberg correction for multiple tests. Ref indicates the reference value for calculating the hazard ratio.

No significant correlation was found between plasma miR-21 levels and clinical variables (**Supplementary Table 4**). Plasma miR-21 levels were strongly correlated with plasma miR-223 levels ($r = 0.71$; $p < 0.001$) (**Supplementary Table 4**).

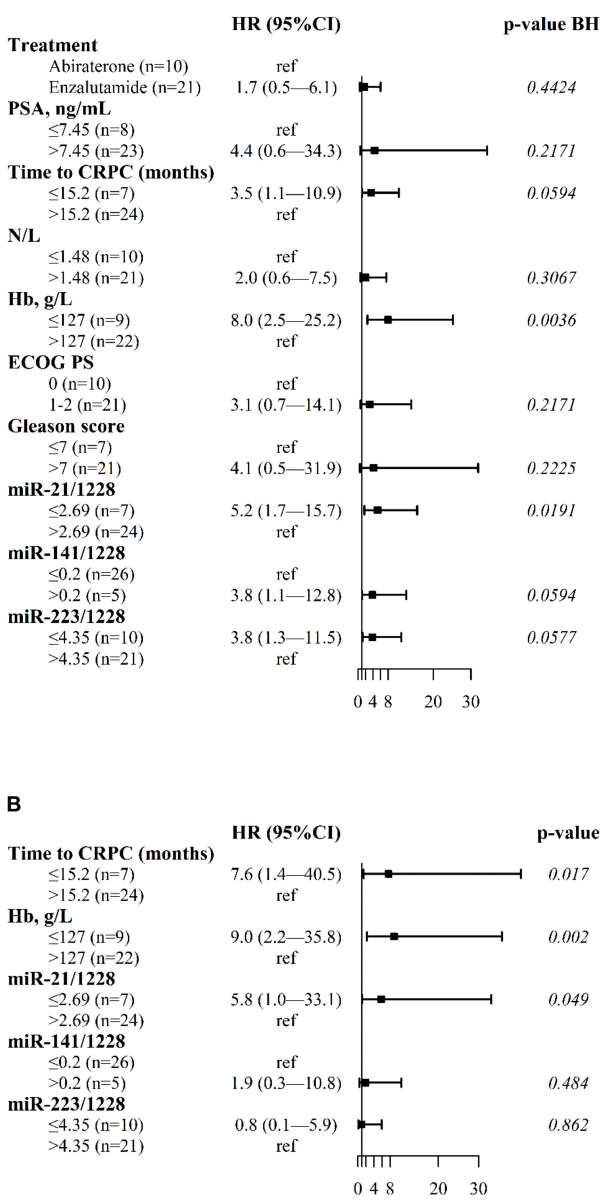

FIGURE 2 | Forest plots of clinical variables and cfmiRNAs associated with OS. **(A)** Univariate Cox regression model **(B)** Multivariable Cox regression model. Indicated are the hazard ratios (HR) and 95% confidence intervals (CI) and corresponding *p*-values; *p*-value BH indicates the *p*-values determined using the Benjamini-Hochberg correction for multiple tests. Ref indicates the reference value for calculating the hazard ratio.

DISCUSSION

The present study explored the relationship between circulating miR-21, miR-141 and miR-223 and clinical outcome of patients with mCRPC treated with ARTA. Among the miRNAs tested, high expression of miR-21 was the best predictor of favorable PFS and OS after treatment with abiraterone or enzalutamide in our cohort of patients.

To date, few studies have analyzed circulating miR-21 in mCRPC. In an analysis of plasma/serum samples from 97 mCRPC patients, Lin et al. (20) found that low levels of miR-21 correlated with a shorter OS following treatment with docetaxel. A recent analysis by Benoist et al. of miRNAs in whole blood samples did not reveal significant differences in the levels of miR-21 or miR-141 in mCRPC patients treated with enzalutamide compared to healthy volunteers (21). However, miRNAs detected in whole blood samples will be predominantly represented by those contained in erythrocytes, platelets and leukocytes, which likely mask the contribution of circulating cell-free miRNAs.

The relationship between miR-21 and androgen-responsive signaling pathways was investigated by Mishra et al. who proposed a positive feedback loop mechanism in prostate cancer cells (22). Androgen receptor (AR) signaling directly enhances miR-21 gene transcription through androgen response elements (AREs) within the miR-21 promoter region (23). miR-21 in turn inhibits expression of the tumor suppressor protein phosphate and tensin homolog deleted on chromosome 10 (PTEN) (24), which negatively controls the AR. Interestingly, PTEN is frequently mutated or deleted in CRPC (25). These feedback connections between miR-21, the AR, and PTEN suggest that high plasma levels of miR-21 might be an indicator of increased AR activity in cancer cells, which is predictive of response to ARTA. This hypothesis is consistent with our results indicating that ARTA-treated patients with high plasma miR-21 levels might have a more favorable PFS and OS compared to those with low levels.

Our finding of higher plasma levels of miR-141 in patients with shorter PFS and OS in the univariate analysis is in line with the results of previous studies showing increased plasma/serum levels of miR-141 in patients with mCRPC compared to healthy/benign prostatic hyperplasia (BPH) subjects (26, 27) or patients with localized prostate cancer (28, 29). A member of the miR-200 family, miR-141 is involved in the epithelial-mesenchymal transition and is thus likely to play an important role in the clinical progression of PC (30). In addition, miR-141 was shown to target the expression of small heterodimer partner (SHP), a corepressor that blunts the activation of target genes by the AR (31). Our findings are coherent with the results of a recent study showing that high plasma levels of miR-141 are associated with shorter PFS/OS in a cohort of mCRPC patients (32).

We previously reported downregulation of cfmiR-223 in plasma from patients with localized PC compared to BPH controls (13), which is consistent with another study that revealed downregulation of miR-223 in CRPC and PC tissues compared to non-PC control samples (33). Consistent with these observations, Kurozumi et al. suggested a tumor suppressor role for this miRNA through regulation of the integrin receptors ITGA3 and ITGB1, a function that might affect the metastatic potential of PC cells (34). There is also evidence that miR-223 is abundantly expressed in macrophages and is transferred to malignant cells, where it inhibits their proliferation (35). Our finding that patients with low PFS/OS exhibit lower plasma levels of miR-223 may

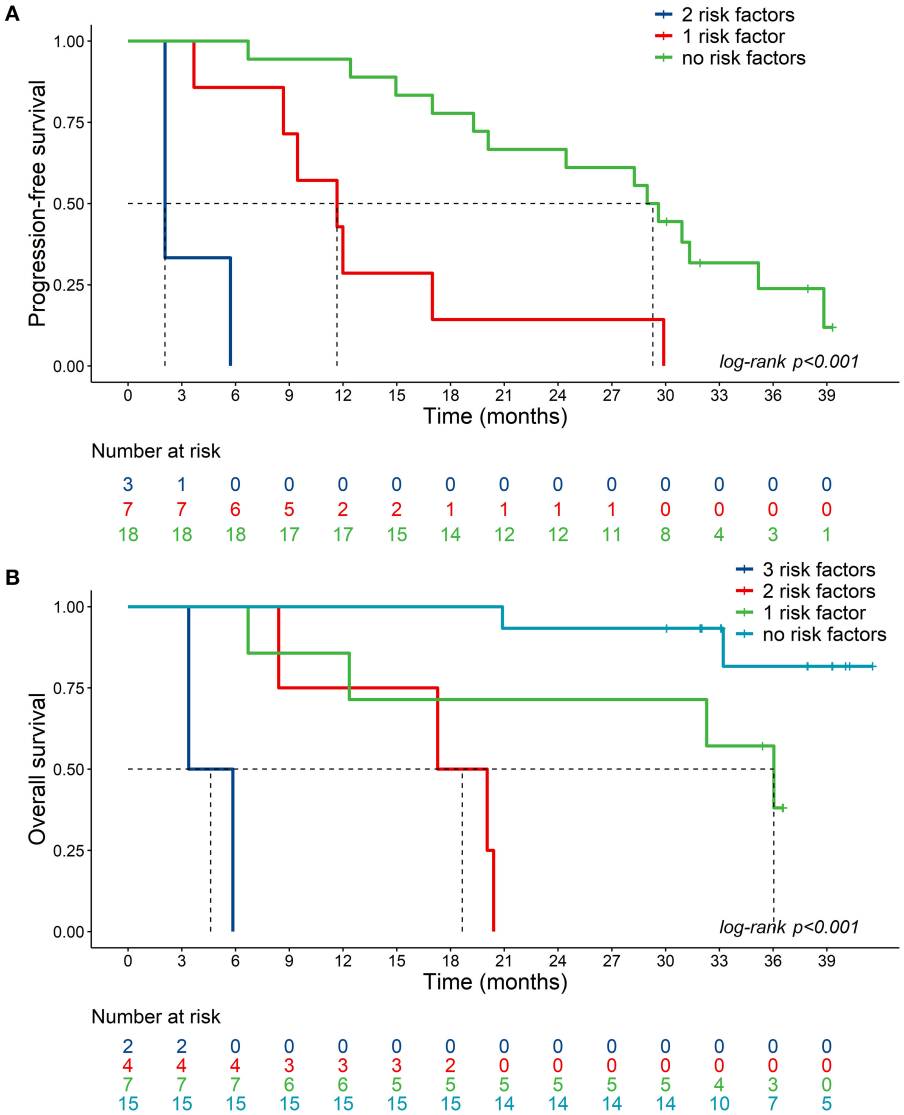

FIGURE 3 | Kaplan-Meier plots. **(A)** Kaplan–Meier plots of PFS in mCRPC patients with high plasma miR-21 levels and long tCRPC (no risk factors, miR-21>2.69, tCRPC>15.2), low plasma miR-21 or short tCRPC (1 risk factor, miR-21≤2.69, tCRPC>15.2, or miR-21>2.69, tCRPC≤15.2), low plasma miR-21 and short tCRPC (2 risk factors, miR-21≤2.69, tCRPC≤15.2); **(B)** Kaplan–Meier plots of OS in mCRPC patients with high miR-21/1228, high hemoglobin and long tCRPC (no risk factors, miR-21>2.69, Hb>127, tCRPC>15.2); low plasma miR-21, or low hemoglobin or short tCRPC (1 risk factor, miR-21≤2.69, Hb>127, tCRPC>15.2 or miR-21>2.69, Hb≤127, tCRPC>15.2 or miR-21>2.69, Hb>127, tCRPC≤15.2); 2 out of 3 of these risk factors (miR-21≤2.69, Hb≤127, tCRPC>15.2 or miR-21≤2.69, Hb>127, tCRPC≤15.2 or miR-21>2.69, Hb≤127, tCRPC≤15.2); low plasma miR-21, low hemoglobin and short tCRPC (3 risk factors, miR-21≤2.69, Hb≤127, tCRPC≤15.2).

thus reflect a reduced immune response in patients with worse clinical outcome.

Multivariable analysis showed that the plasma level of miR-21 (but not miR-223 or miR-141) was associated with outcome (OS and PFS), independently of other clinical variables. In our evaluation of different clinical parameters usually included in prognostic/predictive models of metastatic prostate cancer (36) time to development of castration resistance and Hb levels were confirmed as independent prognostic factors for OS, findings in line with the results of previous studies of mCRPC patients treated with enzalutamide (37). Interestingly, low Hb levels are also associated with poor survival in several other tumor types (38).

The results presented here are promising, but must be considered preliminary, due to the limited number of patients examined, which reflects the exploratory nature of the study that implies the lack of any previous information required to carry out a power analysis and determine the appropriate sample size. In addition, our cohort included five patients who were previously treated with docetaxel. Although it is possible that docetaxel may alter tumor biology and influence

miRNA expression, in the context of our study, docetaxel-treated patients did not show a significant difference in the levels of the cfmiRNA examined compared to chemonaïve patients; furthermore chemotherapy is currently administered at very early stages of disease and is not considered cross-resistant with ARTA.

Taken together, our findings suggest that the integration of the analysis of cfmiR-21 with the clinical parameters tCRPC and Hb levels may provide useful information for the prognostic stratification of mCRCP patients receiving ARTA treatment, and lay the ground for a large prospective validation study.

DATA AVAILABILITY STATEMENT

The original contributions presented in the study are included in the article/**Supplementary Materials**, further inquiries can be directed to the corresponding author/s.

ETHICS STATEMENT

The studies involving human participants were reviewed and approved by Ethics Committee of the Veneto Institute of Oncology. The patients/participants provided their written informed consent to participate in this study.

AUTHOR CONTRIBUTIONS

ES, VC, UB, and MM conceived and designed the experiments. ES performed the experiments. MM, UB, and FP followed the patients, including planning clinical visits and blood sample collection, follow-up and clinical data collection. PDB performed statistical analysis. ES, IC, PDB, VC, MM, and VZ analyzed the results. ES, MM, UB, and VC wrote and revised the paper. All authors reviewed the manuscript.

FUNDING

This study was supported by 5×1000 funding from the Veneto Institute of Oncology IOV – IRCCS and by the BIRD 205490 grant from the University of Padova.

ACKNOWLEDGMENTS

The authors would like to thank Donna M. D'Agostino for discussions.

SUPPLEMENTARY MATERIAL

The Supplementary Material for this article can be found online at: https://www.frontiersin.org/articles/10.3389/fonc.2021.626104/full#supplementary-material

REFERENCES

1. Huang Y, Jiang X, Liang X, Jiang G. Molecular and cellular mechanisms of castration resistant prostate cancer. *Oncol Lett*. (2018) 15:6063–76. doi: 10.3892/ol.2018.8123
2. Hoffman-Censits J, Kelly WK. Enzalutamide: a novel antiandrogen for patients with castrate-resistant prostate cancer. *Clin Cancer Res*. (2013) 19:1335–9. doi: 10.1158/1078-0432.CCR-12-2910
3. Tannock IF, de Wit R, Berry WR, Horti J, Pluzanska A, Chi KN, et al. Docetaxel plus prednisone or mitoxantrone plus prednisone for advanced prostate cancer. *N Engl J Med*. (2004) 351:1502–12. doi: 10.1056/NEJMoa040720
4. Ryan CJ, Smith MR, Fizazi K, Saad F, Mulders PF, Sternberg CN, et al. Abiraterone acetate plus prednisone versus placebo plus prednisone in chemotherapy-naive men with metastatic castration-resistant prostate cancer (COU-AA-302): final overall survival analysis of a randomised, double-blind, placebo-controlled phase 3 study. *Lancet Oncol*. (2015) 16152–60. doi: 10.1016/S1470-2045(14)71205-7
5. Beer TM, Armstrong AJ, Rathkopf D, Loriot Y, Sternberg CN, Higano CS, et al. Enzalutamide in men with chemotherapy-naïve metastatic castration-resistant prostate cancer, extended analysis of the phase 3 PREVAIL study. *Eur Urol*. (2017) 71:151–154. doi: 10.1016/j.eururo.2016.07.032
6. Rescigno P, Dolling D, Conteduca V, Rediti M, Bianchini D, Lolli C, et al. De bono, early post-treatment prostate-specific antigen at 4 weeks and abiraterone and enzalutamide treatment for advanced prostate cancer, an international collaborative analysis. *Eur Urol Oncol*. (2020) 3:176–182. doi: 10.1016/j.euo.2019.06.008
7. Ryan CJ, Shah S, Efstathiou E, Smith MR, Taplin ME, Bubley GJ, et al. Phase II study of abiraterone acetate in chemotherapy-naive metastatic castration-resistant prostate cancer displaying bone flare discordant with serologic response. *Clin Cancer Res*. (2011) 17:4854–61. doi: 10.1158/1078-0432.CCR-11-0815
8. Cochetti G, Rossi de Vermandois JA, Maulà V, Giulietti M, Cecati M, Del Zingaro M, et al. Role of miRNAs in prostate cancer, Do we really know everything? *Urol Oncol*. (2020) 38:623–635. doi: 10.1016/j.urolonc.2020.03.007
9. Razdan A, de Souza P, Roberts TL. Role of microRNAs in treatment response in prostate cancer. *Curr Cancer Drug Targets*. (2018) 18:929–944. doi: 10.2174/1568009618666180315160125
10. Scher HI, Morris MJ, Stadler WM, Higano C, Basch E, Fizazi K, et al. Trial design and objectives for castration-resistant prostate cancer, updated recommendations from the prostate cancer clinical trials working group 3. *J Clin Oncol*. (2016) 34:1402–18. doi: 10.1200/JCO.2015.64.2702
11. Cavallari I, Grassi A, Del Bianco P, Aceti A, Zaborra C, Sharova E, et al. Prognostic stratification of bladder cancer patients with a microRNA-based approach. *Cancers (Basel)*. (2020) 12:3133. doi: 10.3390/cancers12113133
12. Appierto V, Callari M, Cavadini E, Morelli D, Daidone MG, Tiberio P. A lipemia-independent NanoDrop(®)-based score to identify hemolysis in plasma and serum samples. *Bioanalysis*. (2014) 6:1215–26. doi: 10.4155/bio.13.344
13. Sharova E, Grassi A, Marcer A, Ruggero K, Pinto F, Bassi P, et al. A circulating miRNA assay as a first-line test for prostate cancer screening. *Br J Cancer*. (2016) 114:1362–6. doi: 10.1038/bjc.2016.151
14. Thieu W, Tilki D, R. de Vere White and Evans CP. The role of microRNA in castration-resistant prostate cancer. *Urol Oncol*. (2014) 32:517–523. doi: 10.1016/j.urolonc.2013.11.004
15. Zhao H, Ma TF, Lin J, Liu LL, Sun WJ, Guo LX, et al. Identification of valid reference genes for mRNA and microRNA normalisation in prostate cancer cell lines. *Sci Rep*. (2018) 8:1949 doi: 10.1038/s41598-018-19458-z
16. Hu J, Wang Z, Liao BY, Yu L, Gao X, Lu S, et al. Human miR-1228 as a stable endogenous control for the quantification of circulating microRNAs in cancer patients. *Int J Cancer*. (2014) 135:1187–94. doi: 10.1002/ijc.28757
17. Hothorn T, Lausen B. On the exact distribution of maximally selected rank statistics. *Comput. Stat. Data Anal*. (2003) 43:121–137 doi: 10.1016/s0167-9473(02)00225-6

18. Grambsch PM, Therneau TM. Proportional hazards tests and diagnostics based on weighted residuals. *Biometrika*. (1994) 81:515–526. doi: 10.2307/2337123
19. Benjamini Y, Hochberg Y. Controlling the false discovery rate, a practical and powerful approach to multiple testing. *J R Stat Soc. [Ser B]*. (1995) 57:289–300.
20. Lin HM, Castillo L, Mahon KL, Chiam K, Lee BY, Nguyen Q, et al. Circulating microRNAs are associated with docetaxel chemotherapy outcome in castration-resistant prostate cancer. *Br J Cancer*. (2014) 110:2462–71. doi: 10.1038/bjc.2014.181
21. Benoist GE, van Oort IM, Boerrigter E, Verhaegh GW, van Hooij O, Groen L, et al. Prognostic value of novel liquid biomarkers in patients with metastatic castration-resistant prostate cancer treated with enzalutamide, a prospective observational study. *Clin Chem*. (2020) 66:842–851. doi: 10.1093/clinchem/hvaa095
22. Mishra S, Deng JJ, Gowda PS, Rao MK, Lin CL, Chen CL, et al. Androgen receptor and microRNA-21 axis downregulates transforming growth factor beta receptor II (TGFBR2) expression in prostate cancer. *Oncogene*. (2014) 33:4097–106. doi: 10.1038/onc.2013.374
23. Ribas J, Ni X, Haffner M, Wentzel EA, Salmasi AH, Chowdhury WH, et al. Lupold: miR-21: an androgen receptor-regulated microRNA that promotes hormone-dependent and hormone-independent prostate cancer growth. *Cancer Res*. (2009) 69:7165–9. doi: 10.1158/0008-5472.CAN-09-1448
24. Lin HK, Hu YC, Lee DK, Chang C. Regulation of androgen receptor signaling by PTEN (phosphatase and tensin homolog deleted on chromosome 10) tumor suppressor through distinct mechanisms in prostate cancer cells. *Mol Endocrinol*. (2004) 18:2409–23. doi: 10.1210/me.2004-0117
25. Kwabi-Addo B, Giri D, Schmidt K, Podsypanina K, Parsons R, Greenberg N, et al. Haploinsufficiency of the Pten tumor suppressor gene promotes prostate cancer progression. *Proc Natl Acad Sci USA*. (2001) 98:11563–8. doi: 10.1073/pnas.201167798
26. Cheng HH, Mitchell PS, Kroh EM, Dowell AE, Chéry L, Siddiqui J, et al. Circulating microRNA profiling identifies a subset of metastatic prostate cancer patients with evidence of cancer-associated hypoxia. *PLoS ONE*. (2013) 8:e69239 doi: 10.1371/journal.pone.0069239
27. Selth LA, Townley S, Gillis JL, Ochnik AM, Murti K, Macfarlane RJ, et al. Discovery of circulating microRNAs associated with human prostate cancer using a mouse model of disease. *Int J Cancer*. (2012) 131:652–61. doi: 10.1002/ijc.26405
28. Watahiki A, Macfarlane RJ, Gleave ME, Crea F, Wang Y, Helgason CD, et al. Plasma miRNAs as biomarkers to identify patients with castration-resistant metastatic prostate cancer. *Int J Mol Sci*. (2013) 14:7757–70. doi: 10.3390/ijms14047757
29. Nguyen HC, Xie W, Yang M, Hsieh CL, Drouin S, Lee GS, et al. Expression differences of circulating microRNAs in metastatic castration resistant prostate cancer and low-risk, localized prostate cancer. *Prostate*. (2013) 73:346–54. doi: 10.1002/pros.22572
30. Gao Y, Feng B, Han S, Zhang K, Chen J, Li C, et al. The roles of microRNA-141 in human cancers, from diagnosis to treatment. *Cell Physiol Biochem*. (2016) 38:427–48. doi: 10.1159/000438641
31. Xiao J, Gong AY, Eischeid AN, Chen D, Deng C, Young CY, et al. miR-141 modulates androgen receptor transcriptional activity in human prostate cancer cells through targeting the small heterodimer partner protein. *Prostate*. (2012) 72:1514–22. doi: 10.1002/pros.22501
32. Zedan AH, Osther PJS, Assenholt J, Madsen JS, Hansen TF. Circulating miR-141 and miR-375 are associated with treatment outcome in metastatic castration resistant prostate cancer. *Sci Rep*. (2020) 10:227. doi: 10.1038/s41598-019-57101-7
33. Goto Y, Kojima S, Nishikawa R, Kurozumi A, Kato M, Enokida H, et al. MicroRNA expression signature of castration-resistant prostate cancer: the microRNA-221/222 cluster functions as a tumour suppressor and disease progression marker. *Br J Cancer*. (2015) 113:1055–65. doi: 10.1038/bjc.2015.300
34. Kurozumi A, Goto Y, Matsushita R, Fukumoto I, Kato M, Nishikawa R, et al. Tumor-suppressive microRNA-223 inhibits cancer cell migration and invasion by targeting ITGA3/ITGB1 signaling in prostate cancer. *Cancer Sci*. (2016) 107:84–94. doi: 10.1111/cas.12842
35. Aucher A, Rudnicka D, Davis DM. MicroRNAs transfer from human macrophages to hepato-carcinoma cells and inhibit proliferation. *J Immunol*. (2013) 191:6250–60. doi: 10.4049/jimmunol.1301728
36. Armstrong AJ, Eisenberger MA, Halabi S, Oudard S, Nanus DM, Petrylak DP, et al. Biomarkers in the management and treatment of men with metastatic castration-resistant prostate cancer. *Eur Urol*. (2012) 61:549–59. doi: 10.1016/j.eururo.2011.11.009
37. Miyazawa Y, Sekine Y, Shimizu N, Takezawa Y, Nakamura T, Miyao T, et al. An exploratory retrospective multicenter study of prognostic factors in mCRPC patients undergoing enzalutamide treatment, Focus on early PSA decline and kinetics at time of progression. *Prostate*. (2019) 79:1462–1470. doi: 10.1002/pros.23865
38. Zhang YH, Lu Y, Lu H, Zhang MW, Zhou YM, Li XL. Pretreatment hemoglobin level is an independent prognostic factor in patients with lung adenocarcinoma. *Can Respir J*. (2018) 2018:6328127. doi: 10.1155/2018/6328127

Conflict of Interest: The authors declare that the research was conducted in the absence of any commercial or financial relationships that could be construed as a potential conflict of interest.

frontiers in Oncology

REVIEW
published: 16 April 2021
doi: 10.3389/fonc.2021.634316

The Role of Liquid Biopsy in Early Diagnosis of Lung Cancer

Cláudia Freitas[1,2], Catarina Sousa[1], Francisco Machado[1], Mariana Serino[1], Vanessa Santos[1], Natália Cruz-Martins[2,3,4], Armando Teixeira[5,6], António Cunha[7,8], Tania Pereira[7], Hélder P. Oliveira[7,9], José Luís Costa[2,4,10] and Venceslau Hespanhol[1,2,10]*

[1] Department of Pulmonology, Centro Hospitalar e Universitário São João, Porto, Portugal, [2] Faculty of Medicine, University of Porto, Porto, Portugal, [3] Laboratory of Neuropsychophysiology, Faculty of Psychology and Education Sciences, University of Porto, Porto, Portugal, [4] Institute for Research and Innovation in Health (i3S), University of Porto, Porto, Portugal, [5] Institute for Biomedical Sciences Abel Salazar (ICBAS), University of Porto, Porto, Portugal, [6] Faculty of Engineering, University of Porto, Porto, Portugal, [7] Institute for Systems and Computer Engineering, Technology and Science (INESC TEC), Porto, Portugal, [8] Department of Engineering, University of Trás-os-Montes and Alto Douro, Vila Real, Portugal, [9] Faculty of Sciences, University of Porto, Porto, Portugal, [10] Institute of Molecular Pathology and Immunology of the University of Porto (IPATIMUP), Porto, Portugal

OPEN ACCESS

Edited by:
Rui P.L. Neves, University Hospital Düsseldorf, Germany

Reviewed by:
Ella W. Englander, University of Texas Medical Branch at Galveston, United States
Menno Tamminga, University Medical Center Groningen, Netherlands

***Correspondence:**
Cláudia Freitas
claudiaasfreitas@gmail.com

Specialty section:
This article was submitted to Cancer Molecular Targets and Therapeutics, a section of the journal Frontiers in Oncology

Received: *27 November 2020*
Accepted: *19 March 2021*
Published: *16 April 2021*

Citation:
Freitas C, Sousa C, Machado F, Serino M, Santos V, Cruz-Martins N, Teixeira A, Cunha A, Pereira T, Oliveira HP, Costa JL and Hespanhol V (2021) The Role of Liquid Biopsy in Early Diagnosis of Lung Cancer. Front. Oncol. 11:634316. doi: 10.3389/fonc.2021.634316

Liquid biopsy is an emerging technology with a potential role in the screening and early detection of lung cancer. Several liquid biopsy-derived biomarkers have been identified and are currently under ongoing investigation. In this article, we review the available data on the use of circulating biomarkers for the early detection of lung cancer, focusing on the circulating tumor cells, circulating cell-free DNA, circulating micro-RNAs, tumor-derived exosomes, and tumor-educated platelets, providing an overview of future potential applicability in the clinical practice. While several biomarkers have shown exciting results, diagnostic performance and clinical applicability is still limited. The combination of different biomarkers, as well as their combination with other diagnostic tools show great promise, although further research is still required to define and validate the role of liquid biopsies in clinical practice.

Keywords: lung cancer, clinical biomarkers detection, liquid biopsy, cell-free DNA, exosomes, tumor-educated platelets, circulating tumor associated cells

INTRODUCTION

Lung cancer (LC) is the most common type of cancer and the leading cause of cancer-related mortality worldwide (1). The prognosis is closely related to the stage at diagnosis, with most cases being diagnosed at locally advanced and advanced stages, when curative treatment is no longer possible (2, 3). Thus, to achieve the LC curative treatment, improving overall survival and to diminish the healthcare costs and adverse events related to systemic therapies, the development of novel diagnostic methods that improve the early diagnosis accuracy are of huge importance. Liquid biopsy is a non-invasive, easy and accessible tool for tumor cells or tumor-derived products detection in body fluids, with the potential of overcome the limitations of the strategies currently used for LC early detection. Indeed, the molecular assessment of tumor-derived components from peripheral blood is of high clinical value, besides to represent promising clinical biomarkers (4). In this sense, and given the above highlighted aspects, this review provides an overview on the utility of liquid biopsy components as early diagnostic biomarkers.

LIQUID BIOPSY IN EARLY DIAGNOSIS: WHAT IS THE RATIONALE?

Thoracic imaging is the traditional method used for early detection of LC, that occur either as an incidental finding or integrated in a screening program. The National Lung Screening Trial (NLST) showed a reduction of 20% in LC specific mortality rate with chest low dose computed tomography (LDCT) screening among high risk individuals, when compared with chest X-ray (5). Recently, the same trial with a median follow-up of 12 years confirmed consistent benefits in terms of LC-related deaths reduction (6). However, the rate of false positives, overdiagnosis and unnecessary invasive procedures still remain major concerns (7).

Tissue biopsies are essential for LC diagnosis. Despite imaging-guided percutaneous needle biopsy has been considered as a relatively safe procedure for peripheral lesions diagnosis, it is not free of complications (8, 9). Bronchoscopy has also a pivotal role in LC diagnosis, with flexible bronchoscopy being the more useful test for central lesions, whereas navigational bronchoscopy and radial endobronchial ultrasound (EBUS) display higher sensitivities for peripheral lesions (10). Nonetheless, although uncommon, complications may occur (11). Tissue biopsies, although of extreme interest and usefulness, have also limitations. For instance, due to tumor heterogeneity, a single biopsy may not be representative of the entire tumor and may misjudge the complexity of its genetic aberrations (12). Also, the primary tumor and its metastases may have significant inter- and even intra-tumor heterogeneity (12). Thus, the lack of enough tissue sample to carry out a complete tumor characterization, comprising histology, immunohistochemistry and genetic analysis, essential for therapeutic decision and prognosis definition, often represents an issue in clinical practice. Although transthoracic needle aspiration or biopsies perform better than bronchoscopic procedures in peripherical lung lesions diagnosis, this technique only provides the confirmation of diagnosis in 90% of LC cases, with 20–30% false negatives (10).

More recently, other strategies have been explored, with circulating biomarkers being target of an extreme attention and interest. Briefly, biomarker is defined as a feature that can be objectively measured and evaluated as an indicator of biological and pathogenic processes, or pharmacologic responses to therapeutic intervention (13). Circulating or other body fluid, especially respiratory samples biomarkers may be viewed as key strategies for improving LC early diagnosis. In this way, liquid biopsy, as a non-invasive, safe and easy procedure, has the potential to improve the currently used strategies for LC diagnosis, either in screening setting or as an alternative diagnostic tool, either alone or as complementary data for imaging findings. Several clinical applications have been reported in LC, including patients stratification, therapeutic decision, and disease monitoring either after surgery or during systemic therapies, enabling to detect the acquired resistance (14). Although the role of liquid biopsy in LC early detection is not yet defined, there is increasing evidence about its potential applications.

THE BIOLOGY BEHIND LIQUID BIOPSIES

Circulating tumor cells (CTCs) and circulating cell-free DNA (cfDNA) are the most studied liquid biopsy-derived biomarkers, but many others have also been investigated (15) **(Figure 1). Table 1** summarizes their advantages and limitations.

Circulating Cell-Free DNA

Tumor cells release DNA fragments into the bloodstream or other anatomic-related body fluid, such as urine or pleural fluid. It is known that cancer patients have higher levels of cfDNA than healthy individuals and, since the tumor volume correlates with cell turnover and death, circulating tumor DNA (ctDNA) concentration increases with tumor size (15, 27). Probably, most fragments result from apoptosis, as they range from 180 to 200 base pairs (16). In addition, smaller and larger fragments have also been reported, suggesting that necrosis is also a probable source (28). Macrophages seem to contribute to the releasing process after necrotic tumor cells phagocytosis (29). When in circulation, cfDNA can be linked to proteins or, alternatively, be transported by vesicles, such as exosomes or apoptotic bodies, through a process that, although not completely clarified, seems to contribute to distant spreading and metastasis (30, 31). In addition, there is evidence that a fraction of tumor DNA circulates in the blood linked to the blood cells surface (i.e. erythrocytes and leukocytes) (31, 32). The genetic alterations of cfDNA reflect the genomic alterations of the original tumors and include point mutations, rearrangements, amplifications and gene copy variations (15).

Circulating Tumor Cells

CTCs released by the primary tumor can be detected in the bloodstream and represent not only an attractive diagnostic method, as a morphologic analysis can be performed, but also an opportunity for molecular characterization, since DNA, RNA and protein information can be obtained (15). During the metastatic process, the tumor cells separate from the primary tumor, migrate through the surrounding tissue and reach lymphatic or blood circulation (33). Two different ways of tumor cell migration have been proposed (34). First, active migration implies that a single or a cluster of tumor cells has gained the ability to move through the extracellular matrix and basement membranes (35). Second, passive migration refers to the growth of tumor mass that pushes single or clusters of tumor cells into the circulation (36) and, as this process is common in epithelial malignancies, CTC frequently maintains the epithelial phenotype and presents epithelial-specific markers, such as the epithelial cell adhesion molecule (EpCAM) (33, 34). Epithelial malignancies may also shift their phenotype from epithelial to mesenchymal. Although the meaning of the transition is still on debate, an association with the ability of becoming invasive has been suggested (37, 38). In these cells, EpCAM is downregulated

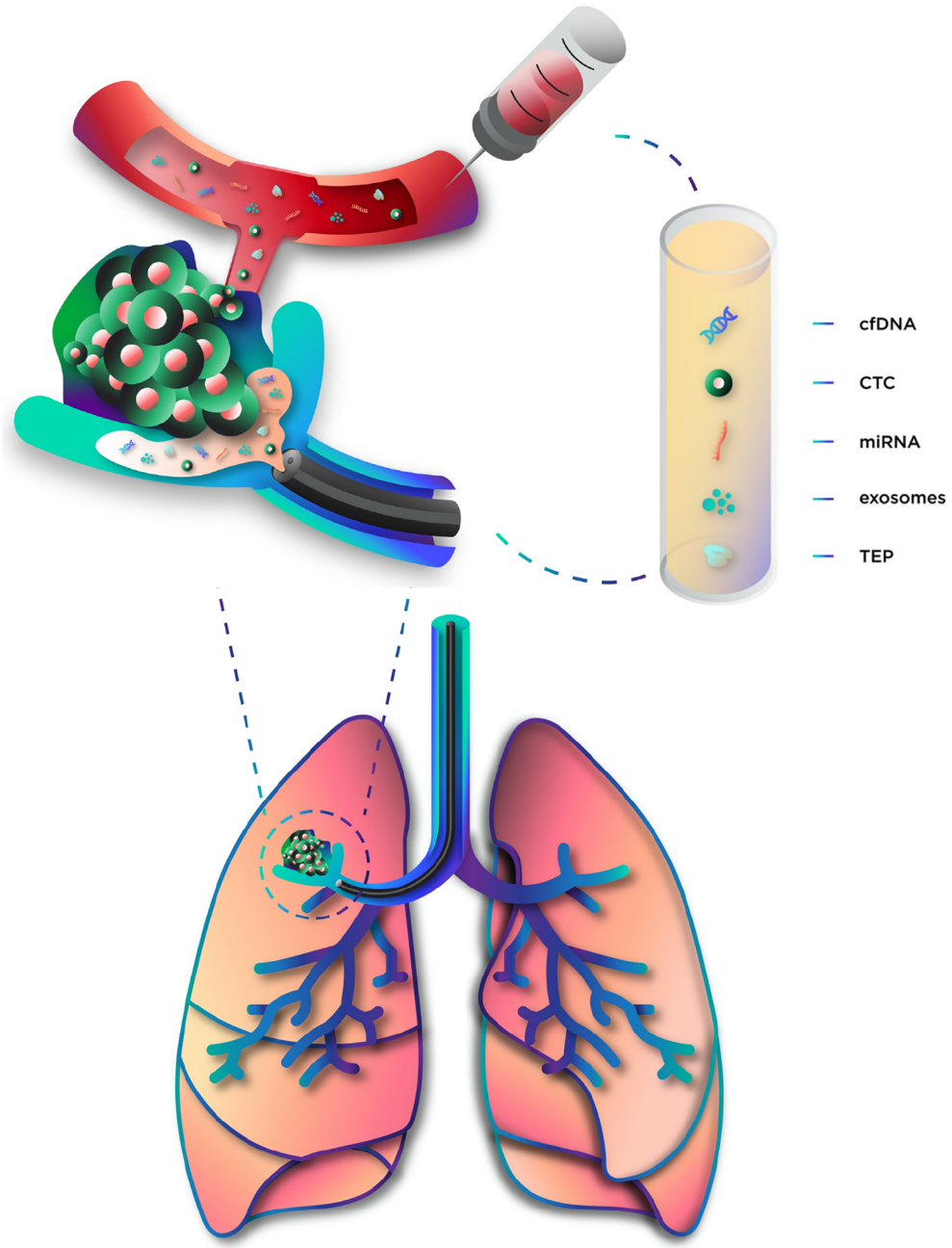

FIGURE 1 | Components of liquid biopsy. cfDNA, circulating cell-free DNA; CTC, circulating tumor cells; miRNA, microRNA; TEP, tumor-educated platelets.

and, thus, cannot be detected by conventional EpCAM-based methods (33). Surviving in the bloodstream is not easy for CTC, since many barriers need to be overcome, namely the forces and stresses created by the blood flow, anoikis and the immune system (33). During this phase, CTCs can be detected in the bloodstream and serve as a biomarker. Tamminga et al. (39) studied the release of CTCs during surgery and identified higher CTCs counts by CellSearch system in the pulmonary vein compared to peripherical circulation, suggesting a clearance mechanism. Since two groups of cells were detected in pulmonary vein samples—the real CTC and benign epithelial cells, the difference between peripherical and central circulation may be explained by the lack of survival ability of benign epithelial cells due to lower tolerance of shearing forces and the mesenchymal environment, leading to their fast clearance or destruction (39). Still, CTCs presence in pulmonary vein at time

TABLE 1 | Summary of advantages and limitations in LC diagnosis according to liquid biopsy-based biomarker.

Biomarkers	Advantages	Limitations	References
cfDNA	• Increased in cancer patients comparing to healthy individuals; • Genetic and epigenetic alterations reflect those of the original tumor; • Representation of tumor heterogeneity and dynamics; • Highly sensitive assays available (PCR, NGS).	• Markedly diluted compared to germline circulating DNA; • Positively correlates with tumor size and staging; • Increased in some benign or premalignant conditions; • High costs.	(16, 17–18)
CTC	• Allows morphologic analysis and tumor molecular characterization; • Correlates with prognosis; • Emerging enrichment and characterization techniques.	• No validated assay; • Rare in bloodstream and surrounded by blood cells; • Epithelial to mesenchymal transition with loss of epithelial-specific markers; • Role in cancer spreading still to be clarified.	(17, 19, 20)
miRNA	• Different profiles among early-stage cancer patients; • Stable in most types of body fluids (e.g. respiratory samples); • Released by several structures (e.g. exosome, TEPs). • Commercial kits available for collection.	• High variability, according to patients and technologies, requiring normalization methods; • Quantification and detection methods need to be validated • Unspecific for a cancer type.	(21–22)
Exosomes	• Contains several types of biomarkers such as proteins and nucleic acids; • Increased in lung cancer patients; • Stable and accessible in most types of body fluids; • Commercial kits available for isolation.	• The extraction approach, detection and characterization methods are challenge and require standardization; • High costs	(23–24)
TEP	• Platelet mRNA profile is distinct in cancer patients; • Abundant; • Easily isolated; • Acquire specific RNA from tumor cells reflecting its genetic alterations; • Dynamic mRNA repertoire due to short life-span.	• No validated assay nor standardized approach; • Reproducibility; • Detection techniques not widely available; • Time consuming and requires extensive computational resources.	(25–26)

of surgery was found to be an independent predictor of LC-specific relapse and their genomic features greatly overlap with those of the metastasis detected 10 months later (19). In fact, extravasion from vessels takes place when blood flow slows down, allowing the CTCs to attach the endothelium (40). Once in the metastatic site, tumor cells can initiate a quiescent state, called cancer dormancy (41), until the new surrounding microenvironment allows proliferation (33).

MicroRNA

In opposition to free RNA molecules that generally do not persist in circulation, cell-free miRNAs can be detected in blood of cancer patients. These fragments of single-stranded non-coding RNA, with a length of 19 to 25 nucleotides, play an important role in gene expression regulation. Mature miRNAs may present in a complex called multiprotein RNA-induced silencing complex (miRISC), which regulates gene expression at a translational level by targeting messenger RNAs (mRNAs) (42). A single miRNA can act on a large number of target mRNAs (43), and a single mRNA target may have multiple miRNA binding sites as well (44), allowing complex combinatorial gene regulation mechanisms. These molecules are involved in several biological processes, such as cell development, differentiation, apoptosis and proliferation (45), and, therefore, changes in the normal cellular miRNA profile can lead to functional abnormalities. In fact, loss or amplification of miRNA genes have been reported in a variety of cancers (46). Since some of the miRNA targets are oncogenes and tumor-suppressor genes, abnormal miRNA levels may result in oncogene activation and/or loss of tumor suppressing mechanisms, which eventually lead to cancer (42). Briefly, distinct miRNAs profiles on tissue and fluid samples seem to discriminate between healthy and tumor tissues (47). MiRNAs are released into the blood stream and surrounding tissues through exosomes, apoptotic bodies, protein–miRNA complexes, and tumor-educated platelets (TEP) (21), which, in conjunction with their remarkable stability (48) makes miRNA profiling a promising tool for cancer detection.

Exosomes

Exosomes are extracellular vesicles, with a diameter of 40–100 nm, derived from the progressive accumulation of intraluminal vesicles that are released into the extracellular space by fusion with plasma membrane (49–51). Its content, such as nucleic acids and proteins, and function are intrinsically related to the cells of origin. Tumor cells are known to release greater amounts of exosomes than healthy cells and these structures can be found in almost all body fluids (23, 51, 52). This vesicles mediate cell-to-cell communication and affect many biological processes in LC, contributing to its progression, angiogenesis and metastasis (53, 54). Several possible mechanisms through which exosomes communicate with target cells have been described. Exosomal membrane proteins can interact directly with the receptors of a target cell and activate intracellular signaling. Additionally,

exosomes can merge with the target cell membrane and release its contents into the target cell. This content, that can include proteins, mRNAs, miRNAs and DNA can promote a multiplicity of signaling events in the target cell (49, 54). In fact, the exosome and its molecular content represent a source of exclusive information on tumor cell.

Tumor-Educated Platelets

Platelets are anucleate cells originating from megakaryocytes in bone marrow, known for their role in hemostasis and thrombosis. Despite that, platelets have emerged as having a major impact in both progression and spreading of several solid tumors, including LC (55, 56). Tumor growth, progression and spreading require specific changes in tumor cells and in the surrounding microenvironment, being many of them similar to the physiological role of platelets (55). Although their exact role in cancer is still under investigation, several hypotheses have been proposed. First, TEPs have the ability to create a favorable tumor microenvironment supporting the proliferative signals release, promoting tumor progression, metastasis and angiogenesis in LC (57). Second, TEPs prevent immune destruction by forming a layer that protects the circulating tumor cells from natural killer, other immune cells and from shear forces of circulatory system (58). This coating mechanism may lead to MHC class I transfer to the tumor cells surface, making them unrecognizable by immune cells (59, 60) and contributing to distant metastasis formation (61, 62). Third, TEPs promote invasion and metastasis through releasing several growth and proangiogenic factors, such as platelet-derived growth factor (PDGF) and transforming growth factor β (TGF-β) (63). Fourth, TEPs seems to induce angiogenesis by delivering proangiogenic factors to the tumor and stimulating the expression of its own angiogenic factors, such as vascular endothelial growth factor (VEGF), platelet-derived growth factor (PDGF) and basic fibroblast growth factor (bFGF) (64, 65). Lastly, TEPs directly interact with tumor cells by acquiring biomolecules, as well as indirectly in response to external signals (55, 66).

LIQUID BIOPSY COMPONENTS AS EARLY DETECTION BIOMARKERS: CURRENT EVIDENCE

Circulating Cell-Free DNA

CfDNA has been extensively studied in LC and its concentration was found to be increased in LC patients (67). However, some important potential limitations have been discussed concerning its utility as an early detection biomarker. First, cfDNA is markedly diluted compared to circulating germline DNA (68) complicating the detection process. Second, it has been estimated that a minimum 10 cm^3 of tumor volume is required to quantify variant allele frequencies of 0.1%, thus hindering early stage tumor detection (69). Definitely cfDNA concentration correlates with tumor size and staging (17), being early-stage LC patients less prone to have representative samples than patients at an advanced stage. Abbosh and colleagues identified several factors related to cfDNA detection, including non-adenocarcinoma histology, high Ki67 expression and lymphovascular invasion. Also, PET FDG avidity was shown to predict cfDNA detection (69). Third, healthy individuals frequently have free DNA in circulation, though in smaller concentrations (70), and benign conditions, such as infections, cardiovascular diseases or other lung diseases are associated to increased cfDNA levels (71–73). However, these limitations may be overcome using highly sensitive genotyping assays, such as digital polymerase chain reaction (PCR) and next-generation sequencing (NGS). Also, a size-based pre-selection of DNA fragments could improve both sensitivity and specificity (74). While PCR methods can only target specific sites in a pre-defined gene and are not able to detect complex genomic alterations, such as gene fusions, NGS-based assays are multiplex methods, also known as massively parallel sequencing assays, allowing a concurrent detection of somatic mutations, including single-nucleotide and copy number variations, gene insertions, deletions or fusions. However, as the portion of sequencing genome increases, a loss of coverage is observed, limiting the ability to call a variant with confidence (75). Thus, the use of panels of primers or probes targeting hotspots or exons of pre-selected genes, such as hybrid capture NGS (76) or amplicon-based NGS (77, 78) is a reasonable strategy for cfDNA detection (79). The correct interpretation of cfDNA genotyping can be challenging, with the major limitation being the rate of false negatives that may result from the assay technical limits or, most importantly, from the cfDNA concentration, especially in early stages (18). On the other side, false positives may also occur due to sequencing errors or by the presence of other tumor or premalignant condition (e.g. in clonal hematopoiesis) (79). One must be aware that considering the primary tumor as reference may lead to misclassification as false positives, since a genetic alteration may be present in a tumor site and absent in other due to tumor heterogeneity (79).

Several studies have addressed the potential of cfDNA for early detection, either focusing in its concentration (**Table 2**) or genetic (**Table 3**) and epigenetic alterations, more specifically methylation patterns (**Table 4**).

cfDNA Concentration

An early study by Sozzi et al. (80) showed that plasma cfDNA concentration was higher among NSCLC patients, mostly with localized disease, than in healthy controls.

Real-time quantitative polymerase chain reaction (RT-PCR) amplification of the human telomerase reverse transcriptase gene (hTERT) was used as an indicator of global amount of plasma cfDNA in several studies (81, 87, 88, 91). The proposed cut-off value to distinguish NSCLC patients from controls ranged from 2 to 25 ng/ml, with sensitivities values varying from 46 to 86% (81, 88, 91). Given this results, cfDNA concentration as a noninvasive strategy for early detection of LC was investigated among 1,035 heavy smokers monitored by annual CT for 5 years by Paci et al., but with disappointing results (87).

Human β-actin gene detected by RT-PCR was another frequent used method for cfDNA detection (83, 85, 86, 89, 90).

TABLE 2 | cfDNA plasma concentration performance as a biomarker for lung cancer diagnosis.

Study	Year	Assay	Study population	Diagnostic performance			
				Cut-off	S	E	AUC
Sozzi (80)	2001	DNA DipStick TM Kit (Invitrogen, Carlsbad, CA)	43 healthy controls 84 patients with radically resected NSCLC (47 ADCs, 25 SCC and 12 others) Stages: IA: 14; IB: 32; II: 15; III: 23	6–25 ng/ml	75%	86%	0.844
Sozzi (81)	2003	RT-PCR using hTERT	100 controls 100 consecutive patients with NSCLC (58 ADC, 34 SCC, 8 others) Stages: IA: 16; IB: 18; IIB: 25; IIIA: 33; IIIB: 5; IV: 3	25 ng/ml	46%	99%	0.940
Gautschi (82)	2004	RT-PCR	46 healthy controls 185 NSCLC patients (81 ADC, 49 SCC, 37 LCC and 18 undifferentiated) Stages: I-II: 19; III: 62; IV: 104	10 ng/ml	–	98%	–
Herrera (83)	2005	RT-PCR using human β-actin gene	11 healthy volunteers; 38 esophageal cancer; 28 GERD 25 NSLC patients undergoing surgery Stages: I: 10; II: 4; III: 3; IV: 1; Unknown: 7	14.0 μg/L	48%	100%	0.630
Ludovini (84)	2008	RT-PCR	66 controls 76 consecutive patients with NSCLC undergoing surgery (37 SCC, 28 ADC and 11 LCC) Stages: I: 20; II: 40; IIIA: 11; IIIB: 5	3.25 ng/ml	80%	61%	0.820
Szpechcinski (85)	2015	RT-PCR using human β-actin	40 healthy volunteers 101 patients with chronic respiratory inflammation (34 COPD, 35 sarcoidosis, 32 asthma) 50 resectable NSCLC patients (24 ADC, 22 SCC and 4 others) Stages: I: 22; II: 20; IIIA: 8	2.80 ng/ml	90%	81%	0.900
Szpechcinski (86)	2016	RT-PCR using human β-actin	16 healthy controls 28 subjects with benign lung tumors 65 NSCLC patients (28 ADC, 27 SCC, 10 others) Stages: I: 30; II: 23, III: 12	2.80 ng/ml	86%	61%	0.800
Sozzi (87)	2009	RT-PCR using hTERT	1035 subjects included in a CT screening program (annually CT). During the 5-year follow-up period, 956 remained cancer free, 38 developed LC, and 41 developed other tumors	–	–	–	0.496
Paci (88)	2009	RT-PCR using hTERT	79 healthy controls. 151 NSCLC patients (65 SCCl, 61 ADC, 12 bronchioloalveolar, 3 LCC, 2 typical carcinoid, 8 others) Stages: IS: 1; IA: 33; IB: 44; IIA: 5; IIB: 12; IIIA: 24; IIIB: 18; IV: 4	2 ng/ml	86%	47%	0.790
Yoon (89)	2009	RT-PCR using human β-actin gene	105 healthy controls 102 LC patients (67 ADC, 16 SCC, 10 SCLC and 9 others) Stages in SCLC: localized: 5; extensive: 4 Stages in NSCLC: I: 8; II: 2; III: 19; IV: 64	–	–	–	0.860
Van der Drift (90)	2010	RT-PCR using human β-actin gene	21 controls 46 untreated NSCLC patients (21 SCC, 20 ADC, 5 LCC) Stages: I: 11; II: 6; III: 12; IV: 15; Unknown: 2	>32 ng/ml	52%	67%	0.660
Catarino (91)	2012	RT-PCR using hTERT	205 controls 104 NSCLC patients (38 SCC, 54 ADC and 12 others) Stages: I/II: 4; III/IV: 100	20 ng/ml	79%	83%	0.880

ADC, adenocarcinoma; AUC, area under the curve; E, specificity; hTERT, human telomerase reverse transcriptase gene; IS, in situ; LC, lung cancer; LCC, large cell carcinoma; NSCLC, non-small cell lung cancer; S, sensitivity; SCC, squamous cell carcinoma; RT-PCR, real time polymerase chain reaction.

While some studies failed in demonstrate the utility of cfDNA (83, 90), others have shown favorable results (85, 86, 89). Szpechcinski and colleagues studied not only LC patients and healthy controls, but also patients with benign lung diseases, found significantly higher plasma cfDNA levels among NSCLC patients than in those with chronic respiratory inflammation and healthy individuals (85, 86). A cut-off value of 2.8 ng/ml was proposed to discriminate NSCLC patients from healthy individuals, with sensitivity and specificity values ranging from 86 to 90% and 61 to 81%, respectively (85, 86).

The relationship between cfDNA levels and tumor histological type or staging is controversial, with several studies reporting no association (84, 86, 88, 90, 91), and others highlighting a difference related to disease staging (82, 83, 87).

cfDNA Genetic Alterations

Single Biomarker

Epidermal growth factor receptor (EGFR) is one of the most studied genes in LC, as the presence of certain mutations in this gene are considered markers of efficacy of target therapies. EGFR mutations detection in cfDNA has been also exploited in diagnostic setting (92–94, 96, 97), and two recent works focused on early stage LC patients. The first one, aimed to determine whether the electric field-induced release and measurement—EFIRM technology was able to detect exon 19 deletions and L858R EGFR mutations in patients with early stage NSCLC (97). The authors obtained a concordance rate between plasma and nodule biopsy of 100% and a global specificity of 95% (97). A second study, by Wan et al. (96) compared EGFR

TABLE 3 | Plasma cfDNA genetic alterations performance as biomarker for lung cancer diagnosis.

Study	Year	Assay	Genetic alteration	Study population	Diagnostic performance		
					S	E	AUC
Single biomarker							
Zhao (92)	2013	Mutant-enriched PCR and sequencing	EGFR mutations (exon 19 and 20) and EGFR exon 19 deletions	111 NSCLC patients including 35 SCC, 73 ADC and 3 others. Stages: I: 22; II: 10; IIIA: 19; IIIB: 14; IV: 46	36%	96%	–
Jing (93)	2014	HRM analysis	EGFR mutations (exons 18, 19, 20 and 21)	120 NSCLC patients including 70 ADC and 50 non-ADC. Stages: I/II: 38; III/IV: 82	78%	97%	–
Uchida (94)	2015	NGS	EGFR mutations (exon 19, 20, 21)	288 NSCLC patients including 274 ADC, 7 SCC, and 7 others Stages: I: 64; II: 19; III: 53; IV: 146	Exon 19 deletions: 51% L858R mutation: 52%	Exon 19 deletions: 98% L858R mutation: 94%	–
Fernandez-Cuesta (95)	2016	NGS	TP53 (exons 2 to 10)	123 non-cancer controls; 51 SCLC patients Stages: I: 7; II: 7; III: 28; IV: 9	49%	89%	–
Wan (96)	2018	ARMS-PCR	EGFR mutations (exon 19 deletion, T790M, L858R)	69 controls; 284 early-stage NSCLC patients (35 ADC, 231 SCC and 18 others) Stages: I: 107; II: 177	14%	92%	–
Wei (97)	2018	EFIRM	EGFR mutations (exon 19 deletion and L858R)	23 patients with benign pulmonary nodules21 early-stage ADC patients (12 L858R and 9 exon19 deletion EGFR variants) Stages: I: 18; II: 3	Exon 19 deletions: 77% L858R mutation: 92%	95%	Exon 19 deletions: 0.978 L858R mutation: 0.973
Combination biomarker							
Newman (98)	2014	CAPP-Seq	139 cancer-related genes	5 healthy controls17 NSCLC patients (14 ADC, 2 SCC and 1 LCC) Stages: I: 4; II: 1; III: 6; IV: 6	85%	96%	0.950
Guo (99)	2016	NGS	50 cancer-related genes	41 NSCLC patients (33 ADC, 6 SCC, 2 others) Stages: I: 23; II: 7; III: 10; IV: 1	69%	93%	–
Chen (100)	2016	NGS	50 cancer-related genes	58 NSCLC patients (51 ADC and seven SCC) Stages: I: 46; II: 12	54%	47%	–
Cohen (101)	2018	CancerSEEK (NGS and protein immunoassay)	8 proteins and 16 cancer-related genes	812 healthy controls1005 patients with stage I to III cancers including 103 NSCLC and 1 SCLC Stages: I: 46; II: 21; III: 31	70%	99%	0.910
Ye (102)	2018	NGS	140 cancer-related genes	35 lung surgery candidate nodule patients (four benign nodule patients, 31 LC patients: 2 ADC IS, 25 ADC, 1 SCC, 3 other) Stages: I: 21; II: 5; III: 4; not defined: 1	33%	100%	–
Peng (103)	2019	NGS	65 cancer-related genes	56 benign lung lesions patients136 LC patients (100 ADC, 28 SCC, 1 SCLC, 7 others) Stages: I: 87; II: 29; III: 17; IV: 3	69%	96%	–
Tailor (104)	2019	NGS		16 benign lung lesion patients17 LC patients (10 ADC, 6 SCC, 1 LCC) Stages: I: 8; II: 2; III: 5; IV: 2	82%	–	–
Leung (105)	2020	COLD–PCR assay coupled with high-resolution melt analysis	KRAS, EGFR, and TP53	26 controls192 patients referred to surgery (106 primary LC, 54 secondary cancer, 6 another primary thoracic malignancy) Stages: I: 52; II: 33; III: 16; IV: 1; Missing: 4	75%	89%	–

ADC, adenocarcinoma; ARMS-PCR, Amplification-refractory-mutation system-based PCR assays; AUC, area under the curve; CAPP-Seq, CAncer Personalized Profiling by deep Sequencing; COLD, Lower denaturation temperature; E, specificity; EFIRM, Electric field-induced release and measurement; HRM, High resolution melting; IS, in situ; LC, lung cancer; LCC, large cell carcinoma; NSCLC, non-small cell lung cancer; S, sensitivity; SCC, squamous cell carcinoma; SCLC, small cell lung cancer.

TABLE 4 | cfDNA hypermethylation performance as biomarker for lung cancer diagnosis.

Study	Year	Assay	Methylated genes	Study population	Sample	Diagnostic performance		
						S	E	AUC
Single-Dual biomarker								
Wang (106)	2007	Methylation-Specific RT-PCR	RASSF1A	15 healthy controls 35 benign pulmonary diseases patients 80 LC patients (40 ADC, 26 SCC, nine adenosquamous carcinoma, five SCLC) Stages: I: 9; II: 18; III: 29; IV: 24	Serum	34%	100%	–
Schmidt (107)	2010	Methylation-Specific RT-PCR	SHOX2	242 controls 281 LC patients (109 ADC, 103 SCC, 37 NOS NSCLC, 29 SCLC, three others) Stages: I: 59; II: 43; III: 108; IV: 62; unknown: 9	Bronchial aspirates	68%	95%	0.860
Kneip (108)	2011	Methylation-Specific RT-PCR	SHOX2	155 controls 188 LC patients (38 SCC, 31 SCC, 15 SCLC, 104 other) Stages: I:37; II:29; III:53; IV:42; unknown:27	Plasma	60%	90%	0.780
Hwang (109)	2011	Pyrosequencing	HOXA9	51 healthy controls 58 benign lung diseases patients 76 LC patients (42 ADC and 34 SCC). Stages: I: 14; II: 5; III: 28; IV: 29	Induced sputum	71%	55%	0.969
Dietrich (110)	2012	Epi proLung BL	SHOX2 and PTGER4	125 controls 125 LC patients (26 ADC, 28 SCC, 40 SCLC, 9 NSCLC NOS, 32 others)	Bronchial aspirates	78%	96%	0.940
Ponomaryova (111)	2013	Methylation-Specific RT-PCR	RARB2and RASSF1A	32 healthy donors 60 NSCLC patients (40 SCC and 20 ADC) Stages: I/II: 20; III: 40	Plasma and cell-surface-bound circulating DNA	85%	75%	–
Powrózek 2014 (112)	2014	Methylation-specific RT-PCR	Septin 9	100 healthy controls 70 LC patients (20 ADC, 20 SCC, 23 SCLC, seven others) Stages: IIA–IIIA: 23; IIIB–IV: 47	Plasma	44%	92%	
Konecny (113)	2016	Epi proLung BL	SHOX2	69 suspected LC patients; 31 excluded LC (controls) and 38 LC confirmed including 28 NSCLC and one SCLC. Stages: I–II: 5; III–IV: 30; unknown: 3	Bronchial lavage Plasma	89% 81%	85% 79%	0.890 0.870
Powrózek (114)	2016	Methylation-specific RT-PCR	DCLK1	95 healthy controls 65 LC patients (22 ADC, 20 SCC, 19 SCLC, four others) Stages: IIA–IIB: 7; IIIA: 21; IIIB–IV: 37	Plasma	49%	92%	–
Ren (115)	2017	Methylation-specific RT-PCR	SHOX2 and RASSF1A	130 controls (112 benign lung disease patients and 18 patients with other malignancies) 52 patients with no exact diagnosis 123 LC patients including 82 ADC, 17 SCC, eight SCLC, 16 others Stages: 0: 4; I: 47; II: 13; III: 19; IV: 25; unknown: 15	Bronchoalveolar lavage	72%	90%	–

(Continued)

TABLE 4 | Continued

Study	Year	Assay	Methylated genes	Study population	Sample	Diagnostic performance		
						S	E	AUC
Nunes (116)	2019	Methylation-specific RT-PCR	4 genes: APC, HOXA9, RARβ2, and RASSF1A	28 benign lung diseases patients 129 LC cancer patients (65 ADC, 42 SCC, 19 SCLC) Stages: I: 15; II: 11; III: 27; IV: 76	Plasma	APC: 25% RASSF1A: 24% APC and RASSF1A: 38%	APC: 96% RASSF1A: 95% APC and RASSF1A: 93%	APC: 0.622 RASSF1A: 0.591
Combination biomarker								
Fujiwara (117)	2005	Methylation-Specific RT-PCR	RARβ, $p16^{INK4a}$, DAPK, RASSF1A, and MGMT	100 non-malignant diseases patients nine other malignancies 91 LC patients (64 ADC, 21 SCC, four SCLC, two carcinoid). Stages: I: 53; II: 7; III: 22; IV: 9	Serum	50%	85%	–
Hsu (118)	2007	Methylation-Specific RT-PCR	BLU, CDH13,FHIT, p16, RARβ, and RASSF1A	36 cancer-free controls 63 NSCLC patients (41 ADCs, 13 SCC) Stages: I–II: 41; III–IV: 21; Not staged: 1	Plasma	73%	82%	
Zhang (119)	2011	Methylation-Specific RT-PCR	9 genes: APC, CDH13, DLEC1, EFEMP1, KLK10, $p16^{INK4A}$, RARβ, RASSF1A, SFRP1	50 cancer-free controls 110 NSCLC patients (Stage I/II)	Plasma	90% APC, RASSF1A, CDH13, KLK10 and DLEC1: 84%	58% APC, RASSF1A, CDH13, KLK10 and DLEC1: 74%	–
Begum (120)	2011	Methylation specific RT-PCR	6 genes: APC, AIM1, CDH1, DCC, MGMT and RASSF1A	30 controls 76 LC patients (36 ADC, 26 SCC, 14 others) Stages: I: 41; II: 17; III: 11; IV: 5; unknown: 2	Serum	84%	57%	–
Nikolaidis (121)	2012	Methylation specific RT-PCR	4 genes: TERT, WT1, p16 and RASSF1	109 controls; 139 LC cases (22 ADC, 31 SCC, 39 SCLC, 16 LCC, 31 others) Stages: T1: 46; T2: 91; T3: 20; T4: 53; N0: 94; N1: 35; N2: 63; N3: 13	Bronchial lavage	82%	91%	–
Diaz-Lagares (122)	2016	Pyrosequencing	4 genes: BCAT1, CDO1, TRIM58, and ZNF177	Bronchial aspirates cohort: -29 cancer-free controls -51 LC patients (17 ADC, 19 SCC, 11 NSCLC NOS, 4 other) Stages: I: 5; II: 6; III: 21; IV: 18; unknown: 1 BAL cohort: -29 cancer-free controls -82 LC patients (25 ADC, 40 SCC, 12 SCLC, 5 others) Stages: I: 17; II: 8; III: 20; IV: 18; unknown: 19 Sputum cohort: -26 cancer-free controls -72 LC patients (38 ADC, 24 SCC, 5 SCLC, 4 other) Stages: I: 12; II: 13; III: 23; IV: 19; unknown: 5	Bronchial aspirates Bronchioalveolar lavages Sputum	84% ~80% ~65%	81% ~80% ~65%	0.910 0.850 0.930

(Continued)

TABLE 4 | Continued

Study	Year	Assay	Methylated genes	Study population	Sample	Diagnostic performance		
						S	E	AUC
Ma (123)	2016	Quantum dots combined with FRET	PCDHGB6, HOXA9 and RASSF1A	50 controls 50 NSCLC patients (24 ADC and 16 SCC) Stages: I: 23; II: 17	Bronchial brushing	80%	100%	0.907
Hulbert (124)	2017	Methylation-specific RT-PCR	6 genes: SOX17, TAC1, HOXA7, CDO1, HOXA9, ZFP42	60 cancer-free controls 150 LC cases (121 ADC, 26 SCC, 3 others) Stages: IA–IB: 136; IIA: 14	Sputum	TAC1, HOXA17 and SOX17: 93% 6 genes, age, PY, COPD and FVC: 91%	TAC1, HOXA17 and SOX17: 89%	TAC1, HOXA17 and SOX17: 0.890 6 genes, age, PY, COPD and FVC: 0.850
					Plasma	CDO1, TAC1 and SOX17: 86% 6 genes, age, PY, COPD and FVC: 85%	CDO1, TAC1 and SOX17:78%	CDO1, TAC1 and SOX17: 0.770 6 genes, age, PY, COPD and FVC: 0.890
Ooki (125)	2017	Methylation-specific RT-PCR	6 genes: CDO1, HOXA9,AJAP1, PTGDR, UNCX, and MARCH11	42 controls 43 primary NSCLC with matched serum samples from stage IA ADC 40 serum samples from stage IA SCC 70 pleural effusions samples 49 ascites samples	Serum Pleural effusions	ADC: 72%SCC: 60% 4-gene panel (CDO1, PTGDR, UNCX, and MARCH11): 70% 5-gene panel (CDO1, AJAP1, PTGDR, UNCX, and MARCH11): 76%	71% 4-gene panel (CDO1, PTGDR, UNCX, MARCH11): 85% 5-gene panel (CDO1, AJAP1, PTGDR, UNCX, MARCH11): 76%	– –
Hubers (126)	2017	Methylation-specific RT-PCR	7 genes: RASSF1A, APC, cytoglobin,3OST2, PRDM14, FAM19A4 and PHACTR3	219 controls 56 LC patients (34 ADC,7 SCC, 2 SCLC, 13 others Stages: I:36, II:4, III:6, IV:10	Sputum	17%	93%	–
Liang (127)	2019	Methyl-seq	9 genes	27 controls 39 LC patients (32 ADC, 6 SCC and 1 other) Stages: IA: 20; IB: 7; IIA: 1; Later stages: 10; unknown: 1	Plasma	80%	85%	0.820

ADC, adenocarcinoma; AUC, area under the curve; COPD, chronic obstructive pulmonary disease; E, specificity; FRET, fluorescence resonance energy transfer; FVC, forced vital capacity; IS, in situ; LC, lung cancer; LCC, large cell carcinoma; NSCLC, non-small cell lung cancer; NOS-NSCLC, not otherwise specified non-small cell lung cancer; PY, pack-years; S, sensitivity; SCC, squamous cell carcinoma; SCLC, small cell lung cancer.

exon 19 deletions, T790M and L858R, using amplification-refractory-mutation system-based PCR assays (ARMS-PCR) in DNA isolated from nanoscale extracellular vesicles and cfDNA in NSCLC patients and controls. Although none of them were correlated with tumor volume, DNA isolated from extracellular vesicles was better than cfDNA for mutation detection among early stage NSCLC patients (96).

As TP53 is inactivated in most SCLC, Fernandez-Cuesta and colleagues (95) assessed the presence of exon 2 to 10 mutations in plasma cfDNA from 51 SCLC patients and 123 controls and showed that, despite their occurrence in control samples due to interference of somatic mutations, they were significantly more frequent in SCLC cases, even when stratified by stage (95).

Combination Biomarker

Despite recurrent point mutations in cancer-related genes, such as EGFR, have been frequently used, a non-negligible proportion of patients have no mutations in these selected genes. Instead of using only a single gene, several studies used multigene panels towards to improve the test performance. An early example is the CAncer Personalized Profiling by deep Sequencing (CAPP-Seq) developed by Newman and collaborators (98). This low-cost method covered multiple classes of somatic alterations and identified mutations in more than 95% of tumors, however showing low sensitivity for stage I patients (98). Nonetheless, in a final analysis, CAPP-Seq showed to potentially improve the low positive predictive value of LDCT screening (98). Cohen et al. (101) described the CancerSEEK, a blood test composed by levels of eight proteins and cfDNA mutations in 16 cancer-related genes that can detect eight frequent types of cancer, including LC. Globally, the results showed a sensitivity of 70% and a specificity of 99%. But a reduced sensitivity among stage I patients and a disappointing sensitivity for LC were noticed (101).

A malignancy prediction model for lung nodules was proposed by Ye et al. (102) in order to complement LDCT screening. Fixing the cut-off values in 4 for mutation score and in 0.3 for tumor mutation burden of cfDNA, the model predicted 33% of malignant adenocarcinoma samples with 100% specificity (102). In the same study, the concordance rate of driver mutations between cfDNA and tumor was low, suggesting that improving sensitivity of early stage LC detection by increasing sequencing depth or coverage may be inappropriate (102). More recently, a pilot investigation by Tailor et al. (104) using whole-exome sequencing (WES) in plasma cfDNA and matched peripheral blood mononuclear cell germline DNA from patients with a CT-detected pulmonary nodules, showed that the number of variants was significantly higher in the LC group than in controls and, when selecting 10 variants, 82% of LC patients were detected, showing the potential role for early LC detection in patients with CT-detected lung lesions (104).

cfDNA Epigenetic Alterations

Single-Dual Biomarker

One of the most studied epigenetic mechanisms is DNA methylation, which consists in the addition of a methyl group at the fifth carbon position of cytosine bases located 5′ to a guanosine in a CpG dinucleotide. Tumor suppressor gene hypermethylation results in gene silencing, occurs at early stages of cancer development, and is easily detected in cfDNA, mostly by methylation-specific PCR technologies (128).

The short stature homeobox 2 gene (SHOX2) is a known chondrocyte hypertrophy regulator, playing important functions in skeleton development, embryogenic pattern formation (129), embryonic morphogenesis, heart and nervous system development (130). SHOX2 methylation was investigated in respiratory (107, 110, 113, 115) and plasma samples (108, 113). When considered as a single biomarker, sensitivities for LC detection ranged from 68 to 89% in respiratory samples (107, 113) and from 60 to 81% in plasma (108, 113). Interestingly, SCLC histology presented the highest and stage I patients the lowest sensitivity values (107, 108). The performance of the *in vitro* diagnostic test kit Epi proLung BL Reflex Assay was assessed both in saccomanno-fixed bronchial and blood samples (110, 113). Analyzing SHOX2 and PTGER4 methylation in bronchial aspirates, Dietrich et al. (110) reported 78% sensitivity and 96% specificity in discriminating 125 LC cases from 125 controls. Interestingly, the sensitivity was higher in cytology positive samples, suggesting that this test may complement traditional investigations (110). Moreover, when respiratory and plasma samples were considered, the sensitivity increases, suggesting advantages in using a combined approach (113).

Methylation of other candidate genes was proposed for diagnostic biomarker in LC, including RASSF1A (106, 111, 116), HOXA9 (109, 116), Septin 9 (112) and DCLK1 (114). Ponomaryova et al. (111) showed that both RARB2, a tumor suppressor gene that encodes a retinoid acid nuclear receptor, and RASSF1A methylation were increased in stage I–III LC patients both in cfDNA and DNA bound to the blood cells surface. The best performance model reported included RARB2 and RASSF1A, both in plasma and bound to blood cells surface. Yet, the highest accuracy was found among stage III patients (111). SHOX2 (107) (108), HOXA9 (116), RASSF1A (116), and DCLK1 (114) hypermethylations seem to be more frequent among SCLC patients.

Combination Biomarkers

Combination of biomarkers seems to be a reasonable option to increase the performance of cfDNA methylation as a diagnostic marker. Nikolaidis et al. (121) suggested a set of four genes (TERT, WT1, p16 and RASSF1) to diagnose LC in bronchial lavage samples and, although sensitivity was improved in cytology-positive samples, the assay seems to be particularly useful in diagnosing cytology-negative LC. Interestingly, SCLC and squamous cell carcinomas were more detectable than adenocarcinomas (121). In a study by Ma and colleagues (123), using quantum dots-based (QDs-based) fluorescence resonance energy transfer (FRET) nanosensor technique to identify hypermethylation of a 3-gene panel, including PCDHGB6, HOXA9 and RASSF1, in bronchial brushings, a robust diagnostic performance for early-stage LC was reported, yet, sensitivity varied according to stage and histotype (123). The analysis of sputum samples of participants from the NELSON trial, demonstrated that, while sputum cytology did not detect

any LC patients, a 3-gene panel, comprising RASSF1A, 3OST2 and PRDM14, detected 28% of cases 2 years before the diagnosis (126). Hulbert and colleagues (124) investigated subjects with suspicious nodules on CT imaging and built prediction models combining gene methylation with clinical information that correctly predicted LC in 91% of subjects using sputum and in 85% using plasma (124). From 20 tumor suppressor genes, Zhang et al. (119) found that nine (APC, CDH13, KLK10, DLEC1, RASSF1A, EFEMP1, SFRP1, RARb and p16INK4A) revealed a higher frequency of hypermethylation in stage I–II NSCLC than in cancer-free plasmas. Additionally, a 5-gene panel, comprising APC, RASSF1A, CDH13, KLK10 and DLEC1 achieved a sensitivity of 84% and specificity of 74% for early LC diagnosis (119).

More recently, Liang and collaborators created a plasma-based 9-marker diagnostic model to distinguish malignant from benign nodules, with a sensitivity of 80% and a specificity of 85%. The model was also very sensitive for early stages, which highlights its utility as complement to imaging methods (127). Interestingly, Ooki and colleagues (125), determined the clinical utility of a set of six genes, including CDO1, HOXA9, AJAP1, PTGDR, UNCX, and MARCH11, for predicting LC diagnosis not only in serum samples but also in pleural effusions and ascites. In serum, the panel reached a specificity of 71%, and a sensitivity of 72 and 60% for stage IA adenocarcinoma and squamous cell carcinoma, respectively. Promoter methylation of the six genes was significantly higher in cytology-positive pleural effusions and, when methylation of at least one of the four genes (CDO1, PTGDR, MARCH11, and UNCX) was considered, the sensitivity and specificity reached 70 and 85%, respectively. When AJAP1 was added to the panel, sensitivity increases and specificity drops, with similar findings for ascites, suggesting the utility of this gene panel for LC detection using different body fluids (125).

In conclusion, cfDNA concentration in plasma or serum samples seems to have diagnostic value in early-stages LC. As tumors-derived cfDNA is likely to represent the whole cancer genomic landscape, its genetic analysis has shown promising results. However, the genetic alteration or, more probably, a set of genetic changes with optimal diagnostic accuracy is still to be defined. Methylation is an early and frequently found epigenetic alteration that can be detected in cfDNA, not only from plasma or serum samples but also from respiratory specimens and other body fluids, representing an excellent opportunity for LC early diagnosis. Further studies are needed to find the optimal biomarker combination. For example, a single tube liquid biopsy allowing simultaneous analysis of cfDNA, tumor-derived extracellular vesicles and CTC with high and low EpCAM expression proved to be useful in predicting survival among advanced NSCLC (131). In the future, a similar combination biomarker strategy may be employed in diagnostic setting.

Circulating Tumor Cells

A meta-analysis demonstrated that CTCs detection seems to be associated to lymph nodal metastasis and staging but not to histology (132). Since CTCs are very rare in bloodstream and are surrounded by normal peripheral blood cells, such as mononuclear and red blood cells (33), several techniques have been developed to selectively enrich CTCs and remove other blood cell components. These assays are classified as label-dependent, which includes EpCAM-based technologies (positive selection) and depletion of CD45-positive leukocytes (negative selection), and label-independent approaches, in which CTCs are separated based on CTCs physical or biological properties. The combination of these approaches may be used. After enrichment, CTCs need to be characterized, usually through the identification of tumor-associated proteins, mRNA or DNA, using several strategies that includes fluorescence immunocytochemistry, RT-PCR, next-generation sequencing (NGS) and whole-genome amplification (33, 133).

Several studies evaluated the utility of CTCs in diagnosing LC (**Table 5**). The CellSearch system, an EpCAM-based technology approved by FDA, has been investigated in LC diagnosis. Allard and collaborators studied a population of healthy subjects, non-malignant diseases, and patients with a variety of metastatic carcinomas, including LC. A cut-off of ≥2 CTCs/7.5 ml blood only identified 20% of LC patients (134). A prospective study showed that CTCs were detected in 30.6% of LC and in 12.0% of non-malignant disease patients and, despite CTC count was significantly higher among the first group, had a low discriminatory capacity (135). However, metastatic and non-metastatic LC patients were successfully distinguished (135).

Isolation by size of epithelial tumor cell (ISET) has been investigated in LC early diagnosis. In 2011, Hofman et al. (136) reported a mean of 42 circulating nonhematologic cells detected in 49% of NSCLC patients undergoing surgery, 37% with malignant features and no cells were found in the control healthy group (136). One year later, the same authors achieved similar conclusions in a larger population (138). Ilie and colleagues (139) examined the presence of CTCs in complement to CT-scan in patients with chronic obstructive pulmonary disease (COPD) in order to identify early LC. CTCs were detected in 5% of COPD patients and all of them developed LC after a mean follow-up period of 3.2 years, suggesting that monitoring CTC-positive COPD patients may allow early LC diagnosis. Importantly, a study comparing CellSearch and ISET methods in LC diagnosis showed that CTCs can be detected by both methods. Moreover, they may complement each other since the percentage of patients with detected CTCs is higher when combining the two methods with a higher number of CTCs detected by ISET (137). Obstacles to CellSearch method include epithelial–mesenchymal transition phenomena and epithelial nontumor cells in circulation (133, 149). Even though CTCs detected by CellSearch are able to predict the prognosis among NSCLC patients reflecting their clinical relevance (150, 151).

Anti–cluster of differentiation, CD45 antibody–coated magnetic beads, have been used for leucocyte depletion and negatively enrich CTCs. Although this method has a high sensitivity (152), CTCs and leucocytes may aggregate and form clusters, or even CTCs may be loss in the process (153). Xu et al. (143) compared this negative enrichment method to an unbiased detection method, in which erythrocytes were lysed and removed and the remaining nucleated cells were bound to substrates, fixed, stained using fluorescence–labeled antibodies

TABLE 5 | Circulating tumor cells (CTC) as biomarker for lung cancer diagnosis.

Study	Year	Assay	Study population	Cut-off	Diagnostic performance		
					S	E	AUC
Allard (134)	2005	CellSearch system	145 healthy women 199 women with non-malignant disease 964 metastatic cancer patients including 99 LC	≥2 CTCs/7.5 ml	20%	99%	–
Tanaka (135)	2009	CellSearch system	25 patients with non-malignant lung disease 125 LC patients (22 SCC, 85 ADC, 9 SCLC, 9 other) Stages: I-III: 94; IV: 31	≥1 CTCs/7.5 ml	30%	88%	0.598
Hofman (136)	2011	ISET method	39 healthy subjects 208 NSCLC (54 SCC, 115 ADC, 39 others) Stages: I: 86; II: 51; III: 58; IV: 13	≥1 CTCs/ml	37%	100%	–
Hofman (137)	2011	CellSearch system vs. ISET method	40 healthy subjects 210 NSCLC (57 SCC, 120 ADC, 33 other) Stages: I: 91; II: 40; III: 60; IV: 19	≥1 CTCs/ml	ISET: 50%CellSearch: 39%Combined: 69%	100%	
Hofman (138)	2012	ISET method	59 healthy subjects 250 NSCLC patients (67 SCC, 150 ADC, 33 others) Stages: I: 111; II: 70; III: 50; IV: 19	≥1 CTCs/ml	41%	100%	–
Ilie (139)	2014	ISET method	77 non-COPD controls (42 smokers and 35 healthy non-smoking individuals) 168 COPD patients	≥1 CTCs/ml	All COPD patients in which CTCs were found (5%) developed LC during follow-up.	Non-COPD controls: 100%COPD controls: 95%	–
Dorsey (140)	2015	Telomerase-promoter immunofluorescence-based assay	Healthy controls 30 NSCLC patients referred for definite RT	≥1 CTCs/ml	65%	100%	–
Fiorelli (141)	2015	Isolation by size method	77 patients with a single lung lesion: 17 benign lesions and 60 with LC (29 ADC, 18 SCC, 13 LCC Stages: I: 25; II: 19; III: 10; IV: 6	>25 CTCs/ml	89%	100%	0.900
Chen (142)	2015	Ligand-targeted PCR for folate receptors	56 healthy volunteers 227 patients with benign lung disease 473 NSCLC patients (293 ADC, 103 SCC, 77 others) Stages I: 18; II: 5; III: 127; IV: 323	≥1 CTCs/3ml	76%	82%	0.813
Xu (143)	2017	Negative enrichment using anti-CD45 coated magnetic beads and CD45 depletion cocktail vs unbiased method	151 non-cancerous controls 83 LC patients Stages: I: 13; II: 10; III: 33; IV: 27	≥1 CTCs/ml	Anti-CD45 coated magnetic beads group: 62%CD45 depletion cocktail group: 47%Unbiased group: 92%	94%	–
Xue (144)	2018	Ligand-targeted PCR for folate receptors	24 patients with benign lung diseases and 2 healthy subjects 72 LC patients (50 ADC, 14 SCC, 8 others) Stages: 0-IS: 2; I: 31; II: 7; III: 12; IV: 14; Uncertain: 6	8.7 CTC/3 mL	82%	73%	0.822
Frick (145)	2020	Telomerase-promoter immunofluorescence-based assay	92 NSCLC undergoing SBRT (22 ADC, 15 SCC, 55 not confirmed) Stages: IA: 81; IB: 11	≥1 CTCs/ml	41%	–	–
He (146)	2017	GILUPI CellCollector *in vivo*	19 healthy volunteers 32 ground-glass nodules patients 15 advanced LC patients	≥1 CTCs/7.5ml	GGN group: 16%Advanced LC patients: 73%	100%	–

(Continued)

TABLE 5 | Continued

Study	Year	Assay	Study population	Cut-off	Diagnostic performance		
					S	E	AUC
Duan (147)	2020	GILUPI CellCollector *in vivo*	20 healthy subjects 44 suspected LC patients including 10 patients diagnosed with benign lung diseases and 34 LC (all ADC)Stages 0: 11/34; IA: 23/34	≥1 CTC/ml	53%	Healthy controls: 100%Benign lung disease: 90%	Benign lung disease: 0.715
He (148)	2020	GILUPI CellCollector *in vivo*	72 matched healthy controls 24 LC patients (6 SCC and 18 ADC) Stages: I: 18/24; II: 6/24	≥1 CTC/ml	63%	100%	–

ADC, adenocarcinoma; AUC, area under the curve; COPD, chronic obstructive pulmonary disease; E, specificity; IS, in situ; ISET, solation by size of epithelial tumor cell; GGN, ground-glass nodules; LC, lung cancer; NSCLC, non-small cell lung cancer; S, sensitivity; SCC, squamous cell carcinoma; SCLC, small cell lung cancer.

and, thereafter examined by microscopy. The results demonstrated that unbiased detection method efficiently detected 92.2% of CTCs among LC patients, and 65% of early-stage LC patients. By contrast, only 40–60% of CTCs were detected by negative enrichment (143). These results suggest that unbiased detection methods may detect CTCs in early-stage LC patients, also revealing a better sensitivity than negative enrichment methods.

More recently, the diagnostic value of detecting folate receptors (FR)-positive CTC by a novel ligand-targeted polymerase chain reaction method in NSCLC patients was investigated (154, 155). Chen and collaborators (142) showed that CTC levels in NSCLC patients were significantly higher than in those with benign lung diseases and in healthy donors. Also, CTC detection was able to identify NSCLC patients (AUC = 0.813). Moreover, a joint model combining CTC, carcinoembryonic antigen, neuron-specific enolase, and Cyfra21-1 was efficient in NSCLC diagnosis (142), showing the interest of combining different types of biomarkers. Later, Xue et al. (142) reported high sensitivity and specificity values using a cut-off value of 8.7 CTC Units/3 ml in discriminating early-stage LC patients from controls (142).

A telomerase-promoter-based assay has shown to be able to overcome the current limitations in detecting CTCs. In a pilot study with 30 patients referred for definite radiotherapy (RT), Dorsay et al. (140) showed a successful detection of CTCs in 65% of patients, being the median CTC counts in patients before RT significantly higher than post-RT values. Interestingly, one patient was exception and developed metastatic disease soon after RT (140). Also in RT setting, 41% of early-stage NSCLC patients had a positive CTC test prior to treatment (145).

Other recent approach is the GILUPI CellCollector *in vivo* examination technique, which consists in a structured and functionalized medical wire that captures CTCs directly from the bloodstream and identifies them through the cytokeratin immunofluorescence intensity signal (156). He and collaborators demonstrated that this strategy was able to identify not only 73.3% of the ad.vanced LC patients as reported before (157), but also 15.6% of the ground-glass nodules (146). In two later studies including early LC patients, sensitivity values of 53–63% were reached (147, 148). Remarkably, the captured CTCs can be separated for NGS or PD-L1 analysis (146–148).

Evidence has shown that CTCs are useful as biomarkers in LC diagnosis. However, techniques for CTCs isolation and counting still need to be optimized and harmonized so that can be possible to validate the ideal detection method. New techniques, such as microfluidic technologies have shown exciting results (158). In order to assess technical validity of emerging CTC detection methods and generate comparative data, a platform was recently created to help to define minimal requirements for performance qualification prior to clinical validation (159).

MicroRNAs

Since miRNA fragments are stable in blood and evidence suggests that their landscape in peripheral circulation correlate with the original tumor (160), they represent a valuable potential biomarker for LC diagnosis.

Serum and Plasma Samples

Notable performances in discriminating between LC patients and healthy and/or benign lesions controls were reported by several authors (**Table 6**.). However, most studies included metastatic and locally advanced patients, and only some of them were restricted to early stages (168, 170, 178, 185, 188).

Foss and collaborators demonstrated that miR-1254 and miR-574-5p were significantly increased in serum samples from early-stage NSCLC, achieving a sensitivity and specificity of 73 and 71%, respectively, in differentiating from controls (168). Fan et al. (179) evaluated the miRNA expression in serum samples of NSCLC patients and healthy subjects firstly by qRT-PCR and, thereafter, they validated the results using the fluorescence quantum dots liquid bead array. They found that five miRNAs including miR-16-5p, miR-17b-5p, miR- 19-3p, miR-20a-5p, and miR-92-3p were significantly downregulated, while miR-15b-5p was upregulated among NSCLC patients. A 3-miRNA profile (miR-15b-5p, miR-16-5p, miR-20a-5p) using bead array showed to be the best diagnostic approach with high sensitivity and specificity values (179). Both serum and plasma samples from 220 early stage NSCLC patients and 220 matched controls were studied by Heegaard et al. (170) who reported that remarkably the expression levels in serum did not correlate with those in plasma, and while in serum samples from NSCLC patients a decreased expression of miR-146b, miR-221, let-7a, miR-155, miR-17-5p, miR-27a and miR-106a and an increased expression of miR-29c were noticed, no significant differences were stated on miRNAs plasma levels.

More recently, the values of plasma miR-486 and miR-150 for LC early diagnosis were also studied by Li et al. (178). The authors found that, individually, these miRNAs were able to distinguish LC patients from healthy volunteers with reported sensitivity and specificity higher than 80% (178). A single-center study reported significantly higher levels of miRNA-17, -146a, -200b, -182, -221, -205, -7, -21, -145, and miRNA-210 in NSCLC nodules comparing with benign ones (185). Later, the same group built a prediction model including 3 miRNAs (miRNA-146a, -200b, and -7) and CT features such as pleural indentation and spiculation, with high diagnostic value in early-stage NSCLC (188).

Circulating miRNAs value in LC screening programs has been widely investigated with promising results. A study by Boeri et al. (167), including participants from two CT-based screening cohorts, INT/IEO and MILD, explored miRNA expression profiles in plasma samples collected from patients 1 and 2 years before CT-detected lesions compared with a control group of heavy-smoking individuals. A signature of 15 miRNAs could discriminate both groups with a sensitivity 80%, and, a specificity of 80 and 90%, respectively (167). Notably, the predictive value of this signature was evaluated to be useful up to 28 months before the disease, with mir-660, mir-140-5p, mir 451, mir-28-3p, mir-30c, and mir-92a being the most frequently deregulated miRNAs (167). The most frequently miRNA deregulated at the time of LC diagnosis were mir-17, mir-660, mir-92a, mir-106a, and mir-19b (167). Later, the same research group analyzed the plasma samples from 939 participants, including 69 LC patients and 870 disease-free individuals in two arms (LDCT and observation) and using a miRNA signature classifier comprising 24 miRNAs reported a diagnostic performance for LC detection of 87% for sensitivity and 81% for specificity for both arms, and a negative predictive value of 99% (171). Furthermore, when combined with LDCT, a significant reduction of LDCT false positives was noticed (171). The BioMILD trial (190) consists in a LC screening program combining LDCT and circulating miRNA which prospectively enrolled 4,119 volunteers from a single center. Preliminary analysis presented in IASLC by Pastorino and colleagues showed a higher LC incidence and overall mortality in subjects with positive LDCT and/or miRNA at baseline and no detrimental effects on stage I LC proportion, resection rates, or interval cancer incidence in the group of subjects that completed 3-year LDCT repetition, suggesting that the combination of these tools is a valuable, safe and reduce unnecessary LDCT repeats (191). After Bianchi et al. (169) developed a serum 34 miRNAs panel able to identify patients with NSCLC in an asymptomatic high-risk population. Montani and colleagues (174) performed a multicenter study enrolling 1,115 high-risk individuals from the Continuous Observation of Smoking Subjects (COSMOS) LC screening program and reduced the original serum 34-miRNA signature to 13 miRNAs (miR-92a-3p, miR-30b-5p, miR-191-5p, miR-484, miR-328-3p, miR-30c-5p, miR-374a-5p, let-7d-5p, miR-331-3p, miR-29a-3p, miR-148a-3p, miR-223-3p, miR-140-5p), maintaining the same performance (174).

A systematic review and metanalysis published in 2017 comprising a total of 134 studies, with 6,919 LC patients and 7,064 controls, confirmed the good diagnostic performance of miRNA (192). Moreover, a subgroup analysis showed that combining miRNAs and Caucasian populations yield higher diagnostic performances, serum might serve as an ideal sample type and that the diagnostic role of miRNAs in early stage LC was high (192). Besides, some miRNAs, such as miR-21-5p, miR-223-3p, miR-155-5p and miR-126-3p, were pointed out as potential biomarkers (192). A more recent review confirmed the high diagnostic performance of miRNA in early detection of LC and also highlighted that multiple miRNA-based panels generally performed better than individual markers (193).

Respiratory Samples

Sputum is the most easily accessible biological fluid and its cytological analysis has been used for LC diagnosis despite its low sensitivity. Molecular analysis of sputum might be more sensitive than cytology (194, 195). Several studies assessed the role of sputum in diagnosis of LC (162, 163, 172, 175, 180, 181, 196).

For example, a panel of three sputum miRNAs (*miRs-21*, *31*, and *210*) allowed to differentiate between malignant and benign nodules, with sensitivity and specificity values higher than 80% (175). Additionally, other specifications were explored: overexpression of *miR-21* was associated with adenocarcinoma, whereas *miR-210* was related to squamous cell carcinoma, and the expression level of *miR-31* associated with smoking. These findings suggested that sputum miRNA biomarkers may

TABLE 6 | MicroRNA (MiRNA) as biomarker for lung cancer diagnosis.

Study	Year	Assay	Tested miRNA	Study population	Sample	Diagnostic performance			
						Best predictors	S	E	AUC
Chen et al. (161)	2008	qRT-PCR and Solexa sequencing	63 miRNAs	75 healthy individuals 152 LC patients	Serum	miR-25, miR-223	–	–	–
Xie et al. (162)	2009	RT-PCR	miR-21 and miR-155	17 healthy individuals 23 NSCLC patients (13 ADC and 10 SCC) Staging: I: 3; II: 5; III: 7; IV: 8	Sputum	miR-21	70%	100%	0.902
Yu et al. (163)	2010	RT-PCR	7 miRNAs (miR-486, miR-126, miR-145, miR-21, miR-182, miR-375, and miR-200b)	Discovery set: 20 stage I ADC Case-control set: 36 healthy individuals 36 stage I ADC Validation set: 58 healthy individuals 64 NSCLC patients (33 ADC and 31 SCC) Validation set staging: I: 16; II: 15; III: 17; IV: 16	Sputum	miR-21, miR-486, miR-375, miR-200b	70%	80%	0.839
Shen et al. (164)	2011	RT-PCR	12 miRNAs (miR-21, 126, 145, 139, 182, 200b, 205, 210, 375, 429, 486-5p, and 708)	29 healthy individuals 58 NSCLC patients including 34 ADC and 24 SCC Staging: I: 15; II: 15; III: 12; IV: 16	Plasma	miRNA-21, -126, -210, and 486-5p	86%	97%	0.926
Shen et al. (165)	2011	RT-PCR	5 miRNAs (miR-21, miR126, miR210, miR375, miR-486-5p)	- 80 benign SPNs patients - 76 malignant SPNs patients including 40 adenocarcinomas and 36 squamous cell carcinomas Staging: I: 24; II: 30; III–IV: 22	Plasma	miR-21, miR- 210, and miR-486-5p	76%	85%	0.855
Zheng et al. (166)	2011	RT-PCR	15 miRNAs (miR-17, -21, -24, -106a, -125b, -128, -155, -182, -183, -197, -199b, -203, -205, -210 and -221)	68 healthy individuals 74 LC patients: -17 SCLC -48 NSCLC (18 ADC, 23 SCC, 7 LCC and 9 others (carcinoid or mixed tumor) Staging: I: 21; II: 12; III: 11; IV: 30	Plasma	miR-155, miR-197, miR-182	81%	87%	0.901
Boeri et al. (167)	2011	TaqMan Microfluidic cards	15 miRNAs	81 heavy smokers' controls 53 LC patients (including 30 ADC) Staging: I: 28; II–III–IV: 25	Plasma	miR-17, miR-660, miR-92a, miR-106a, and miR-19b	75%	100%	0.880
Foss et al. (168)	2011	RT-PCR	11 miRNAs (miR-1268, miR-574-5p, miR-1254, miR-1228, miR-297, miR-1225-5p, miR-923, miR-1275, miR-185, miR-483-5p, miR-320a)	Discovery set: 11 healthy individuals; 11 early-stage (I and II) NSCLC patients Validation set: 31 healthy individuals; 22 early-stage (I and II) NSCLC patients	Serum	miR-1254 and miR-574-5p	73%	71%	0.750
Bianchi et al. (169)	2011	RT-PCR	34 miRNAs	30 healthy individuals 22 ADC 12 SCC Staging: I: 22; II–IV: 12	Serum	–	71%	90%	0.890

(Continued)

TABLE 6 | Continued

Study	Year	Assay	Tested miRNA	Study population	Sample	Diagnostic performance			
						Best predictors	S	E	AUC
Heegaard et al. (170)	2012	RT-PCR	30 miRNAs	220 early-stage NSCLC patients 220 healthy individuals Staging: I: 180; II: 40	Serum	miR-146b, miR-221, let-7a, miR-155, miR-17-5p, miR27a, miR-106a, miR-29c	–	–	0.602
Sozzi et al. (171)	2014	RT-PCR	24 miRNAs	870 healthy individuals (690 smokers) 69 LC patients (55 smokers) Staging: I: 37; II–III: 12; IV: 19	Plasma	–	87%	81%	–
Shen et al. (172)	2014	RT-PCR	12 miRNAs (miRs-21, 31, 126, 139, 182, 200b, 205, 210, 375, 429, 486, and 708)	Training set: 68 cancer-free smokers; 66 LC patients (27 ADC, 26 SCC and 13 SCLC) Training set staging of the NSCLC patients: I: 17; II: 18; III–IV: 18 Testing set: 73 cancer-free smokers; 64 LC patients (30 ADC, 28 SCC, 6 SCLC) Testing set staging of the NSCLC patients: I: 19; II: 19; III–IV: 20	Sputum	miR-31, miR-210	65%	89%	0.830
Wang et al. (173)	2014	RT-PCR	9 miRNAs(miR-20a, miR-25, miR-486-5p, miR-126, miR-125a-5p, miR-205, miR-200b, miR-21, and miR-155)	111 healthy individuals 142 LC patients (including 101 ADC, 22 SCC and 10 SCLC) Staging: I: 70; II: 24; III: 21; IV: 27	Serum	miR-125a-5p, miR-25, and miR-126	88%	83%	0.930
Montani et al. (174)	2015	RT-PCR	34 miRNAs	972 healthy individuals 36 LC patients (28 ADC and 5 SCC) Staging: I: 31; II–III: 5	Serum	miR-92a-3p, miR-30b-5p, miR-191-5p, miR-484, miR-328-3p, miR-30c-5p, miR-374a-5p, let-7d-5p, miR-331-3p, miR-29a-3p, miR-148a-3p, miR-223-3p, miR-140-5p	75%	78%	0.850
Xing et al. (175)	2015	RT-PCR	13 miRNAs (miR205; miR708; miR375; miR200b; miR182; miR155; miR372; miR143; miR486-5p; miR126; miR31; miR21; miR210)	Training set: 62 benign SPNs; 60 malignant SPNs (with 27 ADC and 29 SCC) Training set staging: I: 39; II: 21 Internal Testing set: 69 benign SPNs; 67 malignant SPNs (including 30 ADC and 31 SCC) Internal Testing set staging: I: 45; II: 22 External Testing set: 79 benign SPNs; 76 malignant SPNs (including 34 ADC and 35 SCC) External Testing set staging: I: 51; II: 25	Sputum	miR-21, miR-31, miR-210	82–88%	81–87%	0.920
Wang et al. (176)	2015	RT-PCR	16 miRNAs (miR-193a-3p, miR-214, miR-7, miR-25, miR-483-5p, miR-523, miR-885-5p, miR-520c-3p, miR-	48 healthy individuals 56 benign nodules 108 NSCLC patients (including 52 ADC and 27 SCC) Staging: I: 43; II: 15; III: 29; IV: 17	Serum	miR-483-5p, miR-193a-3p, miR-214, miR-25, and miR-7	95%	84%	0.952

(Continued)

TABLE 6 | Continued

Study	Year	Assay	Tested miRNA	Study population	Sample	Diagnostic performance			
						Best predictors	S	E	AUC
			484, miR-720, miR-133a, miR-337-5p, miR-150, miR-1274b, miR-342-3p, miR-145)						
Kim et al. (177)	2015	RT-PCR	5 miRNAs (miR-21, miR-143, miR-155, miR-210, and miR-372)	10 cancer-free controls 21 early-stage NSCLC patients (13 ADC, 5 SCC and 3 LCC) Staging: I: 12; II: 9	BAL fluid/ Sputum	miR-21, miR-143, miR-155, miR-210, and miR-372	Patients BAL vs controls sputum: 86% Sputum: 68%	Patients BAL vs controls sputum: 100% Sputum: 90%	
Li et al. (178)	2015	RT-PCR	10 miRNAs (miR-126, miR-150, miR-155, miR-205, miR-21, miR-210, miR-26b, miR-34a, miR-451 and miR-486)	11 healthy individuals 11 early-stage NSCLC patients Staging: I–II: 11	Plasma	miR-486 and miR-150 (individually)	miR-486: 91% miR-150: 82%	miR-486: 82% miR-150: 82%	miR-486: 0.926miR-150: 0.752
Fan et al. (179)	2016	Fluorescence quantum dots liquid bead	12 miRNAs (miR-15b-5p, miR-16-5p, miR-17b-5p, miR-19-3p, miR-20a-5p, miR-28-3p, miR-92-3p, miR-106-5p, miR-146-3p, miR-506, miR-579, and miR-664	54 healthy individuals 70 NSCLC patients (56 ADC, 12 SCC and 2 LCC) Staging: I: 49; II–III: 21	Serum	miR-15b-5p, miR-16-5p, miR-20a-5p	94$	94%	0.930
Razzak et al. (180)	2016	RT-PCR	3 miRNAs (miR-21, miR-210, miR-372)	10 healthy individuals 21 Early-stage NSCLC patients (including 13 ADC and 4 SCC) 22 Advanced-stage NSCLC patients (10 ADC and 5 SCC) Staging: I: 14; II: 7; III: 14; IV: 8	Sputum	miR-21, miR-210, miR-372	67%	90%	0.926
Bagheri et al. (181)	2017	RT-PCR	6 miRNAs (miR-223, miR-212, miR-192, miR-3074, SNORD33 and SNORD37)	17 healthy individuals 17 NSCLC patients (11 ADC and 6 SCC) Staging: I: 2; II: 3; III: 5; IV: 7	Sputum	miR-223	82%	95%	0.900
Leng et al. (182)	2017	RT-PCR	54 miRNAs	30 cancer-free smokers 34 NSCLC patients (21 AC and 13 SCC) Staging: I: 19; II: 9; III–IV: 15	Plasma	miRs-126, 145, 210, and 205-5p	92%	97%	0.960
Lu et al. (183)	2018	RT-PCR	13 miRNAs (miR-101, miR-133a, miR-17,miR-190b, miR-19a, miR-19b, miR-205, miR-26b, miR-375, miR-451, miR-601, miR-760, miR-765)	203 normal individuals 258 LC patients (133 ADC, 76 SCC and 49 SCLC) Staging: I: 78; II: 27; III: 40; IV: 64	Plasma	miR-17, miR-190b, miR-19a, miR-19b, miR-26b, and miR-375	80%	80%	0.868

(Continued)

TABLE 6 | Continued

Study	Year	Assay	Tested miRNA	Study population	Sample	Diagnostic performance			
						Best predictors	S	E	AUC
Abu-Duhier et al. (184)	2018	Magnetic bead technology and TaqMan assays	miRNA-21	80 healthy individuals 80 NSCLC patients (60 ADC and 20 SCC) Staging: I: 2; II: 7; III: 26; IV: 46	Plasma	–	80%	80%	0.891
Xi et al. (185)	2018	RT-PCR	12 miRNAs (miRNA-17, -146a, -200b, -182, -155, -221, -205, -126, -7, -21, -145, and miRNA-210)	15 benign pulmonary nodules 42 NSCLC patients Staging: IA: 29; IB: 10; II: 3	Plasma	miRNA-17, -146a, -200b, -182, -221, -205, -7, -21, -145, -210 (individually)	>55%	>60%	>0.680
Li et al. (186)	2019	RT-PCR	4 miRNAs (miRs-126-3p, 145, 210-3p and 205-5p)	245 cancer-free smokers 239 NSCLC cases (111 AC, 102 SCC and 26 LCC) Staging: I: 72; II: 76; III–IV: 91	Plasma	miRs-126-3p, 145, 210-3p and 205-5p	90%	95%	–
Liang et al. (187)	2019	RT-PCR	miRNA-30a-5p	20 healthy individuals 38 lung benign lesions104 LC patients (including 75 ADC, 20 SCC and 5 SCLC) Staging: I–IIA: 62; IIB–IV: 42	Plasma	–	80%	61%	0.820
Xi et al. (188)	2019	RT-PCR	10 miRNAs (miR-17, -146a, -200b, -182, -221, -205, -7, -21, -145, and miR-210)	13 benign pulmonary nodules 39 NSCLC patients staging: 0–IA: 31; IB: 7; IIA: 1	Plasma	miRNA-146a, -200b, and -7	72%	69%	0.781
Liao et al. (189)	2020	RT-PCR	2 miRNAs in sputum (miRs-31-5p and 210-3p)3 miRNAs in plasma (miRs-21-5p, 210-3p, and 486-5p)	55 cancer-free smokers 56 NSCLC patients (31 ADC and 25 SCC) Staging: I: 18; II: 17; III–IV: 21	Plasma and Sputum	Sputum: miRs-31-5p and 210-3pPlasma: miRs-21-5p	84%	91%	0.930

ADC, adenocarcinoma; AUC, area under the curve; BAL, bronchoalveolar lavage; E, specificity; LC, lung cancer; NSCLC, non-small cell lung cancer; RT-PCR, real time polymerase chain reaction; S, sensitivity; SCC, squamous cell carcinoma; SCLC, small cell lung cancer; SPN, solitary pulmonary nodules.

improve LC screening in heavy smokers (175). Also, the same research group showed that a panel of four miRNAs (*miR-21*, *miR-486*, *miR-375*, and *miR-200b*) could distinguished LC patients from controls with high sensitivities and specificity values, without differences among the stage subgroups, with the best prediction for adenocarcinoma (196).

Indeed, CT scan has an important role in LC diagnosis, however with low specificity. Sheng et al. (172) determine whether analysis of the miRNA signatures could improve regular CT scan and concluded that a panel of two miRNAs could cover the major histological types. Taken together, the combination of miRNA biomarkers and CT provided a higher specificity than CT alone (172).

Showing that respiratory samples other than sputum may have value, Kim and collaborators (177) investigated the role of 5 miRNAs (miR-21, miR-143, miR-155, miR-210, and miR-372) in discriminate early NSCLC patients from controls using both sputum and BAL samples and reported better diagnostic performance with BAL (177). Very recently, Liao et al. (189) determined a higher expression level of two sputum miRNAs (*miRs-31-5p* and *210-3p*) and three plasma miRNAs (*miRs-21-5p*, *210-3p*, and *486-5p*) of 76 NSCLC patients and 72 cancer-free smokers. Considered these panels, the authors reported 65.8–75.0% sensitivities and 83.3–87.5% specificities for LC diagnosis (189). Moreover, the expression levels of both *miR-21-5p* and *miR-210-3p* in sputum was correlated to squamous cell carcinoma (189). These results suggest that the combination of markers from different body fluids may play a role.

Overall, it seems that some miRNAs, either in circulation or in respiratory samples, have a role as biomarkers for early cancer diagnosis, especially when used in combination and as a complement to LDCT. However, the current data consist mostly in small sized populations from single-center studies with a great variability in terms of staging, analyzed miRNA and methodologies. Despite the great potential of miRNA, larger validation studies are required in order to define their exact role in clinics.

Exosomes

Exosomes were found to be increased in LC patients compared with healthy controls (197). Several techniques have been used for exosome isolation, including methods based on physical features, such as ultracentrifugation, density gradient separation, ultrafiltration, size exclusion chromatography, chemical precipitation methods, and biological assays such as immune-bead isolation. Transmission electron microscopy and western blot are two examples of frequently used techniques for further exosome characterization. Additionally, commercial kits are available (54).

Exosomal miR-21 is a potential biomarker for cancer diagnosis, including LC. However, may be increased in other types of cancer, as well as in other diseases which suggests that the combination of miRNA panels may provide better results (24). In an early study, Cazzoli et al. (198) reported that a panel of six exosomal miRNAs (miR-151a-5p, miR-30a-3p, miR-200b-5p, miR-629, miR-100 and miR-154-3p) were able to discriminate LC from granuloma patients, with a sensitivity and specificity of 96 and 60%, respectively (AUC = 0.760) (198). Another 6-miRNA panel comprising miR-19b3p, miR-21-5p, miR-221-3p, miR-409-3p, miR-425-5p and miR-584-5p was able to discriminate lung adenocarcinoma patients from healthy controls, achieving an AUC of 0.84 (199). Likewise, Jin et al. (200) selected a panel of exosomal miRNAs (let-7b-5p, let-7e-5p, miR-23a-3p and miR-486-5p) and obtained a sensitivity of 80% and a specificity of 92% (AUC = 0.899), regarding ability to differentiate early-stage NSCLC from non-NSCLC patients. Moreover, adenocarcinoma and squamous cell carcinoma histology was identified by combining miR-181b-5p with miR-361b-5p (AUC = 0.936), and miR-10b-5p with miR-320b (AUC = 0.911), respectively (200). Also exosomes might be useful in identified malignant pleural effusions. Lin et al. (201) demonstrated a higher expression of miR-205p5p and miR-200b in pleural effusions of LC patients comparing with those with infections (201). Exosomes may be also useful in identifying tumor somatic mutations, such as EGFR activating mutations (202, 203). In addition, some studies have explored the potential of exosomal proteins as diagnostic biomarkers (204–207). More recently, Zhang and colleagues (208) demonstrated that a four biomarker panel, including miR-17-5p, carcinoembryonic antigen (CEA), cytokeratin 19 fragment (CYFRA21-1), and squamous cell carcinoma antigen (SCCA), was able to reach an adequate diagnostic performance (AUC = 0.844) (208).

These data suggest that exosomes, specially exosomal miRNAs, due to its stability, may represent valuable diagnostic biomarkers achieving promising sensitivity and specificity results. Although some technical concerns have been raised (209), the technological advances have the potential to overcome these difficulties and to allow the development of more robust assays to be part of the routine clinical practice in the future.

Tumor-Educated Platelets

Evidence have shown that platelet RNA profile is distinct in patients with and without cancer, the later expressing a highly dynamic mRNA repertoire both at cancer onset and progression as well as during the treatment (25, 210). Best et al. (210) prospectively characterized the platelet mRNA profiles in 55 healthy donors and 228 patients with localized and metastasized tumors and concluded that cancer patients could be discriminated from non-cancer individuals with 97% sensitivity, 94% specificity and 96% accuracy (AUC = 0.986). In a multiclass analysis, the authors further distinguished healthy donors from patients with specific types of cancer with an average accuracy of 71% (210). Biomarkers like KRAS, EGFR, MET, HER2 or PIK3CA were also accurately distinguished using surrogate TEP mRNA profiles (210) as well as EML4-ALK rearrangements (211).Other studies have also shown that the analysis of mRNA profiles may allow to detect the primary tumor (212–214). Also, susceptibility to metastasis and staging seems to be possible to predict (25). Calverley et al. (215) identified a subset of platelet-based gene expression that are differentially expressed in individuals with LC metastases (215).

TEPs may have advantages over other blood-based biosources: they are abundant, may be easily isolated and

acquire specific RNA from tumor cells. Since platelets have a median of 7 days of survival, expression of a highly dynamic mRNA repertoire is expected during cancer progression. However, more robust and specific studies are needed to better define the value of TEPs applicability in LC early detection, alone or in combination with other blood-based biomarkers or diagnostic procedures.

FUTURE PERSPECTIVES

While liquid biopsy-derived biomarkers have shown promising results in the early detection of LC, currently, there is no evidence for its use in the screening or diagnosis of LC outside the research setting. These biomarkers are still limited by a significant proportion of false negatives and a negative plasma test still requires a confirmatory tissue biopsy. Indeed, low or absent values of most liquid biopsy components in the very early stages of LC limit their applicability. Due to tumour heterogeneity, to the emergence of different tumours or pre-cancerous conditions and using conventional tissue biopsy as a reference, positive results not related with LC can also be expected, and their clinical significance needs further clarification. The technological advances expected to happen in the next few years may be able to help mitigate these limitations, with the development of more sensitive and specific assays. Biomarker combination and the combined use of biomarkers and other diagnostic tools, such as imaging techniques, seem to be a promising strategy, although the best combinations are still to be defined. Larger and more robust studies are required to define and validate the role of liquid biopsy in the mainstream clinical practice for the screening or diagnosis of LC.

AUTHOR CONTRIBUTIONS

All authors listed have made a substantial, direct, and intellectual contribution to the work and approved it for publication.

FUNDING

This work is financed by the ERDF—European Regional Development Fund through the Operational Programme for Competitiveness and Internationalization—COMPETE 2020 Programme and by National Funds through the Portuguese funding agency, FCT—Fundação para a Ciência e a Tecnologia within project POCI-01-0145-FEDER-030263.

ACKNOWLEDGMENTS

Authors thank Abílio Cunha and Francisco Correia for the illustration work. NC-M acknowledges the Portuguese Foundation for Science and Technology under Horizon 2020 Program (PTDC/PSI-GER/28076/2017).

REFERENCES

1. World Health Organization. Global Cancer Observatory. *Int Agency Res Cancer* (2020).
2. Walters S, Maringe C, Coleman MP, Peake MD, Butler J, Young N, et al. Lung cancer survival and stage at diagnosis in Australia, Canada, Denmark, Norway, Sweden and the UK: a population-based study, 2004–2007. *Thorax* (2013) 68:551–64. doi: 10.1136/thoraxjnl-2012-202297
3. Bannister N, Broggio J. Cancer survival by stage at diagnosis for England (experimental statistics): Adults diagnosed 2012, 2013 and 2014 and followed up to 2015. *Off Natl Stat* (2016): 1–30.
4. Pérez-Ramírez C, Cañadas-Garre M, Robles AI, Molina MÁ, Faus-Dáder MJ, Calleja-Hernández MÁ. Liquid biopsy in early stage lung cancer. *Transl Lung Cancer Res* (2016) 5:517–24. doi: 10.21037/tlcr.2016.10.15
5. Aberle DR, Adams AM, Berg CD, Black WC, Clapp JD, Fagerstrom RM. The National Lung Screening Trial Research Team. Reduced Lung-Cancer Mortality with Low-Dose Computed Tomographic Screening. *N Engl J Med* (2011) 365:395–409. doi: 10.1056/NEJMoa1102873
6. Team TNLSTR. Lung Cancer Incidence and Mortality with Extended Follow-up in the National Lung Screening Trial. *J Thorac Oncol* (2019) 14:1732–42. doi: 10.1016/j.jtho.2019.05.044
7. Patz EFJr, Pinsky P, Gatsonis C, Sicks JD, Kramer BS, Tammemägi MC, et al. Team for the NOMW. Overdiagnosis in Low-Dose Computed Tomography Screening for Lung Cancer. *JAMA Intern Med* (2014) 174:269–74. doi: 10.1001/jamainternmed.2013.12738
8. Richardson CM, Pointon KS, Manhire AR, Macfarlane JT. Percutaneous lung biopsies: A survey of UK practice based on 5444 biopsies. *Br J Radiol* (2002) 75(897):731–5. doi: 10.1259/bjr.75.897.750731
9. Robertson EG, Baxter G. Tumour seeding following percutaneous needle biopsy: The real story! *Clin Radiol* (2011) 66(11):1007–14. doi: 10.1016/j.crad.2011.05.012
10. Rivera MP, Mehta AC, Wahidi MM. Establishing the Diagnosis of Lung Cancer. *Chest* (2013) 143(5):e142S–65S. doi: 10.1378/chest.12-2353
11. Stahl D, Richard K, Papadimos T. Complications of bronchoscopy: A concise synopsis. *Int J Crit Illn Inj Sci* (2015) 5(3):189–95. doi: 10.4103/2229-5151.164995
12. Bambury RM, Power DG, O'Reilly S. Intratumor heterogeneity and branched evolution [4]. *N Engl J Med* (2012) 366:2132–3. doi: 10.1056/NEJMc1204069
13. Definitions B, Group W, Atkinson AJJ, Colburn WA, DeGruttola VG, DeMets DL, et al. Biomarkers and surrogate endpoints: preferred definitions and conceptual framework. *Clin Pharmacol Ther* (2001) 69:89–95. doi: 10.1067/mcp.2001.113989
14. Wang J, Chang S, Li G, Sun Y. Application of liquid biopsy in precision medicine: opportunities and challenges. *Front Med* (2017) 11:522–7. doi: 10.1007/s11684-017-0526-7
15. Bardelli A, Pantel K. Liquid Biopsies, What We Do Not Know (Yet). *Cancer Cell* (2017) 31:172–9. doi: 10.1016/j.ccell.2017.01.002
16. Marques JF, Junqueira-Neto S, Pinheiro J, Machado JC, Costa JL. Induction of apoptosis increases sensitivity to detect cancer mutations in plasma. *Eur J Cancer* (2020) 127:130–8. doi: 10.1016/j.ejca.2019.12.023
17. Bettegowda C, Sausen M, Leary RJ, Kinde I, Wang Y, Agrawal N, et al. Detection of circulating tumor DNA in early- and late-stage human malignancies. *Sci Transl Med* (2014) 6:224ra24–224ra24. doi: 10.1126/scitranslmed.3007094
18. Abbosh C, Birkbak N, Swanton C. Early stage NSCLC - challenges to implementing ctDNA-based screening and MRD detection. *Nat Rev Clin Oncol* (2018) 15:577–86. doi: 10.1038/s41571-018-0058-3
19. Chemi F, Rothwell DG, McGranahan N, Gulati S, Abbosh C, Pearce SP, et al. Pulmonary venous circulating tumor cell dissemination before tumor resection and disease relapse. *Nat Med* (2019) 25:1534–9. doi: 10.1038/s41591-019-0593-1

20. Kapeleris J, Kulasinghe A, Warkiani ME, Vela I, Kenny L, O'Byrne K, et al. The Prognostic Role of Circulating Tumor Cells (CTCs) in Lung Cancer. *Front Oncol* (2018) 8:311:311. doi: 10.3389/fonc.2018.00311
21. Siravegna G, Marsoni S, Siena S, Bardelli A. Integrating liquid biopsies into the management of cancer. *Nat Rev Clin Oncol* (2017) 14:531–48. doi: 10.1038/nrclinonc.2017.14
22. Rijavec E, Coco S, Genova C, Rossi G, Longo L, Grossi F. Liquid Biopsy in Non-Small Cell Lung Cancer: Highlights and Challenges. *Cancers* (2020) 12:1–17. doi: 10.3390/cancers12010017
23. Cui S, Cheng Z, Qin W, Jiang L. Exosomes as a liquid biopsy for lung cancer. *Lung Cancer* (2018) 116:46–54. doi: 10.1016/j.lungcan.2017.12.012
24. Shi J. Considering Exosomal miR-21 as a Biomarker for Cancer. *J Clin Med* (2016) 5:42. doi: 10.3390/jcm5040042
25. Lomnytska M, Pinto R, Becker S, Engström U, Gustafsson S, Björklund C, et al. Platelet protein biomarker panel for ovarian cancer diagnosis. *Biomark Res* (2018) 6:2. doi: 10.1186/s40364-018-0118-y
26. Chen R, Xu X, Qian Z, Zhang C, Niu Y, Wang Z, et al. The biological functions and clinical applications of exosomes in lung cancer. *Cell Mol Life Sci* (2019) 76:4613–33. doi: 10.1007/s00018-019-03233-y
27. Bettegowda C, Sausen M, Leary R, Kinde I, Agrawal N, Bartlett B, et al. Detection of circulating tumor DNA in early- and late-stage human malignancies. *Sci Transl Med* (2014) 6:224ra24. doi: 10.1126/scitranslmed.3007094.Detection
28. Jiang P, Lo YMD. The Long and Short of Circulating Cell-Free DNA and the Ins and Outs of Molecular Diagnostics. *Trends Genet* (2016) 32:360–71. doi: 10.1016/j.tig.2016.03.009
29. Choi J-J, Reich 3CF, Pisetsky DS. The role of macrophages in the in vitro generation of extracellular DNA from apoptotic and necrotic cells. *Immunology* (2005) 115:55–62. doi: 10.1111/j.1365-2567.2005.02130.x
30. Thierry AR, El Messaoudi S, Gahan PB, Anker P, Stroun M. Origins, structures, and functions of circulating DNA in oncology. *Cancer Metastasis Rev* (2016) 35:347–76. doi: 10.1007/s10555-016-9629-x
31. Rykova EY, Morozkin ES, Ponomaryova AA, Loseva EM, Zaporozhchenko IA, Cherdyntseva NV, et al. Cell-free and cell-bound circulating nucleic acid complexes: mechanisms of generation, concentration and content. *Expert Opin Biol Ther* (2012) 12:S141–53. doi: 10.1517/14712598.2012.673577
32. Ponomaryova AA, Rykova EY, Cherdyntseva NV, Skvortsova TE, Cherepanova AV, Morozkin ES, et al. Concentration and Distribution of Single-Copy β-Actin Gene and LINE-1 Repetitive Elements in Blood of Lung Cancer Patients BT2010. In: *Circulating Nucleic Acids in Plasma and Serum*. Dordrecht: Springer Netherlands (2010). p. 41–5.
33. Joosse SA, Gorges TM, Pantel K. Biology, detection, and clinical implications of circulating tumor cells. *EMBO Mol Med* (2015) 7:1–11. doi: 10.15252/emmm.201303698
34. Joosse SA, Pantel K. Biologic challenges in the detection of circulating tumor cells. *Cancer Res* (2013) 73:8—11. doi: 10.1158/0008-5472.can-12-3422
35. Friedl P, Alexander S. Cancer Invasion and the Microenvironment: Plasticity and Reciprocity. *Cell* (2011) 147:992–1009. doi: 10.1016/j.cell.2011.11.016
36. Förnvik D, Andersson I, Dustler M, Ehrnström R, Rydén L, Tingberg A, et al. No evidence for shedding of circulating tumor cells to the peripheral venous blood as a result of mammographic breast compression. *Breast Cancer Res Treat* (2013) 141:187–95. doi: 10.1007/s10549-013-2674-z
37. Thiery JP. Epithelial–mesenchymal transitions in tumour progression. *Nat Rev Cancer* (2002) 2:442–54. doi: 10.1038/nrc822
38. Mimeault M, Batra SK. Molecular biomarkers of cancer stem/progenitor cells associated with progression, metastases, and treatment resistance of aggressive cancers. *Cancer Epidemiol Biomarkers Prev* (2014) 23:234–54. doi: 10.1158/1055-9965.EPI-13-0785
39. Tamminga M, de Wit S, van de Wauwer C, van den Bos H, Swennenhuis JF, Klinkenberg TJ, et al. Analysis of Released Circulating Tumor Cells During Surgery for Non-Small Cell Lung Cancer. *Clin Cancer Res* (2020) 26:1656–66. doi: 10.1158/1078-0432.CCR-19-2541
40. Reymond N, d'Água BB, Ridley AJ. Crossing the endothelial barrier during metastasis. *Nat Rev Cancer* (2013) 13:858–70. doi: 10.1038/nrc3628
41. Uhr JW, Pantel K. Controversies in clinical cancer dormancy. *Proc Natl Acad Sci USA* (2011) 108:12396–400. doi: 10.1073/pnas.1106613108
42. Esquela-Kerscher A, Slack FJ. Oncomirs — microRNAs with a role in cancer. *Nat Rev Cancer* (2006) 6:259–69. doi: 10.1038/nrc1840
43. Lim LP, Lau NC, Garrett-Engele P, Grimson A, Schelter JM, Castle J, et al. Microarray analysis shows that some microRNAs downregulate large numbers of target mRNAs. *Nature* (2005) 433:769–73. doi: 10.1038/nature03315
44. Krek A, Grün D, Poy MN, Wolf R, Rosenberg L, Epstein EJ, et al. Combinatorial microRNA target predictions. *Nat Genet* (2005) 37:495–500. doi: 10.1038/ng1536
45. Bartel DP. MicroRNAs: Genomics, Biogenesis, Mechanism, and Function. *Cell* (2004) 116:281–97. doi: 10.1016/S0092-8674(04)00045-5
46. Calin GA, Croce CM. MicroRNA-Cancer Connection: The Beginning of a New Tale. *Cancer Res* (2006) 66:7390–4. doi: 10.1158/0008-5472.CAN-06-0800
47. Calin GA, Croce CM. MicroRNA signatures in human cancers. *Nat Rev Cancer* (2006) 6:857–66. doi: 10.1038/nrc1997
48. Schwarzenbach H, Nishida N, Calin GA, Pantel K. Clinical relevance of circulating cell-free microRNAs in cancer. *Nat Rev Clin Oncol* (2014) 11:145–56. doi: 10.1038/nrclinonc.2014.5
49. Mathivanan S, Ji H, Simpson RJ. Exosomes: Extracellular organelles important in intercellular communication. *J Proteomics* (2010) 73:1907–20. doi: 10.1016/j.jprot.2010.06.006
50. Raposo G, Stoorvogel W. Extracellular vesicles: exosomes, microvesicles, and friends. *J Cell Biol* (2013) 200:373–83. doi: 10.1083/jcb.201211138
51. Reclusa P, Taverna S, Pucci M, Durendez E, Calabuig S, Manca P, et al. Exosomes as diagnostic and predictive biomarkers in lung cancer. *J Thorac Dis* (2017) 9:S1373–82. doi: 10.21037/jtd.2017.10.67
52. Andre F, Schartz NEC, Movassagh M, Flament C, Pautier P, Morice P, et al. Malignant effusions and immunogenic tumour-derived exosomes. *Lancet* (2002) 360:295–305. doi: 10.1016/S0140-6736(02)09552-1
53. Azmi AS, Bao B, Sarkar FH. Exosomes in cancer development, metastasis, and drug resistance: a comprehensive review. *Cancer Metastasis Rev* (2013) 32:623–42. doi: 10.1007/s10555-013-9441-9
54. Zhang X, Yuan X, Shi H, Wu L, Qian H, Xu W. Exosomes in cancer: small particle, big player. *J Hematol Oncol* (2015) 8:83. doi: 10.1186/s13045-015-0181-x
55. Franco AT, Ware J. G Soff, editor. *Thrombosis and Hemostasis in Cancer*. Cham: Springer International Publishing (2019). p. 37–54. doi: 10.1007/978-3-030-20315-3_3
56. Liu L, Lin F, Ma X, Chen Z, Yu J. Tumor-educated platelet as liquid biopsy in lung cancer patients. *Crit Rev Oncol Hematol* (2020) 146:102863. doi: 10.1016/j.critrevonc.2020.102863
57. Janowska-Wieczorek A, Wysoczynski M, Kijowski J, Marquez-Curtis L, Machalinski B, Ratajczak J, et al. Microvesicles derived from activated platelets induce metastasis and angiogenesis in lung cancer. *Int J Cancer* (2005) 113:752–60. doi: 10.1002/ijc.20657
58. Gay LJ, Felding-Habermann B. Contribution of platelets to tumour metastasis. *Nat Rev Cancer* (2011) 11:123–34. doi: 10.1038/nrc3004
59. Jiang X, Wong KHK, Khankhel AH, Zeinali M, Reategui E, Phillips MJ, et al. Microfluidic isolation of platelet-covered circulating tumor cells. *Lab Chip* (2017) 17:3498–503. doi: 10.1039/c7lc00654c
60. Placke T, Örgel M, Schaller M, Jung G, Rammensee H-G, Kopp H-G, et al. Platelet-Derived MHC Class I Confers a Pseudonormal Phenotype to Cancer Cells That Subverts the Antitumor Reactivity of Natural Killer Immune Cells. *Cancer Res* (2012) 72:440–8. doi: 10.1158/0008-5472.CAN-11-1872
61. Menter DG, Kopetz S, Hawk E, Sood AK, Loree JM, Gresele P, et al. Platelet "first responders" in wound response, cancer, and metastasis. *Cancer Metastasis Rev* (2017) 36:199–213. doi: 10.1007/s10555-017-9682-0
62. Plantureux L, Crescence L, Dignat-George F, Panicot-Dubois L, Dubois C. Effects of platelets on cancer progression. *Thromb Res* (2018) 164:S40–7. doi: 10.1016/j.thromres.2018.01.035
63. Labelle M, Begum S, Hynes RO. Direct signaling between platelets and cancer cells induces an epithelial-mesenchymal-like transition and promotes metastasis. *Cancer Cell* (2011) 20:576–90. doi: 10.1016/j.ccr.2011.09.009
64. Pinedo HM, Verheul HMW, D'Amato RJ, Folkman J. Involvement of platelets in tumour angiogenesis? *Lancet* (1998) 352:1775–7. doi: 10.1016/S0140-6736(98)05095-8
65. Cross MJ, Claesson-Welsh L. FGF and VEGF function in angiogenesis: signalling pathways, biological responses and therapeutic inhibition. *Trends Pharmacol Sci* (2001) 22:201–7. doi: 10.1016/S0165-6147(00)01676-X

66. Nilsson RJA, Balaj L, Hulleman E, van Rijn S, Pegtel DM, Walraven M, et al. Blood platelets contain tumor-derived RNA biomarkers. *Blood* (2011) 118:3680–3. doi: 10.1182/blood-2011-03-344408
67. Leon SA, Shapiro B, Sklaroff DM, Yaros MJ. Free DNA in the Serum of Cancer Patients and the Effect of Therapy. *Cancer Res* (1977) 37:646–50.
68. Diaz LA, Bardelli A. Liquid biopsies: Genotyping circulating tumor DNA. *J Clin Oncol* (2014) 32:579–86. doi: 10.1200/JCO.2012.45.2011
69. Abbosh C, Birkbak NJ, Wilson GA, Jamal-Hanjani M, Constantin T, Salari R, et al. Phylogenetic ctDNA analysis depicts early-stage lung cancer evolution. *Nature* (2017) 545:446–51. doi: 10.1038/nature22364
70. Fiala C, Diamandis EP. Utility of circulating tumor DNA in cancer diagnostics with emphasis on early detection. *BMC Med* (2018) 16:166. doi: 10.1186/s12916-018-1157-9
71. Casoni GL, Ulivi P, Mercatali L, Chilosi M, Tomassetti S, Romagnoli M, et al. Increased Levels of Free Circulating Dna in Patients with Idiopathic Pulmonary Fibrosis. *Int J Biol Markers* (2010) 25:229–35. doi: 10.5301/JBM.2010.6115
72. Chang CP-Y, Chia R-H, Wu T-L, Tsao K-C, Sun C-F, Wu JT. Elevated cell-free serum DNA detected in patients with myocardial infarction. *Clin Chim Acta* (2003) 327:95–101. doi: 10.1016/S0009-8981(02)00337-6
73. Rainer TH, Lam NYL. Circulating Nucleic Acids and Critical Illness. *Ann N Y Acad Sci* (2006) 1075:271–7. doi: 10.1196/annals.1368.035
74. Mouliere F, Chandrananda D, Piskorz AM, Moore EK, Morris J, Ahlborn LB, et al. Enhanced detection of circulating tumor DNA by fragment size analysis. *Sci Transl Med* (2018) 10:eaat4921. doi: 10.1126/scitranslmed.aat4921
75. Gagan J, Van Allen EM. Next-generation sequencing to guide cancer therapy. *Genome Med* (2015) 7:80. doi: 10.1186/s13073-015-0203-x
76. Schwaederlé MC, Patel SP, Husain H, Ikeda M, Lanman RB, Banks KC, et al. Utility of Genomic Assessment of Blood-Derived Circulating Tumor DNA (ctDNA) in Patients with Advanced Lung Adenocarcinoma. *Clin Cancer Res* (2017) 23:5101–11. doi: 10.1158/1078-0432.CCR-16-2497
77. Chang F, Li MM. Clinical application of amplicon-based next-generation sequencing in cancer. *Cancer Genet* (2013) 206:413–9. doi: 10.1016/j.cancergen.2013.10.003
78. Remon J, Caramella C, Jovelet C, Lacroix L, Lawson A, Smalley S, et al. Osimertinib benefit inEGFR-mutant NSCLC patients withT790M-mutation detected by circulating tumour DNA. *Ann Oncol* (2017) 28:784–90. doi: 10.1093/annonc/mdx017
79. Guibert N, Pradines A, Favre G, Mazieres J. Current and future applications of liquid biopsy in nonsmall cell lung cancer from early to advanced stages. *Eur Respir Rev* (2020) 29:190052. doi: 10.1183/16000617.0052-2019
80. Sozzi G, Conte D, Mariani L, Lo Vullo S, Roz L, Lombardo C, et al. Analysis of Circulating Tumor DNA in Plasma at Diagnosis and during Follow-Up of Lung Cancer Patients. *Cancer Res* (2001) 61:4675–8.
81. Sozzi G, Conte D, Leon M, Cirincione R, Roz L, Ratcliffe C, et al. Quantification of Free Circulating DNA As a Diagnostic Marker in Lung Cancer. *J Clin Oncol* (2003) 21:3902–8. doi: 10.1200/JCO.2003.02.006
82. Gautschi O, Bigosch C, Huegli B, Jermann M, Marx A, Chassé E, et al. Circulating Deoxyribonucleic Acid As Prognostic Marker in Non–Small-Cell Lung Cancer Patients Undergoing Chemotherapy. *J Clin Oncol* (2004) 22:4157–64. doi: 10.1200/JCO.2004.11.123
83. Herrera LJ, Raja S, Gooding WE, El-Hefnawy T, Kelly L, Luketich JD, et al. Quantitative Analysis of Circulating Plasma DNA as a Tumor Marker in Thoracic Malignancies. *Clin Chem* (2005) 51:113–8. doi: 10.1373/clinchem.2004.039263
84. Ludovini V, Pistola L, Gregorc V, Floriani I, Rulli E, Piattoni S, et al. Microsatellite Alterations, and p53 Tumor Mutations Are Associated with Disease-Free Survival in Radically Resected Non-small Cell Lung Cancer Patients: A Study of the Perugia Multidisciplinary Team for Thoracic Oncology. *J Thorac Oncol* (2008) 3:365–73. doi: 10.1097/JTO.0b013e318168c7d0
85. Szpechcinski A, Chorostowska-Wynimko J, Struniawski R, Kupis W, Rudzinski P, Langfort R, et al. Cell-free DNA levels in plasma of patients with non-small-cell lung cancer and inflammatory lung disease. *Br J Cancer* (2015) 113:476–83. doi: 10.1038/bjc.2015.225
86. Szpechcinski A, Rudzinski P, Kupis W, Langfort R, Orlowski T, Chorostowska-Wynimko J. Plasma cell-free DNA levels and integrity in patients with chest radiological findings: NSCLC versus benign lung nodules. *Cancer Lett* (2016) 374:202—207. doi: 10.1016/j.canlet.2016.02.002
87. Sozzi G, Roz L, Conte D, Mariani L, Andriani F, Lo Vullo S, et al. Plasma DNA quantification in lung cancer computed tomography screening: five-year results of a prospective study. *Am J Respir Crit Care Med* (2009) 179:69–74. doi: 10.1164/rccm.200807-1068oc
88. Paci M, Maramotti S, Bellesia E, Formisano D, Albertazzi L, Ricchetti T, et al. Circulating plasma DNA as diagnostic biomarker in non-small cell lung cancer. *Lung Cancer* (2009) 64:92–7. doi: 10.1016/j.lungcan.2008.07.012
89. Yoon K-A, Park S, Lee SH, Kim JH, Lee JS. Comparison of circulating plasma DNA levels between lung cancer patients and healthy controls. *J Mol Diagn* (2009) 11:182—5. doi: 10.2353/jmoldx.2009.080098
90. van der Drift MA, Hol BEA, Klaassen CHW, Prinsen CFM, van Aarssen YAWG, Donders R, et al. Circulating DNA is a non-invasive prognostic factor for survival in non-small cell lung cancer. *Lung Cancer* (2010) 68:283–7. doi: 10.1016/j.lungcan.2009.06.021
91. Catarino R, Coelho A, Araújo A, Gomes M, Nogueira A, Lopes C, et al. Circulating DNA: Diagnostic Tool and Predictive Marker for Overall Survival of NSCLC Patients. *PloS One* (2012) 7:1–8. doi: 10.1371/journal.pone.0038559
92. Zhao X, Han R-B, Zhao J, Wang J, Yang F, Zhong W, et al. Comparison of Epidermal Growth Factor Receptor Mutation Statuses in Tissue and Plasma in Stage I–IV Non-Small Cell Lung Cancer Patients. *Respiration* (2013) 85:119–25. doi: 10.1159/000338790
93. Jing C-W, Wang Z, Cao H-X, Ma R, Wu J-Z. High resolution melting analysis for epidermal growth factor receptor mutations in formalin-fixed paraffin-embedded tissue and plasma free DNA from non-small cell lung cancer patients. *Asian Pac J Cancer Prev* (2014) 14:6619—23. doi: 10.7314/APJCP.2013.14.11.6619
94. Uchida J, Kato K, Kukita Y, Kumagai T, Nishino K, Daga H, et al. Diagnostic Accuracy of Noninvasive Genotyping of EGFR in Lung Cancer Patients by Deep Sequencing of Plasma Cell-Free DNA. *Clin Chem* (2015) 61:1191—6. doi: 10.1373/clinchem.2015.241414
95. Fernandez-Cuesta L, Perdomo S, Avogbe PH, Leblay N, Delhomme TM, Gaborieau V, et al. Identification of Circulating Tumor DNA for the Early Detection of Small-cell Lung Cancer. *EBioMedicine* (2016) 10:117–23. doi: 10.1016/j.ebiom.2016.06.032
96. Wan Y, Liu B, Lei H, Zhang B, Wang Y, Huang H, et al. Nanoscale extracellular vesicle-derived DNA is superior to circulating cell-free DNA for mutation detection in early-stage non-small-cell lung cancer. *Ann Oncol* (2018) 29:2379–83. doi: 10.1093/annonc/mdy458
97. Wei F, Strom CM, Cheng J, Lin C-C, Hsu C-Y, Soo Hoo GW, et al. Electric Field–Induced Release and Measurement Liquid Biopsy for Noninvasive Early Lung Cancer Assessment. *J Mol Diagnostics* (2018) 20:738–42. doi: 10.1016/j.jmoldx.2018.06.008
98. Newman AM, Bratman SV, To J, Wynne JF, Eclov NCW, Modlin LA, et al. An ultrasensitive method for quantitating circulating tumor DNA with broad patient coverage. *Nat Med* (2014) 20:548–54. doi: 10.1038/nm.3519
99. Guo N, Lou F, Ma Y, Li J, Yang B, Chen W, et al. Circulating tumor DNA detection in lung cancer patients before and after surgery. *Sci Rep* (2016) 6:33519. doi: 10.1038/srep33519
100. Chen K-Z, Lou F, Yang F, Zhang J-B, Ye H, Chen W, et al. Circulating Tumor DNA Detection in Early-Stage Non-Small Cell Lung Cancer Patients by Targeted Sequencing. *Sci Rep* (2016) 6:31985. doi: 10.1038/srep31985
101. Cohen JD, Li L, Wang Y, Thoburn C, Afsari B, Danilova L, et al. Detection and localization of surgically resectable cancers with a multi-analyte blood test. *Science (80-)* (2018) 359:926–30. doi: 10.1126/science.aar3247
102. Ye M, Li S, Huang W, Wang C, Liu L, Liu J, et al. Comprehensive targeted super-deep next generation sequencing enhances differential diagnosis of solitary pulmonary nodules. *J Thorac Dis* (2018) 10:S820–9. doi: 10.21037/jtd.2018.04.09
103. Peng M, Xie Y, Li X, Qian Y, Tu X, Yao X, et al. Resectable lung lesions malignancy assessment and cancer detection by ultra-deep sequencing of targeted gene mutations in plasma cell-free DNA. *J Med Genet* (2019) 56:647–53. doi: 10.1136/jmedgenet-2018-105825
104. Tailor TD, Rao X, Campa MJ, Wang J, Gregory SG, Patz EFJr. Whole Exome Sequencing of Cell-Free DNA for Early Lung Cancer: A Pilot Study to

Differentiate Benign From Malignant CT-Detected Pulmonary Lesions. *Front Oncol* (2019) 9:317. doi: 10.3389/fonc.2019.00317
105. Leung M, Freidin MB, Freydina DV, Von Crease C, De Sousa P, Barbosa MT, et al. Blood-based circulating tumor DNA mutations as a diagnostic and prognostic biomarker for lung cancer. *Cancer* (2020) 126:1804–9. doi: 10.1002/cncr.32699
106. Wang Y, Yu Z, Wang T, Zhang J, Hong L, Chen L. Identification of epigenetic aberrant promoter methylation of RASSF1A in serum DNA and its clinicopathological significance in lung cancer. *Lung Cancer* (2007) 56:289–94. doi: 10.1016/j.lungcan.2006.12.007
107. Schmidt B, Liebenberg V, Dietrich D, Schlegel T, Kneip C, Seegebarth A, et al. SHOX2 DNA Methylation is a Biomarker for the diagnosis of lung cancer based on bronchial aspirates. *BMC Cancer* (2010) 10:600. doi: 10.1186/1471-2407-10-600
108. Kneip C, Schmidt B, Seegebarth A, Weickmann S, Fleischhacker M, Liebenberg V, et al. SHOX2 DNA Methylation Is a Biomarker for the Diagnosis of Lung Cancer in Plasma. *J Thorac Oncol* (2011) 6:1632–8. doi: 10.1097/JTO.0b013e318220ef9a
109. Hwang S-H, Kim KU, Kim J-E, Kim H-H, Lee MK, Lee CH, et al. Detection of HOXA9 gene methylation in tumor tissues and induced sputum samples from primary lung cancer patients. *Clin Chem Lab Med* (2011) 49:699–704. doi: 10.1515/CCLM.2011.108
110. Dietrich D, Kneip C, Raji O, Liloglou T, Seegebarth A, Schlegel T, et al. Performance evaluation of the DNA methylation biomarker SHOX2 for the aid in diagnosis of lung cancer based on the analysis of bronchial aspirates. *Int J Oncol* (2012) 40:825–32. doi: 10.3892/ijo.2011.1264
111. Ponomaryova AA, Rykova EY, Cherdyntseva NV, Skvortsova TE, Dobrodeev AY, Zav'yalov AA, et al. Potentialities of aberrantly methylated circulating DNA for diagnostics and post-treatment follow-up of lung cancer patients. *Lung Cancer* (2013) 81:397–403. doi: 10.1016/j.lungcan.2013.05.016
112. Powrózek T, Krawczyk P, Kucharczyk T, Milanowski J. Septin 9 promoter region methylation in free circulating DNA—potential role in noninvasive diagnosis of lung cancer: preliminary report. *Med Oncol* (2014) 31:917. doi: 10.1007/s12032-014-0917-4
113. Konecny M, Markus J, Waczulikova I, Dolesova L, Kozlova R, Repiska V, et al. The value of SHOX2 methylation test in peripheral blood samples used for the differential diagnosis of lung cancer and other lung disorders. *Neoplasma* (2016) 63:246–53. doi: 10.4149/210_150419N208
114. Powrózek T, Krawczyk P, Nicoś M, Kuźnar-Kamińska B, Batura-Gabryel H, Milanowski J. Methylation of the DCLK1 promoter region in circulating free DNA and its prognostic value in lung cancer patients. *Clin Transl Oncol* (2016) 18:398—404. doi: 10.1007/s12094-015-1382-z
115. Ren M, Wang C, Sheng D, Shi Y, Jin M, Xu S. Methylation analysis of SHOX2 and RASSF1A in bronchoalveolar lavage fluid for early lung cancer diagnosis. *Ann Diagn Pathol* (2017) 27:57–61. doi: 10.1016/j.anndiagpath.2017.01.007
116. Nunes SP, Diniz F, Moreira-Barbosa C, Constâncio V, Silva AV, Oliveira J, et al. Subtyping Lung Cancer Using DNA Methylation in Liquid Biopsies. *J Clin Med* (2019) 8:1–14. doi: 10.3390/jcm8091500
117. Fujiwara K, Fujimoto N, Tabata M, Nishii K, Matsuo K, Hotta K, et al. Identification of Epigenetic Aberrant Promoter Methylation in Serum DNA Is Useful for Early Detection of Lung Cancer. *Clin Cancer Res* (2005) 11:1219–25.
118. Hsu H-S, Chen T-P, Hung C-H, Wen C-K, Lin R-K, Lee H-C, et al. Characterization of a multiple epigenetic marker panel for lung cancer detection and risk assessment in plasma. *Cancer* (2007) 110:2019–26. doi: 10.1002/cncr.23001
119. Zhang Y, Wang R, Song H, Huang G, Yi J, Zheng Y, et al. Methylation of multiple genes as a candidate biomarker in non-small cell lung cancer. *Cancer Lett* (2011) 303:21–8. doi: 10.1016/j.canlet.2010.12.011
120. Begum S, Brait M, Dasgupta S, Ostrow KL, Zahurak M, Carvalho AL, et al. An epigenetic marker panel for detection of lung cancer using cell-free serum DNA. *Clin Cancer Res* (2011) 17:4494–503. doi: 10.1158/1078-0432.CCR-10-3436
121. Nikolaidis G, Raji OY, Markopoulou S, Gosney JR, Bryan J, Warburton C, et al. DNA methylation biomarkers offer improved diagnostic efficiency in lung cancer. *Cancer Res* (2012) 72:5692–701. doi: 10.1158/0008-5472.can-12-2309
122. Diaz-Lagares A, Mendez-Gonzalez J, Hervas D, Saigi M, Pajares MJ, Garcia D, et al. A Novel Epigenetic Signature for Early Diagnosis in Lung Cancer. *Clin Cancer Res* (2016) 22:3361–71. doi: 10.1158/1078-0432.CCR-15-2346
123. Ma Y, Bai Y, Mao H, Hong Q, Yang D, Zhang H, et al. A panel of promoter methylation markers for invasive and noninvasive early detection of NSCLC using a quantum dots-based FRET approach. *Biosens Bioelectron* (2016) 85:641–8. doi: 10.1016/j.bios.2016.05.067
124. Hulbert A, Jusue Torres I, Stark A, Chen C, Rodgers K, Lee B, et al. Early Detection of Lung Cancer using DNA Promoter Hypermethylation in Plasma and Sputum. *Clin Cancer Res* (2016) 23:clincanres.1371.2016. doi: 10.1158/1078-0432.CCR-16-1371
125. Ooki A, Maleki Z, Tsay J-CJ, Goparaju C, Brait M, Turaga N, et al. A Panel of Novel Detection and Prognostic Methylated DNA Markers in Primary Non-Small Cell Lung Cancer and Serum DNA. *Clin Cancer Res* (2017) 23:7141–52. doi: 10.1158/1078-0432.ccr-17-1222
126. Hubers AJ, Heideman DAM, Duin S, Witte BI, de Koning HJ, Groen HJM, et al. DNA hypermethylation analysis in sputum of asymptomatic subjects at risk for lung cancer participating in the NELSON trial: argument for maximum screening interval of 2 years. *J Clin Pathol* (2017) 70:250–4. doi: 10.1136/jclinpath-2016-203734
127. Liang W, Zhao Y, Huang W, Gao Y, Xu W, Tao J, et al. Non-invasive diagnosis of early-stage lung cancer using high-throughput targeted DNA methylation sequencing of circulating tumor DNA (ctDNA). *Theranostics* (2019) 9:2056–70. doi: 10.7150/thno.28119
128. Balgkouranidou I, Liloglou T, Lianidou ES. Lung cancer epigenetics: emerging biomarkers. *Biomark Med* (2013) 7:49–58. doi: 10.2217/bmm.12.111
129. Yu L, Liu H, Yan M, Yang J, Long F, Muneoka K, et al. Shox2 is required for chondrocyte proliferation and maturation in proximal limb skeleton. *Dev Biol* (2007) 306:549–59. doi: 10.1016/j.ydbio.2007.03.518
130. Blaschke RJ, Monaghan AP, Schiller S, Schechinger B, Rao E, Padilla-Nash H, et al. SHOT, a SHOX-related homeobox gene, is implicated in craniofacial, brain, heart, and limb development. *Proc Natl Acad Sci USA* (1998) 95:2406–11. doi: 10.1073/pnas.95.5.2406
131. de Wit S, Rossi E, Weber S, Tamminga M, Manicone M, Swennenhuis JF, et al. Single tube liquid biopsy for advanced non-small cell lung cancer. *Int J Cancer* (2019) 144:3127–37. doi: 10.1002/ijc.32056
132. Wang J, Wang K, Xu J, Huang J, Zhang T. Prognostic significance of circulating tumor cells in non-small-cell lung cancer patients: a meta-analysis. *PloS One* (2013) 8:e78070–0. doi: 10.1371/journal.pone.0078070
133. Hamilton G, Rath B. Detection of circulating tumor cells in non-small cell lung cancer. *J Thorac Dis* (2016) 8:1024–8. doi: 10.21037/jtd.2016.03.86
134. Allard WJ, Matera J, Miller MC, Repollet M, Connelly MC, Rao C, et al. Tumor cells circulate in the peripheral blood of all major carcinomas but not in healthy subjects or patients with nonmalignant diseases. *Clin Cancer Res* (2005) 10:6897–904. doi: 10.1158/1078-0432.CCR-04-0378
135. Tanaka F, Yoneda K, Kondo N, Hashimoto M, Takuwa T, Matsumoto S, et al. Circulating Tumor Cell as a Diagnostic Marker in Primary Lung Cancer. *Clin Cancer Res* (2009) 15:6980–6. doi: 10.1158/1078-0432.CCR-09-1095
136. Hofman V, Bonnetaud C, Ilie MI, Vielh P, Vignaud JM, Fléjou JF, et al. Preoperative Circulating Tumor Cell Detection Using the Isolation by Size of Epithelial Tumor Cell Method for Patients with Lung Cancer Is a New Prognostic Biomarker. *Clin Cancer Res* (2011) 17:827–35. doi: 10.1158/1078-0432.CCR-10-0445
137. Hofman V, Ilie MI, Long E, Selva E, Bonnetaud C, Molina T, et al. Detection of circulating tumor cells as a prognostic factor in patients undergoing radical surgery for non-small-cell lung carcinoma: comparison of the efficacy of the CellSearch Assay™ and the isolation by size of epithelial tumor cell method. *Int J Cancer* (2011) 129:1651–60. doi: 10.1002/ijc.25819
138. Hofman V, Long E, Ilie M, Bonnetaud C, Vignaud JM, Fléjou JF, et al. Morphological analysis of circulating tumour cells in patients undergoing surgery for non-small cell lung carcinoma using the isolation by size of epithelial tumour cell (ISET) method. *Cytopathology* (2012) 23:30–8. doi: 10.1111/j.1365-2303.2010.00835.x
139. Ilie M, Hofman V, Long-Mira E, Selva E, Vignaud J-M, Padovani B, et al. "Sentinel" circulating tumor cells allow early diagnosis of lung cancer in patients with chronic obstructive pulmonary disease. *PloS One* (2014) 9:e111597. doi: 10.1371/journal.pone.0111597

140. Dorsey JF, Kao GD, MacArthur KM, Ju M, Steinmetz D, Wileyto EP, et al. Simone 2nd CBTracking viable circulating tumor cells (CTCs) in the peripheral blood of non-small cell lung cancer (NSCLC) patients undergoing definitive radiation therapy: pilot study results. *Cancer* (2015) 121:139–49. doi: 10.1002/cncr.28975
141. Fiorelli A, Accardo M, Carelli E, Angioletti D, Santini M, Di Domenico M. Circulating Tumor Cells in Diagnosing Lung Cancer: Clinical and Morphologic Analysis. *Ann Thorac Surg* (2015) 99:1899–905. doi: 10.1016/j.athoracsur.2014.11.049
142. Chen X, Zhou F, Li X, Yang G, Zhang L, Ren S, et al. Folate Receptor–Positive Circulating Tumor Cell Detected by LT-PCR–Based Method as a Diagnostic Biomarker for Non–Small-Cell Lung Cancer. *J Thorac Oncol* (2015) 10:1163–71. doi: 10.1097/JTO.0000000000000606
143. Xu Y, Liu B, Ding F, Zhou X, Tu P, Yu B, et al. Circulating tumor cell detection: A direct comparison between negative and unbiased enrichment in lung cancer. *Oncol Lett* (2017) 13:4882–6. doi: 10.3892/ol.2017.6046
144. Xue Y, Cong W, Xie S, Shu J, Feng G, Gao H. Folate-receptor-positive circulating tumor cells as an efficacious biomarker for the diagnosis of small pulmonary nodules. *J Cancer Res Ther* (2018) 14:1620–6. doi: 10.4103/jcrt.JCRT_905_17
145. Frick MA, Feigenberg SJ, Jean-Baptiste SR, Aguarin LA, Mendes A, Chinniah C, et al. Circulating tumor cells are associated with recurrent disease in patients with early stage non-small cell lung cancer treated with stereotactic body radiation therapy. *Clin Cancer Res* (2020) 26:clincanres.2158.2019. doi: 10.1158/1078-0432.CCR-19-2158
146. He Y, Shi J, Shi G, Xu X, Liu Q, Liu C, et al. Using the New CellCollector to Capture Circulating Tumor Cells from Blood in Different Groups of Pulmonary Disease: A Cohort Study. *Sci Rep* (2017) 7:9542. doi: 10.1038/s41598-017-09284-0
147. Duan G-C, Zhang X-P, Wang H-E, Wang Z-K, Zhang H, Yu L, et al. Circulating Tumor Cells as a Screening and Diagnostic Marker for Early-Stage Non-Small Cell Lung Cancer. *Onco Targets Ther* (2020) 13:1931–9. doi: 10.2147/OTT.S241956
148. He Y, Shi J, Schmidt B, Liu Q, Shi G, Xu X, et al. Circulating Tumor Cells as a Biomarker to Assist Molecular Diagnosis for Early Stage Non-Small Cell Lung Cancer. *Cancer Manag Res* (2020) 12:841–54. doi: 10.2147/CMAR.S240773
149. Hofman VJ, Ilie M, Hofman PM. Detection and characterization of circulating tumor cells in lung cancer: Why and how? *Cancer Cytopathol* (2016) 124:380–7. doi: 10.1002/cncy.21651
150. Tamminga M, de Wit S, Schuuring E, Timens W, Terstappen LWMM, Hiltermann TJN, et al. Circulating tumor cells in lung cancer are prognostic and predictive for worse tumor response in both targeted- and chemotherapy. *Transl Lung Cancer Res Vol 8, No 6 (December 2019). Transl Lung Cancer Res* (2019) 8(6):854–61. doi: 10.21037/tlcr.2019.11.06
151. Lindsay CR, Blackhall FH, Carmel A, Fernandez-Gutierrez F, Gazzaniga P, Groen HJM, et al. EPAC-lung: pooled analysis of circulating tumour cells in advanced non-small cell lung cancer. *Eur J Cancer* (2019) 117:60–8. doi: 10.1016/j.ejca.2019.04.019
152. Liu Z, Fusi A, Klopocki E, Schmittel A, Tinhofer I, Nonnenmacher A, et al. Negative enrichment by immunomagnetic nanobeads for unbiased characterization of circulating tumor cells from peripheral blood of cancer patients. *J Transl Med* (2011) 9:70. doi: 10.1186/1479-5876-9-70
153. Ozkumur E, Shah AM, Ciciliano JC, Emmink BL, Miyamoto DT, Brachtel E, et al. Inertial focusing for tumor antigen-dependent and -independent sorting of rare circulating tumor cells. *Sci Transl Med* (2013) 5:179ra47. doi: 10.1126/scitranslmed.3005616
154. He W, Kularatne SA, Kalli KR, Prendergast FG, Amato RJ, Klee GG, et al. Quantitation of circulating tumor cells in blood samples from ovarian and prostate cancer patients using tumor-specific fluorescent ligands. *Int J Cancer* (2008) 123:1968–73. doi: 10.1002/ijc.23717
155. Parker N, Turk MJ, Westrick E, Lewis JD, Low PS, Leamon CP. Folate receptor expression in carcinomas and normal tissues determined by a quantitative radioligand binding assay. *Anal Biochem* (2005) 338:284–93. doi: 10.1016/j.ab.2004.12.026
156. Saucedo-Zeni N, Mewes S, Niestroj R, Gasiorowski L, Murawa D, Nowaczyk P, et al. A novel method for the in vivo isolation of circulating tumor cells from peripheral blood of cancer patients using a functionalized and structured medical wire. *Int J Oncol* (2012) 41:1241–50. doi: 10.3892/ijo.2012.1557
157. Gorges TM, Penkalla N, Schalk T, Joosse SA, Riethdorf S, Tucholski J, et al. Enumeration and Molecular Characterization of Tumor Cells in Lung Cancer Patients Using a Novel In Vivo Device for Capturing Circulating Tumor Cells. *Clin Cancer Res* (2016) 22:2197–206. doi: 10.1158/1078-0432.CCR-15-1416
158. Nagrath S, Sequist LV, Maheswaran S, Bell DW, Irimia D, Ulkus L, et al. Isolation of rare circulating tumour cells in cancer patients by microchip technology. *Nature* (2007) 450:1235–9. doi: 10.1038/nature06385
159. Neves RPL, Ammerlaan W, Andree KC, Bender S, Cayrefourcq L, Driemel C, et al. Proficiency Testing to Assess Technical Performance for CTC-Processing and Detection Methods in CANCER-ID. *Clin Chem* (2021) 67 (4):631–41. doi: 10.1093/clinchem/hvaa322
160. Mitchell PS, Parkin RK, Kroh EM, Fritz BR, Wyman SK, Pogosova-Agadjanyan EL, et al. Circulating microRNAs as stable blood-based markers for cancer detection. *Proc Natl Acad Sci* (2008) 105:10513–8. doi: 10.1073/pnas.0804549105
161. Chen X, Ba Y, Ma L, Cai X, Yin Y, Wang K, et al. Characterization of microRNAs in serum: a novel class of biomarkers for diagnosis of cancer and other diseases. *Cell Res* (2008) 18:997–1006. doi: 10.1038/cr.2008.282
162. Xie Y, Todd NW, Liu Z, Zhan M, Fang H, Peng H, et al. Altered miRNA expression in sputum for diagnosis of non-small cell lung cancer. *Lung Cancer* (2010) 67:170–6. doi: 10.1016/j.lungcan.2009.04.004
163. Yu L, Todd NW, Xing L, Xie Y, Zhang H, Liu Z, et al. Early detection of lung adenocarcinoma in sputum by a panel of microRNA markers. *Int J Cancer* (2010) 127:2870–8. doi: 10.1002/ijc.25289
164. Shen J, Todd NW, Zhang H, Yu L, Lingxiao X, Mei Y, et al. Plasma microRNAs as potential biomarkers for non-small-cell lung cancer. *Lab Investig* (2011) 91:579–87. doi: 10.1038/labinvest.2010.194
165. Shen J, Liu Z, Todd NW, Zhang H, Liao J, Yu L, et al. Diagnosis of lung cancer in individuals with solitary pulmonary nodules by plasma microRNA biomarkers. *BMC Cancer* (2011) 11:374. doi: 10.1186/1471-2407-11-374
166. Zheng D, Haddadin S, Wang Y, Gu L-Q, Perry MC, Freter CE, et al. Plasma microRNAs as novel biomarkers for early detection of lung cancer. *Int J Clin Exp Pathol* (2011) 4:575–86.
167. Boeri M, Verri C, Conte D, Roz L, Modena P, Facchinetti F, et al. MicroRNA signatures in tissues and plasma predict development and prognosis of computed tomography detected lung cancer. *Proc Natl Acad Sci USA* (2011) 108:3713–8. doi: 10.1073/pnas.1100048108
168. Foss KM, Sima C, Ugolini D, Neri M, Allen KE, Weiss GJ. miR-1254 and miR-574-5p: Serum-Based microRNA Biomarkers for Early-Stage Non-small Cell Lung Cancer. *J Thorac Oncol* (2011) 6:482–8. doi: 10.1097/JTO.0b013e318208c785
169. Bianchi F, Nicassio F, Marzi M, Belloni E, Dall'olio V, Bernard L, et al. A serum circulating miRNA diagnostic test to identify asymptomatic high-risk individuals with early stage lung cancer. *EMBO Mol Med* (2011) 3:495–503. doi: 10.1002/emmm.201100154
170. Heegaard NHH, Schetter AJ, Welsh JA, Yoneda M, Bowman ED, Harris CC. Circulating micro-RNA expression profiles in early stage nonsmall cell lung cancer. *Int J Cancer* (2012) 130:1378—86. doi: 10.1002/ijc.26153
171. Sozzi G, Boeri M, Rossi M, Verri C, Suatoni P, Bravi F, et al. Clinical utility of a plasma-based miRNA signature classifier within computed tomography lung cancer screening: a correlative MILD trial study. *J Clin Oncol* (2014) 32:768–73. doi: 10.1200/JCO.2013.50.4357
172. Shen J, Liao J, Guarnera MA, Fang H, Cai L, Stass SA, et al. Analysis of MicroRNAs in sputum to improve computed tomography for lung cancer diagnosis. *J Thorac Oncol* (2014) 9:33–40. doi: 10.1097/JTO.0000000000000025
173. Wang P, Yang D, Zhang H, Wei X, Ma T, Cheng Z, et al. Early Detection of Lung Cancer in Serum by a Panel of MicroRNA Biomarkers. *Clin Lung Cancer* (2015) 16:313—9.e1. doi: 10.1016/j.cllc.2014.12.006
174. Montani F, Marzi MJ, Dezi F, Dama E, Carletti RM, Bonizzi G, et al. miR-Test: A Blood Test for Lung Cancer Early Detection. *JNCI J Natl Cancer Inst* (2015) 107:1–5. doi: 10.1093/jnci/djv063
175. Xing L, Su J, Guarnera MA, Zhang H, Cai L, Zhou R, et al. Sputum microRNA biomarkers for identifying lung cancer in indeterminate solitary pulmonary nodules. *Clin Cancer Res* (2015) 21:484–9. doi: 10.1158/1078-0432.CCR-14-1873

176. Wang C, Ding M, Xia M, Chen S, Van Le A, Soto-Gil R, et al. A Five-miRNA Panel Identified From a Multicentric Case–control Study Serves as a Novel Diagnostic Tool for Ethnically Diverse Non-small-cell Lung Cancer Patients. *EBioMedicine* (2015) 2:1377–85. doi: 10.1016/j.ebiom.2015.07.034
177. Kim JO, Gazala S, Razzak R, Guo L, Ghosh S, Roa WH, et al. Non-small Cell Lung Cancer Detection Using MicroRNA Expression Profiling of Bronchoalveolar Lavage Fluid and Sputum. *Anticancer Res* (2015) 35:1873–80.
178. Li W, Wang Y, Zhang Q, Tang L, Liu X, Dai Y, et al. MicroRNA-486 as a Biomarker for Early Diagnosis and Recurrence of Non-Small Cell Lung Cancer. *PloS One* (2015) 10:e0134220. doi: 10.1371/journal.pone.0134220
179. Fan L, Qi H, Teng J, Su B, Chen H, Wang C, et al. Identification of serum miRNAs by nano-quantum dots microarray as diagnostic biomarkers for early detection of non-small cell lung cancer. *Tumour Biol* (2016) 37:7777–84. doi: 10.1007/s13277-015-4608-3
180. Razzak R, Bédard ELR, Kim JO, Gazala S, Guo L, Ghosh S, et al. MicroRNA expression profiling of sputum for the detection of early and locally advanced non-small-cell lung cancer: a prospective case-control study. *Curr Oncol* (2016) 23:e86–94. doi: 10.3747/co.23.2830
181. Bagheri A, Khorram Khorshid HR, Mowla SJ, Mohebbi HA, Mohammadian A, Yaseri M, et al. Altered miR-223 Expression in Sputum for Diagnosis of Non-Small Cell Lung Cancer. *Avicenna J Med Biotechnol* (2017) 9:189–95.
182. Leng Q, Lin Y, Jiang F, Lee C-J, Zhan M, Fang H, et al. A plasma miRNA signature for lung cancer early detection. *Oncotarget* (2017) 8:111902–11. doi: 10.18632/oncotarget.22950
183. Lu S, Kong H, Hou Y, Ge D, Huang W, Ou J, et al. Two plasma microRNA panels for diagnosis and subtype discrimination of lung cancer. *Lung Cancer* (2018) 123:44–51. doi: 10.1016/j.lungcan.2018.06.027
184. Abu-Duhier FM, Javid J, Sughayer MA, Mir R, Albalawi T, Alauddin MS. Clinical Significance of Circulatory miRNA-21 as an Efficient Non-Invasive Biomarker for the Screening of Lung Cancer Patients. *Asian Pac J Cancer Prev* (2018) 19:2607–11. doi: 10.22034/APJCP.2018.19.9.2607
185. Xi K-X, Zhang X-W, Yu X-Y, Wang W-D, Xi K-X, Chen Y-Q, et al. The role of plasma miRNAs in the diagnosis of pulmonary nodules. *J Thorac Dis* (2018) 10:4032–41. doi: 10.21037/jtd.2018.06.106
186. Li J, Fang H, Jiang F, Ning Y. External validation of a panel of plasma microRNA biomarkers for lung cancer. *Biomark Med* (2019) 13:1557–64. doi: 10.2217/bmm-2019-0213
187. Liang L-B, Zhu W-J, Chen X-M, Luo F-M. Plasma miR-30a-5p as an early novel noninvasive diagnostic and prognostic biomarker for lung cancer. *Futur Oncol* (2019) 15:3711–21. doi: 10.2217/fon-2019-0393
188. Xi K, Wang W, Wen Y, Chen Y, Zhang X, Wu Y, et al. Combining Plasma miRNAs and Computed Tomography Features to Differentiate the Nature of Pulmonary Nodules. *Front Oncol* (2019) 9:975. doi: 10.3389/fonc.2019.00975
189. Liao J, Shen J, Leng Q, Qin M, Zhan M, Jiang F. MicroRNA-based biomarkers for diagnosis of non-small cell lung cancer (NSCLC). *Thorac Cancer* (2020) 11:762–8. doi: 10.1111/1759-7714.13337
190. Mensah M, Borzi C, Verri C, Suatoni P, Conte D, Pastorino U, et al. MicroRNA Based Liquid Biopsy: The Experience of the Plasma miRNA Signature Classifier (MSC) for Lung Cancer Screening. *J Vis Exp* (2017) 190:56326. doi: 10.3791/56326
191. Pastorino U, Boeri M, Sestini S, Sabia F, Silva M, Suatoni P, et al. PL02.04 Blood MicroRNA and LDCT Reduce Unnecessary LDCT Repeats in Lung Cancer Screening: Results of Prospective BioMILD Trial. *J Thorac Oncol* (2019) 14:S5–6. doi: 10.1016/j.jtho.2019.08.057
192. Yang Y, Hu Z, Zhou Y, Zhao G, Lei Y, Li G, et al. The clinical use of circulating microRNAs as non-invasive diagnostic biomarkers for lung cancers. *Oncotarget* (2017) 8:90197–214. doi: 10.18632/oncotarget.21644
193. Yu H, Guan Z, Cuk K, Brenner H, Zhang Y. Circulating microRNA biomarkers for lung cancer detection in Western populations. *Cancer Med* (2018) 7:4849–62. doi: 10.1002/cam4.1782
194. Thunnissen FBJM. Sputum examination for early detection of lung cancer. *J Clin Pathol* (2003) 56:805–10. doi: 10.1136/jcp.56.11.805
195. Saccomanno G, Archer VE, Auerbach O, Saunders RP, Brennan LM. Development of carcinoma of the lung as reflected in exfoliated cells. *Cancer* (1974) 33:256–70. doi: 10.1002/1097-0142(197401)33:1<256::AID-CNCR2820330139>3.0.CO;2-G
196. Xing L, Todd NW, Yu L, Fang H, Jiang F. Early detection of squamous cell lung cancer in sputum by a panel of microRNA markers. *Mod Pathol* (2010) 23:1157–64. doi: 10.1038/modpathol.2010.111
197. Rabinowits G, Gerçel-Taylor C, Day JM, Taylor DD, Kloecker GH. Exosomal microRNA: A diagnostic marker for lung cancer. *Clin Lung Cancer* (2009) 10:42–6. doi: 10.3816/CLC.2009.n.006
198. Cazzoli R, Buttitta F, Di Nicola M, Malatesta S, Marchetti A, Rom WN, et al. microRNAs Derived from Circulating Exosomes as Noninvasive Biomarkers for Screening and Diagnosing Lung Cancer. *J Thorac Oncol* (2013) 8:1156–62. doi: 10.1097/JTO.0b013e318299ac32
199. Zhou X, Wen W, Shan X, Zhu W, Xu J, Guo R, et al. A six-microRNA panel in plasma was identified as a potential biomarker for lung adenocarcinoma diagnosis. *Oncotarget* (2017) 8:6513–25. doi: 10.18632/oncotarget.14311
200. Jin X, Chen Y, Chen H, Fei S, Chen D, Cai X, et al. Evaluation of Tumor-Derived Exosomal miRNA as Potential Diagnostic Biomarkers for Early-Stage Non–Small Cell Lung Cancer Using Next-Generation Sequencing. *Clin Cancer Res* (2017) 23:5311–9. doi: 10.1158/1078-0432.CCR-17-0577
201. Lin J, Wang Y, Zou Y-Q, Chen X, Huang B, Liu J, et al. Differential miRNA expression in pleural effusions derived from extracellular vesicles of patients with lung cancer, pulmonary tuberculosis, or pneumonia. *Tumor Biol* (2016) 37:15835–45. doi: 10.1007/s13277-016-5410-6
202. Krug AK, Enderle D, Karlovich C, Priewasser T, Bentink S, Spiel A, et al. Improved EGFR mutation detection using combined exosomal RNA and circulating tumor DNA in NSCLC patient plasma. *Ann Oncol Off J Eur Soc Med Oncol* (2018) 29:700–6. doi: 10.1093/annonc/mdx765
203. Thakur BK, Zhang H, Becker A, Matei I, Huang Y, Costa-Silva B, et al. Double-stranded DNA in exosomes: a novel biomarker in cancer detection. *Cell Res* (2014) 24:766–9. doi: 10.1038/cr.2014.44
204. Huang S, Li Y, Zhang J, Rong J, Ye S. Epidermal Growth Factor Receptor-Containing Exosomes Induce Tumor-Specific Regulatory T Cells. *Cancer Invest* (2013) 31:330–5. doi: 10.3109/07357907.2013.789905
205. Clark DJ, Fondrie WE, Yang A, Mao L. Triple SILAC quantitative proteomic analysis reveals differential abundance of cell signaling proteins between normal and lung cancer-derived exosomes. *J Proteomics* (2016) 133:161–9. doi: 10.1016/j.jprot.2015.12.023
206. Sandfeld-Paulsen B, Jakobsen KR, Bæk R, Folkersen BH, Rasmussen TR, Meldgaard P, et al. Exosomal Proteins as Diagnostic Biomarkers in Lung Cancer. *J Thorac Oncol* (2016) 11:1701–10. doi: 10.1016/j.jtho.2016.05.034
207. Jakobsen KR, Paulsen BS, Bæk R, Varming K, Sorensen BS, Jørgensen MM. Exosomal proteins as potential diagnostic markers in advanced non-small cell lung carcinoma. *J Extracell vesicles* (2015) 4:26659. doi: 10.3402/jev.v4.26659
208. Zhang Y, Zhang Y, Yin Y, Li S. Detection of circulating exosomal miR-17-5p serves as a novel non-invasive diagnostic marker for non-small cell lung cancer patients. *Pathol - Res Pract* (2019) 215:152466. doi: 10.1016/j.prp.2019.152466
209. Jarry J, Schadendorf D, Greenwood C, Spatz A, van Kempen LC. The validity of circulating microRNAs in oncology: Five years of challenges and contradictions. *Mol Oncol* (2014) 8:819–29. doi: 10.1016/j.molonc.2014.02.009
210. Best MG, Sol N, Kooi I, Tannous J, Westerman BA, Rustenburg F, et al. RNA-Seq of Tumor-Educated Platelets Enables Blood-Based Pan-Cancer, Multiclass, and Molecular Pathway Cancer Diagnostics. *Cancer Cell* (2015) 28:666–76. doi: 10.1016/j.ccell.2015.09.018
211. Nilsson RJA, Karachaliou N, Berenguer J, Gimenez-Capitan A, Schellen P, Teixido C, et al. Rearranged EML4-ALK fusion transcripts sequester in circulating blood platelets and enable blood-based crizotinib response monitoring in non-small-cell lung cancer. *Oncotarget* (2016) 7:1066–75. doi: 10.18632/oncotarget.6279
212. Li D, Yang W, Zhang Y, Yang JY, Guan R, Xu D, et al. Genomic analyses based on pulmonary adenocarcinoma in situ reveal early lung cancer signature. *BMC Med Genomics* (2018) 11:106. doi: 10.1186/s12920-018-0413-3
213. Sheng M, Dong Z, Xie Y. Identification of tumor-educated platelet biomarkers of non-small-cell lung cancer. *Onco Targets Ther* (2018) 11:8143–51. doi: 10.2147/OTT.S177384
214. Xue L, Xie L, Song X, Song X. [Expression and Significance of ACIN1 mRNA in Platelets of Lung Cancer]. *Zhongguo Fei Ai Za Zhi* (2018) 21:677–81. doi: 10.3779/j.issn.1009-3419.2018.09.05

215. Calverley DC, Phang TL, Choudhury QG, Gao B, Oton AB, Weyant MJ, et al. Significant downregulation of platelet gene expression in metastatic lung cancer. *Clin Transl Sci* (2010) 3:227–32. doi: 10.1111/j.1752-8062.2010.00226.x

Conflict of Interest: The authors declare that the research was conducted in the absence of any commercial or financial relationships that could be construed as a potential conflict of interest.

frontiers in Oncology

ORIGINAL RESEARCH
published: 13 May 2021
doi: 10.3389/fonc.2021.679366

Serum hsa_tsr016141 as a Kind of tRNA-Derived Fragments Is a Novel Biomarker in Gastric Cancer

Xinliang Gu[1,2,3†], *Shuo Ma*[1,2,3†], *Bo Liang*[4*] *and Shaoqing Ju*[1*]

[1] Department of Laboratory Medicine, Affiliated Hospital of Nantong University, Nantong, China, [2] Research Center of Clinical Medicine, Affiliated Hospital of Nantong University, Nantong, China, [3] Medical School of Nantong University, Nantong University, Nantong, China, [4] Department of Medical Ultrasonics, Affiliated Hospital of Nantong University, Nantong, China

Background: Gastric cancer (GC) is one of the most common malignant tumors globally and the third leading cause of cancer-related death. Currently, the sensitivity and specificity of diagnostic markers for GC are low, so it is urgent to find new biomarkers with higher sensitivity and specificity. tRNA-derived small RNAs are a kind of small non-coding RNAs derived from tRNAs. It is abundant in cancer cells and body fluids. Our goal is to find the differentially expressed tRNA-derived small RNAs in GC to explore their potential as a GC biomarker.

Methods: Quantitative real-time PCR was used to detect the expression level of hsa_tsr016141. The molecular characteristics of hsa_tsr016141 were verified by agarose gel electrophoresis, Sanger sequencing, Actinomycin D Assay, and Nuclear and Cytoplasmic RNA Separation Assay. The diagnostic efficiency of hsa_tsr016141 was analyzed through receiver operating characteristic.

Results: The expression level of hsa_tsr016141 in GC tissues and serum was significantly increased. The serum expression level showed a gradient change between GC patients, gastritis patients, and healthy donors and was positively correlated with the degree of lymph node metastasis and tumor grade. ROC analysis showed that the serum expression level of hsa_tsr016141 could significantly distinguish GC patients from healthy donors or gastritis patients. Besides, the expression level of hsa_tsr016141 in GC patients decreased significantly after the operation ($P<0.0001$).

Conclusions: Serum hsa_tsr016141 has good stability and specificity and can be used for dynamic monitoring of GC patients, suggesting that serum hsa_tsr016141 can be a novel biomarker for GC diagnosis and postoperative monitoring.

Keywords: tRNA-derived small RNAs, gastric cancer, hsa_tsr016141, biomarker, diagnosis

OPEN ACCESS

Edited by:
Matteo Bocci,
Lund University, Sweden

Reviewed by:
Christos K. Kontos,
National and Kapodistrian University of Athens, Greece
Fan Yang,
Nanjing Medical University, China

****Correspondence:***
Bo Liang
281692191@qq.com
Shaoqing Ju
jsq814@hotmail.com

[†]These authors have contributed equally to this work and share first authorship

Specialty section:
This article was submitted to Cancer Molecular Targets and Therapeutics, a section of the journal Frontiers in Oncology

Received: *11 March 2021*
Accepted: *20 April 2021*
Published: *13 May 2021*

Citation:
Gu X, Ma S, Liang B and Ju S (2021) Serum hsa_tsr016141 as a Kind of tRNA-Derived Fragments Is a Novel Biomarker in Gastric Cancer. Front. Oncol. 11:679366. doi: 10.3389/fonc.2021.679366

INTRODUCTION

Gastric cancer (GC) is one of the most common malignancies globally, and more than 1 million people are newly diagnosed with GC worldwide every year (1). GC can occur in any part of the stomach. The vast majority of GC is adenocarcinoma, originating from the most superficial glands or mucous membrane of the stomach (2). Although the morbidity and mortality of GC have

declined worldwide in the past 50 years, it is still the third leading cause of cancer-related death (2, 3). The early symptoms of GC are not obvious, and the symptoms of benign gastric diseases such as gastritis and gastric ulcers are easy to be ignored. Due to the lack of specific early diagnostic markers, patients often miss the best opportunity for treatment (4). Therefore, there is an urgent need to find accurate biomarkers and therapeutic targets. Some studies have shown that non-coding RNAs can be used as a biomarker of tumor diagnosis and prognosis. For example, the expression level of miR-425-5p was upregulated in cervical cancer and could be used as a promising prognostic biomarker for cervical cancer (5). In addition, HIF1A-AS2 was a dependable predictor of malignancy and prognosis in GC, and circEHBP1 could act as a promising biomarker for lymphatic metastasis in bladder cancer (6, 7). However, the sensitivity and specificity of the existing diagnostic markers for GC are low, so it is of high clinical significance to search for new biomarkers with high sensitivity and specificity. In recent years, novel small non-coding RNAs called tRNA-derived small RNAs (tsRNAs) have gradually attracted attention, and we have a strong interest in whether they can be used as a promising biomarker.

The discovery of tsRNAs can be traced back to the late 1970s. It was initially considered to be the product of random degradation of tRNAs and did not attract widespread attention (8, 9). However, with the rapid development of high-throughput sequencing technology and the exploration of the role of small RNAs in gene regulation, the research related to small RNAs is increasing (10, 11). In recent years, a large number of experiments and studies have proved that tsRNAs are a derivative fragment produced by specific cleavage of pre-tRNAs or mature tRNAs in a specific environment (12), which can be divided into two types: tRNA-derived fragments (tRFs) and tRNA halves (tiRNAs) according to the cutting position on the pre-tRNAs or mature tRNAs (13, 14). tsRNAs can mainly inhibit the activity of peptidyl transferase by binding to small ribosomal subunits, thus affecting the occurrence and development of tumors. It can also inhibit protein translation through the mechanism of protein sponge (15). Previous studies showed that 5′-tiRNA^{Val} could inhibit the FZD3/Wnt/β-Catenin signaling pathway to suppress the proliferation, migration, invasion, and other functions of tumor cells (16). Zhang found that tRF-3019a could serve as a promising biomarker for GC and target FBXO47 to promote the proliferation, migration, and invasion of GC cells (17). Tong found that the expression of tRF-3017A was increased in GC tissues and cell lines, and it could regulate the migration and invasion of GC cells by targeting NELL2 (18). The research on tsRNAs is mainly on the mechanism presently, but there are few studies on whether they can be good biomarkers in serum. tRFs and tiRNAs have the characteristics of high expression and high stability in a variety of body fluids and are related to a variety of pathological conditions. They have strong discrimination between cancer patients and normal controls, which makes them have the potential to become a new biomarker. Besides, tRFs are usually about 14-30 nucleotides (nt) in length, which was similar to that of microRNAs. According to the different digesting positions of Angiogenin, Dicer, or other RNases on the mature tRNA or pre-tRNA, they can be divided into five types, 5'tRF, 3'tRF, i-tRF, tRF-2 and tRF-1 (15). Among them, 5'tRF has 5′-phosphate, while 3'tRF has 3′-hydroxyl groups, these tRFs can suppress the translation of mRNA by combining the 5' or 3' ends with the conservative region of 3'-UTRs in mRNAs (19). They have attracted more and more attention over the past few years (20). Overall, a growing body of evidence suggests that abnormal expression of tRFs is associated with human tumor disease and may become new diagnostic biomarkers (21). Therefore, we focused on 5'tRF and 3'tRF in all kinds of tsRNAs for the exploration of new GC biomarkers.

In this study, we focused on the potential of hsa_tsr016141 as a tumor marker of GC and analyzed its value in clinical application. We found that hsa_tsr016141 can be used as a useful tumor marker. Compared with normal controls, the expression level of hsa_tsr016141 in tissue and serum of patients with GC was upregulated. Its expression level increased with the increase of lymph node metastasis and tumor grade, showing good diagnostic efficacy for GC patients. It has good stability and specificity in clinical application, and the diagnostic efficiency was the highest after combined diagnosis. At the same time, hsa_tsr016141 can effectively track the postoperative condition of GC, play a dynamic monitoring role in patients with GC. Therefore, hsa_tsr016141 provides a potential possibility for early diagnosis and postoperative monitoring of GC.

Abbreviations: GC, Gastric cancer; BC, Breast cancer; CRC, Colorectal cancer; LC, Lung cancer; TC, Thyroid cancer; tsRNAs, tRNA-derived small RNAs; tRFs, tRNA-derived fragments; tiRNAs, tRNA halves; AGE, agarose gel electrophoresis; CV, coefficient of variation; CEA, carcinoembryonic antigen; CA199, Carbohydrate antigen199; CI, confidence interval; CA724, Carbohydrate antigen724; NSCLC, non-small cell lung cancer.

MATERIALS AND METHODS

Human Serum Samples and Tissue Specimens

All the serum samples in this study included 130 cases of GC patients, 110 cases of healthy donors, 50 cases of gastritis patients, 63 postoperative samples from patients with GC after the operation, and 20 cases of breast cancer (BC), colorectal cancer (CRC), lung cancer (LC), and thyroid cancer (TC) patients were collected in the Clinical Laboratory, Affiliated Hospital of Nantong University. In this study, all patients with GC, BC, CRC, LC, TC and gastritis were clinically diagnosed and did not receive radiotherapy or chemotherapy before. 20 pairs of GC specimens were collected in the Department of Pathology of Affiliated Hospital of Nantong University. All tissue specimens were diagnosed by pathologists as GC and placed immediately into an RNA fixator Bioteke (Nantong, China), after resection and stored at −80°C refrigerator. All participants had obtained informed consent prior to the clinical trial and consented to publication. All of the above samples were collected in accordance with the Code Ethics of the World Medical Association from September 2016 to January 2021. This study was approved by the ethics committee of the local hospital (ethical review report number: 2018-L055).

Cell Culture

Human GC cell lines (MKN-45, AGS, BGC-823, and HGC-27) and human gastric epithelial cells (GES-1) were purchased from the

Chinese Academy of Sciences (Shanghai, China). All of the cells were cultured in RPMI-1640 medium (Corning, USA) with 10% Fetal bovine serum (FBS) (Gibco, USA) and 1% penicillin and streptomycin were added. All cells were culture at 37°C, 5%CO_2.

Total RNA Extraction and cDNA Synthesis

Total RNA in serum of GC patients was extracted using Total RNA Pure and Isolation Kit with Spin Column (BioTeke, Beijing, China), and total RNA in tissues and cells was extracted by TRIzol Reagent (Invitrogen, Germany). Then 20μL cDNA was generated by Revert Aid RT Reverse Transcription Kit (Thermo Fisher Scientific) from 10μL total RNA solution, which was incubated at 42°C for 60 min and 70°C for 5 min.

Real-Time Fluorescent Quantitative PCR

Roche Light Cycler 480 (Roche, Switzerland) was used for the qRT-PCR reaction. The reaction system included 10μL of SYBR Green I Mix (Roche), 1μL of primer, 5μL of cDNA, and 3μL of enzyme-free Water. U6 was used to standardize the relative expression of hsa_tsr016141, and the expression level was calculated through the $2^{-\Delta\Delta CT}$ method. All primers used in this study were synthesized by RiboBio (Guangzhou, China).

Actinomycin D Assay

Actinomycin D at a concentration of 1000μg/mL was diluted to 2.5μg/mL by Complete Medium. The complete medium in the six-well plate was replaced with the above-diluted medium containing actinomycin D and cultured 24 hours. TRIzol was added successively at 0, 2, 4, 8, 12, and 24 hours to extract RNA.

Nuclear and Cytoplasmic RNA Separation Assay

5×10^6 cells were digested by trypsin and placed in a small centrifuge tube after digestion. Then, according to the procedure of the PARIS™ Kit (Thermo Fisher Scientific), the cells were isolated and extracted into 60 μL Nuclear RNA and Cytoplasmic RNA and stored in the refrigerator at -80°C.

Statistical Analysis

Statistical analysis was conducted by SPSS Statistics Version 20.0 (IBM SPSS Statistics, Chicago, USA) and GraphPad Prism v8.0 (GraphPad Software, San Diego, CA). The expression level of hsa_tsr016141 in different groups was expressed by mean ± SD. Two-sided Test was used to compare two independent groups, while one-way analysis of variance was used when compared multiple independent groups. ROC curve area under the curve (AUC) was established and calculated to evaluate the diagnostic performance. $P<0.05$ was considered to have statistical significance.

RESULTS

Database and Tissues Screening of hsa_tsr016141

To explore whether tsRNAs can be used as a good biomarker for GC, we carried out screening in the OncotRF database (http://bioinformatics.zju.edu.cn/OncotRF/). We sorted by the standard of $\log_2$ fold change and selected the top three 3'tRF and 5'tRF with $\log_2$ fold change, and their P values were all less than 0.05. The specific information can be found in **Figure 1A**. Subsequently, the qRT-PCR analysis was performed to verify the differences in the expression levels of these six tRFs between 20 GC tissues and their matching adjacent non-tumor tissues. We found that the expression of 5'-M-tRNA-Gln-TTG-4-1_L29 increased significantly in GC. However, the expression level of 3'-M-tRNA-Asp-ATC-chr6-103_L16, 3'-mito-tRNA-Asp-GTC_L23, 3'-M-tRNA-Ala-TGC-3-2_L25, 5'-M-tRNA-Gly-GCC-1-5_L28, and 5'-tRNA-Arg-TCT-4-1_L20 did not differ significantly between GC tissues and their adjacent non-tumor tissues (**Figure 1B**). Subsequently, we followed up an in-depth study of it and named it as hsa_tsr016141 according to its naming rules in tsRBase (http://tsrbase.org/).

hsa_tsr016141 Is a Kind of tRFs

Using the UCSC Genome Browser database, we found that hsa_tsr016141 was mapped to chromosome 6q24.2 with coordinates of 145,503,859–145,503,887 (**Figure 2A**). According to the basic information of hsa_tsr016141 in OncotRF Database and MINTbase v2.0 (http://cm.jefferson.edu/MINTbase/.). We determined that it is a tRNA-derived fragment with a length of 29nt (5'-GGTCCCATGGTGTAATGGTTAGCACTCTG-3'). Hsa_tsr016141 was a 5'tRF of tRNA-Gln-TTG, which was processed from tRNA-Gln-TTG-1-1, tRNA-Gln-TTG-2-1 and tRNA-Gln-TTG-4-1 (**Figure 2B**). The cleavage sites are all located above the anticodon loop (**Figure 2C**). Then, the product of qRT-PCR was detected by agarose gel electrophoresis (AGE), showing a single electrophoresis band of about 80bp (**Figure 2D**), and confirmed by sequencing that the product contained the full-length sequence of hsa_tsr016141 (**Figure 2E**).

Characterization of hsa_tsr016141 and Its Advantage as a Biomarker for GC

To investigate the stability of hsa_tsr016141, we conducted an actinomycin D experiment, due to actinomycin D can inhibit RNA production by inhibiting the activity of RNA polymerase. We cultured MKN-45 cells and AGS cells in a medium containing actinomycin D for 24 hours. Through qRT-PCR, we found that the expression level of hsa_tsr016141 was not significantly decreased, which confirmed the good stability of hsa_tsr016141 (**Figure 3A**). Subsequently, to investigate the origin of hsa_tsr016141 in serum from GC cells, three GC cells AGS, BGC-823, HGC-27, and gastric epithelial cell GES-1 were cultured for 7 days, and supernatants were collected regularly. The result showed that the expression level of hsa_tsr016141 in AGS, BGC-823, and HGC-27 supernatants increased with the extension of culture time, especially in AGS and BGC-823 cells. However, the expression of hsa_tsr016141 in GES-1 supernatant did not change significantly. It is suggested that hsa_tsr016141 may be released into the blood by GC cells and has the potential to be used as a biomarker (**Figure 3B**). Besides, we selected MKN-45 and HGC-27 cells for Nuclear and Cytoplasmic RNA Separation Assay and found that most hsa_tsr016141 in the two kinds of cells was located in the nucleus (**Figure 3C**). Then, we collected 20 cases of BC, CRC, LC, TC, and 20 cases of healthy donors serum samples, respectively, to detect the expression level of

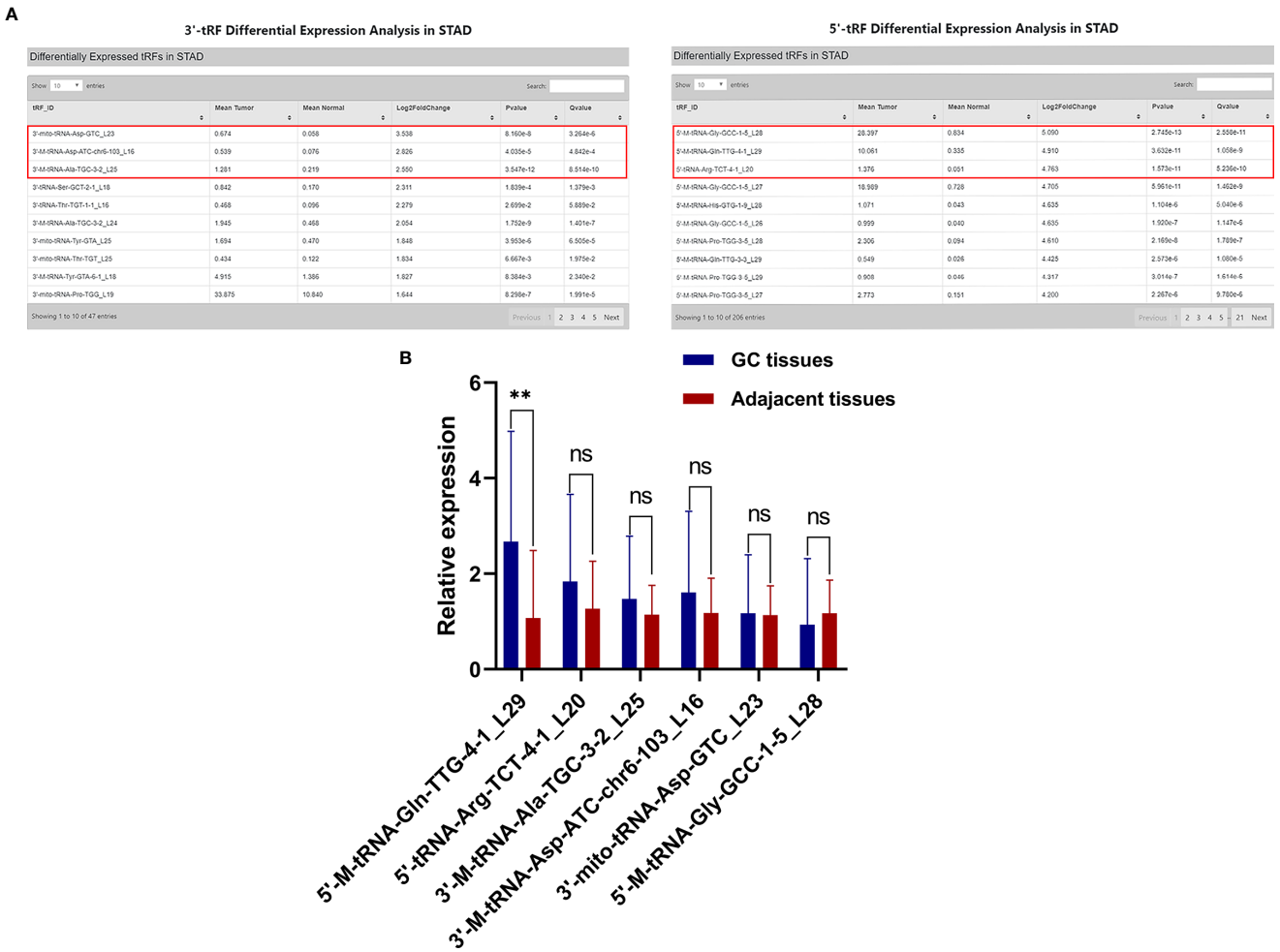

FIGURE 1 | Screening of hsa_tsr016141. **(A)** Three 3'tRF and 5'tRF were sorted by the standard of the most significant $\log_2$ fold change, and their P values were all less than 0.05. **(B)** Expression levels of 6 tRFs in GC tissues. **P < 0.01, ns P > 0.805.

hsa_tsr016141 in these four other cancers. Through the qRT-PCR, we found that there was no statistically significant difference between serum of these four kinds of cancer patients and healthy donors (P-values were 0.4689, 0.0573, 0.1440, and 0.1073) (**Figure 3D**), but we previously found that the expression level of hsa_tsr016141 was significantly increased in GC. In conclusion, the above evidence proves that hsa_tsr016141 has good characteristics as a biomarker for GC.

Methodological Evaluation and Biomarker Potential of hsa_tsr016141 Detection in Serum Samples

To explore whether the detection of hsa_tsr016141 can be used in clinical analysis, we first made an evaluation of its detection methods comprehensively. We used the mixed serum to determine the detection accuracy of hsa_tsr016141 and found that the intra-assay coefficient of variation (CV) and the inter-assay CV performed well (**Table 1**). Subsequently, the mixed serum samples were placed at room temperature for 0, 6, 12, 18, and 24 hours and freeze-thawed repeatedly for 0, 1, 3, 5, and 10 times, and then the relative expression level of hsa_tsr016141 was detected. The results showed no significant difference in its expression level, which revealed that the detection method of hsa_tsr016141 would not be affected by these factors and had good stability and repeatability (**Figures 4A, B**). Besides, the smooth and unimodal specific melting curve also shows the accuracy and specificity of this method (**Figure 4C**). In conclusion, the detection method of hsa_tsr016141 is suitable for clinical analysis.

In order to explore the diagnostic significance of hsa_tsr016141 in the serum of GC, we collected serum samples from 130 patients with GC, 50 patients with gastritis, and 110 healthy controls to explore the difference in their expression levels. We found that the expression level of hsa_tsr016141 in the serum of patients with GC was significantly higher than that of healthy donors (P<0.0001). In addition, the expression level of hsa_tsr016141 in the serum of patients with gastritis was higher than that of healthy donors (P=0.0467) but significantly lower than that of patients with GC

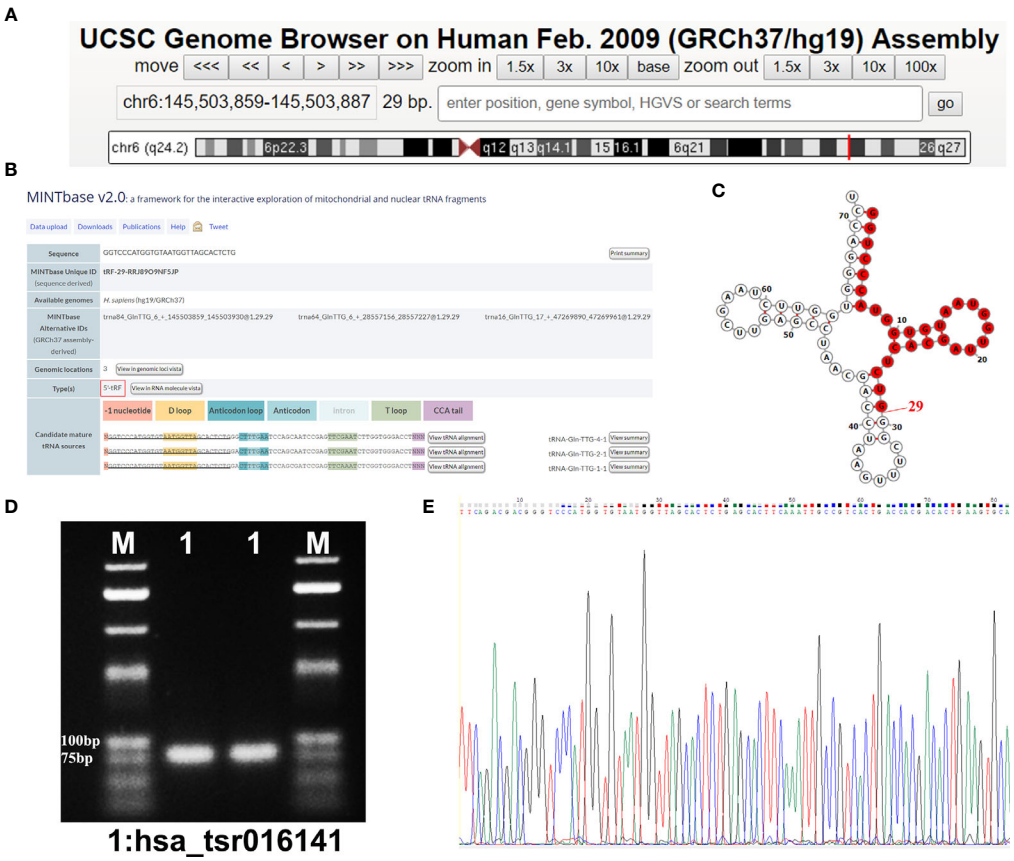

FIGURE 2 | Hsa_tsr016141 is a kind of tRFs. **(A)** hsa_tsr016141 was mapped to chromosome 6q24.2 with coordinates of 145,503,859–145,503,887. **(B)** hsa_tsr016141 was a 5'tRF of tRNA-Gln-TTG, which was processed from tRNA-Gln-TTG-1-1, tRNA-Gln-TTG-2-1, and tRNA-Gln-TTG-4-1. **(C)** Taking tRNA-Gln-TTG-4-1 as an example, the cleavage site of hsa_tsr016141 was located above the anticodon loop. **(D)** The product of qRT-PCR was run on 2% agarose gel, showing a single electrophoresis band. **(E)** The product of qRT-PCR was confirmed by Sanger sequencing that contained the full-length sequence of hsa_tsr016141.

(P<0.0001) **(Figure 4D)**. In order to further explore whether the expression level of hsa_tsr016141 in the serum is related to tumor metastasis or tumor progression, we classified the expression level of hsa_tsr016141 in serum of patients with GC according to lymph node metastasis and TNM stage. The results showed that the expression level of hsa_tsr016141 increased with the increase of lymph node metastasis. Also, the expression level increased as the tumor grade increased (P=0.0001). These results indicated that the serum expression level of hsa_tsr016141 was elevated in patients with GC and positively correlated with lymph node metastasis and tumor grade **(Figures 4E, F)**.

Comparison and Combination of Serum hsa_tsr016141 and Other Tumor Markers in the Diagnosis of GC

Firstly, we further discussed the diagnostic characteristics and efficacy of hsa_tsr016141 as a potential biomarker for GC. It is well known that carcinoembryonic antigen (CEA) and Carbohydrate antigen199 (CA199) are commonly used clinical tumor markers. We used 130 GC patients and 110 healthy donors to perform ROC analysis on hsa_tsr016141, CEA, and CA199 to determine the diagnostic efficacy of hsa_tsr016141 in GC serum. The ROC curve showed that the AUC of hsa_tsr016141 was 0.814 (95% confidence interval (CI): 0.760-0.867), which was higher than 0.705 (95% CI: 0.637-0.774) of CEA and 0.607 (95% CI: 0.535-0.678) of CA199 **(Figure 5A)**. Meanwhile, the sensitivity (75%), specificity (78%), accuracy (76%), positive predictive value (80%), and negative predictive value (72%) of hsa_tsr016141 were also higher than those of CEA and CA199. Subsequently, we analyzed the efficacy of joint diagnosis and found that AUC increased to 0.830 after the combination of hsa_tsr016141 and CEA, and 0.854 after combining of hsa_tsr016141 and CA199. The AUC of the combination of the three was the highest, reaching 0.864 **(Figure 5B)**. Simultaneously, the sensitivity of joint diagnosis was also increasing, and the sensitivity of the combination of the three is up to 90%, which was higher than that of each tumor marker **(Table 2)**. The above analysis results indicate that hsa_tsr016141 may have the potential to become a biomarker of GC and, combined with other tumor markers, can improve the diagnostic efficiency of a single tumor marker. Next, we

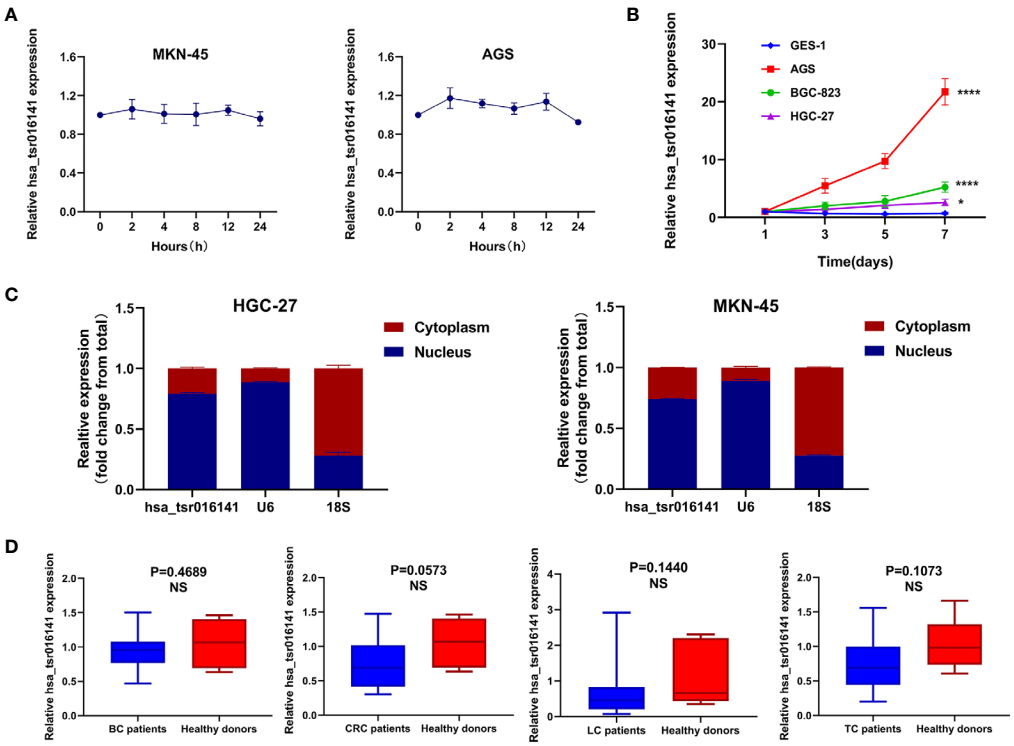

FIGURE 3 | Characterization and advantage of hsa_tsr016141 as a GC biomarker**. (A)** The good stability of hsa_tsr016141 was confirmed by actinomycin D assay. **(B)** The expression level of hsa_tsr016141 in culture supernatants of AGS and BGC-823 increased with time compared to GES-1. **(C)** The location of hsa_tsr016141 in HGC-27 and MKN-45 cells was detected by Nuclear and Cytoplasmic RNA Separation Assay. **(D)** The expression level of hsa_tsr016141 had no significant difference in other tumors. *P < 0.05, ****P < 0.0001, NS P > 0.05.

TABLE 1 | The Intra-Assay CV and the Inter- Assay CV of hsa_tsr016141.

	hsa_tsr016141	U6
Intra assay CV,%	**2.14**	**2.95**
Inter assay CV,%	**1.94**	**3.13**

CV, coefficient of variation.

analyzed whether the expression level of hsa_tsr016141 could distinguish patients with GC from those with gastritis. ROC analysis was performed in 130 patients with GC and 50 patients with gastritis. The ROC curve showed that the AUC of hsa_tsr016141 was 0.692 (95% CI: 0.599-0.785), which was higher than 0.654 of CEA (95% CI: 0.567-0.741) and 0.621 of CA199 (95% CI: 0.522-0.720) (**Figure 5C**). The AUC of hsa_tsr016141 combined with CEA was 0.703, and that of CA199 was 0.683. The highest AUC was the combination of the three of 0.718, and the sensitivity was 81%, indicating that hsa_tsr016141 can also be used as a biomarker to distinguish GC from gastritis (**Figure 5D** and **Table 3**).

Secondly, in patients with GC at different stages, the levels of serum CEA, CA199, and Carbohydrate antigen724 (CA724) may be increased (22), but the positive rate of CA724 is generally higher than that of CEA and CA199 (22–24). Therefore, we further studied and analyzed the difference in diagnostic efficacy between hsa_tsr016141 and CA724. CA724 was detected in 96 of 130 GC patients and 74 of 110 healthy donors. Therefore, we performed a ROC analysis on these 96 GC patients and 74 healthy donors. The results showed that the AUC of hsa_tsr016141 was 0.820 (95% CI: 0.759-0.881), which was slightly higher than 0.780 of CA724 (95% CI: 0.712-0.848) (**Figure 5E**). The sensitivity (66%) and specificity (89%) of hsa_tsr016141 were also slightly higher than that of CA724. Subsequently, we combined the two and found that the AUC increased significantly, reaching 0.893 (**Figure 5F**), and the sensitivity was also higher than the single index reached 82%, indicating that both hsa_tsr016141 and CA724 have high diagnostic efficiency, and after the combination of the two, the diagnostic efficiency would be significantly improved (**Table 4**). CA724 was detected in 35 of 50 gastritis patients, and then we performed a ROC analysis on these 96 GC patients and 35 gastritis patients. It was found that the AUC of hsa_tsr016141 was 0.754 (95% CI: 0.656-0.851), which was slightly higher than 0.716 of CA724 (95% CI: 0.622-0.810) (**Figure 5G**). The AUC increased to 0.802, and the sensitivity significantly increased to 88% after the combination of the two (**Figure 5H**). In conclusion, hsa_tsr016141 has higher diagnostic efficiency than CA724, and the combination of the two would further improve the diagnostic efficiency (**Table 5**).

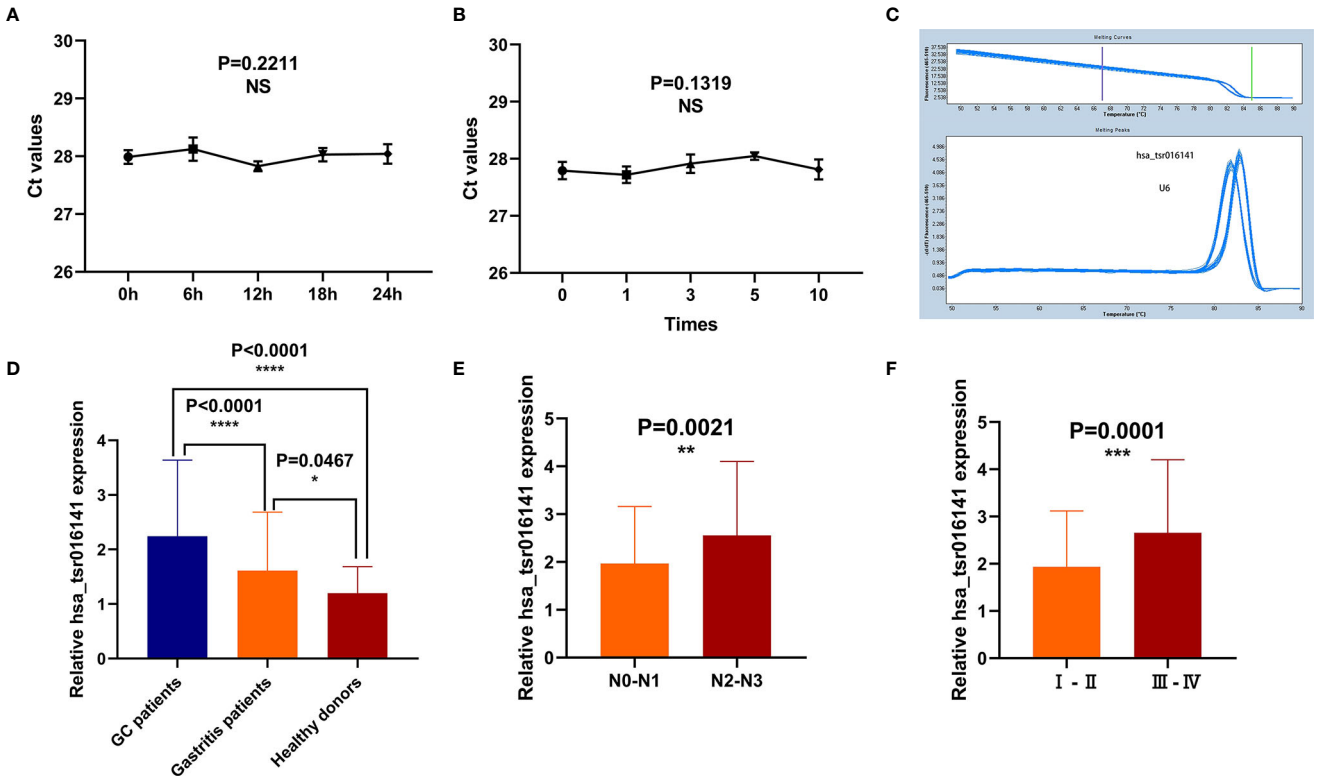

FIGURE 4 | Methodological evaluation and biomarker potential of hsa_tsr016141. **(A, B)** The detection method of hsa_tsr016141 would not be easily affected and had good stability and repeatability. **(C)** The melting curve of hsa_tsr016141. **(D)** The expression level of hsa_tsr016141 in GC patients (n=130), gastritis patients (n=50), and healthy donors (n=110). **(E)** The expression levels of hsa_tsr016141 in serum samples of GC at different stages of lymph node metastasis. **(F)** The expression levels of hsa_tsr016141 in serum samples of GC at different stages of tumor grade. *P < 0.05, **P < 0.01, ***P < 0.001, ****P < 0.0001, NS P > 0.05.

Correlation Between Serum hsa_tsr016141 Expression and Clinicopathological Parameters in Patients With GC

In order to investigate the clinical application value of serum hsa_tsr016141, we collected the clinicopathological data of 130 patients with GC. We divided them into two groups according to the median: higher expression group (expression>1.725, n=65) and lower expression group (expression<1.725, n=65). As shown in **Table 6**, the expression level of hsa_tsr016141 was positively correlated with tumor differentiation grade, T stage, lymph node status, and TNM stage, but not with sex, age, tumor size, and nerve/vascular invasion. The occurrence of GC is caused by many factors, including helicobacter pylori infection, precancerous lesions, diet, or genetic factors. Among them, helicobacter pylori chronic infection is a major cause of stomach cancer, accounting for about 89% of the cases of distal GC in the world (25–27). In order to explore whether the expression level of hsa_tsr016141 is related to Helicobacter pylori infection, we conducted induction analysis in 130 GC patients and found that 83 of 130 GC patients were tested for Helicobacter pylori, of which 52 were positive, with a positive rate of 64.6%. Then, we statistically analyzed the expression level of hsa_tsr016141 in the Helicobacter pylori-positive group and Helicobacter pylori-negative group and found no significant difference in hsa_tsr016141 expression level between the Helicobacter pylori-positive group and Helicobacter pylori-negative group. Similarly, we conducted the same analysis on 50 patients with gastritis. Among the 50 patients with gastritis, 33 cases were tested for Helicobacter pylori, 18 were positive, the positive rate was 54.5%. There was no significant difference in the expression level of hsa_tsr016141 between the Helicobacter pylori-positive and Helicobacter pylori-negative groups in patients with gastritis which indicated that there was no significant correlation between Helicobacter pylori-positive group and hsa_tsr016141 expression level (**Figures 6A, B**).

The Role of Serum hsa_tsr016141 in Dynamic Monitoring of Tumor in Patients With GC

In order to verify the dynamic relationship between serum hsa_tsr016141 expression level and tumor progression, we compared the difference of hsa_tsr016141 expression level before and after surgery in 63 patients with GC. It was found that the serum hsa_tsr016141 expression decreased significantly in the same patient after GC surgery (**Figure 6C**). In addition, the survival curve showed that the survival rate of the low expression group was higher than that of the high expression group, indicating that hsa_tsr016141 can effectively track the postoperative condition of GC and dynamically monitor the patients with GC (**Figure 6D**).

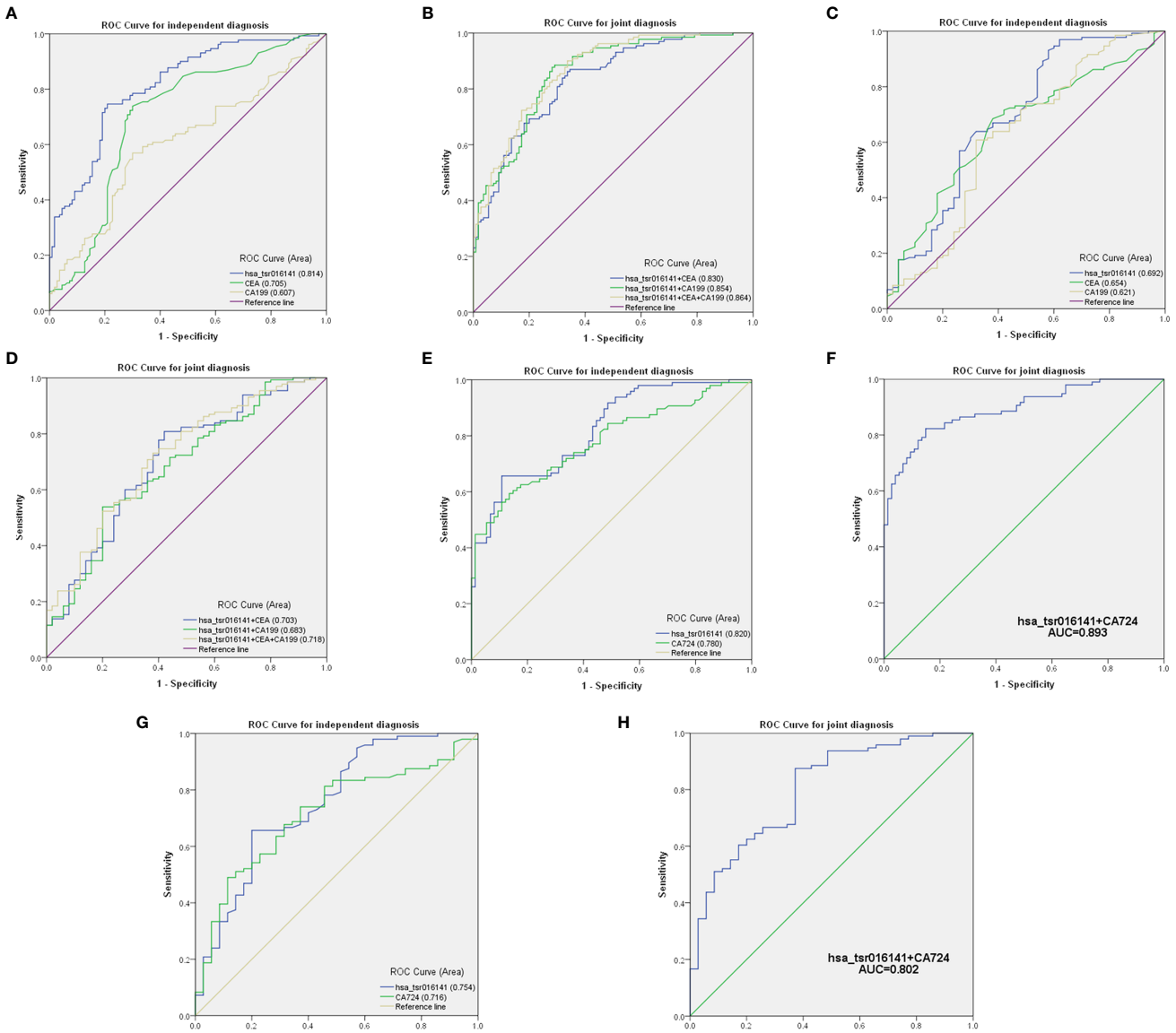

FIGURE 5 | Comparison and combination of serum hsa_tsr016141 and other tumor markers in the diagnosis of GC. **(A)** ROC curve analysis of hsa_tsr016141, CEA, and CA199 in independent diagnosis of GC patients and healthy donors. **(B)** ROC curve analysis of hsa_tsr016141, CEA, and CA199 in joint diagnosis of GC patients and healthy donors. **(C)** ROC curve analysis of hsa_tsr016141, CEA, and CA199 in independent diagnosis of GC patients and gastritis patients. **(D)** ROC curve analysis of hsa_tsr016141, CEA, and CA199 in joint diagnosis of GC patients and gastritis patients. **(E)** ROC curve analysis of hsa_tsr016141 and CA724 in independent diagnosis of GC patients and healthy donors. **(F)** ROC curve analysis of hsa_tsr016141 and CA724 in joint diagnosis of GC patients and healthy donors. **(G)** ROC curve analysis of hsa_tsr016141 and CA724 in independent diagnosis of GC patients and gastritis patients. **(H)** ROC curve analysis of hsa_tsr016141 and CA724 in joint diagnosis of GC patients and gastritis patients.

TABLE 2 | Use the expression levels of hsa_tsr016141, CEA, and CA199 to distinguish GC patients from healthy donors.

	SEN,%	SPE,%	ACCU,%	PPV,%	NPV,%
hsa_tsr016141	0.75(97/130)	0.78(86/110)	0.76(183/240)	0.80(97/121)	0.72(86/119)
CEA	0.68(89/130)	0.73(80/110)	0.70(169/240)	0.75(89/119)	0.66(80/121)
CA199	0.60(78/130)	0.64(70/110)	0.62(148/240)	0.66(78/118)	0.57(70/122)
hsa_tsr016141+CEA	0.86(112/130)	0.66(73/110)	0.77(185/240)	0.75(112/149)	0.80(73/91)
hsa_tsr016141+CEA+CA199	0.90(117/130)	0.66(73/110)	0.79(190/240)	0.76(117/154)	0.66(73/111)

SEN, sensitivity; SPE, specificity; ACCU, overall accuracy; PPV, positive predictive value; NPV, negative predictive value.

TABLE 3 | Use the expression levels of hsa_tsr016141, CEA, and CA199 to distinguish GC patients from gastritis patients.

	SEN,%	SPE,%	ACCU,%	PPV,%	NPV,%
hsa_tsr016141	0.64(83/130)	0.68(34/50)	0.65(117/180)	0.84(83/99)	0.52(34/65)
CEA	0.68(89/130)	0.62(31/50)	0.67(120/180)	0.82(89/108)	0.43(31/72)
CA199	0.60(78/130)	0.68(34/50)	0.62(112/180)	0.83(78/94)	0.40(34/86)
hsa_tsr016141+CEA	0.77(100/130)	0.60(30/50)	0.68(130/180)	0.83(100/120)	0.50(30/60)
hsa_tsr016141+CEA+CA199	0.81(105/130)	0.52(26/50)	0.69(131/180)	0.81(105/129)	0.51(26/51)

SEN, sensitivity; SPE, specificity; ACCU, overall accuracy; PPV, positive predictive value; NPV, negative predictive value.

TABLE 4 | Use the expression levels of hsa_tsr016141 and CA724 to distinguish GC patients from healthy donors.

	SEN,%	SPE,%	ACCU,%	PPV,%	NPV,%
hsa_tsr016141	0.66(63/96)	0.89(66/74)	0.76(129/170)	0.89(63/71)	0.67(66/99)
CA724	0.64(61/96)	0.77(57/74)	0.69(118/170)	0.78(61/78)	0.57(57/92)
hsa_tsr016141+CA724	0.82(79/96)	0.85(63/74)	0.84(142/170)	0.88(79/90)	0.79(63/80)

SEN, sensitivity; SPE, specificity; ACCU, overall accuracy; PPV, positive predictive value; NPV, negative predictive value.

TABLE 5 | Use the expression levels of hsa_tsr016141 and CA724 to distinguish GC patients from gastritis patients.

	SEN,%	SPE,%	ACCU,%	PPV,%	NPV,%
hsa_tsr016141	0.66(63/96)	0.80(28/35)	0.69(91/131)	0.90(63/70)	0.46(28/61)
CA724	0.64(61/96)	0.69(24/35)	0.65(85/131)	0.85(61/72)	0.41(24/59)
hsa_tsr016141+CA724	0.88(84/96)	0.63(22/35)	0.81(106/131)	0.87(84/97)	0.65(22/34)

SEN, sensitivity; SPE, specificity; ACCU, overall accuracy; PPV, positive predictive value; NPV, negative predictive value.

TABLE 6 | Clinicopathological analysis of hsa_tsr016141.

Parameter		No. of patients	hsa_tsr016141(high)	hsa_tsr016141(low)	P-value
Sex	male	94	46	48	0.7907
	female	36	19	17	
Age(year)	<60	40	19	21	0.2111
	≥60	90	46	44	
Tumor size	<5	96	43	53	0.0705
	≥5	34	22	12	
Differentiation grade	Well-moderate	63	24	39	0.0006***
	Poor-undifferentiation	67	41	26	
T stage	T1-T2	72	26	46	0.0004***
	T3-T4	58	39	19	
Lymph node status	Positive	78	45	33	0.0047**
	Negative	52	20	32	
TNM stage	I-II	74	29	45	0.0001***
	III-IV	56	36	20	
Nerve/vascular invasion	Positive	77	42	35	0.0815
	Negative	53	23	30	

**P < 0.05, **P < 0.01, ***P < 0.001, ****P < 0.0001.*

DISCUSSION

GC is one of the most serve malignant tumors in the world, with the highest mortality rate. However, nowadays, tumor markers that can be applied to GC have low sensitivity and specificity, and most patients have reached an advanced stage when GC is found (28). Therefore, it is urgent to find biomarkers with high sensitivity and specificity suitable for the early screening of GC.

tsRNAs are a new member of the family of small non-coding RNAs. Their stable structure and high abundance in body fluids show their potential to be used in liquid biopsy and become a new generation of tumor biomarkers. At present, most of the studies on tsRNAs have described the effects of tsRNAs on tumor cell proliferation, invasion, and migration, as well as their internal pathways and mechanisms. However, there are still few studies on whether tsRNAs can be applied as biomarkers (17, 29, 30). Therefore, in this study, we explored the potential of hsa_tsr016141 as a tumor marker for GC.

We screened out three 5'tRF and 3'tRF with the condition of biggest $\log_2$ fold change and $P<0.05$ through the OncotRF database. By comparing the expression of 5'tRF and 3'tRF in 20 pairs of GC tissues and their matching adjacent non-tumor

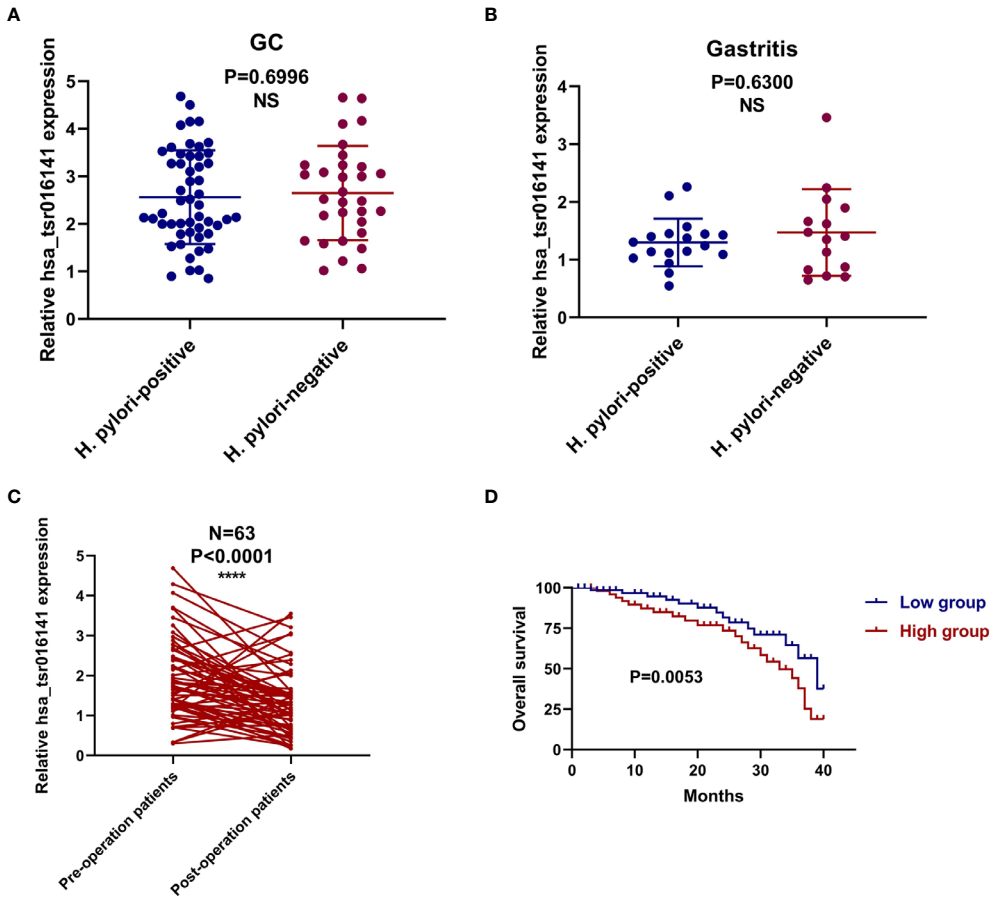

FIGURE 6 | The corresponding relationship with Helicobacter pylori infection and prognostic value of hsa_tsr016141 in GC. **(A)** The expression level of hsa_tsr016141 between the Helicobacter pylori-positive and Helicobacter pylori-negative groups in GC patients. **(B)** The expression level of hsa_tsr016141 between the Helicobacter pylori-positive and Helicobacter pylori-negative groups in gastritis patients. **(C)** The expression levels of the serum hsa_tsr016141 in the 63 GC patients before and after the operation. **(D)** Survival curve verifies the prognostic value of hsa_tsr016141. ****P < 0.0001, NS P > 0.05.

tissues, we selected the most differentially expressed 5'tRF and named it hsa_tsr016141 according to the naming rule of tsRBase. Then we studied its molecular characteristics, confirmed its chromosome location, and verified the PCR amplification products by AGE and Sanger sequencing. Then, through experiments, we found that its stability and specificity were good, and it was mainly located in the nucleus. Subsequently, we found that it was secreted continuously from tumor cells over time, showing its potential as a biomarker. Then, we verified that the detection method of hsa_tsr016141 could be applied to clinical analysis. By analyzing a large sample of hsa_tsr016141, we found that the expression level of hsa_tsr016141 was gradient change in GC patients, gastritis patients, and healthy donors. By classifying the expression levels of these 130 GC patients by N stage and TNM stage, we found that with the increasing of lymph node metastasis and the increasing tumor grade, the expression level of hsa_tsr016141 also increased. After ROC analysis, it was found that hsa_tsr016141 could significantly distinguish GC patients from healthy donors as well as GC patients from gastritis patients. The sensitivity of hsa_tsr016141, CEA, and CA199 in the joint diagnosis of GC is 90%, while the sensitivity of hsa_tsr016141 and CA724 in the joint diagnosis of GC is 82%. After the analysis of clinicopathological data, it was found that the expression level of hsa_tsr016141 was correlated with differentiation grade, T stage, lymph node status, and TNM stage. By comparing the expression level of hsa_tsr016141 in Helicobacter pylori-positive and Helicobacter pylori-negative GC patients and gastritis patients, we found that there was no significant correlation between Helicobacter pylori infection and the expression level of hsa_tsr016141. In addition, through the analysis of the survival curve and the expression level of hsa_tsr016141 in patients with GC patients after operation, we found that hsa_tsr016141 could dynamically monitor the patients with GC after the operation.

Several previous studies have highlighted the potential use of tRFs as biomarkers for diagnosing different types of cancer (16, 31, 32). For example, Mo found that the serum expression level of 5'-tiRNA ^{Val} was significantly decreased in 60 breast cancer patients compared with normal controls, suggesting that it may inhibit the progression of breast cancer (16). Shen detected the expression level

of tRF-33-P4R8YP9LON4VDP in 89 gastric cancer patients and 98 healthy plasma samples. The expression level of tRF-33-P4R8YP9LON4VDP in plasma of gastric cancer patients was significantly lower than that of normal people (32). They have verified the potential of tRFs as tumor biomarkers, but they all have limitations and lack of validation of molecular properties and detection methods. In our research, we conducted a comprehensive analysis of the potential of hsa_tsr016141 as a biomarker for GC, the elevated serum hsa_tsr016141 has good stability and specificity, which makes it have the potential to be used as a good biomarker for GC. Meanwhile, the elevated serum hsa_tsr016141 can effectively track the postoperative situation of GC, dynamically monitor GC patients. Besides, the increased expression level of hsa_tsr016141 is positively correlated with lymph node metastasis and tumor grade, which has high diagnostic efficacy for GC. Its detection method also has good clinical application value. In conclusion, we found that hsa_tsr016141 could be used for the diagnosis and postoperative monitoring of GC patients. In future studies, larger samples are needed to verify the value of the clinical application.

tsRNAs are divided into tRFs and tiRNAs, and tRFs were divided into 5'tRF and 3'tRF according to the different digesting positions. Previous research has shown that 5'tRF is mainly present in the nucleus (33), while 3'tRF is mainly present in the cytoplasm (34). In this study, we found that hsa_tsr016141 belongs to 5'tRF and is mainly located in the nucleus as previous studies had concluded. Some studies have found that tsRNAs can inhibit the translation process (35, 36). For instance, 3'tRF from $tRNA^{Leu\text{-}CAG}$ of non-small cell lung cancer (NSCLC) cells has a similar effect to miRNA and can attenuate protein translation (35). Another study found that 5'$tiRNA^{Ala}$ and 5' $tiRNA^{Cys}$ could inhibit translation by forming intermolecular RNA G quadruplexes (RG4) to replace the translation initiation complex eIF4G/eIF4E which located on mRNA cap (36). Simultaneously, some tsRNAs can influence the occurrence and progression of diseases through the protein sponge mechanism (37, 38). For example, a series of tRFs generated by Glu/Asp/Gly/Tyr tRNAs in the low metastatic breast cancer cell line MDA under hypoxia conditions competitively bind with oncogene YBX1 protein, which reduces the stability of oncogene transcripts and thus inhibits cancer metastasis (37). When it comes to 5'tRF, some researchers believe that both 5'tRF and 3'tRF are involved in RNA silencing, while others believe that 5'tRF can inhibit the protein translation process and is considered a novel gene regulation mechanism (39, 40). Therefore, we predict that the regulation of hsa_tsr016141 on GC might affect protein translation or RNA silencing by binding to downstream mRNA. To our knowledge, this is the first report to elucidate that hsa_tsr016141 could be used in the diagnosis and postoperative monitoring of GC, and there are still no reports on the functional role of hsa_tsr016141 in other types of cancer also. However, the specific mechanism of hsa_tsr016141 is still unclear, which needs to be further studied and verified in the future.

DATA AVAILABILITY STATEMENT

The original contributions presented in the study are included in the article/supplementary material. Further inquiries can be directed to the corresponding authors.

ETHICS STATEMENT

The studies involving human participants were reviewed and approved by The ethics committee of the local hospital (ethical review report number: 2018-L055). The patients/participants provided their written informed consent to participate in this study.

AUTHOR CONTRIBUTIONS

Material preparation, data collection and analysis were performed by XG and SM. The first draft of the manuscript was written by XG, resources and guidance for the paper were provided by BL and SJ, and all authors commented on previous versions of the manuscript. All authors contributed to the article and approved the submitted version.

FUNDING

This project was supported by the National Natural Science Foundation of China (No. 81871720, 82072363).

REFERENCES

1. Thrift A, El-Serag H. Burden of Gastric Cancer. *Clin gastroenterology hepatology Off Clin Pract J Am Gastroenterological Assoc* (2020) 18(3):534–42. doi: 10.1016/j.cgh.2019.07.045
2. Karimi P, Islami F, Anandasabapathy S, Freedman N, Kamangar F. Gastric Cancer: Descriptive Epidemiology, Risk Factors, Screening, and Prevention. *Cancer epidemiology Biomarkers Prev Publ Am Assoc Cancer Research cosponsored by Am Soc Prev Oncol* (2014) 23(5):700–13. doi: 10.1158/1055-9965.Epi-13-1057
3. Ferlay J, Colombet M, Soerjomataram I, Mathers C, Parkin D, Piñeros M, et al. Estimating the Global Cancer Incidence and Mortality in 2018: GLOBOCAN Sources and Methods. *Int J Cancer* (2019) 144(8):1941–53. doi: 10.1002/ijc.31937
4. Ma S, Kong S, Wang F, Ju S. Circrnas: Biogenesis, Functions, and Role in Drug-Resistant Tumours. *Mol Cancer* (2020) 19(1):119. doi: 10.1186/s12943-020-01231-4
5. Sun L, Jiang R, Li J, Wang B, Ma C, Lv Y, et al. Micorna-425-5p is a Potential Prognostic Biomarker for Cervical Cancer. *Ann Clin Biochem* (2017) 54 (1):127–33. doi: 10.1177/0004563216649377
6. Mu L, Wang Y, Su H, Lin Y, Sui W, Yu X, et al. HIF1A-AS2 Promotes the Proliferation and Metastasis of Gastric Cancer Cells Through Mir-429/PD-L1 Axis. *Digestive Dis Sci* (2021) S1525–0016(21):00065–4. doi: 10.1007/s10620-020-06819-w
7. Zhu J, Luo Y, Zhao Y, Kong Y, Zheng H, Li Y, et al. Circehbp1 Promotes Lymphangiogenesis and Lymphatic Metastasis of Bladder Cancer Via Mir-130a-3p/Tgfβr1/VEGF-D Signaling. *Mol Ther J Am Soc Gene Ther* (2021) S1525-0016(21):00065–4. doi: 10.1016/j.ymthe.2021.01.031
8. Borek E, Baliga B, Gehrke C, Kuo C, Belman S, Troll W, et al. High Turnover Rate of Transfer RNA in Tumor Tissue. *Cancer Res* (1977) 37(9):3362–6.
9. Speer J, Gehrke C, Kuo K, Waalkes T, Borek E. Trna Breakdown Products as Markers for Cancer. *Cancer* (1979) 44(6):2120–3. doi: 10.1002/1097-0142(197912)44:6<2120::aid-cncr2820440623>3.0.co;2-6

10. Lee R, Feinbaum R, Ambros V. The C. Elegans Heterochronic Gene Lin-4 Encodes Small Rnas With Antisense Complementarity to Lin-14. *Cell* (1993) 75(5):843–54. doi: 10.1016/0092-8674(93)90529-y
11. Wightman B, Ha I, Ruvkun G. Posttranscriptional Regulation of the Heterochronic Gene Lin-14 by Lin-4 Mediates Temporal Pattern Formation in C. Elegans. *Cell* (1993) 75(5):855–62. doi: 10.1016/0092-8674(93)90530-4
12. Zhu P, Yu J, Zhou P. Role of Trna-Derived Fragments in Cancer: Novel Diagnostic and Therapeutic Targets Trfs in Cancer. *Am J Cancer Res* (2020) 10(2):393–402.
13. Shen Y, Yu X, Zhu L, Li T, Yan Z, Guo J. Transfer RNA-Derived Fragments and Trna Halves: Biogenesis, Biological Functions and Their Roles in Diseases. *J Mol Med (Berlin Germany)* (2018) 96(11):1167–76. doi: 10.1007/s00109-018-1693-y
14. Zhu L, Ge J, Li T, Shen Y, Guo J. Trna-Derived Fragments and Trna Halves: The New Players in Cancers. *Cancer Lett* (2019) 452:31–7. doi: 10.1016/j.canlet.2019.03.012
15. Xie Y, Yao L, Yu X, Ruan Y, Li Z, Guo J. Action Mechanisms and Research Methods of Trna-Derived Small Rnas. *Signal transduction targeted Ther* (2020) 5(1):109. doi: 10.1038/s41392-020-00217-4
16. Mo D, Jiang P, Yang Y, Mao X, Tan X, Tang X, et al. A Trna Fragment, 5'-Tirna, Suppresses the Wnt/Beta -Catenin Signaling Pathway by Targeting FZD3 in Breast Cancer. *Cancer Lett* (2019) 457:60–73. doi: 10.1016/j.canlet.2019.05.007
17. Zhang F, Shi J, Wu Z, Gao P, Zhang W, Qu B, et al. A 3'-Trna-Derived Fragment Enhances Cell Proliferation, Migration and Invasion in Gastric Cancer by Targeting FBXO47. *Arch Biochem biophysics* (2020) 690:108467. doi: 10.1016/j.abb.2020.108467
18. Tong L, Zhang W, Qu B, Zhang F, Wu Z, Shi J, et al. The Trna-Derived Fragment-3017A Promotes Metastasis by Inhibiting NELL2 in Human Gastric Cancer. *Front Oncol* (2020) 10:570916. doi: 10.3389/fonc.2020.570916
19. Zong T, Yang Y, Zhao H, Li L, Liu M, Fu X, et al. Tsrnas: Novel Small Molecules From Cell Function and Regulatory Mechanism to Therapeutic Targets. *Cell proliferation* (2021) 54(3):e12977. doi: 10.1111/cpr.12977
20. Couvillion M, Sachidanandam R, Collins K. A Growth-Essential Tetrahymena Piwi Protein Carries Trna Fragment Cargo. *Genes Dev* (2010) 24(24):2742–7. doi: 10.1101/gad.1996210
21. Zhu L, Liu X, Pu W, Peng Y. Trna-Derived Small Non-Coding Rnas in Human Disease. *Cancer Lett* (2018) 419:1–7. doi: 10.1016/j.canlet.2018.01.015
22. Kim D, Oh S, Oh C, Choi M, Noh J, Sohn T, et al. The Relationships Between Perioperative CEA, CA 19-9, and CA 72-4 and Recurrence in Gastric Cancer Patients After Curative Radical Gastrectomy. *J Surg Oncol* (2011) 104(6):585–91. doi: 10.1002/jso.21919
23. Guadagni F, Roselli M, Cosimelli M, Ferroni P, Spila A, Casaldi V, et al. Correlation Between Positive CA 72-4 Serum Levels and Lymph Node Involvement in Patients With Gastric Carcinoma. *Anticancer Res* (1993) 13:2409–13.
24. Aloe S, D'Alessandro R, Spila A, Ferroni P, Basili S, Palmirotta R, et al. Prognostic Value of Serum and Tumor Tissue CA 72-4 Content in Gastric Cancer. *Int J Biol Markers* (2003) 18(1):21–7. doi: 10.5301/jbm.2008.1151
25. González C, Megraud F, Buissonniere A, Lujan Barroso L, Agudo A, Duell E, et al. Helicobacter Pylori Infection Assessed by ELISA and by Immunoblot and Noncardia Gastric Cancer Risk in a Prospective Study: The Eurgast-EPIC Project. *Ann Oncol Off J Eur Soc Med Oncol* (2012) 23(5):1320–4. doi: 10.1093/annonc/mdr384
26. Lochhead P, El-Omar E. Helicobacter Pylori Infection and Gastric Cancer. *Best Pract Res Clin gastroenterology* (2007) 21(2):281–97. doi: 10.1016/j.bpg.2007.02.002
27. Plummer M, Franceschi S, Vignat J, Forman D, de Martel C. Global Burden of Gastric Cancer Attributable to Helicobacter Pylori. *Int J Cancer* (2015) 136 (2):487–90. doi: 10.1002/ijc.28999
28. Hamashima C. Current Issues and Future Perspectives of Gastric Cancer Screening. *World J gastroenterology* (2014) 20(38):13767–74. doi: 10.3748/wjg.v20.i38.13767
29. Zhang M, Li F, Wang J, He W, Li Y, Li H, et al. Trna-Derived Fragment Trf-03357 Promotes Cell Proliferation, Migration and Invasion in High-Grade Serous Ovarian Cancer. *OncoTargets Ther* (2019) 12:6371–83. doi: 10.2147/ott.S206861
30. Zhu J, Cheng M, Zhao X. A Trna-Derived Fragment (Trf-3001b) Aggravates the Development of Nonalcoholic Fatty Liver Disease by Inhibiting Autophagy. *Life Sci* (2020) 257:118125. doi: 10.1016/j.lfs.2020.118125
31. Zhu L, Li T, Shen Y, Yu X, Xiao B, Guo J. Using Trna Halves as Novel Biomarkers for the Diagnosis of Gastric Cancer. *Cancer Biomarkers section A Dis Markers* (2019) 25(2):169–76. doi: 10.3233/cbm-182184
32. Shen Y, Yu X, Ruan Y, Li Z, Xie Y, Yan Z, et al. Global Profile of Trna-Derived Small Rnas in Gastric Cancer Patient Plasma and Identification of Trf-33-P4R8YP9LON4VDP as a New Tumor Suppressor. *Int J Med Sci* (2021) 18 (7):1570–9. doi: 10.7150/ijms.53220
33. Kumar P, Kuscu C, Dutta A. Biogenesis and Function of Transfer RNA-Related Fragments (Trfs). *Trends Biochem Sci* (2016) 41(8):679–89. doi: 10.1016/j.tibs.2016.05.004
34. Kumar P, Anaya J, Mudunuri S, Dutta A. Meta-Analysis of Trna Derived RNA Fragments Reveals That They are Evolutionarily Conserved and Associate With AGO Proteins to Recognize Specific RNA Targets. *BMC Biol* (2014) 12:78. doi: 10.1186/s12915-014-0078-0
35. Shao Y, Sun Q, Liu X, Wang P, Wu R, Ma Z. Trf-Leu-CAG Promotes Cell Proliferation and Cell Cycle in Non-Small Cell Lung Cancer. *Chem Biol Drug design* (2017) 90(5):730–8. doi: 10.1111/cbdd.12994
36. Kuscu C, Kumar P, Kiran M, Su Z, Malik A, Dutta A. Trna Fragments (Trfs) Guide Ago to Regulate Gene Expression Post-Transcriptionally in a Dicer-Independent Manner. *RNA (New York NY)* (2018) 24(8):1093–105. doi: 10.1261/rna.066126.118
37. Goodarzi H, Liu X, Nguyen H, Zhang S, Fish L, Tavazoie S. Endogenous Trna-Derived Fragments Suppress Breast Cancer Progression Via YBX1 Displacement. *Cell* (2015) 161(4):790–802. doi: 10.1016/j.cell.2015.02.053
38. Krishna S, Yim D, Lakshmanan V, Tirumalai V, Koh J, Park J, et al. Dynamic Expression of Trna-Derived Small Rnas Define Cellular States. *EMBO Rep* (2019) 20(7):e47789. doi: 10.15252/embr.201947789
39. Burroughs A, Ando Y, de Hoon M, Tomaru Y, Suzuki H, Hayashizaki Y, et al. Deep-Sequencing of Human Argonaute-Associated Small Rnas Provides Insight Into Mirna Sorting and Reveals Argonaute Association With RNA Fragments of Diverse Origin. *RNA Biol* (2011) 8(1):158–77. doi: 10.4161/rna.8.1.14300
40. Sobala A, Hutvagner G. Small Rnas Derived From the 5' End of Trna Can Inhibit Protein Translation in Human Cells. *RNA Biol* (2013) 10(4):553–63. doi: 10.4161/rna.24285

Conflict of Interest: The authors declare that the research was conducted in the absence of any commercial or financial relationships that could be construed as a potential conflict of interest.

frontiers | Frontiers in Oncology

ORIGINAL RESEARCH
published: 28 April 2022
doi: 10.3389/fonc.2022.664420

Cerebrospinal Fluid Cell-Free DNA-Based Detection of High Level of Genomic Instability Is Associated With Poor Prognosis in NSCLC Patients With Leptomeningeal Metastases

*Xi Wu[1], Puyuan Xing[2], Min Shi[3], Weihua Guo[3], Fangping Zhao[3], Honglin Zhu[3], Jianping Xiao[4], Jinghai Wan[5] and Junling Li[2]**

[1] General Department, National Cancer Center/National Clinical Research Center for Cancer/Cancer Hospital, Chinese Academy of Medical Sciences and Peking Union Medical College, Beijing, China, [2] Department of Medical Oncology, National Cancer Center/National Clinical Research Center for Cancer/Cancer Hospital, Chinese Academy of Medical Sciences and Peking Union Medical College, Beijing, China, [3] Hangzhou Jichenjunchuang Medical Laboratory Co., Ltd. Hangzhou, China, [4] Department of Radiotherapy, National Cancer Center/National Clinical Research Center for Cancer/Cancer Hospital, Chinese Academy of Medical Sciences and Peking Union Medical College, Beijing, China, [5] Department of Neurosurgery, National Cancer Center/National Clinical Research Center for Cancer/Cancer Hospital, Chinese Academy of Medical Sciences and Peking Union Medical College, Beijing, China*

Introduction: Leptomeningeal metastasis (LM) commonly occurs in non-small cell lung cancer (NSCLC) patients and has a poor prognosis. Due to limited access to leptomeningeal lesions, the genetic characteristics of LM have not been explored to date. Cerebrospinal fluid (CSF) may be the most representative liquid biopsy medium to obtain genomic information from LM in NSCLC.

Methods: CSF biopsies and matched peripheral blood biopsies were collected from 33 NSCLC patients with LM. We profiled genetic alterations from LM by comparing CSF cell-free DNA (cfDNA) with plasma cfDNA. Somatic mutations were examined using targeted sequencing. Genomic instability was analyzed by low-coverage whole-genome sequencing (WGS).

Results: Driver mutations were detected in 100% of CSF cfDNA with much higher variant allele frequency than that in matched plasma cfDNA (57.5%). Furthermore, we found that the proportions of CSF cfDNA fragments below 150 bp were significantly higher than those in plasma cfDNA. These findings indicate enrichment of circulating tumor DNA (ctDNA) in CSF and explain the high sensitivity of mutation detection in the CSF. The absence of some mutations in CSF cfDNA—especially the first-/second-generation mutation T790M, which confers resistance to epidermal growth factor receptor (EGFR)-

OPEN ACCESS

Edited by:
Rui P. L. Neves, University Hospital Düsseldorf, Germany

Reviewed by:
Minggang Fang, University of Massachusetts Medical School, United States
Boxiang Liu, Baidu, United States

***Correspondence:**
Junling Li
lijunling@cicams.ac.cn

Specialty section:
This article was submitted to Cancer Molecular Targets and Therapeutics, a section of the journal Frontiers in Oncology

Received: *05 February 2021*
Accepted: *30 March 2022*
Published: *28 April 2022*

Citation:
Wu X, Xing P, Shi M, Guo W, Zhao F, Zhu H, Xiao J, Wan J and Li J (2022) Cerebrospinal Fluid Cell-Free DNA-Based Detection of High Level of Genomic Instability Is Associated With Poor Prognosis in NSCLC Patients With Leptomeningeal Metastases. Front. Oncol. 12:664420. doi: 10.3389/fonc.2022.664420

Tyrosine kinase inhibitors (TKIs)—that were present in plasma cfDNA samples indicates different mechanisms of cancer evolution between LM and extracranial lesions. In addition, 86.6% of CSF ctDNA samples revealed high levels of genomic instability compared with 2.5% in plasma cfDNA samples. A higher number of large-scale state transitions (LSTs) in CSF cfDNA were associated with a shorter overall survival (OS).

Conclusion: Our results suggest that LM and extracranial lesions develop independently. Both CSF cfDNA genetic profiling and plasma cfDNA genetic profiling are necessary for clinical decision-making for NSCLC patients with LM. Through CSF-based low-coverage WGS, a high level of LSTs was identified as a potential biomarker of poor prognosis.

Keywords: cerebrospinal fluid cfDNA, leptomeningeal metastases, EGFR-TKI resistance, genomic instability, NSCLC

INTRODUCTION

Leptomeningeal metastases (LMs) occur in 3.4%–3.8% of non-small cell lung cancer (NSCLC) patients and are more common (9.4%) in patients whose tumors carry epidermal growth factor receptor (EGFR) mutations, even during EGFR-TKI treatment (1–3). Despite extensive research on extracranial lesions, the role of acquired resistance to EGFR-TKIs in LM has not been well studied due to limited access to leptomeningeal lesions. The prognosis of LM in NSCLC is very poor, with a median overall survival (OS) of 1.9 months if patients are untreated and 3.5–12 months upon treatment with EGFR-TKIs (4). Brain imaging technology (MRI) and cerebrospinal fluid (CSF) cytology are widely used in the diagnosis of LM. Despite CSF cytology being the gold standard, a positive result for this diagnostic method is observed in only 50%–60% of patients with LM at the first CSF examination (5, 6). Early diagnosis and a comprehensive understanding of genetic alterations are essential for accurate assessment of disease progression and a rational exploration of clinical treatments.

With the rapid progress in the application of liquid biopsy in the past few years, cell-free DNA (cfDNA), especially plasma cfDNA, has been used widely for monitoring tumor progression/regression and response to treatments (7, 8). However, plasma cfDNA is not effective in detecting mutations in brain tumors and brain metastasis (9–13). CSF cfDNA-based profiling of tumor-related genetic alterations has also been investigated, with some limitations, depending on the location and stage of tumors, and has shown great advantages in the case of LM (9, 11–14).

Previous studies have shown that CSF-derived cfDNA demonstrates higher sensitivity and better represents the genetic status for LM than plasma-derived cfDNA (11, 13, 15, 16). However, a fundamental understanding of LM genetics remains elusive. In this study, we focused on identifying genetic alterations (both mutations and structural variants) at both gene and genome levels in CSF cfDNA derived from NSCLC patients with LM in order to investigate the molecular mechanism of LMs and identify genetic signatures for improved clinical management.

MATERIALS AND METHODS

Patient Enrollment

This study was conducted in accordance with the Declaration of Helsinki and approved by the Peking University Cancer Hospital Ethics Committee. All patients provided written informed consent for treatment, sample collection, and analysis. Thirty-three lung adenocarcinoma patients with LM were enrolled from March 2017 to August 2019 at the Cancer Hospital Chinese Academy of Medical Sciences. The diagnostic criteria for LM were based on a positive result on brain MRI or CSF cytologic examination. All patients received care at the Cancer Hospital Chinese Academy of Medical Sciences and had been followed for more than 6 months if death did not occur earlier.

Cell-Free DNA Extraction

CSF cfDNA and plasma cfDNA were extracted using QIAamp Circulating Nucleic Acid Kit (Qiagen, USA) in accordance with the manufacturer's instructions. Germline DNA was extracted from the buffy coat of the matched whole-blood samples using a DNeasy Blood and Tissue Kit (Qiagen, USA) and analyzed as a germline reference. DNA was quantified using the Qubit Fluorometer (Invitrogen, USA). Size distribution of cfDNA was determined by low-coverage whole-genome sequencing (WGS), as previously described (17).

Mutation Profiling

Genomic bar-coded DNA libraries were constructed with 20 ng cfDNA or 500 ng genomic DNA using KAPA HyperPrep Kits (Roche, Germany) and captured using probes from three designed lung cancer panels, which covered exons of 137 genes (Geneseeq, China), 520 genes (Burning Rock Dx, China), or 180 genes (Genetron Health, China). High-throughput sequencing was performed on a HiSeq platform (Illumina, USA). Sequencing reads were mapped to a human reference genome (hg19) using the Burrows–Wheeler Aligner (BWA) (18). Duplicate removal, local realignment, and base quality recalibration were performed using PICARD (http://broadinstitute.github.io/picard/) and the Genome Analysis Toolkit (GATK). Mutations with allelic fractions of less than 0.1%, supported by fewer than 4 unique

reads or detected as germline mutations, were disregarded. Mutations in 84 genes, which overlapped between the three lung cancer panels mentioned above, were analyzed in this study (**Table S1**).

Structural Variant Analysis

Copy number variants (CNVs) from targeted sequencing data were called using copy number segments produced by ABSOLUTE v.1.4 and analyzed by GISTIC 2.0 (19).

Low-coverage WGS (3×) was performed using genomic barcoded DNA libraries, which were constructed with KAPA HyperPrep Kits [Genetron Health (Beijing) Co. Ltd.]. PE150 reads were generated using the HiSeq 4000 platform (Illumina, USA) and aligned to the reference human genome hg19.

For a general assessment of genome instability, read counts from the WGS bam files were binned into contiguous 1-Mb windows (sex chromosomes were excluded) and GC bias was corrected using GATK. Stable chromosomal regions were identified if the coverage of each bin in the region was relatively stable and the variant allele fraction (VAF) of heterozygotic germline Single nucleotide polymorphisms (SNPs) in the region remained at about 0.5 using sequencing data from 180-gene lung cancer panel data as a reference. Coverage of each bin was adjusted to the mean coverage of stable chromosomal regions for each sample. For plasma and CSF samples, the coverage in each genomic bin was further divided by the coverage in the corresponding bin of germline DNA from the same patient. The resulting ratios were log2-transformed, and segmentation was performed using the R package DNAcopy (20).

Genomic instability was evaluated based on a number of large-scale state transitions (LSTs) and the genome instability number (GIN). Using low-coverage WGS data, the number of LSTs was quantified as the number of chromosomal breakpoints (change in coverage) between adjacent regions, each of at least 10 megabases (Mb) obtained after smoothing (filtering <3 Mb small-scale copy number variation) (21). Similarly, GIN was quantified as the sum, across all autosomal bins, of the absolute deviation of the normalized genomic representation of a sample to the expected normalized genomic representation of stable chromosome regions of the same sample (22).

Data Availability

The mutation profiling data and raw whole-genome sequence data referenced in this study are available from The National Omics Data Encyclopedia (https://www.biosino.org/node/) under accession code OEP003149 and is available on request.

RESULTS

Patient Information

All diagnoses of LMs were confirmed based on MRI or CSF cytology. Seventeen of 33 patients (51.5%) were men, and the median age of the cohort was 55 years (range, 39–78 years). Driver mutations of primary tumors were determined by qPCR or targeted sequencing: 31 out of 33 primary tumors harbored EGFR mutations (93.9%), 1 primary tumor carried Anaplastic Lymphoma kinase (ALK) rearrangement, and 1 primary tumor carried erb-b2 receptor tyrosine kinase 2 (ERBB2) mutations (**Table 1**). Most patients (31 out of 33) with EGFR alterations had a history of targeted therapies and were switched to a different EGFR-TKI upon the development of resistance (**Table 1**). Ten out of 33 patients showed no brain parenchymal metastases at the time of LM diagnosis; among them, 2 patients showed no extracranial metastases. For genomic profiling, 10 ml of CSF was collected by lumbar puncture and 10 ml of matched peripheral blood was collected by venipuncture, after LM diagnosis, from all 33 patients.

Reliable Detection of Driver Mutations in Cerebrospinal Fluid Cell-Free DNA From Leptomeningeal Metastasis Patients

Examination of mutation profiles in CSF cfDNA and matched plasma cfDNA revealed that driver mutations identified in primary tumors could be detected in all CSF cfDNA samples (33 out of 33) but were only present in 51.5% of plasma cfDNA samples (16 out of 33) (**Figure 1A**); these results are in alignment with previous findings that CSF cfDNA is more sensitive than plasma cfDNA in identifying mutations (9, 11–13). The percentage of VAFs was, in general, much higher in CSF cfDNA than in that in plasma cfDNA (**Figure 1C**), with the median VAFs of driver mutations being 34.7% in CSF cfDNA and 0.1% in plasma cfDNA. In addition, 90.9% (30/33) of CSF samples showed VAFs of driver mutations to be over 20%, and only one plasma sample had a VAF of driver mutations of more than 10% (**Figure 1C**). The extremely high VAFs of driver mutations suggested a high fraction of circulating tumor DNA (ctDNA) in CSF cfDNA.

Furthermore, the presence of driver mutations in plasma cfDNA reflected the status of extracranial lesions because patients whose driver mutations were detected in plasma cfDNA were more likely to be at a progressive stage (9 out of 17) and patients whose driver mutations were not detected in plasma were mostly at a stable/regressive stage (**Figure 1B**). For 2 patients who had no extracranial metastases at the time of sample collection, no driver mutations were detected in plasma cfDNA (P12 and P19) (**Table 1** and **Figure 1B**).

Enrichment of Circulating Tumor DNA in Cerebrospinal Fluid

In plasma cfDNA, ctDNA accounts for a small fraction of cfDNA because most cfDNA is derived from non-cancer cells, especially blood cells (17). It has been reported that cfDNA fragments in the plasma of healthy individuals are significantly longer than those in the plasma of patients with late-stage lung cancer, and therefore, selective sequencing with specific fragment sizes may boost ctDNA detection (17). In a parallel comparison, the yield

TABLE 1 | Clinical information.

Pt NO.	Age at LM, years	Sex	The driver mutations in primary tumor	ECOG PS at LM	Extracranial metastases status	Brain parenchymal metastases status	TKI before CSF collection	OS from LM, months	Genomic profiling test
P01	48	man	EGFR.G719C	2	stable	stable	Icotinib+Erlotinib	16	180 genes panel and WGS
P02	46	man	EGFR.L858R	4	progressive	progressive	Icotinib+Osimertinib	2	180 genes panel and WGS
P03	56	man	EML4-ALK fusion	2	stable	without metastases	Crizotinib+Brigatinib	3	137 genes panel
P04	54	man	EGFR.exon19del	1	stable	without metastases	Gefitinib+Osimertinib+ Erlotinib	16	180 genes panel and WGS
P05	47	man	EGFR.exon19del	1	stable	without metastases	Icotinib	>14	180 genes panel and WGS
P06	62	woman	EGFR.L858R	3	stable	stable	Erlotinib+Osimertinib	12	520 genes panel
P07	75	man	EGFR.L858R	3	stable	without metastases	Erlotinib	11	137 genes panel
P08	49	woman	EGFR.exon19del	2	progressive	regressive	Gefitinib+Osimertinib+ Capmatinib	8	180 genes panel and WGS
P09	45	woman	EGFR.exon19del	2	stable	progressive	Gefitinib	>11	180 genes panel and WGS
P10	57	man	EGFR.exon19del	3	stable	without metastases	Gefitinib+Osimertinib	>13	180 genes panel and WGS
P11	48	woman	EGFR.exon19del	4	stable	progressive	Gefitinib+Osimertinib	15	180 genes panel and WGS
P12	47	woman	EGFR.L858R	3	without metastases	without metastases	Icotinib+Osimertinib+ Erlotinib+Cabozantinib	>19	180 genes panel and WGS
P13	57	woman	ERBB2.G776delinsVV	3	stable	progressive	Afatinib	6	520 genes panel
P14	58	woman	EGFR.exon19del	2	progressive	progressive	Gefitinib+Erlotinib	1	180 genes panel and WGS
P15	48	man	EGFR.L858R	4	progressive	stable	Erlotinib+Osimertinib	7	520 genes panel
P16	56	woman	EGFR.exon19del	1	progressive	without metastases	Gefitinib	>13	180 genes panel and WGS
P17	52	woman	EGFR.exon19del	2	stable	stable	Gefitinib+Osimertinib	>14	180 genes panel and WGS
P18	60	man	EGFR.L858R	3	progressive	stable	Icotinib+Erlotinib+ Osimertinib	3	180 genes panel and WGS
P19	53	man	EGFR.L858R	2	without metastases	progressive	Icotinib	6	137 genes panel
P20	39	man	EGFR.exon19del	2	regressive	without metastases	Gefitinib+Afatinib	>14	180 genes panel and WGS
P21	66	woman	EGFR.L858R	4	progressive	stable	Gefitinib+Osimertinib	0.5	180 genes panel and WGS
P22	60	woman	EGFR.L858R	1	stable	progressive	Gefitinib+Erlotinib+ Osimertinib	8	520 genes panel
P23	60	man	EGFR.L858R	3	progressive	progressive	Gefitinib	9	520 genes panel

(Continued)

TABLE 1 | Continued

Pt NO.	Age at LM, years	Sex	The driver mutations in primary tumor	ECOG PS at LM	Extracranial metastases status	Brain parenchymal metastases status	TKI before CSF collection	OS from LM, months	Genomic profiling test
P24	62	woman	EGFR.exon19del	2	progressive	without metastases	Gefitinib+Erlotinib	9	137 genes panel
P25	55	man	EGFR.exon19del	1	stable	progressive	Gefitinib+Erlotinib+ Osimertinib	8	180 genes panel and WGS
P26	50	woman	EGFR.L858R	2	stable	stable	Osimertinib	>12	180 genes panel and WGS
P27	64	woman	EGFR.exon19del	2	stable	progressive	Erlotinib	>11	180 genes panel and WGS
P28	79	man	EGFR.L858R	2	stable	without metastases	Icotinib	>9	180 genes panel and WGS
P29	50	woman	EGFR.exon19del	2	progressive	progressive	–	11	180 genes panel and WGS
P30	47	man	EGFR.exon19ins	1	progressive	progressive	Gefitinib+Afatinib+ Osimertinib	5	180 genes panel and WGS
P31	64	woman	EGFR.L858R	2	progressive	progressive	–	10	180 genes panel and WGS
P32	66	man	EGFR.L858R	4	stable	stable	Afatinib	3.5	180 genes panel and WGS
P34	60	man	EGFR.L858R	1	progressive	progressive	Gefitinib+Erlotinib	>7	180 genes panel and WGS

LM, leptomeningeal Metastasis; ECOG PS, ECOG performance status; OS, overall survival; TKI, tyrosine kinase inhibitors; CSF, cerebrospinal fluid; WGS, whole genome sequencing.

of cfDNA from CSF was much lower than that from plasma (median yield: 1.75 ng/ml of CSF vs. 8.19 ng/ml of plasma, Wilcoxon test p value = 0.0025) (**Figure 2A**); 53.8% of CSF cfDNA samples showed a size of peak fragments below 160 bp, while the size of peak fragments from all plasma cfDNA samples was over 160 bp (**Figure 2B**). Consistent with this, the proportion of CSF cfDNA in the size range of 20–150 bp was significantly higher than that for plasma cfDNA (**Figure 2C**). A reduction in cfDNA fragment size and extremely high VAFs of driver mutations in CSF provided evidence that ctDNA was more enriched in CSF and better represents LM-associated genetic alterations.

Leptomeningeal Metastases and Extracranial Lesions Acquired Resistance Mutations Independently

As demonstrated by driver mutation detection, plasma cfDNA was not reflective of LM status (**Figure 1**). This finding was further confirmed when comparing more comprehensive genomic profiles between CSF cfDNA and plasma cfDNA. Among all 183 alterations detected in all samples by targeted sequencing, only 29 were present in both CSF cfDNA and matched plasma cfDNA samples (**Figure 3A**, cutoff limit: Mutant allele frequency (MAF) >0.1%), including 28 single-nucleotide variants (SNVs) or indels and 1 CNV (**Figures 2B, C**); 132 were unique to CSF (not present in matched plasma), and 22 mutations were unique to plasma (not present in matched CSF) (**Figure 3A**). The presence of plasma-specific genetic alterations was more striking when considering the high sensitivity of CSF in picking up mutations for LM, suggesting the possibility that CSF cfDNA and plasma cfDNA can be used to detect separate tumors located in different compartments with distinct features.

The large number of CSF-specific mutations, which could not be detected in plasma, might be simply a result of the low sensitivity of mutation detection *via* plasma biopsy. Plasma-specific mutations reveal differences between LM and extracranial lesions. Therefore, we focused on 22 plasma-specific mutations. The EGFR T790M mutation, the most common acquired resistant mutation to first-/second-generation EGFR-TKIs with poor blood–brain barrier (BBB) penetration, was the most frequently detected plasma-specific mutation in this cohort. When tracking the treatment history of these patients, among 28 patients who were treated with first-/second-generation EGFR-TKIs, the EGFR T790M mutation was detected in 5 plasma cfDNA samples (**Figure 3D**; P04, P08, P16, P17, and P20) and in one CSF cfDNA sample (**Figure 3D**, P32). The lack of effective exposure of meningeal metastases to first-/second-generation EGFR-TKIs (23) may be one of the reasons

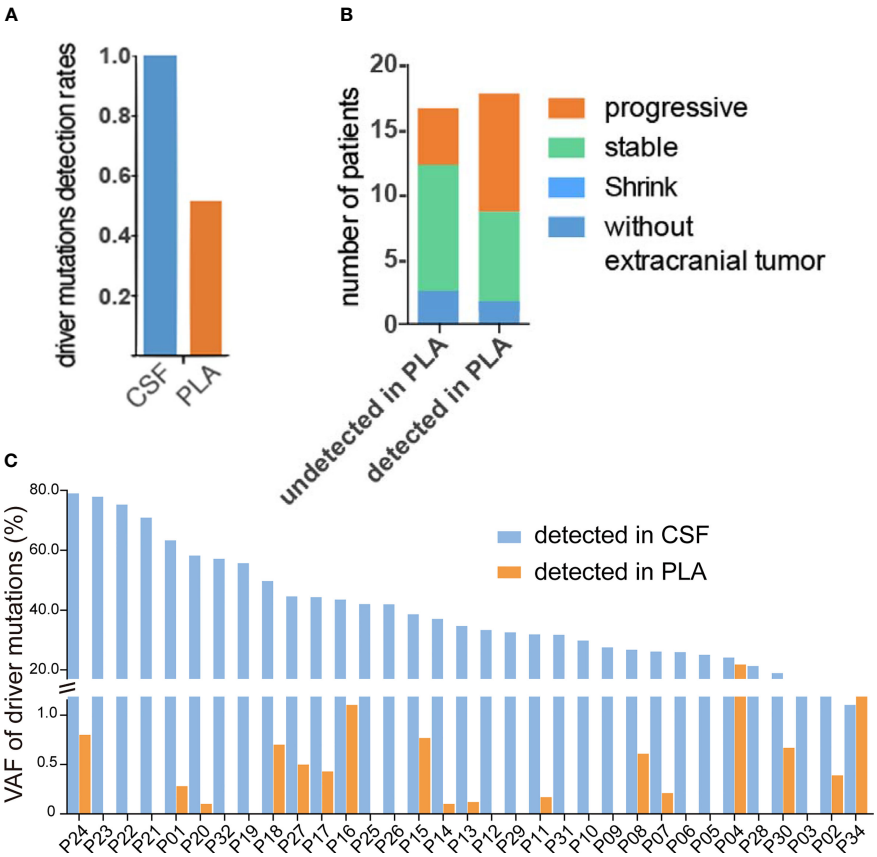

FIGURE 1 | High fraction of ctDNA in CSF. **(A–C)** Targeted sequencing was performed in matched CSF cfDNA and plasma cfDNA, as described in the *Materials and Methods*, and the status of driver mutations was compared in CSF and plasma samples. **(A)** Rates of driver mutation detection in CSF cfDNA and plasma (PLA) cfDNA. **(B)** The association of driver gene mutation detection in PLA cfDNA with extracranial tumor status. The column on the left represents the disease status when driver mutations were not detected and the majority of patients were shown at stable/regression stages. The column on the right represents the disease status when driver mutations were detected and almost 50% of patients were at the progressive stage. **(C)** Variant allele fractions (VAFs) of driver mutations in matched CSF cfDNA or PLA cfDNA samples.

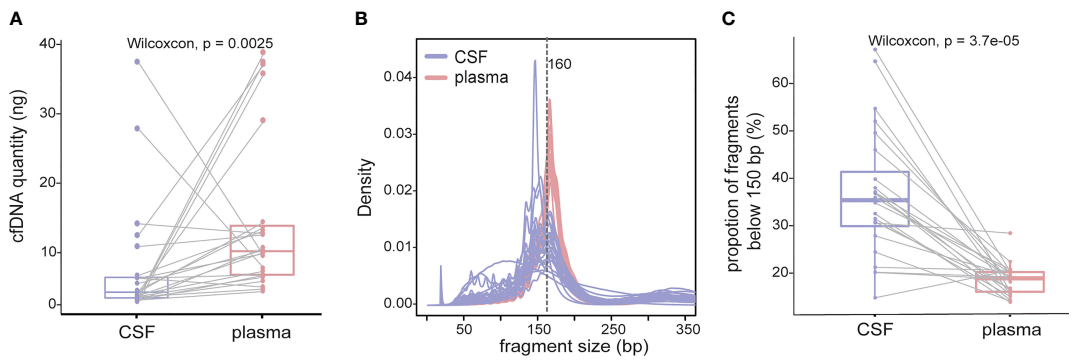

FIGURE 2 | cfDNA fragments are shorter in CSF than those in plasma. cfDNAs were extracted from 24 CSF samples and matched plasma samples, and the size of cfDNA was analyzed by low-coverage WGS (3×). **(A)** cfDNA yield between 5 ml CSF (violet) and 5 ml plasma (red) from 24 NSCLC patients with LM. **(B)** Size distribution of cfDNA fragments between CSF samples and matched plasma samples. **(C)** Proportion of cfDNA fragments below 150 bp in size in CSF samples and matched plasma samples. Each dot represents each sample, and each line connects matching samples.

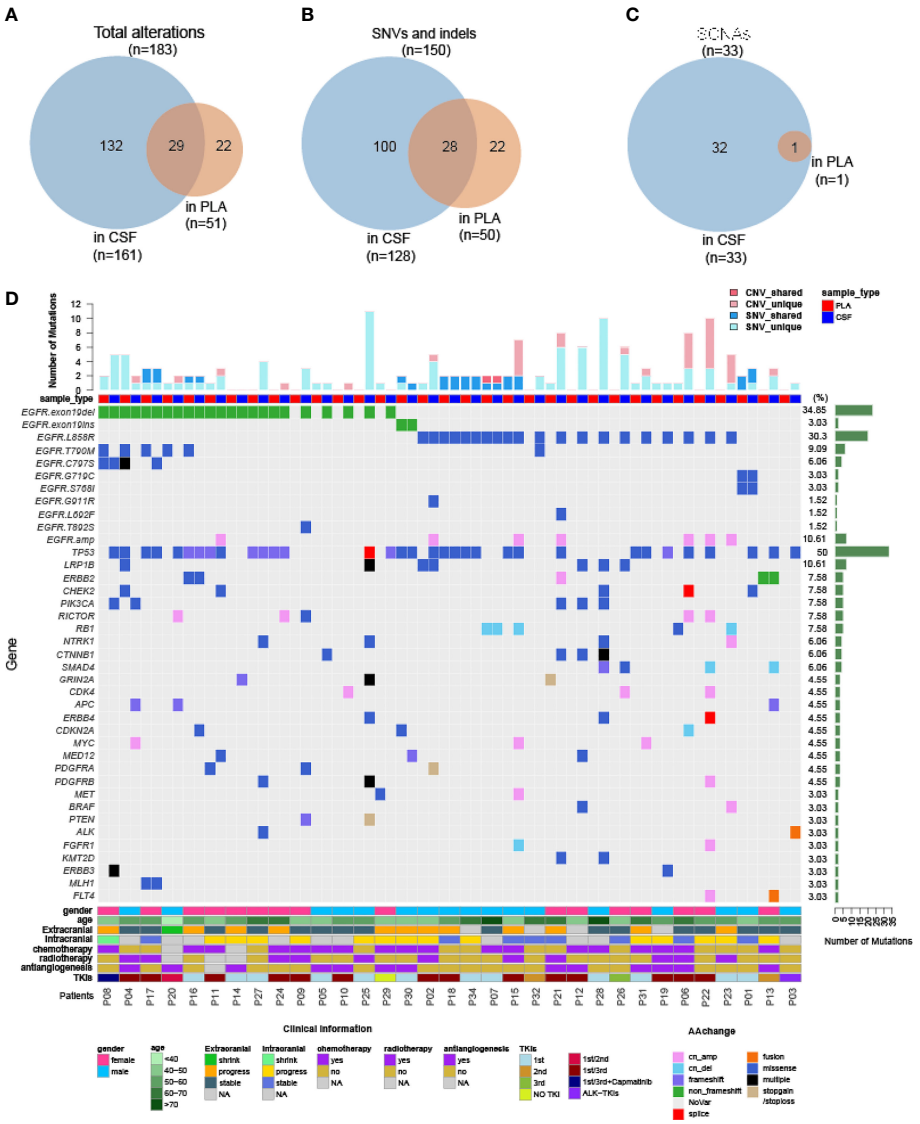

FIGURE 3 | Genomic landscape of CSF and plasma cfDNA in NSCLC with LM. Samples were subject to targeted sequencing by different vendors; a final analysis for 84 core genes was performed, and the results were compared between CSF and plasma. **(A–C)** Venn diagram of genetic alterations for CSF- and plasma-based cfDNA profiling. **(A)** Venn diagram of total alterations detected in CSF cfDNA and plasma (PLA) cfDNA. **(B)** Venn diagram of single-nucleotide variants (SNVs) and indels detected in CSF cfDNA and PLA cfDNA. **(C)** Venn diagram of somatic copy number alterations (SCNAs) detected in CSF cfDNA and PLA cfDNA. **(D)** Mutational landscape in plasma cfDNA and matched CSF cfDNA from individual patients. The number of SNVs and SCNAs are shown at the top of the panel, and clinical information is shown at the bottom of the panel.

for the lesser detection of EGFR T790M mutations in CSF. However, the EGFR C797S mutation was almost evenly distributed in CSF and matched plasma collected from third-generation EGFR-TKI osimertinib-treated patients (n = 15). The incidence of EGFR T790M in plasma and CSF was not significantly different due to the small sample size. Notably, however, the EGFR C797S mutation was detected in both CSF and plasma, but with different nucleotide variants in patient P08. In plasma, EGFR 2390G>C was located in cis to T790M (VAF: 0.5%). But in the CSF, it was replaced by an EGFR 2389T>A (VAF: 8.8%) (**Figures 4A, B**). In other words, LM and extracranial lesions independently acquired resistance mutations in patient P08. In our cohort, EGFR-TKI-resistant mutations with the same nucleotide variant were never present in both CSF and plasma from the same patient.

These results suggest that EGFR-TKI-resistant mutations evolved differently in the extracranial lesion and LM from the same patient, providing further evidence that extracranial and LM lesions progress independently and supporting the notion that both CSF cfDNA and plasma cfDNA are necessary for

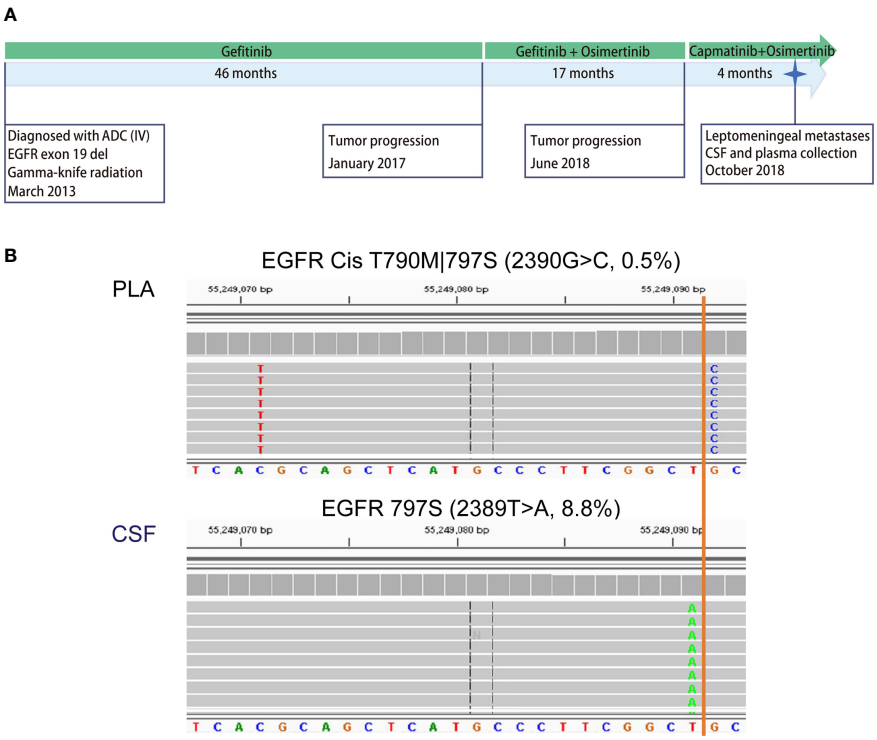

FIGURE 4 | Case analysis: distribution of EGFR-TKI-resistant mutations in P08. Patient P08 was exposed to both first- (gefitinib) and third-generation (osimertinib) EGFR-TKIs before LM diagnosis. **(A)** Disease timeline. P08 was diagnosed with lung adenocarcinoma in March 2013 and received treatment with gefitinib, osimertinib, and capmatinib sequentially. In October 2018, he was diagnosed with leptomeningeal metastasis. CSF and matched peripheral blood were collected subsequently. **(B)** The mutation profiling of CSF cfDNA and plasma cfDNA was performed using a next-generation sequencing (NGS) panel containing 180 genes. The raw reads for two types of EGFR mutations are shown. EGFR C797S 2390G>C was detected in the CSF in cis with T790M 2369C>T in plasma only (0.6%), not in CSF, while C797S 2389T>A was detected in CSF only (8.8%).

comprehensive genetic profiling to make clinical decisions for NSCLC patients with LM.

Chromosomal Instability as a Universal Genetic Characteristic of Leptomeningeal Metastasis

Given the evidence that CSF cfDNA is representative of genetic profiles for LM lesions, we further characterized LM by CSF cfDNA. It is worth noting that in 7 CSF samples (22.6%), VAFs of EGFR mutations were over 50% (**Figure 1C**), indicating a loss of heterozygosity (LOH) of EGFR in LM. Similarly, almost all CNVs were exclusively detected in CSF samples in this cohort (**Figures 3C, D**). The high occurrence rate of both LOH and CNVs in CSF cfDNA suggested a universal genome instability in LM.

To assess genome instability, we performed low-coverage WGS (3×) with matched CSF and plasma cfDNA samples from 24 out of 33 patients. At the whole-genome level, CSF cfDNA demonstrated a much more vibrating pattern (**Figure 5A**). LSTs (longer than 10 Mb) were detected in 23 CSF cfDNA samples (95.8%, 23/24, median number of LSTs is 15.5) compared with only 2 plasma cfDNAs (8.3%, 2/24). The observation of high levels of genomic instability in LM was further confirmed by comparing to primary lung adenocarcinoma tissue samples from a public dataset (24) (**Figures 5B, C**, labeled as LUAD). Both the number of LST and GIN of this cohort were significantly higher in CSF cfDNA than in genomic DNA derived from primary tumor tissues (**Figures 5B, C**).

Association of Large-Scale State Transitions in Cerebrospinal Fluid With Patient Survival

To further understand the relationship between chromosomal instability and the clinical outcome of LM patients, we analyzed data from 24 patients with a follow-up over 6 months (**Figure 5D**) and found that a survival shorter than 6 months was correlated with higher levels of LSTs (**Figure 5E**). In contrast, 6-month survival rates in patients with higher levels of LSTs (≥15.5) and lower levels of LSTs (<15.5) were 60% and 92%, respectively. Median survival was significantly shorter in patients with higher levels of LSTs (10 months vs. 16 months, $p = 0.0304$, **Figure 5F**). GIN levels were not found to be associated with patient survival (**Figure S1**).

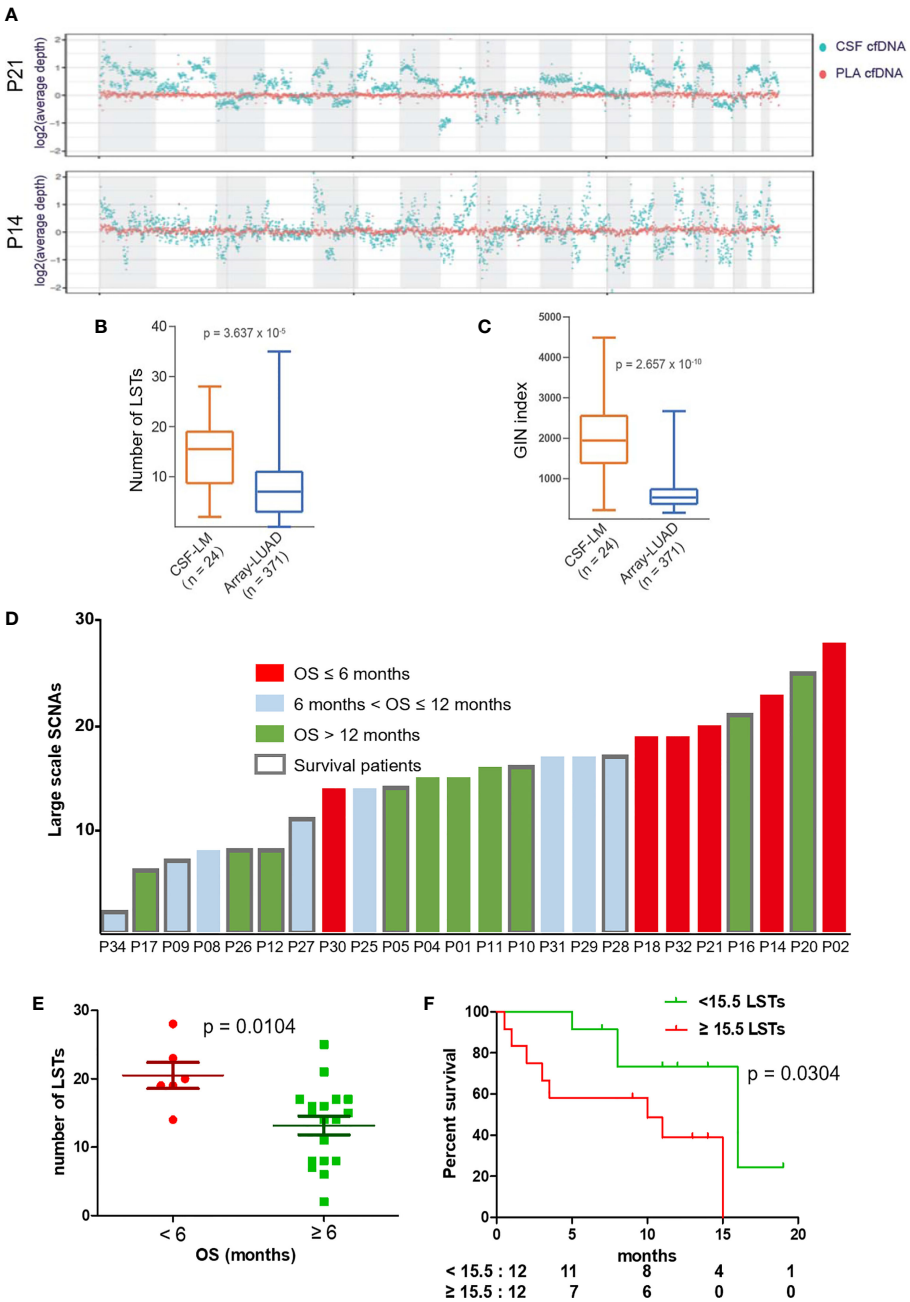

FIGURE 5 | LST as a potential prognostic marker for LM. **(A)** Visualization of genomic instability. The average depths along chromosomes (1M/bin) of CSF cfDNA (teal color) and matched plasma cfDNA (orange color) from 2 representative patients are shown. Plasma samples demonstrated a constant read across the chromosome, while reads from CSF samples varied continuously, indicating extensively affected copy numbers through the whole genome. **(B, C)** Genomic instability was assessed based on the number of large stable transitions [large-scale state transitions (LSTs)] and genome instability number (GIN) using low-coverage WGS data for the current cohort (n = 24, CSF-LM) and compared with a published dataset comprising genomic DNA profiles from primary lung adenocarcinoma tissues [n = 371, Array-LUAD (24)]. Data were analyzed as described in the *Materials and Methods*. **(B)** Comparison of LST between CSF-LM and Array-LUAD. The average level of LSTs in CSF-LM was significantly higher than that in Array-LUAD (15.0 vs. 7.8, $p < 0.001$). **(C)** Comparison of GIN levels between CSF-LM and Array-LUAD. The average level of GIN in CSF-LM was significantly higher than that from Array-LUAD (1,961.4 vs. 681.6, $p < 0.001$). **(D)** Levels of LSTs and survival status in LM patients (n = 24). Each column represented each patient. Columns in red indicate an overall survival of less than 6 months, columns in green indicate an overall survival of over 12 months, columns in gray indicate an overall survival between 6 and 12 months. The columns with borders indicate the patients who were still alive at the time of the data collection and reporting, while the columns without borders indicate patients who had died at the time of data collection. **(E, F)** Association of LSTs with survival. **(E)** The levels of LSTs were significantly lower in patients whose survival was over 6 months ($p = 0.0068$). **(F)** Kaplan–Meier curves of overall survival. With a cutoff at 15.5, the median level of this cohort, patients with higher levels of LSTs demonstrated a short survival (median OS after LM, 10 months vs. 15 months, $p = 0.038$). However, GIN was not associated with survival (**Figure S1**).

DISCUSSION

The rate of detection of mutations in CSF from patients is lower when tumors are located farther away from the cerebral ventricle (25, 26). However, LM is adjacent to CSF, and this study and others reveal that it shows 100% sensitivity in identifying driver mutations through CSF-based biopsy (**Figure 1A**). Compared with plasma cfDNA, the enrichment of ctDNA in CSF could explain its high sensitivity. LMs are normally diagnosed through MRI or CSF cytology with low sensitivity before patients receive lifesaving treatments (5, 6, 27). CSF cfDNA, which contains a high fraction of ctDNA, has shown great promise in diagnosing LM over traditional methods with its high sensitivity as a result of the enrichment of LM-specific mutations. In addition, we found that genome instability is a universal genetic characteristic of LM. CSF cfDNA-based low-coverage WGS might offer an early and sensitive diagnostic tool in LM, especially for patients without hotspot mutations. CSF-based dynamic mutation profiling and low-coverage WGS, in combination with MRI or CSF cytology, could be set up conveniently in a hospital setting to offer an early diagnosis and accurate assessment of disease status.

The difference in detection sensitivity makes the direct comparison between CSF and plasma difficult. Under most conditions, the MAF of a particular genetic change in CSF is 50- to100-fold higher than that in plasma (**Figure 1**). Therefore, it is not surprising that CSF-specific alterations dramatically outnumber plasma-specific alterations (**Figure 3**). At the same time, the difference in detection sensitivity makes plasma-specific alterations more clearly evident. The predominant presence of T790M in plasma cfDNA can be explained by poor BBB penetration of first-/second-generation EGFR-TKIs (23). However, the different nucleotide mutations of C797S detected in CSF and plasma, i.e., 2390G>C only in plasma and 2389T>A only in CSF, from one patient upon treatment with improved BBB-penetrating osimertinib support the independent evolution of extracranial lesions and LMs. In addition to resistance mutations, very few passenger mutations (**Figure 3D**, such as GRIN24 in P21 and CDKN24 in P30) were detected exclusively in plasma, and the mechanism by which tumors in these two compartments behave differently remains unclear. Resolution of this discrepancy requires larger cohort studies.

The potential biomarker LST identified in LM through CSF-based liquid biopsy in this study offers new possibilities for understanding and potentially exploring novel treatment strategies for LM. However, the cutoff value for LST needs to be determined with a larger dataset. Despite the fact that both GIN and LST are considered indicators of chromosomal ploidy, instead of considering all CNVs in GIN index evaluation (22), LSTs only count large-scale CNVs that are longer than 10 Mb (21). LSTs are reported as indicators of homologous recombination deficiency (HRD) and associated with cisplatin and poly ADP ribose polymerase (PARP) inhibitor sensitivity in breast carcinomas (28). This might explain why both LST and GIN were higher in LMs, but only LST was associated with survival (**Figure 5**, **Figure S1**). The findings are expected to guide future investigations of HRD in LM for new therapeutic opportunities (28).

In summary, our study confirms previous findings that CSF is a more sensitive and reliable liquid biopsy tool for LM, suggesting that LM and extracranial lesions arise through independent processes during cancer development and identifying higher levels of LSTs in CSF as a prognostic marker. Based on findings from this study, a simple driver mutation test and low-coverage WGS through CSF biopsy might offer a ready-to-use diagnostic tool for LM. Future larger-scale studies on HRD might lead to new opportunities for the treatment of LM. The discrepancy between extracranial lesion(s) and LM supports the evaluation of the disease *via* a combination-based approach for a more accurate assessment of disease status and clinical intervention.

DATA AVAILABILITY STATEMENT

The datasets presented in this study can be found in online repositories. The name of the repository and accession number can be found below: Bio-Med Big Data Center (BMDC) National Omics Data Encyclopedia (NODE), https://www.biosino.org/node/, OEP003149.

ETHICS STATEMENT

The studies involving human participants were reviewed and approved by The Independent Ethics Committee, National GCP Center for Anticancer Drugs, China. The patients/participants provided their written informed consent to participate in this study.

AUTHOR CONTRIBUTIONS

PX and JL designed and supervised the study. XW and MS xsearched the literature. XW, PX, JX, and JW participated in data acquisition. MS, WG, FZ, and HZ did the data analysis and interpretation. XW and MS drafted the article. WG, FZ, and HZ did statistical analysis. PX and JL performed critical revision of the article for important intellectual content. All authors contributed to the article and approved the submitted version.

SUPPLEMENTARY MATERIAL

The Supplementary Material for this article can be found online at: https://www.frontiersin.org/articles/10.3389/fonc.2022.664420/full#supplementary-material

REFERENCES

1. Remon J, Le Rhun E, Besse B. Leptomeningeal Carcinomatosis in Non-Small Cell Lung Cancer Patients: A Continuing Challenge in the Personalized Treatment Era. *Cancer Treat Rev* (2017) 53:128–37. doi: 10.1016/j.ctrv.2016.12.006
2. Li YS, Jiang BY, Yang JJ, Tu HY, Zhou Q, Guo WB, et al. Leptomeningeal Metastases in Patients With NSCLC With EGFR Mutations. *J Thorac Oncol* (2016) 11(11):1962–9. doi: 10.1016/j.jtho.2016.06.029
3. Flippot R, Biondani P, Auclin E, Xiao D, Hendriks L, Le Rhun E, et al. Activity of EGFR Tyrosine Kinase Inhibitors in NSCLC With Refractory Leptomeningeal Metastases. *J Thorac Oncol* (2019) 14(8):1400–7. doi: 10.1016/j.jtho.2019.05.007
4. Yufen X, Binbin S, Wenyu C, Jialiang L, Xinmei Y. The Role of EGFR-TKI for Leptomeningeal Metastases From Non-Small Cell Lung Cancer. *Springerplus* (2016) 5(1):1244. doi: 10.1186/s40064-016-2873-2
5. Chamberlain MC. Leptomeningeal Metastases in the MRI Era. *Neurology* (2011) 76(2):200; Author Reply 200–201. doi: 10.1212/WNL.0b013e3181fac738
6. Thakkar JP, Kumthekar P, Dixit KS, Stupp R, Lukas RV. Leptomeningeal Metastasis From Solid Tumors. *J Neurol Sci* (2020) 411:116706. doi: 10.1016/j.jns.2020.116706
7. Bronkhorst AJ, Ungerer V, Holdenrieder S. The Emerging Role of Cell-Free DNA as a Molecular Marker for Cancer Management. *Biomol Detect Quantif* (2019) 17:100087. doi: 10.1016/j.bdq.2019.100087
8. Ai B, Liu H, Huang Y, Peng P. Circulating Cell-Free DNA as a Prognostic and Predictive Biomarker in Non-Small Cell Lung Cancer. *Oncotarget* (2016) 7 (28):44583–95. doi: 10.18632/oncotarget.10069
9. De Mattos-Arruda L, Mayor R, Ng CK, Weigelt B, Martinez-Ricarte F, Torrejon D, et al. Cerebrospinal Fluid-Derived Circulating Tumour DNA Better Represents the Genomic Alterations of Brain Tumours Than Plasma. *Nat Commun* (2015) 6:8839. doi: 10.1038/ncomms9839
10. Ge M, Zhan Q, Zhang Z, Ji X, Zhou X, Huang R, et al. Different Next-Generation Sequencing Pipelines Based Detection of Tumor DNA in Cerebrospinal Fluid of Lung Adenocarcinoma Cancer Patients With Leptomeningeal Metastases. *BMC Cancer* (2019) 19(1):143. doi: 10.1186/s12885-019-5348-3
11. Li YS, Jiang BY, Yang JJ, Zhang XC, Zhang Z, Ye JY, et al. Unique Genetic Profiles From Cerebrospinal Fluid Cell-Free DNA in Leptomeningeal Metastases of EGFR-Mutant Non-Small-Cell Lung Cancer: A New Medium of Liquid Biopsy. *Ann Oncol* (2018) 29(4):945–52. doi: 10.1093/annonc/mdy009
12. Seoane J, De Mattos-Arruda L, Le Rhun E, Bardelli A, Weller M. Cerebrospinal Fluid Cell-Free Tumour DNA as a Liquid Biopsy for Primary Brain Tumours and Central Nervous System Metastases. *Ann Oncol* (2019) 30(2):211–8. doi: 10.1093/annonc/mdy544
13. Zheng MM, Li YS, Jiang BY, Tu HY, Tang WF, Yang JJ, et al. Clinical Utility of Cerebrospinal Fluid Cell-Free DNA as Liquid Biopsy for Leptomeningeal Metastases in ALK-Rearranged NSCLC. *J Thorac Oncol* (2019) 14(5):924-32. doi: 10.1016/j.jtho.2019.01.007
14. Wang Y, Springer S, Zhang M, McMahon KW, Kinde I, Dobbyn L, et al. Detection of Tumor-Derived DNA in Cerebrospinal Fluid of Patients With Primary Tumors of the Brain and Spinal Cord. *Proc Natl Acad Sci USA* (2015) 112(31):9704–9. doi: 10.1073/pnas.1511694112
15. Zheng MM, Li YS, Tu HY, Jiang BY, Yang JJ, Zhou Q, et al. Genotyping of Cerebrospinal Fluid Associated With Osimertinib Response and Resistance for Leptomeningeal Metastases in EGFR-Mutated NSCLC. *J Thorac Oncol* (2020) 16(2):250–8. doi: 10.1016/j.jtho.2020.10.008
16. Wang Y, Jiang F, Xia R, Li M, Yao C, Li Y, et al. Unique Genomic Alterations of Cerebrospinal Fluid Cell-Free DNA Are Critical for Targeted Therapy of Non-Small Cell Lung Cancer With Leptomeningeal Metastasis. *Front Oncol* (2021) 11(3563). doi: 10.3389/fonc.2021.701171
17. Mouliere F, Chandrananda D, Piskorz AM, Moore EK, Morris J, Ahlborn LB, et al. Enhanced Detection of Circulating Tumor DNA by Fragment Size Analysis. *Sci Transl Med* (2018) 10(466):eaat4921. doi: 10.1126/scitranslmed.aat4921
18. Li H, Durbin R. Fast and Accurate Short Read Alignment With Burrows-Wheeler Transform. *Bioinformatics* (2009) 25(14):1754–60. doi: 10.1093/bioinformatics/btp324
19. Mermel CH, Schumacher SE, Hill B, Meyerson ML, Beroukhim R, Getz G. GISTIC2.0 Facilitates Sensitive and Confident Localization of the Targets of Focal Somatic Copy-Number Alteration in Human Cancers. *Genome Biol* (2011) 12(4):R41. doi: 10.1186/gb-2011-12-4-r41
20. Seshan VE, Olshen A. *DNAcopy: DNA Copy Number Data Analysis*. (2020). (R package version 1.62.0.). doi: 10.18129/B9.bioc.DNAcopy. Avalable at: https://bioconductor.org/packages/release/bioc/html/DNAcopy.html.
21. Popova T, Manie E, Rieunier G, Caux-Moncoutier V, Tirapo C, Dubois T, et al. Ploidy and Large-Scale Genomic Instability Consistently Identify Basal-Like Breast Carcinomas With BRCA1/2 Inactivation. *Cancer Res* (2012) 72 (21):5454–62. doi: 10.1158/0008-5472.CAN-12-1470
22. Jensen TJ, Goodman AM, Kato S, Ellison CK, Daniels GA, Kim L, et al. Genome-Wide Sequencing of Cell-Free DNA Identifies Copy-Number Alterations That Can Be Used for Monitoring Response to Immunotherapy in Cancer Patients. *Mol Cancer Ther* (2019) 18(2):448–58. doi: 10.1158/1535-7163.MCT-18-0535
23. Colclough N, Chen K, Johnstrom P, Strittmatter N, Yan Y, Wrigley GL, et al. Preclinical Comparison of the Blood-Brain Barrier Permeability of Osimertinib With Other EGFR TKIs. *Clin Cancer Res* (2021) 27(1):189–201. doi: 10.1158/1078-0432.CCR-19-1871
24. Weir BA, Woo MS, Getz G, Perner S, Ding L, Beroukhim R, et al. Characterizing the Cancer Genome in Lung Adenocarcinoma. *Nature* (2007) 450(7171):893–8. doi: 10.1038/nature06358
25. Miller AM, Shah RH, Pentsova EI, Pourmaleki M, Briggs S, Distefano N, et al. Tracking Tumour Evolution in Glioma Through Liquid Biopsies of Cerebrospinal Fluid. *Nature* (2019) 565(7741):654–8. doi: 10.1038/s41586-019-0882-3
26. Pan C, Diplas BH, Chen X, Wu Y, Xiao X, Jiang L, et al. Molecular Profiling of Tumors of the Brainstem by Sequencing of CSF-Derived Circulating Tumor DNA. *Acta Neuropathol* (2019) 137(2):297–306. doi: 10.1007/s00401-018-1936-6
27. Jiang BY, Li YS, Guo WB, Zhang XC, Chen ZH, Su J, et al. Detection of Driver and Resistance Mutations in Leptomeningeal Metastases of NSCLC by Next-Generation Sequencing of Cerebrospinal Fluid Circulating Tumor Cells. *Clin Cancer Res* (2017) 23(18):5480–8. doi: 10.1158/1078-0432.CCR-17-0047
28. Manie E, Popova T, Battistella A, Tarabeux J, Caux-Moncoutier V, Golmard L, et al. Genomic Hallmarks of Homologous Recombination Deficiency in Invasive Breast Carcinomas. *Int J Cancer* (2016) 138(4):891–900. doi: 10.1002/ijc.29829

Conflict of Interest: Authors MS, WG, FZ, and HZ were employed by Hangzhou Jichenjunchuang Medical Laboratory Co., Ltd.

The remaining authors declare that the research was conducted in the absence of any commercial or financial relationships that could be construed as a potential conflict of interest.

Advantages of publishing in Frontiers

OPEN ACCESS
Articles are free to read for greatest visibility and readership

FAST PUBLICATION
Around 90 days from submission to decision

HIGH QUALITY PEER-REVIEW
Rigorous, collaborative, and constructive peer-review

TRANSPARENT PEER-REVIEW
Editors and reviewers acknowledged by name on published articles

Frontiers
Avenue du Tribunal-Fédéral 34
1005 Lausanne | Switzerland

Visit us: www.frontiersin.org
Contact us: frontiersin.org/about/contact

REPRODUCIBILITY OF RESEARCH
Support open data and methods to enhance research reproducibility

DIGITAL PUBLISHING
Articles designed for optimal readership across devices

FOLLOW US
@frontiersin

IMPACT METRICS
Advanced article metrics track visibility across digital media

EXTENSIVE PROMOTION
Marketing and promotion of impactful research

LOOP RESEARCH NETWORK
Our network increases your article's readership